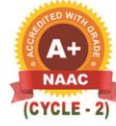




**NARASARAOPETA
ENGINEERING COLLEGE**
(AUTONOMOUS)



PROCEEDINGS

INTERNATIONAL CONFERENCE

EMERGING TRENDS IN MECHANICAL ENGINEERING AND INDUSTRIAL AUTOMATION

NEC-ICETMEIA-2K23

09th & 10th June, 2023

Editors-in-Chief

Dr. M.Sreenivasa Kumar

Principal & Professor, Dept. of Mechanical Engineering

Dr. B. Venkata Siva

Professor, HoD Dept. of ME

Editors

Dr. D.Suneel

Vice-Principal

Dr. D. Jagadish

Professor, Dept. of ME

Dr. P.Suresh Babu

Professor, Dept. of ME

Dr. M.Venkanna Babu

Associate Professor, Dept. of ME

ISBN: 978-93-91420-39-0



Organized by **Department of Mechanical Engineering**

In Association with **The Institution of Engineers (India)**

Indian Society for Technical Education (ISTE)

The American Society of Mechanical Engineers (ASME)



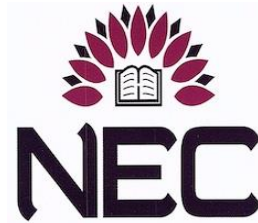
Proceedings of
**International Conference on
Emerging Trends in Mechanical Engineering and Industrial Automation
NEC-ICETMEIA- 2K23
9th – 10th June-2023**

Chief Editors

Dr.M.Sreenivasa Kumar Principal and Professor Department of Mechanical Engineering Narasaraopeta Engineering College Narasaraopet-522601	Dr.B.Venkata Siva Professor & Head Department of Mechanical Engineering Narasaraopeta Engineering College Narasaraopet-522601
---	--

Editors

Dr.D.Suneel
Dr.D.Jagadish
Dr.P.SureshBabu
Dr.M.VenkannaBabu



Organized By

Department of Mechanical Engineering
NARASARAOPETA ENGINEERING COLLEGE (AUTONOMOUS)
NARASARAOPET-522 601, ANDHRA PRADESH, INDIA
www.nrtec.in

Every effort has been made to avoid errors or omissions in this publication. In spite of this, some errors might have crept in. Any mistake, error or discrepancy noted may be brought to our notice which shall be taken care of in the next edition. It is notified that neither the publisher nor the authors or seller will be responsible for any damage or loss of action to any one, of any kind, in any manner, there from.

No part of this book may be reproduced or copied in any form or by any means (graphic, electronic or mechanical, including **Photocopying**, recording, taping, or information retrieval system) or reproduced on any disc, tape, perforated media or other information storage device, etc., without the written permission of the publishers. Breach of this condition is liable for legal action.

For binding mistakes, misprints or for missing pages, etc., the publisher's liability is limited to replacement within one month of purchase by similar edition. All expenses in this connection are to be borne by the purchaser.

"Copying of the book and selling it after photocopying or reselling it as **Second Hand Book** is illegal and is not allowed, under the copyright act".

This book is sold subject to the condition that it shall not, by way of trade or otherwise, be **lent, hired** out, or otherwise circulated without the publisher's prior written consent.

All disputes are subject to Pakala jurisdiction only.

Note: Please inform if any one encourage to photocopy of this book, along with the Proof and get attractive Reward. Names will be kept Confidential.

©Authors

Rs. /-

ISBN: ISBN: 978-93-91420-39-0

First Edition: 2023

Published by Surneni Mohan Naidu for Spectrum Publications and printed at Students Helpline Group, Hyderabad-38



SPECTRUM PUBLICATIONSTM
knowledge at your hands...

#326/C, Surneni Nilayam, Near BK Guda Park, S.R. Nagar

Hyderabad-500038, India

Tel: +914023710657, 32494570, 23800657

Cell: +919440575657, 9392575657

Fax: +914023810657

E-mail: studentshelpline.org@gmail.com

ACKNOWLEDGEMENT

It is my pleasure to record my sincere thanks to **Mr M.S.Chakravarthi, Hon'ble Vice Chairman**, NEC Group for his valuable guidance and encouragement throughout the proceedings of the conference. My sincere thanks to **Dr.M.Sreenivasa Kumar, Principal, NEC, Dr D. Suneel, Vice Principal NEC and Dr.B.Venkata Siva H.O.D., Mech.** for their whole hearted administrative support.

It's my privilege to thank the Keynote Speakers, Invited Speakers and Chairpersons of various technical sessions for their support in organizing the event. My sincere thanks to all the individual members of the Scientific Advisory Committee and Organizing Committee for their constructive ideas while designing the Conference Program. I thank all the participants who submitted the scientific and technical papers for sharing their ideas.

NEC-ICETMEIA 2K23 conference would have been impossible without the support of academic institutions and industrial organizations both in terms of manpower and ideas. This support is greatly acknowledged. I thank my management **Sri M.V.Koteswara Rao** Garu, Chairman and **Sri M.Ramesh Babu** Garu Secretary for their kind support and encouragement for the conference.

My heartfelt thanks to my colleagues and all my research team members whose efforts and hard work in organizing and managing the conference are gratefully acknowledged. I thank Co-Conveners and Organizing Committee for rendering their support to the conference.

I sincerely thank M/S Spectrum Publications Hyderabad for bringing out the Souvenir and Pre Conference Proceedings well in time.

Finally, I thank all the people and institutions who are directly and indirectly involved in organizing the Conference.

I thank one and all

Dr.D.Jagadish

Professor

Department of Mechanical Engineering

Narasaraopeta Engineering College

(Autonomous)

Co-Convener, NEC-ICETMEIA- 2K23

Chief Patron

Sri M.S.Chakravarthi, B.Tech, M.S (US),eMBA(ISB-Hyd)
Vice -Chairman, NEC Group

Patrons

Sri M.V.Koteswara Rao, B.Sc
Chairman, NEC Group

Sri M.Ramesh Babu, B.Com
Secretary, NEC Group

Co-Patrons

Dr.M.Sreenivasa Kumar, M.Tech, Ph.D(UK), MISTE, FIE(I)
Principal, NEC
Dr.D.Suneel, M.Tech, Ph.D, FIE(I),MISTE, MRSI
Vice Principal, NEC

Convener

Dr.B.Venkata Siva, M.Tech, Ph.D, FIE (I), MISTE, ISNT
Head, Dept. of ME

Co-Conveners

Dr.D.Jagadish,M.E, Ph.D,
Professor, Dept. of ME
Dr. P.Suresh Babu,M.Tech, Ph.D
Professor, Dept. of ME

Organizing Committee

Dr.M.Venkanna Babu

Mr.M.Venkaiah

Mr.P.Srinivasa Rao

Mr.Ch.Sekhar

Mr.T.Ashok Kumar

Mr.K.Kiran Chand

TNV Mahesh Babu

Mr.K.JohnBabu

Mr. SK.Nagul Meeravali

Mrs.P.Sravani

Mrs.D.Raghavendra

Mr.Shaik Bajan

Mr.A.Pavan Kumar

Conference Advisory Committee

**Prof. Marina L.Galano,
Dept. of Material Science, UNIVERSITY OF OXFORD, UK**

**Dr.Rukmini Srikant Revuru,
Assoc Prof. University of Northern Iowa, Cedar Falls, IA, USA**

**Jose I.Rojas,
Department of Physics – Division of Aerospace Engineering,
Universitat politecnica de catalunya, Spain**

**Kishore Kumar Sadasivuni,
Department of ME & IE, Qatar University, Qatar**

**Prof. N Siva Prasad,
Pro Vice Chancellor, GITAM University, Hyderabad**

**Dr.K.Srinivasa Reddy,
Professor, Dept of ME, IIT Madras**

**Prof. V.V.Subbarao,
Principal, UCEN, JNTUK, Narasaraopet**

**Dr.A.Gopala Krishna,
Professor, Director (R&D), JNTUK**

**Dr.D.Chakradhar,
Asst. Prof. Dept. of ME, IIT, Palakkad**

**Dr. K.L.Sahoo,
Sr.Principal Scientist, CSIR, NML, Jamshedpur**

**Dr. Y. Ravi Kumar,
Asoc. Prof. Dept. of ME, NIT, Warangal**

**Dr.Y.Naresh,
Asst. Prof. Dept. of ME, SVNIT, Surat**

**Dr.Ramakrishna Ramachandran,
Assoc. Prof. Dept. of D&A, VIT, Vellore**

**Dr. P.S. Rama Sreekanth,
Dept. of ME, VIT, A.P**

**Mr. Jnanananda Rao Kadi,
Deputy Manager, Bharat Dynamics Ltd., Hyderabad**

**Dr.Srinivasu Gangisetty,
Asst. Prof. Dept. of ME, NIT, Raipur**

Conference Papers Review Board

Dr.M.Sreenivasa Kumar, Professor, Principal, NEC

Dr.D.Suneel, Professor, Vice Principal, NEC

Dr.B.Venkata Siva, Professor, Head, Dept. of ME, NEC

Dr.D.Jagadish, Professor

Dr.P.SureshBabu, Professor

Dr.M.Rama Kotaiah, Professor

Dr.B.Ravi Naik, Professor

Dr.M.Naveen Kumar, Associate Professor

Dr.S.Jaya Krishna, Associate Professor

Dr.T.R.Santhosh Kumar, Associate Professor

Dr.M.Venkanna Babu, Associate Professor

M.Venkaiah, Associate Professor

P.Srinivasarao, Assistant Professor

Ch.Sekhar, Assistant Professor

K.Kiran Chand, Assistant Professor

P.Sravani, Assistant Professor

T.Ashok Kumar, Assistant Professor

K.John Babu, Assistant Professor

T.N.V.Mahesh Babu, Assistant Professor

SK.Nagul Meeravali, Assistant Professor

D.Raghavendra, Assistant Professor

PREFACE

International Conference on “Emerging Trends in Mechanical Engineering and Industrial Automation” **NEC-ICETMEIA-2K23** provides an excellent international forum for sharing knowledge and results in theory, methodology and applications impacts and challenges of Mechanical Engineering. The purpose of this conference is to bring together the mechanical engineering community to explore, disseminate and strengthen initiatives in new directions under the broad areas of Manufacturing, Thermal Sciences, Mechanical Design, Robotics, Mechatronics and Industrial Automation.

The objective of this conference is to create an international conglomeration of scientists, engineers and institutional experts. This forum serves as platform where people can share information about latest diverse technological advancements, innovations and achievements in the areas of Mechanical Engineering and allied fields of Engineering. Further it would also facilitate the discussion that centers on the developments and challenges in the fields of design, manufacturing, thermal, robotics, mechatronics fields of Engineering. The focus of this conference is to provide technical platform that encourages the scientific research and educational activities that would cater the needs of both society and the industry. Most importantly, NEC-ICEMEIA-2K23 is invested in the advancement of a common man’s life by utilizing the theory and practice of mechanical engineering and allied streams of Engineering. The conference includes Keynote addresses and guest lectures by eminent speakers around the globe who would deliberate the recent trends and challenges in the fields of Mechanical Engineering and Industrial Automation.

Message from Vice Chairman



I am glad to know that Department of Mechanical Engineering of Narasaraopeta Engineering College is organizing “International Conference on **Emerging Trends in Mechanical Engineering and Industrial Automation [NEC-ICETMEIA2K23]**. I hope this e-conference can congregate academicians, industry personnel and research scholars to share their findings and insights about innovations in Mechanical Engineering. The theme of the conference emphasizes on key aspects of Manufacturing, Thermal Sciences, Mechanical Design, Robotics, Mechatronics and Industrial Automation. I hope this initiative by Department of Mechanical Engineering will pave way to exceptional deliberations and other activities to enhance the power of knowledge and ideology in the field of engineering.

I wish the organizers great success for the conference.

Mr.M.S.Chakravarthi
Vice Chairman
NEC-Group

Message from Principal



I am glad to know that the Department of Mechanical Engineering of Narasaraopeta Engineering College organizing an International Virtual Conference on “**Emerging Trends in Mechanical Engineering and Industrial Automation [NEC-ICETMEIA2K23]**” during 9th& 10th of June 2023. The unprecedented ongoing pandemic situation prevailing all over the globe has driven the professionals to continue their research and knowledge dissemination virtually. I believe that such virtual conferences will be one of the finest opportunities for academicians, scientists, professionals, students and researchers from all over the globe to share and express their views, discuss the practical challenges and possible solutions in Science & Engineering fields.

The theme of the conference emphasizes the necessity of engineering innovation Mechanical Engineering in these difficult times all over the globe. I hope the scientific deliberations, discussions and other activities that happen during the conference will enrich the participants and definitely leave new milestones.

I wish the organizers the very best for the success of the Conference

Dr. M.Sreenivasa Kumar
Principal
Narasaraopeta Engineering College

Message from Vice Principal



It gives immense pleasure to write a message for the International Conference on “**Emerging Trends in Mechanical Engineering and Industrial Automation [NEC-ICETMEIA2K23]**” organized by Department of Mechanical Engineering, Narasaraopeta Engineering College (Autonomous) during 9th& 10th of June 2023. There are truly amazing innovations and breakthrough nowadays in the selected fields of Mechanical Engineering. I expect the present International Conference will explore students and research scholars to focus much on the field of Mechanical Engineering and Industrial Automation. I have gone through some of the abstracts and could see its rich qualitative academic content. I am also able to envisage its great potential to discuss and learn some new innovations in the fields of Mechanical Engineering.

It is important to inculcate an attitude towards research in the minds of younger generation and this conference would be a stepping stone towards this attainment in the field of Mechanical Engineering.

I wish the conference a great success. I am sure the conference is a grand scientific extravaganza and great feast for the student community.

Dr.D.Suneel
Vice Principal
Narasaraopeta Engineering College

Message from Head of the Department



I am very much delighted in welcoming the delegates for the 2 day virtual international conference on “**Emerging Trends in Mechanical Engineering and Industrial Automation [NEC-ICETMEIA2K23]**”. The pursuit for knowledge has been from the beginning of time but knowledge only becomes valuable when it is disseminated and applied to benefit of humankind. The prime focus of this conference is to bring together academicians, researchers and industry professional to join hands in finding the scope, challenges and opportunities and solutions that are encountered in the fields of Mechanical Engineering. Our technical sessions are rich and varied in the domains of **Machine Design, Production Engineering, Thermal Engineering and Automation**. As a conference Convener, I know that the success of the conference depends ultimately on the many people who have worked with us in planning and organizing both the technical program and virtual technical deliberations. In particular, we thank the review and advisory committee for their wise advice and brilliant suggestion on organizing the technical program; the Program Committee for their thorough and timely reviewing of the papers and publishing them in a conference proceeding. It is envisaged that the intellectual discourse will result in future collaborations between Universities, research institutions and industry globally towards the recent technological developments of Mechanical Engineering, during this pandemic situation.

Dr.B.Venkata Siva
Head, Department of ME

LIST OF FULL LENGTH PAPERS SELECTED FOR PROCEEDINGS
International Conference on Emerging Trends in Mechanical Engineering
and Industrial Automation
NEC-ICETMEIA- 2K23

REF. NO.	TITLE OF THE PAPER	Page. No.
NECICETMEIA-R01	Electricity Management and Energy Efficiency With IOT-enabled e-Life Devices	1
NECICETMEIA-R02	Fabrication of Hand Controlled Robot Car	6
NECICETMEIA-R03	Fabrication of Human Following Robot Using Arduino	10
NECICETMEIA-R04	Design And Fabrication of Cam And Follower Using 3D Printer	15
NECICETMEIA-R05	3D Printing of Rack And Pinion Steering Mechanism	18
NECICETMEIA-R06	Simulation of AUV Robotic Vehicle Body Using FEA Method	22
NECICETMEIA-R07	Conception, Fabrication, and Development of a Mechanized Arm for Physically Challenged Individuals	31
NECICETMEIA-R08	Design And Fabrication of MIG 29-K Fighter Jet Using 3D Printer	36
NECICETMEIA-R09	Design And Development of Walking Robot On The Bases of Four Bar And Weight Balance Mechanism	40
NECICETMEIA-R10	Design And Fabrication of Connecting Rod By Using 3d Printer	44
NECICETMEIA-R11	Design And Simulation of Prosthetic Arm	48
NECICETMEIA-R12	Design And Fabrication of Flex Sensor Operator Robot	58
NECICETMEIA-R13	3D Printing of Automotive Differential	66
NECICETMEIA-R14	Design And Fabrication of 3D Engine Model Using 3d Printer	71
NECICETMEIA-T01	Design and Thermal Analysis of Engine Fins Using Ansys	76
NECICETMEIA-T02	The Effect of Titanium Oxide (TiO ₂) Nano Lubricant On The Performance of Single Cylinder Diesel Engine	80

NECICETMEIA-T03	Fabrication And Analysis of Transmission System For Electric Vehicle	84
NECICETMEIA-T04	Design & Fabrication of Braking System For Electric Vehicle	89
NECICETMEIA-T05	A Historical Review on Solar Water Heaters	93
NECICETMEIA-T06	Design & Fabrication of Suspension System For An Electrical Vehicle	96
NECICETMEIA-T07	A Review on Hybrid Electric Vehicles and Types	100
NECICETMEIA-T08	Enhancement of COP in Vapour Compression Refrigeration System	104
NECICETMEIA-T09	Capability of Compression-Ignition Engine Fuelled With Pond Water Algae Biodiesel	109
NECICETMEIA-T10	Optimization And Simulation Analysis Of Subsonic Aircraft Using Aluminum Alloy And Carbon Fiber Composite (CFC)	114
NECICETMEIA-T11	A short review on various strategies for the reduction of CO ₂ emissions from automotive exhausts	128
NECICETMEIA-T12	3D printing Thermo Mechanical Analysis of carburetor for optimized support structure orientation for EOS M 280 Machine	132
NECICETMEIA-T13	Advanced foot step power generation using piezoelectric sensors	136
NECICETMEIA-D01	Design and fabrication of steering gear mechanism for electrical vehicle	140
NECICETMEIA-D02	Design And Analysis of Connecting Rod Using ANSYS	146
NECICETMEIA-D03	Design And Simulation of Gyro Sphere	151
NECICETMEIA-D04	Investigation of Stress Intensity Factors And J-Integrals In Fracture Of Composites Using FEM	158
NECICETMEIA-D05	Design And Fabrication of Electric Vehicle Chassis	159
NECICETMEIA-D06	Finite Element Analysis of Sheet Moulding Compound Panels	165
NECICETMEIA-D07	Design And Fabrication of Mini CNC Drilling Machine	169
NECICETMEIA-D08	Design And Fabrication of 360 Degree Desk Lamp	176
NECICETMEIA-D09	Investigation into the Synergistic Influence of Inclination and Partial Fins on the Melting Process of Phase Change Material in a Rectangular Enclosure Employing CFD	177

NECICETMEIA-D10	Dual Axis Solar Tracking System	186
NECICETMEIA-D11	Developing Face Recognition System Using AI & ML	187
NECICETMEIA-D12	Design And Optimization of HTV Fuel Tank Assembly By Finite Element Analysis	191
NECICETMEIA-D13	Fire and Gas Safety Alarm Prototype Using ARDUINO	197
NECICETMEIA-M01	Characterization of Sugarcane Reinforced Composite	201
NECICETMEIA-M02	Smart Auditorium Using Arduinio	207
NECICETMEIA-M03	Fatigue Characterization of A356-Sic Metal Matrix Nano Composites By Using Stir Casting Method	211
NECICETMEIA-M04	Fabrication of Fatigue Specimen By Using Stir Casting Method	218
NECICETMEIA-M05	Bending of Composite Plates Using Classical Laminate Plate Theory	222
NECICETMEIA-M06	The Automatic Detection of Fishing Vessels For Indian Fishermen	227
NECICETMEIA-M07	Modeling And Reinforcement of a Heavy Vehicle Leaf Spring For The Materials of E- Glasses And Epoxy Composites	232
NECICETMEIA-M08	Multi response optimization of mechanical properties of sponge gourd fiber reinforced polypropylene composites using grey relational analysis	239
NECICETMEIA-M09	Experimental Investigation of AZ31 Metal Matrix Composites	244
NECICETMEIA-M10	Construction of A Motorized Rotary Welding Table	248
NECICETMEIA-M11	Preparation and Characterization of Al-Cu Composite By Using Stir Casting Technique	252
NECICETMEIA-M12	Cruise Control System Using Fuzzy Logic For Autonomous Vehicle	256

ELECTRICITY MANAGEMENT AND ENERGY EFFICIENCY WITH IOT-ENABLED E-LIFE DEVICES

Miranji Katta¹, Yamini Komati¹, Satish Rapaka¹ and R.Sandana Lakshmi²

¹Sir C R Reddy College of Engineering, Eluru, West Godavari District-534007, Andhra Pradesh, India

²Department of Electronics and Communication Engineering, Puducherry Technological University, Pondicherry – 605014

Abstract— Energy conservation is a key challenge nowadays when it comes to living a more sustainable lifestyle. However, it is often ignored because of a lack of knowledge and the inability to predict the lifetime of electric or electronic equipment. Energy conservation is the most cost-effective strategy to cope with energy shortages. It enables the implementation of a product named "E-Life" to solve this problem and promotes public awareness. Electricity-intensive products have their own power specifications and lifespans, yet they usually live far longer than originally anticipated. However, the amount of power that they use is greater than what is stated in the datasheet. This issue is caused by the effects of aging. According to an experimental investigation, a 40-watt incandescent light uses an additional 25% of its original power after its lifespan has ended. The E-life algorithm in an "IoT-enabled small electronic device" integrated into any load to monitor and express product replacement time is proposed to prevent such a problem and be aware of excessive power consumption on all-electric or electronic equipment. The experimental research indicates that the suggested gadget can save over 37% of power over the course of six months for constrained loads.

Keywords— Energy Saving; Efficiency; Energy management; energy conservation; IoT; e-Life

I. INTRODUCTION

In today's world, energy conservation is one of the most difficult and significant aspects of living a green life; despite this, it is often ignored owing to a lack of understanding and an inability to accurately forecast how long electric or electronic items will continue to operate. Because we rely on energy for pretty much everything we do on a daily basis, this topic is incredibly significant to each and every individual. The generation of electricity is typically accomplished through the use of natural resources such as coal and water. Nevertheless, excessive usage of electricity leads to the depletion of these natural resources, which in turn contributes to climate change. Even if it means fewer energy services, energy conservation should result in better environmental quality, increased personal and national economic security, and greater savings[1]. At a somewhat more macro level, energy conservation may represent a very significant component of energy strategy[2]. The most common and cost-effective approach to dealing with energy shortages is to practise energy conservation. We want to design a product/load life indicator that will be known as eLife in order to solve this issue and educate consumers about the amount of power that is used by the electric or electronic items that they own.

Because we frequently consider energy in terms of how much we accomplish each day, it is critical for all of us. The most basic kinds of energy come from the earth itself, and that means things like fossil fuels, water, and air. While coal is responsible for 56.1% of the total power production in India, fossil fuels in general and coal in particular are responsible for 72% of the total power generation throughout the globe. Fossil fuel combustion is responsible for 40 percent of the emissions of carbon dioxide, which, when mixed with mercury and sulphur dioxide, are the primary contributors to acid rain and respiratory diseases. Because of the excessive use of power, the depletion of these natural resources contributes to the warming of the planet. Despite the fact that energy conservation reduces the number of available energy services, it is expected to have a positive impact on environmental greenery, national and personal economic stability, and savings. It's feasible that energy conservation will be an essential part of the energy plan on a much larger scale, and this possibility should not be discounted. A 5-year-old refrigerator uses up to 10% more electricity than it did when you first purchased it. A refrigerator that is ten years old uses twenty percent more power than it did when it was first purchased. After 15 years, the extra electricity utilised amounts to 30 percent.

The power-hungry goods that we often buy each come with their own set of power requirements as well as a lifespan; yet, the vast majority of these products continue to function for a period of time that is far longer than the lifetime that was originally indicated for them. However, the amount of electricity that they use is far greater than what is specified[3]. This is because of a natural process known as ageing. According to the findings of a recent study, a standard light bulb with 40 watts of light uses an additional 25 percent of its power once it has reached the end of its life cycle. Now, when we simply examine the bulb, this may not seem like a very significant issue; but, when we consider a whole home, street, town, district, or state, it becomes clear that this is a significant issue. In order to address the problem that was described earlier, a single portable, compact, and cost-effective electronic circuit that consists of two indications known as "safe" and "replace" was used. This enabled the issue to be fixed.

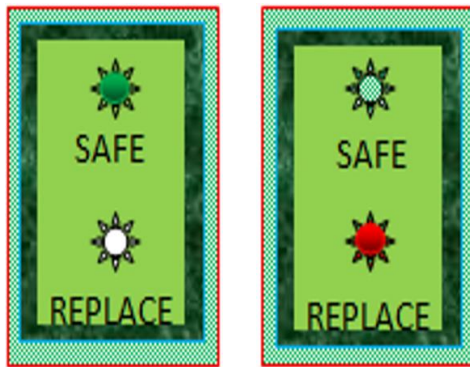


Figure 1. Life indicator of appliance

If the product uses the amount of power that is mentioned in the datasheet, then it will be displayed by a green LED that says "SAFE." If it uses more power than its specifications allow for or if the product is not functioning properly, then it will notify you with a red LED that it needs to be replaced. If any power-consuming device already has this suggested electronic circuit built in, then it will be extremely simple to determine when the product should be replaced and whether or not it is safe to use according to the indications. This mode's presentation is the most user-friendly, so everyone can understand what's being said. By increasing people's knowledge of the need to replace a product before it reaches the end of its useful life at the appropriate time, this strategy helps minimise overall power usage.

A monitoring system for individual home appliances' power usage based on the internet of things.

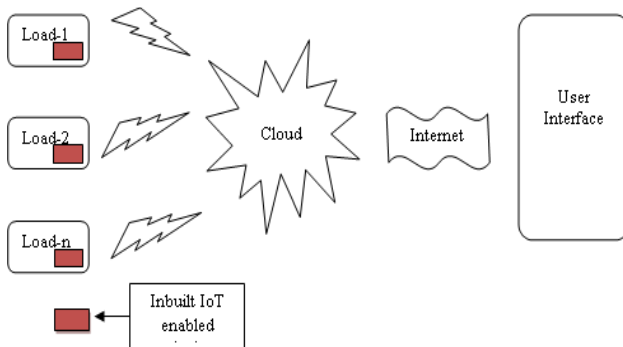


Figure 2. Basic Block Diagram of Enabled IoT in Loads

The power consumption of each individual gadget in the home may be tracked because of the built-in circuits that are present in each appliance. The power consumption of each appliance is measured by the integrated circuit, and the data is then sent to the neighbourhood server. Any user may log in to his or her energy bill payment website and check the consumption as well as the bill that was collected for it by accessing the data that is saved on the local server and uploading it into a central database as well as the cloud.

II. . LITERATURE SURVEY

[4] Refers to an automatic detection of appliances. The energy monitor device is embedded electrical appliances to monitor power consumption. The user may choose to opt-in to certain energy saving programs such as receiving notifications of sales on energy saving appliances, receiving recommendations and advice on repair or replacement aging appliances based on energy usage information. The user connect the monitoring device to mobile which is having an internet connection to identify the information stored in the monitoring device.

[5] Refers to a system and method for monitoring electrical appliance. The cloud server allows the monitoring device to connect the electrical appliance to monitor the abnormal state (electrical leakage, overcurrent etc.) or the aging condition of the electrical appliance according to the safe usage standard. If the overcurrent occurs on the appliance then the control unit of the monitoring device determines the abnormal state or aging condition by using load boundary and sends a warning to the user. Whether the electric appliance is abnormal whenever necessary, or detect the aging condition of the electric appliance in order to maintain or replace the electric appliance. The load current of the appliance displayed on the user interface display or cloud server.

[6] Refers to a meter for measuring and displaying the power consumption of an electrical appliance and the time period of such power consumption. The meter is provided as an integral part or built into an appliance and also comprises a row of five LED's. The two red LED's on the right side, two green LED's on the left side. When the electrical appliances consumes very high power then the rightmost red LED's will be lit up. When electrical appliances consumes very light power then the leftmost green LED's will be lit up. The power meter comprising a computer interface for downloading the measurement results of the power meter to an external computer for processing the results.

[7] Refers to an electricity energy consumption data management system. The indicator group connected to the control host to facilitate the visual observation of the energy consumption of each device, an abnormal load is found in time. The indicator light is a red and green two-colour indicator light, which can indicate three colour states of red, green, and orange, so that the current energy consumption of the device detected by the detection node to which it belongs is higher, lower, and flatter than the historical history of the device. The Ethernet interface and the serial communication interface are also connected to the control host.

III. MATERIALS AND METHODS

The current sensor and the energy metering module are both parts of the power measurement module. In order to measure power, the energy metering module needs to know the mains voltage and current.

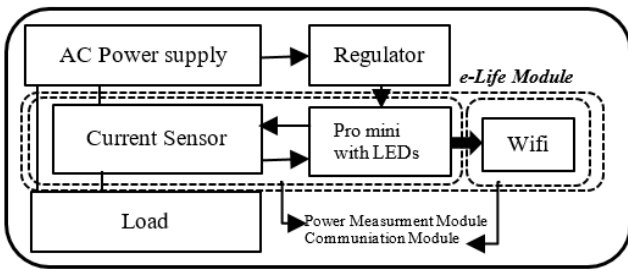


Figure 1. Basic Block Diagram of e-Life Module and Associated connections

The amount of current that is moving through the wire that is connected to the device whose power consumption is being monitored. The transformer that is used to provide power for the functioning of the current sensor also has an extra secondary tap that is accessible, and this tap is used to measure the voltage.

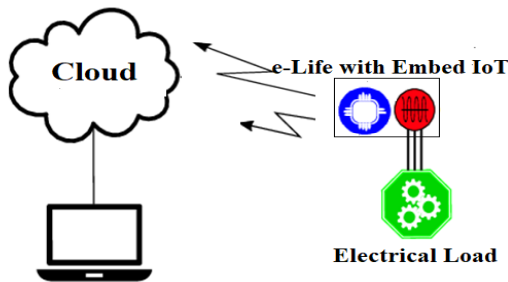


Figure 2. Cloud interface with Load via e-life

Both invasive and non-invasive types of current sensors are available, in this experiment, investigators use hall effect based current sensor (ACHS-719x) is used. This Unified Hall-effect-oriented standalone linear current sensors are used to detect AC or DC current in industry and communications systems. Each ACHS-719x integrated circuit contains a small, accurate linear Hall circuitry with a metal conduction route located near the chip's surface. When an external current is sent over this copper conductor, a magnetic field is produced. Differential Hall sensors then take this magnetic field and transform it into an electric signal. Because of the closeness of the magnetic pulse to the Hall sensors, the accuracy of the device is maintained regardless of the operating temperature of the surrounding environment. During operation, there will be no core movement since the case has a click-fit structure that secures the cores in their proper positions. Because of the way the case is designed, users are able to effortlessly detach the e- life device from one wire and reattach it to another without causing any disruption to the mains wiring. The current sensor and associated circuitry linked to the energy measurement module. Then, the output of the energy metering module is sent to the processing module, where the power value is calibrated, encrypted, and sent[8].

B. Communication Module

A Wi-Fi System on Chip is used to accomplish the processing and communication functions. It is a compact Wi-Fi chip that has a high level of integration, and it is easy to programme using a variety of software, such as the Arduino IDE [8], the ESPRESSIF SDK [9], and NodeMCU [10]. For the sake of simplicity and since there is existing support available, we have programmed the Wi-Fi module using the

Arduino IDE. Here investigator used segregated modules for Monitoring and communication for better functionality and user friendly. This has allowed us to perform functions such as power measurement and data communication. The output of the energy metering module is delivered into the processing module, which is where the power value is computed and calibrated according to the parameters that have been saved for calibration.

C. Elife Algorithm

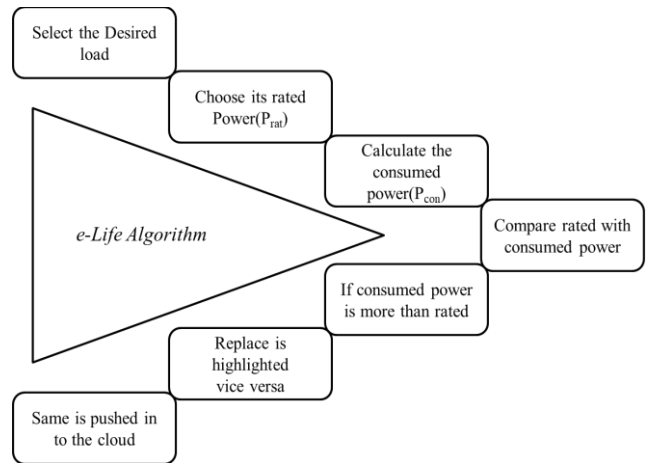


Figure 3. E-Life Algorithm

Elife algorithm is based on rated power (P_{rat}) and consumed power (P_{con}) of given electrical appliance. Any electrical appliance has its own data sheet, where manufacturer mentioned how much power it consumed and life time of each of these appliance according to switching count. But most of these appliances works well even its life time vanished, the fore most important point here is, these appliances consumes more than rated power after specified life span. According to E-life algorithm, if consumed power is more than rated power ($P_{con} > P_{rat}$) then appliance life span is over and the same is indicated with RED Colour glow LED by means of ready to replace the appliance. Otherwise it shows Green Colour glow LED is showing by means of Safe, no need to replace the appliance [].

C. Cloud Environment

Here Google firebase cloud environment is used for storing periodical data from e-life device. This cloud environment has SSID and password for the wireless network already registered for data storage. It is necessary to have these characteristics in order to connect the power monitoring sensor to the Wi-Fi network and guarantee permitted access. In order to transfer the encrypted value of the instantaneous power to the distant server, we have the option of using either the Transmission Control Protocol (TCP) or the User Datagram Protocol (UDP). TCP's transmissions have proven to be more reliable than those of UDP, which is why we chose to adopt it.

D. Remote Data Logging Unit

The remote data logging unit is made up of a computer that has a server programme installed and is operating on it. This computer is linked to the same network as the power monitor sensor. After being encrypted, the power values are sent to the server, where they are received and then decrypted using the

same pre-shared key that was used during encryption. In addition, a one-of-a-kind sensor ID is encoded into each elife device, and this ID is sent to the server with each load power consumption. This will make it easier for the server to do an individual analysis of the power data coming from each sensor or, if necessary, from a collection of sensors. The server may also have connectivity to the Internet, allowing the data to be accessed and analysed at a distant location. All the information may be mapped with according to their Geo locations are also possible with GUI.

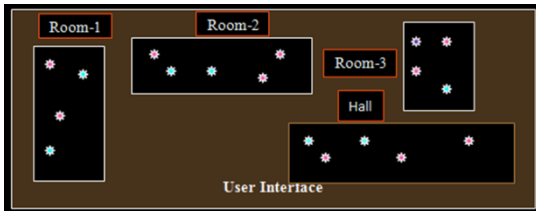


Figure 4. Geo Mapping with e-Life devices

On these data, which are kept on a server and can be accessed via a browser, as seen in Figure 4, one may do a variety of analyses. A graphical analysis of the data has been supplied by us so that you may view the time-based trend of the power usage (refer to Fig. 5). These power figures may also be used to compute the total amount of electric energy that is used over a certain period of time. This can be done by calculating the area under the curve that represents the instantaneous power. In addition to this, we have built an application for Android that makes viewing analysis simple and improves the overall user experience all of the components, including the current sensor, processing module, and communication module, are contained inside a small shell that was developed and built using 3D printing technology. This makes the device very user-friendly. The current sensor is located on the top deck of the casing, while the processing and communication module is located on the lower deck of the casing. The casing is divided into two portions.

IV. RESULTS AND DISCUSSIONS

The functionality of the suggested power monitoring system is evaluated, and some insights on the basis of reliability, efficiency, and the cost of the necessary materials are provided below.

E-Life experimental setup and Measurement

The development of a secured Wi-Fi-based power monitor sensor that is simple, compact, and inexpensive is proposed. It has been effectively installed all around the college premises, and it has been tested there as well. It has been shown that the precision of power measurement is sufficient for the reliable use as a life monitoring sensor. Numerous sensors may be used to monitor the power consumption of multiple electrical appliances at the same time. Due to their compact size, low cost, and ease of use, multiple sensors are ideal for this task. Consumers will be able to monitor safe operating period of electrical appliance more efficiently.

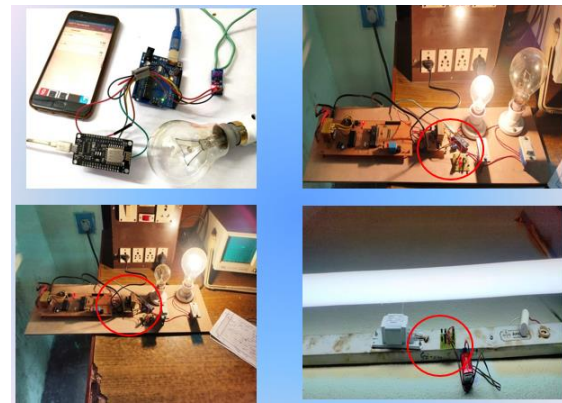


Figure 5. Experimental setup and Installation

The experimental setup, shown above in Figure 7, is intended to investigate the typical lifetime of electrical loads. The average lifetime of a load may be obtained directly from the manufacturer by referencing the relevant datasheet. Even after the specified life has elapsed, the equipment continues to function normally but consumes more power than was initially expected. Table 1 lists the most commonly used electrical loads, as well as the amount of electricity they consume and an estimate of their typical life span.

Table 1. Rated power and average life time of most common loads

Type of load	Rated power	Life time
Incandescent Lamp	60W	750-1000
Tube Light	40W	7000-15000
Fan(Speed 5)	75W	4-6 years
Motor(0.2hp)	150W	5 years

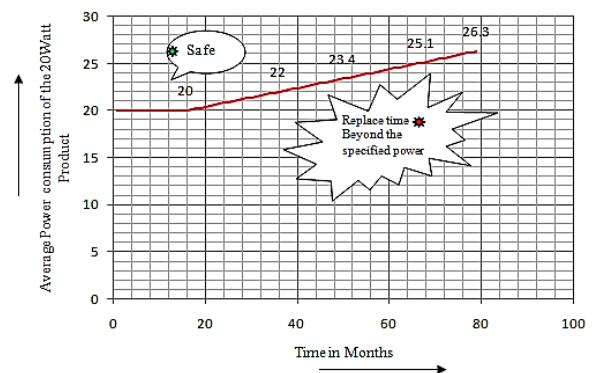


Figure 6. Experimental results shows load replacement time

The findings of the experiments demonstrate that after 18 months of the bulb's stated life, it begins to use more electricity than it was designed to and continues to do so every month until it finally dies shown in figure 8.

The results of a simulation showing the power consumption of a load as measured by a Pico power analyser are shown in Figure 9. The simulation study reveals that the calculated power of the load once it has reached its specified

life time is always higher than the rated power, and its value continues to rise over time. This is due to the ageing process. If the same information were to be transmitted via visual presentation, the user could be able to understand precisely when the replacement time is, similar to the time needed to change the batteries in water filters. By presenting the information in this way, the customers are at least made aware of the need to replace power-hungry loads on schedule and to save electricity through more efficient consumption.



Figure 7. Experimental and Simulated outputs



Figure 8. Google Fire Base Analytics Window

The data was collected from the e-life gadget installed on the load and transmitted using the IoT Module ESP8266. The Google Firebase analytical window can be used to monitor the collected data and perform an analysis of the rated and actual power consumption. According to analytics, the loads listed in Table 1 use 37% more power than what is specified after their lifetime has passed. According to the findings of the research, the appliance that is being recommended may help users save more than 37% of the power that is being used by constrained loads.

V. CONCLUSION

In this article, a simple, compact, and low-cost method for fabricating a reliable IoT-based life monitoring sensor is proposed. It has been effectively installed all around the college campus, and it has been tested there as well. The precision of power measurement between rated and consumed has been demonstrated to be sufficient for reliable use as a life monitoring device. Numerous sensors may be used to monitor the power consumption of multiple electrical appliances at the same time. Due to their compact size, low cost, and ease of use, multiple sensors are ideal for this task. Consumers are able to use energy in a more efficient manner by observing visible indications on the e-life device, and geo-mapping makes the exact location and indication of replacement times

accurate. With this proposed e-life device, electricity management becomes quite easy and can improve energy efficiency significantly.

REFERENCES

- [1] H. L. M. do Amaral, A. N. de Souza, D. S. Gastaldello, F. Fernandes, and Z. Vale, "Smart meters as a tool for energy efficiency," in *2014 11th IEEE/IAS International Conference on Industry Applications*, Juiz de Fora, Dec. 2014, pp. 1–6. doi: 10.1109/INDUSCON.2014.7059413.
- [2] Q. Liu and W. Feng, "Research on the Efficiency and Economic Impact of Energy-Saving Transformation of Residential Buildings in Different Climatic Regions of China," *Adv. Mater. Sci. Eng.*, vol. 2015, pp. 1–9, 2015, doi: 10.1155/2015/634904.
- [3] S. Perumal and S. Rajendiran, "Operational Load Forecasting Using Machine Learning Algorithms," *SSRN Electron. J.*, 2021, doi: 10.2139/ssrn.3883192.
- [4] M. Cirrincione *et al.*, "Intelligent energy management system," in *2009 7th IEEE International Conference on Industrial Informatics*, Cardiff, Wales, UK, Jun. 2009, pp. 232–237. doi: 10.1109/INDIN.2009.5195809.
- [5] A. Joshi and S. Venugopal, "Energy Management Systems in India," vol. 03, no. 11.
- [6] T. Knayer and N. Kryvinska, "An analysis of smart meter technologies for efficient energy management in households and organizations," *Energy Rep.*, vol. 8, pp. 4022–4040, Nov. 2022, doi: 10.1016/j.egyr.2022.03.041.
- [7] A. K. Aliyu, A. L. Bukar, J. G. Ringim, and A. Musa, "An Approach to Energy Saving and Cost of Energy Reduction Using an Improved Efficient Technology," *Open J. Energy Effic.*, vol. 04, no. 04, pp. 61–68, 2015, doi: 10.4236/ojee.2015.44007.
- [8] K. Yamini, K. S. N. Raju, and K. Miranji, "Low Power Data Compression Algorithm For Wireless Sensor Networks Using VHDL," vol. 3, no. 11, p. 6, 2014.

FABRICATION OF HAND CONTROLLED ROBOT CAR

B. Venkata Siva , G. Anil, K. Naveen, V. Koteswara Rao, K. Ajith Kumar, Ch. Karunakar

Narasaraopeta Engineering College, Narasaraopet, Palnadu (Dist.), A.P., India

ABSTRACT -Any object can be moved by some external force which is generally human efforts. Moving distant physical objects just by little movements of hands can be achieved by our project. A small amount of motion is amplified on a larger scale. This concept can bring much comfort, convenience and physical cost reduction in daily life as well as industries.

In this project a Robotic project is developed hand-controlled car that takes readings from an accelerometer which is placed on a human hand. The direction of the car can be changed by moving the hand in a particular direction, each movement generates the values in its corresponding axis. Generated values by accelerometer are sent to the Arduino UNO, HT12E encoder which is connected to Arduino will encode the values and send it to a receiver through RF433 transmitter.

HT12D placed on the car will decode the values and give it to the L293D motor driver, which will instruct the motors to move the vehicle. This project can be very helpful for physically challenged people as they can move certain objects with less physical movement.

Keywords- *Arduino IDE, Robot, sensor control system, Automation system.*

I. INTRODUCTION

Technology is the word coined for the practical application of scientific knowledge in the industry. The advancement in technology cannot be justified unless it is used for leveraging the user's purpose. The society as a whole is exquisitely dependent on science and technology. Technology has played a very significant role in improving the quality of life. One way through which this is done is by automating several tasks using complex logic to simplify the work.

Gesture recognition has been a research area which received much attention from many research communities such as human computer interaction and image processing. The increase in human- machine interactions in our daily lives has made user interface technology progressively more important. Physical gestures as intuitive expressions will greatly ease the interaction process and enable humans to more naturally command computers or machines. Now a day's robots are controlled by remoter cell phone or by direct wired connection. If we thinking about cost and required hardware's all this thing increases the complexity, especially for low level application.

II. LITERATURE REVIEW

[1] The major goal of this study is to design and implement energy-saving measures in public spaces such as auditoriums, shopping malls, and theatres. A human or a controlling system is required to control and monitor all of these devices or appliances.

[2] The primary goal of this study is to conserve energy. Manual control methods are preferred over automatic control systems. Controlling electrical and electronic gadgets, appliances, and other devices is possible with the design of power control and saving projects.

[3] In our project, we used Arduino to create a control system that is easier to use than other microcontrollers. They proposed a technique to analyse the power usage in the gathering by building a visitor counter and an automatic fan control system.

[4] An effective innovation technology in enhancing teaching and learning of knowledge using ict methods, international journal of contemporary research in computer science and technology

[5] The objective of this paper is to build a gesture-controlled robot that can be controlled by gesture wirelessly. User is able to control motions of the Robot by wearing the controller glove and performing predefined gestures.

III. PROPOSED METHOD

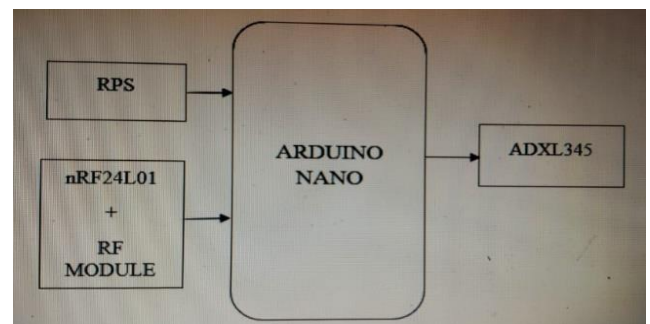


Fig.1: Block diagram of Transmitter



Fig.2: Block diagram of Receiver

The objective of this paper is to build a gesture-controlled robot that can be controlled by gesture wirelessly. User is able to control motions of the Robot by wearing the controller glove and performing predefined gestures. This Robot can detect block objects and stop automatically; in addition, feedback messages are sent to the controller and warn the user. The robot also senses surrounding temperature and human presence. This project provides a basic platform for many potential applications such as wireless controlled car racing games, gesture human-machine interfacing, and etc.

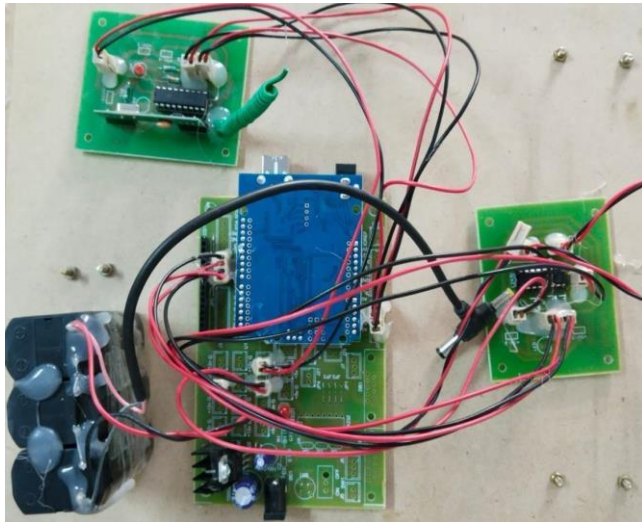


Fig.3: Circuit diagram of the Receiver

The ATmega328P-based Arduino UNO is a microcontroller board. It has 14 digital I/O pins (of which 6 can be used as PWM outputs), 6 analogue inputs, a ceramic resonator operating at 16 MHz, a USB connection, a power jack, an ICSP header, and a reset button. It comes with everything you need to support the microcontroller; simply connect it to a computer via USB or power it via an AC-to-DC adapter or battery to get started.



Fig.4: Arduino Uno

The **Arduino Nano** is a small, complete, and breadboard-friendly board based on the **ATmega328**. It has more or less the same functionality of the **Arduino Duemilanove**, but in a different package. It lacks only a DC power jack, and works with a **Mini-B USB** cable instead of a standard one.

It comes with an operating voltage of 5V; however, the input voltage can vary from 7 to 12V. **Arduino Nano Pinout** contains 14 digital pins, 8 analog Pins, 2 Reset Pins & 6 Power Pins. Each of these Digital & Analog Pins are assigned with multiple functions but their main function is to be configured as input or output. The analog pins come with a total resolution of 10bits which measure the value from zero to 5V.

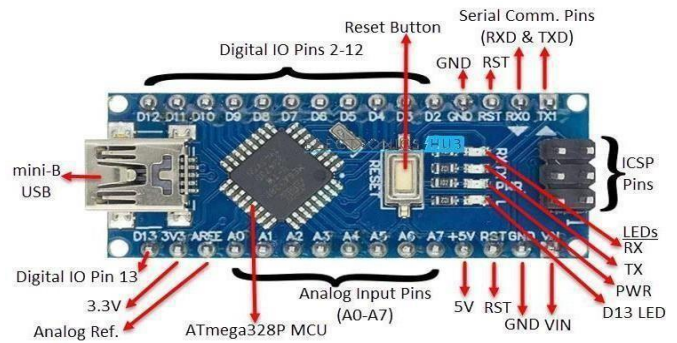


Fig.5.Arduino NANO

The speed of a DC motor can control in three ways: By varying the flux, and by varying the current through field winding. By varying the armature voltage, and the armature resistance. Through the supply voltage.



Fig.6. DC Motor

RF module (short for radio-frequency module) is a small electronic device used to transmit and receive radio signals between two devices. In an embedded system it is often desirable to communicate with another device wirelessly.

RF modules are most often used in medium and low volume products for consumer applications such as garage door openers, wireless alarm or monitoring systems, industrial remote controls, smart sensor applications, and wireless home automation systems. They are sometimes used to replace older infrared communication designs as they have the advantage of not requiring line-of-sight operation.

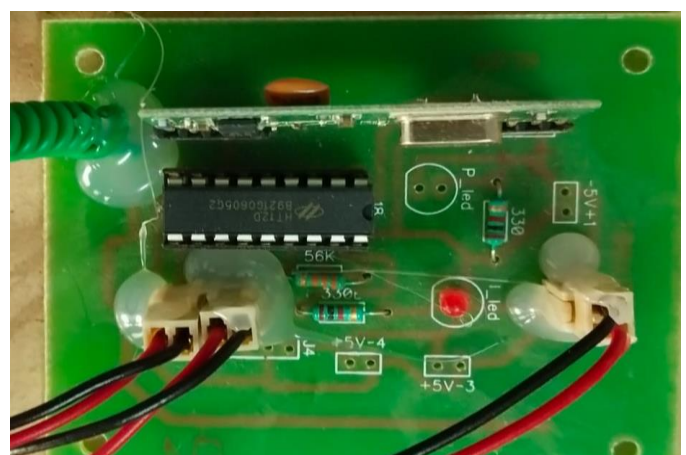


Fig.7: RF module

The ADXL345 is a small, thin, low power, complete 3-axis accelerometer with signal conditioned voltage outputs. The product measures acceleration with a minimum full-scale range of $\pm 16g$.

ADXL345 works on the principle of capacitive. It works on the principle of when the acceleration is applied to the sensor, the capacitance inside the sensor changes. The change in capacitance is then used to measure the acceleration of the object.



Fig.8: ADXL345

The L293D is designed to provide bidirectional drive currents of up to 600-mA at voltages from 4.5 V to 36 V. Both devices are designed to drive inductive loads such as relays, solenoids, DC and bipolar stepping motors, as well as other high-current/high-voltage loads in positive-supply applications.



Fig.9: L293D Module

SOFTWARE IMPLEMENTATION:

The Arduino Integrated Development Environment or Arduino Software (IDE) contains a text editor for writing code, a message area, a text console, a toolbar with buttons for common functions and a series of menus. The language used is based on C and C++, there are a couple of small differences designed to make Arduinos as easy to use as possible. The Arduino IDE will do some pre-processing to the code to avoid some unwanted errors but other than that it's C and C++

Installation of Software:

To begin, download the Arduino IDE from the Arduino website. Make sure to select the right version for your Operating System (OS). For a full getting started guide for each OS, please refer to the Arduino guide. Once the arduino.zip file has been downloaded, extract the file to a folder somewhere on your computer. There is no install - simply open the folder and double click the .exe



Fig.10: Arduino Software

IV. RESULT

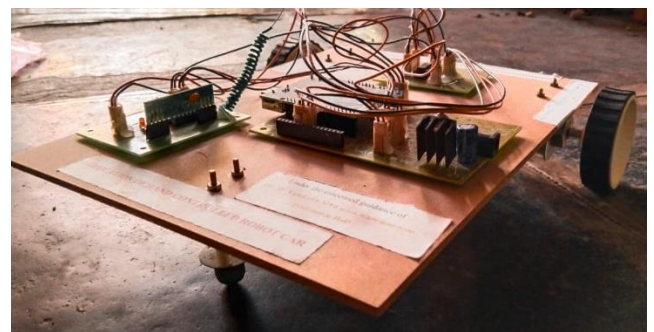
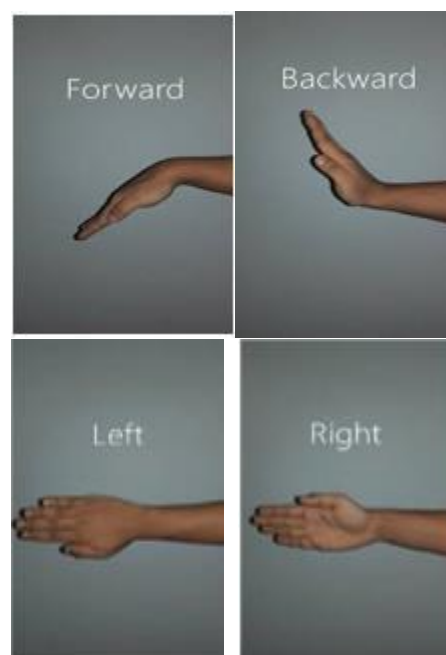


Fig.11: Implemented circuit

The movement of robot is as follows: -

- The robot moves **Forward**, when the X-axis of ADXL345 is less than 250.
- The robot moves **Backward**, when the X-axis of ADXL345 is greater than 300.
- The robot moves **Left**, when the Y-axis of ADXL345 is less than 250.
- The robot moves **Right**, when the Y-axis of ADXL345 is greater than 300.



V. ADVANTAGES

Our Project aims at creating Smart environment and “Smart Hospitals” along with the ever-growing smart technology. It can easily overcome the drawbacks of the traditional methods of using bells, sirens and buzzers at hospitals. This project eases the life of patients and their family members

VI. APPLICATIONS

- These robots are used in military applications to operate robots
- These robots are used in medical applications for the purpose of surgery
- This robotics are used in the construction field.
- This robotics are used in industries to control trolley and lift

VII. CONCLUSION & FUTURE SCOPE

MEMS based hand-controlled robot” has a future enhancement, the MEMS accelerometer can be even programmed in Z axis so the robot can be made to move in Z direction with additional hardware equipment’s. Another improvement can be done in this, which enables the user to be used in high performance applications are by replacing the PIC microcontroller with ARM processor.

The on-board batteries occupy a lot of space and are also quite heavy. We can either use some alternate power source for the batteries or replace the current DC Motors with ones which require less power. The proposed system is applicable in hazardous environment where a camera can be attached to the robot and can be viewed by the user who is in his station. This system can also be employed in medical field where miniature robot are created that can help doctors for efficient surgery operations for more efficient response, threshold values can be used to detect gesture and advanced features such as finger counts that provide different functional commands can be used. Entertainment applications – Most videogames today are played either on game consoles, arcade units or PCs, and all require a combination of input devices. Gesture recognition can be used to truly immerse a player in the game world like never before. Automation systems – In homes, offices, transport vehicles and more, gesture recognition can be incorporated to greatly increase usability and reduce the resources necessary to create primary or secondary input systems like remote controls, car entertainment systems with buttons or similar.

REFERENCES

- [1] Y. Yan, Y. Qian, H. Sharif, and D. Tipper, “A survey on smart grid communication infrastructures: Motivations, requirements and challenges,” *IEEE Communications Surveys and Tutorials*. 2013.
- [2] D.V. Nicolae and A. A. Jimoh (2007), “A Three-Phase Induction Motor with Power Electronic Controlled Single-Phase Auxiliary Stator Winding”, *IEEE Power Electronics Specialists Conferences (PESC 2007)*, pp. 98-103
- [3] *The Internet of Things (The MIT Press Essential Knowledge series) – 20 March 2015.*
- [4] *The Fourth Industrial Revolution Hardcover – January 3, 2017, by Klaus Schwab (Author).*
- [5] *Getting Started with the Internet of Things: Connecting Sensors and Microcontrollers to the Cloud (Make: Projects) 1st Edition, Kindle Edition by Cuno Pfister (Author)*
- [6] X. Fang, S. Misra, G. Xue, and D. Yang, “Smart grid -The new and improved power grid: A survey,” *IEEE Communications Surveys and Tutorials*. 2012
- [7] “The Smart Grid,” in *The Internet of Things: Key Applications and Protocols*, 2011.
- [8] N. Komninos, E. Philippou, and A. Pitsillides, “Survey in smart grid and smart home security: Issues, challenges and countermeasures,” *IEEE Communications Surveys and Tutorials*. 2014.
- [9] J. L. Hernández-Ramos, M. V. Moreno, J. B. Bernabé, D. G. Carrillo, and A. F. Skarmeta, “SAFIR: Secure access framework for IoT-enabled services on smart buildings,” in *Journal of Computer and System Sciences*, 2015.
- [10] A. R. Metke and R. L. Ekl, “Security technology for smart grid networks,” *IEEE Trans. Smart Grid*, 2010.
- [11] M. Yigit, V. C. Gungor, and S. Baktir, “Cloud Computing for Smart Grid applications,” *Computer Networks*. 2014.

FABRICATION OF HUMAN FOLLOWING ROBOT USING ARDUINO

Ch. Sekhar, J.Nagendra babu, J. Jayanth kumar, .T. Vinay kumar, A. Raghu Rami Reddy, M. Rakesh.

Narasaraopeta Engineering College, Narasaraopet, Palnadu(Dist.),A.P,India.

Abstract - A robot which can help us in many fields like carrying items, work with more accuracy in lesser time in every kind of works. A robot that can help us in a hospital or bringing medical items in any emergency case will be more helpful for a doctor in emergency cases. This type of robot having so many benefits and it will be helpful in the future. This type of robot can be close to humans is much possible. This useful project is made to attempts to follow the right human or obstacle. In this robot, Infrared sensors are used to move the robot in both the direction and ultrasonic sensor for both the forward and reverse direction. the Arduino Uno microcontroller as the brain of this project. This robot is driven with four Dc motors and it is controlled by a motor driver shield with L293d. The main objective of designing this useful project is to make our life better and luxurious. In this project robotic car sense the human by IR sensor automatically and follow the human and obstacles. This type of robot will be more useful and it will be a trend in the future. A person come near to the robot, it starts to follow the human. here 4 motors attached to the wheels. There are three sensors i.e., Ultrasonic sensor and two IR sensors are mounted on the robot. sensors left and right to the ultrasonic sensor. If the human turns the hand to the left side the **Arduino robot** moves on the left side, and similarly, in the right the robot will move in the right direction. when the human put the hand in front of the ultrasonic sensor then the sensor detects person and sends this information to the Arduino

I.INTRODUCTION

Microcontrollers are widely used in Embedded Systems. An Embedded product uses the microprocessor (or microcontroller) to do only one task at a time. A printer is an example of embedded system since the processor inside it performs one task only, namely getting the data and printing it. Although microcontroller is preferred choice for many embedded systems, there are times that a microcontroller is inadequate for the task. For this reason, in recent years many manufactures general-purpose microprocessors

such as INTEL, Motorola, AMD & Cyrix have targeted their microprocessors for the high end of embedded market. One of the most critical needs of the embedded system is to decrease power consumptions and space. This can be achieved by integrating more functions into the CPU chips. All the embedded processors have low power consumptions in additions to some forms of I/O, ROM all on a single chip. In higher performance embedded system, the trend is to integrate more & more function on the CPU chip & let the designer decide which feature he/she wants to use.

II.LITERATURE SURVEY

In this high technology, a robot must be able to detect and follow humans. A robot that can detect and follow human or obstacle within a specific range is called 'Human Following Robot'. Robots are used to change people's lives and make people's life luxurious. A robot that can use in shopping time which carries items and follow human without any remote more useful. A robot that can use in the hospital to bring medicine with more accuracy and fast. The human following robot has many works like work as trolley, structure in hospital, and a small basket with a car and so on. Now in this changing world, people are started to live with robot-like humans following robots for their luxurious life. This project named called human following robot because it can follow humans with the help of IR sensors and can co-exist with humans and help humans in any kind of work with more accuracy and in lesser time. The human following robot can use in the defence sector also to carry weapons for the soldiers. This type of robot can sense obstacles and humans automatically and it can use in the future in our cars. An human following robot can be modified in the future with more developed components and can make it more advance. This robot can be enhanced by structure by adding more components like camara, tracking device and make it more beautiful and workable . This robot will be more trend in our future.

III. Hardware Integration



Fig:1 Arduino Uno

It is the brain of our project. It can give all the command to their sub ordinate components which should by operated by the human behaviour . And it also gives feedback to the other components and

human. So that it can be used as a medium of communication between human and robots & vice versa. It has specification of 8-bit CPU, 16 MHz clock speed, 2 KB SRAM 32 KB flash Memory, 1 KB EEPROM.

2. DC Motors:



Fig:2 DC motor

DC Motor is a device that converts any form of energy into mechanical energy or imparts motion. In constructing a robot, motor usually plays an important role by giving movement to the robot. Here 4 DC motor are used to drive the robot.

3 Motor Shield: The Motor Shield is a driver module for motors that allows you to use Arduino to control. the working speed and direction of the motor. The Motor Shield can either be powered by Arduino directly or by an external 6V~15V power supply via the terminal input. Here Motor Driver Board is designed to Work with L293D IC.



Fig:3 Motor Shield

4. Ultrasonic sensor:

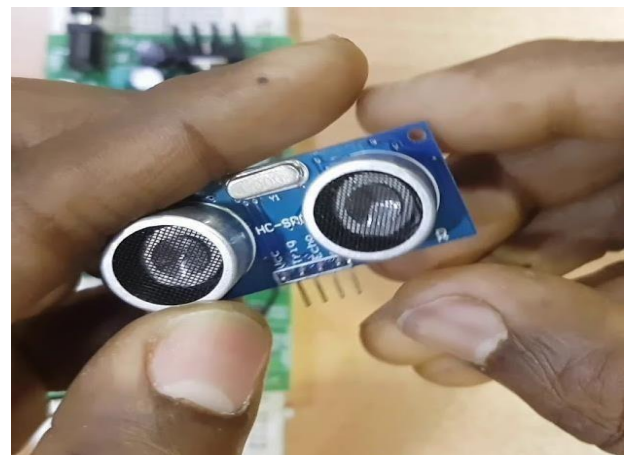


Fig:4 Ultrasonic sensor

An ultrasonic sensor is an instrument that measures the distance to an object using ultrasonic sound waves. The working principle of this module is simple, it sends an ultrasonic pulse out at 40kHz which travels through the air and if there is an obstacle or object, it will bounce back to the sensor. By calculating the travel time and the speed of sound, the distance can be calculated.

5. IR Sensor:

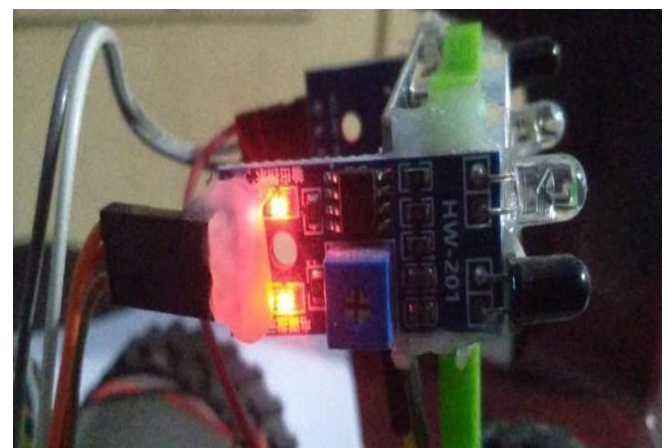


Fig:5 IR Sensor

IR sensor is an electronic device, that emits the light in order to sense some object of the surroundings. An IR sensor can measure the heat of an object as well as detects the motion. Usually, in the infrared spectrum, all the objects radiate some form of thermal radiation. These types of radiations are invisible to our eyes, but infrared sensor can detect these radiations. The emitter is simply an IR LED (Light Emitting Diode) and the detector is simply an IR photodiode.

6. ON-OFF SWITCH:

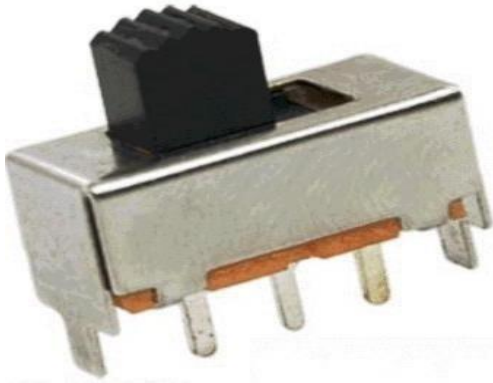


Fig:6 ON-OFF SWITCH

A Switch is a device which is designed to interrupt the current flow in a circuit. In simple words, a Switch can make or break an electrical circuit. Every electrical and electronics application uses at least one switch to perform ON and OFF operation of the device. So, switches are a part of the control system and without it, control operation cannot be achieved. A switch can perform two functions, namely fully ON or fully OFF.

7. CHASSIS:

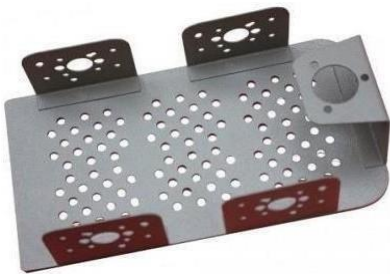


Fig:7 Chassis

Features of 4-Wheel Robot Chassis:

- Simple mechanical structure, easy for installation.
- Adopts 4 DC motors for better power, speed and load capacity.
- Large and stable Chassis, easy for expansion.
- Easy interface with Arduino development platform
 - Enormous space between middle & bottom chassis.

8. RECHARGABLE BATTERIES:



Fig:8. LI-ON RECHARGABLE BATTERIES

1. In rechargeable batteries, energy is induced by applying an external source to the chemical substances.
2. The chemical reaction that occurs in them is reversible.
3. Internal resistance is comparatively low.
4. They have a high self-discharge rate comparatively.
5. They have a bulky and complex design.
6. They have high re sell value.

9. SERVO MOTOR:

A **servo motor** is a type of motor that can rotate with great precision. Normally this type of motor consists of a control circuit that provides feedback on the current position of the motor shaft, this feedback allows the servo motors to rotate with great precision.



Fig.:9 SERVO MOTOR

SOFTWAREIMPLEMENTAON:

The Arduino Integrated Development Environment or Arduino Software (IDE) contains a text editor for writing code, a message area, a text console, a toolbar with buttons for common functions and a series of menus. The language used is based on C and C++, there are a couple of small differences designed to make Arduinos as easy to use as possible. The Arduino IDE will do some pre-processing to the code to avoid some unwanted errors but other than that it's C and C++

IV. Installation of Software:

To begin, download the Arduino IDE from the Arduino website. Make sure to select the right version for your Operating System (OS). For a full getting started guide for each OS, please refer to the Arduino guide. Once the arduino.zip file has been downloaded, extract the file to a folder somewhere on your computer. There is no install - simply open the folder and double click the .exe



Fig: Arduino Software

V.RESULT

TESTING OF HUMAN FOLLOWING ROBOT USING ARDUINO:

CASE(I):

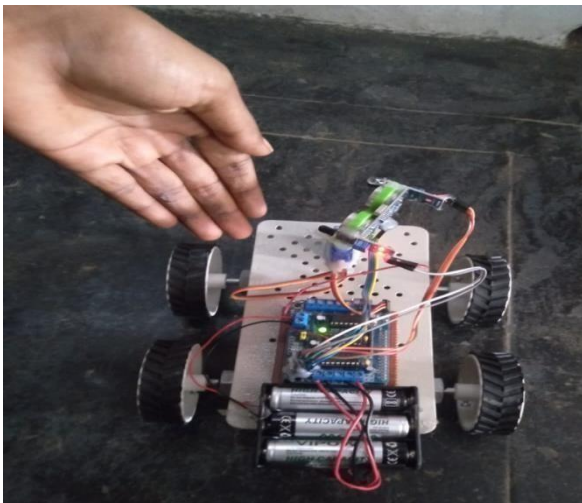


Fig: 10 Testing the Robot in left direction

The human following ROBOT turn left when left IR sensor in position left side sense the human or object then ROBOT take left turn.

CASE(II):

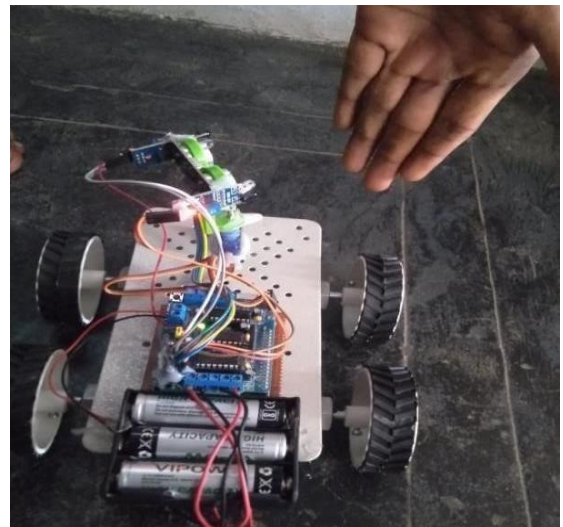


Fig :11 Testing the robot in right direction

The human following ROBOT turn right when left IR sensor in position right side sense the human or object then ROBOT take left turn.

CASE (III):

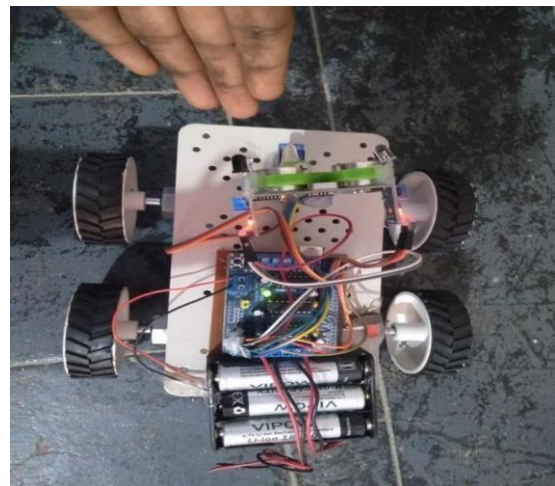


Fig:12 Testing the Robot in Forward direction

The human following ROBOT move Forward when left IR sensor in position at stable sense the human or object then ROBOT take left turn.

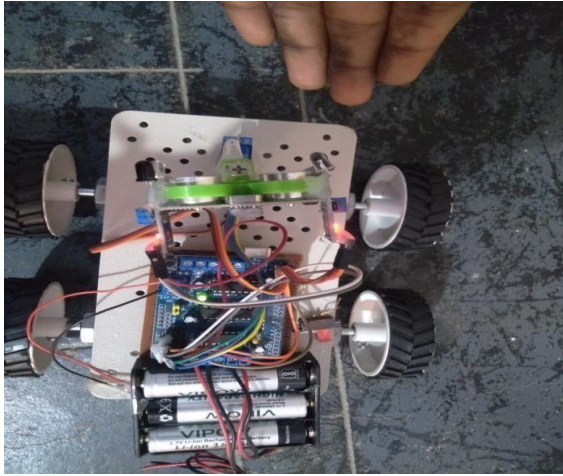
CASE (IV):

Fig: 14 Testing the Robot in Backward direction

The human following ROBOT turn left when left IR sensor in position at stable sense the human or object then ROBOT take left turn.

VI.CONCLUSION:

A successful implementation of a prototype of human following robot is illustrated in this project. This robot does not only have the detection capability but also the following ability as well. While making this prototype it was also kept in mind that the functioning of the robot should be as efficient as possible. Tests were performed on the different conditions to pinpoint the mistakes in the steps and to correct them. The different sensors that were integrated with the robot provided an additional advantage. The human following robot is an automobile system that has ability to recognize obstacle, move and change the robot's position toward the subject in the best way to remain on its track.

VII.REFERENCES

- [1] Waqar Farooq, Nehal butt, shamed shukat, Nouman alibaig, shiek Muhammad ahmed "wirelessly controlled mines detection robot". IEEE transactions systems, man, and cybernetics, 2016 IEEE international conference.
- [2] Gini M.L, ohnishi k, and pagello E advances in autonomous robots for service and entertainment. Robotics and Autonomous systems, 58(7): 829-832.
- [3] Muthukumar .N and Ravi .R, 'Hardware Implementation of architecture techniques for fast efficient loss less image compression system', wireless personal communication, volume 90, No.3, pp. 1291-1315, October 2016, SPRINGER.
- [4] Muthukumar N and ravi R," The performance analysis of fast efficient lossless satellite image compression and decompression for W velet based algorithm', wireless personal communications, volume. 81, No.2, pp.839-859, March 2015, SPRINGER.

- [5] Antonelli G, fossen T, and yoerger D. R, (2008). Under water robotics in (siciliano and khatib, (2008) pages 987-1008.
- [6] Corke P.I, Roberts J.M, Cunningham j, and Hainsworth D, (2008). Mining robotics in (siciliano and khatib,2008), pages 1127-1150
- [7] K. Morioka, J.-H. Lee, and H. Hashimoto, "Human-following mobile robot in a distributed intelligent sensor network," *IEEE Trans. Ind. Electron.*, vol. 51, no. 1, pp. 229–237, Feb. 2004.
- [8] Y. Matsumoto and A. Zelinsky, "Real-time face tracking system for human-robot interaction," in *1999 IEEE International Conference on Systems, Man, and Cybernetics, 1999. IEEE SMC '99 Conference Proceedings, 1999*, vol. 2, pp. 830–835 vol.2.

DESIGN AND FABRICATION OF CAM AND FOLLOWER USING 3D PRINTER

K. John Babu, P. Naveen, K. Sai Raghu Vamsi, K. Ashok, P. Ganesh, M. Vamsi, D. Hema Gurunadh.

Narasaraopeta Engineering College, Narasaraopet, Palnadu(Dist), A.P, India.

Abstract- This project describes the design and fabrication of a cam and follower mechanism using 3D printing technology. The cam and follower mechanism is a common mechanical system used in various engineering applications, including automotive engines, industrial machinery, and robotic systems. The mechanism consists of a rotating cam and a translating follower that follows the contour of the cam surface. The design and optimization of the cam profile are critical to achieving desired motion characteristics of the follower. The design process started with creating the cam profile, followed by the follower profile. The two profiles were then integrated into a functional mechanism using the CAD software. After the design was complete, the 3D printing process was initiated to create a physical model of the cam and follower mechanism. 3D printing technology is the most advanced manufacturing process which is trending now a day which help in printing component at high speed and reduces production cost. In this project work, design is done by using FUSION 360 software and then file is transformed to STL format which is used for production of the component in 3D printing machine. Ultimaker Cura software is used for slicing of the component produced in FUSION 360 and it also helps in adjustment of dimensions, solidification time, material selection, printing speed and printing time. In this project PLA material is used for the production of the component in 3D printing machine. The total time taken to print the parts is 23 hours 21 minutes. The final product was a fully functional cam and follower mechanism that demonstrated smooth and efficient linear motion. The 3D printing process allowed for easy replication of the design, and the Fusion 360 software made it possible to create intricate designs with precision and accuracy. Overall, this project demonstrated the powerful combination of modern software tools and 3D printing technology to create complex mechanical designs.

Keywords – 3D Printer, Fusion360, Cam and Follower.

INTRODUCTION

The starting point for any 3D printing process is a 3D digital model, which can be created using a variety of 3D software programmes in industry this is 3D CAD, for Makers and Consumers there are simpler, more accessible programmes available or scanned with a 3D scanner. The model is then 'sliced' into layers, there by converting the design into a file readable by the 3D printer. The material processed by the 3D printer is then layered according to the design and the process. As stated, there are a number of different types of 3D printing technologies, which process different materials in different ways to create the final object. Functional plastics, metals, ceramics and sand are, now, all routinely used for industrial prototyping and production applications. Research

is also being conducted for 3D printing bio materials and different types of food. Generally speaking though, at the entry level of the market, materials are much more limited. Plastic is currently the only widely used material usually ABS or PLA, but there are a growing number of alternatives, including Nylon.

LITERATURE SURVEY

Design and Analysis of Cam and Follower Mechanisms" by **G. Ambekar and S. Kadam**: This study presents a comprehensive review of the design and analysis of cam and follower mechanisms. The authors discuss various types of cam profiles, the selection of cam materials, and the kinematics and dynamics of cam and follower systems.

A Review of Cam and Follower Mechanisms for Industrial Applications" by **M. R. Azimi and M. J. Nategh**: This review paper focuses on the applications of cam and follower mechanisms in various industrial fields, such as automotive, aerospace, and manufacturing. The authors discuss the advantages and disadvantages of different cam and follower designs and their suitability for specific industrial applications.

"Performance Analysis of a Cam and Follower Mechanism for a Novel Hydraulic Hybrid System" by **K. D. Mohapatra and S. K. Acharya**: This research study analyzes the performance of a cam and follower mechanism used in a hydraulic hybrid system. The authors investigate the effect of different cam profiles on the system's energy efficiency and provide recommendations for optimizing the design of the cam and follower mechanism.

"Optimization of the Design of a Cam and Follower Mechanism Using Genetic Algorithms" by **M. J. Seo and J. H. Kim**: This study presents an optimization approach for designing cam and follower mechanisms using genetic algorithms. The authors demonstrate the effectiveness of their approach by optimizing the design of a cam and follower mechanism used in a textile machine.

"Development and Evaluation of a Cam and Follower-Based Active Balancing Mechanism for Rotating Machines" by **Robert L. Mott, Edward M. Vavrek, Jyhwen Wang**: This research study presents the development and evaluation of a cam and follower-based active balancing mechanism for rotating machines. The authors demonstrate the effectiveness of their mechanism in reducing the vibration and noise levels of rotating machines.

In a study by **B. S. Srinivasan (2012)** the authors used Fusion 360 to design a cam and follower mechanism for a multi-degree of freedom robotic arm. The authors used a combination of 2D and 3D sketches to create the cam and follower profiles, and then used the software's simulation tools to analyze the performance of the mechanism. The

authors concluded that Fusion 360 was an effective tool for designing and testing cam and follower mechanisms.

In a study by **R. L. Norton** (2010), the authors used 3D printing to create a cam and follower mechanism for a gripper used in a robotic arm. The authors designed the mechanism in Fusion 360, and then printed the parts using a 3D printer. The authors were able to successfully assemble the mechanism and test its functionality, demonstrating the effectiveness of 3D printing for prototyping mechanical parts. The use of Fusion 360 for designing cams and followers has become increasingly popular in recent years, with the software's powerful tools allowing for complex designs and simulations. Additionally, the application of 3D printing technology has made it possible to quickly prototype these designs with high precision, allowing for faster design iterations and a shorter time to market. As these technologies continue to advance, it is likely that we will see even more innovative designs and applications of cam and follower work .

EXPERIMENTATION

Step 1: Initially the components to be prepares are drawn using FUSION 360 software by using sketcher tool.

Step 2: Once the component is drawn as per required dimension, then the file is saved as STL file in FUSION 360software.

Step 3: After completion of above procedure, STL file is loaded into cura software. **Step 4:** Once the STL file is loaded, required parameters are set in cura software that is material used, layer thickness, infill density, infill shapes, fan speed, nozzle temperature, bed temperature, extrusion temperature, supports required all are selected and modified as per the requirement.

Step 5: After selection of the above parameters slicing is done by using slice option. **Step 6:** Once slicing is done STL file is converted into G codes which is readable by 3D printer.

Step 7: G-code file is loaded in 3D printer by using pen drive and printing is done.

Step 8: Assembly of Printed Components.

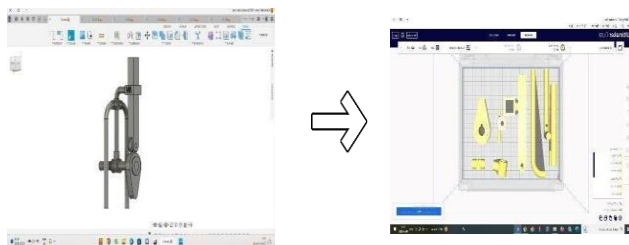


Fig: Design in Fusion 360& Slicing Ultimakers Cura

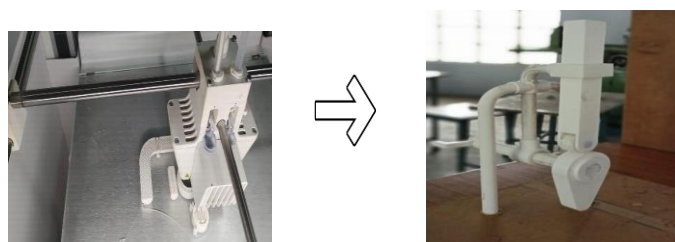


Fig: 3D Printing

Fig: Final Assembly

snap pin head be sure to remove these to ensure the snap pin seats well. When all are placed on the body parts which are called stands place another body part on top of the set up.

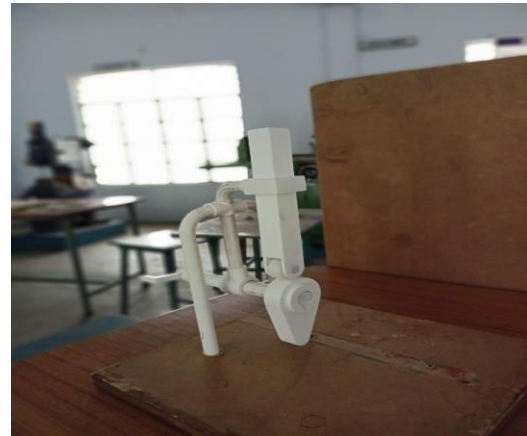


Fig : Assembly of Cam and Follower

The above figure shows the final assembly of cam and follower mechanism printed in 3D printer.

RESULT

Check the gears and crank for any defects. Small pieces of filament sometimes droop in the rectangular recess for the The key advantages and disadvantages of the technology Are summarised below: FDM is the most cost-effective way of producing custom thermoplastic parts and prototypes. The lead times of FDM are short (as fast as next-day- delivery), due to the high availability of the technology. A wide range of thermoplastic materials is available, suitable for both prototyping and some non-commercial functional applications. FDM has the lowest dimensional accuracy and resolution compared to other 3D printing technologies, so it is not suitable for parts with intricate details. FDM parts are likely to have visible layer lines, so post processing is required

II. APPLICATIONS

- IC Engines
- Children Toys
- Automatic Lathe Machines
- Spinning and Weaving machines
- Paper Cutting machineries
- Printing control mechanisms
- Diesel fuel pumps
- Wall clocks

CONCLUSION & FUTURE SCOPE

In conclusion, designing and printing a cam and follower using Fusion 360 and 3D printing technology can be a cost-effective and efficient way to prototype and test mechanical systems. By using computer-aided design software like Fusion 360, designers can easily create precise and complex cam and follower shapes that can be difficult or time-consuming to create by hand.

3D printing technology allows for the rapid production of physical prototypes from these designs, allowing designers to quickly test and refine their designs. Additionally, 3D printing allows for the creation of complex shapes that may not be possible with traditional manufacturing methods, making it a valuable tool for prototyping. However, it is important to note that 3D printed parts may not be as durable as traditionally manufactured parts, and may not be suitable for high-stress or high-temperature applications. Therefore, it is important to carefully consider the intended use of the cam and follower and choose appropriate materials and printing parameters for the 3D printing process.

Overall, using Fusion 360 and 3D printing technology to design and create a cam and follower can be a useful and effective way to prototype mechanical systems, but it is important to carefully consider the limitations and suitability of 3D printed parts for the intended application. In this project work, design is done using FUSION 360 software and then file is transformed to STL format which is used for production of the component in 3D printing machine. CURA software is used for slicing of the component produced in FUSION 360 and it also helps in adjustment of dimensions, solidification time, material selection, printing speed and printing time. In this project PLA material is used for the production of the component in 3D printing machine. The total time taken to print the Cam and Follower is 23 hours 21 minutes and components are successfully assembled.

REFERENCES

- 1.G. Ambekar and S. Kadam. (2004). Design of Machinery: An Introduction to the Synthesis and Analysis of Mechanisms and Machines. New York: McGraw Hill.
- 2.M. R. Azimi J.E., M. J. Nategh, C.R., and Budynas, R.G. (2003). Mechanical Engineering Design. New York: McGraw Hill. Bryce, E. (January 19, 2014). How a 3D printer gave a teenage bomb victim a new arm – and a reason to live.
- 3.Erdman, K. D. Mohapatra and S. K. Acharya, G.N. (1997). Mechanism Design: Analysis and Synthesis. Prentice Hall. Burke. (January 16, 2014). 3D Printing Is the Future, But Safety Comes First. In Information Week.
- 4.M. J. Seo and J. H. Kim (2013). Manufacturing Engineering and Technology. Pearson.
- 5.Robert L. Mott, Edward M. Vavrek, Jyhwen Wang (2011). Machine Elements in Mechanical Design. Prentice Hall.
- 6.B. S. Srinivasan (2012). Theory of Machines. New

Age International..

- 7.Joseph Edward Shigley, Charles R. Mischke, and Thomas H. Brown (1989). Standard Handbook of Machine Design. McGraw Hill.
- 8.J. J. Uicker, G. R. Pennock and J. E. Shigley (2003). Theory of Machines and Mechanisms.
- 9.R. L. Norton (2010). Kinematics and Dynamics of Machinery. McGraw Hill.
- 10.Robertson. (May 20, 2013). New 'Lulz Liberator' pistol proves guns can be made on cheap 3D printers. In the Verge

3D PRINTING OF RACK AND PINION STEERING MECHANISM

T.Ashok Kumar, D.Venkata Gopal, M.Sai Vinay, M.Jayanth Kumar, Balachandar M, V. Naga Seshu, J. Karunakar

Department of Mechanical Engineering, Narasaraopet engineering College, Narasaraopet, Palnadu(Dist.), A.P. India.

Abstract— A Rack-and-Pinion steering mechanism includes a hand wheel, a main-shaft, universal joints, and an intermediate shaft. When the steering is rotated, rotation is transferred by the shafts to the pinion. The pinion is meshed with the teeth of the rack, so pinion rotation moves the rack from left to right or right to left. The rack and pinion Steering system is based on the conversion of the rotating motion of the steering wheel into a linear motion onto the wheels and consists of two gears namely, rack and pinion which assist in turning the vehicle relative to the driver's needs.

I. INTRODUCTION.

3D Printing also known as additive manufacturing has been quoted in the Financial Times and by other sources as potentially being larger than the Internet. Some believe this is true. Many others urge that this is part of the extraordinary hype that exists around this very exciting technology area. So, what really is 3D printing, who generally uses 3D printers and what for. The term 3D printing covers a host of processes and technologies that offer a full spectrum of capabilities for the production of parts and products in different materials. Essentially, what all of the processes and technologies have in common is the manner in which production is carried out layer by layer in an additive process which is in contrast to traditional methods of production involving subtractive methods or molding/casting processes.

II. LITERATURE REVIEW

Many modern cars use rack and pinion steering mechanisms. This literature review will focus on this steering system which is mostly used maximum number of automobiles. When the steering wheel turns the pinion gear, the pinion moves the rack, converting circular motion into linear motion along the transverse axis of the car (side to side motion), kind of like a gear mechanism. This motion applies steering torque to the swivel pin ball joints (that replaced previously used kingpins) of the stub axle of the steered wheels via tie rods and a short

BMW began to use rack and pinion steering systems in the 1930s with many other European manufacturers later adopting the technology.

lever arm called the steering arm. The rack and pinion design has the advantages of a direct steering "feeling".

Older designs use two main principles: the worm and sector design and the screw and nut. Both types were enhanced by reducing the friction; for screw and nut it is the recirculating ball mechanism, which is still found on trucks and utility vehicles. The steering column turns a large screw, which meshes with the nut by recirculating balls. The nut moves a sector of a gear, causing it to rotate about its axis as the screw is turned; an arm attached to the axis of the sector moves the Pitman arm, which is connected to the steering linkage and thus steers the wheels.

III. METHODS AND MATERIALS

3D printable models may be created with a computer-aided design (CAD) package, via a 3D scanner, or by a plain digital camera and photogrammetry software. 3D printed models created with CATIA result in relatively fewer errors than other methods. Errors in 3D printable models can be identified and corrected before printing.[48] The manual modelling process of preparing geometric data for 3D computer graphics is similar to plastic arts such as sculpting. 3D scanning is a process of collecting digital data on the shape and appearance of a real object, creating a digital model based on it. CATIA models can be saved in the stereolithography file format (STL), a de facto CATIA file format for additive manufacturing that stores data based on triangulations of the surface of CATIA models..

A crowd favourite in our 3D printing materials guide is PLA, which can, under certain commercially attainable conditions, biodegrade. (You're not going to be able to compost it at home.). First and foremost, Polylactic Acid (PLA) is easy to print with. It has a low printing temperature, doesn't need a heated bed.

is that it doesn't give off an off-putting odour during printing (unlike ABS). Moreover, it is a suitable 3D printing material for single-use food contact. However, PLA is less durable than ABS or PETG and susceptible to heat. So, for any type of engineering part, you'll be better off with the latter. Avoid using it when making items that might be bent, twisted, or repeatedly dropped, such as phone cases, high-wear toys, or tool handles.

PLA means Polylactic Acid

ABS means Acrylonitrile Butadiene Styrene

PVA means Polyvinyl Alcohol

- A. PLA is available in a broad range of colors and also comes in a variety of composites from glow-in-the-dark, glittery, or color changing.
- B. ABS, Remember the quality of Lego bricks? Then you can relate to why Acrylonitrile butadiene styrene (ABS) is one of the most popular 3D printing materials to date. Made from petroleum, ABS is commonly used in injection molding and is found in many household items, such as those rock-hard Lego bricks, phone cases, or bicycle helmets – due to its durability, robustness, and temperature resistance.
- C. PVA, Polyvinyl alcohol (PVA) is soluble in water, and that's exactly what commercial applications take advantage of. Popular uses include packaging for dishwasher detergent “pods” or bags full of fishing bait. (Throw the bag in water and watch it dissolve, releasing the bait.)
- D. Nylon, Nylon, a branch of synthetic polymers, is a tough and durable material originally seen in textiles. The technical name for the material is polyamide (PA), while the common name is “nylon” (despite some still associating it with stockings). The material stands out for its toughness and its resistance to high temperatures and impacts.

IV. MODELLING

- CATIA stands for Computer Aided Three-Dimensional Interactive Application. It was developed by Dassault Systems, France. It is a complete re-engineered, next generation family of CAD/CAM/CAE software solution for PLM (Product Lifecycle Management).
- CATIA V5 delivers innovative technologies for maximum productivity and creativity. It allows the flexibility of using feature-based design and parametric design.

Components printed are:

- The dimensions of the axle shaft are 50 mm x 28.5mm x 60mm. Axle shafts are primarily responsible for transferring the transmission's rotational force and power to make the vehicle move. When the force from the transmission causes the axle shaft to rotate, the wheels connected to it also turn
- The dimensions of the crank are 9mm x 10mm x 33mm. A crank is an arm attached at a right angle to a rotating shaft by which circular motion is imparted

to or received from the shaft. When combined with a connecting rod, it can be used to convert circular motion into reciprocating motion, or vice versa.

- The dimensions of track support are 113.271mm x 36.5mm x 47.5mm. A track rod – also called a tie rod – is located at either end of the rack. Each track rod is attached to a steering arm which is attached to the wheel hub, to which the wheel is bolted. As the rack moves, all these connections ensure the wheels turn together.
- The dimensions of gear are 10mm x 33.711mm x 33.897mm. The pinion gear is attached to the steering shaft so that when the steering wheel is turned, the gear spins, moving the rack. The axial rod at each end of the rack connects to the tie rod end.

V. CURA SOFTWARE

Cura is an open-source slicing application for 3D printers. It was created by David Braam who was later employed by Ultimaker, a 3D printer manufacturing company, to maintain the software. Cura is available under LGPLv3 license. Cura was initially released under the open source Affero General Public License version 3, but on 28 September 2017 the license was changed to LGPLv3. This change allowed for more integration with third-party CAD applications. Development is hosted on GitHub. Ultimaker Cura is used by over one million users worldwide and handles 1.4 million print jobs per week. It is the preferred 3D printing software for Ultimaker 3D printers, but it can be used with other printers as well.



Figure 1: Cura logo

Stages of 3d printing:

1. Modeling
2. 3d file export
3. Slicing file export

MODEL VIEWS IN CURA

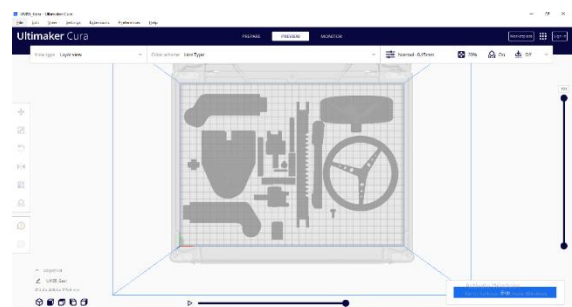


Figure 2: Preview of the components

Cura’s default view enables you to get a good idea of how the model will look when printed. It will show you the size and shape related to the print platform.

this feature is great for when prints go wrong and quickly enables you to see parts of the internal structure of your print. Where it really comes in handy is if your print is suffering from manifold edges — edges that intersect other edges. Cura’s X-Ray enables you to see what needs to be reworked.

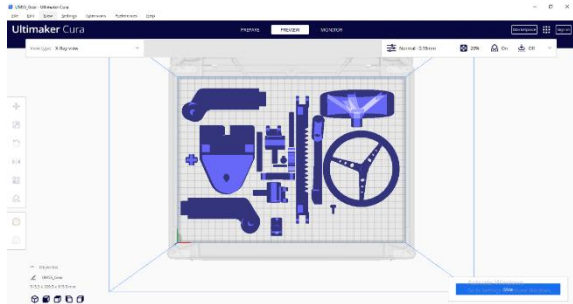


Figure 3: layers (x-ray)

Under Preview, if a print is failing every time at a certain point, or you’ve done something clever and just want to check that part of the print is OK, you can switch to Layer view. An accurate way to do this is with the arrow keys. Alternatively, there’s a slider for quickly looking through all of the layers that build up your print.



Figure 4: Ultimaker 3D printer (S5pro model)

The Ultimaker S5 is the first member of Ultimaker's "S-line" printer family. It has the biggest build volume of an Ultimaker printer to date by all dimensions and the build volume is consistent with both nozzles and dual extrusion. The Ultimaker S5 has a 4.7" colour touchscreen replacing the older LCD screen and rotary wheel, a feeder system that pauses when material runs out and is compatible with glass and carbon fibre composites, among many other materials, and a pair of hinged glass doors.

A. Processing catia model using cura software

STL file prepared in CATIA software and loaded into a Cura software which is a free print preparation software for the ultimaker 3D printers. Slicing is done using this software. After slicing the file is save in G codes format

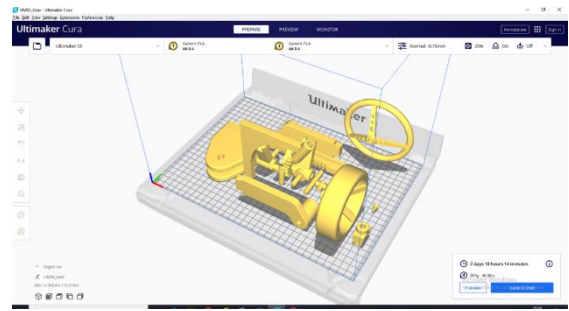


Figure 5: Rack and Pinion steering in STL file in Cura

Using ultimaker cura software were used for the analysing the different parameters like infill density, infill shapes, layer height and top layers, etc. and after the analysing the different parameters select one parameter which gives good strength, saves time and money.

Table 1: Analysed cura parameters

	fast	normal	fine	Extra fine
Quality Layer height	0.2mm	0.15mm	0.1mm	0.06mm
Walls Wall thickness	1mm	1.3mm	1.3mm	1.3mm
Wall count line	3	4	4	4
Top/bottom				
Top/bottom thickness	1.2mm	1.2mm	1.2mm	1.2mm
Top thickness	1.2mm	1.2mm	1.2mm	1.2mm
Top layer	6	8	12	20
Bottom thickness	1.2mm	1.2mm	1.2mm	1.2mm
Bottom layer	6	8	12	20
In fill				
Infill density	20%	20%	20%	20%
Infill pattern	triangles	triangles	triangles	triangles
material				
Printing temperature	250°C	245°C	240°C	235°C
Build plate temperature	85°C	85°C	85°C	85°C
Speed				

Print speed	60mm/s ec	60mm/s ec	55mm/s ec	50mm/s ec
Time				
Estimated time	48hr 50 min	46hr 5min	44hr 35min	42hr 15min
Material consumption	445g 36.17m	153g 36.87m	160g 21.93m	165g 22.1m

Printing of objects using 3d printer

1. Once the modelling is done then STL file is loaded into cura software and slicing is done. After completion of the above process the G code file loaded in to 3D printer by using SD card or Pen drive.
2. In order to print the component filament is loaded into the machine (PLA filament is used).
3. Initially bed is prepared by cleaning it with alcohol-based solvent.
4. After cleaning bed is preheated to 60C temperature.
5. Before printing the component, glue stick is applied because of avoiding the warping
6. Once the above procedure is done select the G code file from the SD card by using select option.
7. Each and every parameter setting is visible on the machine screen. Check for any errors and parameters and do modifications if necessary.
8. After checking the parameters printing is started by giving start option in the machine.
9. After completion of the component wait for at least 30 minutes in order to remove the component from the machine bed.
10. Post processing is done to the components by removing of excess material and component supports.



Figure 6: assembled components

VII. CONCLUSION

Though 3D printing is still a growing technology, it already has many benefits and drawbacks. While many people agree that this technology could change the world, there are also those who believe it could have extreme consequences if it is not researched and tested

thoroughly. As the technology beings to grow more and more throughout the next couple of years there will be more information and data that will determine whether it is a technology that is here to stay or it is something that will simply not make it. The total time and material taken to print the Rack and Pinion steering Forty-six hours and five minutes and 434 grams (36 mts) material is used to print the components and components are successfully assembled.

REFERENCES

1. "3D printing scales up". *The Economist*. 5 September 2013.
2. Excell, Jon (23 May 2010). "The rise of additive manufacturing". *The Engineer*. Retrieved 30 October 2013.
3. "Learning Course: Additive Manufacturing – Additive Fertigung". *tmg-muenchen.de*.
4. Lam, Hugo K.S.; Ding, Li; Cheng, T.C.E.; Zhou, Honggeng (1 January 2019). "The impact of 3D printing implementation on stock returns: A contingent dynamic capabilities perspective". *International Journal of Operations & Production Management*. 39 (6/7/8): 935–961. doi:10.1108/IJOPM-01-2019-0075. ISSN 0144-3577. S2CID 211386031.
5. "3D Printing: All You Need to Know". *explainedideas.com*. Retrieved 11 August 2022.
6. "Most used 3D printing technologies 2017–2018 | Statista". *Statista*. Retrieved 2 December 2018.
7. "Google Ngram Viewer". *books.google.com*.
8. "ISO/ASTM 52900:2015 – Additive manufacturing – General principles – Terminology". *iso.org*. Retrieved 15 June 2017.
9. Zelinski, Peter (4 August 2017), "Additive manufacturing and 3D printing are two different things", *Additive Manufacturing*, retrieved 11 August 2017.
10. M. Leinster, *Things Pass By, in The Earth In Peril* (D. Wollheim ed.). Ace Books 1957, USA, List of Ace SF double titles D-205, p.25, story copyright 1945, by Standard Magazines Inc.

Simulation of AUW Robotic vehicle body using FEA method

SKCM Subhani¹, Pilli Sravani²

¹Assistant Professor, Department of Mechanical Engineering, Eswar College of Engineering, Narasaraopet, AP.

²Assistant Professor, Department of Mechanical Engineering, Narasaraopeta Engineering College (Autonomous), Narasaraopet, AP.

ABSTRACT:

An Autonomous Underwater Robotic Vehicle (AUWRV) is a robot that travels underwater without requiring input from an operator. AUWRVs constitute part of a larger group of undersea systems known as unmanned underwater vehicles, the structure of an Autonomous Underwater Robotic Vehicle (AUWRV), usually composed of a cylindrical shell, may be exposed to high hydrostatic pressures where buckling collapse occurs before yield stress failure. In conventional submarines, welded stiffeners increase the buckling resistance, however, in small AUWRVs, they reduce the inner space and cause residual stresses. The Aim of the project work presents an innovative concept for the structural design of an AUWRV Pressure vessel, proposing the use of sliding stiffeners that are part of the structure used to accommodate the electronics inside it.

Design of AUWRV pressure vessel using Catia software and analysis using Ansys software using sand which beam material in this project taken total 4 cases.

CASE 1: 2mm Steel + 2mm Rubber +2mm Steel

CASE 2: 2.5mm Steel + 1mm Rubber +2.5mm Steel

CASE 3 :2mm Ti64Al + 2mm Rubber +2mm Ti64Al

CASE 4: 2.5mm Ti64Al + 1mm Rubber +2.5mm Ti64Al

Finally concluded the which material is suitable on pressure vessel based on the stresses, strains, deformation, shear stress in static analysis and in modal analysis find out the modes at Total deformation in different Frequency

KEYWORDS: AUWRV, ANSYS, CATIA, Analysis, Materials

I. INTRODUCTION

1.1. INTRODUCTION OF AUTONOMOUS UNDERWATER ROBOTIC VEHICLE (AUWRV)

Autonomous Underwater Vehicles (AUWRVs) are programmable, robotic vehicles that, depending on their design, can drift, drive, or glide through the ocean without real-time control by human operators. Some AUWRVs communicate with operators periodically or continuously through satellite signals or underwater acoustic beacons to permit some level of control.

AUWRVs allow scientists to conduct other experiments from a surface ship while the vehicle is off collecting data elsewhere on the surface or in the deep ocean.

Some AUWRVs can also make decisions on their own, changing their mission profile based on environmental data they receive through sensors while under way.

The first AUWRV was developed at the Applied Physics Laboratory at the University of Washington as early as 1957 by Stan Murphy, Bob Francois and later on, Terry Ewart. The term light hull (casing) is used to describe the outer hull of a submarine, which houses the pressure hull, providing hydro dynamically efficient shape, but not holding pressure difference.

The term pressure hull is used to describe the inner hull of a submarine, which holds the difference between outside and inside pressure.



Figure 1: Autonomous Underwater Robotic Vehicles

1.2 PRESSURE HULL

Inside the outer hull there is a strong hull, or pressure hull, which actually withstands the outside pressure and has normal atmospheric pressure inside. The pressure hull is generally constructed of thick high-strength steel with a complex structure and high strength reserve, and is separated with watertight bulkheads into several compartments. The pressure and light hulls aren't separated, and form a three-dimensional structure with increased strength. The inter hull space is used for some of the equipment which doesn't require constant pressure to operate. The list significantly differs between submarines, and generally includes different water/air tanks. In case of a single-hull submarine, the light hull and the pressure hull are the same except for the bow and stern. The constructions of a pressure hull require a high

degree of precision. This is true irrespective of its size. Even a one inch (25 mm) deviation from cross-sectional roundness results in over 30 percent decrease of hydrostatic load. Minor deviations are resisted by the stiffener rings, and the total pressure force of several million longitudinally oriented tons must be distributed evenly over the hull by using a hull with circular cross section.

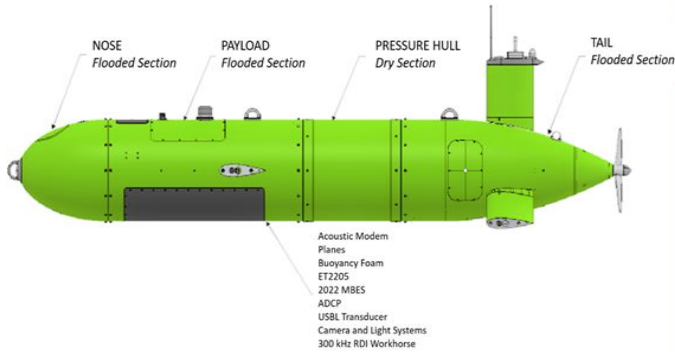


Figure 2 :Outer part of AUWRV

1.3 PARTS OF AUWRV

There are several aspects in AUWRV electrical and mechanical design need to be looked at closely so that the design will be successful. In order to design any underwater vehicle AUWRV, it is essential or compulsory to have strong background knowledge, fundamental concepts and theory about the processes and physical laws governing the underwater vehicle in its environment.

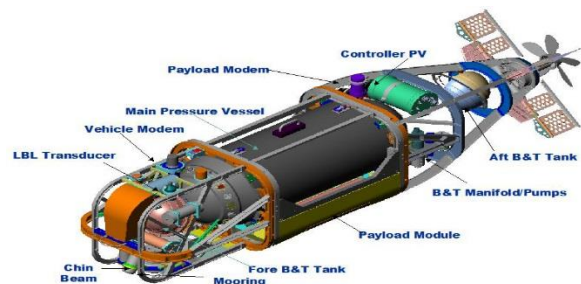


Figure 3 : Parts of AUWRV

1.4 APPLICATIONS

1. The oil and gas industry uses AUWRVs to make detailed maps of the seafloor before they start building subsea infrastructure; pipelines and subsea completions can be installed in the most cost-effective manner with minimum disruption to the environment.
2. A typical military mission for an AUWRV is to map an area to determine if there are any mines, or to monitor a protected area (such as a harbor) for new unidentified objects. AUWRVs are also employed in anti-submarine warfare, to aid in the detection of manned submarines.
3. Scientists use AUWRVs to study lakes, the ocean, and the ocean floor. A variety of sensors can be affixed to AUWRVs to measure the concentration of various elements or compounds, the absorption or reflection of light, and the presence of microscopic life.
4. Autonomous Underwater Vehicles are today a vital part of marine geosciences. They have eliminated so many challenges to exploring the underwater and have made a lot of difficult underwater tasks easier.

They, however, cannot operate with 100% efficiency in some areas. Some areas prove to be more violence and overpower the AUWRV in the tide. For instance,



Figure 4 Various applications of Autonomous Under water vehicle

2. METHODOLOGY

- Design of pressure hull done using CATIA & CAD software. Design of pressure hull completed based on ISO standard drawing sheet.
- These stresses are calculated for Four different materials of pressure hulls .
- Pressure hull design imported in Ansys software for analysis purpose. Structural analysis of hull done for and different material types (steel, Ti6al4v).
- Perform the static and modal analysis
- Consider the 65 bar applied the external because of this is the hydro static pressure.
- From these results, concluded the suitable pressure hull proposed under radial pressure conditions with 4 materials.
- with a length of 1000mm were developed in ANSYS 17.0. a) Rules of Mixture adopted to find the material properties like tensile strength, elastic modulus, density etc.
- Different composites used to investigate their failure criteria to provide optimum strength. The basic details like cross sectional dimensions, number of stiffeners used are kept constant for all models.

2.2 SCOPE OF THE PROJECT:

1. Study the different Journals Related to the AUWRV, Pressure vessel and sandwich materials.
2. Study the complete design analysis concepts about the pressure hull.
3. Study the different materials CASE 1: 2mm C40Steel + 2mm Rubber +2mm C40Steel, CASE 2: 2.5mm C40Steel + 1mm Rubber +2.5mm C40Steel, CASE 3 :2mm Ti-6Al-4V + 2mm Rubber +2mm Ti-6Al-4V, CASE 4: 2.5mm Ti-6Al-4V + 1mm Rubber +2.5mm Ti-6Al-4V.
4. Create Finite element model of the pressure hull using ANSYS software.
5. Perform static and modal analysis for the hydrostatic pressure of 65 bars.
6. Perform Modal analysis to calculate natural frequencies and mass participations.
7. Implement modifications on the pressure hull based on the results obtained from modal analysis to shift the fundamental natural frequency.
8. Perform structural static analysis for the hydrostatic pressure of 65 bars on the modified model.

9. Perform Modal analysis to calculate natural frequencies and mass participations on the modified model. Perform analysis of the modified pressure hull in X, Y and Z directions.
10. Perform transient dynamic analysis of the modified pressure hull in X, Y and Z directions.

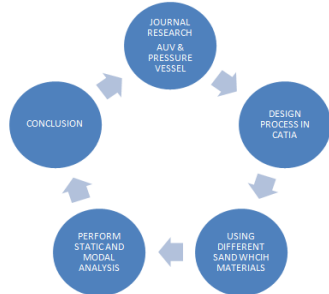


FIGURE 5:SCOPE OF THE PROJECT

2.3 DESIGN SPECIFICATIONS OF PRESSURE HULL

- Length overall = 1.8 m.
- Pressure hull diameter = 0.4 m.
- Layout = double diameter ring stiffened cylinder.
- Submerged displacement =1015 tones.
- Thickness of the pressure vessel =6mm

TABLE 1: MATERIAL PROPERTIES

3. MODELLING OF PRESURE HULL IN CATIA

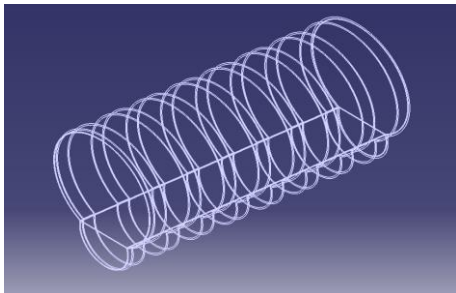


FIGURE6 : PRESSURE HUB IN WIRE FRAME VIEW

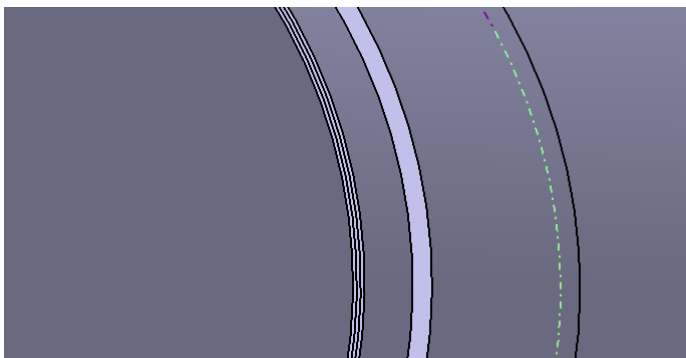


FIGURE 7: LAYER BY LAYER SAND WHICH MATERIAL

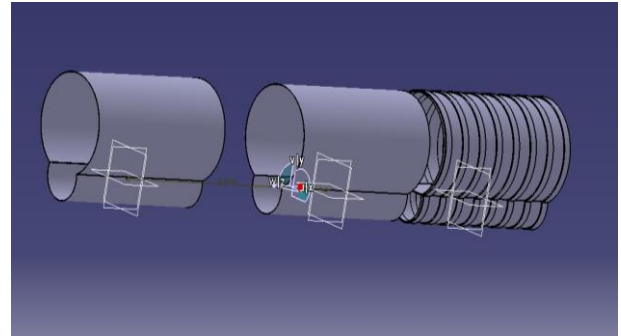


FIGURE 8: EXPLODED VIEW IN ASSEMBLY WORKBENCH

MATERIAL PROPERTIES	Density(g/cm ³)	Possion's ratio(μ)	Young's Modulus (Gpa)
Ti-6Al-4v	4.429	0.30	206
C40 Steel	7.80	0.29	200
Rubber-Core	1.10	0.48	0.2

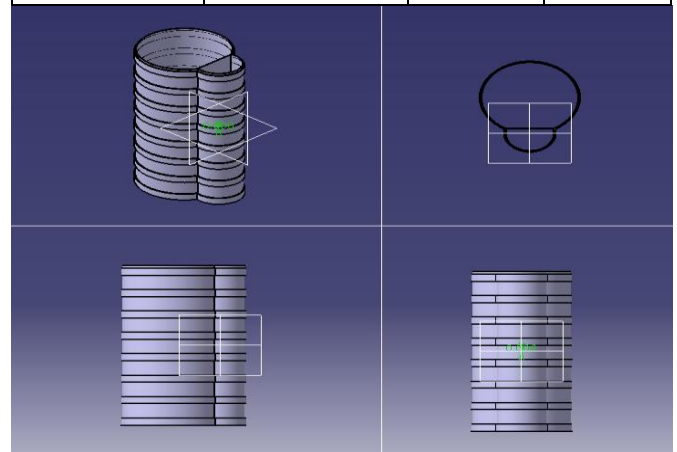


FIGURE 9: MULTI VIEW IN CATIA WORKBENCH

4. ANALYSIS OF PRESSURE HULL

Structure static analysis was done on the pressure hull for external pressure of 65 bars to determine the stresses and deflections. The ends of the pressure hull are fixed in all dof and the external pressure of 65bars @ 6.5Mpa is applied on the shells of the pressure hull. The boundary conditions and loading applied on the pressure hull is shown in the figure.

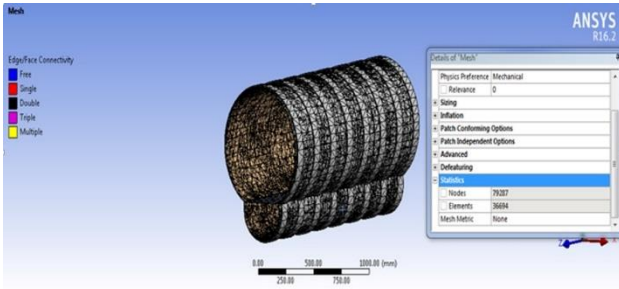


FIGURE 10: MESH IN ANSYS WORKBENCH NODES:79287, ELEMENTS:36694

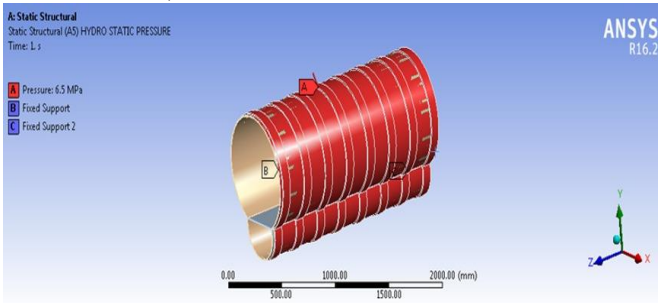


FIGURE 11: BOUNDARY CONDITIONS IN STATIC

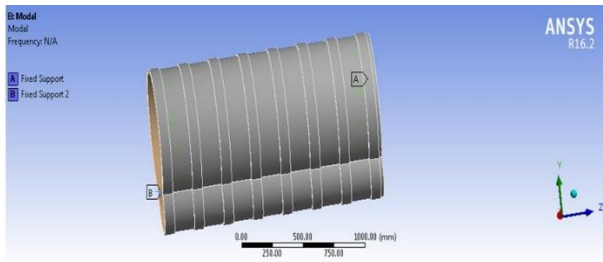


FIGURE 12: BOUNDARY CONDITIONS IN MODAL

RESULTS AND DISCUSSION
 Structure static and modal analysis was done on the pressure hull for external pressure of 65 bars to determine the stresses and deformations. The ends of the pressure hull are fixed in all dof and the external pressure of 65bars is applied on the shells of the pressure hull. The boundary conditions and loading applied on the pressure hull is shown in the figure.

5.1 2.5MM C40 STEEL+1MM RUBBER+2.5MM C40 STEEL MATERIAL:

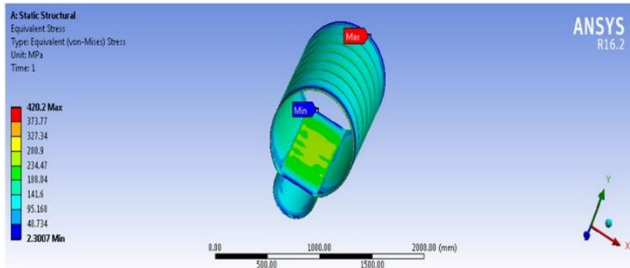


FIGURE 13: VON-MISSES STRESS OF C40 STEEL+1MM RUBBER+2MM C40 STEEL MATERIAL

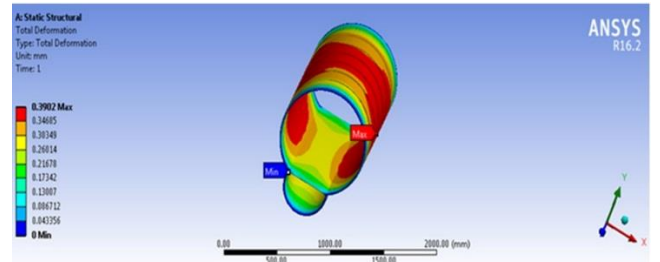


FIGURE 14: TOTAL DEFORMATION OF C40 STEEL+1MM RUBBER+2MM C40 STEEL MATERIAL

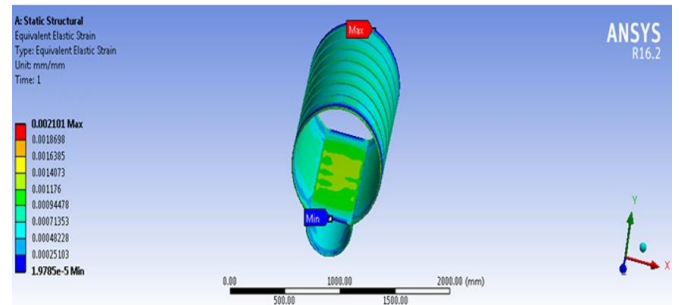


FIGURE 15: STRAIN OF C40 STEEL+1MM RUBBER+2MM C40 STEEL MATERIAL

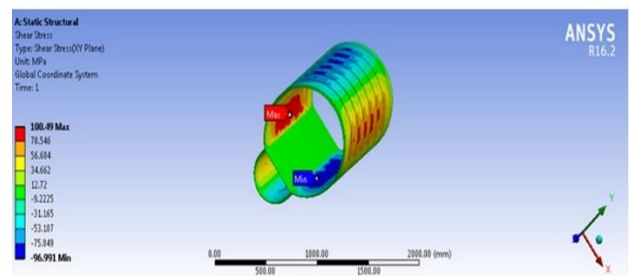


FIGURE 16: SHEAR STRESS OF C40 STEEL+1MM RUBBER+2MM C40 STEEL MATERIAL

5.2 2MM C40 STEEL+2MM RUBBER+ 2MM C40 STEEL MATERIAL:

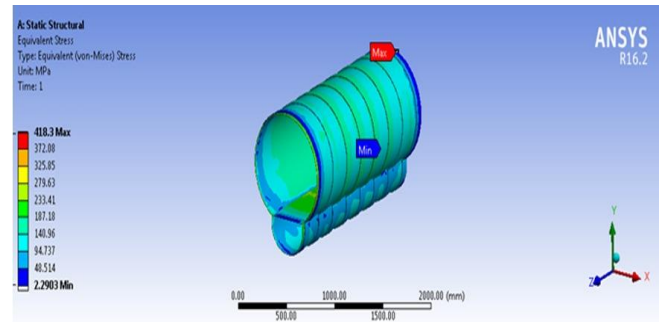


FIGURE 17: VON-MISSES STRESS OF 2MM C40 STEEL+2MM RUBBER+ 2MM C40 STEEL

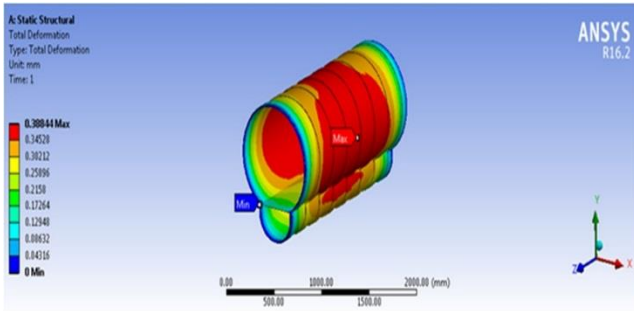


FIGURE 18: TOTAL DEFORMATION OF 2MM C40 STEEL+2MM RUBBER+ 2MM C40 STEEL

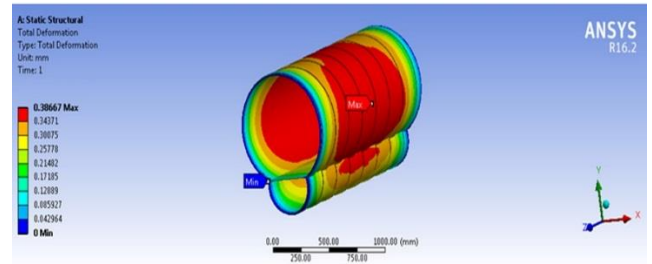


FIGURE 22: TOTAL DEFORMATION OF 2.5MM TI-6AL-4V +1MM RUBBER +2.5MMTI-6AL-4V

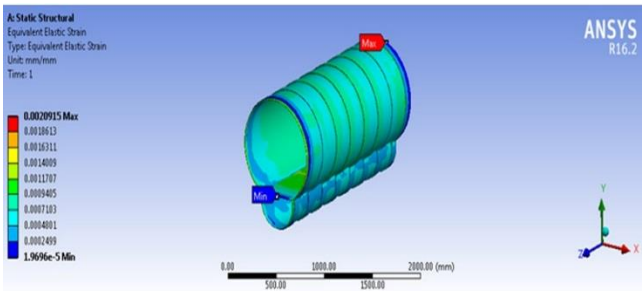


FIGURE 19: STRAIN OF 2MM C40 STEEL+2MM RUBBER+ 2MM C40 STEEL MATERIAL

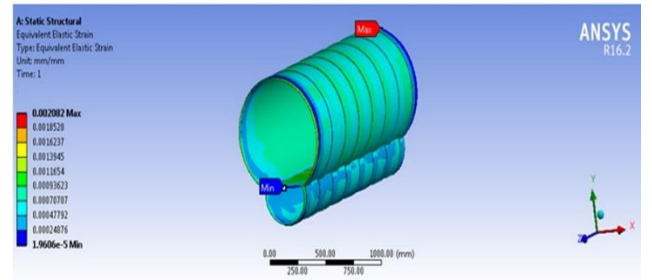


FIGURE 23: STRAIN OF 2.5MM TI-6AL-4V +1MM RUBBER +2.5MMTI-6AL-4V

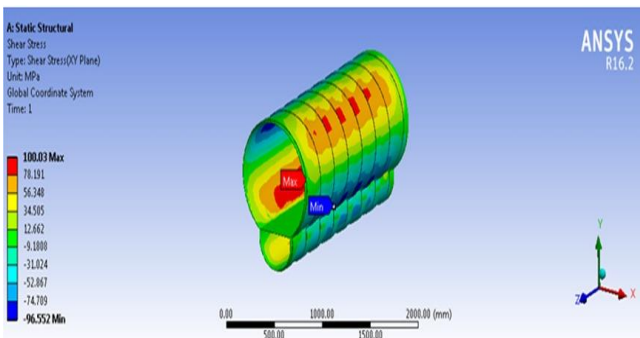


FIGURE 20: SHEAR STRESS OF 2MM C40 STEEL+2MM RUBBER+ 2MM C40 STEEL MATERIAL

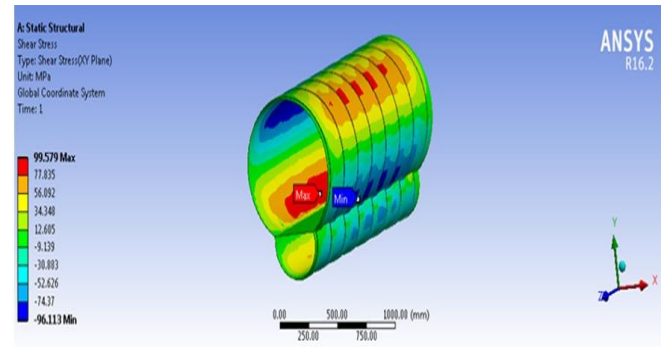


FIGURE 24: SHEAR STRESS OF 2.5MM TI-6AL-4V +1MM RUBBER +2.5MMTI-6AL-4V

5.3 2.5MM TI-6AL-4V +1MM RUBBER +2.5MMTI-6AL-4V:

5.4 2MM TI-6AL-4V +2MM RUBBER +2MMTI-6AL-4V:

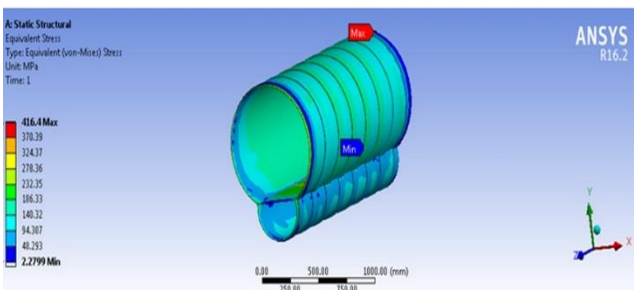


FIGURE 21: VON-MISSES STRESS OF 2.5MM TI-6AL-4V +1MM RUBBER +2.5MMTI-6AL-4V

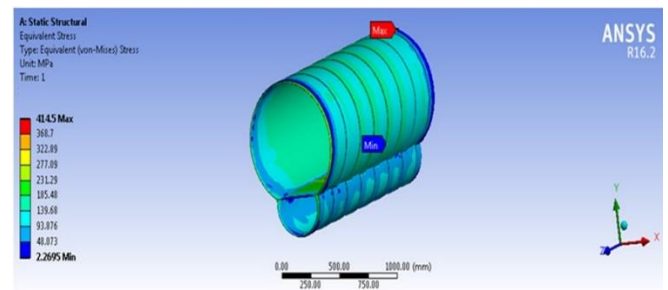


FIGURE 25: VON-MISSES STRESS OF 2MM TI-6AL-4V +2MM RUBBER +2MMTI-6AL-4V

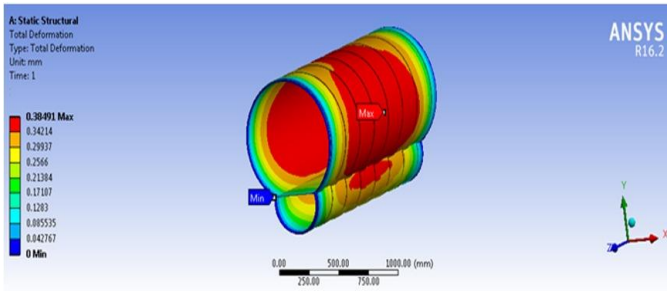


FIGURE 26: TOTAL DEFORMATION OF 2MM TI-6AL-4V +2MM RUBBER +2MMTI-6AL-4V

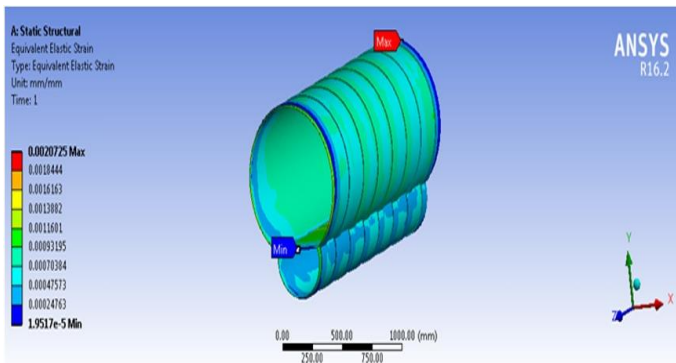


FIGURE 27: STRAIN OF 2MM TI-6AL-4V +2MM RUBBER +2MMTI-6AL-4V

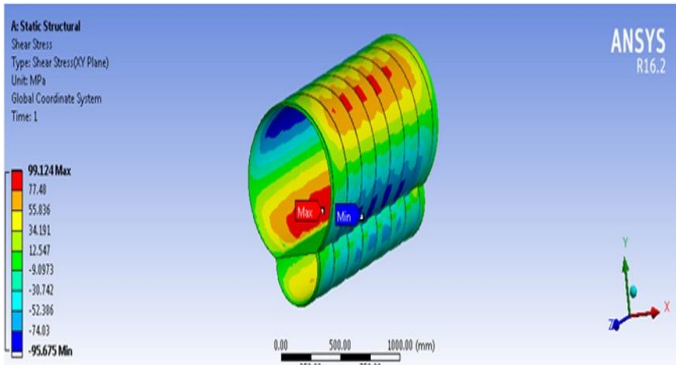


FIGURE 28: SHEAR STRESS OF 2MM TI-6AL-4V +2MM RUBBER +2MMTI-6AL-4V

5.5 MODAL ANALYSIS:

Here find out the Total deformations with different frequencies, we are consider totally 3 modes as shown below graph

5.6 Modal analysis of 2mm Steel + 2mm Rubber +2mm Steel

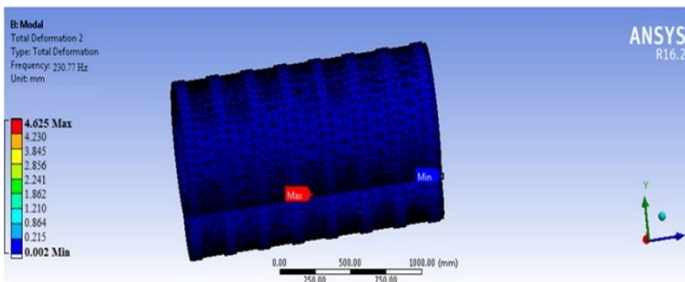


FIGURE 29: MODE 1 OF 2MM STEEL + 2MM RUBBER +2MM STEEL MATERIAL

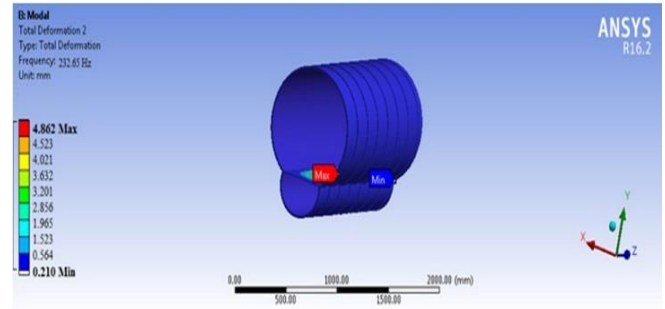


FIGURE 30: MODE 2 OF 2MM STEEL + 2MM RUBBER +2MM STEEL MATERIAL

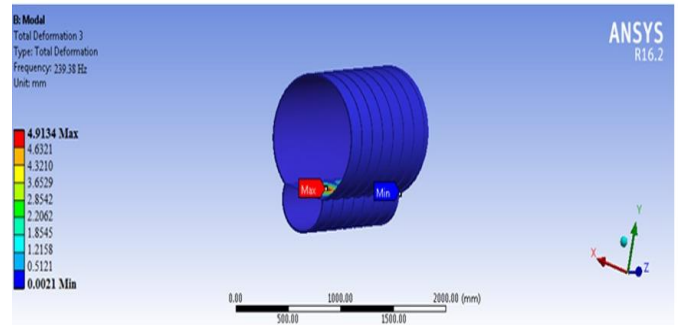


FIGURE 31: MODE 3 OF 2MM STEEL + 2MM RUBBER +2MM STEEL MATERIAL

5.7 2.5mm Steel + 1mm Rubber +2.5mm Steel:

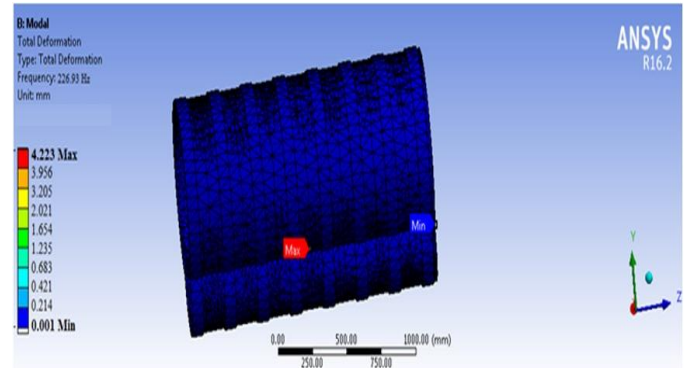


FIGURE 32: MODE 1 OF 2.5MM STEEL + 1MM RUBBER +2.5MM STEEL

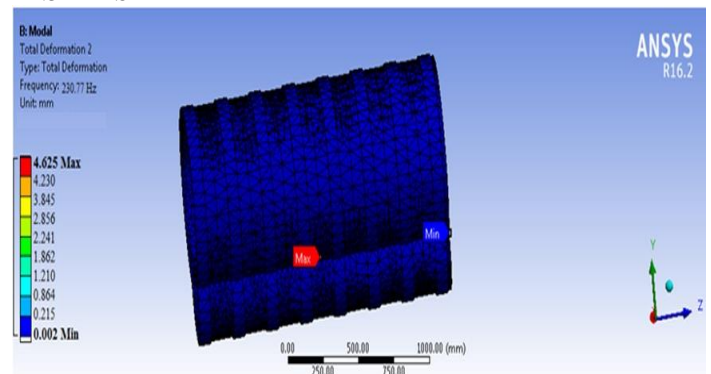


FIGURE 33: MODE 2 OF 2.5MM STEEL + 1MM RUBBER +2.5MM STEEL

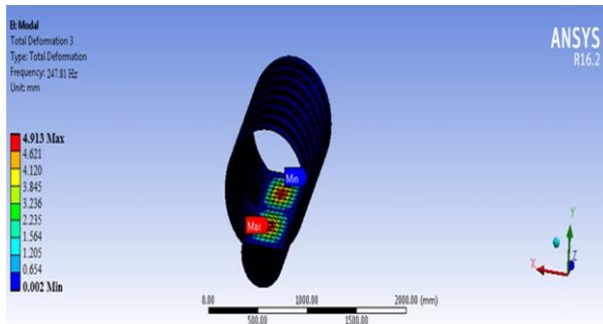


FIGURE 34: MODE 3 OF 2.5MM STEEL + 1MM RUBBER +2.5MM STEEL

5.8 2MM TI-6AL-4V + 2MM RUBBER + 2MM TI-6AL-4V:

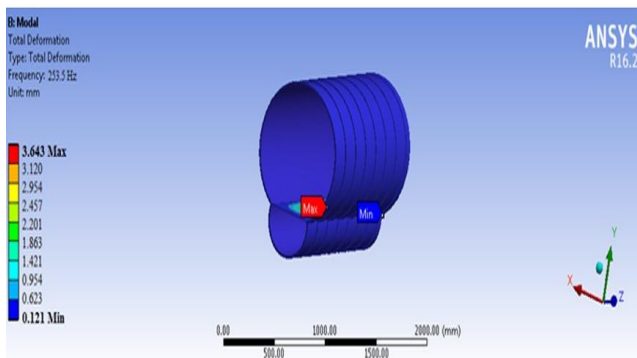


FIGURE 35: MODE 1 2MM TI-6AL-4V + 2MM RUBBER + 2MM TI-6AL-4V

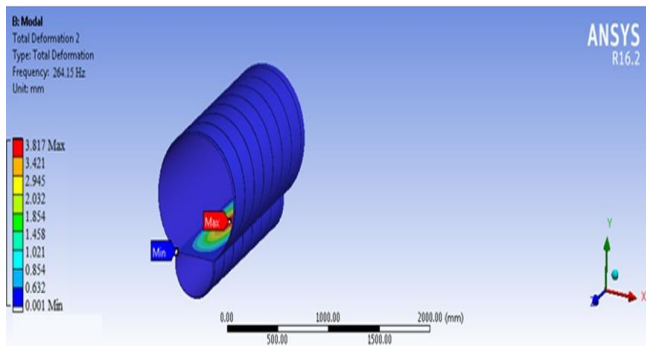


FIGURE 36: Mode 2 2MM TI-6AL-4V + 2MM RUBBER + 2MM TI-6AL-4V

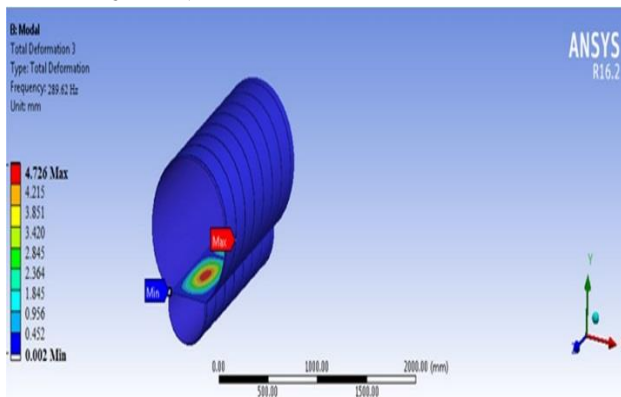


FIGURE 37: Mode 3 2MM TI-6AL-4V + 2MM RUBBER + 2MM TI-6AL-4V

5.9 7.5.4 2.5mm Ti-6Al-4V + 1mm Rubber +2.5mm Ti-6Al-4V:

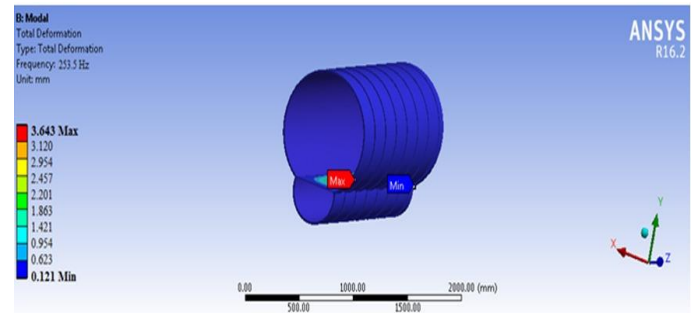


FIGURE 38: MODE 1 2.5MM TI-6AL-4V + 1MM RUBBER +2.5MM TI-6AL-4V

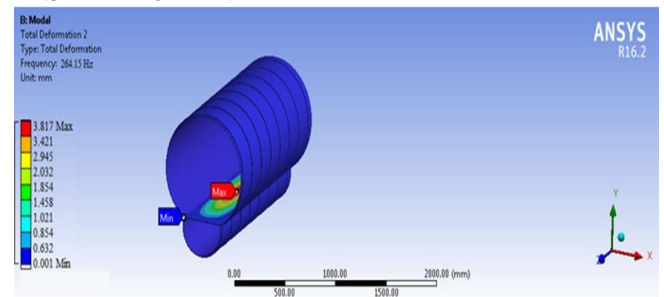


Figure 39: MODE 2 2.5MM TI-6AL-4V + 1MM RUBBER +2.5MM TI-6AL-4V

984
;LK

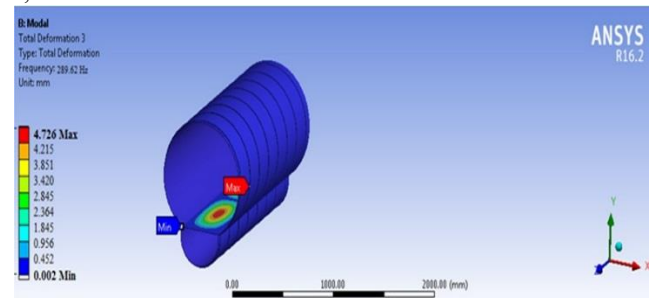


Figure 40: Mode 3 2.5MM TI-6AL-4V + 1MM RUBBER +2.5MM TI-6AL-4V

5.10 GRAPHS

The static structural analysis of Sand which materials with different layers like 2.5mm Ti-6Al-4v + 1mm Rubber + 2.5Ti-6Al-4V, 2mm Ti-6Al-4v + 2mm Rubber + 2mmTi-6Al-4V, 2.5mm C40 Steel + 1mm Rubber + 2.5mm C40 Steel, 2mm C40 Steel + 2mm Rubber + 2mm C40 Steel are done we are taking load conditions are fixed at two Ends and applied hydro static pressure at outside of the pressure hub results are obtained for Equivalent (Von-Mises) stress, shear stress, total deformation. These results are plotted graphically and a comparison is made between these results.

5.10.1 VON-MISES STRESS GRAPH:

We can observe that in case of equivalent (von-mises) stress, Sand which materials with different layers like 2.5mm Ti-6Al-4v + 1mm Rubber + 2.5Ti-6Al-4V, 2mm Ti-6Al-4v + 2mm Rubber + 2mmTi-6Al-4V, 2.5mm C40 Steel + 1mm Rubber + 2.5mm C40 Steel, 2mm C40 Steel + 2mm Rubber + 2mm C40 Steel. Finally concluded the 2mm Ti-6Al-

4v + 2mm Rubber + 2mmTi-6Al-4V is the less Von-misses stress compared with remaining materials.

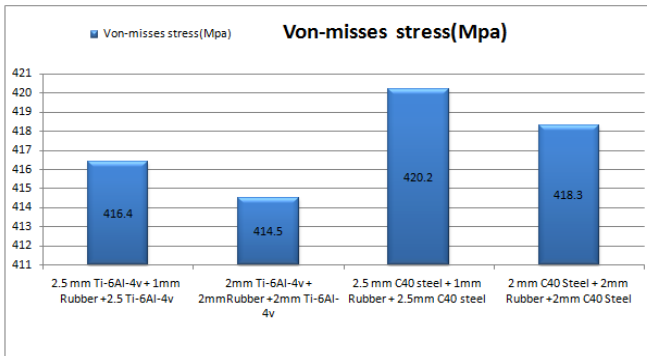


FIGURE 41: VON-MISSES STRESS GRAPH

5.10.2 TOTAL DEFORMATION GRAPH:

We can observe that in case of Total deformation, Sand which materials with different layers like 2.5mm Ti-6Al-4v + 1mm Rubber + 2.5Ti-6Al-4V, 2mm Ti-6Al-4v + 2mm Rubber + 2mmTi-6Al-4V, 2.5mm C40 Steel + 1mm Rubber + 2.5mm C40 Steel, 2mm C40 Steel + 2mm Rubber + 2mm C40 Steel. Finally concluded the 2mm Ti-6Al-4v + 2mm Rubber + 2mmTi-6Al-4V is the less Total deformation compared with remaining materials.

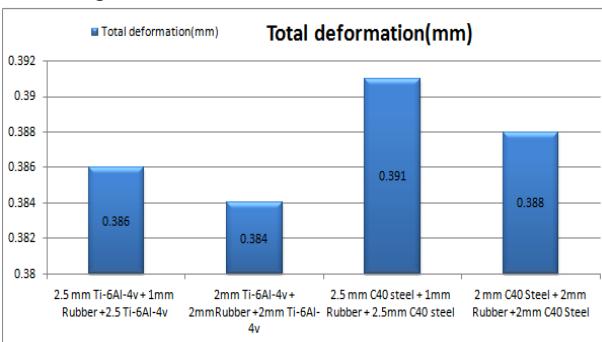


FIGURE 42: TOTAL DEFORMATION GRAPH

5.10.3 STRAIN GRAPH

We can observe that in case of Strain, Sand which materials with different layers like 2.5mm Ti-6Al-4v + 1mm Rubber + 2.5Ti-6Al-4V, 2mm Ti-6Al-4v + 2mm Rubber + 2mmTi-6Al-4V, 2.5mm C40 Steel + 1mm Rubber + 2.5mm C40 Steel, 2mm C40 Steel + 2mm Rubber + 2mm C40 Steel. Finally concluded the 2mm Ti-6Al-4v + 2mm Rubber + 2mmTi-6Al-4V is the less Strain compared with remaining materials.

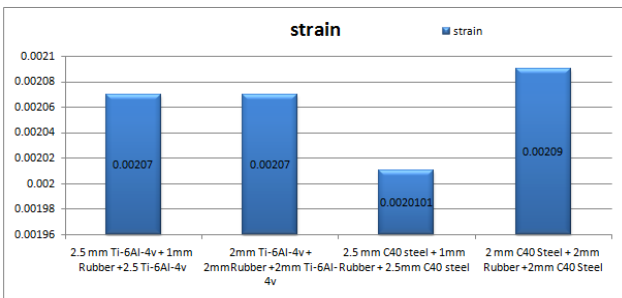


FIGURE 43: STRAIN GRAPH

5.10.4 SHEAR STRESS GRAPH

We can observe that in case of equivalent Shear stress, Sand which materials with different layers like 2.5mm Ti-6Al-4v + 1mm Rubber + 2.5Ti-6Al-4V, 2mm Ti-6Al-4v + 2mm Rubber + 2mmTi-6Al-4V, 2.5mm C40 Steel + 1mm

Rubber + 2.5mm C40 Steel, 2mm C40 Steel + 2mm Rubber + 2mm C40 Steel. Finally concluded the 2mm Ti-6Al-4v + 2mm Rubber + 2mmTi-6Al-4V is the less Shear stress compared with remaining materials.

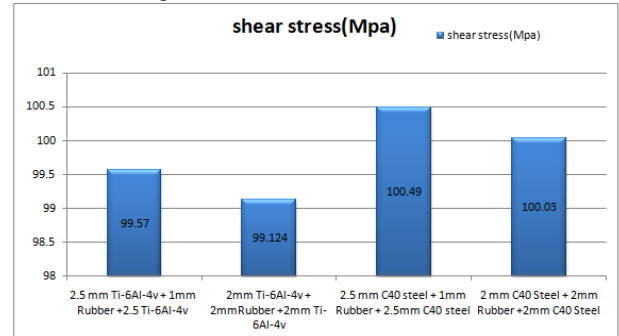


FIGURE 44: SHEAR STRESS GRAPH

5.10.5 MODAL ANALYSIS GRAPH:

The graph drawn between the different modes of different Frequencies at different deformation as shown below graphs.

7.7.1 2mm C40 Steel + 2mm Rubber + 2mm C40 Steel Material:

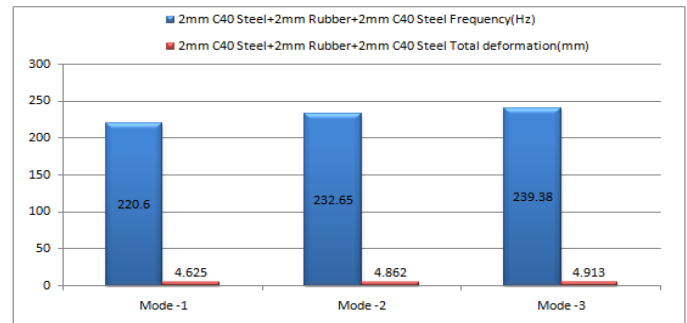


FIGURE 45: MODAL ANALYSIS OF 2MM C40 STEEL + 2MM RUBBER + 2MM C40 STEEL MATERIAL

5.10.6 2.5mm C40 Steel + 1mm Rubber + 2.5mm C40 Steel Material:

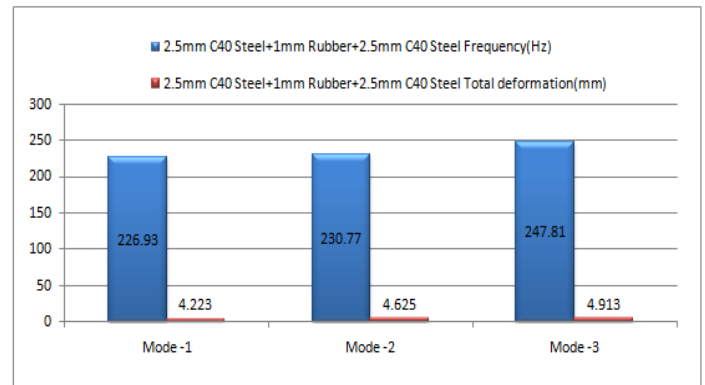


FIGURE 46: MODAL ANALYSIS OF 2.5MM C40 STEEL + 1MM RUBBER + 2.5MM C40 STEEL MATERIAL

5.10.7 2.5mm Ti-6Al-4v + 1mm Rubber + 2.5Ti-6Al-4V Material:

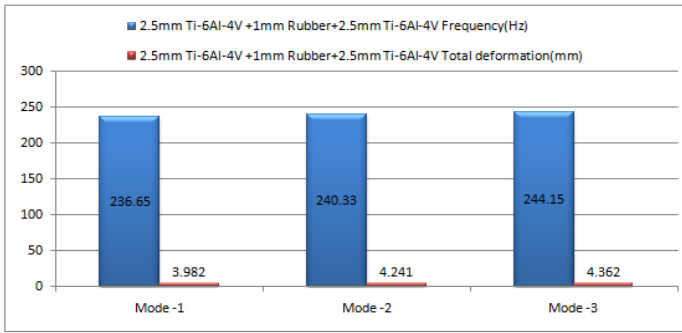


FIGURE 47: MODAL ANALYSIS OF 2.5MM TI-6AL-4V + 1MM RUBBER + 2.5TI-6AL-4V MATERIAL

5.10.8 2mm Ti-6Al-4v + 2mm Rubber + 2mmTi-6Al-4V Material:

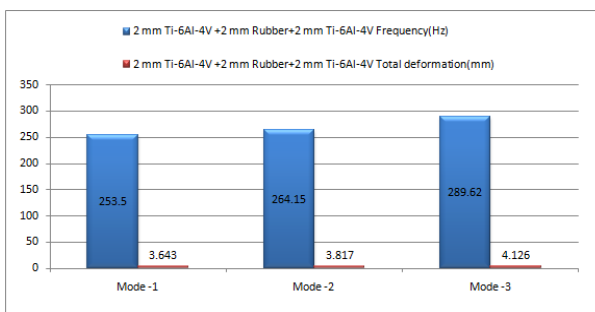


FIGURE 48: MODAL ANALYSIS OF 2MM TI-6AL-4V + 2MM RUBBER + 2MMTI-6AL-4V M

6. CONCLUSION

An Autonomous Underwater Robotic Vehicle (AUWRV) is a robot that travels underwater without requiring input from an operator. AUWRVs constitute part of a larger group of undersea systems known as unmanned underwater vehicles, Design and analysis of AUWRV Pressure vessel, perform the static and modal analysis. Design of AUWRV pressure vessel using Catia software and analysis using Ansys software using sand which beam material, in this project taken total 4 cases sand which beam material. CASE 1: 2mm Steel + 2mm Rubber +2mm Steel, CASE 2: 2.5mm Steel + 1mm Rubber +2.5mm Steel, CASE 3 :2mm Ti64Al + 2mm Rubber +2mm Ti64Al, CASE 4: 2.5mm Ti64Al + 1mm Rubber +2.5mm Ti64Al.

Finally concluded the Ti64Al + 2mm Rubber +2mm Ti64Al sand which material is suitable on pressure vessel based on the stresses, strains, deformation, shear stress in static analysis and in modal analysis find out the modes at Total deformation and in different Frequency this material is suitable for the pressure hull because of less stresses, strains, deformation, shear stress, better with stand capability in dynamic conditions.

7. REFERENCES

1. Project thesis of Roberts Tompkins submitted to TAMU University- Visco elastic analysis of Sandwich beam having Aluminum and Fiber reinforced polymer skins with polystyrene foam core- December 2009,
2. Y. Swathi and Sd Abdul Kalam, "Sandwich Treatment in FRP beams: Static and Dynamic Response". IJERT, voll 9,2012, pp 2-5.
3. Noor AK and Burton WS, "Stress and free vibration analysis of multilayered composite panels" Compos Structures, voll1,1989, pp 183-204

4. Frosting Y, Baruch M, Vainly O and Scheinman I, "High order theory for sandwich beam behavior with transversely flexible core", J Eng. Mech, vol 1 18, 1992, pp1026-1043.
5. Kant T and Swaminathan K, "Analytical solutions for the static analysis of laminated composite and sandwich plates based on a higher order refined theory", Compos Structures, vol56, 2002, pp. 329-344.
6. Pandit MK, Sheikh AH and Singh BN, "Analysis of laminated sandwich plates based on improved higher order zig zag theory", J Sandwich Struct Mater, Vol 12 2010, pp.307- 326.
7. K. Malek Zadeh, M. R. Khalili and R.K. Mittal, "Local and Global Damped Vibrations of Plates with a viscoelastic soft flexible core: An improved high order approach", Journal of sandwich structures and materials, vol7 2005, pp 431.
8. Ju F, Lee HP, Lee KH, "Finite element analysis free vibration of delaminated composite plates". Compose Eng.1995,5(2), pp,195-209.
9. Ahrari, E. (2010) 'Transformation of America's Military and Asymmetric War', Comparative Strategy, 29 (3), pp. 223 - 244.
10. Andrewes. (2010). Element Aspect Ratio. Available: <http://andreweib.wordpress.com/2010/12/14/element-aspectratio/>. Last accessed 20 April 2011.
11. British Standards Institution. (2009) 'PD 5500'. [in Specification for unfired fusion welded pressure vessels. London: BSI.
12. Burcher, R. & Rydill, L. (1994) Concepts in submarine design. Cambridge ocean technology series. Cambridge University Press.
13. FAS. (1999). Dry Deck Shelters—Deploying Special Operations Forces from Submarines. Available: <http://www.fas.org/man/dod-101/sys/ship/docs/990100-drydeck.htm>. Last accessed 20 April 2011.
14. 'Fewer dragons, more snakes' (2010), Economist, 397 (8708), pp. 27-30.
15. Freedman, L. (1998) 'The changing forms of military conflict', Survival, 40 pp. 39-56.
16. Geiger, V. (2009) 'The Submarine as a Potent Weapon For Littoral Water Operations'. www.sea-technology.com. [Online]. Available at: http://sea-technology.com/features/2009/1109/submarine_littoral.html. Last accessed 20 April 2011.
17. Germanischer Lloyd. (2007). World's First Submarine in Class. Available: http://www.glggroup.com/pdf/bravo_zulu_2007-01_E.pdf. Last accessed 20 April 2011.
18. Germanischer Lloyd. (2008) 'Rules for Classification and Construction - Naval Ship Technology'. [in Hamburg: Germanischer Lloyd.
19. Graham, D. (2007) 'Predicting the collapse of externally pressurized ring-stiffened cylinders using finite element analysis', Marine Structures, 20 (4), pp. 202-217.
20. Hoffman, F. G. (2006) 'Complex Irregular Warfare: The Next Revolution in Military Affairs', Orbis, 50 (3), pp. 395- 411.

Conception, Fabrication, and Research & Development of a Mechanized Arm for Physically Challenged Individuals

Sivasankara Raju Rallabandi^{1*}, Lakshmi Srinivas², Hari Kiran Vuddagiri³, And Timothy Pandi⁴

¹Department of Mechanical Engineering, Aditya Institute of Technology and Management, Tekkali-532201, Andhra Pradesh, India,

²Department of Mechanical Engineering, Bapatla Engineering College, Bapatla, Andhra Pradesh, India,

³Department of Mechanical Engineering, Avanti Institute of Engineering and Technology, Narsaipatnam, Andhra Pradesh, India.

⁴Department of Mechanical Engineering, Lendi Institute of Engineering and Technology, Vizianagaram, Andhra Pradesh, India.

Abstract. This study primarily focuses on individuals who have lost a hand as a result of a fatal accident, a paralytic condition, or who have become incapacitated as a result of high-priced prosthetic hands supplied by the medical sector. Using additive manufacturing, this work aims to produce a prosthetic hand-made thing for the least amount of money. GRAPHITE SOFTWARE and ONSHAPE were used to design the model. The planned mechanical hand is a user-friendly model robot designed to help individuals, especially those who have lost one hand. It is capable of performing a wide range of duties without a person's help. These tasks require lifting and moving objects. The automated hand is constrained by five servo engines, one for each finger. These servo engines can be moved around and positioned wherever is required. These servo engines are linked to the main control unit (MCU). Due to its MCU's reliance on Arduino, the robot can be controlled by clients up to 10 meters away. Here, two methods of controlling the growth of an automated hand were used: a flex sensor and the elimination of hand muscle impulses. **Keywords-** Arduino IDE, Robot, sensor control system, Automation system.

Keywords: Robotics, hand, control system, grippers, sensing, motors, PLA

I. INTRODUCTION

Mechanical arms intended for handicapped people are assistive gadgets that can be constrained by people who have restricted or no versatility in their arms or hands. These gadgets are intended to assist individuals with disabilities perform regular errands that would somehow or another be testing or unthinkable, like eating, drinking, and getting objects. A mechanical arm commonly comprises of a few enunciated joints, permitting it to impersonate the developments of a human arm. The arm is regularly controlled utilizing a joystick, switch, or other info gadget that the client can work with their excess actual capacities. A few mechanical arms could be controlled utilizing mind PC interfaces or other high level control frameworks[1–3].

There are various sorts of automated arms accessible for debilitated people, each with its own arrangement of elements and capacities. Some are intended to be utilized at home, while others are more reasonable for use in clinical or restoration settings. Eventually, the decision of automated arm will rely upon the particular requirements and capacities of the singular client. Generally speaking, mechanical arms can give a huge lift in freedom and personal satisfaction for individuals with handicaps. By empowering people to perform undertakings that would somehow or another be testing or incomprehensible, these gadgets can assist with advancing more noteworthy independence and confidence, as well as diminishing the requirement for help from guardians or relatives[4,5].

Kawasaki et al. [6] are committed to designing technologies that help people with disabilities take charge of their own rehabilitation in order to speedily reclaim lost abilities. The system relies on therapists providing guidance tailored to each patient's specific needs for it to function properly. Mouri et al. [7] are developed new design approaches mimic disabled human hands in a robot hand. Distributed tactile sensors can be used to assess a disabled person's joint torque. It introduces a model of contracture joints with tendon adhesion. Torque-based force control controls the contracture-jointed robot hand. Experimental evidence supports the efficacy of the proposed approach.

Ramiro et al. [2] came up with an improved plan for the robotic hand that doesn't move much. Three of the fingers of this robotic hand are articulated, and they may move to fit the thing it is holding. The auctioning and finger movement are both powered by a single dc motor. The command sequences are straightforward and can be transmitted from any computer. The ASIBOT Robot incorporates the robotic hand's mechanism, electrical control, and 250-gram-weight actuator, making it a unique piece of technology.

The Fuzzy PID Control of a Wearable Rehabilitation Robotic Hand Powered by Pneumatic Muscles was developed by Jun Wu and Jian Huang[8]. For people who have survived stroke and traumatic brain injury, intensive task-oriented repeated physical therapy must be delivered through tailored contact between the patients and the rehabilitation specialists. The development of a unique wearable device for robotically aided repetitive hand rehabilitation is the aim of this study. We created a wearable therapy device powered by pneumatic muscles (PM) that delivers the supportive forces needed for grasping and finger extension.

The primary objective of a robotic arm designed for disabled persons is to provide individuals with limited or no mobility in their arms or hands with greater independence and autonomy in performing everyday tasks. By mimicking the movements of a human arm, a robotic arm can assist users with a wide range of activities, such as eating, drinking, and picking up objects. The only goal of the project is to integrate into society and improve the quality of life of persons with disabilities. The use of robotic arms also frees human workers from performing tasks that present a risk of bodily injury. Robotic arms are used to provide an alternative method to engage in joint play activities Working Principal and Methods

Contact sensors are a key component of a mechanical hand's operating principle for people with disabilities. These sensors detect pressure or force applied to the skin's outer layer and then

translates this information into signals that can be used to control the mechanical hand's growth. The mechanical hand typically has several separate fingers, each of which is restrained by a distinct engine. The touch sensors, which are located on the skin of the client's remaining appendage or on a special glove the client is wearing, are connected to the engines. The touch sensor recognizes when the client is exerting pressure or power on it and sends a message to the corresponding engine. The engine then repeats the development that the client would make if they truly had their own hand by moving the corresponding finger of the automated hand at that stage. High-level touch sensors can also provide other information, such as the surface's temperature or texture. The precision and awareness of the mechanical hand can be improved with the help of this data.

In general, using touch sensors in a mechanical hand for people with disabilities considers a more natural and regular approach to controlling the hand's movements, and it can extraordinarily further develop the client's personal satisfaction by allowing them to perform tasks that sound difficult or unimaginable. The use of sensors to detect changes and strain imposed by the client's remaining appendage is part of the operating guidelines for a mechanical hand for disabled individuals that uses touch sensors. The prosthetic hand's outside is covered with sensors that are linked to a microprocessor. When the user moves their residual appendage, the sensors detect the movement and send data to the microprocessor, which then activates the engines that move the mechanical hand's fingers and wrist. In order to mimic the natural movements of a human hand, the engines move the fingers and wrist in a predetermined manner.

The following methods have been followed for attaining of mechanical arm.

Identify customer needs. The most important step in prosthesis promotion is to identify your customers' needs. This includes an assessment of the client's withdrawal rate, the permanent nature of the appendage, and useful need for a prosthetic arm.

Construction: A prosthetic plan is created according to the customer's needs. This includes making an ergonomic prosthetic by selecting the right materials and components such as motors, sensors, and actuators.

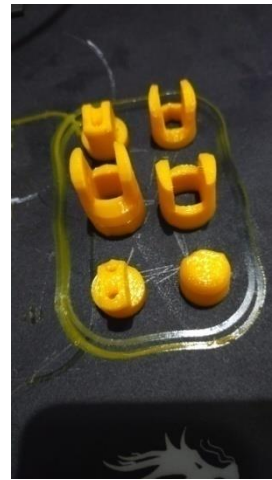
Model Evolution: A prosthetic hand model was created using PC-aided drawings. The design is optimized using Cura software and 3D printing innovation. Consider iterative and experimental plans to improve the usefulness and availability of prosthetic arms.

Testing: Evaluate usability and ease of use by testing the model. This includes checking the hand's ability to hold and manipulate an object and evaluating the client's execution of the plan.

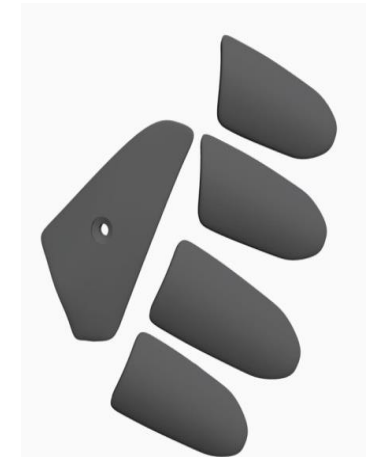
Refined: Plans are refined and updated based on test results and circumstances. This can include getting familiar with the materials or details used, as well as fine-tuning the shape and presence of the hands. **Implementation:** Execute the prosthetic hand when the plan is stopped. This includes putting all the pieces together and completing the hand.

Fitting and Preparation: The prosthetic arm is fitted to the client's permanent appendage and preparation is performed

using the most efficient arm technique. This may include demonstrating to the client how to control the arm with electromechanical signals, and preparing the best way to actually focus on and follow the prosthetic arm.



(a) Fingers



(b) Cover



(c) Bolt entireties



(d) holding surfaces



(e) Rob cap



(f) Rob cap joint

Figure 1 list of components are prepared with 3D printing and used for mechanical hand

List of Components Used in Mechanical Arm

Planning a mechanical hand utilizing PLA material and Ultimaker Cura 3D printing programming should be possible in a few stages. The arm parts are created utilizing different assembling cycles like projecting, fashioning, machining, or 3D printing. These cycles might be acted in-house or moved to particular producers. The Figure 1 shows the lists of 3d printed components were used in mechanical hand.

The fingers (vide in Figure 1a) of a mechanical hand are the most noticeable piece of the gadget, and they are liable for holding and controlling items. The quantity of fingers can shift contingent upon the plan of the hand, however most mechanical hands have somewhere in the range of three and five fingers.

Holding surfaces and covers: The grasping surfaces of a mechanical hand are the parts that come into contact with the items being controlled, shown in Figure 1(b)- Figure 1(f). They can be produced using various materials, like elastic or silicone, to give a solid grasp on objects of various shapes and sizes.

Joints: The joints of a mechanical hand permit the fingers to move in various ways, like twisting and pivoting, it can be observed in Figure 1(c) and Figure 1(e). The quantity of joints can likewise fluctuate contingent upon the plan of the hand, yet most automated hands have no less than one joint for every finger.

Plan the hand: Utilize a 3D demonstrating programming to make a plan for the mechanical hand. The plan ought to think about the scope of movement expected for the hand, as well as the size and state of the singular fingers. Convert the plan to a STL record: When the plan is finished, send out it as a STL document. This record design is viable with most 3D printing programming, including Ultimaker Cura[2].

Actuators: Actuators are the parts of a mechanical hand that create the power expected to move the fingers and joints. They can be controlled by power, hydrodynamics, or pneumatics, contingent upon the plan of the hand[9].

The Arduino Nano (vide in Figure 2(a)) is compatible with the Arduino IDE (Integrated Development Environment), which provides an easy-to-use interface for programming and uploading code to the board. It can be programmed using C++ language and the Arduino programming language, which is based on Wiring. The board includes a USB interface for programming and communication, as well as a power regulator to provide a stable 5V supply from the input voltage. The digital I/O pins can be used to control external devices such as LEDs, motors, and sensors, while the analog input pins can be used to read analog signals from sensors such as temperature and light sensors[10,11].

Sensors: Sensors are utilized to recognize the position, direction, and power applied by the fingers of the mechanical hand, shown in Figure 2(b). The data is utilized to control the development of the hand and guarantee that it holds objects with the right measure of power. Motion sensors can be utilized in a mechanical hand for impaired people to give extra criticism and command over the prosthetic hand's developments. Motion sensors are gadgets that action changes in attractive transition, which can be utilized to identify the position and development of items[12,13].

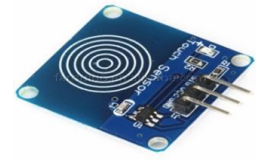
Relay module: A 4-channel 12V relay module is an electronic device that allows you to control up to four high voltage or high current devices using low voltage signals from a microcontroller or other control system, shown in Figure 2(c). The module consists of four individual relays mounted on a PCB (printed circuit board) along with supporting electronics.

Control framework: The control arrangement of a mechanical hand incorporates the product and equipment used to work the hand[12,14]. It can incorporate sensors, processors, and correspondence frameworks that permit the hand to be controlled from a distance or modified to perform explicit undertakings. The MG995 can convey up to 13 kg-cm of force at 6V, making it reasonable for

undertakings that require elevated degrees of power, for example, lifting and grasping articles, shown in Figure 2(d).



(a)Arduino nano



(b) Flex sensor



(c)Relay



(d) Servo motor

Figure 1 list of electrical components used in mechanical hand

Program Used to Control Mechanical Arm

C programming can be utilized to control a mechanical arm by sending orders to the arms control board. Here are the essential strides for programming a mechanical arm utilizing C. Interface with the control board: Prior to programming the mechanical arm, you want to lay out an association with the arms control board utilizing a chronic or USB link. The particular association strategy will rely upon the kind of control board utilized. Compose a C program that sends orders to the control board to control the development of the mechanical arm. This program ought to incorporate capabilities to move the arm's joints and control the end effectors (the device or gripper toward the finish of the arm). The following test the program to guarantee that it is working accurately. This might include physically testing the arm's development or utilizing a reproduction program to test the program's usefulness.

```
#include <Servo.h>
// Define the pin for the touch sensor
const int touchPin1 = 2;
const int touchPin2 = 3;
const int touchPin3 = 4;
const int touchPin4 = 5;
int servopin1=6; // Attach the servo to pin 6
int servopin2=7; // Attach the servo to pin 7
int servopin3=8;

if (digitalRead(touchPin3) == HIGH) {
    // Move the servo to a new position
    if (servoPosition3 == 0) {
        servo3.write(90);
        servoPosition3 = 1;
    } else {
        servo3.write(0);
        servoPosition3 = 0;
    }
    // Delay to allow the servo to move to the new position
    delay(500);
}

void loop() {
    // Wait for the touch sensor input
    if (digitalRead(touchPin1) == HIGH) {
        // Move the servo to a new position
    }
}
```


<https://doi.org/10.1080/09638280410001704278>.

- [4] A. Hussain, R. Wenbi, A.L. Da Silva, M. Nadher, M. Mudhish, *Health and emergency-care platform for the elderly and disabled people in the Smart City*, *J. Syst. Softw.* 110 (2015) 253–263. <https://doi.org/10.1016/j.jss.2015.08.041>.
- [5] A. Kargov, T. Asfour, C. Pylatiuk, R. Oberle, H. Klosek, S. Schultz, K. Regenstein, G. Bretthauer, R. Dillman, *Development of an anthropomorphic hand for a mobile assistive robot*, in: *Proc. 2005 IEEE 9th Int. Conf. Rehabil. Robot.*, 2005: pp. 182–186. <https://doi.org/10.1109/ICORR.2005.1501080>.
- [6] H. Kawasaki, T. Komatsu, K. Uchiyama, *Dexterous anthropomorphic robot hand with distributed tactile sensor: Gifu hand II*, *IEEE/ASME Trans. Mechatronics.* 7 (2002) 296–303. <https://doi.org/10.1109/TMECH.2002.802720>.
- [7] T. Mouri, H. Kawasaki, Y. Nishimoto, T. Aoki, Y. Ishigure, *Development of robot hand for therapist education/training on rehabilitation*, in: *IEEE Int. Conf. Intell. Robot. Syst.*, 2007: pp. 2295–2300. <https://doi.org/10.1109/IROS.2007.4399377>.
- [8] J. Wu, J. Huang, Y. Wang, K. Xing, Q. Xu, *Fuzzy PID control of a wearable rehabilitation robotic hand driven by pneumatic muscles*, in: *20th Anniv. MHS 2009 Micro-Nano Glob. COE - 2009 Int. Symp. Micro-NanoMechatronics Hum. Sci.*, 2009: pp. 408–413. <https://doi.org/10.1109/MHS.2009.5352012>.
- [9] S.R. Rallabandi, S.K. Adapa, *Evaluation Of Thermo-Mechanical Behavior Of Hemp Fiber Polymer*, *Compos. Mech. Comput. Appl. An Int. J.* 13 (2022) 113–132. <https://doi.org/10.1615/CompMechComputApplIntJ.2022043103>.
- [10] M.A. Kumar, S.A.K. Jilani, U. Sreenivasulu, S.J. Hussain, *Automated Color Recognition System for Visually Challenged and Achromatopsia People using Arduino and Mobile App*, *Int. J. Adv. Res. Electron. Commun. Eng.* 4 (2015) 2106–2110.
- [11] S. Vandana, K. Shamukha Sri Sai, P. Rohila, V. Manideep, *PLC Operated Colour Based Product Sorting machine*, *IOP Conf. Ser. Mater. Sci. Eng.* 1119 (2021) 012016. <https://doi.org/10.1088/1757-899x/1119/1/012016>.
- [12] S.R. R. Jagadish, C.J. Rao, S. Kumar, S. Yanda, S. Kumar Aadapa, S. Yanda, *Predication of temperature distribution and strain during FSW of dissimilar Aluminum alloys using Deform 3D*, *Mater. Today Proc.* 59 (2022) 1760–1767. <https://doi.org/10.1016/j.matpr.2022.04.371>.
- [13] H.K. Vuddagiri, S. Vadapalli, J. Sagari, R.S. Raju, S.R. R., *Fabrication and Modelling of Tribological Performance of Al-Si/12Al2O3/2MoS2 Composite using Taguchi Technique*, *Int. J. Automot. Mech. Eng.* 18 (2021) 8959–8977. <https://doi.org/10.15282/ijame.18.3.2021.09.0686>.
- [14] S. Raju, L. Srinivas, S. Rao Gunji, T. Srinag, M.C. Sekhar, T. Pandi, *Estimation of Effect of Cold Forging Deformational Behavior on Al-2024 Alloy Reinforced with Fly-Ash Particulates*, *Adv. Sci. Technol.* 120 (2022) 3–14. <https://doi.org/10.4028/p-609250>.
- [15] A.A.M. Faudzi, J. Ooga, T. Goto, M. Takeichi, K. Suzumori, *Index Finger of a Human-Like Robotic Hand Using Thin Soft Muscles*, *IEEE Robot. Autom. Lett.* 3 (2018) 92–99. <https://doi.org/10.1109/LRA.2017.2732059>.
- [16] M.M.R. Rana, M.F. Zaman, S.K. Ray, J. Al Faysal, *Prototype Design and Development of Flex Sensor Controlled Bionic Arm for the Handicapped Person*, *Int. J. Comput. Appl.* 183 (2021) 1–4. <https://doi.org/10.5120/ijca2021921410>.

DESIGN AND FABRICATION OF MIG 29-kFIGHTERJET USING 3D PRINTER

D.Raghavendra, SK. Mahammad Bilal, B.Prasanna Kumar, N.Anwar Basha, G.Ravi, K.Nagendra Babu
 Department of Mechanical Engineering,
 Narasaraopeta Engineering College, Narasaraopet, Palnadu(Dist.), A.P., India

Abstract - The MiG-29K is based on the 'basic' MiG-29K airframe, but it is lighter in order to meet the Indian Navy's requirement for the smallest possible dimensions in order to maximise use of space on the aircraft carrier Vikramaditya (formerly Admiral Gorshkov). The plane is based on the original MiG-29K airframe, but it lacks the expensive welded aluminium lithium fuel tanks and forward fuselage. The fuel tanks on the MiG-29K are located in the dorsal spine fairing and wing leading-edge root extensions. This is said to give the aircraft a 50% performance boost over the land-based MiG-29. 3D printing technology is the most advanced manufacturing process currently in use, allowing for the rapid printing of components while lowering production costs. In this project, the design is completed using FUSION 360 software, and the file is then converted to STL format, which is used for component production in a 3D printing machine. Ultimaker Cura software is used for slicing FUSION 360 components, as well as for adjusting dimensions, solidification time, material selection, printing speed, and printing time. In this project, PLA material is used to create the component in a 3D printing machine.

Formula: The total time required to print the fighter jet was 13 hours and 21 minutes.

The total amount of material used to print the fighter jet is 82 grammes. a height of 10.37 metres

Keywords- MiG-29K airframe, 3D printing, FUSION

I. INTRODUCTION

Additive Manufacturing is the formalised term for what was previously known as Rapid Prototyping and is now commonly known as 3D Printing. Rapid prototyping (or RP) is a term used in many industries to describe a process for quickly creating a system or part representation prior to final release or commercialization. In other words, the emphasis is on quickly producing something, with the output being a prototype or basis model from which further models and, eventually, the final product will be derived. Both management consultants and software engineers use the term Rapid Prototyping to describe a method of developing business and software solutions in stages, allowing clients and other stakeholders to test ideas and provide feedback during the development process. A 3D digital model serves as the foundation for any 3D printing process. This model can be developed using a variety of 3D

software programmes, such as 3D CAD for industry, or it can be scanned with a 3D scanner for Makers and Consumers. The model is then "sliced" into layers, resulting in a file that the 3D printer can read. The 3D printer then layers the material in accordance with the method and design.

II. EXISTING DESIGN

Printing is accomplished by first applying ink onto the raised areas. The inked roller is then pressed against the material to be printed causing the ink color to be transferred from the surface of the raised design onto a moving web of wallcoverings. One roller is required for each color.



Fig 1: Printing Machine

III. PROPOSED METHOD



Fig 2: Autodesk Fusion

Printing of Objects using 3D Printing

Step 1: Once the modelling is done then STL file is loaded into cura software and slicing is done. After completion of the above process the G code file loaded in to 3Dprinter by using SD card or Pen drive.

Step 2: In order to print the component filament is loaded into the machine

Step 3: Initially bed is prepared by cleaning It with alcohol based solvent.

Step 4: After cleaning bed is preheated to 85°C temperature.

Step 5: Before printing the component, glue stick is applied because of avoiding the warping

Step 6: Once the above procedure is done select the G code file from the SD card by using select option.

Step 7: Each and every parameter setting is visible on the machine screen. Check for any errors and parameters and do modifications if necessary.

Step 8: After checking the parameters printing is started by giving start option in the machine.

Step 9: After completion of the component wait for at least 30 minutes in order to remove the component from the machine bed.

Step 10: Post processing is done to the components by removing of excess material and component supports



Fig 5: Ultramixer

The Ultimaker S5 Pro Bundle is made up of three breakthrough devices: Ultimaker S5 – our award-winning, composite-ready dual extrusion FFF 3D printer. Material Station – a 6-spool prefeeder with humidity control that automatically switches between materials.

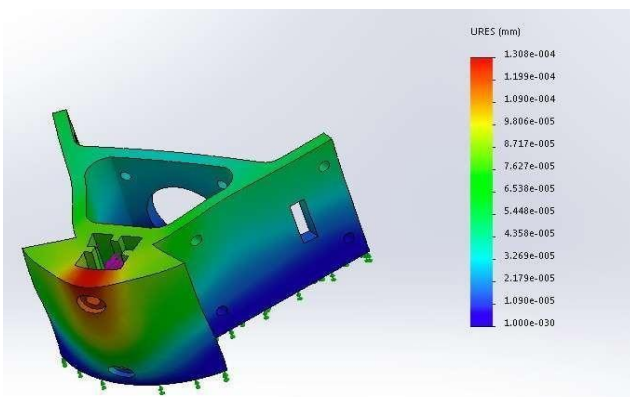


Fig 3: Analysis of MIG 29 K wings

These can prevent a prominent Z-Seam on the 3D model surface. Sometimes, the printer will leave a mark on the model surface at the start of each layer. When these marks all align, the 3D model will have a prominent spurious line on its outer wall. This line is called a Z-Seam. The Z-Seam Alignment setting lets you choose where in the 3D model surface this line appears or lets you get rid of the line altogether.

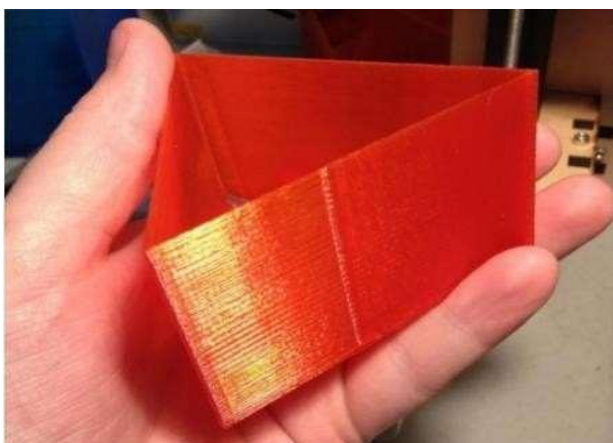


Fig 4: Z Seam Alingment

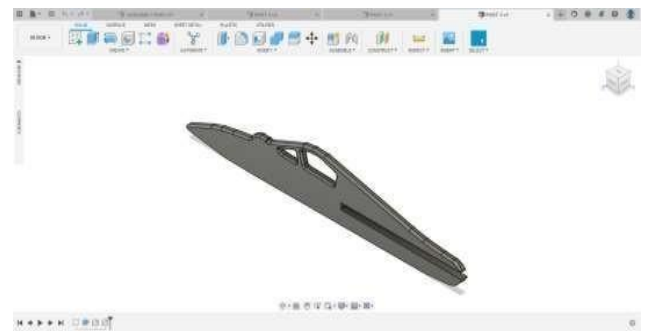


Fig 6: Nose Radome

The above figure shows the Nose radome file. Design in a FUSION 360 and saved in the .prt format because if any changes or modifications required to the above component .prt file is editable and after again saved in the .stl (stereolithography) format this format is used for the 3D printers and next transfers into cura software.

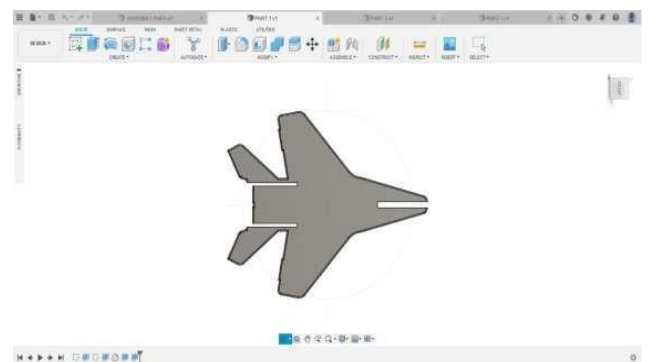


Fig 7: Central Chest

The above figure shows the Central chest file. Design in a FUSION 360 and saved in the .prt format because if any changes or modifications required to the above component .prt file is editable and after again saved in the .stl (stereolithography) format this format is used for the 3D printers and next transfers into cura software. Cura converts .stl file into machine understandable file i.e. a G code in .gcode format.

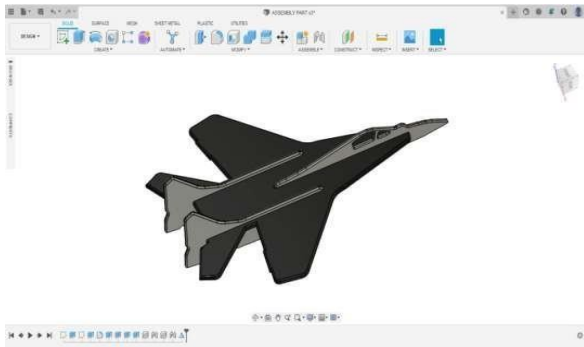


Fig 8: Combine Jet

The above figure shows the Central chest file. Design in a FUSION 360 and saved in the .prt format because if any changes or modifications required to the above component .prt file is editable and after again saved in the .stl (sterolithography) format this format is used for the 3D printers and next transfers into cura software. Cura converts .stl file into machine understandable file i.e. a G code in .gfp format

SOFTWARE IMPLEMENTATION:

STL file prepared in FUSION 360 software and loaded into a Cura software which is a free print preparation software for the ultimaker 3D printers. Slicing is done using this software. After slicing the file is saved in G codes format and with it is used as input for 3D printer for printing of the components. Each and every parameter required is modified as per the requirement in cura software.

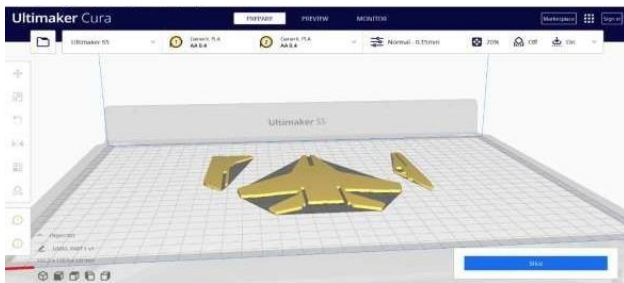


Fig 9: Fighter jet STL file in Cura

In order to see if my design for the 3D printer corner bracket would perform better than the existing 3D printed one, I needed to be able to run tests to gauge each design's performance. The main criteria I chose to focus on with my experimentation was deflection, since the overall goal of my project was to design a part that would deflect less when subject to the loads that occur during the operation of the printer.

IV. RESULT



Fig 10: Components while 3D Printing



Fig 11: Fighter jet

Total time taken for this print is 11 hours 9 minutes and the material consumed by the printer for this project is 85 grams. In cura software, arrangement of components were done in the effective way to reduce the time and material wastage.

Remove the parts from the build plate



Fig 12: 3D Printed Components

Check the gears and crank for any defects. Small pieces of filament sometimes droop in the rectangular recess for the snap pin head be sure to remove these to ensure the snap pin seats well. When all are placed on the body parts which are called stands place another body part on top of the set up.



Fig 13: Assembled component

V. ADVANTAGES

1. Flexible Design. 3D printing allows for the design and print of more complex designs than traditional manufacturing processes.
2. Rapid Prototyping.
3. Print on Demand.
4. Strong and Lightweight Parts.
5. Fast Design and Production.
6. Minimising Waste.
7. Cost Effective.
8. Ease of Access.

VI. APPLICATIONS

- Education
- Prototyping and Manufacturing
- Medicine
- Construction
- Art and Jewelry
- Custom art and design

VII. CONCLUSION & FUTURE SCOPE

With the help of FUSION 360, design of fighter jet is developed including few sub- assemblies and fabrication gears and other components completed by using 3D printing machine. 3D printing technology is the most advanced manufacturing process which is trending now a day which help in printing component at high speed and reduces production cost. In this project work, design is done using FUSION 360 software and then file is transformed to STL format which is used for production of the component in 3D printing machine. CURA software is used for slicing of the component produced in FUSION 360 and it also helps in adjustment of dimensions, solidification time, material selection, printing speed and printing time. In this project PLA material is used for the production of the component in 3D printing machine. The total time taken to print the fighter jet is 13 hours 21 minutes and components are successfully assembled.

• Layer height	0.15mm
• Wall thickness	0.8mm
• Wall countline	2
• Top/bottom thickness	1.0mm
• Top thickness	1.0mm
• Top layers	7
• Bottom thickness	1.0mm
• Bottom layer	7
• Infill density	20%
• Infill pattern	Triangles
• Printing temperature	200oc
• Build plate temperature	60oc
• Print speed	70mm/sec
• Estimated time	13 hrs 21min
• Material consumption	82 grams

REFERENCES

- [1] *Russia to deliver five MiG-29K fighters to India by year end*". RIA Novosti. 13 August 2011. Archived from the original on 25 November 2011.
- [2] Karnozov, Vladimir (1 November 2012). "MiG- 29K carrier trials for India completed". Flightglobal.com.
- [3] Johnson, Reuben F. (7 July 2016). "Indian Navy reports problems with Russian carrier aircraft". IHS Jane's Defence Weekly. Archived from the original on 8 July 2016.
- [4] Raghuvanshi, Vivek (8 August 2017). "Report: India's Russian-made MiG-29K Fighters Face Problems". Defense News. Retrieved 26 September 2017.
- [5] Rogoway, Tyler (17 July 2017). "Indian Navy MiG- 29Ks Make Low Approaches To USS Nimitz During "Malabar" Drills". The Drive. Retrieved 26 September 2017.
- [6] Sen, Sudhi Ranjan (27 July 2016). "Auditor's Report Card Fails Navy's New Flagship Fighter, MiG-29K". NDTV. Retrieved 30 July 2016.
- [7] "All Issues Pertaining to Serviceability of MiG-29K Sorted Out - Indian Navy". IndianDefense News. 5 December 2018. Retrieved 22 January 2022.
- [8] Bedi, Rahul (1 February 2017). "India issues RFI for 57 carrier-borne fighters". Jane's Defence Weekly. 54 (5)
- [9] "It's Official: Indian Navy Wants 57 Carrier-borne Fighters". LiveFistDefence.com. 25 January 2017. Archived from the original on 2 March 2017. Retrieved 1 March 2017.
- [10] "Report: Indian Navy Expresses Confidence in MiG- 29K Naval Fighters; Jets to Deploy From Carriers Vikrant and Vikramaditya". MilitaryWich Magazine. 5 December 2018. Retrieved 5 December 2018.
- [11] "'Sea Flankers' prepare for Syria". Combat Aircraft. 30 September 2016. Archived from the original on 6 October 2016.
- [12] Castells, M (1996). *The Rise of the Network Society, The Information Age: Economy, Society and Culture Vol. I*. Cambridge, MA; Oxford, UK: Blackwell.
- [13] Chua, K. Leong, K. Lim, C. (2003). 'Rapid Prototyping: Principles and Applications' (2nd edition). World Scientific Publishing Company Singapore, 2003, P124
- [14] Corney, J. (2005), 'The Next and Last Industrial Revolution?'. *Assembly Automation* Vol.25, No.4, p.257
- [15] Flaherty, N. (2007), 'Moral Dimension to Prototyping System'. *Electronics Weekly* No.2299 (Aug 1, 2007), p.3
- [16] Gershenfeld, N. (2005), 'The Coming Revolution on Your Desktop: From Personal Computers to Personal Fabricators', Basic Books, New York, NY, April.
- [17] Schumpeter, J A, 'Economic Theory and Entrepreneurial History' reprinted in Hugh G.J Aitken (ed.), *Explorations in Enterprise* (1965)
- [18] Tapscott, D. Williams, A (2008). *Wikinomics: how mass collaboration changes everything.* .: Atlantic Books.

DESIGN AND DEVELOPMENT OF WALKING ROBOT ON THE BASES OF FOUR BAR AND WEIGHT BALANCE MECHANISM

Dr. Bazani Shaik^a, Dr.V.Srinivasa Rao^b, K. Bhavanarayana^c, B.Sudhakar Rao^d, Dr. J. Ranga^e,

B. Ashok Kumar^f, R. Sai Ram^g

a,b,c,d,e,f,g Ramachandra college of Engineering, Vatluru ,Eluru and 534007, India.

ABSTRACT

A walking machine (robot) is a type of locomotion that operates by means of legs and/or wheels on rough terrain or flat surface. The performance of legged machines is greater than wheeled or tracked walking machines on an unstructured terrain. These types of machines are used for data collections in a variety of areas such as large agricultural sector, dangerous and rescue areas for a human. The leg mechanism of a walking machine has a different joint in which a number of motors are used to actuate all degrees of freedom of the legs. In the synthesis of walking machine reported in this article, the leg mechanism is developed using integration of linkages to reduce the complexity of the design and it enables the robot to walk on a rough terrain. We made this model by using ploy acidic material, servo motor, on/off switch, Creo software, fused deposition 3d modeling machine. And our project is based on weight balance mechanism also.

Key Words: *Four bar mechanism, weight balance mechanism, walking robot, creo-software and fused deposition 3d modeling machine*

I. INTRODUCTION

This “Design and development of walking robot on the bases of four bar mechanism and weight balance mechanism”. By using this model, we gain a knowledge about four bar and weight balance mechanism and also 3d modeling. Nowadays, the expansion of using robots in human life is becoming a more attractive area of research and development. This expansion has led many to start advancing automated machinery aimed at different applications. Over the past periods, science and technology in robotics developed and improved from fiction to reality, particularly in design and production of robots. Different applications within diverse disciplines such as computer science, medical application, fields of engineering and automation played a great role in the advancements within robotics. A locomotion over a soft or hard surface by means of limbs, legs and/or wheels at low

speed can be defined as a walking machine. The design and development of these machines have been widely studied by NASA for planetary exploration since the 1960s. Based on the surface on which they operate, NASA developed and used three basic types of walking machines; namely wheeled, tracked and legged walking machine or robot.

Walking machines that can operate under different conditions are used for planetary, medical, engineering, agricultural task, etc. to speed up or replace human works. The establishment of the walking machine technology started since ancient times of human civilization for conquering the machines on rough terrain surface. Recently, developed multi-legged robots are widely used locomotion principles in a biological system to achieve the surface mobility. The legs of the robots have three degrees of freedom (DOF) which perform walking motions by adapting the body system to surface structure. In the history of the walking machine, Massachusetts Institute of Technology (MIT) contributed widely to the development of walking machines design including the hopping robot. MIT humanoid Robotics group developed the concept of subsumption architecture, which is based on a strong coupling between actuators and sensors, promoting a more reactive behavior than in the classical control approaches. Based on this concept, six-legged walking machines were designed in late 1980s, which were designed with two DOF to achieve simplicity in the mechanism and low weight.

II. METHODOLOGY

FOUR BAR MECHANISM

In the study of mechanisms, a four-bar linkage, also called a four-bar, is the simplest closed-chain Figure.1

movable linkage. It consists of four bodies, called bars or links, connected in a loop by four joints. Generally, the joints are configured so the links move in parallel planes, and the assembly is called a planar four-bar linkage. Spherical and spatial four-bar linkages also exist and are used in practice. The synthesis, or design, of four-bar mechanisms is important when aiming to produce a desired output motion for a specific input motion. In order to minimize cost and maximize efficiency, a designer will choose the simplest mechanism possible to accomplish the desired motion. When selecting a mechanism type to be designed, link lengths must be determined by a process called dimensional synthesis. Dimensional synthesis involves an iterate-and-analyze methodology which in certain circumstances can be an inefficient process however, in unique scenarios, exact and detailed procedures to design an accurate mechanism may not exist.

III. WEIGHT BALANCE MECHANISM

A number of methods can be found in the literature to gravity balance a machine. In this model we use hybrid method to achieve gravity balancing. Hybrid method employs a mechanism to locate center of mass of the robot in conjunction with legs. This method is used to develop a rotating device, which compensates the effect of gravity on a human leg. This data showed that the machine could be used for gravity balancing of the leg and could be potentially used for study purpose. The invention relates to a device for balancing the weight carried by a robot leg. Said device comprise of rotating body and a control device for controlling the movements of the robot. Said device and the method provided for by the invention permit the exact adjustment and balancing of the movements of the robot by its legs.

IV. 3D MODELING

Rapid prototyping of complex and intricate shapes has become easier, quicker and cost effective with the introduction of additive manufacturing process. Fused deposition modeling technique is a popular additive manufacturing process, which is used to develop the complex biomedical apparatus without the use of more

no. of tools, fixtures and complex systems. The addition of copper and silver nanoparticles into the PLA material improves the biomedical and mechanical properties of various prosthetic appliances. Addition of desired percentage of copper and silver improves properties and usage of anti-bacterial PLA material significantly.

The basic methodology for all current rapid prototyping techniques can be summarized as follow. A CAD model is constructed, and then converted to STL format. The resolution can be set to minimize stair stepping. The RP machine processes the STL file by creating sliced layers of the model. The first layer of the physical model is created. The model is then lowered by the thickness of the next layer, and the process is repeated until completion of the model. The model and any supports are removed. The surface of the model is then finished and cleaner. The CAD Mode There are many different CAD packages capable of producing an STL file. For rapid prototyping it is essential that parts are complete and have continuity, i.e., the part to be built must be represented as closed surfaces that unambiguously define an enclosed volume.

CATIA REVIEW

CATIA v5 is an Integrated Computer Aided Engineering tool which incorporates: CAD, CAM, CAE and other applications. CATIA v5 is a native Windows application. User friendly icon based graphical user interface. Encourages design flexibility and design reuse. Supports knowledge-based design.

V. ASSEMBLY



Figure 1. Assembly of prototype

Chassis Assembly

To assemble the chassis, I performed the following steps:

- Pressed "Bevel, Gear, Motor.stl" onto the motor shaft.
- Pressed the motor assembly into "Chassis.stl".
- Positioned "Bevel, Gear, Axle.stl" in the chassis assembly and secured it in place with two "Axle, Gear, Bevel.stl" (a small dot of glue may assist in retaining these components).
- Inserted the four AAA batteries into the battery pack.
- Placed double sided sticky tape on the side of the battery pack opposite of the switch.
- Centered the battery back into "Battery Case Holder.stl" and secured it in place.
- Slid the battery pack holder onto the chassis assembly.
- Soldered the battery case wires to the motor such that the motor shaft rotated counter clockwise when viewed from the motor shaft end of the motor.
- Adjusted the motor position such that the motor gear aligned with the axle bevelgear.
- Applied a thin strip of double-sided sticky tape to the battery case holder top rail.
- Secured the battery wires to the tape.

Track Assembly

To assemble the track, I performed the following steps:

- Threaded two "Standoff, Leg.stl" into one "Mount, Legs.stl", then repeated the process with the remaining leg axles and mount.
- Attached the four "Leg.stl" onto the leg mounts using four "Axle, Leg.stl", making certain the legs rotated smoothly on the axles.
- Pressed each leg assembly into "Track.stl".

VIWORKING PROCEDURE



Figure 2. Working prototype

The model Figure 2. incorporates a motorized chassis hanging from an oval track having free rotating legs. When the chassis passes beyond the front pair of legs, its weight is tuned just enough to flip the oval track over bringing the previously rear legs to the front to repeat the process.

Designed using PTC Creo, sliced using Ultimaker Cura 4.12.1, and 3D printed in PLA on Ender 3.

With assembly complete, I proceed to weight and balance the chassis. The weight of the chassis has to overcome the mechanical advantage of the track and legs behind it. In order to accomplish this, I added few M10 nuts to the top of the battery pack which is 38 grams, bringing the final weight of my chassis was 150 grams until the model operated properly. Also, the chassis must be level, so I slid the battery pack fore and aft until the chassis was level, then secured the battery pack to the chassis double sided tape.

And that is how WE 3D printed and assembled "WALKING ROBOT".

PROTOTYPE AND DISCUSSION

By the end of the project, we made our prototype Figure 3. by the bases of four bar and weight balance mechanism. And also, we gain some knowledge about the 3D modeling and fused deposition process. We calculated the displacement of geometric from above

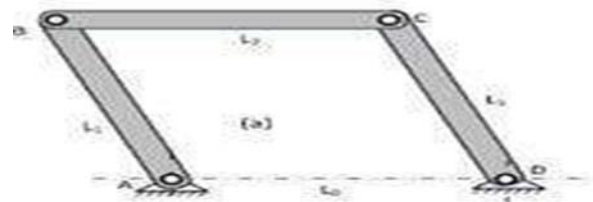


Figure 3. line diagram of prototype

$$L0 = L1 = L2 = L3$$

One or more data of the frequency of oscillation, the speed at different positions and range of motion of the slider may be provided.

Then, the required task will be finding the dimensions of the members of the leg mechanism and position of the slider such as to have the desired motion of the leg mechanism. The relation between the link lengths of the crank mechanism is determined from Fig. parametrically to formulate the general equation of its dimensions as given.

Applying Cosine law (referring to Fig. 2) gives

Upon using trigonometric identities and simplifications, the displacement s is expressed as a function of the geometric parameters r , l and q as

This is the final equation we developed from geometric calculations of displacement(s), length of the links(l) etc.

CONCLUSION

By the end of this we conclude that

1. Special types of four-bar mechanisms are used to enable effective motion of the walking machine leg mechanism for walking operation.

Simple linkage integration is proposed in the synthesis to generate motion path for the leg mechanism of a walking machine

2020;10(1):22. <https://doi.org/10.3390/nano10010022>.

7. Maróti P, Kocsis B, Ferencz A, Nyitrai M, Lőrinczy D. Differential thermal analysis of the antibacterial effect of PLA-based materials planned for 3D printing. *J Therm Anal Calorim.* 2020;139(1):367–74. <https://doi.org/10.1007/s10973-019-08377-4>.

8. Ghozali M, Fahmiati S, Triwulandari E, Restu WK, Farhan D, Wulansari M, et al. PLA/metaloxide biocomposites for antimicrobial packaging application. *Polym Plast Technol Eng.*2020:1–11. <https://doi.org/10.1080/25740881.2020.1738475>.

9. Minoshima M, Lu Y, Kimura T, Nakano R, Ishiguro H, Kubota Y, et al. Comparison of the antiviral effect of solid state copper and silver compounds. *J Hazard Mater.* 2016; 312:1–7. <https://doi.org/10.1016/j.jhazmat.2016.03.023>.

10. Ingle AP, Duran N, Rai M. Bioactivity, mechanism of action, and cytotoxicity of copper-based nanoparticles: a review. *Appl Microbiol Biotechnol.* 2014; 98(3):1001–9. <https://doi.org/10.1007/s00253-013-5422-8>.

11. I. Zamalloa, R. Kojcev, A. Hernández, I. Muguruza, L. Usategui, A. Bilbao, V. Mayoral, Cornell University, [arXiv:1704.08617](https://arxiv.org/abs/1704.08617) (2017).

1. Song, Y.; Li, Y.; Song, W.; Yee, K.; Lee, K.-Y.; Tagarielli, V.L. Measurements of the mechanical response of unidirectional 3D-printed PLA. *Mater. Des.* 2017, 123, 154–164.

2. Asadi S, Bouvier N, Wexler AS, Ristenpart WD. The coronavirus pandemic and aerosols: does COVID-19 transmit via expiratory particles? *Aerosol Sci Technol.* 2020;54(6):635–8. <https://doi.org/10.1080/02786826.2020.1749229>.

3. Livingston E, Desai A, Berkwitz M. Sourcing personal protective equipment during the COVID-19 pandemic. *JAMA.* 2020. <https://doi.org/10.1001/jama.2020.5317>.

4. Paxton NC, Forrestal DP, Desselle M, Kirrane M, Sullivan C, Powell SK, et al. N95 respiratory masks for COVID19: a review of the literature to inform local responses to global shortages. 2020.

5. Sandler N, Salmela I, Fallarero A, Rosling A, Khajeheian M, Kolakovic R, et al. Towards fabrication of 3D printed medical devices to prevent biofilm formation. *Int J Pharm.* 2014;459(1–2):62–4. <https://doi.org/10.1016/j.ijpharm.2013.11.001>.

6. Sonseca A, Madani S, Rodríguez G, Hevilla V, Echeverría C, Fernández-García M, et al. Multifunctional PLA blends containing chitosan mediated silver nanoparticles: thermal, mechanical, antibacterial, and degradation properties. *Nanomaterials.*

DESIGN AND FABRICATION OF CONNECTING ROD BY USING 3D PRINTER

D. Venkata Rao¹, K. John Babu², Chintada Naveen Kumar¹, Bolla Krishna¹

¹Department of Mechanical Engineering, Kallam Haranadhareddy Institute of Technology(Autonomous), AP, India

²Department of Mechanical Engineering, Narasaraopeta Engineering College, Narasaraopet, India

Abstract— The connecting rod is a major link inside of combustion engine. It connects the piston to the crankshaft and is responsible for transferring power from the piston to the crankshaft. It has to work on high r.p.m. because of which it has to bear severe stresses which make its design vital for internal combustion engine. In this paper, a connecting rod for two wheeler is designed by analytical method. On the basis of that design a physical model is created in CATIA V5 Connecting rod interconnects piston to crankshaft and it is responsible for transferring power from piston to the crankshaft and sending it to the transmission.

Connecting rods are traditionally manufactured using mould casting method which has high moulding cost and requires highly skilled designer to design the mould which is also more costly. So there is a need to optimise the manufacturing process of connecting rod. In this project work, Objective is to use advance manufacturing processes to produces connecting rod using 3d printing methods.

Keywords: Catia, Cura Slicing software, 3D Printing Methods, Connecting Rod, Poly Lactic Acid (PLA)

INTRODUCTION

Polymers are made of long, repeating chains of molecules. polymers include a range of materials with a variety of properties, depending on the type of molecules being bonded and how they are bonded. Polymers touch almost every aspect of modern life. The term polymer is often used to describe plastics, which are synthetic polymers. However, natural polymers also exist. Polymers are giant molecules of high molecular weight, called macromolecules, which are build up by linking together of a large number of small molecules, called monomers. The reaction by which the monomers combine to form polymer is known as polymerization. The product is called polymer and the starting material is called monomer

CLASSIFICATION OF POLYMERS

Polymers cannot be classified under one category because of their complex structures, different behaviours, and vast applications. Therefore, we classify polymers based on the following considerations

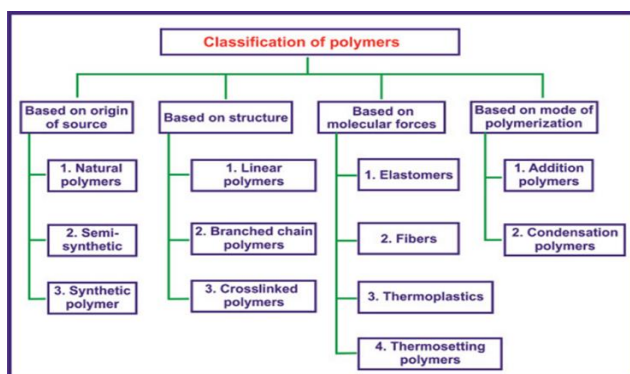


Fig. 1: Classification of polymers

CATIA V5 R21: CATIA is a multi-platform 3D software suite encompassing CAD, CAM as well as CAE Tools. Dassault is a French engineering giant active in the field of aviation, 3D design, 3D digital mock-ups, and product lifecycle management (PLM) software. CATIA is a Rectilinear modelling tool that unites the 3D parametric features with 2D tools and also addresses every design-to-manufacturing process.

CURA SOFTWARE: Cura is a Software used for Slicing the CAD File and converting them into G - Codes, for printing the Components. It only takes the.STL File and selects the Printer for printing and starts slicing after giving the Infill Pattern and Infill Density to the software. Components can be printed directly by connecting to the computer or by saving the file in G- Code Format in pen drive. The pen drive is connected to printer through a Pen drive. It also shows the Time for printing the Component.

3D Printing Technology: 3D printing can create physical objects from a geometrical representation by successive addition of materials 3D printing technology has originated from the layer by layer fabrication technology of three-dimensional (3D) structures directly from computer-aided design (CAD) drawing. 3D printing technology is a truly innovative and has emerged as a versatile technology stage. It opens new opportunities and gives hope to many possibilities for companies looking to improve manufacturing efficiency. Conventional thermoplastics, ceramics, graphene-based materials, and metal are the materials that can be printed now by using 3D printing technology. 3D printing technology has the potential to revolutionize industries and change the production line. The adoption of 3D printing technology will increase the production speed while reducing costs. At the same time, the demand of the consumer will have more influence over production.

LITERATURE REVIEW

Arshad Mohamed Gani P, Vinithra Banu T [1] “The connecting rod is the intermediate member between the piston and the Crankshaft. Its primary function is to transmit the push and pull from the piston pin to the crank pin, thus converting the reciprocating motion of the piston into rotary motion of the crank. Existing connecting rod is manufactured by using Carbon steel. This paper describes modeling and analysis of connecting rod. In this project connecting rod is replaced by Aluminum reinforced with Boron Silicide for Suzuki GS150R motorbike. A 2D drawing is drafted from the calculations. A parametric model of connecting rod is modelled using CATIA V5 software. Analysis is carried out by using ANSYS Workbench software. The best combination of parameters like Von misses stress and strain, Deformation, Factor of safety and weight reduction for two wheeler piston were done in ANSYS software. Compared to carbon steel, and aluminum boron carbide

Durgesh Yadav1 , Mr. Avinash Nath Tiwari [2] “Connecting rod is the vital part of an I.C.Engine. It is designed to withstand stresses from the combustion and movement of the piston. The purpose of a connection rod is to provide fluid movement between pistons and a crankshaft. When building a high performance engine, great attention is paid to the connecting rods. The most effective feature of a connecting rod is that it should be of uniform shape and lighter in weight. The main purpose of this paper is to analyse the stresses developed in connecting rod of four stroke petrol engine under static loading conditions. And then look forward for weight reduction along with material optimization. The model of the connecting rod is developed using CATIA V5 (dimensions are measured from Hero Splendor 100cc bike connecting rod) and ANSYS is used for stresses analysis by simulation (this method is also known as Finite Element Analysis by simulation). This is the cost and time effective method of analysis. Al 360 and Carbon steel are two material considered as the optimizing material

MATERIAL SELECTION

Polylactic Acid (PLA) is one of the most extensively researched 3D printing material. It has good Printability and high stiffness and Tensile Strength, besides available at cheap cost. PLA filament provides aesthetic 3D printing experience. It has better reliability and good surface quality. PLA is safe, easy to print with and it serves a wide range of applications for both novice and advanced users. easy to work with at high print speeds, user-friendly for both home and office environments, PLA allows the creation of high-resolution parts. There is a wide range of color options available. PLA is more Environmental-Friendly and Is Compositable.

Types of internal structures:

A variety of filling patterns that are used printing of components in additive manufacturing like honeycomb, rectilinear, solid, triangular, hillbert curve, Archimedean Chords, Octa gram spiral, concentric etc...Based on Filling pattern the properties of components of same material will change. . Infills play an essential role in the overall strength of an object, connecting the outer shells and supporting the upper surfaces too Our project mainly focuses on two infill patterns i.e Honey-Comb and Rectilinear with same infill densities, and comparing their mechanical properties.

Rectilinear Structure:

The rectilinear grid pattern is drawing of inclined continuous lines between the shells. Rectilinear has linear structures drawn inclined over another with different infill densities varying from 5% to 100%. It has a good strength on fatigue properties.

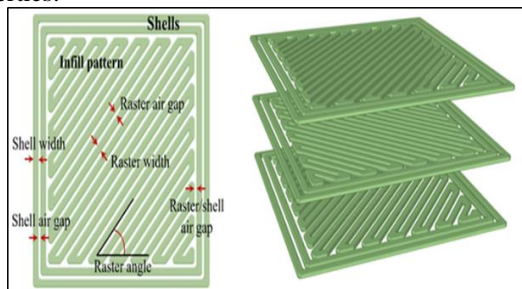


Fig 2: Rectilinear Structure

Honeycomb structure:

In 3D printing, the honeycomb is also a familiar structure, particularly for infills. 3D printed objects are typically not 100% Rectilinear and are instead held together by a lattice structure called an infill. Most 3D printed parts on FFF

(FDM, Material Extrusion) 3D printers are only 20 to 30% full.

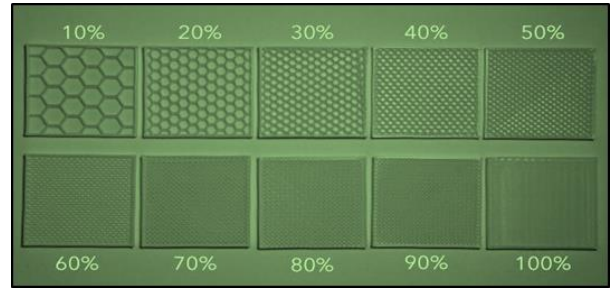


Fig. 3 : Honeycomb structure

METHODOLOGY

- Step 1:** Initially the components to be prepares are drawn using CATIA software by using sketcher tool.
- Step 2:** Once the component is drawn as per required dimensions then the file is saved as STL file in CATIA software
- Step 3:** After completion of above procedure, STL file is loaded into cura software.
- Step 4:** Once the STL file is loaded, required parameters are set in cura software that is material used, layer thickness, infill density, infill shapes, fan speed, nozzle temperature, bed temperature, extrusion temperature, supports required all are selected and modified as per the requirement.
- Step 5:** After selection of the above parameters slicing is done by using slice option.
- Step 6:** Once slicing is done STL file is converted into G codes which is readable by 3D Printer.
- Step 7:** G-code file is loaded in 3d printer by using pen drive and printing is done.
- Step 8:** Assembly of Printed Components

3D PRINTER USED

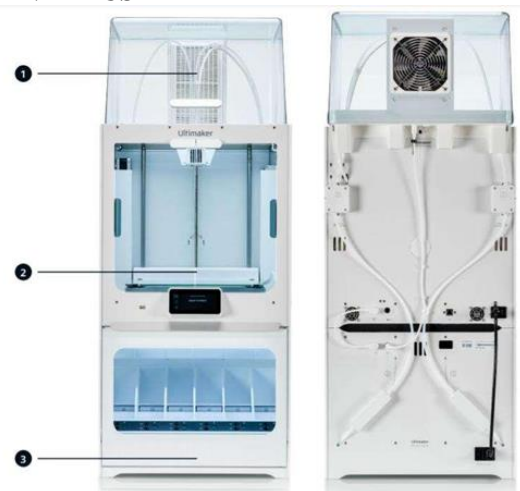


Fig. 4 : Ultimaker S5 Pro Bundle 3D Printer

Modelling Of Connecting Rod in Ic Engine

USES OF CATIA:

- ✓ Shape designing.
- ✓ Styling.
- ✓ Surface workflow.
- ✓ Modelling and simulation.

INDUSTRIES USING CATIA

- ✓ Automobile.
- ✓ Defence
- ✓ Ship building.

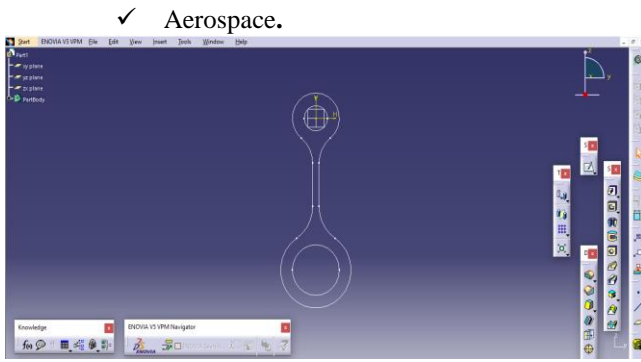


Fig 5 : connecting rod in IC Engine

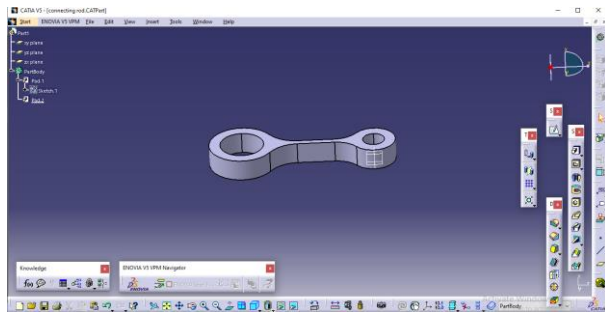


Fig 6 : conversion of 2D surface to 3D surface

CURA SOFTWARE

Cura 3D is slicing software for 3D printers. It takes a 3D model and slices it into layers to create a file known as G-Code, which is the code that a 3D printer understands. Cura slices 3D models. It translates the 3D STL, OBJ or 3MF file into a format that the printer can understand. Fused filament fabrication (FFF) 3D printers print one layer upon another to build up the 3D object. Cura 3D takes the 3D model and works out how those layers are placed on the print bed and creates a set of instructions for the printer to follow layer on layer. Cura generates instructions for your 3D printer. They are called G-Code, a text document that ends with the file extension.ufp. Open the file and you'll actually be able to read through quite a bit of the code and understand what it's telling the printer to do. Here's a small snippet. Three Stages Of 3d Printing

There are three basic stages to preparing files for 3D printing **Modeling:** This is carried out in any 3D modelling application such as Tinker cad or Sketch Up, which are just two of many example applications. These applications have their own file format and these enable you to open, edit, save, and export those 3D printer files from the application.

3D File Export: Once you have created your model, it then needs to be exported as either an STL, OBJ, or 3MF file. These are the file formats that are recognized by Cura. They differ from the file formats that are native to the 3D modelling applications as they just hold the final geometry and not the individual primitives and editable content. Still, you can change the size of the 3D model, but not the geometry.

Slicing File Export: The STL or OBJ file can then be imported into the Cura software where it is sliced and output as G-Code. This G-Code is just a text document (in essence) with a list of commands for the 3D printer to read and follow such as hot-end temperature, move to the left this much, right that much etc.

Adding A 3D Printer Model to Cura:

Once you have set up Cura for your printer, it's time to import a model into the Cura software. To import a model,

you can either click on the floating folder icon on the left or select *File > Open File(s)* from the top menu. Select an STL, OBJ, or 3MF file from your computer and Cura will import it.

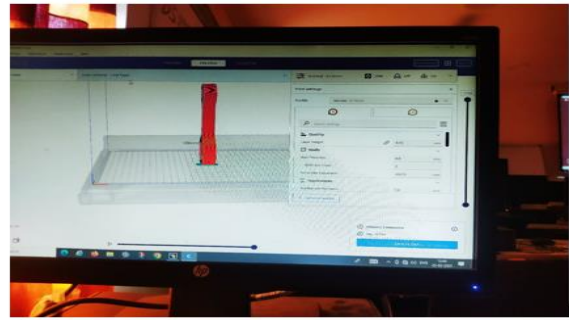


Fig 7 : Loading Model into Cura

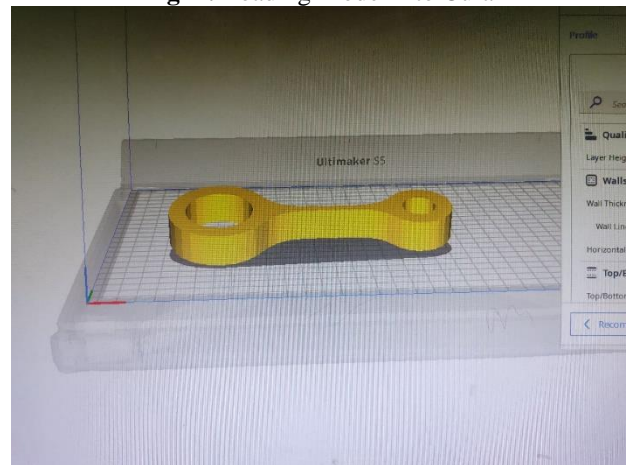


Fig 8 : Model in Ultimaker Cura

Printing Of Connecting Rod Using 3d Printer

The following steps are to be follow and to complete the 3d printing process

1. Once the modelling is done then STL file is loaded into Cura software and slicing is done. After completion of the above process the G code file loaded in to 3D printer by using SD card or Pen drive.
2. In order to print the component filament is loaded into the machine
3. Initially bed is prepared by cleaning it with alcohol based solvent.
4. After cleaning bed is preheated to 85°C temperature.
5. Before printing the component, glue stick is applied because of avoiding the warping
6. Once the above procedure is done select the G code file from the SD card by using select option.
7. Each and every parameter setting is visible on the machine screen. Check for any errors and parameters and do modifications if necessary.
8. After checking the parameters printing is started by giving start option in the machine.
9. After completion of the component wait for at least 30 minutes in order to remove the component from the machine bed.
10. Post processing is done to the components by removing of excess material and component supports.

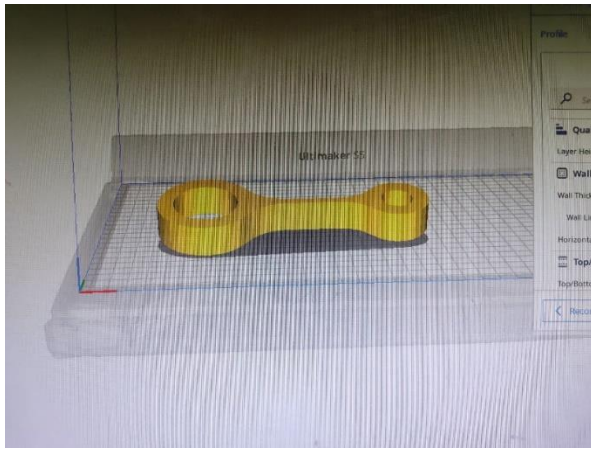


Figure 9 : Components while 3D Printing

Components Printed Using 3d Printer



Figure 10 : printing of connecting rod



Figure 11 : final printing of connecting rod

Total time taken for this print is 11 hours 9 minutes and the material consumed by the printer for this project is 85 grams. In cura software, arrangement of components were done in the effective way to reduce the time and material wastage. After completion of a print, wait for the sometime to remove the materials from the build plate because the build plate temperature is high and wait until the bed cools and use scrapper for the removing parts carefully. Completion of cooling display shows please remove the components. The cooling time is depends upon the print material size and temperature.

Conclusion

Connecting rod is designed and 3D printed by using Fused Deposition Modeling. The final 3D printed object is a prototype of connecting rod made by 3D printing to identify the minute errors and solve them to manufacture a perfect model of connecting rod. In this project modeling of a Connecting rod is carried out with the of CATIA v5 Software by using of machine design. After creating model we save

the component in stl. File. Import the component into the Cura Software 3D Printing slicing and then we apply the G-CODES to the component. And then we load the PLA material to get the final component.

Future Scope

This concept of Advance manufacturing can be used for different mechanical parts manufacturing like gears and Mold manufacturing for composite materials. These types of manufacturing can be used in Biology where 3D printed body parts can significantly enhance learning. Feeling the texture of a brain is differently from seeing it in a book or on screen. Complex structures of protein molecules in DNA can be very easily appreciated with 3d prints.

REFERENCES

[1] Arshad Mohamed Gani P, Vinithra Banu T, —Design and Analysis of Metal Matrix Composite Connecting Rod, International Journal of Engineering Research and General Science, Volume 3, Issue 2, March-April, 2015, ISSN 2091-2730, 672, www.ijergs.org.

[2] Sushant, Victor Gambhir, —Design Fabrication and Analysis of A Connecting Rod with Aluminum Alloys and Carbon Fiber, —International Journal Of Innovative Research In Science Engineering and Technology, Vol. 3, Issue 10, October 2014.

[3] N. Yadagiri Mohd Wajeed Ali Mohd Ilyas Mohd Abdul Aslam Pasha - Design and 3D Printing of Connecting Rod IJSRD - International Journal for Scientific Research & Development| Vol. 7, Issue 09, 2019 | ISSN (online): 2321-0613

[4] Anand D. Tale1 , Abhijit S. Shingane , Pranav P. Shingane , Suhas P. Thakare , M. V. Wasekar A Review on Comparison of Connecting Rod Made by 3D Printing Method International Journal of Research in Engineering, Science and Management Volume-2, Issue-2, February-2019 www.ijresm.com | ISSN (Online): 2581-5792.

[5] B. Naresh , G. Bhagyaraj , P. Vineeth Kumar , S. Nagendar Reddy , M. Srinath Modelling and Analysis of Connecting Rod International Journal for Research in Applied Science & Engineering Technology (IJRASET) ISSN: 2321-9653; IC Value: 45.98; SJ Impact Factor: 7.177 Volume 7 Issue XI, Nov 2019-Available at www.ijraset.com.

[6] Leela Krishna Vegil , Venu Gopal Veg Design And Analysis of Connecting Rod Using Forged steel International Journal of Scientific & Engineering Research, Volume 4, Issue 6, June-2013 2081 ISSN 2229-5518

[7] Nikhil U. Thakare, Nitin D. Bhusale, Rahul P. Shinde, Mahesh M. Patil, —Finite Element Analysis Of Connecting Rod Using ANSYSI, Proceedings of ISER 2nd International Conference, Singapore, 19th July 2015

[8] Mohamed Abdulalam Hussin, Er. Prabhat Kumar Sinha, Dr. Arvind Saran Darbari, —Design and Analysis of Connecting Rod Using Aluminum Alloy 7068 T6, T6511, —International Journal of Mechanical Engineering and Technology, Volume 5, Issue 10, October (2014).

[9] Mr. F. A. Pathan, Prof. M. K. Wasekar, "Static Analysis of Connecting Rod for Weight Optimization", International Research Journal of Engineering and Technology, volume: 02, Issue: 03 June-2015.

[10] Nikhil U. Thakare, Nitin D. Bhusale, Rahul P. Shinde, Mahesh M. Patil, —Finite Element Analysis Of Connecting Rod Using ANSYSI, Proceedings of ISER 2nd International Conference, Singapore, 19th July 2015.

DESIGN AND SIMULATION OF PROSTHETIC ARM

Md.JabihullaShariff Y Srinivasa Reddy

Department of Mechanical Engineering, PACE Institute of Technology and Sciences Ongole, Andhra Pradesh, India.

Abstract--- The continuous increase in industrialization, lack of awareness of safety parameters, and cases of disconnection are increasing. The search for safer, simpler and more automated prostheses for upper limb treatment is expected. From simple belt actuation to automated mechanisms with a variety of control options, continuous efforts have been made to design and develop prostheses. However, due to cost constraints, automatic prostheses are still out of the reach of those in need. Recent data show that there is ample room to develop cheap and lightweight upper limb prostheses. This overview summarizes the various design methods, mechanisms, control systems, and their advances developed by researchers. Equally important is to develop acceptance of the prosthesis and educate the patient to use it for the most basic desirable functions of the human hand, post-amputation care, and improving the patient's independent living. In conclusion, the adaptive finger opening and closing mechanism using other methods of path and position synthesis can be interpreted as having a wide range of designs. You can optimize cost factors with a simple mechanism and few components. To reduce the weight of the prosthesis, use polymers used in engineering applications. Control systems continue to be a never-ending challenge for researchers, but it is important to maintain simplicity from the patient's perspective.

Keywords---Amputation, Prosthetic arm, automated prosthesis.

1. INTRODUCTION

3D design environments have grown rapidly in popularity among student groups, 3D design aficionados, artists, and engineers during the previous ten years. This was made feasible by the general citizenry's open access to computer-aided design (CAD) tools that, in addition to the fundamental design and modelling skills, include support for assembly, the application of restrictions between 3D objects, and, most importantly, the creation of 3D models. Export to a 3D printable format immediately.

Combining these benefits, many studies have focused on prototyping 3D devices that overcome the limitations of traditional prostheses and can easily fit the human arm, especially given the fact that amputation of a limb can have both physical and psychological consequences, wreaking havoc on a patient's quality of life. As a result, replacing a human body part can be a difficult operation, and it is required to duplicate the human part as closely as possible to reality, taking into account the growing number of scenarios that need amputees of the upper limbs throughout the world. The most common amputations were undertaken for car accident victims, with an incidence of 86.9% on upper limbs, according to pilot research conducted in the Kingdom of Saudi Arabia over 2.5 decades.

Dyscalculic disease and cancer are two major causes of upper extremity amputations on a global scale, with 2.2 million amputations expected in the United States alone by 2020.

Scientists have attempted to restore missing limbs with traditional human-made technologies over time. The initial prostheses were considered passive devices that did not give many options for control and movement and served more of an aesthetic than a practical purpose.

There are various kinds of prosthetic devices on the market or in the research phase, typically categorized by the device's method: passive prostheses, mechanical/body control prostheses, myoelectric controlled prostheses, and direct brain interface.

2. PROSTHETIC ARM

PASSIVE PROSTHETICS

Passive prostheses are devices that try to replicate the original form of an amputated part, and they are divided into two categories: pure aesthetic and functional prosthetics for sports and work. Because the force necessary to modify the gripping mechanism must be delivered externally, this form of the prosthesis is only suited for a select set of patients, particularly those who have had their hands amputated.

MECHANICAL PROSTHESIS

The mechanical prosthesis is controlled by the user's body. They are usually basic devices, such as a mechanical hook that moves with the elbow or shoulder. Even though they are basic gadgets, this is the most popular.

MYOELECTRICAL PROSTHESES

When compared to mechanical prostheses, myoelectrical prostheses have several advantages, including the use of motors and batteries as actuation means, a better resemblance to anatomical hands, and the elimination of the need for heavy belts or harnesses, which, in addition to being visible, can damage the user's clothing

These prostheses are custom-made to fit the remaining limb and be connected to it. It has the benefit of using electronic electromyography (EMG) sensors for muscle activity once connected, resulting in a movement that is as similar to natural as possible, with the user being able to adjust the strength and pace of the motions.

PROSTHETICS CONTROLLED DIRECTLY BY THE BRAIN

The most sophisticated control mechanism in this field is currently brain control. A brain- computer interface (BCI), sometimes known as a Brain-machine Interface (BMI), is a technology that allows someone to control a calculator using only their thoughts.

Electrical activity in the nerve cells of the brain is generated by the phenomenon linked to thoughts, which may be identified in the form of impulses depending on brainwave frequency. A chip can be implanted directly at the brain level or a non-invasive method based on a network of electrodes inserted at the scalp level to read brain signals.

This technology has the advantage of being able to target a wide variety of users, including those who have had limbs amputated, but more crucially, those who have severe.

3. LITERATURE SURVEY

This section will discuss the previous works on the design and development of the prosthetic arm. This literature will give some path to investigate the physical characteristics, design parameters and topologies of the previous design . These journals gave an idea about the prosthetic arm and its application in various fields.

1] James Burck et al. at John Hopkins University Applied Physics Laboratory (APL) and Defense Advanced Research Projects Agency DARPA have worked to develop a smartest arm driven by neural inputs and sensory feedback technologies to enable the perception of physical inputs such as pressure, force

and temperature in addition to adaptive gripping. Figure 12 depicts APL Smart hand. 194 The Modular Prosthetic Limb features:

- Anthropomorphic (lifelike) form factor and appearance
- Human-like strength and dexterity
- High-resolution tactile and position sensing
- Neural interface for intuitive and natural closed-loop control.

The two prototype limbs developed for the DARPA program use Targeted Muscle Reinnervation, a technique pioneered by Dr. Todd Kuiken of the Rehabilitation Institute of Chicago. This technique involves the transfer of residual nerves from an amputated limb to unused muscle regions near the injury. In a clinical evaluation, the first prototype enabled a patient to complete a variety of functional tasks, including pulling a credit card from a pocket.

2] The cyber hand project was funded by the Future and Emerging Technologies (FET) arm of the IST Program, it aimed at exploring theories and solutions in the fields of neuroscience and robotics, in order to develop a cybernetic prosthetic hand, paper presented by Roccella, Carozza, Cappiello, Cabibihan, Laschi, Dario, Takanobu, Matsumoto, Miwa, Itoh et al. (2007). Six partners from four countries Scuola Superiore Sant'Anna University Pisa Italy, INAIL Prosthetic Centre Pontedera Italy, Institute of Microelectronics of Barcelona IMB-CNM Barcelona Spain, Fraunhofer Institute for Biomedical Engineering St. Ingbert Germany, Universidad Autonoma de Barcelona, Spain and Center for Sensory Motor Interaction, Aalborg University, Denmark Collaborated on this project. The objective project was focused on the development of a new kind of hand able to re-create the natural link which exists between the hand and the Central Nervous System. The project was targeted towards developing a bionic hand close to natural one.

3] The new hand, SARAH (Self Adaptive Robotic Auxiliary Hand) designed with 12- 278 DOF. The earlier robotic hands developed in the laboratory had an under-actuation 279 only in the fingers. Each finger was actuated by its own motor. In 1998 the company 280 MDA Space Missions contacted the laboratory in order to request the development 281 of a hand for the well-known Canadarm. One of the specifications requested for 282 this new hand was that it should be actuated by only two motors. This led to the 283 principles of a hand featuring under actuation among the fingers the opening and 284 closing of the fingers is controlled by only one motor. The study shows only one 285 motor is sufficient as it is not necessary for all three fingers to close independently, 286 because all fingers will close to grasp an object as firmly as possible. If one finger 287 is firmly wrapped around an object, the other fingers will continue to close until 288 all fingers are firmly closed. The under actuation among the fingers is achieved 289 through an innovative gear differential mechanism.

4] Burck, Zeher, Armiger and Beaty (2009) DARPA Johns Hopkins University Applied Physics Laboratory (APL) is a leading worldwide team which included government agencies, universities, and private companies whose mission was to develop a prosthetic arm that far exceeds any prosthetic available today. The final version of the arm will have control algorithms driven by neural inputs that enable the wearer to move with the speed, dexterity, and force of a real arm. Advanced sensory feedback technologies will enable the perception of physical inputs, such as pressure, force and temperature. The two prototype limbs developed for the Defense Advanced Research Projects Agency (DARPA)

program used Targeted muscle reinnervation, a technique pioneered by Dr. Todd Kuiken of the Rehabilitation Institute of Chicago. This technique involves the transfer of residual nerves from an amputated limb to unused muscle regions near the injury. In a clinical evaluation, the first prototype enabled a patient to complete a variety of functional tasks, including pulling a credit card from a pocket. No information on mechanism design and mathematical modelling.

5] Chang, Tseng and Wu (2004) In their paper presented an auxiliary methodology called the creative mechanism design was introduced into the innovation of gripping devices for prosthetic hands. An existing gripping device (Teh Lin ATG-5F prosthetic hand) constructed by a planar six-bar linkage with one degree of freedom was dealt with by using this methodology. Through the processes of generalization, number synthesis, specialization and particularization for the existing design, five new mechanisms were created for anthropomorphic prosthetic hands.

4. INTRODUCTION TO ANATOMY OF HUMAN HAND

A prosthetic upper limb is a man-made device that replaces a partially or completely missing hand or arm as a result of an accident, injury, disease, or congenital abnormality. They are available in a variety of forms, sizes, and patterns. To replicate the connection of the limb to a joint or ball and socket, a prosthetic hand or arm generally consists of shafts, sockets, and components. With the use of cables, it may be fastened to the body.

Cosmetic, functional, or both prostheses are available. A cosmetic prosthesis is generally created solely to make the limb appear natural, and it has little or no utility. A functional prosthesis, on the other hand, can assist an amputee in doing tasks that might otherwise be difficult or impossible once a limb is lost. However, it usually does not provide much in the way of aesthetic concealment.

There are five prosthetic solutions available to those with congenital abnormalities or lost upper limbs. You must examine several criteria when determining which alternative is best for you, including your amount of limb loss, the purpose of using a prosthesis, and your lifestyle.

There is no requirement for prosthetic arms or hands. They are, nonetheless, strongly recommended since they can assist amputees in resuming daily tasks. If you've just had an upper-limb amputation, knowing how to create a custom prosthetic hand or arm is critical.

A prosthetist, the person who develops, measures, and fits the prosthesis, is the first step in the process of constructing a prosthetic arm. Based on your specific circumstances and demands, this medical professional collaborates with you and your doctor to find the best prosthetic arm design for you.

Several days after the amputation, the prosthetic arm design process begins. The prosthetist will often measure the stump's length and compare it to the length of the remaining healthy limb. Following the completion of the measurements

Your prosthesis will be linked to the stump and organised and positioned until it fits precisely during the fitting appointment. It may be required to make numerous modifications at times. Prosthetic hand design and manufacture follow the same procedure.

The price of an upper-limb prosthesis can range from less than \$5,000 to more than \$100,000. The cost is mostly determined by the type of prosthesis you select. A simply aesthetic prosthetic arm is usually the cheapest, but a myoelectric prosthetic arm is frequently the costliest. Prosthetic arm costs are often greater than prosthetic hand costs for the same type of prosthesis.

4. ANATOMY OF THE HUMAN HAND

Hand The movements of the human hand are accomplished by two sets of each of these issues. They can be subdivided into two groups: the extrinsic and intrinsic muscle groups. The extrinsic muscle groups are the long flexors and extensors. They are called extrinsic because the muscle belly is located on the forearm. The intrinsic muscle groups are the thenar and hypothenar muscles (thenar referring to the thumb, hypothenar to the small finger), the lumbrical muscles and the interosseus muscles. These muscles arise from the deep flexor (and are special because they have no bony origin) and insert into the dorsal extensor hood mechanism.

- The thenar muscles include the abductor pollicis brevis, flexor pollicis brevis and opponens pollicis and are chiefly responsible for the movement known as the opposition of the thumb.
- The hypothenar muscles include the abductor digit minimi, flexor digit minimi brevis, and opponens digit minimi and deal with the movement of the 5th digit.
- The interosseous muscles are located between the metacarpal bones and are responsible for the abduction of the digits. They also assist the actions of the lumbrical muscles.
- The lumbrical muscles are responsible for flexion of the digits; there are 4 slender lumbrical muscles, one for each digit.

The fingers have two long flexors, located on the underside of the forearm. They insert by tendons to the phalanges of the fingers. The deep flexor attaches to the distal phalanx, and the superficial flexor attaches to the middle phalanx. The flexors allow for the actual bending of the fingers. The thumb has one long flexor and a short flexor in the thenar muscle group. The human thumb also has other muscles in the thenar group (opponents and abductor’s muscle), moving the thumb in opposition, making grasping possible.

The extensors are located on the back of the forearm and are connected in a more complex way than the flexors to the dorsum of the fingers. The tendons unite with the interosseous and lumbrical muscles to form the extensor hood mechanism. The primary function of the extensors is to straighten out the digits.

The thumb has two extensors in the forearm. Also, the index finger and the little finger have an extra extensor, used for instance for pointing. The extensors are situated within 6 separate compartments. The 1st compartment contains abductor pollicis longus and extensor pollicis Brevis. The 2nd compartment contains extensors carpi radialis longus and brevis. The 3rd compartment contains extensor pollicis longus. The extensor digitorum indices and extensor digitiform communis are within the 4th compartment. Extensor digits minima are in the fifth, and extensor carpi ulnar is in the 6th.

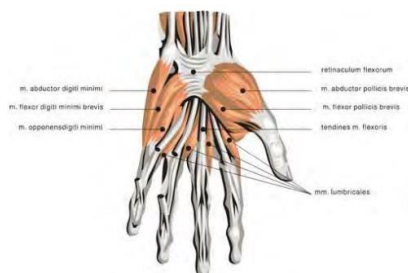


Figure 4 Human hand Muscular version

The thumb has two extensors in the forearm. Also, the index finger and the little finger have an extra extensor, used

for instance for pointing. The extensors are situated within 6 separate compartments. The 1st compartment contains abductor pollicis longus and extensor pollicis Brevis. The 2nd compartment contains extensors carpi radialis longus and brevis. The 3rd compartment contains extensor pollicis longus. The extensor digitorum indices and extensor digitiform communis are within the 4th compartment. Extensor digits minima are in the fifth, and extensor carpi ulnar is in the 6th.

4.1 BONES IN THE HAND

The bones of the hand provide support and flexibility to the soft tissues. They can be divided into three categories:

- Carpal bones (Proximal) – A set of eight irregularly shaped bones. These are located in the wrist area.
- Metacarpals – There are five metacarpals, each one related to a digit
- Phalanges (Distal) – The bones of the fingers. Each finger has three phalanges, except for the thumb, which has two.

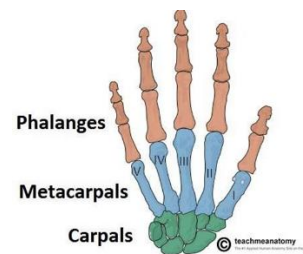


Figure 4.1 Overview of the bones of the hand.

4.1.1 CARPAL BONES

The carpal bones are a group of eight, irregularly shaped bones. They are organised into two rows: proximal and distal. Collectively, the carpal bones form an arch in the coronal plane. A membranous band, the flexor retinaculum, spans between the medial and lateral edges of the arch, forming the carpal tunnel. Proximally, the scaphoid and lunate articulate with the radius to form the wrist joint (also known as the ‘radio-carpal joint’). In the distal row, all of the carpal bones articulate with the metacarpals.

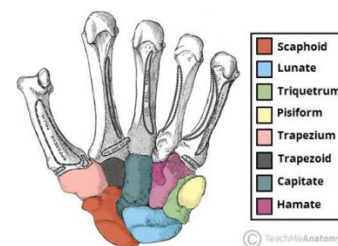


Figure 4.1.1 Palmar view of the carpal bones of the left hand.

4.1.2 Metacarpal Bones

The metacarpal bones articulate proximally with the carpals, and distally with the proximal phalanges. They are numbered, and each associated with a digit:

Metacarpal I – Thumb.

Metacarpal II – Index finger.

Metacarpal III – Middle finger.

Metacarpal IV – Ring finger.

Metacarpal V – Little finger.

Each metacarpal consists of a base, shaft and head. The

medial and lateral surfaces of the metacarpals are concave, allowing attachment of the interossei muscles.

4.1.3 PHALANGES

Each finger except the thumb consists of three bones – the proximal, middle, and distal phalanx. The thumb has only two phalanges – the proximal and the distal.

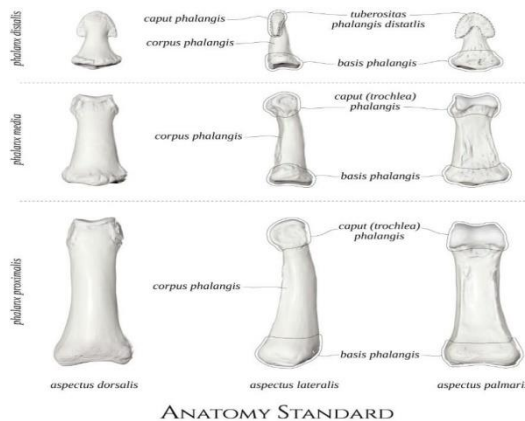


Figure 4.1.3 anatomy of phalanges

Sesamoid bones (ossa sesamoid) seen in both previous pictures are the rounded bones embedded in the muscle's tendons to protect them from excessive friction and redirect the tendon's attachment vector, so the muscle action is more effective. These bones are almost invariably present in front of the first metacarpophalangeal joint. They are also frequently observed in front of the fifth metacarpophalangeal joint and the thumb's interphalangeal joint.

4.2 WRIST JOINT

The wrist is the region between the forearm and the hand, known as the carpus. The wrist joint is a condyloid joint – one in which an ovoid head of one bone moves in an elliptical cavity of another. The wrist joint allows for 3 degrees of freedom of movement (flexion, extension, supination, pronation and circumduction). The wrist has three main joints: Radiocarpal Joint – the radiocarpal joint is formed by the radius, radioulnar disk, and 3 bones in the proximal carpal row: the scaphoid, lunate, and triquetrum. The proximal joint surface is a single biconcave curvature. It is long and shallow in the frontal plane (side to side) while being shorter and sharper in the frontal plane (anteroposterior). The curvature of the distal joint surface is sharper in both directions. The incongruity thus created in the joint allows for a greater range of motion at this joint than if there were greater congruency. It allows two degrees of freedom based on five types of movements: flexion, extension, abduction, adduction and circumduction. The most important movements are those of flexion and extension both with an angle of movement between 0-60° [14]. From an anatomical point of view, the wrist and hand contain many bones and joints to connect the forearm to the hand. The wrist is connected to the forearm through the proximal bones radius and ulna as presented in Fig. 4. It consists of 8 carpal bones arranged in two rows, four are more proximal: scaphoid, lunate, triquetrum, pisiform and four are more distal: trapezium, trapezoid, capitates and hamate. Midcarpal Joint – the midcarpal joint is a functional rather than anatomical unit as it has no uninterrupted articular surface. However, the articular surface is generally concave-convex and has been considered a condyloid joint allowing 2 degrees of freedom of movement. It consists proximally of the scaphoid, lunate, and triquetrum articulating with the

distal carpal row: the trapezium, trapezoid, capitate, and hamate.

Carpometacarpal Joint – the carpometacarpal joints are the articulations between the distal row of carpals and the bases of the first through fifth metacarpals. The first carpometacarpal joint is the articulation between the first metacarpal and the trapezium.

This articulation is a saddle joint, the first metacarpal is convex anterior/posterior and concave medial/lateral. The second metacarpal articulates primarily with the trapezoid and secondarily with the trapezium and capitate. The third metacarpal articulates with the capitate. The fourth metacarpal articulates with the capitate and hamate and the fifth metacarpal articulates with the hamate. Intercarpal Joints – the intercarpal joints are the articulations between the individual carpal bones. They are plane synovial joints. The small amount of movement between the carpal bones at these joints contributes to total wrist mobility. The carpals together form an arch in the transverse plane that is concave primarily. This arch deepens with wrist flexion and flattens with wrist extension.

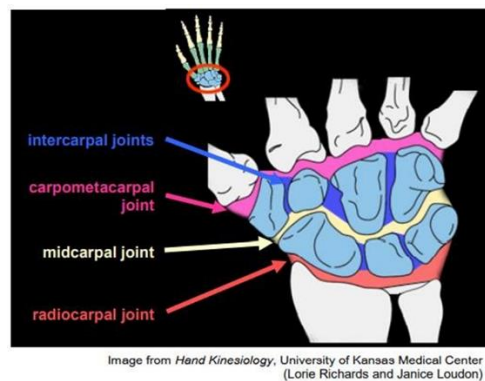


Figure 4.2 Wrist joint

4.3 CAD MODEL OF PROSTHETIC ARM

The main aim of this project is to design a biomimetic prosthetic arm in CAD design software and simulate it. The cad model is designed in the Autodesk Fusion 360 which is a cloud-based CAD modelling software. We designed every part as an individual part in software and assembled them all in one file to animate the joints and links.

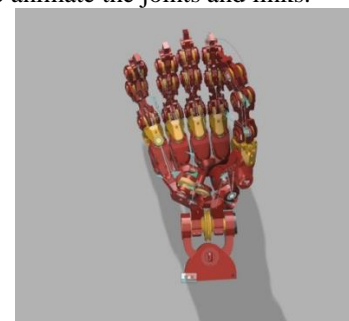


Figure 4.3 CAD Rendered model of prosthetic arm

4.4 WRIST JOINT

We used 2 resolutory joints at the XY plane and in the XZ- plane, which are covered to drive the entire hand with the maximum degree of freedom as a human can do with his normal hand. These joints are connected to two pullies for each of their own with their plane of action parallel to the plane of arrangement. These are moved in terms of both sides either in negative or positive directions to move in both ways. These pullies are moved with a string fastened to a

servo motor which has a feedback loop to make sure there is no error in revolution and to give precise output while using these pullies. We used nylon, polyvinylidene fluoride (PVDF, also called fluorocarbon), polyethylene, Dacron and UHMWPE strings to withstand the tensile strengths while lifting weights and operating. The wrist joint is a critical joint there we used two sections to hold the joint components and integrated 5mm bearings in that sections to complement the motion freely. And to relieve some frictional forces the bearings are supported by wedged circular bearing holders with slotted circumference.

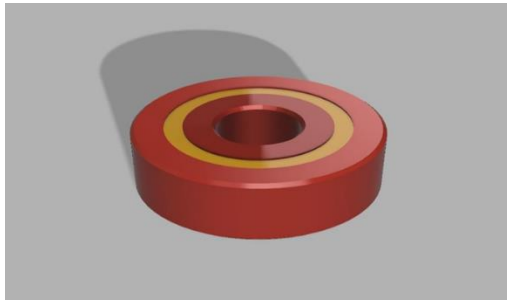


Figure 4.4.1 permanently lubricated stainless steel bearing



Figure 4.4.2 wrist movement in negative Z- direction.

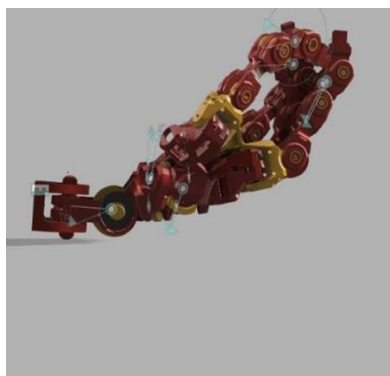


Figure 4.4.3 wrist movement in positive Z- direction.

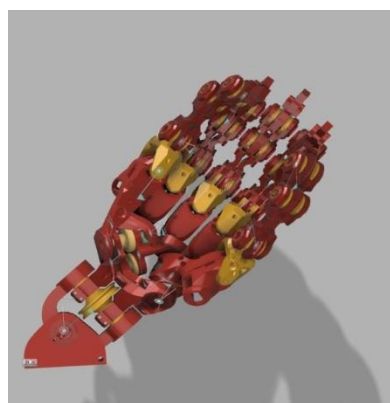


Figure 4.4.4 wrist movement along positive X- direction

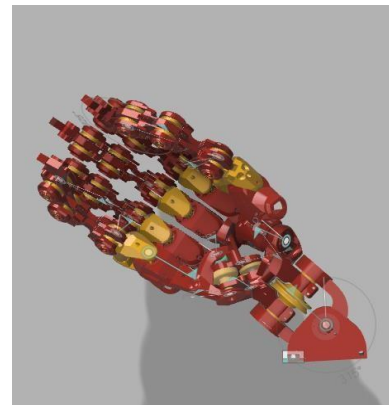


Figure 4.4.5 wrist movement along negative x-direction

4.5 META CARPAL JOINTS

To achieve the rotary motion in meta carpal joints, we used custom made gear boxes for each figure set, to achieve the desired mechanism as realistically as possible.

The meta carpal joints are the rigid structures in the human hand which are the support for the wrist to fingers these joints contain all muscular mass in the palm and neurons. The center of gravity and mass of the arm falls in this region. The use of a custom-made gear box for metacarpal joints made all the desired motions come into action. These are custom made for every finger.

4.5.1 META CARPAL JOINT DESIGN FOR FINGERS

These joints are powered by mini brushless DC motors which have enough torque to complete the task and to be precise in terms of motion along the rotational axis. We integrated a carpal gear box to mimic the child muscle movement of other main fingers, when we move the ring figure the pinkie figure also moves in the direction to support the muscles of the ring figure and to balance the centre of mass. We can mimic the same motion with the carpal gear box which gives a 2:1 ratio of rotation for these fingers.



Figure 4.5.1 Meta carpal joint for all fingers

4.5.2 THUMB META CARPAL JOINT

The meta carpal joint for the thumb is different from the other meta carpals because it supports the strongest finger than other fingers. This supports from both sides as the thumb rotation is done by using the spinner along the axis. This is constructed stronger than the other joints to spin while handling the bigger and heavier items. This joint has to include two rotational joints to mimic the exact motion of the thumb, one is along the perpendicular plane of the rotational axis, and the other is along the plane of the rotational axis.

4.6 PHALANGES

These joints are the actual fingers we use in our daily life. We use these phalanges to hold objects and make grip and sense of touch in the real world. These joints are very well known as the combination of three links and two joints in which two joints are partially constrained to angular displacement.

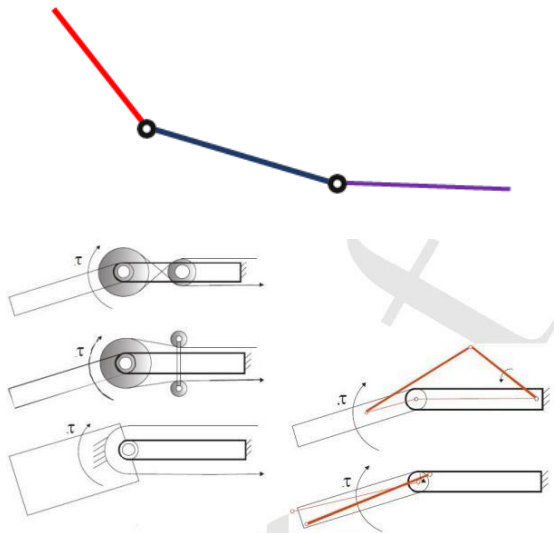


Figure 4.6.1 2-bar link mechanism in phalanges

Figure 4.6.2 pulley driven mechanism and link driven mechanism

A two-bar linkage, which is described in differential dynamical equations, can perform nonlinear behaviors due to system parameters or external input. As a basic component of a robot system, the investigation of its behavior can improve robot performance, control strategy, and system parameters.

These joints are created by using two pulleys to rotate the joints clock and anti-clockwise. These are attached to a hub which is included with a displacement sensor. All parts are connected with the bearings and the shaft attached to connect them all through the center of the axis.

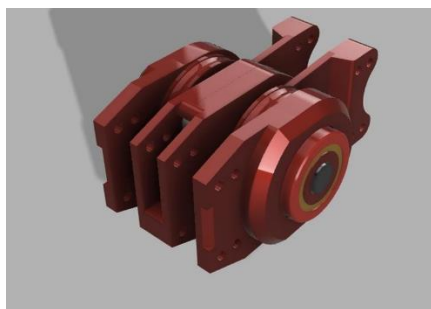


Figure 4.6.2 joint assembly in the finger



Figure 4.6.3 finger assembly manipulated

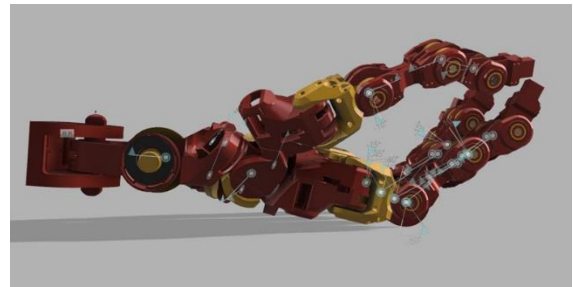


Figure 4.6.4 thumb outmost down position

4.7 OVERVIEW: MECHANISM AND CONTROL OF THE PROSTHETIC ARM



Figure 4.7.2 Motion in internal phalanges

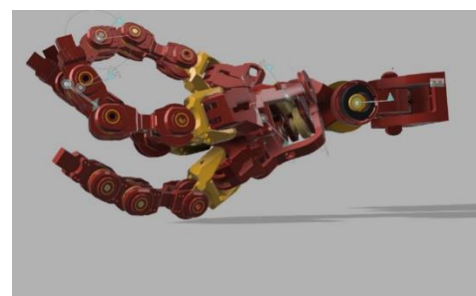


Figure 4.7.3 motion of the internal phalanges towards back knuckles

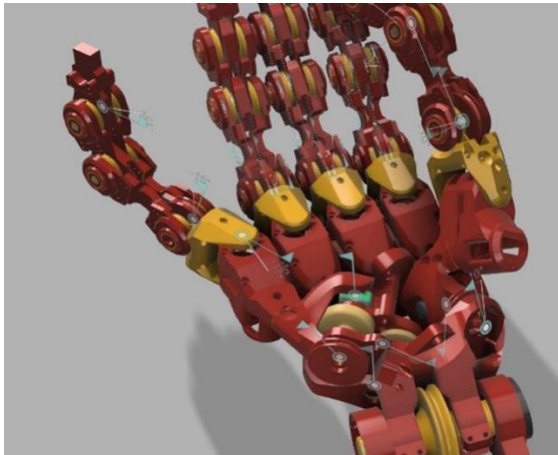


Figure 4.7.4 External phalanges rotation in y direction

5. SIMULATION OF THE PROSTHETIC ARM.

Simulation means exploring the basic working nature of the product which is being simulated in the virtual environment, by recreating the physical properties of the product and the nature of the surroundings in the nature we can create a simulating model.

5.1 SIMULATION TOOLS.

We used the famous tools used by robotics engineers to simulate robotics in industrial level. Those are ROS and MATLAB.

5.1.1 ROS

The Robot Operating System (ROS) is a set of software libraries and tools that help you build robot applications. From drivers to state-of-the-art algorithms, and with powerful developer tools, ROS has what you need for your next robotics project. And it's all open source. It is a Linux based software which runs in a kernel it uses the kernel to simulate a virtual environment. i.e. "Gazebo" is a virtual environment to manipulate the joints and the links in the robot. This is mainly used in the sector because it gives accurate results and it is open source and is very easy to use. This includes a visualization tool called RVIZ to visualize the properties of the model.

This accepts the data in the format of XML which is a web based language and it contains all properties in vector forms.

5.1.2 MATLAB.

MATLAB is a programming platform designed specifically for engineers and scientists to analyze and design systems and products that transform our world. The heart of MATLAB is the MATLAB language, a matrix-based language allowing the most natural expression of computational mathematics.

5.2 URDF.

URDF, or Unified Robotics Description Format, is an XML specification used in academia and industry to model multibody systems such as robotic manipulator arms for manufacturing assembly lines and animatronic robots for amusement parks. URDF is especially popular with users of ROS, or Robotics Operating System a framework that offers standard support for URDF models. You can import

URDFmodels into the simecape multibody environment, for example, for simulation, analysis, and control design tasks. See the Humanoid Robot featured example for a simple use case.

Like other types of XML files, URDF files comprise various XML elements, such as <robot>, <link>, <joint>, nested in hierarchical structures known as XML trees. For example, the <link> and <joint> elements are said to be children of the <robot> element and, reciprocally, the <robot> element the parent of the <link> and <joint> elements.

<robot>

<link>

...

</link>

<link>

...

</link>

<joint>

...

</joint>

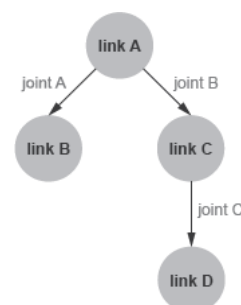
</robot>

Child elements, such as <link> and <joint> under <robot>, can in turn have child elements of their own. For example, the <link> element has the child elements <inertial> and <visual>. The <visual> element has the child elements <geometry> and <material>. And the <material> element has the child element <color>. Such chains of child elements are essential to define the properties and behavior of the parent elements.

URDF links connect through joints in hierarchical structures not unlike those formed by nesting XML elements in a URDF file. <joint> elements enforce these hierarchies through <parent> and <child> elements that identify one link as the parent and the other as the child. Parent links can themselves be children—and child links parents—of other links in the model.

You can visualize the connections between links using a schematic known as a connectivity graph. The figure shows an example. Circles denote links and arrows denote joints. The arrow roots identify the parent nodes and the arrow tips the child nodes. The connectivity graph reveals the topology of the underlying model—here a simple kinematic tree with two branches.

Connectivity Graph of a Kinematic Tree:



As we designed the cad model in the Fusion 360 we used the “Fusion2URDF” extension to convert the whole entity into the URDF code.

5.2.1 URDF FILE

```
<package format="2">
<name>Arranemgent 2 v40 v10</name>
<version>1.0.0</version>
<description>
<p>URDF Description package for Arranemgent 2 v40 v10</p>
<p>This package contains configuration data, 3D models and launch files for Arranemgent 2 v40 v10 robot</p>
</description>
<author>TODO</author>
<maintainer email="TODO@email.com" />
<license>BSD</license>
<buildtool_depend>catkin</buildtool_depend>
<depend>roslaunch</depend>
<depend>robot_state_publisher</depend>
<depend>rviz</depend>
<depend>joint_state_publisher_gui</depend>
<depend>gazebo</depend>
<export>
<architecture_independent />
</export>
</package>
```

5.2.2 GAZEBO LAUNCH FILE

```
<package format="2">
<name>Arranemgent 2 v40 v10</name>
<version>1.0.0</version>
<description>
<p>URDF Description package for Arranemgent 2 v40 v10</p>
<p>This package contains configuration data, 3D models and launch files for Arranemgent 2 v40 v10 robot</p>
</description>
<author>TODO</author>
<maintainer email="TODO@email.com" />
<license>BSD</license>
<buildtool_depend>catkin</buildtool_depend>
<depend>roslaunch</depend>
<depend>robot_state_publisher</depend>
<depend>rviz</depend>
<depend>joint_state_publisher_gui</depend>
<depend>gazebo</depend>
<export>
<architecture_independent />
</export>
</package>
```

5.2.3 ROS PACKAGE CODE

```
<package format="2">
<name>Arranemgent 2 v40 v10</name>
<version>1.0.0</version>
<description>
<p>URDF Description package for Arranemgent 2 v40 v10</p>
<p>This package contains configuration data, 3D models and launch files for Arranemgent 2 v40 v10 robot</p>
```

```
</description>
<author>TODO</author>
<maintainer email="TODO@email.com" />
<license>BSD</license>
<buildtool_depend>catkin</buildtool_depend>
<depend>roslaunch</depend>
<depend>robot_state_publisher</depend>
<depend>rviz</depend>
<depend>joint_state_publisher_gui</depend>
<depend>gazebo</depend>
<export>
<architecture_independent />
</export>
</package>
```

5.3 MATLAB

MATLAB Simulink is powered with multi-disciplinary tools which are used in both simulation and control and logic. MATLAB is the most powerful tools for ROS simulation we created the nodes for using XML sheets from the CAD models.

5.3.1 MATLAB SIMULATION

These MATLAB trees are made out from the XML sheet from the Simscape , multimedia tool.

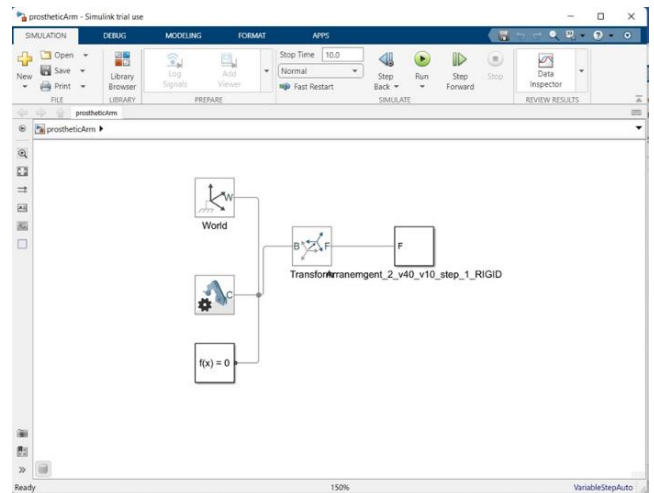


Figure 5.3.1 SLX format of the prosthetic arm

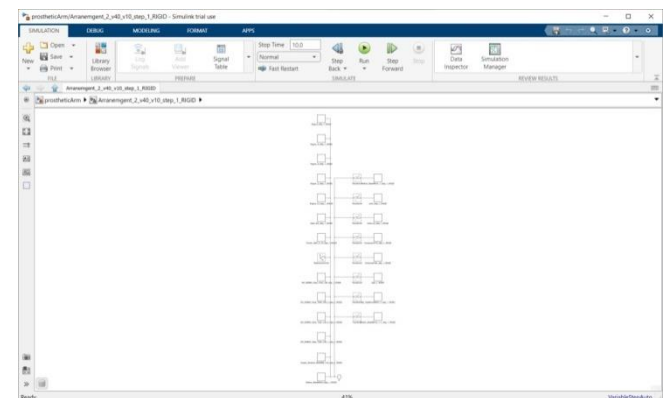


Figure 5.3.2 SLX format of the prosthetic arm in branched view

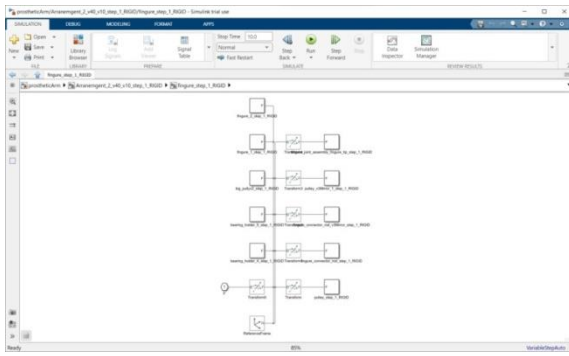


Figure5.3.3 SLX format of the finger model with joints

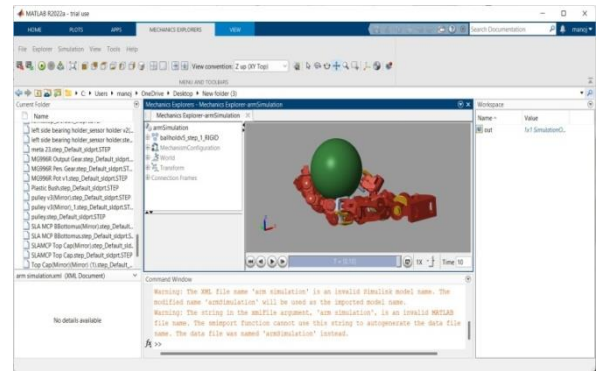


Figure 5.3.7 Simulated model of prosthetic arm holding an object

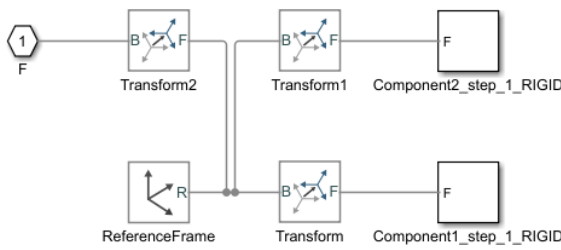


Figure5.3.4 SLX format of the joints of the phalanges

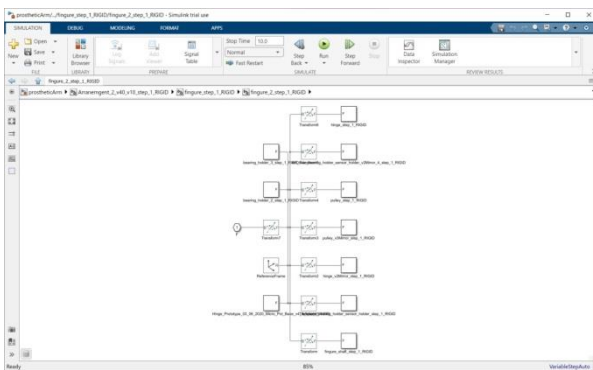


Figure 5.3.5 SLX format of the joints of the internal phalanges

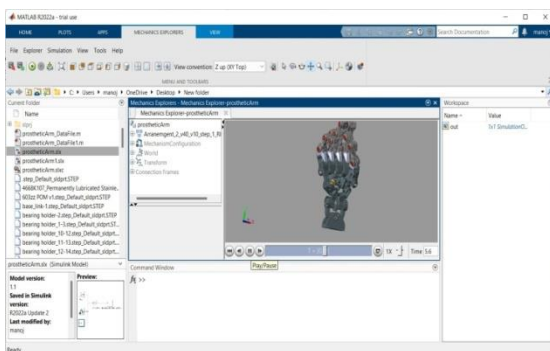


Figure 5.3.6 Simulation model of the Prosthetic Arm

These images are the SLX formatted XML code of the STEP extension file for the CAD file. This data is sufficient to simulate the file in the MATLAB. The final result is shown in figure5.3.7.

6. CONCLUSION

These above process of designing and simulation all went as expected and the desired results are obtained. In this work, a new human-like low-cost prosthetic arm has been designed. This device is formed by a three-DOF spherical manipulator at the wrist, which are connected in a serial architecture. The spherical manipulator at allows sharing the load, and therefore, the required torque and the power consumption of the motors are lower than those in other solutions. The use of small motors has the benefit that its weight is low and it is possible to create a design with a reduced cost and easier to afford than existing solutions. That mechanism makes it possible to place the actuator of the elbow close to the shoulder, and in this way, the inertial effects are reduced, in comparison to common solutions where the elbow is actuated with big motors placed at the elbow. The synthesis of this mechanism allows the locking of the arm when it is fully extended or flexed; then the consumption of the wrist actuator can be reduced in these common positions. The wrist mechanism has a suitable range of motion to perform ADLs using small actuators. The selection of the mechanism makes it possible to have a prototype with a total weight of 1350 g, not including the hand. This weight is lower than the average weight of a human arm that is approximately 5 kg. The numerical and experimental evaluations show that the prototype can perform natural movements of the human arm. Despite the feasibility of this device being demonstrated, further work needs to be done: this includes performing structural analysis in order to determinate the most suitable materials and dimensions of the main elements of the prosthesis aiming to assure its structural integrity.

REFERENCES

- [1] A.J.Metzger, A.W.Dromerick, R.J.Holley and P.S.Lum, "Characterization of compensatory trunk movements during prosthetic upper limb reaching tasks," *Archives of Physical Medicine and Rehabilitation*, vol. 93, no. 11, pp.2029–2034,2012.View at: [Publisher Site](#)/[Google Scholar](#)
- [2] H. Burger and G. Vidmar, "A survey of overuse problems in patients with acquired or congenital upper limb deficiency," *ProstheticsandOrthoticsInternational*,vol.40, no. 4,pp. 497–502, 2016.View at: [PublisherSite](#)/[Google Scholar](#)
- [3] K.Østlie,I.M.Lesjø,R.J.Franklin,B.Garfelt,O.H.Skjeldal and P.Magnus, "Prosthesis rejection in acquired major upper-limb amputees: a population-based survey," *Disability and Rehabilitation. Assistive Technology*, vol. 7, no.4,pp. 294–303, 2012.View at: [Publisher Site](#)/[Google Scholar](#)
- [4] T. R. Dillingham, L. E. Pezzin, and E. J. MacKenzie, "Limb amputation and limb deficiency: epidemiology and recent trends in the United States,"*Southern Medical Journal*,vol.95,no.8,pp.875–883,2002. View at: [Google](#)

- Scholar.
- [5] D.A.Zlotolow and S.H.Kozin, "Advances in upper extremity prosthetics," *Hand Clinics*, vol.28, no.4, pp.587–593, 2012. View at: [Publisher Site/Google Scholar](#)
- [6] M.S.Johannes, J.D.Bigelow, J.M.Burck, S.D.Harshbarger, M.V. Kozlowski, and T. Van Doren, "An overview of the developmental process for the modular prosthetic limb," *Johns Hopkins APL Technical Digest*, vol.30, no.3, pp. 207–216, 2011. View at: [Google Scholar](#)
- [7] L.Resnik, F.Acluche, S.LiebermanKlinger, and M.Borgia, "Does the DEKA Arm substitute for or supplement conventional prostheses," *Prosthetics and Orthotics International*, 2017. View at: [Publisher Site/Google Scholar](#)
- [8] L.Resnik, S.L.Klinger, and K.Etter, "The DEKA Arm: its features, functionality, and evolution during the Veterans Affairs study to optimize the DEKA Arm," *Prosthetics and Orthotics International*, vol.38, no.6, pp.492–504, 2014. View at: [Publisher Site/Google Scholar](#)
- [9] L.He, C.Xiong, and K.Zhang, "Mechatronic design of an upper limb prosthesis with a hand," in *Intelligent Robotics and Applications. ICIRA 2014*, X.Zhang, H. Liu, Z. Chen, and N. Wang, Eds., vol. 8917 of *Lecture Notes in Computer Science*, Springer, Cham, Switzerland, 2014. View at: [Publisher Site/Google Scholar](#)
- [10] J. A. Leal-Naranjo, M. Ceccarelli, and C. R. T. S. Miguel, "Mechanical design of a prosthetic human arm and its dynamic simulation," in *Advances in Intelligent Systems and Computing*, Springer, Cham, 2017. View at: [Publisher Site/Google Scholar](#)
- [11] J.-A. Leal-Naranjo, M. Ceccarelli, C.-R. Torres-San-Miguel, L.-A. Aguilar-Perez, G. Urriagoitia-Sosa, and G. Urriagoitia-Calderón, "Multi-objective optimization of a parallel manipulator for the design of a prosthetic arm using genetic algorithms," *Latin American Journal of Solids and Structures*, vol. 15, no.3, 2018. View at: [Publisher Site/Google Scholar](#)
- [12] T. Mashimo, T. Urakubo, and T. Kanade, "Singularity-based four-bar linkage mechanism for impulsive torque with high energy efficiency," *Journal of Mechanisms and Robotics*, vol.7, no.3, article 031002, 2015. View at: [Publisher Site/Google Scholar](#)
- [13] R.L.Norton, *Machine Design: an Integrated Approach*, vol.4, Pearson Prentice Hall Publishers, USA, 2006.
- [14] C. Gosselin and J. Angeles, "The optimum kinematic design of a spherical three-degree-of-freedom parallel manipulator," *Journal of Mechanisms Transmissions and Automation in Design*, vol. 111, no. 2, p. 202, 1989. View at: [Publisher Site/Google Scholar](#)
- [15] J.Ryu, W.P.Cooney III, L.J.Askew, K.-N.An, and E.Y.S.Chao, "Functional ranges of motion of the wrist joint," *The Journal of Hand Surgery*, vol. 16, no.3, pp. 409–419, 1991. View at: [Publisher Site/Google Scholar](#)
- [16] J.A.Lealndash, C.R.Torres-SanMiguel, F.Carbajalndash and L.Martinez-Saez, "Structural numerical analysis of a three fingers prosthetic hand prototype," *International Journal of Physical Sciences*, vol. 8, no. 13, pp. 526–536, 2013. View at: [Publisher Site/Google Scholar](#)
- [17] S. P. Won and F. Golnaraghi, "A triaxial accelerometer calibration method using a mathematical model," *IEEE Transactions on Instrumentation and Measurement*, vol.59, no.8, pp.2144–2153, 2010. View at: [Publisher Site/Google Scholar](#)

DESIGN AND FABRICATION OF FLEX SENSOR OPERATOR ROBOT

Chandra Sekhar Kukkambakam, Venkata Subbarao Chilukuri, D.Sarath Kumar

Department of Mechanical Engineering, QIS College of Engineering and Technology, Ongole, AP-523272

Abstract— It is estimated that by the year 2030, 800 million workers all over the world be replaced by robots. This is evident that Robotic revolution is happening in a large scale. Robots eliminate dangerous jobs for humans because they are capable of working in hazardous environments. They can handle lifting heavy loads, toxic substances and doing repetitive tasks. They have helped to prevent many accidents, also saving time and money. Recent advancements in embedded systems have opened up a vast area of research and. This project deals with the design and development of a robotic hand with real time control, which is precise and cost-effective. This five fingered robotic arm mimics a small degree of dexterity and could be used for other applications such as prosthesis for leprosy patients. This will allow them to get a higher degree of freedom and will help in their day to day life.

The aim was to investigate how well the robotic hand could imitate the movements of a user-worn controller glove as well as grip objects, both through wireless communication.

Keywords— *Robotic Hand, Flex sensors.*

INTRODUCTION

A robotic arm consists of several sections connected together by linkages that help the arm to travel specifically in a designed pattern, with sensors ensuring that all movements are exactly of the similar pattern. They are endowed with several degrees-of-freedom, giving them the flexibility to move in many directions through multiple angles with utmost ease and agility. The study of robotics originates back to ancient Egypt where priests created masks that moved as a way to intimidate their worshippers. Robotics, as we know it today, originated half a century ago with the creation of a robot named “Unimate”. This Robot was created by George Devol and Joseph Engelberger. Unimate was created with the intention of being used in industry at a General Motors plant, working with heated Die-casting machines. In recent years the development of humanoid robots has become a larger area of focus for the engineering community. Humanoid robots are precisely what their name would lead you to expect, robots designed to look and act like humans. While their Current use is primarily within the entertainment industry, there are hopes that one day they will be able to be used in a broader domain. Modern investigations into humanoid robot development have led to the desire to create

a robot that can not only walk from one destination to another, but also discern Objects in front of it and be able to compensate for that by moving around them. This was where the current project came into play. The purpose of this project was to design and build a humanoid robot that was capable of walking smoothly. Due to constant advances in technology, humanoid robots of the future will be capable of helping mankind by accomplishing tasks that may too dangerous, dirty, dull or even physically impossible, such as exploring other planets. Though there is still room for improvement for the locomotion of these robots to become more and more similar to that of a human, the future looks bright for the development of the next generation of Humanoid robots.

LITERATURE SURVEY

- The design of grasping mechanisms has been the aim of several researches in the field of Robotics. These researches have addressed attention to a physical interface between a robotic system and its environment. This interface provides interaction with objects and offers dexterity manipulation and grasping functionalities. Developments of industrial robotics have produced 3 several types of gripper mechanisms. Robotic grippers are employed in robotic manipulators that perform repetitive tasks. These grippers can only execute limited and specific manipulation tasks, [Penisi et al., 2003]. They are limited to objects that are very similar in terms of shape, weight and manipulation requirements, [Chen, 1982]. The use of grippers is also limited to the grasping of objects with regular geometries. Considerable disadvantages of industrial grippers have been found as regarding with the stability of the grasping of objects with irregular geometries or complex manipulation operations. Due to these limitations, research efforts have been dedicated to the development of multiple finger robotic hands. These devices try to mimic one or more characteristics of the human hand.

- The phase that involves identification of applications for a robotic hand is fundamental. It allows focusing the design problem in a more specific way by referring to technological and market requirements. Many of the research efforts for conception of dexterous hands have been oriented to specific applications, [Banks, 2001]. Some of these applications can be listed as:
 - Prosthesis;
 - Manipulators for Astronautic Purposes;
 - Humanoid Robotics;
 - Industrial Manipulators.
 Human prostheses and astronautic manipulators seem to be the most demanding and ambitious applications. For example, the design that is oriented to develop infant or adult prosthesis is a complex problem for robotic hand design, since geometric, ergonomic and functional characteristics of human hands have to be matched in order to develop successful hand prosthesis. The hand structure and material are important aspects to consider for aeronautical applications because of the hard conditions in the working environment.
- In general, the anthropomorphic characteristics of a design are not strong requirements, as are precision of control system and dexterous capabilities of manipulation, as pointed out for example in [Martin et al., 2004].
- A design problem for a robot hand with similar complexity can be the application for a sub-system in a humanoid robot, as discussed in [Ceccarelli, 2003]. A design objective for a grasping sub-system of a humanoid robot can be to generate an autonomous, flexible and anthropomorphic design. In the case of prosthesis, the autonomy cannot be established as a design requirement, as illustrated in [Suares & Grosch, 2004].
- Human hands are universal grasping mechanisms with great flexibility in manipulation, [Belforte, 1985]. The dexterity of this complex biological mechanism is capable for a great diversity of applications. The sensory system of human hand permits to identify a cognitive representation of grasped objects that is a much desired ability for medical prosthesis as well as in advanced developments in mobile and humanoid robotics. Anthropomorphism and dexterity are two of the main desirable characteristics for robot hands.

- In particular, in [Buchholz & Armstrong, 1991] a kinematical model is presented for simulating of finger positions that are required for grasping objects with known geometry. This work presents measured sizes of the metacarpal and carpal bones that can be directly used as dimensional restrictions for a robot hand design. Further analysis is required on the sensory capabilities of human hand and human nervous system to identify requirements for sensory and control systems of robot hands [Banks, 2001]. The next phase in a design process consists in mechanical synthesis that is closely related to the topology of the main functional elements; which are the fingers, palm and wrist. The synthesis process provides the geometric characteristics, materials and actuators for a robot hand.

Components

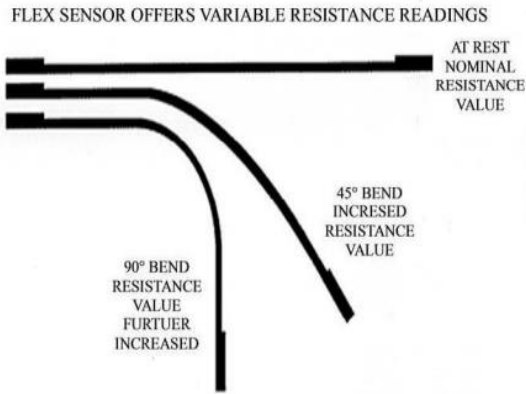
- ARDUINO
- ACCERELOMETER SENSOR
- TRANSCEIVER MODULE
- 9V BATTERY
- DC MOTOR DRIVE MODULE
- GRIPPER

FLEX SENSORS

Flex sensors are passive resistive devices that can be used to detect bending or flexing. The flex sensor shown in this figure. is a bi-directional flex sensor that decreases its resistance in proportion to the amount it is bent in either direction. The sensor we are building is about 3/8" wide by 5" long. The ranges of the flex sensor are 10k Ω to 40k Ω . The Flex sensor offers variable resistance readings, resistance for the unflexed is 10k Ω and for the flexed the resistance is 40k Ω . Flex sensors are analogue resistors. They work as variable analogue voltage dividers. The flex sensor shown in is the unidirectional. Flex sensor is a unique component that changes resistance when flexed. Flex sensor is bent in one direction the resistance gradually increases.

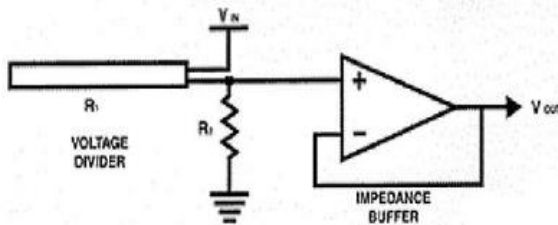
HOW IT WORKS

Flex sensors are analogue resistors, they works as variable analogue voltage divider. Inside the flex sensors are carbon resistive elements within a thin flexible substrate. More carbon means less resistance, when the substrate is bent the sensor produces a resistance output relative to the bent radius. The higher the resistance value yielding smaller radius.



FLEX SENSOR CIRCUIT

BASIC FLEX SENSOR CIRCUIT:

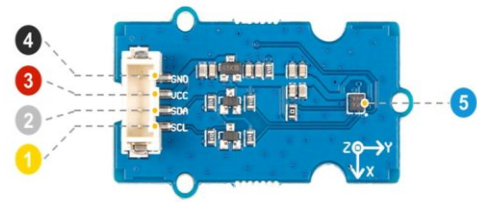


APPLICATIONS

Flex sensors may be used in robotics to determine joint movement or placement. They may also be used like whiskers for wall detection. The sensors we are making are also pressure sensitive so they can also be used as bumper switches for wall detection or pressure switches on robotic grippers. For bio-metrics, the sensor can be placed on a moving joint of athletic equipment to provide an electrical indication of movement or placement. A few of the sensors can be incorporated onto a glove to make virtual reality glove.

ACCELEROMETER SENSOR

An accelerometer is a tool that measures proper acceleration. Proper acceleration is the acceleration (the rate of change of velocity) of a body in its own instantaneous rest frame; this is different from coordinate acceleration, which is acceleration in a fixed coordinate system. For example, an accelerometer at rest on the surface of the Earth will measure an acceleration due to Earth's gravity, straight upwards (by definition) of $g \approx 9.81 \text{ m/s}^2$. By contrast, accelerometers in free fall (falling toward the center of the Earth at a rate of about 9.81 m/s^2) will measure zero.



- 4 GND: connect this module to the system GND
- 3 VCC: you can use 5V or 3.3V for this module
- 2 SDA: I²C serial data
- 1 SCL: I²C serial clock
- 5 The BMA400 module

Accelerometers have many uses in industry and science. Highly sensitive accelerometers are used in inertial navigation systems for aircraft and missiles. Vibration in rotating machines is monitored by accelerometers. They are used in tablet computers and digital cameras so that images on screens are always displayed upright. In unmanned aerial vehicles, accelerometers help to stabilise flight.

TRANSCEIVER MODULE

In radio communication, a transceiver is an electronic device which is a combination of a radio transmitter and a receiver, hence the name. It can both transmit and receive radio waves using an antenna, for communication purposes. These two related functions are often combined in a single device to reduce manufacturing costs. The term is also used for other devices which can both transmit and receive through a communications channel, such as optical transceivers which transmit and receive light in optical fiber systems, and bus transceivers which transmit and receive digital data in computer data buses.

9V BATTERY

The nine-volt battery, or 9-volt battery, is an electric battery that supplies a nominal voltage of 9 volts. Actual voltage measures 7.2 to 9.6 volts, depending on battery chemistry. Batteries of various sizes and capacities are manufactured; a very common size is known as PP3, introduced for early transistor radios.



The PP3 has a rectangular prism shape with rounded edges and two polarized snap connectors on the top. This type is commonly used for many applications including household uses such as smoke and gas detectors, clocks, and toys.

DC MOTOR DRIVE MODULE

Motor drive means a system that includes a motor. An adjustable speed motor drive means a system that includes a motor that has multiple operating speeds. A variable speed motor drive is a system that includes a motor and is continuously variable in speed. If the motor is generating electrical energy rather than using it – this could be called a generator drive but is often still referred to as a motor drive.

GRIPPER

Grippers, sometimes called hand grippers, are primarily used for testing and increasing the strength of the hands; this specific form of grip strength has been called crushing grip, which has been defined as meaning the prime movers are the four fingers, rather than the thumb.

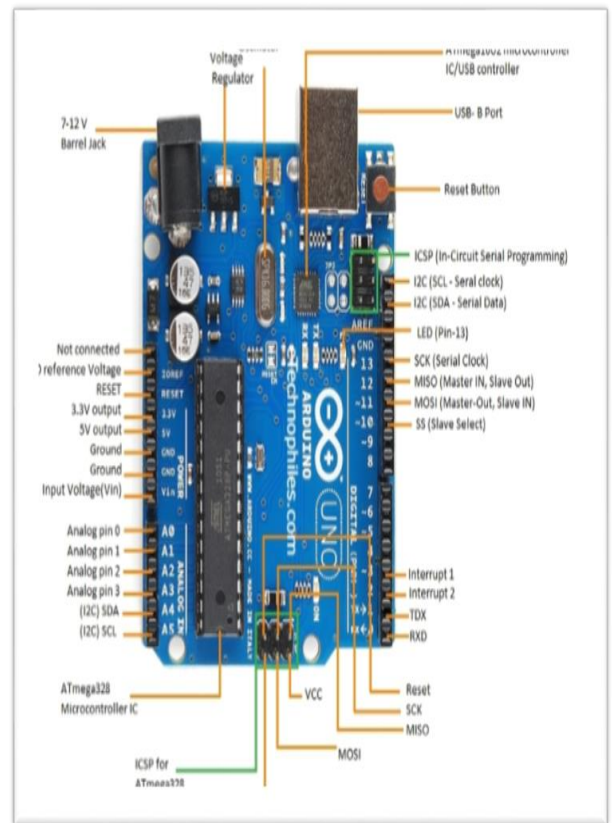


There are differences from brand to brand, but the common features of standard grippers are that they use a torsion spring fitted with two handles. The exact dimensions of these elements vary, as well as the materials used to make them; the springs are made from various types of steel, and the handles are generally made from wood, plastic, steel or aluminum.

ARDUINO

The Arduino Uno is an open-source microcontroller board based on the Microchip ATmega328P microcontroller and developed by Arduino.cc. The board is equipped with sets of digital and analog input/output (I/O) pins that may be interfaced to various expansion boards (shields) and other circuits.^[1] The board has 14 digital I/O pins (six capable of PWM output), 6 analog I/O pins, and is programmable with the Arduino IDE (Integrated Development Environment), via a type B USB cable. It can be powered by the USB cable or by an external 9-volt battery, though it accepts voltages between 7 and 20 volts. It is similar to the Arduino Nano and Leonardo. The hardware reference design is distributed under a Creative Commons Attribution Share-Alike 2.5 license and is available on the Arduino website. Layout and production files for some versions of the hardware are also available.

PIN DIAGRAM



GENERAL PIN FUNCTIONS

- **LED:** There is a built-in LED driven by digital pin 13. When the pin is high value, the LED is on, when the pin is low, it is off.
- **VIN:** The input voltage to the Arduino/Genuino board when it is using an external power source (as opposed to 5 volts from the USB connection or other regulated power source). You can supply voltage through this pin, or, if supplying voltage via the power jack, access it through this pin.
- **5V:** This pin outputs a regulated 5V from the regulator on the board. The board can be supplied with power either from the DC power jack (7 - 20V), the USB connector (5V), or the VIN pin of the board (7-20V). Supplying voltage via the 5V or 3.3V pins bypasses the regulator, and can damage the board.
- **3V3:** A 3.3 volt supply generated by the on-board regulator. Maximum current draw is 50 mA.
- **GND:** Ground pins.
- **IOREF:** This pin on the Arduino/Genuino board provides the voltage reference with which the microcontroller operates. A properly configured shield can read the IOREF pin voltage and select the appropriate power source, or enable voltage translators on the outputs to work with the 5V or 3.3V.

- Reset: Typically used to add a reset button to shields that block the one on the board.

CODING

```
#include <SoftwareSerial.h>

SoftwareSerial HC12(11, 12); // HC-12 TX Pin, HC-12 RX
Pin

int x_axis_1, y_axis_1, x_axis_2, y_axis_2;

void setup()
{
  Serial.begin(9600);      // Serial port to computer
  HC12.begin(9600);       // Serial port to HC12
}

void loop()
{
  x_axis_1 = analogRead(A0);
  y_axis_1 = analogRead(A1);
  x_axis_2 = analogRead(A2);
  y_axis_2 = analogRead(A3);
  HC12.write('%');
  HC12.write(x_axis_1/100%10+48);
  HC12.write(x_axis_1/10%10+48);
  HC12.write(x_axis_1/1%10+48);
  HC12.write(',');
  HC12.write(y_axis_1/100%10+48);
  HC12.write(y_axis_1/10%10+48);
  HC12.write(y_axis_1/1%10+48);
  HC12.write(',');
  HC12.write(x_axis_2/100%10+48);
  HC12.write(x_axis_2/10%10+48);
  HC12.write(x_axis_2/1%10+48);
  HC12.write(',');
  HC12.write(y_axis_2/100%10+48);
  HC12.write(y_axis_2/10%10+48);
  HC12.write(y_axis_2/1%10+48);
  HC12.print("#\r\n");
  delay(100);
}
```

```
#include <SoftwareSerial.h>

SoftwareSerial HC12(11, 12); // HC-12 TX Pin, HC-12 RX
Pin

const int IN1 = 9;
const int IN2 = 8;
const int IN3 = 6;
const int IN4 = 7;
const int IN5 = 5;
const int IN6 = 4;
const int IN7 = 3;
const int IN8 = 2;

int x_axis_1, y_axis_1, x_axis_2, y_axis_2;

unsigned char inByte;

unsigned char arr[20], ii, start_flag = 0, over_flag = 0;

void setup()
{
  Serial.begin(9600);      // Serial port to computer
  HC12.begin(9600);       // Serial port to HC12

  pinMode(IN1, OUTPUT); digitalWrite(IN1, LOW);
  pinMode(IN2, OUTPUT); digitalWrite(IN2, LOW);
  pinMode(IN3, OUTPUT); digitalWrite(IN3, LOW);
  pinMode(IN4, OUTPUT); digitalWrite(IN4, LOW);
  pinMode(IN5, OUTPUT); digitalWrite(IN5, LOW);
  pinMode(IN6, OUTPUT); digitalWrite(IN6, LOW);
  pinMode(IN7, OUTPUT); digitalWrite(IN7, LOW);
  pinMode(IN8, OUTPUT); digitalWrite(IN8, LOW);
}

void loop()
{
  while(HC12.available()) // If HC-12 has data
  {
    inByte = HC12.read();
    //Serial.write(inByte)

    if(start_flag == 0)
    {
      if(inByte == '%')
```

```

{
  ii = 0;
  start_flag = 1;
}
else if(start_flag == 1)
{
  if(inByte == '#')
  {
    over_flag = 1;
    start_flag = 0;
  }
  else
  {
    arr[ii++] = inByte;
  }
}
if(over_flag == 1)
{
  x_axis_1 = (((int)arr[ 0] - 48) * 100) + (((int)arr[ 1] - 48)
* 10) + (((int)arr[ 2] - 48) * 1);
  y_axis_1 = (((int)arr[ 4] - 48) * 100) + (((int)arr[ 5] - 48)
* 10) + (((int)arr[ 6] - 48) * 1);
  x_axis_2 = (((int)arr[ 8] - 48) * 100) + (((int)arr[ 9] - 48)
* 10) + (((int)arr[10] - 48) * 1);
  y_axis_2 = (((int)arr[12] - 48) * 100) + (((int)arr[13] -
48) * 10) + (((int)arr[14] - 48) * 1);
  /*
  Serial.write(x_axis_1/100%10+48);
  Serial.write(x_axis_1/10%10+48);
  Serial.write(x_axis_1/1%10+48);
  Serial.write(',');
  Serial.write(y_axis_1/100%10+48);
  Serial.write(y_axis_1/10%10+48);
  Serial.write(y_axis_1/1%10+48);
  Serial.write(',');
  Serial.write(x_axis_2/100%10+48);

```

```

Serial.write(x_axis_2/10%10+48);
Serial.write(x_axis_2/1%10+48);
Serial.write(',');
Serial.write(y_axis_2/100%10+48);
Serial.write(y_axis_2/10%10+48);
Serial.write(y_axis_2/1%10+48);
Serial.print("\r\n");
*/
  if( (x_axis_1 > 290 && x_axis_1 < 370) &&
(y_axis_1 > 290 && y_axis_1 < 370) )
  {
    //Serial.write('S');
    digitalWrite(IN1, LOW); digitalWrite(IN2, LOW);
    digitalWrite(IN3, LOW); digitalWrite(IN4, LOW);
  }
  else if( !(x_axis_1 > 290 && x_axis_1 < 370) &&
(y_axis_1 > 290 && y_axis_1 < 370) )
  {
    if(x_axis_1 <= 290)
    {
      //Serial.write('R');
      digitalWrite(IN1, LOW); digitalWrite(IN2, HIGH);
      digitalWrite(IN3, HIGH); digitalWrite(IN4, LOW);
    }
    else if(x_axis_1 >= 370)
    {
      //Serial.write('L');
      digitalWrite(IN1, HIGH); digitalWrite(IN2, LOW);
      digitalWrite(IN3, LOW); digitalWrite(IN4, HIGH);
    }
  }
  else if( (x_axis_1 > 290 && x_axis_1 < 370) &&
!(y_axis_1 > 290 && y_axis_1 < 370) )
  {
    if(y_axis_1 <= 290)
    {
      //Serial.write('F');
      digitalWrite(IN1, LOW); digitalWrite(IN2, HIGH);

```

```

digitalWrite(IN3, LOW); digitalWrite(IN4, HIGH);
}
else if(y_axis_1 >= 370)
{
//Serial.write('B');
digitalWrite(IN1, HIGH); digitalWrite(IN2, LOW);
digitalWrite(IN3, HIGH); digitalWrite(IN4, LOW);
}
}
if( (x_axis_2 > 290 && x_axis_2 < 370) &&
(y_axis_2 > 290 && y_axis_2 < 370) )
{
//Serial.write('E');

digitalWrite(IN5, LOW); digitalWrite(IN6, LOW);
//gripper
digitalWrite(IN7, LOW); digitalWrite(IN8, LOW);
//shoulder
}
else if( !(x_axis_2 > 290 && x_axis_2 < 370) &&
(y_axis_2 > 290 && y_axis_2 < 370) )
{
if(x_axis_2 <= 290)
{
//Serial.write('A');
digitalWrite(IN5, LOW); digitalWrite(IN6, HIGH);
//gripper
}
else if(x_axis_2 >= 370)
{
//Serial.write('B');
digitalWrite(IN5, HIGH); digitalWrite(IN6, LOW);
//gripper
}
}
else if( (x_axis_2 > 290 && x_axis_2 < 370) &&
!(y_axis_2 > 290 && y_axis_2 < 370) )
{
if(y_axis_2 <= 290)

```

```

{
//Serial.write('C');
digitalWrite(IN7, LOW); digitalWrite(IN8, HIGH);
//shoulder
}
else if(y_axis_2 >= 370)
{
//Serial.write('D');
digitalWrite(IN7, HIGH); digitalWrite(IN8, LOW);
//shoulder
}
}
over_flag = 0;
}
}
}

```

CONCLUSION

The overall system performs reasonably well. The user is able to carry out comfortable and precise functions of the robotic Hand through the use of a sensor based control glove. Furthermore, the robotic Hand is capable to carry normal routine function as human hand does. The microcontroller accepts inputs from the sensor and generates the proper control signals based on those inputs. The usable lifetime of the flex sensors seems to be limited. The sensors themselves are very fragile and easily wear out from overuse. Careful maintenance and protection of the flex sensors is crucial to successful operation of the system. The robotic hand was able to imitate the hand motions of the controller glove and grip objects through wireless communication. The robotic hand was able to grip objects.

FUTURE SCOPE

We will work on this project in future and make it an essential component of all factories involving movement of hazardous substances and chemicals. Further robotic hand will be made for more advanced technologies when it will be wireless and can be used from far places without hindrance. Now, sensors are used for moving fingers afterwards we will make it auto for all those works which need not variable instructions. Another form of this hand will be access from software wirelessly without sensors which will reduce cost as well.

REFERENCES

- [1] M. Nore and C. Westerberg, *Robotic arm controlled by arm movements*, URN: urn:nbn:se:kth:diva-264509, 2019.
- [2] F. Hardell and J. Tjomsland, *Motorized tensioner system for prosthetic hands*, URN: urn:nbn:se:kth:diva-230144, 2018.
- [3] R. Nilsson and A. Winquist de Val, *Hand gesture controlled wheelchair*, URN: urn:nbn:se:kth:diva-264512, 2019.
- [4] R. J. Schwarz and C. Taylor, "The anatomy and mechanics of the human hand", *Artificial limbs*, vol. 2, no. 2, pp. 22–35, 1955.
- [5] C. Sollerman and A. Ejeskär, "Sollerman hand function test. a standardised method and its use in tetraplegic patients.", *Scandinavian journal of plastic and reconstructive surgery and hand surgery*, vol. 29 2, pp. 167–76, 1995.
- [6] Arduino, *What is arduino?*, <https://www.arduino.cc/en/guide/introduction>, [Online; accessed 03-February-2020].
- [7] Arduino Uno Rev3, <https://store.arduino.cc/arduino-uno-rev3>, [Online; accessed 03-February-2020].
- [8] Arduino Nano, <https://store.arduino.cc/arduino-nano>, [Online; accessed 25-March-2020].
- [9] TowerPro, *MG996R Robot servo 180° Rotation*, <http://www.towerpro.com.tw/product/mg995-robot-servo-180-rotation/>, [Online; accessed 07-February-2020].
- [10] J. Gieras, *PERMANENT MAGNET MOTOR TECHNOLOGY: DESIGN AND APPLICATIONS*. Jan. 2010, isbn: 978-1-4200-6440-7.

3D PRINTING OF AUTOMOTIVE DIFFERENTIAL

SK.Nagur meeravali, D.Anil, L.Gopireddy, R.kishore, SK.N.Althaf hussain, G.Nagaiah

Department of Mechanical Engineering,
Narasaraopeta Engineering College, Narasaraopet, Palnadu(Dist.), A.P., India

Abstract : In automobiles and other wheeled vehicles, the differential permit each of the driving wheels to rotate at different speeds, while for most vehicles supplying equal torque to each of them. A vehicle's wheels rotate at divergent speeds, mainly when turning corners. 3D Printing or Additive manufacturing is a novel method of manufacturing parts directly from digital model by using layer by layer material build-up approach. This tool-less manufacturing method can produce fully dense metallic parts in short time, with high precision. Features of additive manufacturing like freedom of part design, part complexity, light weighting, part consolidation and design for function are garnering particular interests in metal additive manufacturing for aerospace, oil & gas, marine and automobile applications.

I. INTRODUCTION

Additive Manufacturing is the formalized term for what used to be called rapid Prototyping and what is popularly called 3D Printing. The term Rapid Prototyping (or RP) is used in a variety of industries to describe a process for rapidly creating a system or part representation before final release or commercialization. In other words, the emphasis is on creating something quickly, and that the output is a prototype or basis model from which further models and eventually the final product will be derived. Management consultants and software engineers both also use the Rapid Prototyping to describe a process of developing business and software solutions in a piecewise fashion that allows climates and other stakeholders to test ideas and provide feedback during the development process. In a product development context, the term Rapid Prototyping was used widely to describe technologies which created physical prototypes directly from digital model data. This texts about these latter technologies, first developed for prototyping but now used for many more purposes.

II. THE GENERIC AM PROCESS

AM involves a number of steps that move from the virtual CAD description to the physical resultant part. Different products will involve AM in different ways and to different small, visualization models. It is widely believed that 3D printing or additive manufacturing (AM) has the vast potential to become one of the technologies. 3D printing has now been covered across many television channels, in mainstream newspapers and across online resources. What really is this 3D printing that some have claimed will put an end to traditional manufacturing as we know it,

geopolitics, economic, social, demographic, and environmental and security implications to our everyday lives.

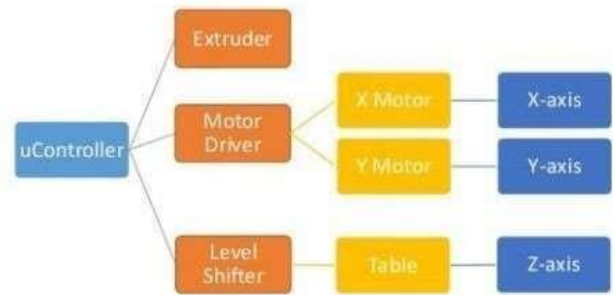


Fig.1:Control Unit

III. HISTORY OF 3D PRINTING TECHNOLOGY

The earliest 3D printing technologies first became visible in the late 1980's, at which time they were called Rapid Prototyping (RP) technologies. This is because the processes were originally conceived as a fast and more cost-effective method for creating prototypes for product development within industry. As an interesting aside, the very first patent application for RP technology was filed by a Dr Kodama, in Japan, in May 1980. Unfortunately for Dr Kodama, the full patent specification was subsequently not filed before the one year deadline after the application, which is particularly disastrous considering that he was a patent lawyer! In real terms, however, the origins of 3D printing can be traced back to 1986, when the first patent was issued for stereo lithography apparatus (SLA). This patent belonged to one Charles (Chuck) Hull, who first invented his SLA machine in 1983. Hull went on to co-found 3D Systems.

IV. 3D PRINTING TECHNOLOGY NOWADAYS

The starting point for any 3D printing process is a 3D digital model, which can be created using a variety of 3D software programs in industry this is 3D CAD, for Makers and Consumers there are simpler, more accessible programs available or scanned with a 3D scanner. The model is then 'sliced' into layers, there by converting the design into a file readable by the 3D printer. The material processed by the 3D printer is then layered according to the design and the process. As stated, there are a number of different types of 3D printing technologies, which process different materials in different ways to create the final object. Functional plastics, metals, ceramics and sand are, now, all routinely used for industrial prototyping and production applications.

Research is also being conducted for 3D printing bio materials and different types of food. Generally speaking though, at the entry level of the market, materials are much more limited. Plastic is currently the only widely used material usually ABS or PLA, but there are a growing number of alternatives, including Nylon.

V. FUSED DEPOSITION MODELLING

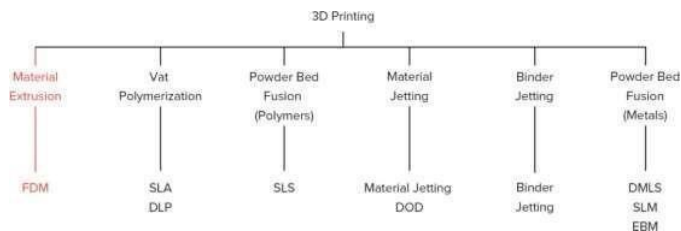


Fig.2: 3D printing technologies

Fused Deposition Modelling (FDM), or Fused Filament Fabrication (FFF), is an additive manufacturing process that belongs to the material extrusion family. In FDM, an object is built by selectively depositing melted material in a pre-determined path layer-by-layer. The materials used are thermoplastic polymers and come in a filament form.

FDM is the most widely used 3D Printing technology: it represents the largest installed base of 3D printers globally and is often the first technology people are exposed to. In this article, the basic principles and the key aspects of the technology are presented

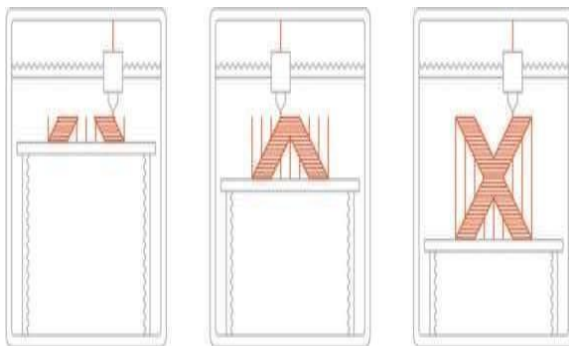


Fig.3.FDM process

VII. METHODOLOGY

Step 1: Initially the components to be prepared are drawn using CATIA-V5 software using sketcher tool.

Step 2: Once the component is drawn as per required dimensions then the file is saved as STL file in CATIA-V5 software

Step 3: After completion of above procedure, STL file is loaded into cura software.

Step 4: Once the STL file is loaded, required parameters are set in cura software that is material used, layer thickness, infill density, infill shapes, fan speed, nozzle temperature, bed temperature, extrusion temperature, supports required all are selected and modified as per the requirement.

Step 5: After selection of the above parameters slicing is done by using slice option.

Step 6: Once slicing is done STL file is converted into G codes which is readable by 3D printer.

Step 7: G-code file is loaded in 3d printer by using pen drive and printing is done.

Step 8: Assembly of Printed Components

VI. 3D PRINTER MAIN COMPONENTS

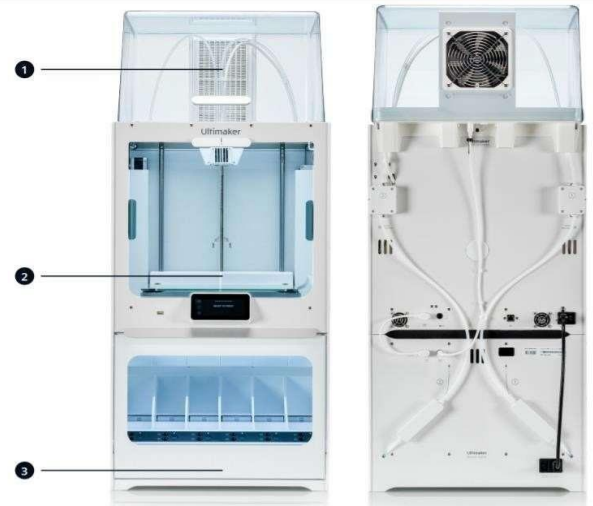


Fig.4: 3D Ultimaker S5 pro bundle bundle 3D printer

1. Air Manger
2. Ultimaker s5
3. Material station

VIII. MODELING OF AUTOMOTIVE DIFFERENTIAL



USES OF CATIA-V5:

- Sharp designing
- Styling
- Surface workflow
- Modelling and simulation

PARTS IN AUTOMOTIVE DIFFERENTIAL:

- Differential Piston
- Differential Ring gear

- Differential Stand
- Differential Carrier
- Differential Carrier cover
- Differential Arm
- Differential Left shift
- Differential Right shaft
- Differential Spider shaft
- Differential Spider
- Differential Wheel
- Differential Side
- Differential Motor cover

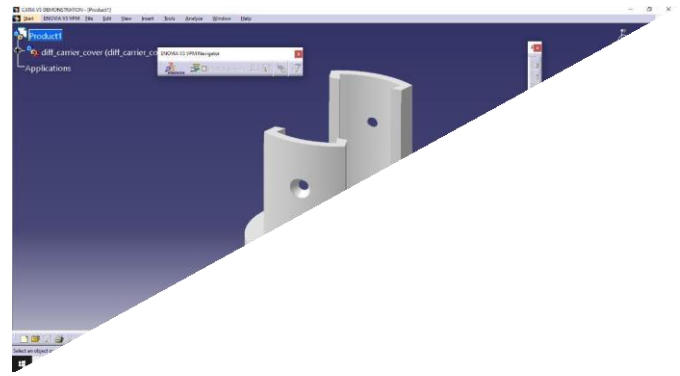


Fig.5: Differential Carrier

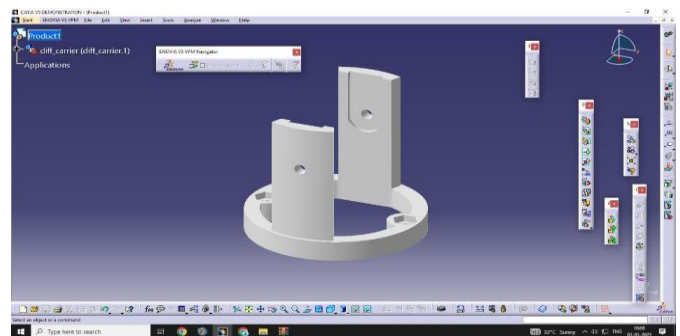


Fig.9: Differential Carrier cover

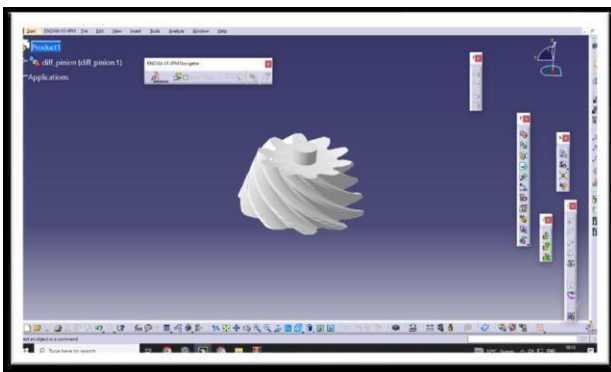


Fig.6: Differential Piston

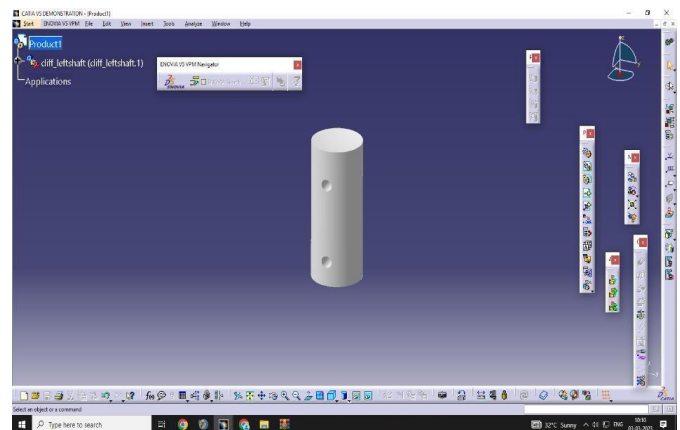


Fig.10: Differential Left shaft

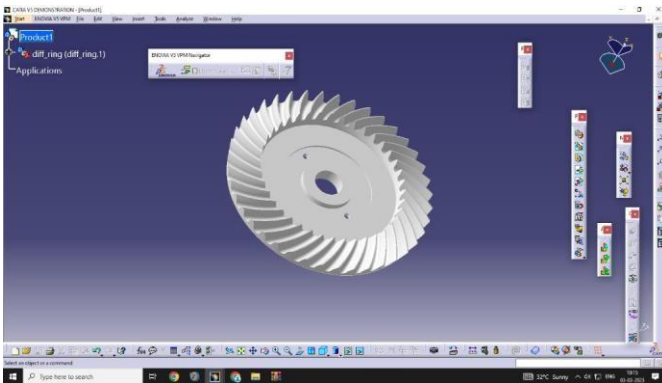


Fig.7: Differential Ring gear

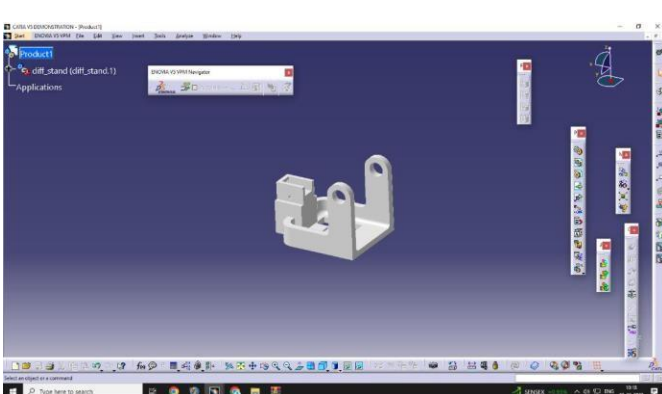


Fig.8: Differential Stand

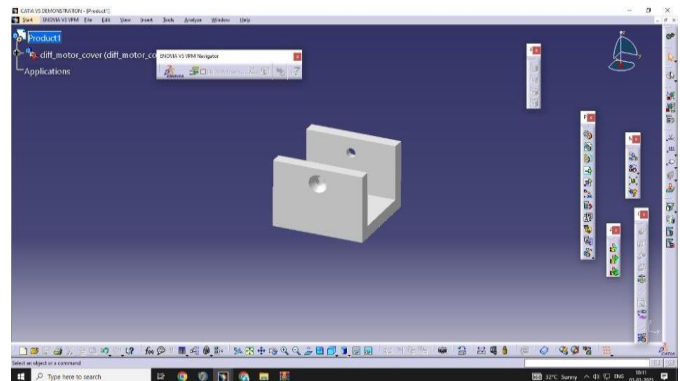


Fig.11: Differential Motor cover

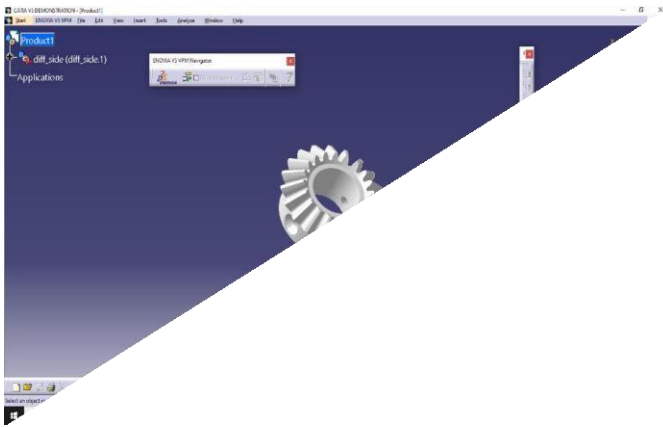


Fig.12: Differential Side

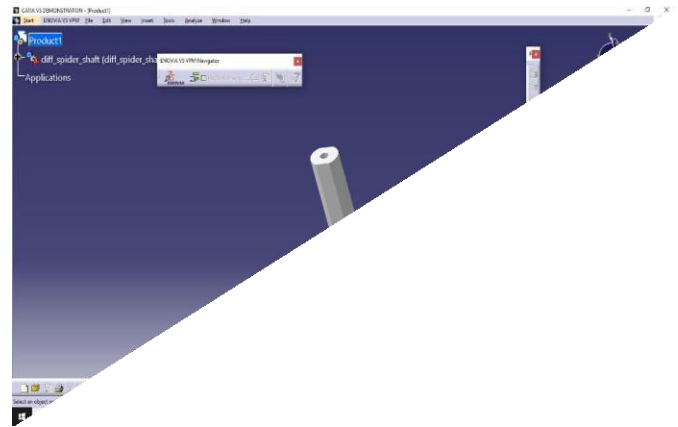


Fig.15: Differential Shaft

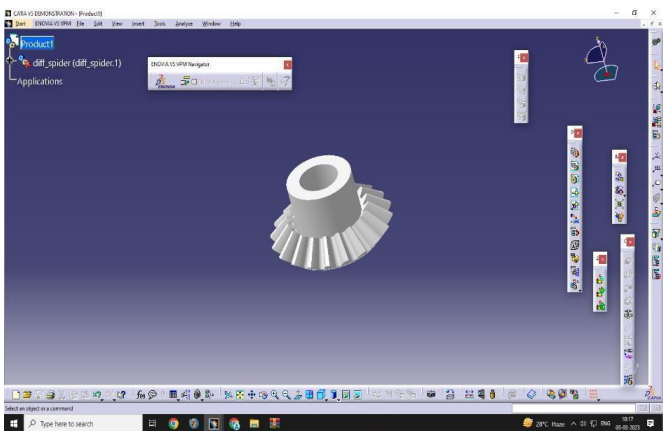


Fig.13: Differential Spider

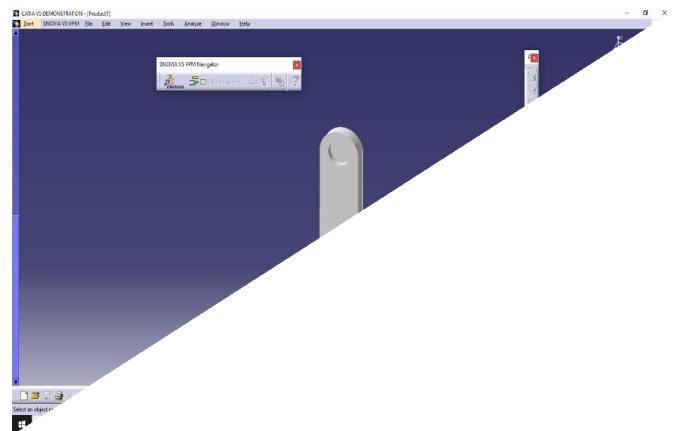


Fig.16: Differential Stand

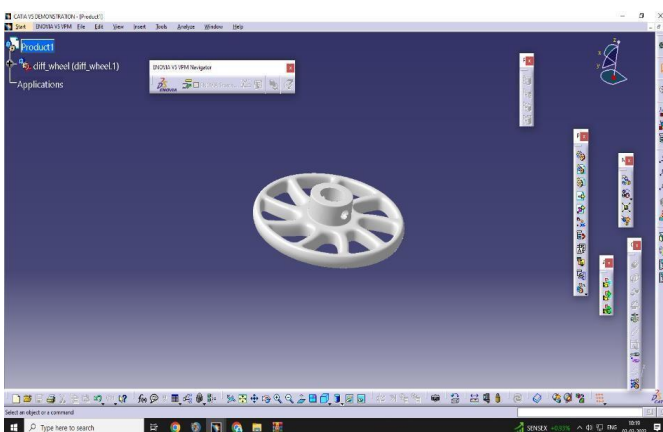


Fig.14: Differential Wheel

IV. PROCESSING CATIA-V5 MODEL USING CURA SOFTWARE

STL file prepared in catia-v5 software and loaded into a Cura software which is a free print preparation software for the ultimaker 3D printers. Slicing is done using this software. After slicing the file is save in G codes format and with is used as input for 3D printer for printing of the components. Each and every parameter required is modified as per the requirement in cura software

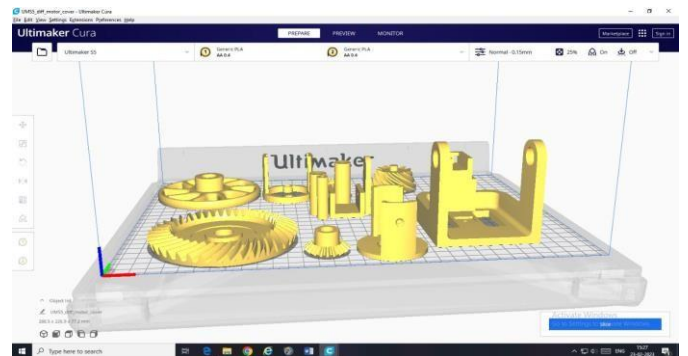


Fig.17: Automotive Differential STL file in Cura

X. RESULT



Fig.18: Final assembled Automotive Differential

V. ADVANTAGES

- Both driving wheels can rotate in the same direction at the same speed.
- Both driving wheels can rotate in the same direction at different speeds.
- Both driving wheels can rotate in the opposite direction at the same speed.
- Both driving wheels can rotate in the opposite direction at a different speed.

VI. APPLICATIONS

- permits power from the engine to be transmitted to a pair of driving wheels
- allows the outer drive wheel to rotate faster than the inner drive wheel during a turn.
- pair of driving wheels.
- used in two input axles in train.

□

VII. CONCLUSION & FUTURE SCOPE

With the help of CATIA-V5, design of automotive differential is developed including few sub- assemblies and fabrication gears and other components completed by using 3D printing machine. 3D printing technology is the most advanced manufacturing process which is trending now a day which help in printing component at high speed and reduces production cost. In this project work, design is done using CATIA-V5 software and then file is transformed to STL format which is used for production of the component in 3D printing machine. CURA software is used for slicing of the component produced in CATIA- V5 and it also helps in adjustment of dimensions, solidification time, material selection, printing speed and printing time. In this project PLA material is used for the production of the component in 3D printing machine. The total time taken to print automotive differential is 31 hours 21 minutes and components are successfully assembled. The total PLA material is consumed to print automotive differential is 290 grams (28.38 meters).

REFERENCES

1. Shashank pandey, Nikhilesh N. sing & Dr. rabhatkumar sinha, 2017, "Modelling and design of differential gear box through FEM, SOLIDWORKS WORKBENCH", *International Journal of Engineering Sciences and Research Technology*.
2. T. Loknadh, DR. P. S. S. Vasu, Design a crown wheel gear of differential gear box used in heavy vehicles for structural loads, *International Journal of Science, Engineering and Technology Research (IJSETR)*, Volume 4, Issue 7, July 2015
3. D. A., Espalin, D., & Wicker, R. B., "3D printer selection: A decision making evaluation and ranking model", *Virtual and Physical Prototyping*, 2013, 8:3, 201-212
4. Lee, I. and Kim, Y., "The Recent Patent Analysis and Industrial Trend of 3D Printing", *Indian Journal of Science and Technology*, Vol 8(S8), 70-73, April 2015
5. Thompson
4. S. M., Bianc, L., Shamsaei, N., & Yadollahia, A., " An overview of Direct Laser Deposition for additive manufacturing; Part I: Transport phenomena, modeling and diagnostics", *Additive Manufacturing* 8 (2015) 36– 62, <http://dx.doi.org/10.1016/j.addma.2015.07.001>
5. Shamsaei, N., Yadollahia, A., Bianc, L., & Thompson S.M., " An overview of Direct Laser Deposition for additive manufacturing; Part II: Mechanical behavior, process parameter optimization and control", *Additive Manufacturing* 8(2015)1235, <http://dx.doi.org/10.1016/j.addma.2015.07.002>

DESIGN AND FABRICATION OF 3D ENGINE MODEL USING 3D PRINTER

SK.Nagul Meeravali , K.Nikhil Kumar, V.Ayyappa, M.Baji Vali, G.Harikrishna Reddy, K.Venkata krishna
 Department of Mechanical Engineering,
 Narasaraopeta Engineering College, Narasaraopet, Palnadu(Dist.), A.P., India

Abstract In automobiles and other wheeled vehicles, the differential permit each of the driving wheels to rotate at different speeds, while for most vehicles supplying equal torque to each of them. A vehicle's wheels rotate at divergent speeds, mainly when turning corners. 3D Printing or Additive manufacturing is a novel method of manufacturing parts directly from digital model by using layer by layer material build-up approach. This tool-less manufacturing method can produce fully dense metallic parts in short time, with high precision. Features of additive manufacturing like freedom of part design, part complexity, light weighting, part consolidation and design for function are garnering particular interests in metal additive manufacturing for aerospace, oil & gas, marine and automobile applications.

I. INTRODUCTION

Additive Manufacturing is the formalized term for what used to be called rapid Prototyping and what is popularly called 3D Printing. The term Rapid Prototyping (or RP) is used in a variety of industries to describe a process for rapidly creating a system or part representation before final release or commercialization. In other words, the emphasis is on creating something quickly, and that the output is a prototype or basis model from which further models and eventually the final product will be derived. Management consultants and software engineers both also use the Rapid Prototyping to describe a process of developing business and software solutions in a piecewise fashion that allows climates and other stakeholders to test ideas and provide feedback during the development process. In a product development context, the term Rapid Prototyping was used widely to describe technologies which created physical prototypes directly from digital model data. This texts about these latter technologies, first developed for prototyping but now used for many more purposes.

II. THE GENERIC AM PROCESS

AM involves a number of steps that move from the virtual CAD description to the physical resultant part. Different products will involve AM in different ways and to different small, visualization models. It is widely believed that 3D printing or additive manufacturing (AM) has the vast potential to became one of the technologies. 3D printing has now been covered across many television channels, in mainstream newspapers and across online resources. What really is this 3D printing that some have claimed will put an end to traditional manufacturing as we know.

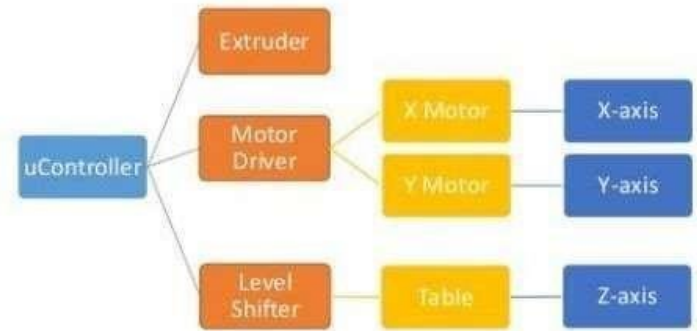


Fig.1:Control Unit

III. HISTORY OF 3D PRINTING TECHNOLOGY

The earliest 3D printing technologies first became visible in the late 1980's, at which time they were called Rapid Prototyping (RP) technologies. This is because the processes were originally conceived as a fast and more cost-effective method for creating prototypes for product development within industry. As an interesting aside, the very first patent application for RP technology was filed by a Dr Kodama, in Japan, in May 1980. Unfortunately for Dr Kodama, the full patent specification was subsequently not filed before the one year deadline after the application, which is particularly disastrous considering that he was a patent lawyer! In real terms, however, the origins of 3D printing can be traced back to 1986, when the first patent was issued for stereo lithography apparatus (SLA). This patent belonged to one Charles (Chuck) Hull, who first invented his SLA machine in 1983. Hull went on to co-found 3D Systems.

IV. 3D PRINTING TECHNOLOGY NOWADAYS

The starting point for any 3Dprinting process is a 3D digital model, which can be created using a variety of 3D software programs in industry this is 3D CAD, for Makers and Consumers there are simpler, more accessible programs available or scanned with a 3D scanner. The model is then 'sliced' into layers, there by converting the design into a file readable by the 3D printer. The material processed by the 3Dprinteris then layered according to the design and the process. As stated, there are a number of different types of 3D printing technologies, which process different materials in different ways to create the final object. Functional plastics, metals, ceramics and sand are, now, all routinely used for industrial prototyping and production applications.

Research is also being conducted for 3Dprinting bio materials and different types of food. Generally speaking though, at the entry level of the market, materials are much more limited. Plastic is currently the only widely used material usually ABS or PLA, but there are a growing number of alternatives, including Nylon.

V. FUSED DEPOSITION MODELLING

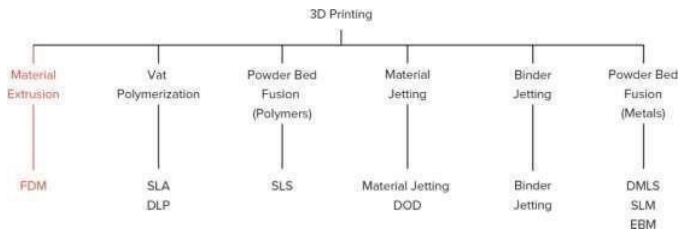


Fig.2: 3D printing technologies

Fused Deposition Modelling (FDM), or Fused Filament Fabrication (FFF), is an additive manufacturing process that belongs to the material extrusion family. In FDM, an object is built by selectively depositing melted material in a pre-determined path layer-by-layer. The materials used are thermoplastic polymers and come in a filament form.

FDM is the most widely used 3D Printing technology: it represents the largest installed base of 3D printers globally and is often the first technology people are exposed to. In this article, the basic principles and the key aspects of the technology are presented

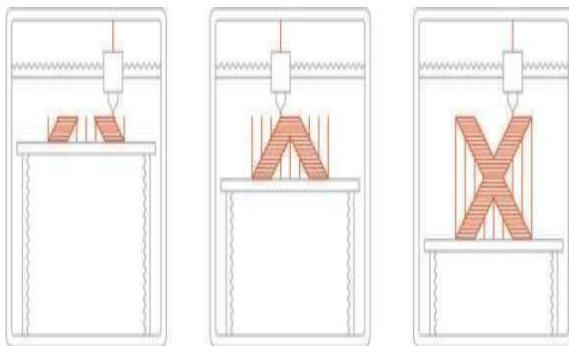


Fig.3.FDM process

VI. METHODOLOGY

Step 1: Initially the components to be prepares are drawn using CATIA-V5 software using sketcher tool.

Step 2: Once the component is drawn as per required dimensions then the file is saved as STL file in CATIA-V5 software

Step 3: After completion of above procedure, STL file is loaded into cura software.

Step 4: Once the STL file is loaded, required parameters are set in cura software that is material used, layer thickness, infill density, infill shapes, fan speed, nozzle temperature, bed temperature, extrusion temperature, supports required all are selected and modified as per the requirement.

Step 5: After selection of the above parameters slicing is done by using slice option.

Step 6: Once slicing is done STL file is converted into G codes which is readable by3D printer.

Step 7: G-code file is loaded in 3d printer by using pen drive and printing is done.

Step 8: Assembly of Printed Components

VII. 3D PRINTER MAIN COMPONENTS

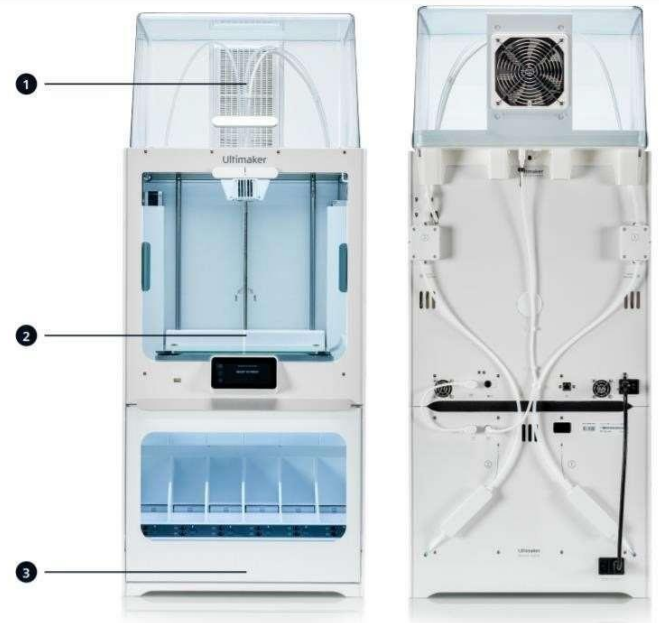


Fig.4: 3D Ultimaker S5 pro bundle bundle 3D printer

- 1. Air Manger
- 2. Ultimaker s5
- 3. Material station

VIII. MODELING OF AUTOMOTIVE DIFFERENTIAL



USES OFCATIA-V5:

- Sharp designing
- Styling
- Surface workflow
- Modelling and simulation

PARTS IN AUTOMOTIVE DIFFERENTIAL:

- Differential Piston
- Differential Ring gear

- Differential Stand
- Differential Carrier
- Differential Carrier cover
- Differential Arm
- Differential Left shift
- Differential Right shaft
- Differential Spider shaft
- Differential Spider
- Differential Wheel
- Differential Side
- Differential Motor cover

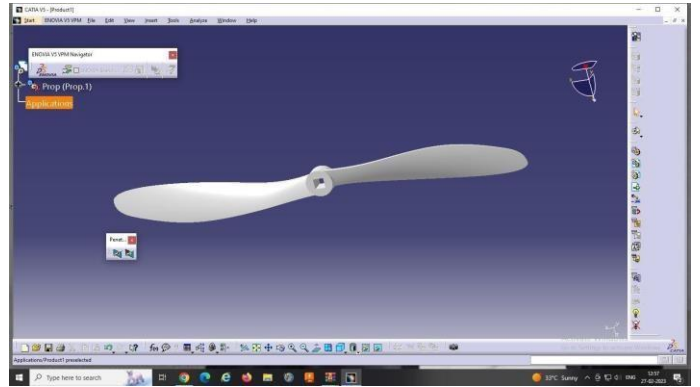


Fig.8: Propeller

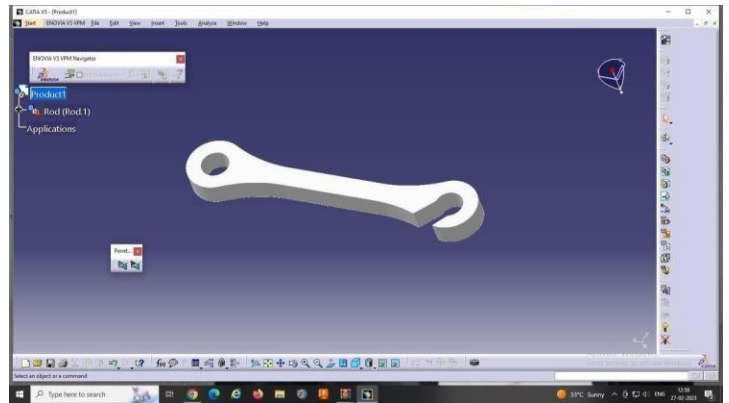


Fig.9: Connecting rod

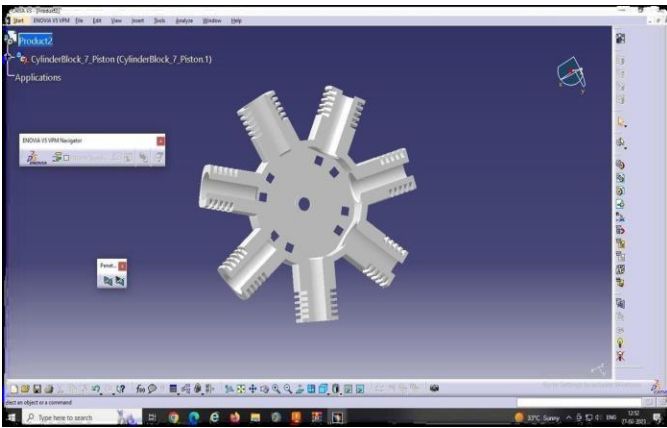


Fig.5: Cylinder block

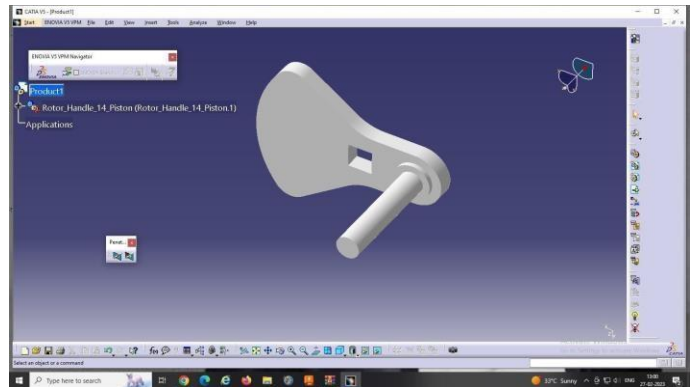


Fig.10: Rotor handle

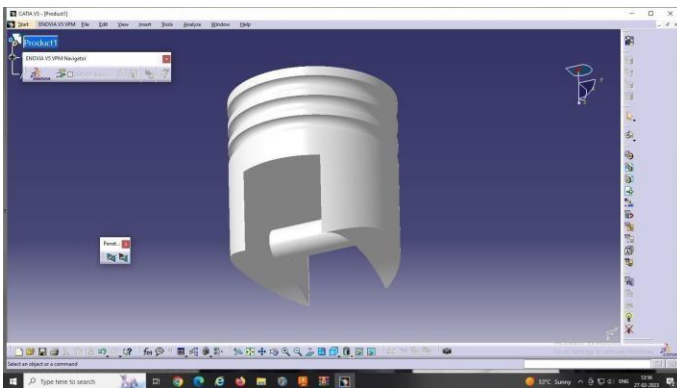


Fig.6: Piston modeling

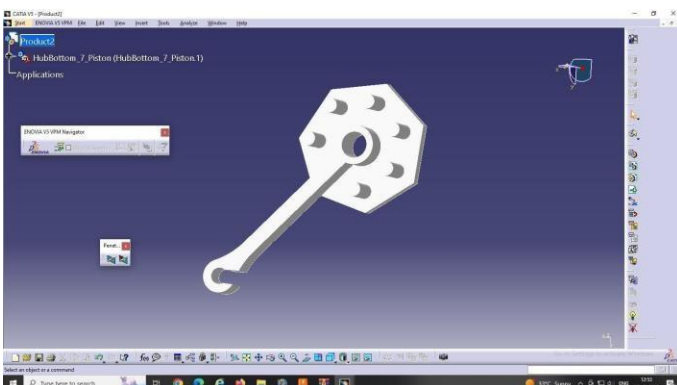


Fig.7: Hub Bottom

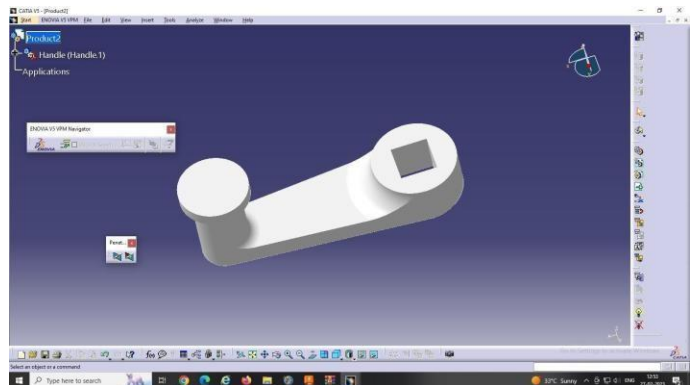


Fig.11: Rotor handl

IX. PROCESSING CATIA-V5MODEL USING CURA SOFTWARE

STL file prepared in catia-v5 software and loaded into a Cura software which is a free print preparation software for the ultimaker 3D printers. Slicing is done using this software. After slicing the file is save in G codes format and with is used as input for 3D printer for printing of the components. Each and every parameter required is modified as per the requirement in cura software

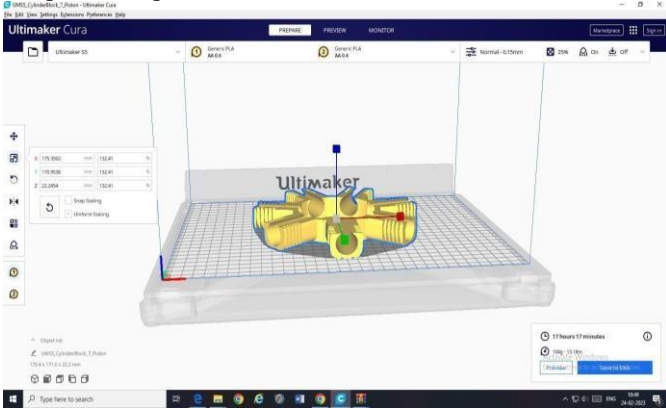


Fig.12: Automotive Differential STL file in Cura

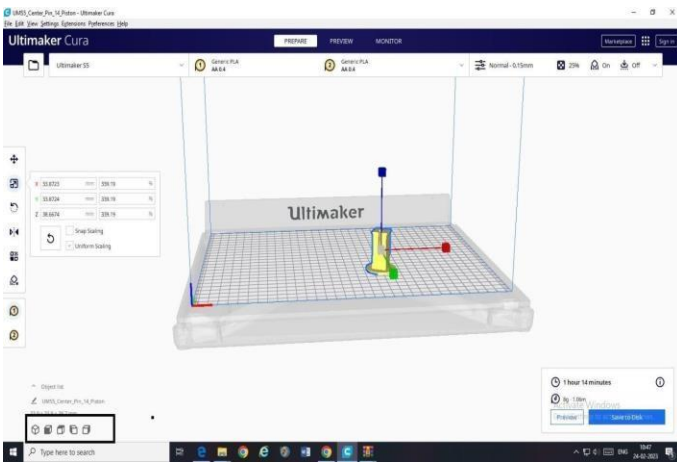


Fig.13: viewing angle bars

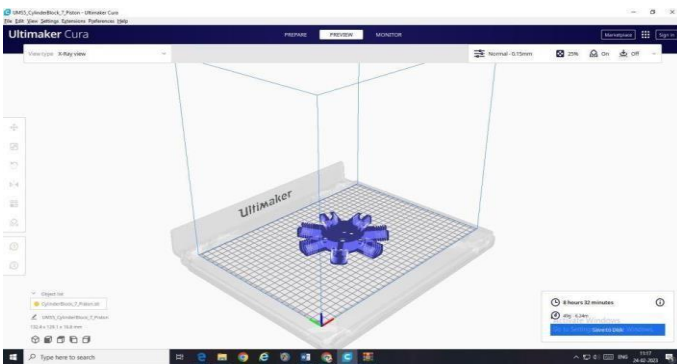


Fig.14: X-RAY VIEW

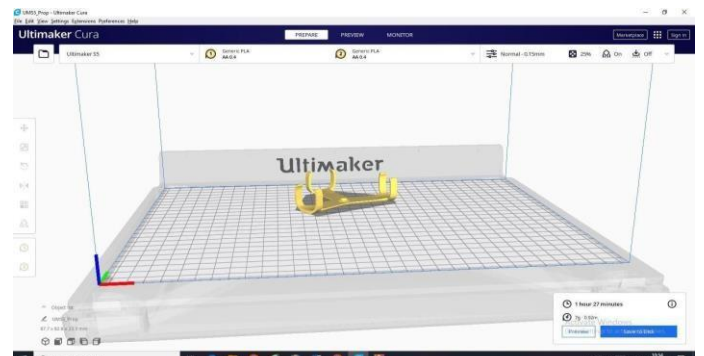


Fig.15: Layer view in CURA

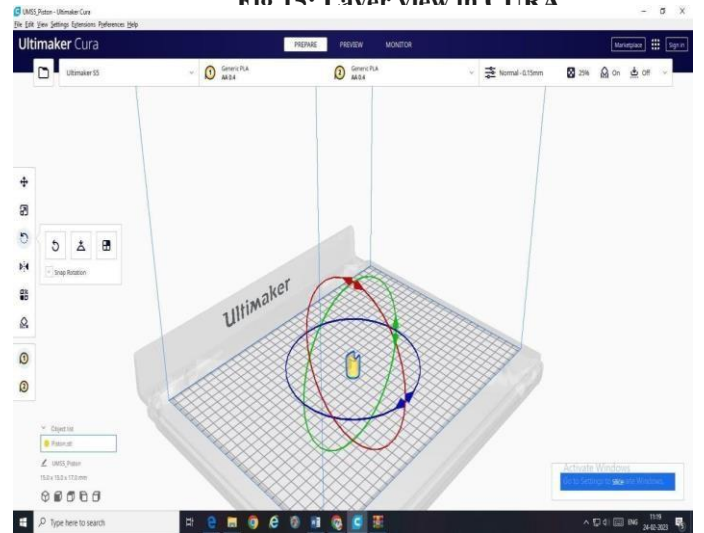
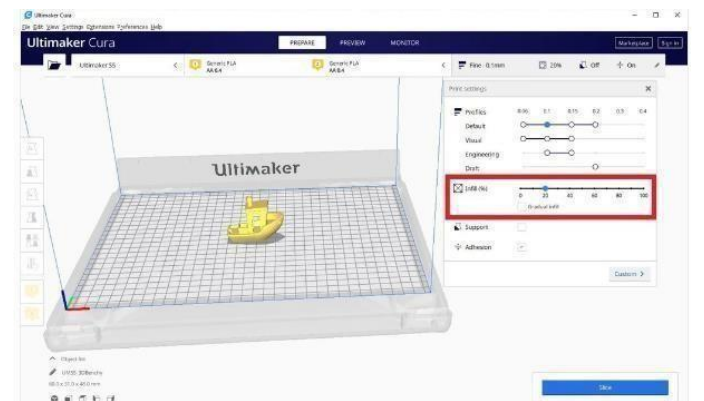


Fig.16: Moving or Rotating the model in CURA



X. RESULT

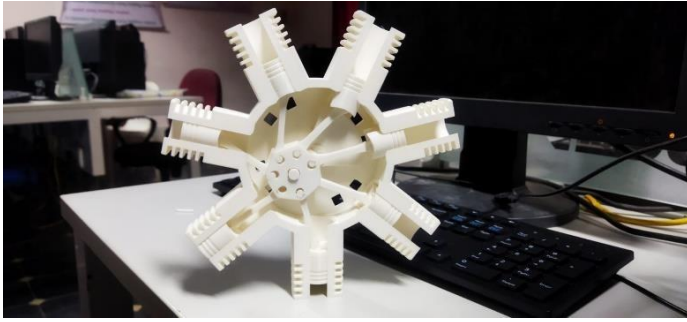


Fig.18: Final assembled Automotive Differential

XI. ADVANTAGES

- Rapid Prototyping.
- Print on Demand
- Strong and Light weight parts.
- Cost Effective.
- Ease of Access.
- Minimizing Waste.
- Fast Design and Production.

XII. APPLICATIONS

- Education
- Prototyping and Manufacturing
- Medicine
- Construction
- Art and Jewellery
- Custom art and design

XIII. CONCLUSION & FUTURESCOPE

With the help of CATIA-V5, design of automotive differential is developed including few sub- assemblies and fabrication gears and other components completed by using 3D printing machine. 3D printing technology is the most advanced manufacturing process which is trending now a day which help in printing component at high speed and reduces production cost.

In this project work, design is done using CATIA-V5 software and then file is transformed to STL format which is used for production of the component in 3D printing machine. CURA software is used for slicing of the

component produced in CATIA-V5 and it also helps in adjustment of dimensions, solidification time, material selection, printing speed and printing time. In this project PLA material is used for the production of the component in 3D printing machine. The total time taken to print automotive differential is 31 hours 21 minutes and components are successfully assembled. The total PLA material is consumed to print automotive differential is 28.38 meters.

REFERENCES

1. Shashank pandey, Nikhilesh N. sing & Dr. rabhatkumar sinha, 2017, "Modelling and design of differential gear box through FEM, SOLIDWORKS WORKBENCH", *International Journal of Engineering Sciences and Research Technology*.
2. T. Loknadh, DR. P. S. S. Vasu, *Design a crown wheel gear of differential gear box used in heavy vehicles for structural loads, International Journal of Science, Engineering and Technology Research (IJSETR), Volume 4, Issue 7, July 2015*
3. Roberson, D. A., Espalin, D., & Wicker, R. B., "3D printer selection: A decision making evaluation and ranking model", *Virtual and Physical Prototyping*, 2013, 8:3, 201-212
4. Lee, I. and Kim, Y., "The Recent Patent Analysis and Industrial Trend of 3D Printing", *Indian Journal of Science and Technology*, Vol 8(S8), 70-73, April 2015
5. Thompson S. M., Bianc, L., Shamsaei, N., & Yadollahia, A., " An overview of Direct Laser Deposition for additive manufacturing; Part I: Transport phenomena, modeling and diagnostics", *Additive Manufacturing* 8 (2015) 36– 62, <http://dx.doi.org/10.1016/j.addma.2015.07.001>
6. Shamsaei, N., Yadollahia, A., Bianc, L., & Thompson S.M., " An overview of Direct Laser Deposition for additive manufacturing; Part II: Mechanical behavior, process parameter optimization and control", *Additive Manufacturing* 8(2015) 12– 35, <http://dx.doi.org/10.1016/j.addma.2015.07.002>
7. Berman, B., "3-D printing: The new industrial revolution", *Business Horizons*(2012) 55, 155–162
8. <https://www.stratasysdirect.com/manufacturingservices/3d-printing>
9. <https://www.designtechcadacademy.com/knowledgebase/catia-training>
10. <https://grabcad.com/tutorials/catia-v5-basic-tutorial->

DESIGN AND THERMAL ANALYSIS OF ENGINE FINS USING ANSYS

Mrs. P.Sravani, Mr.U.Shanmukharao, Mr.I.Nagulmeeravali, Mr.K.Bhanuprasad, Mr.D.Mahesh Reddy, Mr.K.Johny

*Department of Mechanical Engineering,
Narasaraopeta Engineering College, Narasaraopet, Palnadu(Dist.), A.P., India*

Abstract - Heat transfer is a process variant in most heat generation methods, applying two-wheeler heat conduction fins. IC engine fins Assemblies with in a reacting power transmission Mechanisms in this engine Assembly, which requires heat removal to ensure proper operation. The aim of this project investigates alternative cooling methods for an engine fins Assembly. IC engine fins Assembly temperatures by worth of conduction cooling are needed for operating pressure. Enhanced design Stack Assembly designs which utilize fins, straight fins and internal cooling cavities are required to reduce or eliminate cooling. Steady state heat transfer finite element analyses are performed using Ansys Workbench™ Version 14.5, utilizing 3-D models and heat transfer material properties of current engine fins Assemblies. Ansys results from modified fins Assembly designs are compared to baseline geometry Ansys results. Baseline cooling analyses are performed to validate the FEA models. Then comparing constant natural materials to take AL 6061, AL 200, CE17, CE17M it's considering take thermal distribution analysis in transient conditions to solving problems it's defined. An average temperature reduction of 150°C at the inner surfaces of the fins is achieved using fin arrays with a total additional surface area of 0.16 m² per Fins Stack Assembly. To consider forced convection to solving heat flux with distribution along the distance with respect to time to be calculating with result and discussed.

Keywords – IC Engines, Fins, Ansys

I. INTRODUCTION

Fins are basically mechanical structures which are used to cool various structures via the process of convection. Most part of their design is basically limited by the design of the system. But still certain parameters and geometry could be modified to better heat transfer. In most of the cases simple fin geometry is preferred such as rectangular fins and circular fins. Many experimental works have been done to improve the heat release of the internal combustion engine cylinder and fin efficiency. A numerical investigation has been carried for a finned metal cylinder using CFD and is validated against the experiments carried out. A transient numerical analysis is carried out with wall cylinder temperature of 423 K initially and the heat release from the cylinder is analyzed for zero wind velocity. The heat release from the cylinder which is calculated numerically is validated with the experimental results. In the present paper an effort is made to study the effect of fin parameters on fin array performance which includes variation in pitch and fin material. In addition, the current paper considers the effect of air flow velocity on different fin pitch. With the help of the available numerical results, the design of the internal combustion engine cooling fins can be altered for better efficiency [1].

In this study, the effective thermal conductivity of aluminum filled high-density polyethylene composites are investigated numerically as a function of filler concentration. The obtained values are compared with experimental results and the existing

theoretical and empirical models. The thermal conductivity is measured by a modified hot-wire technique. For numerical study, the effective thermal conductivity of particle-filled composite was calculated numerically using the micro structural images of them. By identifying each pixel with a finite difference equation and accompanying appropriate image processing, the effective thermal conductivity of composite material is determined numerically. As a result of this study, numerical results, experimental values and all the models are close to each other at low particle content. For particle content greater than 10%, the effective thermal conductivity is exponentially formed. All the models fail to predict thermal conductivity in this region. But numerical results give satisfactory values in the whole range of aluminum particle content.

II. PROBLEM IDENTIFICATION

The heat that is generated produced (or) developed in the system that conducts through the walls or boundaries is to be continuously dissipated to the surroundings or environment to keep the system in steady state condition. Large quantities of heat must be dissipated from small area as heat transfer by convection between a surface and the fluid surroundings. It can be increased by attaching thin strips of metals called fins to the surface of the system. In that case the design model of fin is to be changed in various model fin blades

III. METHODOLOGY

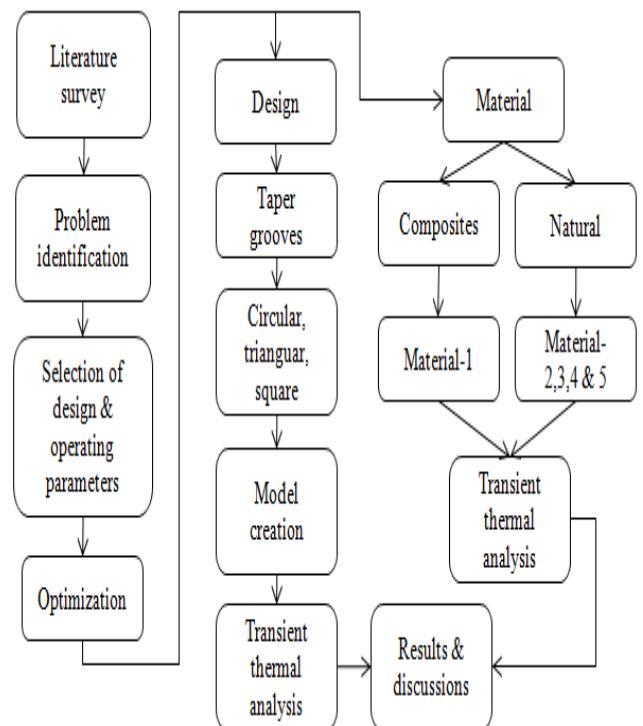


Fig. 1: Block diagram of the Design and Analysis

IV. MATERIALS

Any materials made up of iron with about 2% or more of carbon is cast iron. Most commercial alloys contain from about 2.5% to 3.8% carbon. There are four types of cast iron that are usually produced.

- Aluminum
- Grey cast iron
- Nodular iron
- White cast iron
- Malleable iron

V. MODELING

Fins improve heat transfer in two ways. One way is by creating turbulent flow through fin geometry, which reduces the thermal resistance (the inverse of the heat transfer coefficient) through the nearly stagnant film that forms when fluid flows parallel to a solid surface. A second way is by increasing the fin density, which increases the heat transfer area that encounters the fluid. Fin geometries and densities that create turbulent flow and improve performance also increase pressure drop, which is a critical requirement in most high-performance applications. The optimum fin geometry and fin density combination is then a compromise of performance, pressure drop, weight, and size. A figure-of-merit comparison based on performance, pressure drop, weight, and size among common fin types is described in “Air Cooled Compact Heat Exchanger Design for Electronics Cooling.” Aside from fin geometry, parameters such as thickness, height, pitch, and spacing can also be altered to improve performance. Typically, fin thicknesses vary from 0.004 in (0.1 mm) to 0.012 in (0.3 mm), heights vary from 0.035 in (0.89 mm) to 0.6 in (15.24 mm), and densities vary from 8 to 30 FPI (Fins per Inch).



Fig No :2(a)

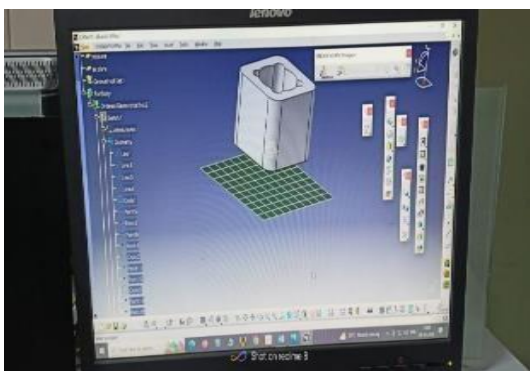


Fig No: 2(b)

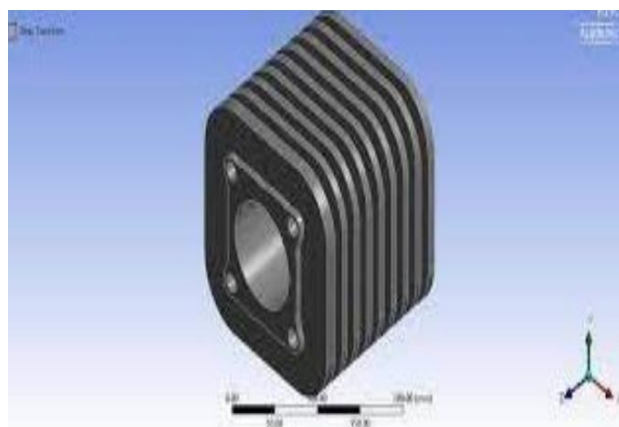


Fig No:2(C) Design of Cylinder Fins

VI. ANALYSIS

A. Meshing

The Engine Fins models are analyzed using ANSYS Workbench Version 14.5 as outlined in Section 2.0. The models are meshed using the ANSYS default settings for path conforming volume with a relevance of 0.5 on a scale of -100 to 100. The resulting mesh is shown in Figure 6. Similar setting the mesh relevance to a maximum of 100 refines the mesh to 185237 nodes and 95422 elements, an almost three-fold increase in number of mesh nodes. The refined mesh is shown in Figure 7. Introducing the Half circle, Triangular, Square, and Trapezoidal. While the default mesh parameters are acceptable, the maximum mesh refinement Table no elements of the different shapes of component. Parameters are used when possible, in order to produce more accurate results. In the convection cooling analyses involving assembly fins, complex model geometries and computing resources available require the models to be reduced to a quarter section of the original geometry. This is acceptable due to the ax symmetric nature of the IC engine Fins -assemblies. The model is conservatively sectioned so that the quarter geometry contains the least cooling surface area of the four quarters possible. Figure 8 shows the plan view of the meshed quarter section model. In all ANSYS cases, the model is first meshed, boundary conditions are applied and then the analysis is performed.

B. FEA model inputs

The FEA model boundary conditions, are calculated in Sections 3.1.1 and 3.1.2 based upon empirical. The intent is to mimic those boundary conditions experienced by the Engine Fins during normal plant operation. It is important to note that heat transfer coefficients are calculated for the regions shown in Figure 5: (1) the internal surfaces of the Pressure Housing, (2) the external surfaces of the Pressure Housing below the Engine Fins, (3) the external surfaces of the Engine Fins and (4) the external surfaces of the Pressure Housing above the Engine Fins. The Engine Fins heat transfer coefficient is calculated by treating the Engine Fins as a flat plate; therefore all four Engine Fins surfaces have the same heat transfer coefficient. Additionally, testing and operating plant data have shown an approximate 210K temperature increase in the cooling air temperature as it passes over the height of the Engine Fins. This 50 °F temperature increase is assumed to occur in a linear fashion such that it is incorporated into the FEA models in 10 °F increments.

C. Conductive Cooling Analyses – fins with optimization shapes in different material

The convective cooling analyses of engine fin cooling effects are performed by applying the heat loads and convective cooling loads on the quarter section ANSYS model Pressure Housing and Engine Fins components including the added engine fins.

Since the amount of convective cooling is dependent on surface area, it is expected that the cooling convective heat transfer will increase as the area increases due to the addition of Engine fins. An increase in cooling convection will result in lower Engine Fins component temperatures. The Engine fin sizes and spacing are shown in Figure 12. The cooling air flow over the external Pressure Housing and Engine Fins surfaces is to be turbulent. It is assumed that the air flow acts on all external surfaces of the Engine Fins.

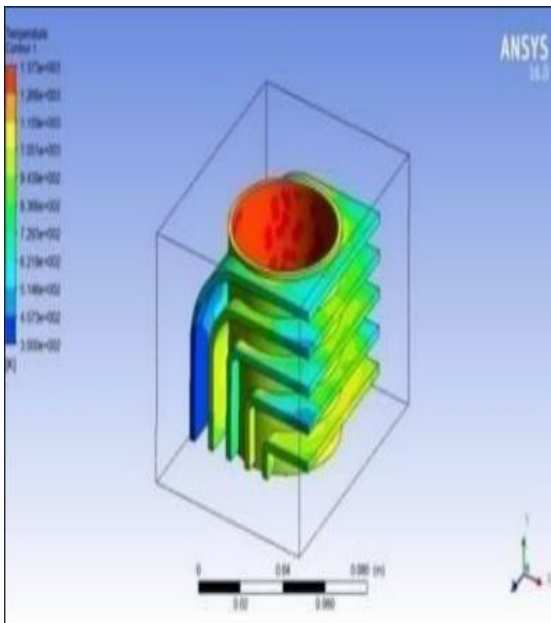


Fig.No:3 Angular Fin

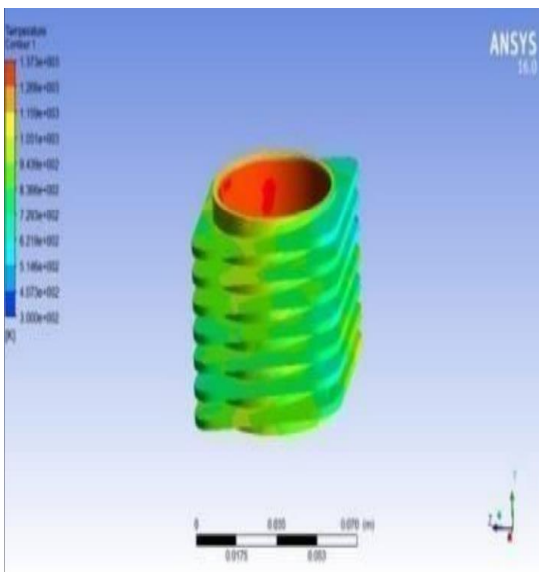


Fig No:4 Curved Fins

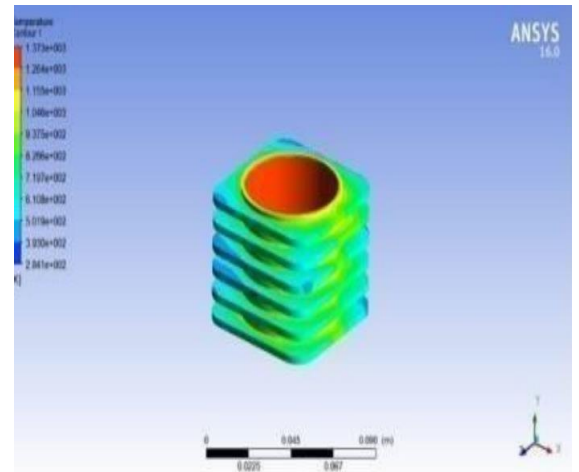


Fig No:4 Rectangular fins

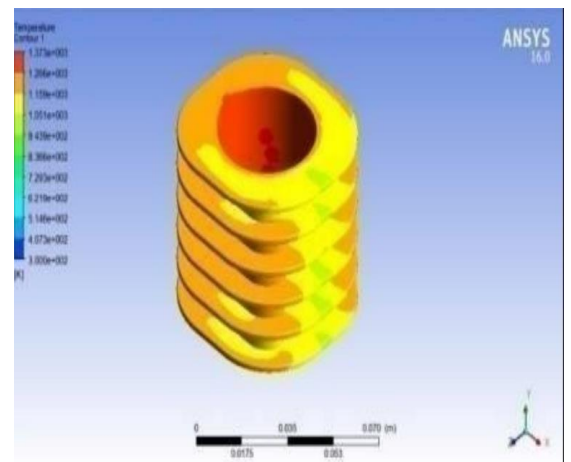


Fig No:4 Cylindrical fins

VII. RESULTS AND DISCUSSION

From the following tabulation the following graphs are drawn and the comparison is carried out for different cross section with shapes on materials. The comparison is carried out for, factor of safety and heattransfer rate.

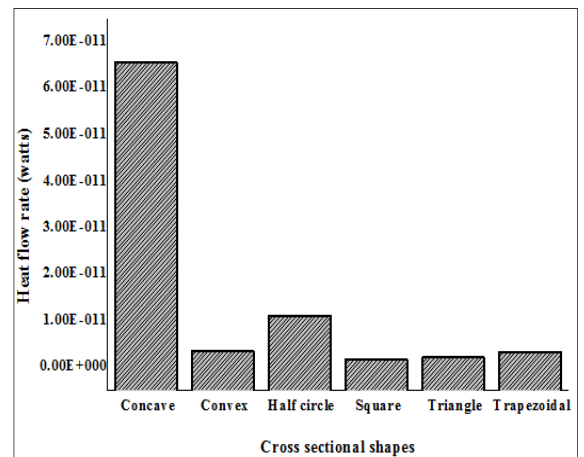


Fig:5 Heat flow rates of AL6061 material for different shapes.

Table No: 1 Results of Thermal Analysis of Fins

	Rectangular	Circular	Curved	Angular
Engine temperature (K)	1200	1200	1200	1200
Heat transfer coefficient (W/m ² K)	1000	1500	1700	1500
Ambient temperature (K)	300	300	300	300
Velocity (m/s)	20	20	20	20
Pressure (atm)	1	1	1	1

VIII. CONCLUSION & FUTURESCOPE

Engine Fins assembly the positions of straight within a reactor core and are vital to the operation of medium air. In order to ensure reliable operation, the of the Engine fins system, a significant amount of heat must be removed from the IC engine fins. This project evaluated several different shapes with material optimization heat removal methods for the using it. IC engine s through utilization of ANSYS finite element analysis software. First, a baseline analysis was performed to verify the FEA model and calculated boundary conditions. Next, conductive cooling apparatuses were analyzed by holding specified surfaces at a constant temperature within the FEA model. Conductive cooling analyses were performed for two cases: a simple apparatus which fit along the flat surfaces of the fin’s walls and a second case in which the apparatus conformed to the external surface profiles of the walls surface. Enhanced convective cooling analyses were then performed to determine the effect of various shapes fin arrays and straight fin arrays on fins coil temperatures. Lastly, an analysis was performed to determine the effect of internal cooling cavities on IC engine coil temperatures. From the analysis the materials it’s best comparing its AL200 compared to AL6061 produces the better thermal behavior than the existing material. Then the best optimization of the shape it find out concave on the best crossection.

Future Scope

The shape of the cylinder fin body is modified and proven analytically that it can be used. But more experiments must be done on that modified model to check the feasibility of the arrangement in the two-wheeler. Since the shape of the fins of modified model is curved, the cost for manufacturing is also to be considered. Since to manufacture this model, if the cost is very high, it is not preferable since it may increase the cost of two-wheeler.

IX. REFERENCES

1. D.G.Kumbhar, et al. “Finite Element Analysis and Experimental Study of Convective Heat Transfer Augmentation from Horizontal Rectangular Fin by

- Triangular Perforations”, Proceedings of the International Conference on Advances in Mechanical Engineering (2009).
2. P.Agarwal, et al. “Heat Transfer Simulation by CFD from Fins of an Air- C o l e d Motorcycle Engine under Varying Climatic Conditions”, Proceedings of the World Congress on Engineering (2011).
3. Yoshida Masao, et al. "Air-Cooling Effects of Fins on a Motorcycle Engine." Nippon Kikai Gakkai Ronbunshu B Hen (Transactions of the Japan Society of Mechanical Engineers Part B)(Japan) 17(9): 2324-2330. (2005).
4. Biermann, A. E. and B. Pinkel.” Heat Transfer from finned metal cylinders in an air stream”, NACA Report No.488.
5. J.C.Sanders, et al. “Cooling test of an air-cooled engine cylinder with copper fins on the barrel”, NACA Report E-103.
6. Denpong Soodphakdee, et al. "A Comparison of Fin Geometries for Heatsinks in Laminar Forced Convection Part 1 - Round, Elliptical, and Plate Fins in Staggered and In-Line Configurations", The International Journal of Microcircuits and Electronic Packaging 24(1). (2001).
7. Fernando Illan and M. Alarcon . "Optimization of Annular Cylindrical and Spherical Fins in an Internal Combustion Engine under Realistic Conditions." Journal of Thermal Science and Engineering Applications 2. (2002).
8. A.Bassam and K. A. Hijleh. "Enhanced Forced Convection Heat Transfer from a Cylinder Using Permeable Fins", ASME Journal of Heat Transfer 125 (2003).
9. C.Han-Taw and C. Jui-Che "Investigation of natural convection heat transfer coefficient on a vertical square fin of finned-tube heat exchangers", International Journal of Heat and Mass Transfer 49(17- 18): 3034-3044. (2006).
10. A.Mohammadi, et al. "Analysis of local convective heat transfer in a spark ignition engine", International Communications in Heat and Mass Transfer 35. (2008).

THE EFFECT OF TITANIUM OXIDE (TiO₂) NANO LUBRICANT ON THE PERFORMANCE OF SINGLE CYLINDER DIESEL ENGINE

P.SrinivasaRao, K.ParameswaraRao, G. ChandraSekhar, CH.Lakshmi Sumanth, Sk.Jilani, P.Ameer Khan
*Department of Mechanical Engineering,
 Narasaraopeta Engineering College, Narasaraopet, Palnadu (Dist.), A.P., India*

Abstract -This work aims to characterize TiO₂-SAE 20W40 engine oil nanolubricant and its performance evaluation in 4- stroke diesel engine. Dynamic light scattering test display the presence of mild agglomeration of particles in nanolubricants. Density and viscosity of nanolubricants are measured with varying particle volume fraction and temperature. The overall performance of nanolubricant is tested on a 4-stroke diesel engine. The nanolubricant with 0.2% mass fraction of TiO₂ nanoparticles shows less frictional power loss and hence higher brake thermal efficiency as compared to other nanolubricants. Increases the engine life. Diesel engines are widely being used in heavy machinery and automobiles due to high power production, high thermal efficiency, and fuel economy. Increase in use of diesel fuel consumption, which also contribute in the depletion of environment and natural fuel sources, put forward a need of efficient utilization of it. Viscosity of base lubricant is significantly modified with the dispersion of nanoparticles. Frictional energy losses inside an internal combustion engine arise from shearing force of lubricant films, which are influenced by the viscosity of the lubricant. The variation of density of TiO₂ - 20W40 nanolubricants with nanoparticles mass fraction is almost uniform. Experimental results of viscosity TiO₂- engine oil nanolubricants do not follow the classical models for viscosity prediction.

Keywords – *Engine oil, four stroke single cylinder diesel Engine.*

I. INTRODUCTION

Diesel engines are widely being used in heavy machinery and automobiles due to high power production, high thermal efficiency and fuel economy. Increase in use of diesel fuel consumption, which also contribute in the depletion of environment and natural fuel sources, put forward a need of efficient utilization of it. widely investigated to enhance the base oil's thermo physical properties. A number of metallic oxide nanoparticles such as alumina (Al₂O₃), silicon oxide (SiO₂) and titanium oxide (TiO₂) has been dispersed in lubricating and engine oils, and a comprehensive study of their effect on, thermophysical and combustion performance has been performed in recent studies., in which Mn showed better performance by increasing cetane number and reducing exhaust gases, viscosity. Viscosity of base lubricant is significantly modified with the dispersion of nanoparticles. Frictional energy losses inside an internal combustion engine arise from shearing force of lubricant films, which are influenced by the viscosity of the lubricant. Engine bench test with nanolubricant display actual performance. Single cylinder diesel engine oil by dispersing titanium oxide

(TiO₂) nanoparticles with results showing that dispersion of 1.5wt% of TiO₂ nanoparticles displayed significant improvement in fuel consumption and throttle position by 2.75 and 3.87%, respectively. Whereas, when TiO₂ nanoparticles were dispersed

in jatropha biodiesel 5% increase in brake thermal efficiency. A similar study has also been performed for biodiesel prepared from jatropha oil by dispersing TiO₂ nanoparticles and CNT. The results shows 15% decrease in heat release with 4% increase in brake thermal efficiency .

Dispersion of graphene in lubricating oils has shown significant increase in thermal properties but only in optimum concentration range of graphene nanoparticle volume fraction as after certain concentration value, the solution shows agglomeration of graphene which contributes in decrease of lubricating properties by forming lumps between the surfaces and causing high friction and wear.

Dispersion of multi-walled carbon nano tubes has considerably improved the engine oil performance by increasing the brake thermal efficiency by 16% along with decreasing fuel consumption by 15% and reducing harmful gas emissions 1% fuel economy has also been achieved by dispersion of MoS₂ nanoparticles in engine oil. Several comparative studies have also been performed to compare different nanoparticle additives. performed the comparative 2 study by dispersing TiO₂ nanoparticles in engine oil (SAE 20W40) and found 0.4% enhancement in brake thermal efficiency. nanoparticles showing better results. Another comparative study was also performed taking TiO₂ nanoparticle 0.4% (nanoparticles, respectively).

Also a maximum 7% improvement in fuel consumption is also obtained in case of TiO₂ nanoparticles In the present work, SAE 20W40-engine oil nanolubricant is characterized and tested in a single cylinder diesel engine rig. Aging test is performed to test stability of nanolubricant.

FTIR spectra of nanolubricants ensure its chemical stability.. Density and Viscosity of nanolubricant are tested by varying the temperature and nanoparticle volume fraction. In addition, viscosity of nanolubricants is also tested with varying shear rate. Single cylinder diesel engine test has been used to test the brake thermal performance of nano lubricants.

2. Characterization of nanolubricant

Titanium oxide (TiO₂) nanoparticles (M/s Alfa Aesar) having nominal diameter of 45 nm and density 3.965 g/cc are used in present study. The morphology of nanoparticles as observed from FESEM is spherical along with particle diameter of around 42–45 nm, which is in agreement with size (40 nm) quoted by the supplier as shown in Fig. 1. Moisture content in nanoparticles affects their miscibility in lubricant; therefore, it is removed by drying them in an oven at 80–100 for half an hour.

TiO₂ nanoparticles with volume fraction ranging from 0.3 to 1.5% are dispersed in engine oil to formulate the nanolubricants. Appropriate mass of TiO₂ nanoparticles for each volume fraction is measured by an electronic weighing machine with a least count of 0.001 mg. SAE 20W40 engine oil is a commercial lubricant which contains some dispersant and hence no additional dispersant is used.

Homogenization of nanoparticles in base oil is done by magnetic stirring for 1h at 500 rpm. To increase the stability and prevent agglomeration of nanoparticles which affects the nanolubricant's properties, nanolubricants are subjected to 1 h ultrasonication (20 kHz) to deagglomerate nanoparticles. The test samples were cleaned by toluene to remove any oil content and after that samples were kept in a heater at 80–100 to vaporize the solvent. The morphologies of TiO₂ nanoparticle in plain and dispersed state. It can be observed that TiO₂ nanoparticles retain their spherical morphology even after dispersion in SAE 20W40 engine oil base lubricant.

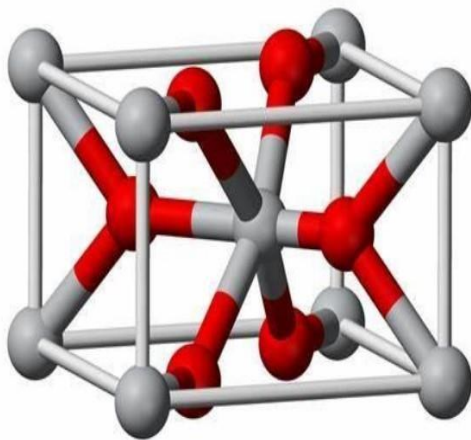


Fig:1 TiO₂(titanim oxide)

3. performance test

Performance test were conducted on a single cylinder 4-stroke diesel engine test rig with rated power of 5HP at 3000 RPM and was connected with an electrical transmission The schematic diagram and actual image of the engine test setup. The detailed specification of engine is reported in Table 1. Experiments are performed in a controlled environment of a laboratory with specification as: temperature 25 C, pressure 1 bar, RH 80%. Initially test was performed with plain engine oil, then Nanolubricant are used in increcingmental nanoparticles volume fraction. Measurements were taken out at steady state. To avoid the heating effects of consecutive testing, an interval of 1 h is taken between two convective tests. The uncertainty in the experimental measurements defined as the error may arise from the instrument type, calibration and observation.

Assume a set of measurements are made and this measurements are used to calculate the desired results of the experiments. To estimate the uncertainty in the calculated result on the basis of uncertainties in the primary experiments, the methodology adopted was this: The result R represents the given function of the independent variables X₁, X₂, X₃,... X_n. Thus, $R = R(X_1, X_2, X_3, \dots X_n)$. W_R is the uncertainty in the result and W₁, W₂, W₃,... W_n are the uncertainties in the independent variables. The percentage of uncertainty of various parameters was calculated by the above mentioned. 4. Engine performance has been tested with plain 20W40, 0.2, 0.4 and 0.6% SAE-20W40 nanolubricants. The overall variation in frictional power can be interpreted from the intercepts of fuel consumption characteristics with the brake power abscissa.

Hence, to obtain the intercept at brake power abscissa for fuel consumption characteristic curves are extrapolated. Figure shows the variation of fuel consumption with brake at different loads. It has been observed that 0.3% of SAE - 20W40 nanolubricant shows substantially reduction in frictional power as compared to plain 20W40 and other nanolubricant. The reason may be the presence of spherical TiO₂ nanoparticles contributed in the ball bearing and mending effect.

However, at higher nanoparticle volume fraction, viscous friction starts dominating. the variation in Brake specific fuel consumption (BSFC) at different brake power. It has been observed from the figure that the BSFC decreases with increase in brake power. It has been observed that 0.2% of SAE-20W40 nanolubricant shows least BSFC, because it produces higher brake power with lesser fuel consumption.

It has been observed form figure that the brake thermal efficiency increases with increasing in brake power. In addition, 0.3% of TiO₂- 20W40 nanolubricant. shows higher brake thermal efficiency compared to plain 20W40 and other nanolubricant.

4. Engine Specefications:

- Make - kirloskar Bore - 80mm
- Stroke - 110mm
- Rated speed - 1500rpm
- Max B.P - 3.7kw (5H.P)
- Compression ratio - 16.5:1
- Orifice diameter - 20mm
- Fuel - Diesel
- Density of diesel - 827Kg/ m³,
- Specific gravity of diesel - 0.827
- Calorific value of diesel - 43400 kj/kg
- Brake drum diameter - 360mm
- Rope diameter - 12mm
- Equivalent diameter - 375mm
- Coefficient of discharge - 0.62



Fig:2 actual engine experimental test rig

CONCLUSION

In the present study, the thermo physical properties of SAE-20W40 nanolubricants with varying nanoparticles volume fraction and temperature have been discussed.

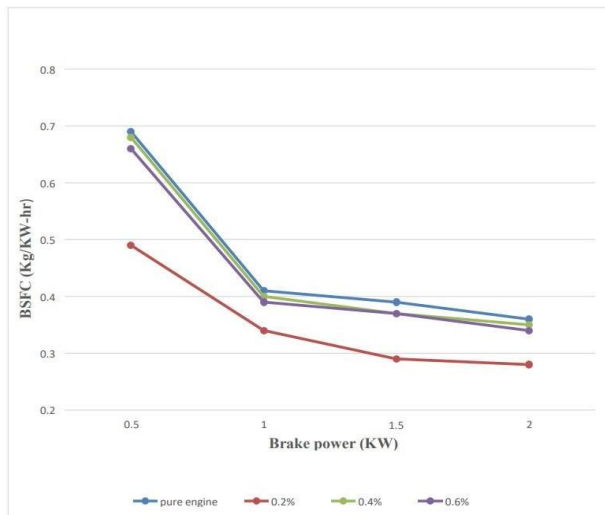


Fig:3 variation of brake specific fuel consumptions with brake power

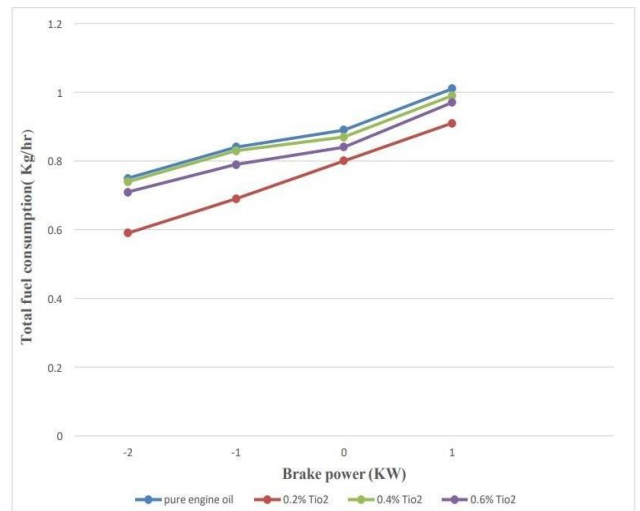


Fig :5 variation of fuel consumption with brake power

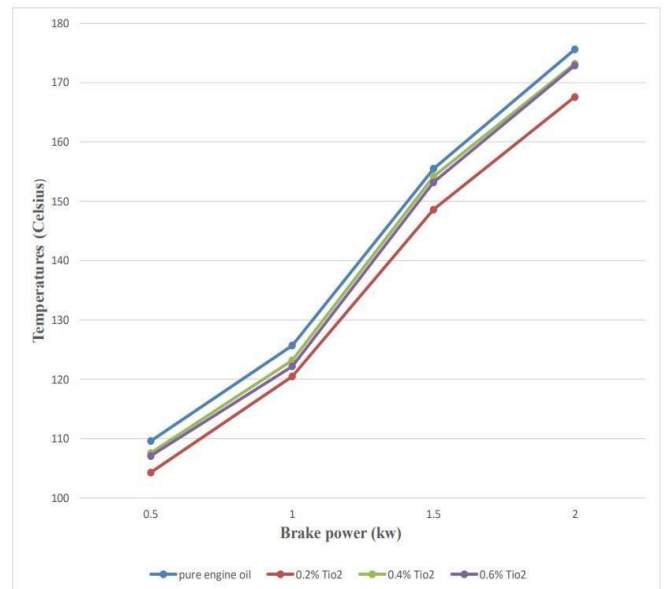


Fig :6 variation of exahust temperature with brake power

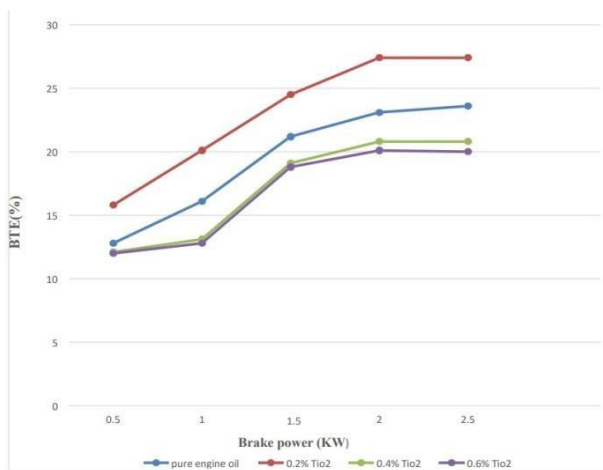


Fig: 4 variation of brake thermal efficiency with brake power

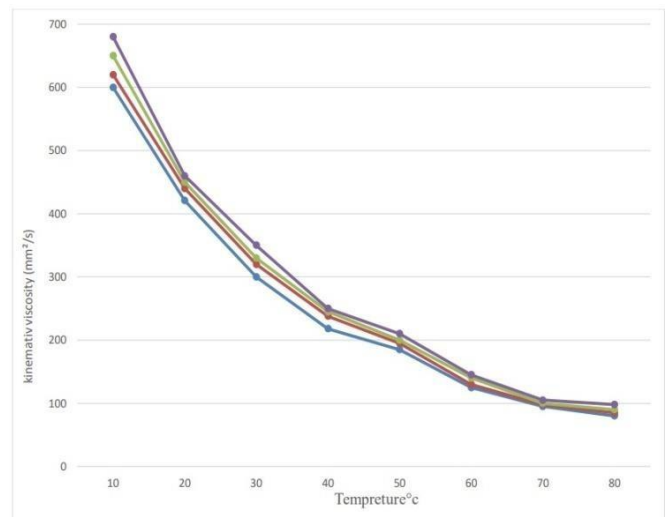


Fig :7 variation of kinematic viscosity with temperature

- In the present study, the thermophysical properties of TiO₂-20W40 nanolubricants with varying nanoparticles volume fraction and temperature have been discussed.
- The performance evaluation of nanolubricant has also been tested in a 4-stroke diesel engine. The test observations are as follow.
- The variation of density of TiO₂ - 20W40 nanolubricants with nanoparticles mass fraction is almost uniform. Experimental results of viscosity TiO₂-engine oil nanolubricants do not follow the classical models for viscosity prediction.
- 0.2% of TiO₂- 20W40 nanolubricant shows substantially reduction in frictional power. This resulted in higher brake thermal efficiency of 0.2% of TiO₂-20W40 nanolubricant as compared to other lubricants.
- Less fuel consumption of comparing to other lubricants.
- Increase the engine life.

12. Holman JB (2004) Experimental techniques for engineers. TataMcGraw Hill, New Delhi. 41 Luo T, Wei X, Huang X, Huang L, Yang F (2014) Diesel operties of TiO₂ nanoparticles as lubricating oil additives. *CeramInt* 40(5):7143–7

REFERENCE

1. Spikes H (2008) Low-and zero-sulphated ash, phosphorus and sulphur anti-wear additives for engine oils. *Lubr Sci* 20(2):103–136.
2. Mehta RN, Chakraborty M, Parikh PA (2014) Nanofuels: combustion, engine performance and emissions. *Fuel* 120:91–97.
3. Mohan N, Sharma M, Singh R, Kumar N (2014) Tribological properties of automotive lubricant SAE 20W-40 containing nano TiO₂ articles. SAE technicalpaper.
4. Kotia A, Ghosh SK (2015) Experimental analysis for rheological properties of aluminium oxide (TiO₂)/gear oil (SAE EP-90) nanolubricant used in HEMM. *Ind Lubr Tribol* 67(6):600–605.
5. Vasheghani M, Marzbanrad E, Zamani C, Aminy M, Raissi B, Ebadzadeh T, Barzegar-Bafrooei H (2011) Effect of TiO₂ phases on the enhancement of thermal conductivity and viscosity of nanofluids in engine oil. *Heat Mass Transfer* 47(11):1401–1405.
6. Shenoy BS, Binu KG, Pai R, Rao DS, Pai RS (2012) Effect of nanoparticles additives on the performance of an externally adjustable fluid film bearing. *Tribol Int* 45:38–42.
7. Patil SJ, Patil DP, Shrotri AP, Patil VP (2014) A review on effect of addition of nano particles on tribological properties of lubricants. *Int J Mech Eng Technol* 5(11):120–129.
8. Mariano A, Pastoriza-Gallego MJ, Lugo L, Mussari L, Pinheiro MM (2015) Co₃O₄ ethylene glycol-based nanofluids: thermal conductivity, viscosity and high pressure density. *Int J Heat Mass Tfransfer* 85:54–60.
9. Wasp EJ, Kenny JP, Gandhi RL (1978) Solid-liquid flow slurry pipeline transportation. *Bulk Mater Handl* 1:56–58. Batchelor GK (1977) The effect of Brownian motion on the bulk stress in a suspension of spherical particles. *J Fluid Mech* 83:97–117.
10. Rashin MN, Hemalatha J (2013) Synthesis and viscosity studies of novel ecofriendly ZnO– coconut oil nanofluid. *Exp Thermal Fluid Sci* 51:312–318.
11. Lue Y-F, Hung Y-H, Li F-S, Teng T-P, Chen S-Y, Wu C-H, OuY-C (2016) Performance assessment and scooter verification of nano-alumina engine oil. *Appl Sci*6(9):258.

FABRICATION AND ANALYSIS OF TRANSMISSION SYSTEM FOR ELECTRIC VEHICLE

M.Venkanna Babu, R. Sivanjaneyulu, Y. Rakesh, R. Surya Prakash, G. Venkata Bhaskar, E. Ashok
*Department of Mechanical Engineering,
 Narasaraopeta Engineering College, Narasaraopet, Palnadu (Dist.), A.P., India*

I. BASIC DESIGN

Abstract - Electric vehicles use electricity to charge their batteries instead of using fossil fuels like petrol or diesel. Electric vehicles are more efficient, and that combined with the electricity cost means that charging an electric vehicle is cheaper than filling petrol or diesel for your travel requirements. The power generated in the electric vehicle motor is transferred to a drive wheel via gearbox. The EV uses single-speed transmission because the motor is efficient in wide range of condition. Electric cars do not require multi-speed transmissions because of the so-called "engine" in an electric car, an electric motor.

This project work, includes the study of the components of transmission system and assembling the transmission system in golf cart electric vehicle by using the components. The 2D and 3D modelling is being done by using catiaV5 Software. The present analysis of transmission system components consists of top speed, acceleration and time, total tractive effort, rolling resistance, grade resistance, distance. From this project obtained the knowledge of components of transmission system of golf cart vehicle.

I. INTRODUCTION

The Engine of a conventional IC Engine Car is replaced by an electrical Motor and the fuel tank is replaced by the Battery Pack. Of all the components only the Battery Pack and Motor alone contributes to about more than 50% of the total cars weight and the price. As you can see the Battery Pack, Battery Management System (BMS) Controller, Motor and the Transmission unit forms the major components in an EV.

The Battery Pack is the fuel source of the car, since there are hundreds of cells arranged to form a battery pack a special circuit is required to monitor these cells, this circuit is called as the Battery Monitoring circuit.

The DC voltage from battery cannot be used to drive a motor we need the controller which drives the motor, and the Transmission system transfers the rotational energy from motor on to the wheels through some gear arrangements. A single lithium cell voltage and Ah rating is not enough to drive an EV, so these cells are connected in series and parallel configuration to increase the resulting system voltage. This pack is called as a module. For people who are new to batteries the term.

For now, you can think of Ah as the fuel range of an EV more the Ah more the mileage we can get out of there. Now that we have known about Batteries in EV the follow up would be to know about battery Management system. Transmission system transfers the rotational energy from motor on to the wheels through some gear arrangements.

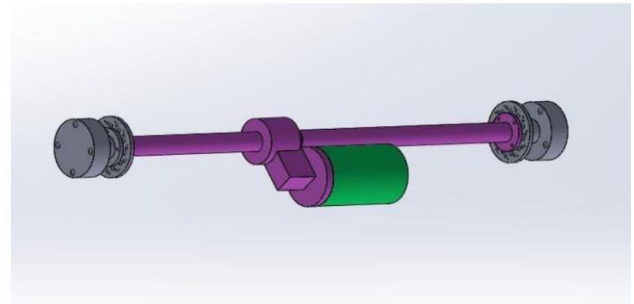


Fig.1: Basic design of Transaxle with motor disc brake & hub assembly

As mentioned above, the EVs have only one driving gear because an electric induction motor is efficient from 0 RPM all the way up to around 6,000 RPM (a speed which a car will perhaps never need to run at!). The opposite of ICs, induction motors generate most of their torque, which is needed for acceleration, at 0 RPM, and are most efficient at power generation at high RPM, which is needed for cruising. In a frictionless world, it would be helpful – but still not necessary – for an EV to have multiple gears, as fuller advantage could be taken of the motor's peak efficiency.

II. COMPONENTS OF TRANSMISSION SYSTEM



Fig.2: Controller

The main objective for the speed controller is, as the name implies, to control the vehicle speed. Any time you apply throttle, the full battery current and voltage is sent to the motor. doing this would cause violent take-offs, bad enough your neck would snap back. This would be awesome on the race track, but dangerous in a neighborhood.

Every time you hit the gas you would only get full battery power. If your golf cart is running an Ac Brushless DC motor, you will not be going anywhere without a speed controller. In these specific types of motors, electrical signals fire back and forth. This must stay consistent, and must be timed precisely with the motor's rotation.



Fig 3: Motor

Electric motors may be classified by considerations such as power source type, construction, application, and type of motion output. They can be powered by AC or DC, be brushed or brushless, single-phase, two-phase, or three-phase, axial or radial flux, and may be air-cooled or liquid-cooled.

An electric motor is an electrical machine that converts electrical energy into mechanical energy. Most electric motors operate through the interaction between the motor's magnetic field and electric current in a wire winding to generate force in the form of torque applied on the motor's shaft.



Fig 4: Batteries

A battery is a source of electric power consisting of one or more electrochemical cells with external connections for powering electrical devices. When a battery is supplying power, its positive terminal is the cathode and its negative terminal is the anode. The terminal marked negative is the source of electrons that will flow through an external electric circuit to the positive terminal.

A battery consists of some number of voltaic cells. Each cell consists of two half-cells connected in series by a conductive electrolyte containing metal cations. One half-cell includes electrolyte and the negative electrode, the electrode to which anions (negatively charged ions) migrate; the other half-cell includes electrolyte and the positive electrode, to which cations (positively charged ions) migrate.



Fig 5: Battery Rechargeable Machine

Charge your batteries for 8 to 10 hours with the proper style of golf cart battery charger. The best practice is to charge overnight after you are done using your cart for the day. Even if you only used the cart for 5 min, you will want to give the golf cart batteries a good charge. Rechargeable batteries typically initially cost more than disposable batteries but have a much lower total cost of ownership and environmental impact, as they can be recharged inexpensively many times before they need replacing. A rechargeable battery, storage battery, or secondary cell is a type of electrical battery.



Fig 6: DC to DC Converter

A DC-to-DC converter is an electronic circuit or electromechanical device that converts a source of direct current (DC) from one voltage level to another. It is a type of electric power converter. Power levels range from very low. DC-to-DC converters are used in portable electronic devices such as cellular phones and laptop computers.

DC-to-DC converters which are designed to maximize the energy harvest for photovoltaic systems and for wind turbines are called power optimizers. Transformers used for voltage conversion at mains frequencies of 50–60 Hz must be large and heavy for powers exceeding a few watts. In these DC-to-DC converters, energy is periodically stored within and released from a magnetic field in an inductor or a transformer, typically within a frequency range of 300 kHz to 10 MHz.

III. MODELLING OF DIFFERENTIAL BYCATIA V5 SOFTWARE



Fig 7: Physical Switches

We placed the kill switch next to where the passenger sits for easy access for the user just in case a problem occurs. If the key is turned counter-clockwise, the key will be disconnected from the system, which turns off the motor. The wireless kill switch is mounted next to the series batteries and the parallel charger.

We used the double-sided tape in order to secure the component. If the user holds down the button on the remote, the motor circuitry is disconnected and the cart is unable to accelerate. The wireless kill switch is mounted next to the series batteries and the parallel charger. Physical kill switch mounted in place, as well as the remote kill switch hanging off it.

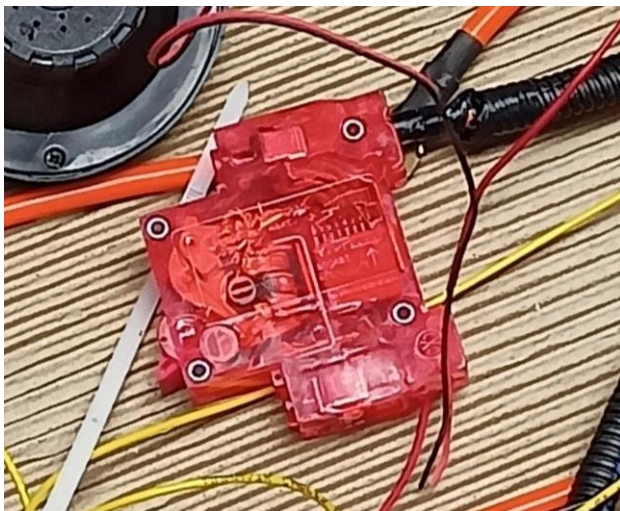


Fig 8: Miniature Circuit Breaker

An MCB works by detecting the current flowing through an electrical circuit. If the current exceeds the maximum level set for the MCB, it will automatically trip and interrupt the circuit. The right MCB for a specific application depends on factors such as the current rating of the circuit, the type of load being powered, and the type of protection required.

It is important to consult with a qualified electrician or engineer to determine the appropriate MCB for a specific application. There are several types of MCBs available, including thermal magnetic MCBs, electronic MCBs, and adjustable trip MCBs.

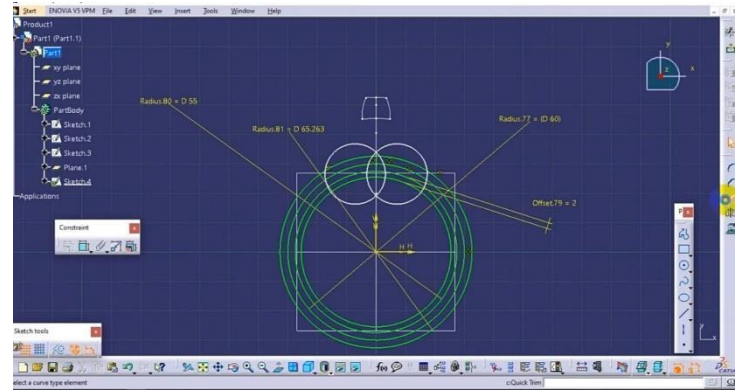


Fig 9: 2D Design

Dimensions Of Design:

- Diameter of outer circle – 65mm
- Diameter of middle circle – 60mm
- Diameter of inner circle – 55mm
- Length – 20mm
- Angle between two circles – 45
- Offset distance between 2 circles – 30mm

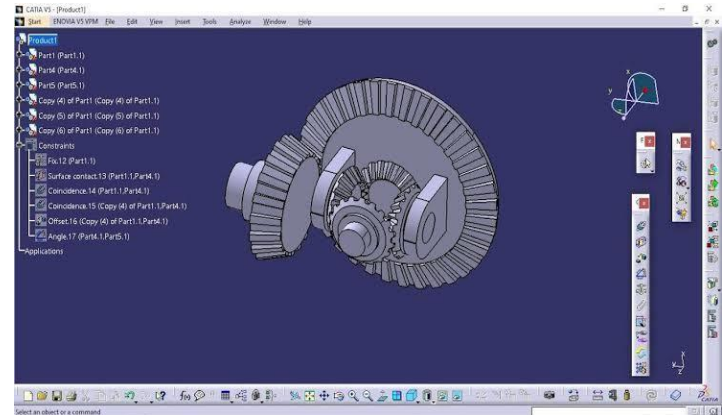


Fig 10: 3D Model of Differential

Before starting the actual design, it is essential to define the requirements of the differential, such as its load capacity, torque transfer, and gear ratios. Software is used to increase the productiveness of the clothier, improve the great of layout, improve communications via documentation, and to create a database for production. D output is frequently within the form of digital documents for print, machining, or other manufacturing operations.

The term CADD is also used. CATIA V5 provides a scalable platform for collaborative product creation and product data management. It offers highly intuitive tools to create, modify, and validate any freeform and mechanical surfaces. Start by creating the main body of the differential using a 3D modeling tool. Use sketches, extrusions, and other geometry tools to create the basic shape of the differential. Once the main body is created, add the gears to the differential. You can use the "gear" tool in CATIAV5 to create spur or helical gears, or import pre-made gear models. Place the gears in their respective positions based on the required gear ratios.

IV. ASSEMBLE OF TRANSMISSION SYSTEM TO ELECTRIC VEHICLE

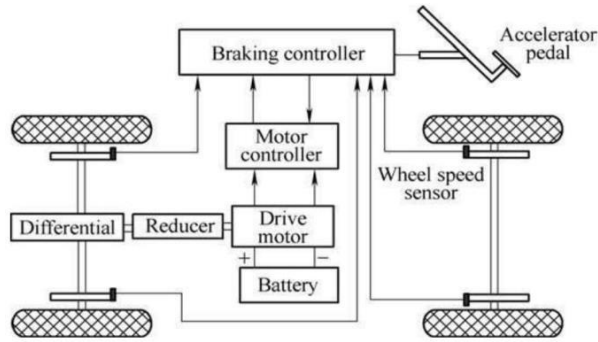


Fig 11: layout of transmission system

A transmission is a system which transmits power and provides controlled application over that power. In layman terms a transmission usually consists of a set of a gearbox that uses gears and gear trains to provide speed and torque conversions from a rotating power source to the output. The main components of our transmission assembly are Transaxle, Motor, and its Controller.

1. Motor – 4kw Dc brushed 3000 rpm (set rpm for transaxle ratio) 14 Nm torque
2. Transaxle with reduction ratio 10.45
3. Curtis’s controller

	Parameter	Values
1	Available Battery Voltage	48V, 60V,72V
2	Available Motor Power	1.2KW - 5KW
3	Phase Peak Current (Few Seconds)	210 A (The bigger, the higher torque)
4	Continue Current	40 A Peak 80A
5	Available Motor Angle	60 / 120
6	Working Frequency	15.6KHz
7	Working Efficiency	< 90 %
8	Control Method	Throttle; Potentiometer (Customized)
9	Default Throttle Working Voltage Range	0.8V - 3.8V, others have to customized
10	Mosfet’s /Pieces	Domestic 24 Tubes
11	Case Material / Color	Aluminum /Sliver

Fig 12: Controller Specification

The 4kw BLDC motor drive is a high performance, cost-effective 3phase BLDC motor drive, which can provide power output Max 210 ah. The design is based on advanced DSP technology and feature high torque, low noise, low vibration, PID speed loop, PID current loop, over current protection, over load protection and a combined use of manual speed adjustment and automatic speed adjustment. These motor controllers are used to control the speed output and rpm set of the motor.

V. RESULT AND ANALYSIS

1. TOPSPEED CALCULATION:

INPUTS:

Rpm of Motor = 3000rpm.

Transaxle reduction = 10.45.

Rpm of Wheel = $\frac{\text{Rpm of Motor}}{\text{Transaxle reduction}}$

$$= \frac{3000}{10.45} = 287.081 \text{ rpm} \dots\dots (1)$$

Rpm / 60 = rps hence

$$= \frac{278.081}{60} = 4.78\text{rps} \dots\dots (2) \text{ [Speed =Rps x Circumference of the tire]}$$

Speed = 4.78 × (π × 18 × 25. 5/ 10 00 × 0.95)

$$\text{Top Speed} = 6.53 \text{ m/s or } 23.5 \text{ km/hr}$$

OUTPUT = 23.5 km/hr

2. ACCELERATION & TIME FOR IT:

INPUTS:

- Front area of the golf cart = (1825x1200 mm) height x breadth
- Motor torque – 14 Nm
- Reduction ratio – 10.45

Torque on wheel = Motor torque x Total gear reduction

$$\text{ratio } T = 14 \times 10.45 = 146.3\text{Nm} \dots\dots (3)$$

Now using formula

Torque on wheel = Force x Radius of tire Where,

$$\text{Radius of tire} = 9 \times 0.95 \times 25.4/1000=0.21717\text{m}$$

Therefore,

$$F = T/R = 146.3/0.21717 = 673.66\text{N} \dots (4)$$

Total resistance losses = Rolling resistance + aerodynamic resistance

$$= \mu mg + 1/2 \rho Av^2cd$$

$$= 0.04 \times 950 \times 9.81 + 0.5 \times 1.2 \times 2.16 \times 6.53^2 \times 0.4$$

$$= 394.88 \text{ N}$$

$$s = u t + 1/2 at^2$$

where, S is distance expressed in meters

Since initial velocity is 0,

$$s = 1/2 at^2$$

$$s = 1/2 * 0.295 * 22.13^2$$

$$= 72.23\text{m}$$

OUTPUT = 72.23m

3. TOTAL TRACTIVE EFFORT CALCULATION:

Gross vehicle weight (Gawk) - 500kg

Weight on each drive wheel 118kg/1165N

Radius of wheel r - 9inch 43

Top speed - 23.05km/h

Acceleration time - 22.13s

Inclination gradient -20%

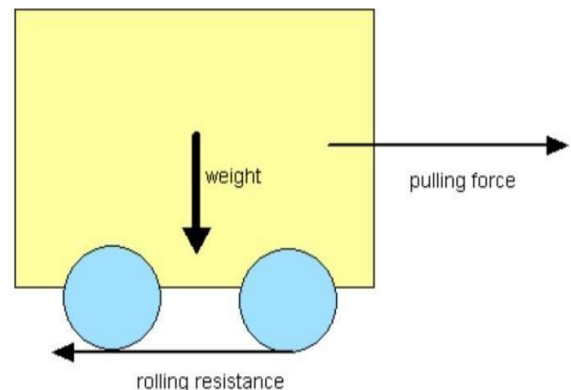


Fig 13: Force & Resistance Direction

4. DETERMINING GRADE RESISTANCE (GR):

$$Gr = Gvw \times \sin \alpha$$

where α is inclination considered 20% in this case $Gr = 950 \times \sin (20) = 324.91 \text{ kg} \times 9.81 = 3187.45\text{N}$

$$Gr = 3187.45\text{N}$$

OUTPUT = 3187.4N

5. TOTAL TRACTIVE EFFORT CALCULATION:

The Total Tractive Effort (TTE) is the sum of the forces calculated in steps 1, 2, and 3

[Rolling resistance + Gradient Resistance + Acceleration force]

$$465.97 + 3187.45 + 280.25 = 3933.67\text{N}$$

$$\text{TTE} = 3933.67$$

OUTPUT = 3933.67N

6. DETERMINING THE TORQUE REQUIRED ON THE WHEEL (TW):

$$Tw = \text{TTE} \times r \times Rf$$

Where, r is radius

Rf is Resistance factor (between 1.1-1.15) losses between caster wheel's axles and bearings

$$Tw = 3933.67 \times 0.229 \times 1.12 = \mathbf{1008.97\text{Nm}}$$

FINAL OUTPUT VALUES:

Parameters	Results
Top speed of golf cart	23.5 km/h
Force transmitting	278.78N
Acceleration	0.295 m/s ²
Time	22.13s
Distance	72.23m
Total Tractive Effort	3933.67N
Grade Resistance	3187.45N
Rolling Resistance	465.97N

Fig 14: Results

VI. CONCLUSION & FUTURE SCOPE

In this project transmission system in golfcart electric vehicle is assembled. The 3d modelling of a transmission system by using Catia and studied the components of transmission system in electric vehicle, by using this component assembled the golf cart electric vehicle is done successfully. From this analysis of the transmission system, top speed, acceleration and time, total tractive effort, rolling resistance, grade resistance, torque required on the wheel is well calculated successfully. From this project the top speed of the vehicle is 23.5 km/h, Battery capacity is 12V * 4, Weight of the vehicle is 500KG, Seating capacity of the vehicle is 06 and Mileage of the vehicle is 80kmph. Acceleration and time of the vehicle is 22.13s, total tractive effort of the vehicle is 3933.6N, grade resistance of the vehicle is 3187.45N, rolling resistance of the vehicle is 465.97N Is done Successfully.

1. Increased range: One of the main limitations of current golf cart electric vehicles is their limited range. Future advancements in battery technology and vehicle design may allow for longer ranges and more efficient use of energy.

2. Improved performance: With advances in electric motor technology and vehicle design, golfcart electric vehicles could become faster, more powerful, and better suited for a wider range of applications.

3. Autonomous operation: As self-driving technology becomes more advanced and affordable, it is possible that golf cart electric vehicles could become fully autonomous, allowing for more efficient and convenient transportation around golf courses, resorts, and other areas.

VII. REFERENCES

[1] Saiful Hasan (2021) attempted to predict consumer intent to purchase electric vehicles. Consumer satisfaction with EV benefits, such as cost, range, recharge, policy measure, environmental qualities, symbolic attributes, and model availability motivate consumers to repurchase EVs, according to the study.

[2] Varghese (2021) and others investigated consumer perceptions of electric vehicles in India, as well as their purchase intentions. According to the findings, increased awareness leads to EV perception development. Environmental benefits and government programs for environmental improvement are well known among consumers.

[3] Parmar and Pradhan (2021) identify consumer knowledge and decision criteria for purchasing an electric vehicle. According to their research, most customers are aware of the internet as a key source of information in addition to television and newspapers.

[4] Selva and Arimachi (2020) set out to determine customer perceptions of electric vehicles and the global market, as well as the effectiveness of electric vehicles and their global market.

[5] Ankita Nagpal (2020) attempts to uncover consumer perceptions of electric vehicles in the Indian setting in her study. The study's goal is to look at the elements that influence consumer purchasing intent. lower maintenance costs, and government measures to incentivize consumers all contribute to higher purchase intent.

[6] Rajper S. Z. (2020) and colleagues analyzed the literature on electric vehicle potential in poor nations. The study investigated electric two-wheelers (E2Ws), hybrid vehicles, and electric four-wheelers (E4Ws). E2Ws are more affordable for developing countries due to their low purchase price and low operating costs

[7] Monica and Mifzala (2019) investigated customer perceptions in Bangalore by learning about their attitudes, feelings, and perceptions. The researchers discovered the level of EV knowledge and the elements that influence client purchase decisions.

DESIGN & FABRICATION OF BRAKING SYSTEM FOR ELECTRIC VEHICLE

D.Jagadish, SK.Dastagiri, K.Akash, SK.TH.Mastan Vali, P.Rajesh, Y.Rajesh
*Department of Mechanical Engineering,
 Narasaraopeta Engineering College, Narasaraopet, Palnadu (Dist.), A.P., India*

Abstract - Present work deals with design and fabrication of an electric vehicle with the available parts. The work is carried out at mechanical engineering lab with the main aim of making the electric vehicle of 6 seating capacity with pay load of 800 kg. The weight of the vehicle is 500 kg. The aim of this project is to design the braking system of electric vehicle. The vehicle is having four wheels and the brakes are provided at back two wheels. The brakes used are drum type. The length of the brake and the effort required to stop the vehicle are calculated. The vehicle is running at speed of 20 mph, and the torque of the vehicle is estimated as 30 Nm. The effort of brakes is thus analysed and the brakes are arranged. The brake length obtained as 32 mm. Heat generated through the braking also estimated as 133 J.

I. INTRODUCTION

An Electric vehicle (EV) is a vehicle that uses one or more electric motors for propulsion. It can be powered by a collector system, with electricity from extravehicular sources, or it can be powered autonomously by a battery (sometimes charged by solar panels, or by converting fuel to electricity using fuel cells ora generator).

EVs include, but are not limited to, road and rail vehicles, surfaceand underwater vessels, electric aircraft and electric spacecraft. For road vehicles,togetherwith other emerging automotive technologies such as autonomous driving, connectedvehicles and shared mobility, EVs form a future mobility vision called Connected, Autonomous, Shared and Electric (CASE) Mobility.

EVs first came into existence in the late 19th century, when electricity was among thepreferred methods for motor vehicle propulsion, providing a level of comfort and easeof operation that could not be achieved by the gasoline cars of the time. Internal combustion engines were the dominant propulsion method for cars and trucks for about100 years, but electric power remained commonplace in other vehicle types, such as trains and smaller vehicles of all types.

Government incentives to increase adoption were first introduced in the late 2000s, leading to a growing market for the vehicles in the 2010s. Increasing public interest and awareness and structural incentives, such as those being built into the green recovery from the COVID-19 pandemic, is expected to greatly increase the electric vehicle market. Electric vehicle sales may increase from 2% of global share in 2016 to30% by 2030.

II.PARTS OF ELECTRIC VEHICLE

An electric vehicle battery (EVB, also known as a traction battery) is a rechargeable battery used to power the electric motors of a battery electric vehicle (BEV) or hybrid electric vehicle (HEV). Typically, lithium-ion batteries, they are specifically designed for high electric charge or energy capacity.

1) BATTERY SYSTEM

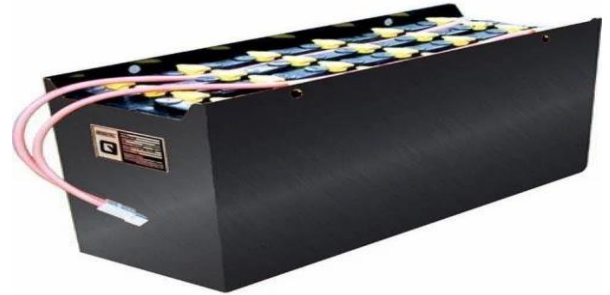


Fig.1:Battery system

Stores electricity for use by the electric traction motor. Transmission electric the transfer’s mechanical power from the electric traction motor to drive the wheels. If it senses one whee spinning a lot faster than the others indicating a loss of traction, a signal is sent to the engine electronics that power be reduced so the wheel can regain grip, regardless of whether the driving is pressing the accelerator. The basic purpose of traction control isto detect when a tyre loses grip, causing the wheel to spin, and then work to stop or slow down the rate of spin.

2) DC-DC CONVERTER

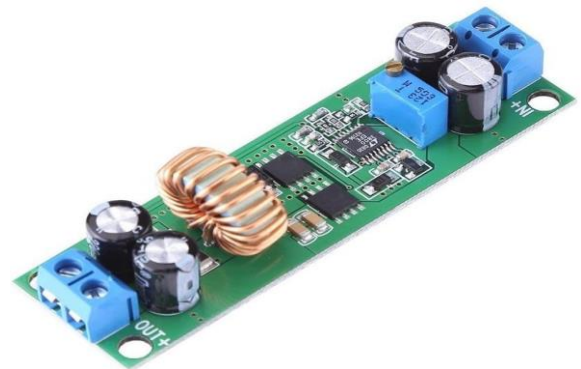


Fig.2:Dc-Dc Converter

The working principle of the DC-to-DC converter is that the inductor in the inputresistance has the unexpected variation in the input current. If the switch is on, then the inductor feeds the energy from the input and it DC- DC converter is a critical component in the architecture of a BEV, where it is used to convert power from the high voltage bus to the 12V Low Voltage bus to charge the LV battery and power the on-board electric devices. The DC-DC power converters are the electronic devices that condition the source voltage of one level to the output.

3) Electric motor



Fig.3: Electric motor

An electric motor is an electrical machine that converts electrical energy into mechanical energy. Most electric motors operate through the interaction between the motor's magnetic field and electric current in a wire winding to generate force in the form of torque applied on the motor's shaft. Electric motors can be powered by direct current DC sources, such as from batteries, or rectifiers, or by alternating current AC sources, such as a power grid, inverters or electrical generators.

4) POWER INVERTER



Fig.4: power inverter

A power inverter, inverter or inverter is a power electronic device or circuitry that changes direct current DC to alternating current AC. The resulting AC frequency obtained depends on the particular device employed. Inverters do the opposite of the The input voltage, output voltage and frequency, and overall power handling depend on the design of the specific device or circuitry. The inverter does not produce any power; the power is provided by the DC source. A power inverter can be entirely electronic may be a combination of mechanical effects and electronic circuitry.

Static inverters do not use moving parts in the conversion process Power inverters are primarily used in electrical power applications where high currents and voltages are present; circuits that perform the same function for electronics signals, which usually have very low currents and voltages, are called oscillators. Circuits that perform the opposite function, converting AC to DC, are called rectifiers.

Braking system for electric vehicle

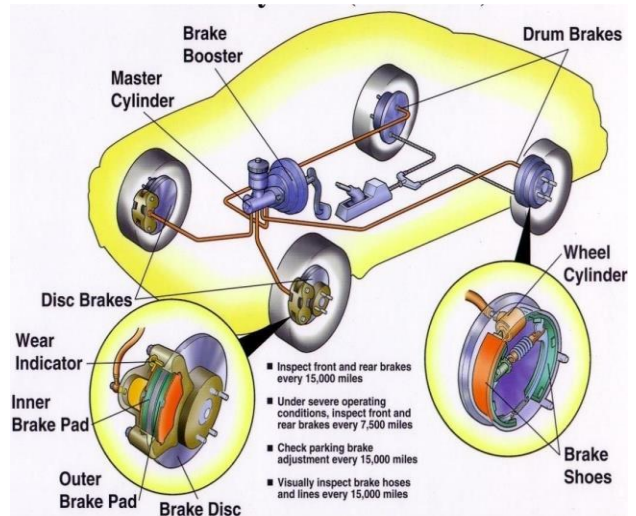


Fig.5: Braking system for electric vehicle

A brake is a mechanical device which inhibits motion. Most commonly brakes use friction to convert kinetic energy into heat, though other methods of energy conversion may be employed. For example, regenerative braking converts much of the energy to electrical energy, which may be stored for later use. Other methods convert kinetic energy into potential energy in such stored forms as pressurized air or pressurized oil. Eddy current brakes use magnetic fields to convert kinetic energy into electric current in the brake disc, fin, or rail, which is converted into heat. Still other braking methods even transform kinetic energy into different forms, for example by transferring the energy to a rotating flywheel.

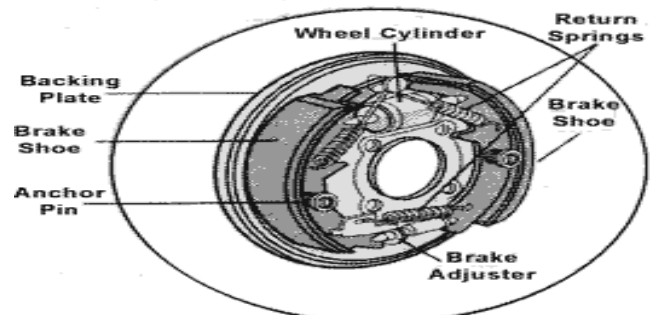


Fig.6. Drum Brake

In cars with rear drum brakes the emergency brake cable usually actuates these drums mechanically much less force than is available through the hydraulic system. A number of production vehicles have been made with a separate drum brake on the transmission tail shaft. This has an advantage of being completely independent of other braking systems. As long as the drive train is intact propeller shaft, differential, and axle shafts this is effective. However, there are examples of electric vehicle with rear disc brakes in which the emergency brake actuates a small drum brake housed within the hub assembly of electric vehicle.

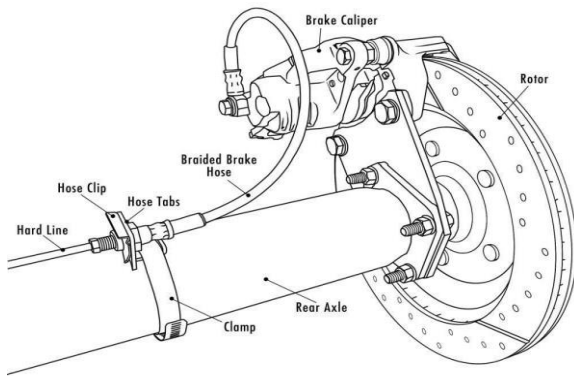


Fig.7:Disc Brake

In cars with rear disc brakes, the emergency brake most often actuates the disc calipers (again, with much less force). A disc brake is a wheel brake which slows rotation of the wheel by the friction caused by pushing brake pads against a brake disc with a set of calipers. The brake disc is usually made of cast iron, but may in some cases be made of composites such as reinforced carbon-carbon or ceramic matrix composites. This is connected to the wheel and/or the axle. To stop the wheel, friction material in the form of brake pads forced.



Fig:8: Hand Brake

In cars, the hand brake also known as the emergency brake, e-brake, park brake, or parking brake is a supplementary system that can be used if the vehicle's primary brake system usually hydraulic brakes have a failure. Automobile e-brakes usually consist of a cable usually adjustable for length directly connected to the brake mechanism on one end. *The lever is traditionally and more commonly a hand-operated system hence the hand brake name, the most common configuration being a handle on the floor between the driver and front passenger, and less commonly being a handle bar located on the lower portion of the dashboard somewhere close to the steering wheel column.*



Fig.9:Braking System Assembly

Electric vehicles are the need for the hour; hence they should also possess excellent brakes along with durable steering knuckle with minimum weight in order to attain high efficiency. Perfect functioning of brakes in all conditions is a necessity for the safety of passengers. There are various types of brakes available right from drum brakes to Pneumatic and Hydraulic brakes. Disc brakes are more efficient than drum brakes, with better heat dissipation but their cost is high. The Braking system works on the principle of conservation of energy, the Kinetic Energy of the vehicle is converted to heat which is then dissipated to the surrounding. Also, these brakes are based on the principle of Pascal's law which states, "The pressure exerted anywhere in a mass of confined liquid is transmitted undiminished in all directions throughout the liquid". When the brake pedal is pressed, the force is transferred to the master cylinder to the brake fluid and then to the pistons in the caliper, which in turn squeezes the brake pads against each other. Disc brakes have a smaller number of sub-components drum brake



Fig.10: Drum Brake

Drum brakes are used primarily to decrease rolling resistance. The disc brake pads have the tendency to slightly drag on the rotors as the vehicle is coasting. Drum brakes, just by nature of their design

I. ADVANTAGES

- No fuel required so you save money on gas.
- Environmental friendly as they do not emit pollutants.
- Lower maintenance due to an efficient electric motor.
- Better performance.

II. APPLICATIONS

- Road ways
- Small weightage can be adopted
- industry
- No emission
- Public places

III. CONCLUSION & FUTURE SCOPE

Electric vehicles are more efficient, and that combined with the electricity cost means that charging an electric vehicle is cheaper than filling petrol or diesel for travel requirements. Using renewable energy sources can make the use of electric vehicles more eco-friendly. Electric vehicles produce less life cycle emissions than traditional cars. Electric vehicles can be best in future because they are more energy efficient than internal combustion engines. Design the braking system of electric vehicle is carried out in this work. The vehicle is having four wheels and the brakes are provided at back two wheels. The brakes used are drum type. The length of the brake and the effort required to stop the vehicle are calculated using standard design calculations. The vehicle is running at average speed of 20 mph, and the torque of the vehicle is calculated as 30 Nm. The effort of brakes is analyzed and the brakes are arranged to the Electric vehicle. The brake size obtained as 32 mm. Heat generated through the braking also estimated as 133 J. The values are within the range.

REFERENCES

- 1) Hamid, Umar Zakir Abdul (2022). "Autonomous, Connected, Electric and Shared Vehicles: Disrupting the Automotive and Mobility Sectors". Retrieved 11 November 2022.
- 2) Asif Fazio Christopher S. Weaver; Michael P. Walsh (1996). Air Pollution from Motor Vehicles: Standards and Technologies for Controlling Emissions. World Bank Publications. p. 227. ISBN 978-0-8213-3444-7. Archived from the original on 4 July 2021. Retrieved 4 December 2017.
- 3) Mom, Gijs (15 February 2013). The Electric Vehicle: Technology and Expectations in the Automobile Age. JHU Press. ISBN 978-1-4214-1268-9.
- 4) See Loeb, A.P., "Steam versus Electric versus Internal Combustion: Choosing the Vehicle Technology at the Start of the Automotive Age," Transportation Research Record, Journal of the Transportation Research Board of the National Academies, No.1885, at 1.
- 5) Belles (2006) the early years the history of electric vehicles about.com archived from the original on 4 July 2021, retrieved 6 July 2006.
- 6) Richardson, D.B. (March 2013). "Electric vehicles and the electric grid: A review of modelling approaches, Impacts, and renewable energy integration". Renewable and Sustainable Energy Reviews.
- 7) Wilmer, Martin (2015). "Electric vehicle traction motors without rare earth magnets". Sustainable Materials and Technologies.
- 8) David Sandolo, ed. (2009) Washington? The. pp. 2–5. ISBN 978-0-8157-0305-
- 9) Archived from the original on 28 March 2019. Retrieved 7 July 2013. See definition on pp.

A Historical Review on Solar Water Heaters

A. Renuka Prasad¹, Donepudi Jagadish² and B.Omprakash³

¹Department of Mechanical Engineering, Sai Rajeswari Institute of Technology, Proddatur, India

² Department of Mechanical Engineering, Narasaraopeta Engg. College, Narasaraopeta, India

³ Department of Mechanical Engineering, JNTUA College of Engg, Anantapuramu, India

Abstract-In the present review paper, the existing solar water heating systems are studied with their applications. Solar energy is free, environmentally clean, and therefore it is accepted as one of the most promising alternative energy sources. The effective use of solar energy is hindered by the intermittent nature of its availability, limiting its use and effectiveness in domestic and industrial applications especially in water heating. Now a day, plenty of hot water is used for domestic, commercial and industrial purposes. Various resources i.e. coal, diesel, gas etc, are used to heat water and sometimes for steam production. Solar energy is the main alternative to replace the conventional energy sources. The size of the systems depends on availability of solar radiation, temperature requirement of customer, geographical condition and arrangement of the solar system, etc. Therefore, it is necessary to design the solar water heating system as per above parameters. The available literature is reviewed to understand the construction, arrangement, applications and sizing of the solar thermal system.

I. INTRODUCTION

We are blessed with Solar Energy in abundance at no cost. The solar radiation incident on the surface of the earth can be conveniently utilized for the benefit of human society. One of the popular devices that harness the solar energy is solar hot water system (SHWS). The solar energy is the most capable of the alternative energy sources. Due to increasing Demand for energy and rising cost of fossil type fuels (i.e., gas or oil) solar energy is considered an attractive source of renewable energy that can be used for water heating in both homes and industry. Heating water consumes nearly 20% of total energy consumption for an average family. Solar water heating systems are the cheapest and most easily affordable clean energy available to homeowners that may provide most of hot water required by a family. Solar heater is a device which is used for heating the water, for producing the steam for domestic and industrial purposes by utilizing the solar energy. Solar energy is the energy which is coming from sun in the form of solar radiations in infinite amount, when these solar radiations falls on absorbing surface, then they gets converted into the heat, this heat is used for heating the water. This type of thermal collector suffers from heat losses due to radiation and convection. Such losses increase rapidly as the temperature of the working fluid increases.

II. SOLAR WATER HEATING SYSTEM

SWH systems are generally very simple using only sunlight to heat water. A working fluid is brought into contact with a dark surface exposed to sunlight which causes the temperature of the fluid to rise. This fluid may be the water being heated directly, also called a direct system, or it may be a heat transfer fluid such as a glycol/water mixture that is passed through some form of heat exchanger

called an indirect system. These systems can be classified into three main categories.

III. TYPES OF SOLAR WATER HEATING SYSTEM:

- 1) Natural circulation solar water heater
- 2) Forced circulation solar water heater

A. Natural Circulation Solar Water Heater

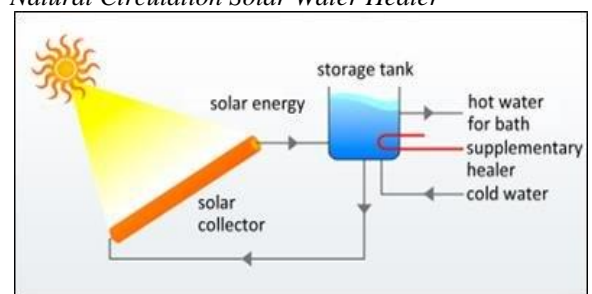


Fig.1: Natural Solar Water Heater

The storage tank is well insulated and is placed at higher level than collector. In this case no pump is required to circulation water through the system. When the water in the collector is heated up to by the sun radiation, it becomes less dense and flows automatically to the top of the tank while high density cold water flows from the bottom of the tank to the collector by the gravity. This water in turn is heated and raises up into tank [3-6]. As long as the sun shines. The water circulation is maintained. Hot water can be taken out from the top of the tank while fresh water may be supplies to the tank from the source. This natural circulation solar water heater is used for domestic usage.

B. Forced Circulation Solar Water Heater

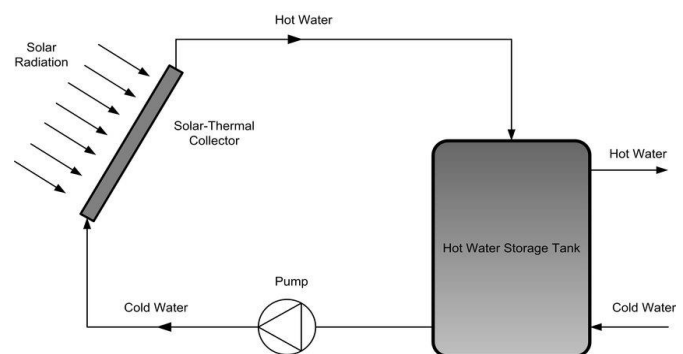


Fig.2: Forced Circulation System.

Solar water heater with forced circulation is used when a large quantity of hot water is required in this case there is

no need to locate the tank above the collector. This type of heater uses a pump to circulate water through the solar collector [7-10]. Pump is operated by switch on and off controller which senses the temperature difference between collector on the tank. Pump is switched on when the temperature difference exceeds certain value and switched off when the difference falls below certain value. A check valve is provided to prevent reverse flow of water it so provided with auxiliary heater to the water leaving the tank to the load. The level of the water in a tank can be maintained by the float control. This forced circulation solar water heaters are used for hotels, hospital, hostels and factories

IV. COMPONENTS OF SOLAR WATER HEATING SYSTEM

SWH generally consists of a solar radiation collector panel, a storage tank, a pump, a heat exchanger, piping units, and auxiliary heating unit. Some of important components are described in the next sections.

A. Flat Plate Collectors

A flat-plate collector (FPC) is a device to collect solar energy and transform it into thermal energy (low-grade energy) by using water as a working fluid [11, 12]. It is a heart of solar thermal devices that has many applications in a medium temperature range $\cong 100$ °C from domestic to preheating to industrial sectors

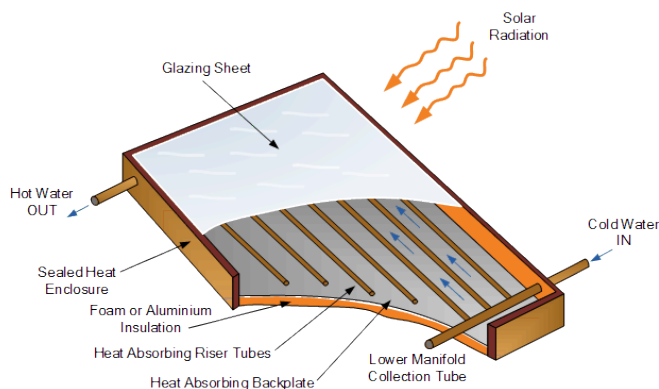


Fig.3: Solar Flat Plate Collector.

B. Storage tank

Most commercially available solar water heaters require a well-insulated storage tank. Thermal storage tank is made of high pressure resisted stainless steel covered with the insulated fiber and aluminum foil[13-16]. Some solar water heaters use pumps to recirculation warm water from storage tanks through collectors and exposed piping. This is generally to protect the pipes from

freezing when outside temperatures drop to freezing or below.

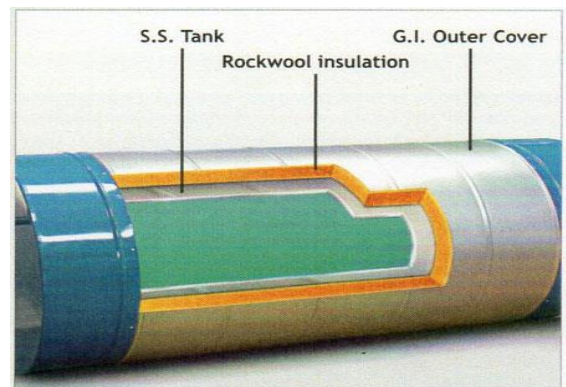


Fig.4: Storage Tank.

C. Heat Transfer Fluid

A heat transfer fluid is used to collect the heat from collector and transfer to the storage tank either directly or with the help of heat exchanger. In order to have an efficient SHW configuration, the fluid should have high specific heat capacity, high thermal conductivity, low viscosity, and low thermal expansion coefficient, anti-corrosive property and above all low cost [17-19]. Among the common heat transfer fluids such as water, glycol, silicon oils and hydrocarbon oils, the water turns out to be the best among the fluids. Water is the cheapest, most readily available and thermally efficient fluid but does freeze and can cause corrosion.

V. APPLICATIONS

1. Swimming pools
2. Residential houses
3. Textile industries
4. Boiler house
5. Hospital and nursing home
6. Dairies and food processing industries
7. Textile factory
8. Hotels and restaurants

VI. ADVANTAGES

1. Simple to construct and install
2. No or negligible running cost
3. Almost free from maintenance
4. It saves time and high grade form of electrical energy
5. Cost is low and economically competitive
6. They are efficient, approximately 80percent radiation is turned into heat energy

VII. DISADVANTAGES:

1. Need large enough space for the solar collectors
2. Solar collectors must be exposed to the sun
3. Freezing problem
4. Solar thermal panels can only heat water

CONCLUSION

At Present, Solar water heating systems are installed with different configurations and arrangements. The basic technology concrete of these systems are studied and it is found that there is a need to work on the generated design procedure to select, install and monitor the solar water heating system as per the availability.

REFERENCES

- [1] Dilip Johari, Ashok Yadav, Ravi Verma —Study of solar water heaters based on exergy analysisl Proceedings of the National Conference on Trends and Advances in Mechanical Engineering, YMCA University of Science & Technology, Faridabad, Haryana, Oct 19-20, 2012.
- [2] Soteris A. Kalogirou, —Solar thermal collectors and applications., Progress in Energy and Combustion Science 30 (2004) 231–295.
- [3] Mustafa AKTAŞ, Olhan CEYLAN, Hikmet DOĞAN — The Thermal Effectiveness Compression Of The Classical And Finned Solar Systeml Isı Bilimi ve Tekniđi Dergisi, 26, 2, 29-33, 2006. J. of Thermal Science and Technology ©2006 TIBTD Printed in Turkey ISSN 1300-3615.
- [4] El-Sebail A.A., Enein Aboul S., Ramadan M. R. I., and El-Gohary H. G. “Experimental investigation of an indirect type natural convection solar dryer”. Energy Conversion and Management, 2002, 43, 2251-2266.
- [5] Arjunan T.V. , Aybar H.S. “ An Experimental study on the effect of the energy storage materials in solar still”. Proceedings 20th National and 9th ISHMT-ASME Heat and Mass Transfer conference, 2010, 259, 981-986.
- [6] Hans Vishavjee Singh, Saini R.P. and Saini J.S. “Experimental investigation of heat transfer and friction characteristics of a multiple V-rib roughened solar air heater”. Proceedings 20th National and 9th ISHMTASME Heat and Mass Transfer conference, 2010, 152, 546-551.
- [7] Jain Dilip. “Modelling the performance of the reversal absorber with packed bed thermal storage natural convection solar crop dryer”. Journal of Food Engineering, 2006, 78, 637-647.
- [8] Forson F.K., Nazha A. A. M., and Rajakaruna H. “Experimental and simulation studies on a single pass double duct solar air heater”. Energy Conversion and Management, 2003, 44, 1209-1227.
- [9] Janjai S., Srisittipokakun N. and Bala B. K. “Experimental and modeling performances of a roof integrated solar drying system for drying herbs and spices”. Energy, 2008, 33, 91-103.
- [10] Almeida F., Naylor D. and Oosthuizen P.H. “An interferometric study of free convection in a window with a heated between-panes blind”. Proceedings 3rd Solar building research network and Solar and sustainable energy society of Canada, 2008, Inc. 33rd joint conference, Fredericton.
- [11] Solanki S.C., Dubey swapnil, and Tiwari Arvind. “ Indoor simulation and testing of photovoltaic thermal (PV/T) air collectors”. Applied Energy, 2009, 86, 2421.
- [12] Karmare S.V., and Tikekar A.N. “Analysis of fluid flow and heat transfer in a rib grit roughened surface solar air heater using CFD”. Energy, 2010, 84, 409– 417.
- [13] Goppert Stefan, Lohse Rolf, Urbaneck Thorsten, Schirmer Ulrich, Platzer Bernd, and Steinert Philip. “New computation method for stratification pipes of solar storage tanks”. Solar Energy, 2009, 83, 1578-1587.
- [14] Pangavhane Dilip R., Sawhney R.L., and Sarsavadia P.N. “Design, development and performance testing of a new natural convection solar dryer”. Energy, 2002, 27, 579–590.
- [15] Koyuncu Turhan. “Performance of various designs of solar air heater for crop drying applications”. Renewable Energy, 2006, 31, 1073–1088.
- [16] Karim M.A. and Hawlader M.N.A. “Development of solar air collectors for drying applications”. Energy Conversion and Management, 2004, 45, 329–344.
- [17] Ezekoye B. A. and Enebe O. M. “Development and performance evaluation of modified integrated passive solar grain dryer”. The pacific journal of science and technology, 2006, 7, 185-190.
- [18] Hossain M. A. and Bala B.K. “Drying of hot chilli using solar tunnel drier”. Solar Energy, 2007, 81, 85-92.
- [19] Fargali M. Hanaa, El-Shafy Abd, Nafeh A., Fahmy H. Faten, and Hassan A. Mohamed. “Medicinal herb drying using a photovoltaic array and a solar thermal system”. Solar Energy, 2008, 82, 1154-1160.

DESIGN & FABRICATION OF SUSPENSION SYSTEM FOR AN ELECTRIC VEHICLE

M.Venkaiah, N.Rakesh, Ch.Sriram, SK.Ameer, M.Ajay kumar, I.Ratnam raju

*Department of Mechanical Engineering,
Narasaraopeta Engineering College, Narasaraopet, Palnadu(Dist.), A.P., India*

Abstract - The main aim of the project is to design and fabricate a suspension system for an electric vehicle. An electric vehicle, also known as an EV. is a vehicle that is powered by one or more electric motors using electricity stored in batteries or another energy storage device. In this project leaf springs are designed which are used as a suspension for an electric vehicle and also analyzed and identified the load carrying capacity of a leaf spring on different load conditions also identified the stress, elongation, & modulus of elasticity and safe load etc. the leaf spring suspension with components are installed and fitted to the electric vehicle.

Keywords –Electric vehicle, Master Leaf, Eye bolts & perches, Manufacturing process, wheel axles, wheel bearings etc.

I. INTRODUCTION

A leaf spring is a simple form of spring commonly used for the suspension in wheeled vehicles. Originally called a laminated or carriage spring, and sometimes referred to as a semi-elliptical spring, elliptical spring, or cart spring, it is one of the oldest forms of vehicle suspension. A leaf spring is one or more narrow, arc-shaped, thin plates which are attached to the axle and chassis in a way that allows the leaf spring to flex vertically in response to irregularities in the road surface.

Lateral leaf springs are the most commonly used arrangement, running the length of the vehicle and mounted perpendicular to the wheel axle, but numerous examples of transverse leaf springs exist as well. Leaf springs can serve multiple functions location, springing, and to extent damping as well through inter leaf friction, however this friction well controlled, resulting in stiction and irregular suspension motion. For this reason some manufacturers choose mono-leaf springs. The longest leaf is also known as the main, master, or No. 1 leaf, with leaves numbered in descending order of length. The eyes at the end of the leaf spring are formed into the masterleaf.

In general, aside from the main leaf, the other leaves are tapered at each end. The leaf spring acts as a linkage to hold the axle in position and thus separate linkages are not necessary. The result is a suspension that is simple and strong. Inter-leaf friction dampens the spring's motion and reduces rebound, which, until shock absorbers were widely adopted, was a very significant advantage over helical springs.

BASIC DESIGN

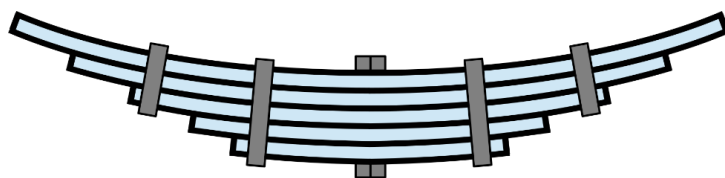


Fig.1: Basic design of leaf spring

A basic design of leaf spring as shown in the above figure that there is a linkage of combination of several sizes of leaves to accommodate and to absorb or to withstand the different types of loads.

I. MANUFACTURING PROCESS OF LEAF SPRINGS



Fig.2: Leafsprings production

1. HEATING FOR HARDENING: Any metal, or alloy which can be hard drawn, or rolled to fairly high strength and retains sufficient ductility to form, may be used for springs, or any alloy which can be heat treated to high strength and good ductility, nonmagnetic characteristics, resistance to corrosion, elevated temperatures and drift require special considerations. leaves are heated to critical temperature in an Oil-fired hardening furnace. Usually temperature is maintained in between 850 and 950 degree Celsius.

2. CAMBERING: The top leaf is known as the master leaf. The eye is provided for attaching the spring with another machine member. The amount of bend that is given to the spring from the central line, passing through the eyes, is known as camber.



Fig 3 : Quenching of leafs

3. QUENCHING: Hot bent leafs kept in tray and quenched in oil bath to get martensite structure. Martensite is the hardest form of steel crystalline structure. Martensite is formed in carbon steels by rapid cooling that is quenching of austenite form of iron. Machine used is conveyerized quench oil bath. Fire point of quenching oil is around 200°C .after quenching the structure of leaf spring becomes very strong at last to remove hardness tempering is done.

4. TEMPERING : Tempering is a process of heat treating, which is used to increase the toughness. Quenched leaves are reheated to drop hardness to required level. Electric heated temperature furnace is used for this process. Hardness of the leaves is found out using Brinell hardness testing. This process is also done to relieve stresses. Temperature inside the machine is maintained between 540 and 680°C.

II. COMPONENTS OF A LEAFSPRING SUSPENSION



Fig 4 : Master leaf

Leaf Spring Suspension are an integral part of your vehicle's suspension system. They are installed to help support the entire weight of your car or truck. Leafsprings also help to maintain the tyres grip on the road and regulate the wheelbase lengths



Fig 5 : Degree Shims

Axle shims are thin pieces of metal that are placed between an axle and a leafspring to adjust the pinion angle of the vehicle's axle. Commonly offered in 2- to 8- degree angles, axle shims are designed to be bolted to the bottom of the leaf spring pack and held in place both by an interference fit between the spring and spring pad on the axle, as well as the center bolt of the spring pack.



Fig 6 : Shackles

Leaf spring shackles help the vehicle's springs to travel through long ways when you drive through different road surfaces like rocks, bumps, potholes, uneven dirt and rocks. It ensures the length of the leaf springs changes appropriately during the movements of the suspension. Another purpose of this component is to keep the vehicle balanced. Shackles are located at the rear end of each leaf spring in the suspension system of any vehicle.



Fig 7 : Spring eyebolts

Spring eyebolts are grade 8, should be the only spring eyebolt/shackle bolt used due to the increased strength and torquing ability needed when installing the suspension. Leaf spring suspension requires a much harder and stronger spring eyebolt than most other applications. Eyebolts are a type of fastener with a looped, circular head (the "eye") that can be screwed or bolted into an object for the purpose of attaching a rope, cable, or chain.

IV .DESIGN & ANALYSIS OFLEAF SPRINGS

Calculations for radius and lengths for a pre specified electric vehicle is given by,

When n=10,

Rear Overall length of the spring = 2L1 = 1372mm

Width of each leaf = 76.2 = 80mm(approx.)

2W = 800*9.8 = 7840N

2W = total load /no of springs

W = 980N

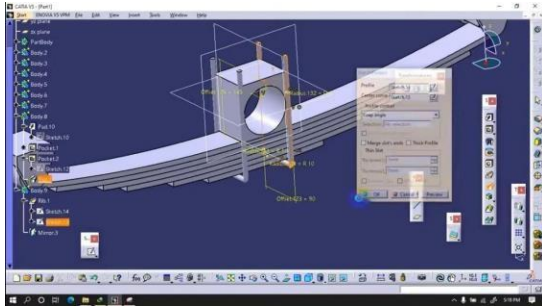
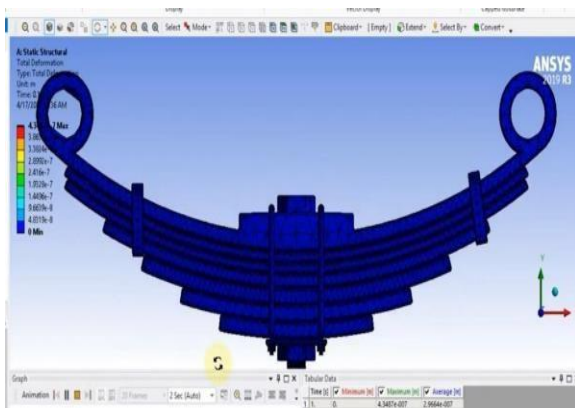


Fig 8 : Design of leaf spring

CATIA V5, the most popular and the most used CATIA version. V5 is a CAD software used for parametric and non-parametric modeling. CATIA V4 essentially replaces it by including more functions such as additional platform support, ease of use, etc. highly intuitive tools to create, modify, and validate any freeform and mechanical surfaces. Its architecture delivers advanced design control for Start of thert engineering. D output is frequently within the form of digital documents for print, machining, or other manufacturing operations. The term CADD is also used.



.Fig 9 : Analysis on leaf spring

Structural & fatigue analysis on leaf spring

- Material - Mild Steel
- Density: 785kg/m³
- Young's modulus : 20000Mpa
- poissons ratio : 0.3

→→→Ansys → Workbench→ Select analysis system → static structural → double click→→Select geometry → right click → import geometry → select browse→open part→ ok→→ select mesh on work bench → right click →edit

Total deformation

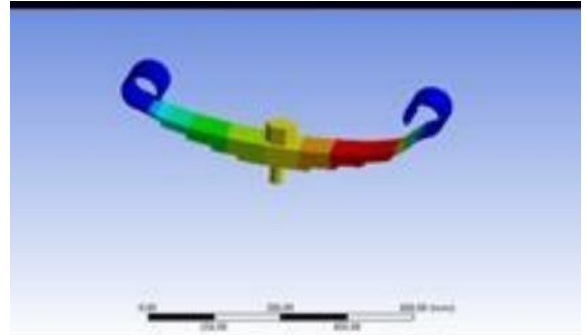


Fig 10 : Total Deformation

According to the contour plot, the maximum deformation0.091808 mm at masterleaf because of load applied on the area and minimum deformation at eyes because offixed on areas.

V. FINAL RESULTS & DISCUSSIONS

The leaf spring material of mild steel which is having the input values of density - 0.00000785kg/mm³ & poisons ratio is given as 0.3,spring rate – 32.7N/mm after analysing by the final results are

Deformation in mm	-	0.091808
Stress in N/mm ²	-	61.715
Strain	-	0.00030971

INSTALLATION OF SUSPENSIONSYSTEM FOR ELECTRIC VEHICLE

- Installation & Fitting of Front Wheel Suspension



Fig 11 : Installation front wheel suspension

Fully loosen the two rack and pinion unit lock nuts , one near the bellow sand one on therear side ofthe rack and pinion unit, until only one thread is engaged remove .the lock nut and washer from the long bolt and discard lock nut. The rack and pinion unit is now loose. Remove the two 1 3/4" long bolts and lock nuts securing driver side spring to axle and discard lock nuts . Hold nut with wrench and loosen long bolt . Note location of washer and thread long bolt out as far as possible to remove the washer,nut and spacer.

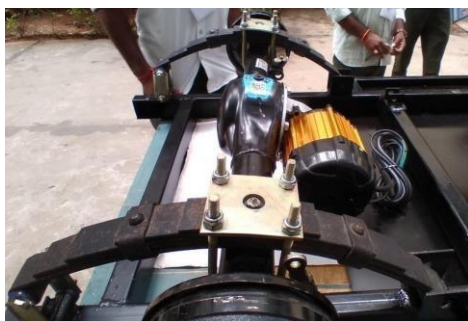


Fig.12.Installation of rear leaf springs

Spring installation is in the reverse order of disassembly. The shock absorbernuts(must be tightened until the shock absorber bushings expand to the diameter of the shock absorber washer tighten front and rear spring mounting hardware to 18 – 23 ft lbs (24-31)mm torque .



Fig 13 :Final Assembly

The above picture is the final assembly of master leafs, centre pins, shackles, eye bolts & axle shims assembly of a leaf spring suspension fitted at the both front and rear axles of an electric vehicle.

VI. ADVANTAGES

- leaf springs are designed to be strong and durable, making them ideal for heavy-duty applications. They can withstand heavy loads and provide a long life.
- leaf springs are capable of supporting heavy loads making them ideal for commercial and heavy duty applications.
- leaf springs provide good stability and control, particularly when the vehicle is heavily loaded or towing.

VII. APPLICATIONS

- Commercial vehicles
- Off- road vehicles
- Military vehicles
- Railway rolling stock
- Agricultural equipment
- Vintage cars

VIII.CONCLUSION & FUTURE SCOPE

By the resultant values the leaf spring suspension can withstand the loads of approximately 800-850kgs .Below the 800 kgs of load the leaf spring suspension can withstand and absorbs the sudden and impact loads during travelling and keeps the vehicle safe. By the theoretical values the leaf spring suspension are designed & successfully fitted and installed to the electric vehicle, Therefore the project Design & fabrication of suspension system for an electric vehicle is successfully completed.

The leaf spring is designed, fabricated, tested experimentally the leaf spring made of mild steel reinforcement polymer material shows higher strength and life when compared to conventional leaf spring. The leaf spring compared to conventional leaf spring, the achievement of the tests and analysis on leaf spring indicates that and analysis on composite leaf spring indicates that alternate to conventional leaf spring. the wheelbase lengths when it is speeding up or slowing down. To control the height of the ride and axle therefore damping leaf springs are very important.

IX REFERENCES

1. "IS 1135(1995): Leaf Springs Assembly for Automobiles". Bureau of Indian standards, retrieved 13 october 2022.
2. Stockel, Martin W.; Stockel, Martin T.; Johanson, Chris (1996). Auto Fundamentals. Tinley Ark: The Goodheart- Willcox Company, Inc. P. 455. ISBN 156637145
3. "Springs – A simple study of car suspension". The Automotor Journal: 936–937.aug 10 1912
4. Felton, William (1796). A treatise on carriages; comprehending coaches, chariots, phaetons article are accurately stated.
5. Reuleaux, Franz (1861). Der Konstrukteur. Braunschweig: F. Vieweg. Retrieved 13october 2022.
6. Rowland, E.K. (1911). "Leaf Springs". Transactions. Society of Automobile 6: 156–191. JSTOR 44579553
7. "Kamis, Khukuri makers of Nepal". Himalayan-imports.com. Retrieved 2011-11-06.
8. Ajitabhateriya, Mudassir Khan, Structural and thermal analysis of spring loaded protection Valve using FEM, International journal of mechanical engineering and robotics research, Four (1), 430-434. [3]. Pozhilarasu V. And T parameshwarao.

A REVIEW ON HYBRID ELECTRIC VEHICLES AND TYPES

A. Renuka Prasad¹ and Donepudi Jagadish²

¹Assistant professor, Department of Mechanical Engineering, SRIT, Proddatur, India

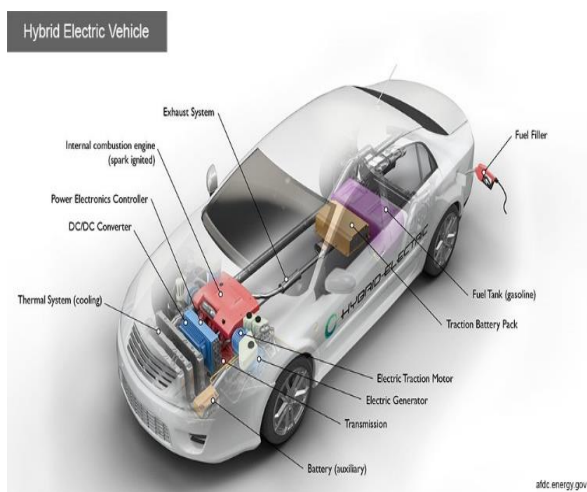
²Professor, Department of Mechanical Engineering, NEC, Narasaraopeta, India

Abstract: With the increase of per capita energy consumption, environmental pollution is worsening. Using new alternativesources of energy, reducing the use of conventional fuel-powered engines is imperative. Due to the short period, pureelectric vehicles cannot be mass-produced and there are many problems such as imperfect charging facilities. Therefore,the development of hybrid electric vehicles is particularly important in a certain period. In this paper, the classification ofhybrid vehicle, research status of hybrid vehicle and future development trends of hybrid vehicles is introduced. It isconducive to the public understanding of hybrid electric vehicles, which has a certain theoretical significance.

I. INTRODUCTION

Hybrid electric vehicles are powered by an internal combustion engine and an electric motor, which uses energy stored in batteries. A hybrid electric vehicle cannot be plugged in to charge the battery. Instead, the battery is charged through regenerative braking and by the internal combustion engine. The extra power provided by the electric motor can potentially allow for a smaller engine[1]. The battery can also power auxiliary loads and reduce engine idling when stopped. Together, these features result in better fuel economy without sacrificing performance.

II. TYPES OF HYBRID VEHICLES



A. Parallel Hybrid Vehicle:

In this most common design, the electric motor(s) and gasoline engine are connected in a common transmission that blends the two power sources. That transmission can be an automatic, a manual, or a continuously variable transmission (CVT). One very popular hybrid transmission is a power-split CVT, which is used by the Toyota Prius and Chevrolet Volt [2-3]. Transmission type and the size of the gasoline engine are the main factors that determine how a parallel hybrid will accelerate, sound, and feel.

B. Series Hybrid Vehicle:

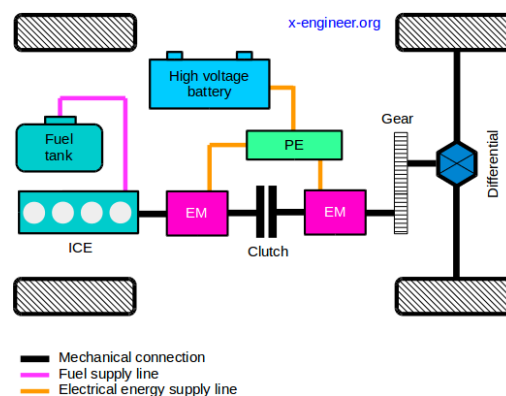


Fig. 1: Series of Hybrid Vehicle.

In this design, the electric motor(s) provides all the thrust, and there is never a physical mechanical connection between the engine and the wheels. The gasoline engine is just there to recharge the battery. This results in a driving experience that's more indicative of an electric car, with smoother, powerful acceleration [4-8]. There's typically less vibration when the gasoline engine engages. However, that engagement doesn't always happen in concert with what your right foot is doing (remember, the battery is making the demands), so the engine might be revving up while the car is cruising at a steady speed. Some find this behaviour disconcerting.

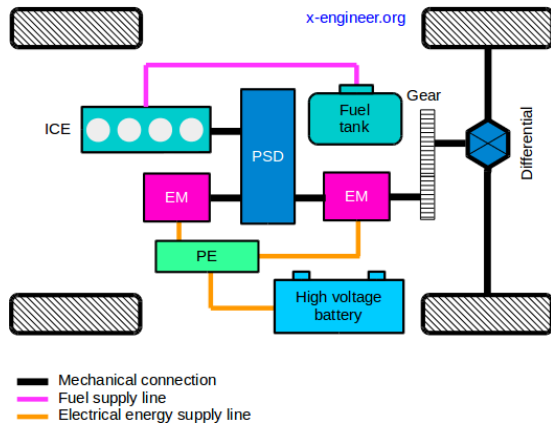


Fig.2: Series of Parallel Hybrid Vehicle.

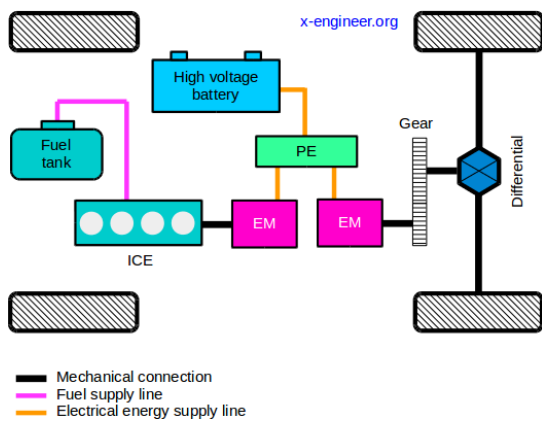


Fig.3: Power Split Hybrid Vehicle

C. Series-Parallel Hybrid Vehicle:

A series hybrid becomes a series-parallel hybrid by adding a mechanical connection (clutch) between the two electric machines [9,10]. The advantage of this architecture is that at low speeds, with the clutch open, the powertrain behaves as a series hybrid, running the engine at the most efficient operating point. At high vehicle speed, the clutch is closed and the engine can transmit torque to the driving wheel thus the powertrain becoming a parallel hybrid.

Compared with the series hybrid, the series-parallel hybrid has the advantage of a smaller power rating of the generator since the excess power of the engine can be transferred directly to the drive wheels. The disadvantage is that, by adding a mechanical connection (clutch), we lose the flexibility in terms of packaging.

In terms of powertrain functions, a series-parallel hybrid is capable of:

- Engine stop & start
- Energy recuperation
- Torque assist/boost
- Electric driving
- Charge at standstill

Compared with a parallel hybrid, a series-parallel hybrid uses two electric machine and performs the same tasks. For these reasons, the series-parallel powertrain architecture with a clutch connection between the two electric machine is not widely used by automotive manufacturers.

D. Power Split Hybrid Vehicle:

A hybrid vehicle with a power-split architecture combines the characteristics of a parallel hybrid with those of a series hybrid [11,12]. A power-split hybrid powertrain mechanically links an internal combustion engine and two electric machines using a power split device (PSD). The power-split device is usually a single planetary gear set (PSG) or multiple PSGs.

The internal combustion engine has the highest rated power, compared with the electric machines. A part of the engine power is converted by one electric machine into electrical energy, the excess power being transmitted to the drive wheel, in parallel with the second electric machine power.

Except Coasting, a power-split hybrid powertrain performs all the functions of a full hybrid:

- Engine stop & start
- Energy recuperation
- Torque assist/boost
- Electric driving
- Charge at standstill

Since the engine is always connected to the drive wheels through the planetary gear set, its speed can only be adjusted within certain limits, depending on the PSG gear ratios and the speed of the two electric machines. The combination of the internal combustion engine[13-18], two electric machines and the PSG gives the overall behaviour of a continuously variable transmission (CVT). For this reason, a power-split hybrid electric vehicles is advertised as having an electric continuously variable transmission (ECVT).

III. WORKING PRINCIPLE OF HYBRID VEHICLES

A. Pulling Away From the Stop

The car is moved initially with the help of an electric motor, which draws on the hybrid battery for power.

B. Normal Cruising

When cruising at high speeds, both the electric motor and petrol engine can work together or independently.

C. Heavy Acceleration

During heavy acceleration and high speeds, the power provided to the car comes from the petrol engine.

D. Braking and Deceleration

When slowing down and braking, kinetic energy turns into electric energy to replenish the battery pack [19]. Also, the car’s electric motor goes into a reverse mode upon applying brakes, causing its wheels to slow down.

E. Coming to a Complete Stop

Both the petrol and electric motors shut down when the vehicle comes to a stop. However, its battery still keeps working, allowing vehicle systems, such as light, air conditioning, and radio to run.

When looking for petrol hybrid cars following the above mechanisms, you might come across numerous SUVs.

If in a dilemma, go for hybrid SUVs such as MG Hector and Mahindra Scorpio to experience the ultimate thrill with optimum performance [20].

IV. ADVANTAGES OF HYBRID VEHICLES

1. Fuel economy: Whether you care about the earth or not, increased fuel economy means fewer trips to the gas station and more money in your pockets.
2. Environmentally friendly: The entire point of hybrid vehicles is to reduce emissions and protect the environment through better fuel efficiency.
3. Performance: In certain applications such as the Acura NSX, gasoline and electricity work in tandem to produce increased performance through extra power, extra torque, wheel control, traction, and braking.
4. Unique trimmings: Manufacturers often want to alert the world that its hybrids are hybrids, so these models are often fitted with unique exterior lighting, extra badging, limited colors, wild designs, and eco-friendly alternative materials. Everybody knows the Prius because nothing else looks like it.
5. No range anxiety: One of the primary reasons consumers avoid electric vehicles is the fear the car will die and leave its occupants stranded. It’s a phenomenon known as range anxiety, and it’s completely eliminated on hybrid vehicles with backup gas power.

V. DISADVANTAGES OF HYBRID VEHICLES

1. Price: Thanks in part to the extra costs of researching and implementing their technology, hybrid models often cost more than the traditional base gasoline variants of the same model.
2. Performance: When fuel economy is prioritized over fun and engagement, enthusiasts will see themselves out.
3. Packaging: Although variety is increasing in the hybrid market due to increased saturation, hybrids are often built to specific parameters for specific people. Unfortunately, this means the buyer has less flexibility in choosing the trims and features he or she wants. For example, Toyota only recently drastically expanded its Prius audience by introducing an all-wheel drive option.
4. Complex to wrench on: Hybrids are generally more complex and more difficult to fix than traditional combustion cars. If a person isn’t comfortable working on their own vehicle, he or she might end up spending more money at the shop.
5. Rare-earth metals and mining: It can be true that hybrids are both helpful and harmful to the environment at the same time. Although they reduce emissions and greenhouse gases, large batteries in hybrids and electric vehicles utilize materials that are harvested and mined from the earth. The increase in hybrid popularity means these materials are mined at a greater rate, and in some cases, the mining operations are unfair and unsafe to its workers.
6. Batteries die: Until batteries can be efficiently and cost-effectively recycled, there will be concern about how to dispose of millions of large dead battery packs.
7. Looks: This is changing, but there aren’t many legitimately beautiful hybrid vehicles out there, and a cool affordable mass-market hybrid still does not exist. The new Ford Bronco hybrid could change that.

CONCLUSION

Hybrid cars are definitely more environmentally friendly than internal-combustion vehicles. Batteries are being engineered to have a long life. When the hybrid cars become more widespread, battery recycling will become economically possible. Research into other energy sources such as fuel cells and renewable fuels make the future look brighter for hybrid cars.

REFERENCES

[1] R.Senthilkumar, K.Ramadoss and R.Manimaran., “[Experimental Investigation](#) of Performance and Emission Characteristics by Different Exhaust Gas Recirculation Methods used in Diesel Engine”, Global J. of Mechanical and Mechanics Engineering, Vol.13, no.1, pp. 57-62, 2013.

- [2] He Ma, Hong-Ming Xu and Ji-Hong Wang., “[Real-time Control Oriented HCCI Engine Cycle-to-cycle Dynamic Modelling](#)”, Int. J. of Automation and Computing, Vol.8, no.3, pp. 317-325, 2011.
- [3] Dr.P.M.Diaz, N.Austin, Dr.K.Maniysundar and M.Julie Emerald Jiju., “[Numerical and Experimental Investigation on CNG Fueled HCCI Engine with EGR](#)”, Life science Journal, Vol.10, no.7s, pp. 1178-1181, 2013.
- [4] Giuseppe Genchi and Emiliano Pipitone., “[Preliminary Experimental Study on Double Fuel HCCI combustion](#)”, Energy Procedia, no.81, pp. 784-793, 2015.
- [5] Khashayar Ebrahimi, Masoud Aliramezani and Charles Robert Koch., “[An HCCI Control Oriented Model that includes Combustion Efficiency](#)”, International Federation of Automatic Control, Vol.49, no.11, pp. 327-332, 2016.
- [6] S.Gowthaman and A.P. Sathiyagnanam., “[Effects of charge temperature and fuel injection pressure on HCCI engine](#)”, Alexandria Engineering Journal, no.55, pp. 119-125, 2016.
- [7] Aravind. I. Garagad., “[Homogeneous Charge Compression Ignition \(HCCI\) Engines](#)”, Int. J. of Engg. Tech., Management and Applied Sciences, Vol.4, no.8, pp. 170-174, 2015.
- [8] Sunil Kumar PAndey, Muralitharan N and Ravikrishna R.V., “[Quasi-Dimensional Modelling and Parametric Studies of a Heavy-Duty HCCI Engine](#)”, Journal of combustion, Vol.2011, pp. 1-10, 2013.
- [9] Suyin Gan, Hoon Kiat Ng and Kar Mun Pang., “[Homogeneous Charge Compression Ignition \(HCCI\) combustion: Implementation and effects on pollutants in direct injection diesel engines](#)”, Journal of Applied Energy, Vol.88, pp. 559-567, 2011.
- [10] D.Ganesh and G.Nagarajan., “[Homogeneous Charge Compression Ignition \(HCCI\) combustion of Diesel Fuel with External Mixture Formation](#)”, SAE International Journals, no.01, pp. 07-15, 2009.
- [11] Bellanca, R.Mauss and Wang.H., “[Automatic Optimization of Detailed KINETIC Mechanism for HCCI Engine Simulation](#)”, Division of Fuel chemistry, Vol.49, no.1, pp. 267-268, 2004.
- [12] Faming Sun, Xiang Chen, David S-K Ting and Andrzej Sobiesiak., “[Modelling Operation of HCCI Engines Fueled with Ethanol](#)”, American Control Conference, pp. 1003-1009, 2005.
- [13] Ali Alqahtani., “[Thermodynamic simulation comparison of AVL BOOST and Ricardo WAVE for HCCI and SI engines optimisation](#)”, Journal of combustion engines, no.161(2), pp. 68-72, 2015.
- [14] S.Voglsam and F.Winter., “[A Global Combustion Model for Simulation of Gasoline HCCI Engines](#)”, Division of Fuel chemistry, Vol.49, no.1, pp. 267-268, 2004.
- [15] M. Nazoktabar and S.A. Jazayeri., “[Controlling the Power Output and Combustion Phasing in an Homogeneous Charge Compression Ignition Engine](#)”, Int. Journal of Engineering, Vol.27, no.11, pp. 1757-1766, 2014.
- [16] Nick J. Killingsworth, Salvador M. Aceves and Daniel L., “[HCCI Engine Combustion – Timing Control: Optimizing Gains and Fuel Consumption Via Extreme Seeking](#)”, IEEE Transactions on Control Systems Technology, Vol.17, No.6, pp. 1350-1361, 2009.
- [17] B.Bahri, A.Abdul Aziz, A.Salavati Z and V. Esfahanian., “[The effect of ethanol combustion on HCCI engine performance and emissions](#)”, The Journal of Engine Research, Vol.41, pp. 21-30, 2016.
- [18] A. Delorme, A Rousseau, T Wallner, E Ortiz Soto and D Assanis., “[Evaluation of Homogeneous Charge Compression Ignition Engine Fuel Savings for Various Electric Drive Powertrains](#)”, The 25th World Battery Symposium & Exhibition, 2010.
- [19] Krzysztof Motyl, Tadeusz and J. Rychter., “[HCCI Engine – A Preliminary Analysis](#)”, Journal of KONES Internal Combustion Engines, Vol.10, no.1, pp. 267-274, 2003.
- [20] P.V.Ramana, D.Maheswar and B.Uma Maheswar Gowd., “[Development of Alternative fuels for HCCI Engine Technology](#)”, Int. J. of Engineering Development and Research, Vol.3, no.2, pp. 108-119, 2015.

ENHANCEMENT OF COP IN VAPOUR COMPRESSION REFRIGERATION SYSTEM

R.Jyothu Naik¹, P.Srinivasarao²

¹ *Department of Mechanical Engg., Rayalaseema University, Kurnool-518001, A.P, India.*

² *Department of Mechanical Engg., Narasaraopeta engineering college, Narasaraopet-522601, A.P, India.*

Abstract: Experimental analysis on vapour compression refrigeration (VCR) system with R-12 refrigerant was done and their results were recorded. The effects of the main parameters of performance analysis such as mass flow of refrigerant, degree of sub cooling and super heating on the refrigerating effect, coefficient of performance (COP) and power required to run the compressor for various evaporating temperatures, percentage increase in COP and percentage reduction of power required to run the compressor for VCR are dealt. Further the investigations are carried out by introducing shell and coil heat exchanger at the end of compressor.

Keywords: Vapour compression refrigeration, Heat exchanger, COP, power.

I. INTRODUCTION

Vapour compression refrigeration system is based on vapour compression cycle. Vapour compression refrigeration system is used in domestic refrigeration, food processing and cold storage, industrial refrigeration system, transport refrigeration and electronic cooling etc. So improvement of performance of system is too important for higher refrigerating effect or reduced power consumption for same refrigerating effect. By sub-cooling using heat exchanger at condenser inlet refrigerating effect increases and power consumption or work input decreases. Thus performance of cycle is improved. Along with this waste heat also recovered. The essential quantity of heat recovered is not the amount but it is value.

Lokapure and Joshi [1] In their article dealt energy conservation by using technique of utilizing waste heat from air-conditioning system and increasing COP. They said that the refrigeration heat recovery device is indirect type of system in which a refrigerant to water heat exchanger is installed between the host refrigeration system compressor and condenser. In this case they achieved their goal by recovering energy and improving COP up to 13%. Khurmi and Gupta [2] in their book gave evidence that the process of under cooling is also brought about by employing a heat exchanger. This increases refrigerating effect and finally improved coefficient of performance in vapour compression refrigeration system. Domanski [3] investigated the effect of LLSL-HX (Liquid line/ Suction line heat exchanger) on system performance by taking liquid refrigerant from condenser to exchange heat with vapor refrigerant from evaporator. They reported that coefficient of performance was increased after installing LLSL-HX. Jain et al. [4] analyzed a complex system in

order to utilize waste heat rejected by condenser to the atmosphere by installing additional water cooled condenser. Baskaran and Mathews [5] described systems including various refrigerants improved by analyzing the effect of the super heating / sub cooling case. Better performance coefficient values (COP) than those of non-super heating /sub cooling case are obtained. Rajput [6] in his book concluded that sub-cooling results in increase of C.O.P and said that no further energy has to be spent to obtain the extra cold coolant. Thirumaleswar [7] proposed correlations for overall heat transfer coefficient for parallel and counter flow heat exchangers. Coronel and Sandeep [8] determined convective heat transfer coefficient in both helical and straight tubular heat exchangers under turbulent flow conditions. The experiments were conducted in helical heat exchangers and their study shows that the heat transfer coefficient in coiled tubes is higher than that in straight tubes.

II. SYSTEM DESCRIPTION AND DESIGN

Heat flows naturally from hot to colder body. But, in refrigeration system there is opposite phenomena i.e. heat flows from a cold to a hotter body. This is achieved by using a substance called a refrigerant. The refrigerant (R-12) absorbs heat and hence evaporates at a low pressure to form a gas. This gas is then compressed to a higher pressure, such that it transfers the heat it has gained to ambient air or water and turns back (condenses) into a liquid. Thus, heat is absorbed, or removed, from a low temperature source and transferred to a higher temperature source. The refrigeration cycle can be broken down into the following stages as in Fig 1.

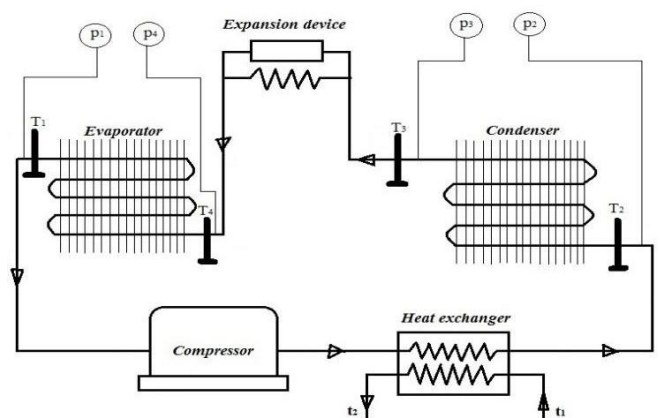


Fig.1: Schematic diagram of a proposed VCR System

Considering Fig.2,

1-2, the saturated vapour enters the compressor where its pressure is raised. There will also be a big increase in temperature, because a proportion of the energy input into the compression process is transferred to the refrigerant.

2-3, the high pressure superheated vapour passes from the compressor into the condenser. There will be decrease in temperature due to condensation process. The cooling for this process is usually achieved by using air. After condensation, refrigerant enters the expansion device.

3'-3, shell and coil heat exchanger is installed between the host refrigeration system compressor and condenser. Water is circulated through one side of heat exchanger and hot refrigerant gas from the compressor is routed through the other side. Heat is transferred from the hot refrigerant gas to the water thus refrigerating effect increases and power consumption or work input decreases. Thus performance of cycle is improved. Along with this waste heat also recovered.

3-4, the high-pressure liquid refrigerant passes through the expansion device, which both reduces its pressure and controls the flow into the evaporator.

4-1, Low pressure liquid refrigerant in the evaporator absorbs heat from its surroundings. During this process it changes its state from a liquid to a gas, and at the evaporator exit is slightly superheated.

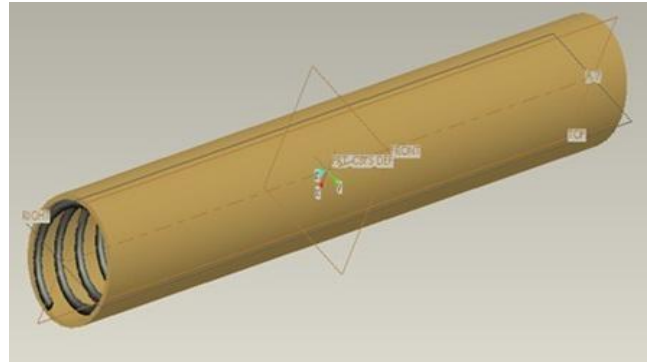


Fig.3: HEAT EXCHANGER COIL (modeled in Pro-E)

(B) Heat Exchanger Unit:

1) Overall heat transfer coefficient.

$$1/U = 1/h_i + 1/h_o + dx/k + F_r + F_w \quad (1)$$

2) Outlet temperature of water

$$t_2 = (Q / (m C_p)) + t_1 \quad (2)$$

3) Log mean temperature difference. = ΔT_m

$$\Delta T_m = (\Delta T_1 - \Delta T_2) / \ln (\Delta T_1 / \Delta T_2) \quad (3)$$

4) Area of Heat Exchanger

$$A = Q / U \times \Delta T_m \quad (4)$$

5) Length of the Tube,

$$L = A / \pi \times D_o \quad (5)$$

III. ANALYSIS OF THE PROBLEM

Based on T-s diagram of basic VCR as shown in Fig.4

1. Refrigerating effect = $h_1 - h_{f3}$ (6)

2. Degree of superheat = $T_2 - T_3$ (7)

3. $h_{2\text{ sup}} = h_{2'} + C_{pv} (T_2 - T_{2'})$ (8)

where $h_{2\text{ sup}}$ = enthalpy of vapour at superheated state
 C_{pv} (specific heat at constant pressure for the superheated vapour)

4. Compressor work (W_{comp}) = $h_{2\text{ sup}} - h_1$ (9)

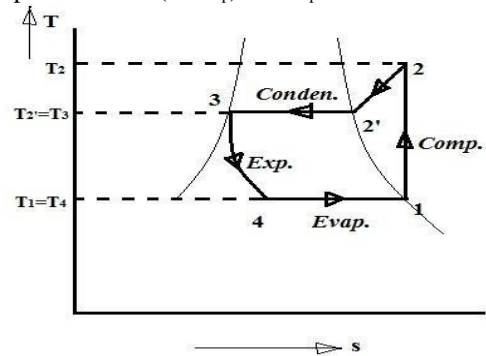


Fig.4: T-s diagram of basic VCR

$$\begin{aligned} \text{COP}_1 &= \frac{\text{Refrigeration Effect}}{\text{Work done by compressor}} \\ &= \frac{(h_1 - h_{f3})}{(h_{2\text{ sup}} - h_1)} \end{aligned} \quad (10)$$

Coefficient of performance of vapour compression Refrigeration system without heat exchanger

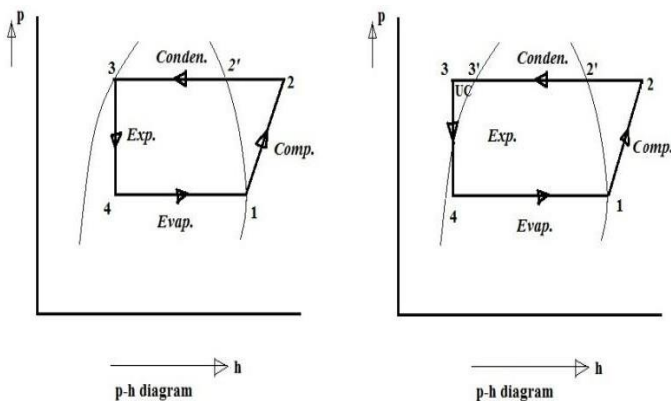


Fig.2: p-h diagram of a basic VCR and VCR with heat exchanger

(A) Shell and Coil Heat Exchanger:

Heat transfer in curved and helical circular tubes has been the subject of several studies due to the relatively high heat transfer coefficients associated with them. Flow in curved tubes is different from flow in straight tubes because of the presence of centrifugal forces. The centrifugal forces generate a secondary flow, normal to the primary direction of flow, with circulatory effects, that increases both the friction factor and the rate of heat transfer. The helically coiled heat exchangers generate a lot of turbulence thus a higher heat transfer coefficient obtained. If the unit is vertically installed, this reduces space requirements. Fig.3 shows heat exchanger coil which is modeled in Pro-E.

6. Mass flow of refrigerant,

$$m_R = \frac{\text{Refrigerating capacity}}{60 \times W_{\text{comp}} \times \text{COP}_1} \quad (11)$$

Where W_{comp} = Compressor work

7. Heat available for desuperheating
 $(Q) = m_R (h_{2 \text{ sup}} - h_2)$ (12)

8. Outlet temperature of water in heat exchanger
 $(t_2 \text{ }^\circ\text{C}) = (Q / (m C_p)) + t_1$ (13)

Where C_p is specific heat of water
 t_1 = inlet temperature of the water
 t_2 = outlet temperature

9. Degree of under cooling(DUC) = $t_2 - t_1$ (14)

10. $h_{f3} = h_{f3'} - C_{pl} \times \text{DUC}$ (15)

Where h_{f3} =Enthalpy of liquid refrigerant (VCR with heat exchanger)
 C_{pl} =Specific heat at constant pressure for the superheated liquid

11. $\text{COP}_2 = \frac{\text{Refrigeration Effect}}{\text{Work done by compressor}}$
 $= \frac{(h_1 - h_{f3})}{(h_{2 \text{ sup}} - h_1)}$ (16)

Where COP_2 = coefficient of performance of vapour compression refrigeration system with heat exchanger

12. % increase in COP = $\frac{(\text{COP}_2 - \text{COP}_1)}{\text{COP}_1} \times 100$ (17)

13. $m_{R1} = \frac{\text{Refrigerating capacity}}{60 \times W_{\text{comp}} \times \text{COP}_1}$
 14. (18) $m_{R1} = \frac{\text{Refrigerating capacity}}{60 \times W_{\text{comp}} \times \text{COP}_2}$

m_{R1} =Mass flow of refrigerant when VCR with heat exchanger

15. $P_1 = \frac{\text{Refrigerating capacity}}{60 \times \text{COP}_1}$ (19)

Where P_1 = Power required to run the compressor when VCR without heat exchanger

16. $P_2 = \frac{\text{Refrigerating capacity}}{60 \times \text{COP}_2}$ (20)

Where P_2 = Power required to run the compressor when VCR with heat exchanger

17. % reduction of power required to run the compressor = $\frac{(P_1 - P_2)}{P_1} \times 100$ (21)

$$\frac{(P_1 - P_2)}{P_1}$$

The results are extended to refrigerating capacity of 2 TR

IV. RESULTS AND DISCUSSION

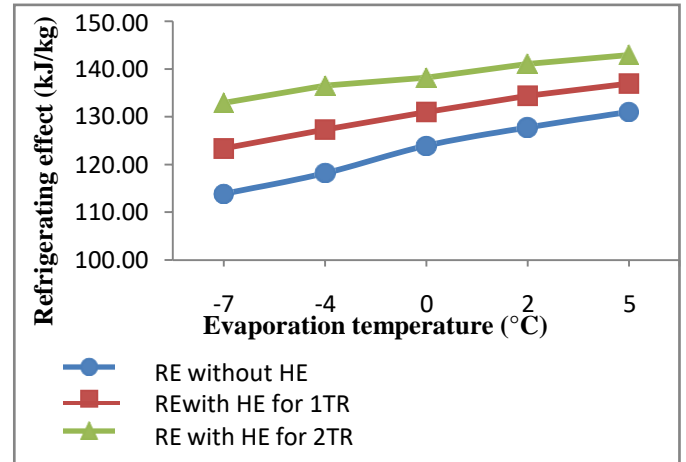


Fig.5: Evaporation temperature (°C) Vs Refrigerating effect (kJ/kg)

The results in above Fig.5 reveal that refrigerating effect increases when the heat exchanger is attached to VCR. This refrigerating effect further increases as the refrigerating capacity is increased from 1 TR to 2 TR.

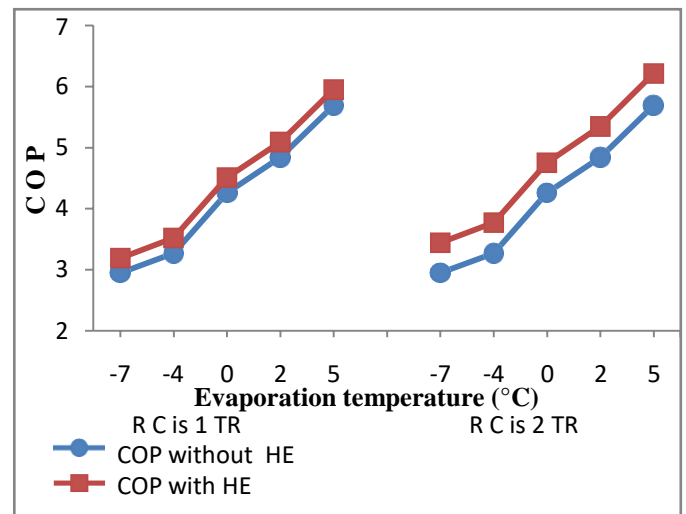


Fig.6: Evaporation temperature (°C) Vs COP

The results in above Fig.6 reveal that the coefficient of performance increases when the VCR is connected to heat exchanger. This is further increases when the refrigerating capacity (RC) increased from 1 TR to 2TR.

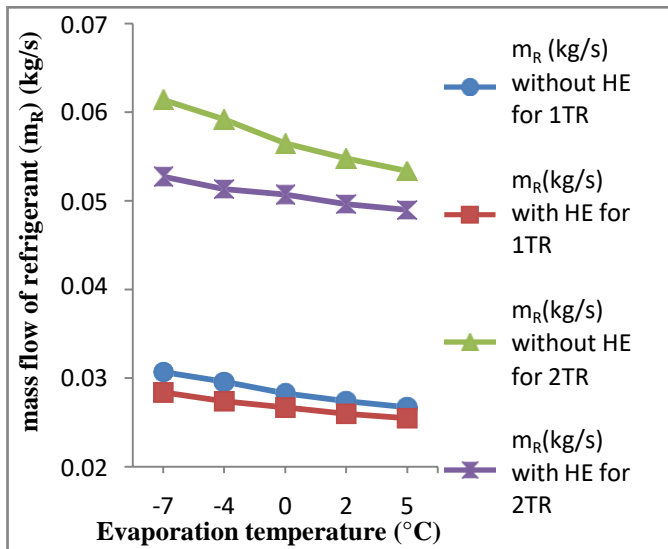


Fig.7: Evaporation temperature (°C) Vs Mass flow of refrigerant (kg/s)

The results in above Fig.7 reveal that Mass flow of refrigerant is decreases when the VCR is connected to heat exchanger. This graph is plotted by taking VCR without heat exchanger, with heat exchanger for refrigerating capacities of 1 TR and 2 TR.

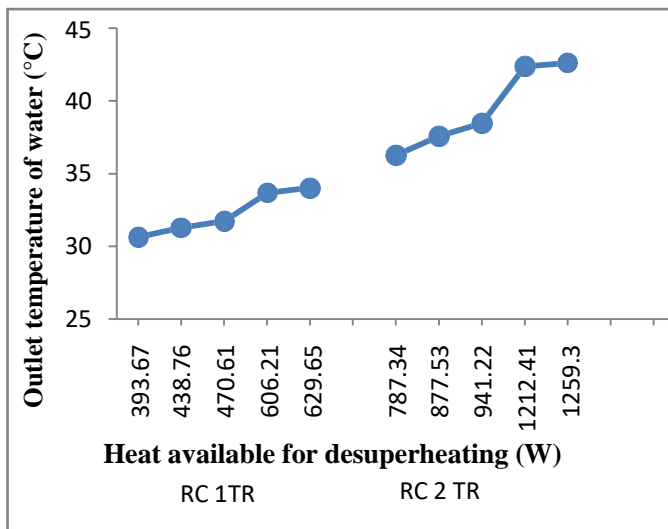


Fig.8: Heat available for desuperheating (W) Vs Outlet temperature of water (°C)

The results in above Fig.8 reveal that as the heat available for desuperheating increases, the outlet temperature of water in heat exchanger also increases.

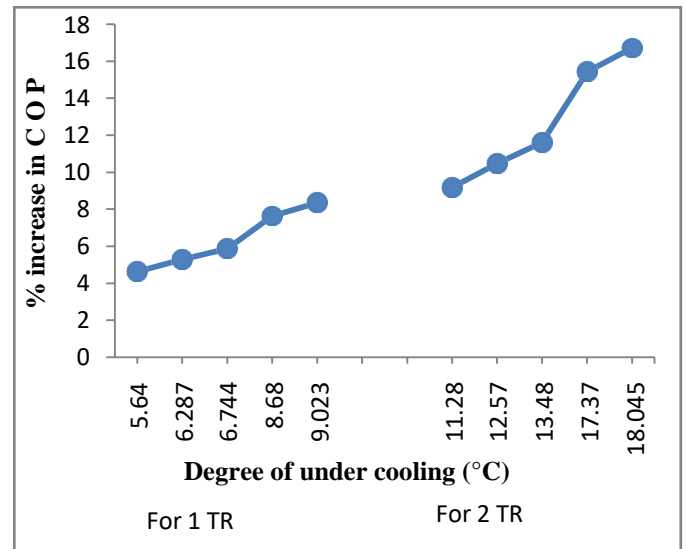


Fig.9: Degree of under cooling (°C) Vs percentage increase in COP

The results in above Fig.9 reveal that as the degree of under cooling increases the % increase in coefficient of performance also increases up to 16%. This is plotted by taking refrigerating capacities of 1 TR and 2TR.

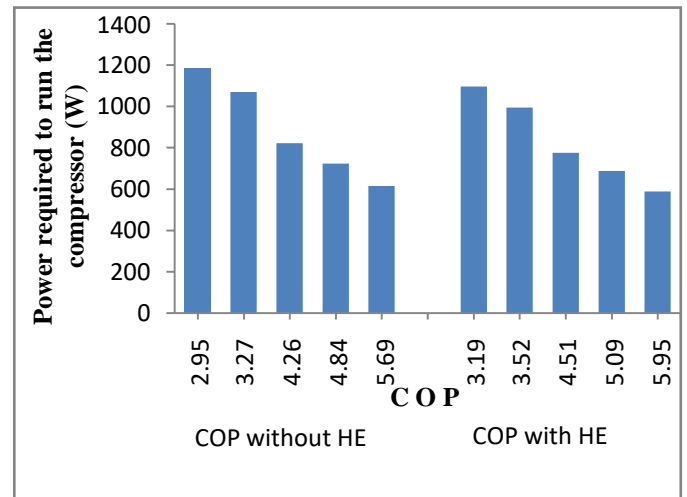


Fig.10: COP Vs Power required to run the compressor (W)

The power required to run the compressor is reduced up to 7.5% when the VCR (having refrigerating capacity of 1 TR) is attached to heat exchanger. The power required to run the compressor for a VCR without heat exchanger and VCR with heat exchanger both were plotted and shown in Fig.10

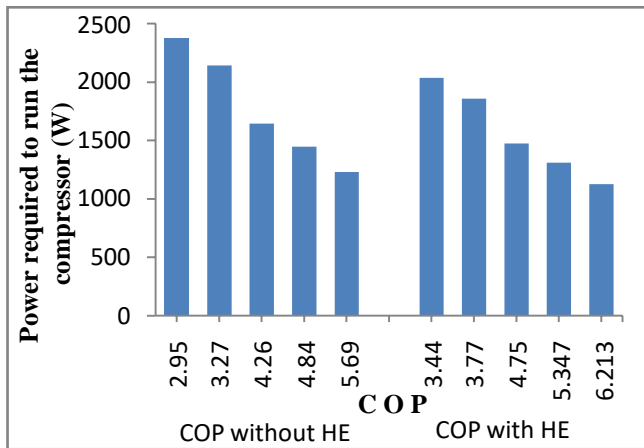


Fig.11: C O P Vs Power required to run the compressor (W)

The power required to run the compressor is reduced up to 14% when the VCR (having refrigerating capacity of 2 TR) is attached to heat exchanger. The power required to run the compressor for a VCR with and without heat exchanger were plotted and shown in Fig.11

V. CONCLUSIONS

The following conclusions are arrived from the VCR system connected with heat exchanger when the evaporation temperature decreases to -7°C:

1. The refrigeration effect of the system is increased up to 16% using the heat exchanger with vapour compression refrigeration system.
2. The C O P (coefficient of performance) of the system is increased up to 16% using the heat exchanger with vapour compression refrigeration system.
3. Mass flow of refrigerant (m_R) is reduced up to 14% using the heat exchanger with vapour compression refrigeration system.
4. Heat available for desuperheating (Q) increases as the evaporation temperature decreases. So by attaching heat exchanger to the vapour compression refrigeration system and regulating water into heat exchanger, outlet temperature of the water (t_2) in heat exchanger increases. That hot water can be used for useful purpose.
5. Power required to run the compressor is reduced up to 14% by using the heat exchanger with vapour compression refrigeration system.

ACKNOWLEDGMENT

We, authors express gratitude to all the anonymous reviewers for their affirmative annotations among our paper. Thanks to every reviewer for reviewing our paper and give valuable suggestions.

REFERENCES

[1] R.B. Lokapure and J.D.Joshi., Waste Heat Recovery through Air Conditioning System, International Journal of Engineering Research and Development, Vol 5, Issue 3, pp: 87-92, Dec 2012.
 [2] R.S.Khurmi and J.K. Gupta., Refrigeration and Air Conditioning, Eurasia publishing house Pvt Ltd, New Delhi, 2006.
 [3] P.A Domanski, Evaluation of Suction-Line/Liquid-Line Heat Exchanger in the Refrigeration Cycle, pp. 10-11, USA, 1995.
 [4] Rakesh Jain, Devendra Dandotiya and Abhishek Jain, Performance improvement of a Boiler through Waste Heat Recovery from an Air Conditioning Unit, International Journal of

Innovative Research in Science, Engineering and Technology, Vol. 2, Issue 2, pp: 405-412, Feb 2013.
 [5] A.Baskaran and P.Koshy Mathews., A Performance Comparison of Vapour Compression Refrigeration System using Eco Friendly Refrigerants of Low Global Warming Potential, International Journal of Scientific and Research Publications, Vol. 2, Issue 9, pp: 4-7, Sept 2012.
 [6] R.K.Rajput, Thermal Engineering, Laxmi publications Pvt Ltd., 2006.
 [7] M. Thirumaleshwar, Fundamentals of Heat and Mass Transfer, Pearson Publications, New Delhi, 2006.
 [8] Pablo Coronel, K.P. Sandeep., Heat Transfer Coefficient in Helical Heat Exchangers under Turbulent Flow Conditions, International Journal of Food Engineering, Vol 4, Issue 1, pp. 1-5, 2008
 [9] Yunus A.Cengel, Heat and Mass Transfer, Third Edition, Tata McGraw-Hill Publication, 2000.
 [10] Frank P.Incropera and David P. Dewitt., Fundamentals of Heat and Mass Transfer, Wiley India Pvt Ltd, 2010

CAPABILITY OF COMPRESSION-IGNITION ENGINE FUELLED WITH POND WATER ALGAE BIODIESEL

N.Vijay Kumar¹, P.Sravani², A.Pavan Kumar³,

¹*Department of Mechanical Engineering, PACE institute of technology & Sciences, Ongole, AP, India.*

^{2,3}*Department of Mechanical Engineering, Narasaraopeta Engineering College, Narasaraopeta, AP, India*

Abstract: Algae are the fast-growing florae around the globe. Microalgae are largely a diverse group of microorganisms comprising leukaryotic photoautotrophic protists and prokaryotic cyanobacteria (sometimes called blue-green algae). These microbes contribute to half of global photosynthetic activity and are virtually found in euphotic niches. The viability of biodiesel from pond water algae (PWA) as a third-generation biodiesel feedstock is examined in current investigation. Primarily, the oil is extracted from the algal biomass and then it is subjected to two stage transesterification technique. Ethanol is mixed up with the attained algal bio oil in order to reduce its viscosity. The processed algal oil is blended with diesel in various proportions. Later, by direct-injection into compression-ignition, the engine's performance and emission characteristics are assessed at varying loads (25, 50 and 100%) and CRs (15.5, 16.5, 17.5 and 18.5) using these prepared blends. Results have depicted that performance indices of engine are enhanced and emission parameters are reduced with the increase of algal biodiesel proportion in diesel fossil fuel.

Keywords: *Selective catalytic reactor, honeycomb, catalyst, space velocity, Nox conversion efficiency, ammonia slip.*

I. INTRODUCTION

Energy executes a noteworthy role in development. The fiscal development of any nation relies on its energy consumption. It is vital in every sector around the world, i.e., transportation, manufacturing, agriculture sector, etc. BP Statistical Review reported that primary energy consumption by fuel is 13276.3 Mtoe. However, total proven oil reserves are 1706.7 thousand million barrels in the world till the end of 2016, which is sufficient to meet 5 to 6 decades of world energy demand [1]. The world energy consumption is drastically increased from ~1687.7 kg in 2003 to 1873.7 kg in 2010 (per capita kg of oil equivalent). However, diesel fuel consumption per capita increased by ~37% between 2003 and 2010 for the automotive diesel engine [2,3]. It has been found

900 million vehicles (except two-wheelers) throughout the world that produces almost 26% greenhouse gases (GHGs) emissions [4]. Nearly all types of automobiles operated by diesel and petrol play a vital role in air pollution. To curb out pollution hazards, many countries adopted and implemented the updated emission standards, and made a policy to use alternative energy sources. In India, Bharat Stage VI (BS-VI) standards are going to be implemented from 2020, surpassing BS-V to control the continuous increasing pollution hazards from automobiles. Various worldwide emission standards (Bharat Stage, China, and Euro) for cars and light trucks (diesel vehicles) for the last decade are shown in Fig. 1 [5]. A flowchart of transportation activities and their emission are presented in Fig. 2, and the vehicle population growth (commercial ~ 29.6% and passenger ~ 34.9) from 2010 to 2020 are shown in Fig. 3 [6].

II. REVIEW OF LITERATURE

Sahar et al. [19] studied the technique for biodiesel production and analysis from used cooking oil with feedstock pretreatment method, transesterification process, whereas Mohadesi et al. [20] examined the impact of KOH/Clinoptilolite as a catalyst to produce biodiesel using used cooking oil. Kassaby and Allah [21] examined the effect of varying compression ratios (CR14, CR16, CR18) at different speeds (1000, 1250, 1500, 1750, and 2000 rpm) on CI engine fueled with different blends (B0, B10, B20, B30, B50) and ensured that the 20% biodiesel blended safely with diesel fuel and delivered almost the same performance and exhaust emissions when compared with diesel.

III. EXPERIMENTAL INVESTIGATION

A. Biodiesel preparation

Blends of fossil fuel diesel, PWA oil and ethanol are employed in CI engine as fuels. Initially, Algae was collected from local pond (PWA) present in Krishna district of Andhra Pradesh state, India. Preparation of PWA biodiesel is depicted through Fig. 6. Collected PWA were ground with motor as much as possible. The ground PWA were dried for 20 min at 80°C

incubator for releasing water. Hexane and ether solution (20 and 20 mL) were mixed with the dried PWA to extract oil. Then the mixture was kept for 24 h for settling. The biomass was collected after filtration and weighted.

The extracted oil was evaporated in vacuum to release hexane and ether solutions using rotary evaporator.

0.25 g NaOH was mixed with 24 mL methanol and stirred properly for 20 min. The mixture of catalyst and methanol was poured into the algal oil in a conical flask in order to lessen its viscosity. Later, transesterification reaction process is carried out. The conical flask containing solution was stirred for 3 h by electric shaker at 300 rpm. The reaction process step is indicated in Fig. 1.

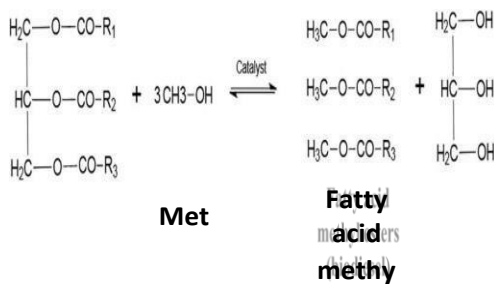


Fig. 1. Transesterification reaction

A. Engine setup and instrumentation

Fig. 8 depicts the schematic of computerized multifuel 4-stroke VCR engine. This setup comprises single-cylinder, variable compression ratio direct-injection compression-ignition engine which the loading is done by dynamometer of eddy current type. There is no need to stop the engine in order to alter its compression ratio (CR). Air box fitted with orifice plate makes the way for air to enter the engine. The instrumentation box comprises gaging instruments for engine speed, air & fuel consumption, torque, temperature and coolant flow rates. Sensors will record these parameters and values will be sent to data acquisition device, which exhibits these data in computer using LabView software. The technical specifications of engine are tabulated in Table 2.

Specification	Details
Make	Kirloskar
Engine cylinder/stroke	1/4
Maximum fuel injection pressure	220 bar
D * L	87.5 * 110 mm
Compression ratio	15.5-18.5
Rated output	4.5 kW at 1500 rpm
Rated speed	1500 rpm

IV. EXPERIMENTAL TEST PROCEDURE

The prepared fuel blends are tested under various engine loads. Prior to each experimentation, the engine is run with diesel for 10 min to ensure the reliability of attained data. The experiment values are taken after the engine reached to a steady state condition. The stationary multi fuel engine employed here is operated to run at its maximum speed of 1500 rpm. The temperature and relative humidity of intake air is measured with the aid of RTD sensors and the velocity is measured using velocity sensors.

All tailpipe exhausts are evaluated in a real-time manner. Fig. 9 illustrates various PEC conducted. The engine load was managed via the load cell. The engine's fuel consumption was estimated by calculating the decrease in the fuel level and in the measurement container over a specified period of time.

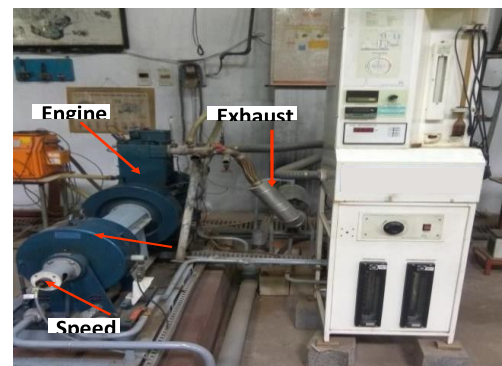
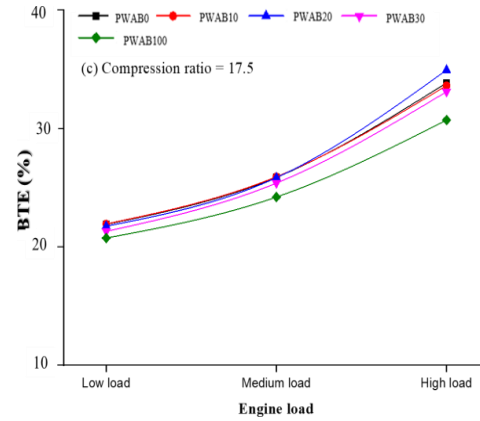
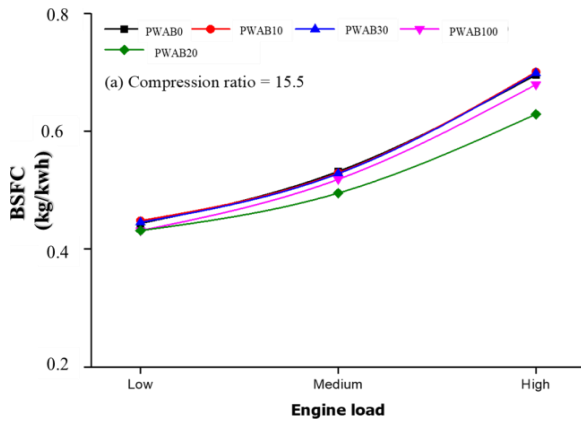


Fig. 8. Engine setup

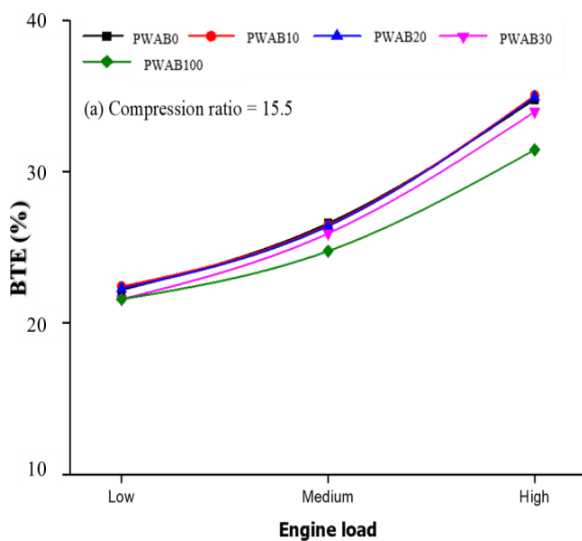
V. RESULTS

A. Brake specific fuel consumption



The prepared blends (PWAB0, PWAB100, PWAB10, PWAB20 and PWAB30) are examined experimentally using VCR diesel engine at various CRs of 15.5 and 17.5 at different engine loads of 25, 50 and 100% and by maintaining uniform speed of 1500 rpm. The performance attributes viz., BTE and BSFC and emission parameters viz., EGT, CO₂, PM, and NO_x are investigated for analyzing the PEC of the engine.

B. Brake thermal efficiency



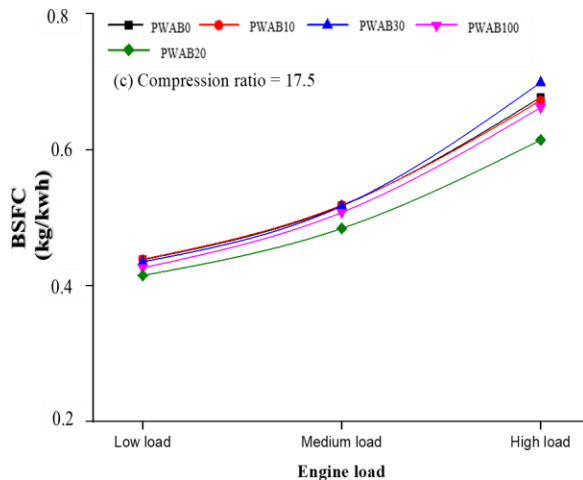


Fig. 2. BSFC at various engine load with different Compression Ratio

The variation of fuel NOX emission with engine load for the engine compression ratio at 15.5 and 17.5 are given in Figure 12 (a, c). The comparison of NOX emission with the low, medium and high engine load shows for PWAB0 (diesel), PWAB10 (90% diesel + 10 PWA oil), PWAB20 (80% diesel + 20% PWA oil), PWAB30 (70% diesel + 30% PWA oil) and PWAB100 (100% PWA biodiesel). The NOX emission of a blend of PWAB10, PWAB30 and PWAB100 found to be lower from those of diesel and PWAB20 for the entire range of engine load. NOX emission raised with enhancement in engine load due to elevated combustion temperature. The increasing compression ratio in the engine than NOX emission increased due to the improved combustion characteristics [50-52]. The NOX emission (ppm) produced for PWAB0 is 3663.9 at CR15.5, 3828.4 at CR17.5 . The NOX emission (ppm) for PWAB10 is 3941.9 at CR15.5, 4061.5 at CR17.5 , and PWAB20 is 2588.4 at CR15.5, 1960.5 at CR17.5 and 1703.1 at full load condition.

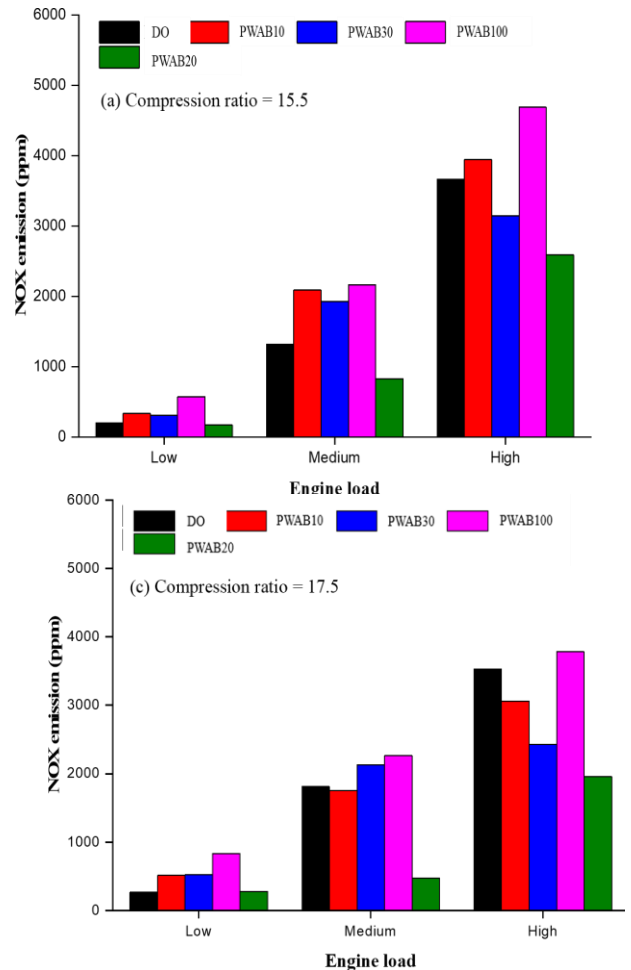


Figure 3. Engine load Vs. Nox emission with different compression ratio

VI. SUMMARY AND CONCLUSIONS

According to the investigation results obtained from the present study, performance and emission characteristics of BTE, BSFC and PM, CO₂, EGT & NOX emissions of CI engine charged with pond water algae-diesel for various engine loads and CR has been summarized below.

- The reduction in exhaust gas temperature has been found for the PWA biodiesel blends than diesel fuel at all engine loads. Maximum EGT was observed at 15.5 CR, 1500 rpm and high engine load.
- charged with diesel at all engine loads.

- PM from tail pipe of CI engine has been declined with the addition of PWA biodiesel to the diesel fuel. PM emissions decrease with increased compression ratio in the present investigation.
- Due to increase in compression ratio of the engine, CO₂ emission decreases as thermal efficiency increases and fuel consumption reduces.
- Escalation of CR from 15.5 to 17.5 leads to increase in NO_x emission by 5.04% and 3.57% for diesel fuel and PWA biodiesel blend (PWAB10), respectively, indicating improved biodiesel combustion at higher CR. NO_x emission escalates with rise in the engine load due to elevated combustion temperature.
- The rise in engine CR escalates the tail pipe emissions because of improvement in combustion of biodiesel in engine at higher CR.

VII. REFERENCES

1. Dudley B DS. BP Statistical Review of World Energy :49. n.d.
2. Energy use (kg of oil equivalent per capita) n.d.<https://data.worldbank.org/indicator/EG.USE.PCAP.KG.OE> (accessed April 1, 2021).
3. Chintala V, Subramanian KA. Assessment of maximum available work of a hydrogen fueled compression ignition engine using exergy analysis. *Energy* 2014; 67:162–75.
4. Nesamani KS. Estimation of automobile emissions and control strategies in India. *Sci Total Environ* 2010; 408:1800–11.
5. Emission Standards - Summary of worldwide engine and vehicle emission standards n.d. <https://www.dieselnets.com/standards/> (accessed April 3, 2021).
6. Wagner I. Number of passenger cars and commercial vehicles in use worldwide from 2006 to 2015 in (1,000 units) n.d. <https://www.statista.com/statistics/281134/number-of-vehicles-in-use-worldwide/> (accessed April 3, 2021).
7. Venkanna, B. K., and Venkataramana Reddy, C., 2011. Performance, emission and combustion characteristics of DI diesel engine running on blends of calophyllum inophyllum linn oil (hone oil)/diesel fuel/kerosene. *Int. J. Renewable Energy Technology*, 2(3): 294-305.
8. Silvio, C.A. de A., Belchior, C.R., Nascimento, M.V.G., Vieira, L. dos S.R. and Fleury, G. 2002, Performance of a diesel generator fuelled with palm oil, *Fuel*, 81:2097–2102.
9. Nwafor, O.M.I., Rice, G. and Ogbonna, 2002. Effect of advanced injection timing on the performance of rapeseed oil in diesel engines, *Renewable Energy*, 21:433–444.

OPTIMIZATION AND SIMULATION ANALYSIS OF SUBSONIC AIRCRAFT USING ALUMINIUM ALLOY AND CARBON FIBER COMPOSITE (CFC)

Y Srinivasa Reddy, Md.JabihullaShariff

*Department of Mechanical Engineering
PACE Institute of Technology and Sciences Ongole, AndhraPradesh, India.*

Abstract— Due to the demands of personal travels and entertainments, light airplanes and small business aircrafts are developing rapidly. Light airplane structure is simple; however, it lacks crashworthiness design, especially the considerations on the impact of energy absorption. Therefore, in an event of accident, significant damage to passengers will be usually incurred. Airplanes made of composite materials structurally have high specific strength and good aerodynamic configuration. These materials have become the primary choice for new airplane development. This study mainly explores the Design and optimization analysis of the light aircraft’s wing made of carbon fibre composite. The wings are usually straight or with low sweep angle. The main group of materials used in aircraft wing construction has been steel, aluminium alloys and more recently titanium alloys and fibre reinforced composites. Composite materials are well known for their excellent combination of high structural stiffness and low weight. This paper compares the compression amounts in the original models of carbon fibre composite material and aluminum alloy with the model optimization during the crash-landing, in order to investigate the safety of aircraft wing made of different materials after structural optimization under the dynamic crashing. This study found that the energy absorbed by the aluminum alloy wing during crash-landing is still higher than that by the carbon fibre composite. On the other hand, the aluminum alloy wing after optimization could have an energy absorption capability enhanced by 40%, as compared to carbon fibre composite. Moreover, it is estimated that replacement of aluminium alloy by CFC results in 52.96% saving in the total structural weight of the aircraft wing.

Keywords— *strength and good aerodynamic configuration, carbon fibre composite, aluminium alloys, fibre reinforced composites, absorption capability, structural weight.*

1 INTRODUCTION

Wings develop the major portion of the lift of a heavier-than-air aircraft. Wing structures carry some of the heavier loads found in the aircraft structure. The particular design of a wing depends on many factors, such as the size, weight, speed, rate of climb, and use of the aircraft. The wing must be constructed so that it holds its aerodynamics shape under the extreme stresses of combat makeovers or wing loading. Wing construction is similar in most modern aircraft [1]. In its simplest form, the wing is a framework made up of spars and ribs and covered with metal. The construction of an aircraft wing, Spars is the main structural members of the wing. They extend from the fuselage to the tip of the wing. The entire load carried by the wing is taken up by the spars. The spars are designed to have great bending strength. Ribs give the wing section its shape, and they transmit the air load from the wing covering to the spars. Ribs extend from the leading edge to the trailing edge of the wing. In addition to the main spars, some wings have a false spar to support the ailerons and flaps. Most aircraft wings have a removable tip, which streamlines the outer end of the wing [2].

Most Navy aircraft are designed with a wing referred to as a wet wing. This term describes the wing that is constructed so it can be used as a fuel cell. The wet wing is sealed with a

fuel-resistant compound as it is built. The wing holds fuel without the usual rubber cells or tanks. The wings of most naval aircraft are of all metal, full cantilever construction. Often, they may be folded for carrier use. A full cantilever wing structure is very strong. The wing can be fastened to the fuselage without the use of external bracing, such as wires or struts [3]. A complete wing assembly consists of the surface providing lift for the support of the aircraft. It also provides the necessary flight control surfaces.



FIG 1.1 STRUCTURE OF AIRCRAFT WING

1.1 Wing Configurations:

Wings are air foils that, when moved rapidly through the air, create lift. They are built in many shapes and sizes. Wing design can vary to provide certain desirable flight characteristics. Control at various operating speeds, the amount of lift generated, balance, and stability all change as the shape of the wing is altered. Both the leading edge and the trailing edge of the wing may be straight or curved, or one edge may be straight and the other curved. One or both edges may be tapered so that the wing is narrower at the tip than at the root where it joins the fuselage. The wing tip may be square, rounded, or even pointed. The wings of an aircraft can be attached to the fuselage at the top, mid-fuselage, or at the bottom [4]. They may extend perpendicular to the horizontal plain of the fuselage or can angle up or down slightly. This angle is known as the wing dihedral. The dihedral angle affects the lateral stability of the aircraft.

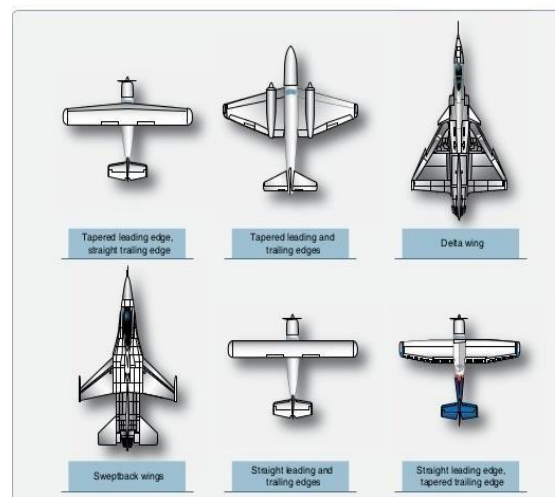


Figure 1.1.1 various aircraft wing design shapes

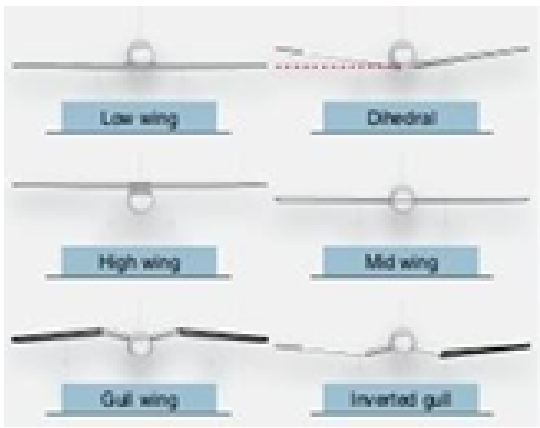


Figure 1.1.2 Aircraft wing shapes and attach points

1.2 Wing Structure:

The wings of an aircraft are designed to lift it into the air. Their particular design for any given aircraft depends on a number of factors, such as size, weight, use of the aircraft, desired speed in flight and at landing, and desired rate of climb. The wings of aircraft are designated left and right, corresponding to the left and right sides of the operator when seated in the cockpit. Often wings are of full cantilever design. This means they are built so that no external bracing is needed. They are supported internally by structural members assisted by the skin of the aircraft. Other aircraft wings use external struts or wires to assist in supporting the wing and carrying the aerodynamic and landing loads. Wing support cables and struts are generally made from steel [5]. Many struts and their attach fittings have fairings to reduce drag. Short, nearly vertical supports called jury struts are found on struts that attach to the wings a great distance from the fuselage. This serves to subdue strut movement and oscillation caused by the air flowing around the strut in flight. Figure 1.3 shows samples of wings using external racing, also known as semi cantilever wings. Cantilever wings built with no external bracing are also shown.



Fig.1.2.1 Left” and “right” wing of an aircraft to the perspective of a pilot sitting in the cockpit

Aluminium is the most common material from which to construct wings, but they can be wood covered with fabric, and occasionally a magnesium alloy has been used. Moreover, modern aircraft are tending toward lighter and stronger materials throughout the airframe and in wing construction. Wings made entirely of carbon fibre or other composite materials exist, as well as wings made of a combination of materials for maximum strength to weight performance. The internal structures of most wings are made up of spars and stringers running spanwise and ribs and formers or bulkheads running chordwise (leading edge to trailing edge) [6]. The spars are the principle structural

members of a wing. They support all distributed loads, as well as concentrated weights such as the fuselage, landing gear, and engines. The skin, which is attached to the wing structure, carries part of the loads imposed during flight. It also transfers the stresses to the wing ribs. The ribs, in turn, transfer the loads to the wing spars.

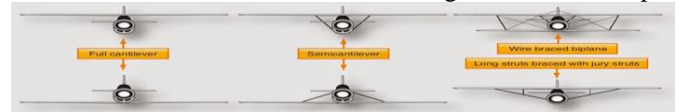


Fig.1.2.2 Full, Semi and Wire braced biplane cantilever aircraft wing structures

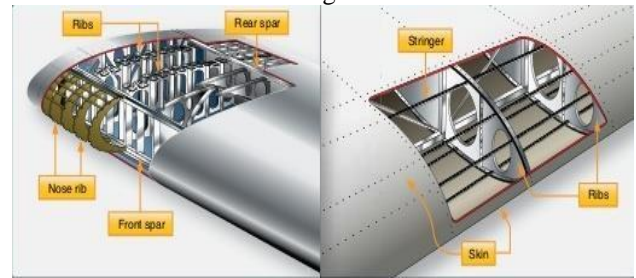


Figure 1.2.3 Wing structure with nomenclature.

In general, wing construction is based on one of three fundamental designs:

1. Monospar
2. Multispar
3. Box beam

Modification of these basic designs may be adopted by various manufacturers. The monospar wing incorporates only one main spanwise or longitudinal member in its construction. Ribs or bulkheads supply the necessary contour or shape to the air foil. Although the strict monospar wing is not common, this type of design modified by the addition of false spars or light shear webs along the trailing edge for support of control surfaces is sometimes used. The multispar wing incorporates more than one main longitudinal member in its construction [7]. To give the wing contour, ribs or bulkheads are often included. The box beam type of wing construction uses two main longitudinal members with connecting bulkheads to furnish additional strength and to give contour to the wing. A corrugated sheet may be placed between the bulkheads and the smooth outer skin so that the wing can better carry tension and compression loads. In some cases, heavy longitudinal stiffeners are substituted for the corrugated sheets. A combination of corrugated sheets on the upper surface of the wing and stiffeners on the lower surface is sometimes used. Air transport category aircraft often utilize box beam wing construction.

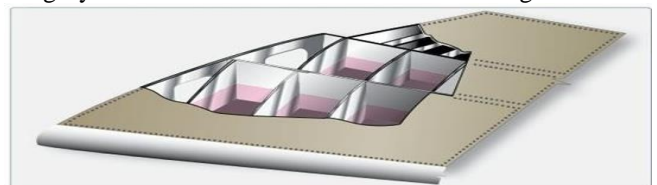


Figure 1.2.4. Box beam construction of aircraft wing

1.3 Wing Spars:

Spars are the principal structural members of the wing. They correspond to the longerons of the fuselage. They run parallel to the lateral axis of the aircraft, from the fuselage toward the tip of the wing, and are usually attached to the fuselage by wing fittings, plain beams, or a truss. Spars may be made of metal, wood, or composite materials depending on the design criteria of a specific aircraft. Wooden spars are usually made from spruce. They can be generally classified into four different types by their cross-sectional configuration. As shown in Figure

1.8, they may be (A) solid, (B) box shaped, (C) partly hollow, or (D) in the form of an I-beam. Lamination of solid wood spars is often used to increase strength. Laminated wood can also be found in box shaped spars. The spar in Figure 1.8 has had material removed to reduce weight but retains the strength of a rectangular spar. As can be seen, most wing spars are basically rectangular in shape with the long dimension of the cross-section oriented up and down in the wing [8].

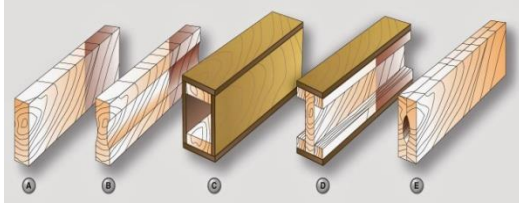


Figure 1.3. Typical wooden wingspar cross-sections

1.4 Wing Ribs:

Ribs are the structural crosspieces that combine with spars and stringers to make up the framework of the wing. They usually extend from the wing leading edge to the rear spar or to the trailing edge of the wing. The ribs give the wing its cambered shape and transmit the load from the skin and stringers to the spars. Similar ribs are also used in ailerons, elevators, rudders, and stabilizers. Wing ribs are usually manufactured from either wood or metal. Aircraft with wood wing spars may have wood or metal ribs while most aircraft with metal spars have metal ribs. Wood ribs are usually manufactured from spruce. The three most common types of wooden ribs are the plywood web, the lightened ply wood web, and the truss types. Of these three, the truss type is the most efficient because it is strong and lightweight, but it is also the most complex to construct [12]. Figure 1.14 shows wood truss web ribs and a lightened plywood web rib. Wood ribs have a rib cap or cap strip fastened around the entire perimeter of the rib. It is usually made of the same material as the rib itself. The rib cap stiffens and strengthens the rib and provides an attaching surface for the wing covering. In Figure 1.14A, the cross-section of a wing rib with a truss-type web is illustrated. The dark rectangular sections are the front and rear wing spars. Note that to reinforce the truss, gussets are used. In Figure 1.14B, a truss web rib is shown with a continuous gusset. It provides greater support throughout the entire rib with very little additional weight. A continuous gusset stiffens the cap strip in the plane of the rib. This aids in preventing buckling and helps to obtain better rib/skin joints where nail-gluing is used. Such a rib can resist the driving force of nails better than the other types [13].

2. LITERATURE SURVEY

This study examines the progress in aircraft and aircraft engines from the standpoint of the role that better materials and processing has played. Such progress includes the relatively recent transformation of the aircraft industry from purely performance driven products to products that are driven by customer value. It is demonstrated that advances in materials and processing technology and understanding have enabled much of the progress that has been made since the inception of manned, heavier than air flight. The recent constraints of cost, as determined by customer value, have changed the way new materials are introduced and these trends appear to be the new paradigm for the aircraft and aircraft engine industry. A recent trend in the transportation industry is to improve customer value through creation of

products that incorporate advanced structural materials and benefit from new manufacturing technologies [21]. The objective is to create value by improving performance, reducing ownership costs, extending the system life and reducing environmental impact. Improved performance, as determined by materials, typically translates into higher structural efficiency, resulting in reduced product weight. Structural efficiency is the combined result of materials capability and design methodology. For example, a stiffness limited component may incorporate a higher modulus material using the same design or it may use a new design that increases the section modulus or both. Honeycomb construction used in aircraft is an example of an increased section modulus design.

2.1 Materials for aerospace Applications

Since the first days of powered flight, aircraft designers have focused on achieving minimum weight, both in airframes and in propulsion systems. For example, the original Wright Flyer employed an engine with an aluminum block, which was virtually unheard of at the turn of the 20th century. From 1903 to about 1930 absolute minimum weight was necessary for practical flight, due in large part to the limited capability of the available propulsion systems. Consequently, the strength/weight ratio was the prime driver for materials selection for both engines and aircraft. While this consideration continues to be of first order importance, light weight is now necessary but not sufficient. Current design criteria are much more complicated, as mentioned in the Introduction, and winning products require new design methods as well as improved materials and processing methods [24]. The transition from internal combustion, piston engines to turbines represented a major "game changer" in aircraft. Beginning in the early 1940's with the German Messerschmitt Me-262 fighter aircraft, turbines became the preferred type of propulsion system. The performance of the early turbine engines was severely limited by materials capability, especially in terms of operating temperature. Jet powered fighters were in operation in the late 40's but large jet aircraft, e.g., bombers and transports did not become feasible until nearly a decade later, largely because of the increased difficulty of producing large turbine engines with adequate reliability. As will be described later, turbine technology has evolved and, today, propulsion technology is not the limiting factor it once was [25].

2.2 Aluminium based Alloy Materials

Although high performance composites such as carbon fibre are receiving increasing interest, aluminium alloys still make up a significant proportion of aerospace structural weight as demonstrated in the examples of materials distribution for some typical Boeing planes. The relatively high specific strength and stiffness, good ductility and corrosion resistance, low price and excellent manufacturability and reliability make advanced aluminium alloys a popular choice of lightweight materials in many aerospace structural applications, e.g. fuselage skin, upper and lower wing skins, and wing stringers, etc. The development of heat treatment technology provides high strength aluminium alloys that remain competitive with advanced composites in many aerospace applications. Aluminium alloys can offer a wide range of material properties meeting diverse application requirements, through adjusting compositions and heat treatment methods. The most extensively used aluminium alloys in aerospace industry are the Al-Cu alloys (2xxx series), Al-Zn alloys (7xxx series) and Al-Li alloys. 2xxx series alloys are used where high damage tolerance and fracture toughness

are the predominant criteria. AA2024 is one of the most commonly used Al alloys in fuselage structure due to its excellent damage tolerance at T3 condition. But its poor yield strength and fracture toughness restrict its application and it has been replaced by AA2524-T3 in the fabrication of many aircraft such as Boeing 777 aircraft, which has 15% to 20% improved fracture toughness resulting in 30% to 40% weight reduction. AA2224 and AA2324 provide enhanced strength and are used in the lower wing skin. AA2026 is considered an excellent replacement of AA2024 because of its better damage tolerance and fatigue resistance, as well as higher strength [27].

2.3 Titanium based Alloys Materials

Titanium alloys have many advantages over other metals, such as high specific strength (e.g. the specific strength of Beta C titanium alloy, ca. 260 kN·m/kg, is around three times that of CoMo steel 4130 and 1.27 times that of high strength aluminium alloy 7075-T6), high stiffness, good fracture toughness and fatigue resistance, as well as very good corrosion resistance, heat resistance, cryogenic embrittlement resistance, and low thermal expansion. These advantages make titanium alloys an excellent alternative to steels and aluminium alloys in airframe and engine applications. However, the poor manufacturability and high-cost result in the restriction of titanium alloys being extensively used [31]. Hence, the titanium alloys are used where high strength is required but limited space is available, as well as where high corrosion resistance is required. The current applications of titanium alloys in aerospace industry are mainly in airframe and engine components. Titanium alloys can, generally, be categorized as α -alloys, $\alpha+\beta$ -alloys and β -alloys, according to the percentage of α - phase and β -phase in the alloy. In the alloys, the α -phase has lower density and the β - phase can improve strength. Ti-6Al-4V ($\alpha+\beta$ -alloys) is currently the most extensively used titanium alloy. Its applications include airframes structures such as windows frames, and gas turbine engine components such as discs and blades for the fan and compressor. Ti-3Al-2.5 V is an α -alloy that is used in place stainless steel in high pressure hydraulic tubing, saving 40% structural weight . The β -alloy, Ti-10V-2Fe-3Al, is used to fabricate the main landing gear of Boeing 777, which results in a weight reduction of 270 kg for the airplane.

2.4 Composite Materials in Aircraft Structures

The study of composite materials started in the early 1960s when they were first developed at the Royal Aircraft Establishment at Farnborough, UK. The initial application of composite materials in the aeronautical field was in the secondary structures of military aircraft, such as fairings, small doors and control surfaces. As the technology evolved and the production costs were reduced, the use of composite materials extended to the commercial transport aircraft applications as both secondary and primary structural components such as wings and fuselage. The composite materials usage trend for commercial transport aircraft is shown in Figure 2.1. One of the main drives to use composite materials is their high stiffness to weight ratio; which offers potentials for great improvement in the overall performance and reduction in costs. However, their application as primary aircraft components are still today always cautiously evaluated, as they behave differently from metallic structures and the methods to accurately predict the damage mechanism and structural failure have not yet been fully explored [32]. Many of the conventional design and

analysis methods have been reviewed to include the anisotropic properties of composites and also to take in to account the additional considerations such as effect of the laminate stacking sequence, through thickness effects, interlaminar stresses and delimitation. Extensive research has therefore been conducted to study how these composite structural components react under various types of loadings and how they behave when they are assembled together.

2.5 Selection of Aerospace Materials

The selection of materials for an aerospace system is based on the operating conditions of the specific component or system, such as loading conditions, operating temperatures, moisture, corrosion conditions, noise in combination with consideration of economic and regulatory factors. For example, wings mainly sustain bending during service, as well as tension, torsion, vibration and fatigue. Hence, the main constraints for wing materials are stiffness, tensile strength (lower wing structures), compressive strength (upper wing structures), and buckling strength and vibration modes [34]. Combustion chambers are subjected to high temperature and pressure operation, and associated fluid-structure interactions, and the materials selection constraints are principally thermal properties and oxidation resistance presents a brief comparison of some commercial aerospace materials. According to Table 2.2, composites such as CFRPs and GLAREs usually have much higher specific strength and stiffness than metals, which makes composites an attractive choice for light-weighting design for many aerospace components and systems. However, metals have the advantage of ease of manufacture and availability, as well as much lower cost, making them still extensively used in many aerospace applications [35].

3 DESIGN OF AIRCRAFT WING

Introduction to ANSYS: For all engineers and students coming to finite element analysis or to ANSYS software for the first time, this powerful hands-on guide develops a detailed and confident understanding of using ANSYS's powerful engineering analysis tools. The best way to learn complex systems is by means of hands-on experience. With an innovative and clear tutorial- based approach, this powerful book provides readers with a comprehensive introduction to all of the fundamental areas of engineering analysis they are likely to require either as part of their studies or in getting up to speed fast with the use of ANSYS software in working life. Introduction to the finite element method Getting started with ANSYS software stress analysis dynamics of machines fluid dynamics problems thermos mechanics contact and surface mechanics exercises, tutorials, worked examples With its detailed step-by-step explanations, extensive worked examples

Root chord length	13m
Tip chord length	3.5m
Thickness of rib	0.2m
Length of front spar	31m
Length of mid spar	30.6m
Length of rear spar	30.2m

and sample problems, this book will develop the reader's understanding of FEA and their ability to use ANSYS's software tools to solve their own particular analysis problems, not just the ones set in the book [36].

ANSYS Mechanical software offers a comprehensive product solution for structural linear/nonlinear and dynamics analysis. The product offers a complete set of elements behavior, material models and equation solvers for a wide range of

engineering problems. In addition, ANSYS Mechanical offers thermal analysis and coupled-physics capabilities involving acoustic, piezoelectric, thermal-structural and thermal-electric analysis. ANSYS Structural software addresses the unique concerns of pure structural simulations without the need for extra tools. The product offers all the power of nonlinear structural capabilities - as well as all linear capabilities -in order to deliver the highest-quality, most reliable structural simulation results available. ANSYS Structural easily simulates even the largest and most intricate structures. ANSYS Professional software offers a first step into advanced linear dynamics and nonlinear capabilities. Containing the power of leading simulation technology in an easy-to-use package, ANSYS Professional tools provide users with high-level simulation capabilities without the need for high-level expertise. ANSYS Design Space software is an easy-to-use simulation software package that provides tools to conceptualize design and validate ideas on the desktop. A subset of the ANSYS Professional product, ANSYS design space allows users to easily perform real-world, static structural and thermal, dynamic, weight optimization, vibration mode, and safety factor simulations on all designs without the need for advanced analysis knowledge.

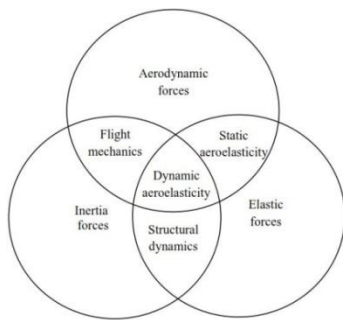


Fig 3(a) Summary of the Field of Aeroelasticity

Fig 3(b) Wing Structural Design Process

Table 3(a) Simulation Dimensions of the Aircraft Wing

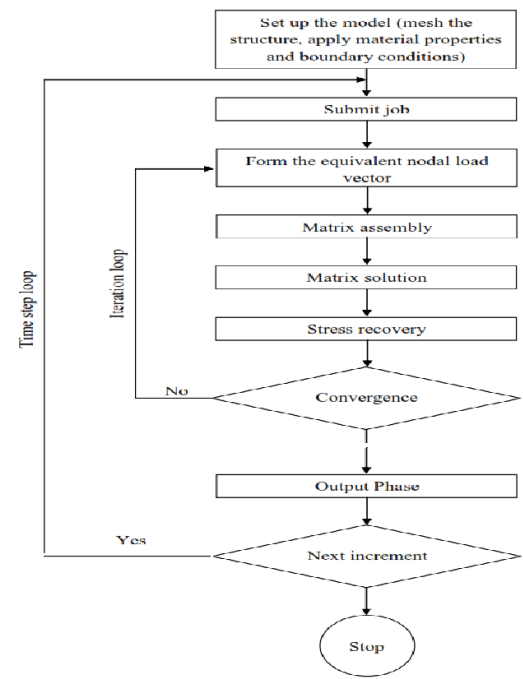


Fig 3(c) Process for Design of Aircraft wing using ANSYS

Table 3(b) Properties of Aluminum Alloy and CFC

Property	Aluminium Alloy	CFC
Density (G/Cm3)	2.7	1.6
Youngs Modulus (GPa)	68.9	127
Shear Modulus (GPa)	26	9.1
Passion's Ratio	0.33	0.31

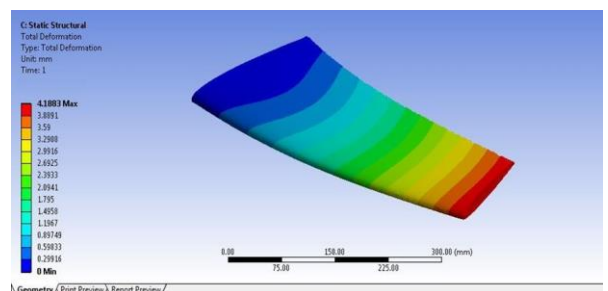
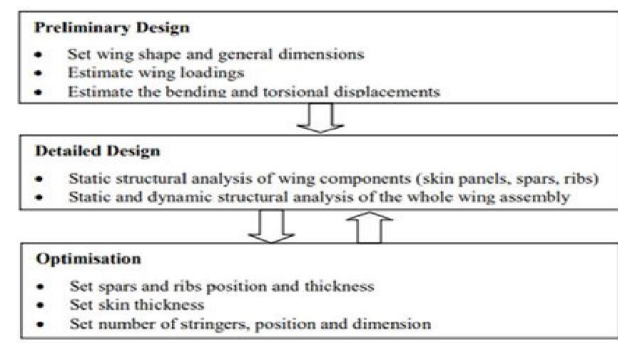
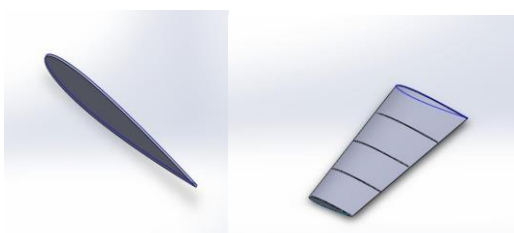


Fig 3(d) Cross-section View of Aircraft Wing Design, Structural View of Aircraft Wing Design

3.1 ANALYSIS OF AIRCRAFT WING

In this study, the 3D model for the aircraft wing structure was built using the ANSYS software. Then, the parameter setting and the structural topology optimization of aluminum alloy and CFC were conducted using the optimization. The output results were imported into Abaqus/Explicit to establish a dynamic crash-landing simulation for comparing the differences in the overall safety and the compression amount of fuselage at each direction between the original model and the optimized model for the light aircraft structure of the two different materials under dynamic impact. The structural optimization simulation for the impact resistance capability or the crashworthiness design of light aircraft studied in this paper is mainly based on the crashing parameters 1.3V so and 30° nose-down angle, laid out by AGATE and the ASTM F2245; we also take the minimum safety standard as the term drafted by the MIL-STD -1290A, whereby the allowable deformation amount of cockpit in the horizontal direction, vertical direction, or lateral direction shall not be more than 15%. The optimization simulation in this study takes minimizing the strain energy as the objective function, that is, the minimum strain satisfied under the above-mentioned crashing condition. The structure optimization of this simulation takes the minimum volume that fulfils the wing rationalization design as the constraint [43].

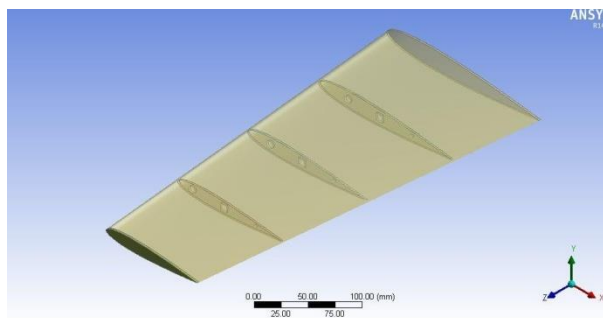


Fig 3.1(a) Design Module of Structural Aircraft Wing

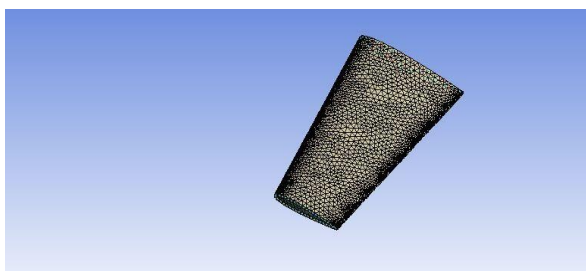


Fig 3.1(b) Meshing applies on the wing

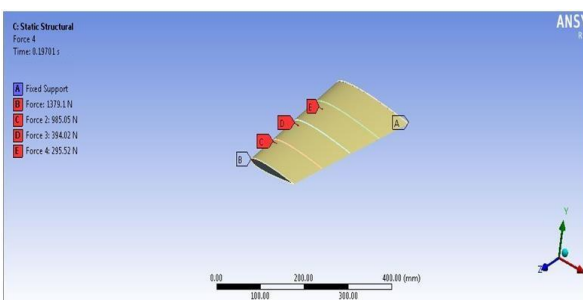


Fig 3.1(c) Load/Forces apply on the wing

Project	
First saved	22 May 2022
Last saved	28 May 2022
Product version	14.5
Save project before solution	Yes
Save project After Solution	Yes

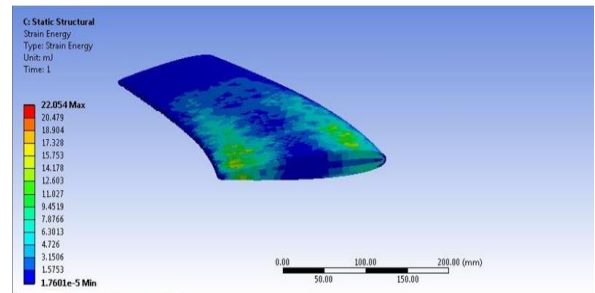
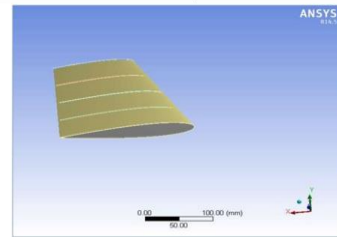


Fig 3.1(d) Total Deformation on Aircraft wing After Load

Fig 3.1(e) Total Strain Energy on Aircraft wing After Load

3.2 Result of Static Analysis on Wing

Contents

- [Units](#)
- [Model \(C4\)](#)
 - [Geometry](#)
 - [Parts](#)
 - [Layered Section](#)
 - [Coordinate Systems](#)
 - [Connections](#)
 - [Contacts](#)
 - [Contact Regions](#)
 - [Mesh](#)
 - [All Triangles Method](#)
 - [Static Structural \(C5\)](#)
 - [Analysis Settings](#)
 - [Loads](#)
 - [Solution \(C6\)](#)
 - [Solution Information](#)
 - [Results](#)
- [Material Data](#)
 - [cfc](#)

Units

Unit System	Metric (mm, kg, N, s, mV, mA) Degrees rad/s Celsius
Angle	Degrees
Rotational Velocity	rad/s
Temperature	Celsius

Model (C4)

Geometry

Model (C4) > Geometry	
Object Name	Geometry
State	Fully Defined
Definition	
Source	D:\wing\lap_files\dp0\SYS-2\DM\SYS-2.agdb
Type	DesignModeler
Length Unit	Millimeters
Element Control	Program Controlled
Display Style	Body Color
Bounding Box	
Length X	200. mm
Length Y	23.856 mm
Length Z	410. mm

Properties	
Volume	N/A
Mass	N/A
Scale Factor Value	1.
Statistics	
Bodies	6
Active Bodies	6
Nodes	10339
Elements	11136
Mesh Metric	None
Basic Geometry Options	
Parameters	Yes
Parameter Key	DS
Attributes	No
Named Selections	No
Material Properties	No
Advanced Geometry Options	
Use Associativity	Yes
Coordinate Systems	No
Reader Mode Saves Updated File	No
Use Instances	Yes
Smart CAD Update	No
Attach File Via Temp File	Yes
Temporary Directory	C:\Users\cheri\AppData\LocalTemp
Analysis Type	3-D
Decompose Disjoint Geometry	Yes
Enclosure and Symmetry Processing	Yes

TABLE 3
Model (C4) > Geometry > Parts

Object Name	Solid	Solid	Solid	Solid	Solid
State					
					Meshed
Graphics Properties					
Visible	Yes				
Transparency	1				
Definition					
Suppressed	No				
Stiffness Behavior	Flexible				
Coordinate System	Default Coordinate System				
Reference Temperature	By Environment				
Material					
Assignment	cfc				
Nonlinear Effects	Yes				
Thermal Strain Effects	Yes				
Bounding Box					
Length X	200. mm	120. mm	174.6 mm	135.8 mm	155.2 mm
Length Y	23.856 mm	14.314 mm	20.827 mm	16.199 mm	18.513 mm
Length Z	2. mm				
Properties					
Volume	6482.4 mm ³	2333.7 mm ³	4691.6 mm ³	2739.8 mm ³	3654.7 mm ³
			8.2102e-003		6.3957e-003

Mass	1.1344e-002 kg	4.0830e-003 kg	kg	4.7946e-003 kg	kg
Centroid X	83.103 mm	89.9 mm	85.629 mm	89.316 mm	86.033 mm
Centroid Y	-3.9131e-004 mm	9.1072e-003 mm	1.0799e-002 mm	6.862e-003 mm	9.0264e-003 mm
Centroid Z	1. mm	400. mm	103. mm	307. mm	205. mm
Moment of Inertia Ip1	0.35815 kg mm ²	4.6884e-002 kg mm ²	0.20531 kg mm ²	7.406e-002 kg mm ²	0.12744 kg mm ²
Moment of Inertia Ip2	24.081 kg mm ²	3.1235 kg mm ²	13.877 kg mm ²	4.7215 kg mm ²	8.3901 kg mm ²
Moment of Inertia Ip3	24.432 kg mm ²	3.1675 kg mm ²	13.877 kg mm ²	4.7924 kg mm ²	8.5134 kg mm ²
Statistics					
Nodes	695	398	1425	1188	1298
Elements	76	40	168	137	151
Mesh Metric	None				

TABLE 4
Model (C4) > Geometry > Parts

Object Name	Surface Body
State	Meshed
Graphics Properties	
Visible	Yes
Transparency	1
Definition	
Suppressed	No
Stiffness Behavior	Flexible
Coordinate System	Default Coordinate System
Reference Temperature	By Environment
Thickness	5. mm
Thickness Mode	Manual
Offset Type	Middle
Material	
Assignment	cfc
Nonlinear Effects	Yes
Thermal Strain Effects	Yes
Bounding Box	
Length X	200. mm
Length Y	23.856 mm
Length Z	410. mm
Properties	
Volume	6.6914e+005 mm ³
Mass	1.171 kg
Centroid X	98.853 mm
Centroid Y	1.3559e-008 mm
Centroid Z	187.92 mm
Moment of Inertia Ip1	16117 kg mm ²
Moment of Inertia Ip2	18789 kg mm ²
Moment of Inertia Ip3	2791.5 kg mm ²
Surface Area(approx.)	1.3383e+005 mm ²
Statistics	
Nodes	5337
Elements	10564
Mesh Metric	None

Model (C4) > Geometry > Layered Section

Object Name	Layered Section
State	Fully Defined
Scope	
Scoping Method	Geometry Selection
Geometry	1 Face
Definition	
Coordinate System	Body Coordinate System
Offset Type	Middle
Layers	Worksheet
Suppressed	No
Material	
Nonlinear Effects	Yes
Thermal Strain Effects	Yes
Graphics Properties	
Layer To Display	All Layers
Properties	
Total Thickness	5.6 mm
Total Mass	1.3111 kg

Model (C4) > Geometry > Layered Section

Layer	Material	Thickness (mm)	Angle (°)
(+Z)			
7	cfc	0.8	0
6	cfc	0.8	45
5	cfc	0.8	0
4	cfc	0.8	-45
3	cfc	0.8	0
2	cfc	0.8	45
1	cfc	0.8	0
(-Z)			

Coordinate Systems

TABLE 6
Model (C4) > Coordinate Systems > Coordinate System

Object Name	Global Coordinate System
State	Fully Defined
Definition	
Type	Cartesian
Coordinate System ID	0.
Origin	
Origin X	0. mm
Origin Y	0. mm
Origin Z	0. mm
Directional Vectors	
X Axis Data	[1. 0. 0.]
Y Axis Data	[0. 1. 0.]
Z Axis Data	[0. 0. 1.]

Connections

TABLE 7
Model (C4) > Connections

Object Name	Connections
State	Fully Defined
Auto Detection	
Generate Automatic Connection On Refresh	Yes
Transparency	
Enabled	Yes

TABLE 8
Model (C4) > Connections > Contacts

Object Name	Contacts
State	Fully Defined
Definition	
Connection Type	Contact
Scope	
Scoping Method	Geometry Selection
Geometry	All Bodies
Auto Detection	
Tolerance Type	Slider
Tolerance Slider	0
Tolerance Value	1.142 mm
Use Range	No
Face/Face	Yes
Face/Edge	No
Edge/Edge	No
Priority	Include All
Group By	Bodies
Search Across	Bodies

TABLE 9
Model (C4) > Connections > Contacts > Contact Regions

Object Name	Contact Region	Contact Region 2	Contact Region 3	Contact Region 4	Contact Region 5
State	Fully Defined				
Scope					
Scoping Method	Geometry Selection				
Contact	1 Face				
Target	1 Face				
Contact Bodies	Solid				
Target Bodies	Surface Body				
Target Shell Face	Program Controlled				
Shell Thickness Effect	No				
Definition					
Type	Bonded				
Scope Mode	Automatic				
Behavior	Program Controlled				
Trim Contact	Program Controlled				
Trim Tolerance	1.142 mm				
Suppressed	No				
Advanced					
Formulation	Program Controlled				
Detection Method	Program Controlled				
Penetration Tolerance	Program Controlled				
Elastic Slip Tolerance	Program Controlled				
Normal Stiffness	Program Controlled				
Update Stiffness	Program Controlled				
Pinball Region	Program Controlled				

Mesh

TABLE 10
Model (C4) > Mesh

Object Name	Mesh
State	Solved
Defaults	
Physics Preference	Mechanical
Relevance	1
Sizing	
Use Advanced Size Function	On: Curvature
Relevance Center	Fine
Initial Size Seed	Active Assembly
Smoothing	Medium
Transition	Fast
Span Angle Center	Coarse
Curvature Normal Angle	Default (30.0 °)
Min Size	Default (1.68560 mm)
Max Face Size	Default (8.42780 mm)
Max Size	Default (8.42780 mm)
Growth Rate	Default
Minimum Edge Length	2.0 mm
Inflation	
Use Automatic Inflation	None
Inflation Option	Smooth Transition
Transition Ratio	0.272
Maximum Layers	5
Growth Rate	1.2
Inflation Algorithm	Pre
View Advanced Options	No
Patch Conforming Options	
Triangle Surface Mesher	Program Controlled
Advanced	
Shape Checking	Standard Mechanical
Element Midside Nodes	Program Controlled
Straight Sided Elements	No
Number of Retries	Default (4)
Extra Retries For Assembly	Yes
Rigid Body Behavior	Dimensionally Reduced
Mesh Morphing	Disabled
Defeaturing	
Pinch Tolerance	Default (1.5170 mm)
Generate Pinch on Refresh	No
Sheet Loop Removal	No

Automatic Mesh Based Defeaturing	On
Defeaturing Tolerance	Default (1.26420 mm)
Statistics	
Nodes	10339
Elements	11136
Mesh Metric	None

TABLE 11
Model (C4) > Mesh > Mesh Controls

Object Name	All Triangles Method
State	Fully Defined
Scope	
Scoping Method	Geometry Selection
Geometry	1 Body
Definition	
Suppressed	No
Method	Triangles
Element Midside Nodes	Use Global Setting

Static Structural (C5)

TABLE 12
Model (C4) > Analysis

Object Name	Static Structural (C5)
State	Solved
Definition	
Physics Type	Structural
Analysis Type	Static Structural
Solver Target	Mechanical APDL
Options	
Environment Temperature	22 °C
Generate Input Only	No

TABLE 13
Model (C4) > Static Structural (C5) > Analysis Settings

Object Name	Analysis Settings
State	Fully Defined
Step Controls	
Number Of Steps	1
Current Step Number	1
Step End Time	1. s
Auto Time Stepping	Program Controlled
Solver Controls	
Solver Type	Program Controlled
Weak Springs	Program Controlled
Large Deflection	Off
Inertia Relief	Off
Restart Controls	
Generate Restart Points	Program Controlled
Retain Files After Full Solve	No
Nonlinear Controls	
Force Convergence	Program Controlled

Moment Convergence	Program Controlled
Displacement Convergence	Program Controlled
Rotation Convergence	Program Controlled
Line Search	Program Controlled
Stabilization	Off
Output Controls	
Stress	Yes
Strain	Yes
Nodal Forces	No
Contact Miscellaneous	No
General Miscellaneous	No
Store Results At	All Time Points
Max Number of Result Sets	Program Controlled
Analysis Data Management	
Solver Files Directory	D:\wing\tap_files\tdp0\SYS-2\MECH\
Future Analysis	None
Scratch Solver Files Directory	
Save MAPDL db	No
Delete Unneeded Files	Yes
Nonlinear Solution	No
Solver Units	Active System
Solver Unit System	mm

TABLE 14
Model (C4) > Static Structural (C5) > Loads

Object Name	Fixed Support	Force	Force 2	Force 3	Force 4
State	Fully Defined				
Scope					
Scoping Method	Geometry Selection				
Geometry	1 Face				
Definition					
Type	Fixed Support	Force			
Suppressed	No				
Define By	Vector				
Magnitude	7000. N (ramped)	5000. N (ramped)	2000. N (ramped)	1500. N (ramped)	
Direction	Defined				

FIGURE 1
Model (C4) > Static Structural (C5) > Force

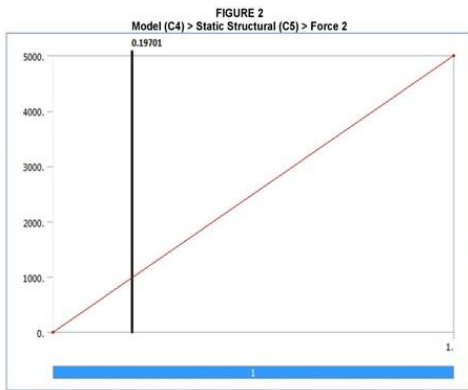
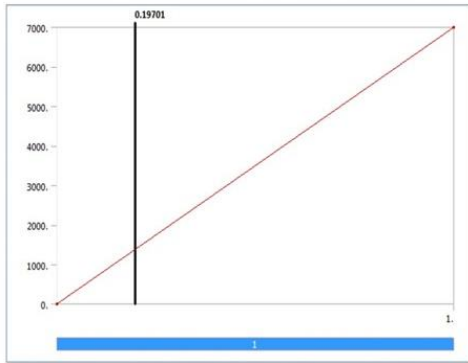


TABLE 15
Model (C4) > Static Structural (C5) > Solution

Object Name	Solution (C6)
State	Solved
Adaptive Mesh Refinement	
Max Refinement Loops	1.
Refinement Depth	2.
Information	
Status	Done

TABLE 16
Model (C4) > Static Structural (C5) > Solution (C6) > Solution Information

Object Name	Solution Information
State	Solved
Solution Information	
Solution Output	Solver Output
Newton-Raphson Residuals	0
Update Interval	2.5 s
Display Points	All
FE Connection Visibility	
Activate Visibility	Yes
Display	All FE Connectors
Draw Connections Attached To	All Nodes
Line Color	Connection Type
Visible on Results	No
Line Thickness	Single
Display Type	Lines

TABLE 17
Model (C4) > Static Structural (C5) > Solution (C6) > Results

Object Name	Total Deformation	Maximum Shear Stress	Equivalent Stress	Strain Energy
State	Solved			
Scope				
Scoping Method	Geometry Selection			
Geometry	All Bodies			
Shell	Top/Bottom			
Layer	Entire Section			
Definition				
Type	Total Deformation	Maximum Shear Stress	Equivalent (von-Mises) Stress	Strain Energy
By	Time			
Display Time	Last			
Calculate Time History	Yes			
Identifier				
Suppressed	No			
Results				
Minimum	0. mm	6.8192e-002 MPa	0.11844 MPa	1.7601e-005 mJ
Maximum	4.1883 mm	744.34 MPa	1456.3 MPa	22.054 mJ
Minimum Occurs On	Solid			
Maximum Occurs On	Surface Body			

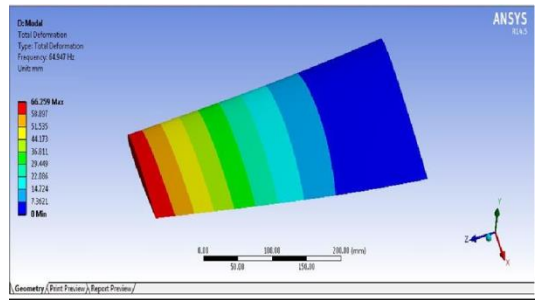


Fig 3.2(a) Total Deformation at 64.947 Hz Frequency

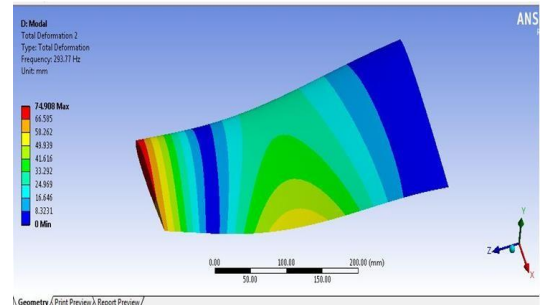


Fig 3.2(b) Total Deformation at 293.77 Hz Frequency

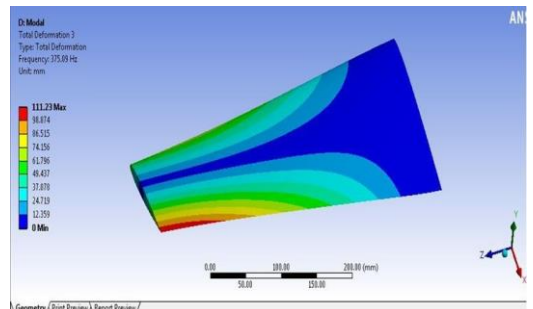


Fig 3.2(c) Total Deformation at 375.09 Hz Frequency

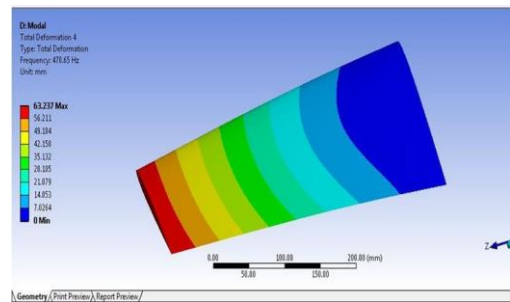


Fig 3.2(d) Total Deformation at 478.65 Hz Frequency

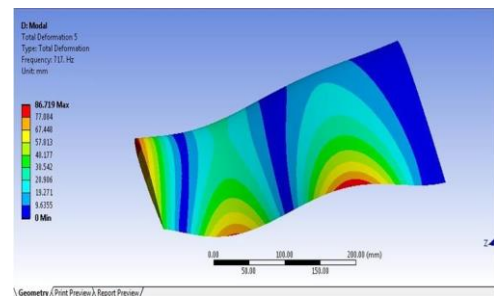


Fig 3.2(e) Total Deformation at 717 Hz Frequency

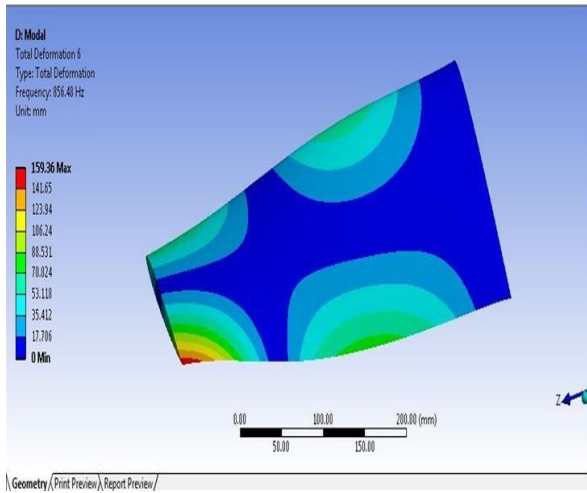


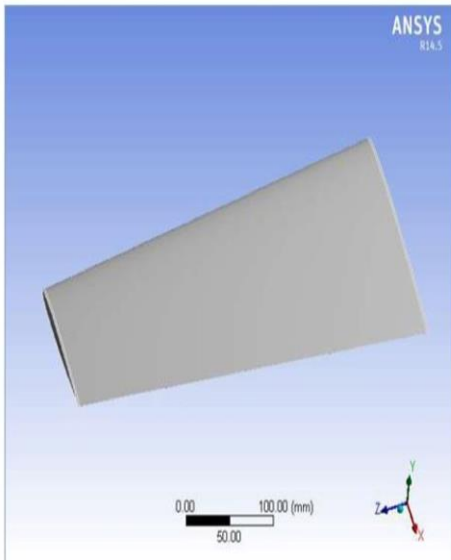
Fig 3.2(f) Total Deformation at 856.48 Hz Frequency

3.3 Results of the Model Analysis on Wing



Project

First saved	22 May 2022
Last saved	28 May 2022
Product version	14.5
Save project before solution	Yes
Save project After Solution	Yes



Contents

- Units
- Model (D4)
 - Geometry
 - Solid
 - Coordinate Systems
 - Mesh
 - Model (DS)
 - Pre-Stress (None)
 - Analysis Settings
 - Fixed Support
 - Solution (DS)
 - Solution Information
 - Results
- Material Data
 - cfc

Units

TABLE 1

Unit System	Metric (mm, kg, N, s, mV, mA)	Degrees	rad/s	Celsius
Angle		Degrees		
Rotational Velocity		rad/s		
Temperature				Celsius

Model (D4)

Geometry

TABLE 2

Model (D4) > Geometry

Object Name	Geometry
State	Fully Defined
Definition	
Source	D:\wing\ap_files\ip2\SYS-3\DM\SYS-3.aptb
Type	DesignModeler
Length Unit	Millimeters
Element Control	Program Controlled
Display Style	Body Color
Bounding Box	
Length X	200. mm
Length Y	23.856 mm
Length Z	410. mm
Properties	
Volume	8.6805e+005 mm ³
Mass	1.5191 kg
Scale Factor Value	1.

Statistics

Bodies	1
Active Bodies	1
Nodes	27809
Elements	5120
Mesh Metric	None
Basic Geometry Options	
Parameters	Yes
Parameter Key	DS
Attributes	No
Named Selections	No
Material Properties	No
Advanced Geometry Options	
Use Associativity	Yes
Coordinate Systems	No
Reader Mode Saves Updated File	No
Use Instances	Yes
Smart CAD Update	No
Attach File Via Temp File	Yes
Temporary Directory	C:\Users\chen\AppData\LocalTemp
Analysis Type	3-D
Decompose Disjoint Geometry	Yes
Enclosure and Symmetry Processing	Yes

TABLE 3

Model (D4) > Geometry > Parts

Object Name	Solid
State	Meshed
Graphics Properties	
Visible	Yes
Transparency	1
Definition	
Suppressed	No
Stiffness Behavior	Flexible
Coordinate System	Default Coordinate System
Reference Temperature	By Environment
Material	
Assignment	cfc
Nonlinear Effects	Yes
Thermal Strain Effects	Yes
Bounding Box	
Length X	200. mm
Length Y	23.856 mm
Length Z	410. mm
Properties	
Volume	8.6805e+005 mm ³
Mass	1.5191 kg
Centroid X	86.049 mm
Centroid Y	4.7738e-004 mm
Centroid Z	171.15 mm
Moment of Inertia Ip1	19661 kg mm ²
Moment of Inertia Ip2	21926 kg mm ²
Moment of Inertia Ip3	2333.5 kg mm ²

Statistics	
Nodes	27609
Elements	5120
Mesh Metric	None

Coordinate Systems

TABLE 4
Model (D4) > Coordinate Systems > Coordinate System

Object Name Global Coordinate System	
State	Fully Defined
Definition	
Type	Cartesian
Coordinate System ID	0.
Origin	
Origin X	0. mm
Origin Y	0. mm
Origin Z	0. mm
Directional Vectors	
X Axis Data	[1. 0. 0.]
Y Axis Data	[0. 1. 0.]
Z Axis Data	[0. 0. 1.]

Mesh

TABLE 5
Model (D4) > Mesh

Object Name Mesh	
State	Solved
Defaults	
Physics Preference	Mechanical
Relevance	0
Sizing	
Use Advanced Size Function	Off
Relevance Center	Coarse
Element Size	Default
Initial Size Seed	Active Assembly
Smoothing	Medium
Transition	Fast
Span Angle Center	Coarse
Minimum Edge Length	244.720 mm
Inflation	
Use Automatic Inflation	None
Inflation Option	Smooth Transition
Transition Ratio	0.272
Maximum Layers	5
Growth Rate	1.2
Inflation Algorithm	Pre
View Advanced Options	No
Patch Conforming Options	
Triangle Surface Mesher	Program Controlled
Advanced	

Stress	No
Strain	No
Nodal Forces	No
Calculate Reactions	No
General Miscellaneous	No
Analysis Data Management	
Solver Files Directory	D:\wing\lap_files\dp\SYS-3\MECH\
Future Analysis	None
Scratch Solver Files Directory	
Save MAPDL db	No
Delete Unneeded Files	Yes
Solver Units	Active System
Solver Unit System	mm

TABLE 9
Model (D4) > Modal (D5) > Leads

Object Name Fixed Support	
State	Fully Defined
Scope	
Scoping Method	Geometry Selection
Geometry	1 Face
Definition	
Type	Fixed Support
Suppressed	No

Solution (D6)

TABLE 10
Model (D4) > Modal (D5) > Solution

Object Name Solution (D6)	
State	Solved
Adaptive Mesh Refinement	
Max Refinement Loops	1
Refinement Depth	2
Information	
Status	Done

The following bar chart indicates the frequency at each calculated mode.

FIGURE 1
Model (D4) > Modal (D5) > Solution (D6)

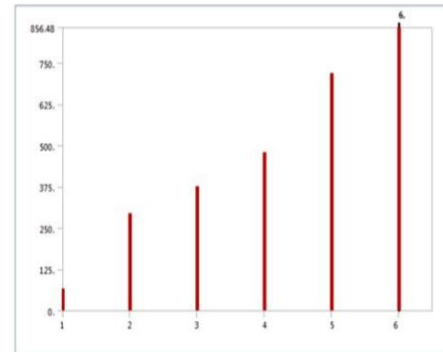


TABLE 11
Model (D4) > Modal (D5) > Solution (D4)

Mode	Frequency [Hz]
1.	64.947
2.	293.77
3.	375.09
4.	478.65
5.	717
6.	856.48

Shape Checking	Standard Mechanical
Element Midside Nodes	Program Controlled
Straight Sided Elements	No
Number of Retries	Default (4)
Extra Retries For Assembly	Yes
Rigid Body Behavior	Dimensionally Reduced
Mesh Morphing	Disabled
Defeaturing	
Pinch Tolerance	Please Define
Generate Pinch on Refresh	No
Automatic Mesh Based Defeaturing	On
Defeaturing Tolerance	Default
Statistics	
Nodes	27609
Elements	5120
Mesh Metric	None

Modal (D5)

TABLE 6
Model (D4) > Analysis

Object Name Modal (D5)	
State	Solved
Definition	
Physics Type	Structural
Analysis Type	Modal
Solver Target	Mechanical APDL
Options	
Environment Temperature	22. °C
Generate Input Only	No

TABLE 7
Model (D4) > Modal (D5) > Initial Condition

Object Name Pre-Stress (None)	
State	Fully Defined
Definition	
Pre-Stress Environment	None

TABLE 8
Model (D4) > Modal (D5) > Analysis Settings

Object Name Analysis Settings	
State	Fully Defined
Options	
Max Modes to Find	6
Limit Search to Range	No
Solver Controls	
Damped	No
Solver Type	Program Controlled
Rotordynamics Controls	
Control Effect	Off
Campbell Diagram	Off
Output Controls	

TABLE 12
Model (D4) > Modal (D5) > Solution (D6) > Solution Information

Object Name Solution Information	
State	Solved
Solution Information	
Solution Output	Solver Output
Newton-Raphson Residuals	0
Update Interval	2.5 s
Display Points	All
FE Connection Visibility	
Activate Visibility	Yes
Display	All FE Connectors
Draw Connections Attached To	All Nodes
Line Color	Connection Type
Visible on Results	No
Line Thickness	Single
Display Type	Lines

TABLE 13
Model (D4) > Modal (D5) > Solution (D6) > Results

Object Name	Total Deformation	Total Deformation 2	Total Deformation 3	Total Deformation 4	Total Deformation 5
State	Solved				
Scope					
Scoping Method	Geometry Selection				
Geometry	All Bodies				
Definition					
Type	Total Deformation				
Mode	1.	2.	3.	4.	5.
Identifier					
Suppressed	No				
Results					
Minimum	0. mm				
Maximum	66.259 mm	74.908 mm	111.23 mm	63.237 mm	86.719 mm
Information					
Frequency	84.947 Hz	293.77 Hz	375.99 Hz	478.85 Hz	717. Hz

TABLE 14
Model (D4) > Modal (D5) > Solution (D6) > Total Deformation

Mode	Frequency [Hz]
1.	84.947
2.	293.77
3.	375.99
4.	478.85
5.	717.
6.	856.48

TABLE 15
Model (D4) > Modal (D5) > Solution (D6) > Total Deformation 2

Mode	Frequency [Hz]
1.	84.947
2.	293.77
3.	375.99
4.	478.85
5.	717.
6.	856.48

TABLE 16
Model (D4) > Modal (D5) > Solution (D6) > Total Deformation 3

Mode	Frequency [Hz]
1.	84.947
2.	293.77
3.	375.99
4.	478.85
5.	717.
6.	856.48

TABLE 17
Model (D4) > Modal (D5) > Solution (D6) > Total Deformation 4

Mode	Frequency [Hz]
1.	84.947
2.	293.77
3.	375.99
4.	478.85
5.	717.
6.	856.48

Total deformation (mm)	64.97	68.025	66.259
	293.77	79.17	74.908
	375.09	112.25	111.23
	478.65	64.021	63.237
	717	88.92	86.719
	856.48	95.678	92.36

4 CONCLUSION

Light-weighting materials represent an effective way to achieve energy consumption reduction and performance enhancement. This concept has been well accepted and utilized in many industries, especially in aerospace component and system design. Light-weighting design involves the use of advanced lightweight material and numerical structural optimization, enabled by advanced manufacturing methods. Structural optimization can effectively improve the performance of aerospace components and systems by optimizing the material distribution to achieve maximum weight reduction, and enhance structural performance such as strength, stiffness and vibration performance. Conventional structural optimization methodologies include sizing, shape and topology optimization. Computer aided software products have been developed to enable optimization. Lattice structural optimization enables multi-scale optimization that could further optimize the weight and performance of objects. One of the major challenges of numerical optimization approaches is the large number of variables. Efficient algorithms are needed to increase the efficiency of numerical optimization.

Since preliminary design of the wing structures carried out as per the industrial practices for the given applied loads by iteration process and we carried out 3 iterations for metallic structure and at iteration 3 we got the optimum structure and in iteration 4 the metallic wing skin, bottom and top is replaced with CFC and we have seen there is a weight saving of 52.96% as still there is a scope for weight reduction of this wing structure by replacing the metallic ribs and spars by composites. This is considered for the future scope of the project. The attention instead, was focused on how this structure can be improved by increasing its strength and load carrying capability without adding significant weight penalty. In particular the following solutions were found:

1. The stress concentrations on spars and ribs webs, caused by the presence of cutouts, can be reduced by optimizing the cutout shape or by bonding reinforcement rings around the edges of the cutout.
2. Significant stress reduction is achieved by using these CFC wings and their effectiveness depends on their stiffness. In particular, the use of carbon fiber tow

3.4 Comparative Model Analysis of Al Alloy and CFC

Table 3.4(a) Model Analysis Results

Objective name	Total deformation(mm)	Total deformation(mm)	Total deformation(mm)	Total deformation(mm)	Total deformation(mm)	Total deformation(mm)
Minimum	0					
Maximum	66.259	74.908	111.23	63.237	86.719	92.36
Frequency	64.97	293.77	375.09	478.65	717	856.48

Table 3.4(b) Comparison of Aluminum Alloy and CFC of Model Analysis Results

Property	Frequency (Hz)	AluminiumAlloy [31]	CFC (Max)
----------	----------------	---------------------	-----------

placements enables to maximize the ratio of stress reduction and added structural weight.

3. The CFC wings also have the capability of increasing the web buckling stability.
4. In order to increase the strength of a composite joint in pulling the stiffness of the base panel must be maximized and good quality bonding must be used between the wings and base panels in order to maximize the load transfer.
5. By implementing these findings in the design of the reference composite wing, it was possible to obtain a failsafe design supporting the aircraft wing structure. It was important to ensure that the wing was stiff enough to withstand the aerodynamic loads as the leading edge did not contribute in adding stiffness to the overall wing.

5 REFERENCES

- [1] M. Marino, R. Sabatini, Advanced lightweight aircraft design configurations for green operations, in: PRCC 2014, Engineers Australia, 2014.
- [2] L. Maurice, D. Lee, Assessing Current Scientific Knowledge, Uncertainties and Gaps in Quantifying Climate Change, Noise and Air Quality Aviation Impacts, final report of the International Civil Aviation Organization (ICAO) Committee on Aviation and Environmental Protection (CAEP) Workshop. Washington DC and Manchester: US Federal Aviation Administration and Manchester Metropolitan University, 2009.
- [3] X. Zhu, Z. Guo, Z. Hou Solar-powered airplanes: a historical perspective and future challenges *Progress. Aero's. Sci.*, 71 (2014), pp. 36-53.
- [4] J. Li, B. Wu, C. Myant, The Current Landscape for Additive Manufacturing Research, 2016.
- [5] Blended wing body architecting and design: current status and future prospects *Procedia Compute. Sci.*, 28 (2014), pp. 619-625.
- [6] Y.Q. Chen, S.P. Pan, M.Z. Zhou, D.Q. Yi, D.Z. Xu, Y.F. Xu Effects of inclusions, grain boundaries and grain orientations on the fatigue crack initiation and propagation behavior of 2524-T3 Al alloy.
- [7] S.T. Kim, D. Tardive, H.T. Yang Fatigue life prediction under random loading conditions in 7475-T7351 aluminum alloy using the RMS model *Int. J. Damage Mech.*, 15 (1) (2006), pp. 89-102.
- [8] Germany Government Funded Research Project on Cabin Safety for Light Aircraft, C4 News Release, Flight Design USA, 2014.
- [9] Light Fixed and Rotary-Wing Aircraft Crash Resistance, MIL-STD- 1290A(AV), 1988.
- [10] EU FP7 Collaborative and Robust Engineering using Simulation Capability Enabling Next Design Optimization (CRESCENDO) <http://www.crescendo-fp7.eu/> (accessed on 21 February 2017).
- [11] Gardiner, G. Topology optimization, *Composites World*, 2011.
- [12] Laplace, I.; Chertier, C.; Baron, A.; Maczka, M. Review of US Civil Aviation Accidents Calendar Year 2011, NTSB/ARA-14/01, PB2014-101453, National Transportation Safety Board, 2014.
- [13] D2.1 Potential Transfer of Passenger Demand to Personal Aviation by 2020, ASA6-CT-2006-044549, European Personal Air Transportation System, 2008.
- [14] Roy, R.; Hinduja, S.; Teti, R. Recent Advances in Engineering Design Optimization: Challenges and Future Trends, *CIRP Annals - Manufacturing Technology*, 2008, 57, 697-715.
- [15] Krog, L.; Tucker, A.; Kemp, M.; Boyd, R., Topology Optimization of Aircraft Wing Box Ribs, 10 AIAA/ISSMO Multidisciplinary Analysis and Optimization Conference, AIAA 2004-4481, Albany, New York, 2004.
- [16] Hall, A.; Mayer, T.; Wuggetzer, I.; Childs, P.R.N. Future Aircraft Cabins and Design Thinking: Optimization vs. Win-Win Scenarios, *Propulsion and Power Research*, 2008, 2, 85-95.
- [17] Schumacher, G.; Murra, I.; Wang, L.; Laxander, A.; O'Leary, O.; Herold, M. Multidisciplinary Design optimization of a Regional Aircraft Wing Box, AIAA 2002-5406, 9th AIAA/ISSMO Symposium on Multidisciplinary Analysis and Optimization, Atlanta, Georgia, 2002.
- [18] Piperni, P.; Adbo, M.; Kafyeke, F. The Application of Multi-Disciplinary Optimization Technologies to the Design of a Business Jet, 10th AIAA/ISSMO Multidisciplinary Analysis and Optimization Conference, AIAA 2004-4370, Albany, New York, 2004.
- [19] Hurley, T.R.; Vandenburg, J.M. Small Airplane Crashworthiness Design Guide, AGATE-WP3.4-034043-036, April 12, 2002.
- [20] Hooper, S.; Henderson, M.; Seneviratne, W. Design and Construction of a Crashworthy Composite Airframe, AGATE-WP3.4-034026-089, Rev. A, March 1, 2002.
- [21] Feraboli, P. Development of a Corrugated Test Specimen for Composite Materials Energy Absorption, *J. Compos. Mater.* 2008, 42, 229-256.
- [22] Feindler, N.; Döll, J.; Drechsler, K. Test Method to Analyze the Energy Absorption of Composite Material using Flat Coupon Testing, 5th International Conference on Composites Testing and Model Simulation, EPFL, Lausanne, 2011.
- [23] Zhou, M.; Fleury, R.; Patten, S.; Stannard, N.; Mylett, D.; Gardner, S. Topology Optimization – Practical Aspects for Industrial Applications, 9th World Congress on Structural and Multidisciplinary Optimization, Shizuoka, Japan, June 13-17, 2011.
- [24] Liu, D.; Lohse-Buschl, H.; Toropov, V.; Hühne, C.; Armani, U. Detailed Design of a Lattice Composite Fuselage Structure by a Mixed Optimization Method, *Engineering Optimization*, 2016, 48, 1707-1720.
- [25] Giordano, V.; Coiro, D.P.; Nicolosi, F.; Leo, L.D. Design and Aerodynamic Optimization of a New Reconnaissance Very Light Aircraft Through Wind- Tunnel Tests, Aerodynamic Design and Optimization of Flight Vehicles in a Concurrent Multi-Disciplinary Environment, RTO AVT Symposium, Ottawa, Canada, October 18-21, 1999, 34.1-34.8.
- [26] Ahamed S.N.; Kumar, J.V.; Sravani, P. Weight Optimization of Empennage of Light Weight Aircraft, *International Journal of Scientific & Technology Research*, vol. 3, issue 4, April 2014.
- [27] ASTM F2245-16a, Standard Specification for Design and Performance of a Light Sport Airplane, ASTM International, West Conshohocken, PA, 2016.
- [28] Salu Kumar Das and Sandipan Roy 2018 IOP Conf. Ser.: Mater. Sci. Eng. 402012077.M. Young, *The Technical Writer's Handbook*. Mill Valley, CA: University Science, 1989.
- [29] Sohel Rana, Raul Figueiro, "Advanced Composite Materials for Aerospace Engineering". Woodhead Publishing, 2016. Elsevier Ltd.
- [30] Sivarama Prasad Peruru, Suman Babu Abbisetti, "DESIGN AND FINITE ELEMENT ANALYSIS OF AIRCRAFT WING USING RIBS AND SPARS". 2017, IRJET.
- [31] Kathiravan.T, Mohammed Huda.A, Parthiban.K, "STRUCTURAL AND MODAL ANALYSIS OF SUBSONIC AIRCRAFT WING USING ANSYS WORKBENCH". 2018, IRJET.
- [32] Rabbej, M. Fazlay, et al. "Structural Deformation and Stress Analysis of Aircraft Wing by Finite Element Method." *Advanced Materials Research*, vol. 906, Trans Tech Publications, Ltd., Apr. 2014, pp. 318–322. Crossref, doi: 10.4028/www.scientific.net/amr.906.318. R. Nicole, "Title of paper with only first word capitalized," *J. Name Stand. Abbrev.*, in press.
- [33] Behaghel P-F, Starke EA, Jr., The effects of processing and microstructure on two aluminum alloys for aerospace applications, *Journal of Advanced Materials*, (in press).
- [34] Troeger LP, Starke Jr. EA. Microstructural and mechanical characterization of a superplastic 6XXX aluminum alloy. *Materials Science and Engineering* 2000; A277:102–13.
- [35] Wadley HNG, Fleck NA, Evans AGI. Fabrication and structural performance of periodic cellular metal sandwich structures, *Composites Science and Technology*, (in press).
- [36] Hinrichsen J. Airbus A3XX: Design features and structural technologies review, Presented at the International School of Mathematics, G. Stampacchia, 28th Workshop: Advanced Design Problems in Aerospace Engineering, Galileo Galilei Celebrations, Eric-Sicily, Italy, 11–18 July 1999.
- [37] Hinrichsen J. The material down-selection process for A3XX, Key Note Address at the 19th European Conference on Materials for Aerospace Applications: Confederation of European Aerospace Societies (CEAS) Munchen, Germany, 6–8 December 2000.
- [38] Hinrichsen J. Airbus A380: Requirements for the selection of materials and manufacturing technologies, Presented at Aluminum in the Aerospace Industries, Gosselies, Belgium, 8 March 2001.
- [39] Starke Jr. EA. Aerospace materials for future technologies. *Journal of the Japan Institute of Light Metals* 2001;51:77–85. [18] Polmear II, Couper MJ. Design and development of an experimental wrought aluminum alloy for use at elevated temperatures. *Metall Trans* 1988;19A:1027.
- [40] Hyatt MV. Program to improve the fracture toughness and fatigue resistance of aluminum sheet and plate for airframe applications, Boeing Commercial Airplane Company, Technical Report AFML-TR-73-224, Wright-Patterson Air Force Base, 1973.
- [41] Warner TJ, Shahani RA, Lassince P, Raynaud GM, Aluminum alloy

developments for affordable airframe structures, Paper presented at the ASM International Conference, Paris, France, June, 1997.

- [42] Zhu AW, Gable BM, Shiflet GJ, Starke Jr. EA. The intelligent design of age hardenable wrought aluminum alloys. *Advanced Engineering Materials* 2002; 4:839–46.
- [43] Zhu AW, Csontos A, Starke Jr. EA. Computer experiment on superposition of strengthening effects of different particles. *Acta Materialia* 1999; 47:1713–21.
- [44] Zhu AW, Starke Jr. EA. Strengthening effect of untearable particles of finite size: A computer experimental study. *Acta Materialia* 1999; 47:3263–9.

A SHORT REVIEW ON VARIOUS STRATEGIES FOR THE REDUCTION OF CO₂ EMISSIONS FROM AUTOMOTIVE EXHAUSTS

V. Krishna Koundinya , D Sameer Kumar

Department of Mechanical Engineering, Bapatla Engineering College, Bapatla, AP, INDIA

Abstract— The automotive sector is one of the most promising research areas, with plenty of prospects for advancement. This industry constantly throws difficulties at engineers and expects quick solutions for a better environment. The CO₂ emissions produced during the combustion process are a global issue in the vehicle industry. These contaminants are promptly causing ozone layer depletion, which has a negative impact on quality of life. As a result, attempting to persuade CO₂ emissions is a beneficial research to protect the atmosphere. The authors of this work tried to explore various options for lowering CO₂ emissions along with future research in this field.

Index Terms— *Ozone layer depletion, Green house effect, CO₂emissions , CO₂ arrester , combustion pollutants , Global Warming , Exhaust contaminants.*

I. INTRODUCTION

The reduction of carbon dioxide (CO₂) emissions from automotive exhausts has become an urgent priority due to the significant role of the transportation sector in contributing to global greenhouse gas emissions. The steady increase in the number of vehicles on the road, coupled with the rising concerns about climate change and air pollution, necessitates the exploration of various strategies to mitigate the environmental impact of automobile emissions. This manuscript provides a concise review of different strategies that have been proposed and implemented to address CO₂ emissions from automotive exhausts.

To comprehend the diverse range of strategies, it is essential to understand the significance of CO₂ emissions from vehicles. Automobiles are a major source of CO₂ emissions, accounting for a substantial portion of global greenhouse gas emissions. According to the International Energy Agency (IEA), the transportation sector accounted for approximately 24% of global energy-related CO₂ emissions in 2020 [1]. This alarming figure underscores the need to focus on reducing CO₂ emissions from automotive sources to achieve sustainability targets and mitigate climate change effects. The sources of green house gases by vehicles is neatly presented in Figure 1.

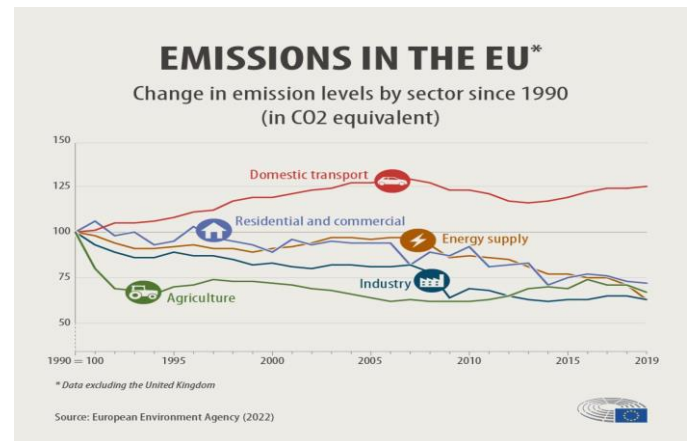


Fig 1 . Transport emissions in EU [2]

Numerous approaches have been explored to tackle the challenge of reducing CO₂ emissions from automotive exhausts. This review paper will discuss several key strategies, including technological advancements in engine design, alternative fuels, hybrid and electric vehicles, and vehicle efficiency improvements. Each strategy offers unique opportunities and challenges, and an in-depth understanding of their effectiveness and limitations is crucial for informed decision-making and policy development.

The objective of this manuscript is to present a comprehensive overview of the current state-of-the-art strategies employed for the reduction of CO₂ emissions from automotive exhausts. By synthesizing information from a variety of sources, including scholarly journals, industry reports, and books, the authors aim to provide a valuable resource for researchers, policymakers, and automotive engineers involved in the pursuit of sustainable transportation solutions.

In the subsequent sections, the authors will delve into each strategy, highlighting the technological advancements, research findings, and case studies that demonstrate their efficacy in reducing CO₂ emissions. Additionally, the explore the associated challenges, and regulatory frameworks that play a pivotal role in the successful implementation of these strategies.

Through this review, the authors hope to contribute the collective knowledge base and foster further research and

innovation in the field of automotive emissions reduction. By understanding and implementing effective strategies, we can move closer to a greener, more sustainable future, mitigating the adverse environmental impacts of the transportation sector.

II. DISCUSSION

The increase in carbon dioxide (CO₂) emissions from automotive exhausts has posed significant environmental challenges, calling for effective strategies to mitigate their impact. This article explores a range of strategies that have been proposed and implemented to reduce CO₂ emissions from vehicles. By understanding and implementing these strategies, the environment will be more greener and sustainable in the future.

Technological Advancements

Technological advancements in engine design have played a crucial role in improving fuel efficiency and reducing CO₂ emissions from automotive exhausts. Direct injection, turbocharging, and variable valve timing are among the notable advancements that have significantly contributed to these improvements. Direct injection enables a more precise fuel delivery system, leading to better combustion efficiency and reduced fuel consumption. Turbocharging increases the engine's power output by compressing the intake air, allowing for smaller engine sizes without sacrificing performance. This downsizing approach not only improves fuel efficiency but also reduces CO₂ emissions. Variable valve timing optimizes the opening and closing of the engine's valves, enhancing combustion efficiency across different operating conditions. By incorporating these advancements, automotive engines can achieve higher levels of efficiency, resulting in reduced fuel consumption and lower CO₂ emissions [3][4]. These technologies are instrumental in the pursuit of sustainable transportation solutions, and further research and development in engine design continue to drive advancements for even greater environmental benefits.

Alternate fuel for lower emissions

The exploration of alternative fuels presents a promising avenue for reducing CO₂ emissions from automotive exhausts. Biofuels, such as ethanol and biodiesel, derived from renewable sources, offer the potential to significantly lower carbon emissions. These fuels can be blended with conventional gasoline and diesel, reducing the overall carbon footprint of transportation. Hydrogen, another alternative fuel, has gained attention due to its high energy density and zero direct emissions when used in fuel cell vehicles. With advancements in hydrogen production and infrastructure, it holds promise as a clean fuel option. Natural gas, particularly compressed natural gas (CNG) and liquefied natural gas (LNG), offers lower carbon emissions compared to conventional fuels. It can be used in dedicated natural gas vehicles or blended with gasoline or diesel. The potential of these alternative fuels in reducing CO₂ emissions is significant, and ongoing research and development are essential to overcome challenges and realize their full potential in the transportation sector [5][6].

Hybrid and Electrical Vehicles

Hybrid and electric vehicles have emerged as key solutions in the quest to reduce CO₂ emissions and improve energy efficiency in the automotive industry as shown in Fig 2. Hybrid vehicles combine an internal combustion engine with an electric motor and battery, allowing for more efficient fuel utilization and reduced emissions. They employ regenerative braking to capture and store energy that would otherwise be wasted, further enhancing their energy efficiency. Electric vehicles (EVs), on the other hand, operate solely on electric power, producing zero tailpipe emissions. By relying on electricity as their primary energy source, EVs significantly reduce CO₂ emissions and contribute to cleaner air quality. The advancements in battery technology have extended the range and performance of electric vehicles, making them a viable alternative to traditional internal combustion engine vehicles. The increasing availability of charging infrastructure and government incentives further support the adoption of hybrid and electric vehicles, contributing to a greener and more sustainable transportation system [7][8].

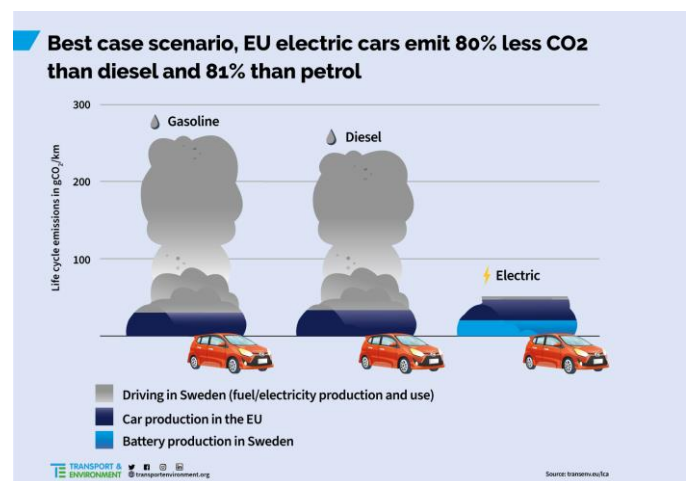


Fig 2 . Co2 emissions from EV and other sources [9]

Vehicle efficiency improvements

Improving vehicle efficiency is a crucial aspect of reducing CO₂ emissions from automotive exhausts. Various strategies have been employed to enhance efficiency and minimize environmental impact. One such strategy involves the use of lightweight materials, such as aluminum, carbon fiber, and high-strength steel, to reduce the overall weight of vehicles. This reduction in weight leads to improved fuel economy and lower CO₂ emissions. Additionally, aerodynamic designs optimize airflow around the vehicle, reducing drag and improving efficiency. By incorporating features like streamlined body shapes, active grille shutters, and underbody panels, vehicles can achieve better fuel efficiency. Moreover, low rolling resistance tires reduce the energy required to propel the vehicle, resulting in reduced fuel consumption and CO₂ emissions. These vehicle efficiency improvements, along with advancements in engine technologies, contribute to a more sustainable transportation system [10][11].

Intelligent Transportation Systems and Eco-Driving Practices

Intelligent transportation systems (ITS) and eco-driving practices both play significant roles in minimizing CO₂ emissions from automotive exhausts. ITS utilizes advanced technologies, such as traffic sensors, smart traffic signals, and real-time data analysis, to optimize traffic flow and reduce congestion. By improving the efficiency of transportation networks, ITS reduces the time vehicles spend idling or in stop-and-go traffic, thereby decreasing fuel consumption and CO₂ emissions. Furthermore, eco-driving practices focus on adopting driving behaviors that maximize fuel efficiency and minimize emissions. These practices include smooth acceleration and deceleration, maintaining proper tire pressure, reducing unnecessary idling, and avoiding rapid speed changes. By implementing eco-driving techniques, drivers can achieve significant fuel savings and reduce their carbon footprint. Both intelligent transportation systems and eco-driving practices contribute to a more sustainable and environmentally friendly transportation system, making them vital in the effort to mitigate CO₂ emissions [12-15]

Policy and Regulatory approaches

Policy and regulatory approaches play a crucial role in addressing CO₂ emissions from automotive exhausts. Governments and regulatory bodies worldwide have implemented various measures to promote cleaner fuels and stricter emission standards. This includes the introduction of regulations that mandate the reduction of CO₂ emissions from vehicles, setting specific targets for automakers to meet. These policies not only encourage the development and adoption of cleaner technologies but also incentivize the production and use of low-emission vehicles. Additionally, policies promoting renewable and alternative fuels, such as biofuels and hydrogen, help diversify the energy sources in the transportation sector and reduce the overall carbon footprint. By establishing clear guidelines and standards, policymakers create a framework that encourages the automotive industry to invest in research and development for cleaner and more sustainable vehicles.

Furthermore, policy and regulatory approaches encompass incentives and subsidies to accelerate the adoption of low-emission vehicles. Governments may provide financial incentives, such as tax credits or rebates, to individuals or businesses that purchase electric or hybrid vehicles. These incentives help reduce the upfront costs of such vehicles and make them more affordable for consumers. In addition to financial incentives, policies can include preferential treatment for low-emission vehicles, such as access to carpool lanes, reduced toll fees, and free parking. By providing tangible benefits to owners of low-emission vehicles, policymakers create a positive environment that encourages the transition towards greener transportation options. Such measures not only help reduce CO₂ emissions but also contribute to improving air quality and public health in urban areas [16][17]. The three

keyways to reduce CO₂ emissions is mentioned in the figure 3.

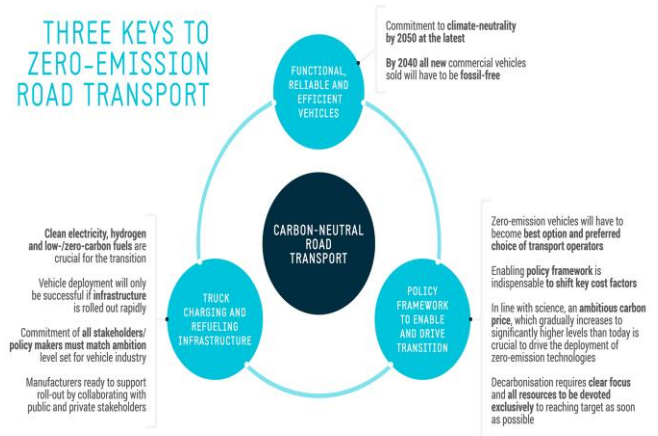


Fig 3. Three important factors to reduce emissions [18]

III. FUTURE OF CO₂ EMISSION STRATEGIES

The future of CO₂ emission reduction strategies holds tremendous potential as emerging technologies and ongoing research pave the way for a sustainable future. One notable area of focus is fuel cell vehicles (FCVs). These vehicles utilize hydrogen as a fuel source, which, when combined with oxygen, produces electricity to power the vehicle, emitting only water vapor as a byproduct. FCVs offer zero-emission transportation and have the potential to revolutionize the automotive industry. Ongoing research aims to improve the efficiency of fuel cells, reduce costs, and develop a robust hydrogen infrastructure to support widespread adoption. As these advancements progress, FCVs have the potential to play a significant role in reducing CO₂ emissions and achieving a greener transportation system.

Another promising avenue for CO₂ emission reduction is carbon capture and storage (CCS). This technology involves capturing CO₂ emissions from industrial processes, such as power plants, and permanently storing them underground. CCS not only prevents CO₂ from being released into the atmosphere but also has the potential to remove CO₂ from the air. Ongoing research focuses on optimizing CCS technologies, improving capture efficiency, and identifying suitable storage sites. By effectively capturing and storing CO₂ emissions, CCS can contribute to significant reductions in greenhouse gas emissions and help mitigate the impacts of climate change.

In addition to specific technologies, the future of CO₂ emission reduction strategies also revolves around sustainable energy sources. The transition towards renewable energy, such as solar and wind power, plays a pivotal role in decarbonizing the transportation sector. Electric vehicles (EVs) charged by renewable energy sources offer a clean and sustainable transportation solution. Furthermore, the integration of renewable energy into the power grid enables the charging infrastructure necessary for widespread EV adoption. Ongoing research focuses on improving the efficiency and cost-effectiveness of renewable energy systems and exploring innovative approaches, such as vehicle-to-grid technology, where EVs can feed excess energy back into the grid. By embracing sustainable energy sources, we can significantly

reduce CO₂ emissions from transportation and create a more sustainable and environmentally friendly future [19][20].

IV. CONCLUSIONS

The following conclusions have been drawn from the present investigation

- The reduction of CO₂ emissions from automotive exhausts is a pressing global challenge. By implementing various strategies such as technological advancements, alternative fuels, hybrid/electric vehicles, and improved vehicle efficiency, we can make significant progress towards a greener transportation system.
- Additionally, intelligent transportation systems, eco-driving practices, sustainable urban planning, and supportive policies are vital in achieving substantial CO₂ emission reductions. The future holds promising advancements, and continued research and innovation are essential in creating a sustainable, low-carbon future.

REFERENCES

- [1] International Energy Agency (IEA). "CO₂ Emissions from Fuel Combustion Highlights 2021." IEA, 2021.
- [2] Information from <https://www.europarl.europa.eu/news/en/headlines/society/20190313STO31218/co2-emissions-from-cars-facts-and-figures-infographics> accessed on 21.06.2023.
- [3] Liu, Y., & Karim, G. A. "Direct injection diesel engine: An overview." SAE Technical Paper, 1999.
- [4] Heywood, J. B. "Internal combustion engine fundamentals." McGraw-Hill Education, 1988.
- [5] Chu, S. "Beyond fossil fuel." Science, 2009.
- [6] Purnell, M., & Howes, J. "Hydrogen as an automotive fuel: Challenges and opportunities." Sustainable Materials and Technologies, 2020.
- [7] Sapin, P., & Chaumette, P. "Hybrid electric vehicle: A review on technologies." International Journal of Automotive Technology, 2017.
- [8] Zhang, X., & Mi, C. "Electric vehicles and renewable energy: Integration perspectives." Applied Energy, 2010.
- [9] Information from <https://www.transportenvironment.org/discover/does-electric-vehicle-emit-less-petrol-or-diesel/>
- [10] Zervomanidis, G. "Lightweight materials for automotive applications." Materials Today, 2021.
- [11] Marland, G., & Cole, N. "What is a low rolling resistance tire?" Transportation Research Part D: Transport and Environment, 2001.
- [12] Millionig, A., & Antoniou, C. "Urban travel demand modeling." Elsevier, 2018.
- [13] Murray-Tuite, P., et al. "Evaluation of the traffic flow impacts of an adaptive signal control system." Transportation Research Part C: Emerging Technologies, 2010.
- [14] Vasic, A., et al. "Eco-driving: Energy, emissions, and human factors." Energy Efficiency, 2014.
- [15] Yan, X., et al. "Eco-driving: A critical review on factors influencing fuel economy of passenger cars." Applied Energy, 2021.
- [16] European Commission. "European Union emission standards for cars and light commercial vehicles." European Commission, 2021.
- [17] Kousoulidou, M., et al. "A comprehensive review of automotive emission regulations and technologies." Science of The Total Environment, 2020.
- [18] Information from <https://www.acea.auto/publication/position-paper-review-of-co2-emission-standards-regulation-for-heavy-duty-vehicles/>
- [19] Ritter, T. "Fuel cell vehicles and hydrogen infrastructure: Status 2020." International Journal of Hydrogen Energy, 2021.
- [20] Yang, M., et al. "Recent advances and remaining challenges of carbon capture and storage: A review." Applied Energy, 2017

3D PRINTING THERMO-MECHANICAL ANALYSIS OF CARBURETOR FOR OPTIMIZED SUPPORT STRUCTURE ORIENTATION FOR EOS M 280 MACHINE

BUSA SRINIVASA RAO, P.SYAM

Department of Mechanical Engineering, Newton's institute of science and technology, Palnadu (Dist.), A.P., India.

Abstract— Carburetor plays major role in mixing the air fuel ratio in SI engine. Due to complexity of geometrical features of the carburetor the manufacturing takes more time. Here we would like to manufacture the carburetor by using metal LPBF process.

Metal AM process is rapidly growing technology. In metal AM process the complexity of the object is not considered. The quality of the final printed parts depends on the so many factors like laser power, scanning strategy, scanning speed, scanning strategy, hatch distance, layer height etc... among all the process parameters print orientation plays major role in consumption of support material and support printing time to avoid this we performed 3D printing simulation for different orientation to study the material consumption, printing time, and thermos mechanical properties to analyze the best orientation for printing the carburetor and by optimizing the printing orientation cost also reduces. **Keywords**— Carburetor, geometrical features 3D printing simulation,

1. INTRODUCTION

Engine works on fuel. The earliest form of fuel supply mechanism for modern automobile is carburetor. The primary function of carburetor is to provide the air-fuel mixture to the engine in the required proportion. The goal of a carburetor is to mix just the right amount of gasoline with air so that the engine runs properly. If there is not enough fuel mixed with the air, the engine "runs lean" and either will not run or potentially damages the engine.

OPERATING PRINCIPLE

The carburettor is located upstream of the inlet manifold. Air from the atmosphere enters the carburettor (usually via an air cleaner), has fuel added within the carburettor, passes through the inlet valve(s) and then enters the combustion chamber. Most engines use a single carburettor shared between all of the cylinders, though some high-performance engines have used multiple carburettors.

The carburetor works on Bernoulli's principle: the static pressure of the intake air reduces at higher speeds, drawing more fuel into the airstream. In most cases (except for the accelerator pump), the driver pressing the throttle pedal does not directly increase the fuel entering the engine. Instead, the airflow through the carburetor increases, which in turn increases the amount of fuel drawn into the intake mixture.

The main disadvantage of basing a carburetor's operation on Bernoulli's Principle is that being a fluid dynamic device, the pressure reduction in a venturi tends to be proportional to the square of the intake airspeed. The fuel jets are much smaller and fuel flow is limited mainly by the fuel's viscosity so that the fuel flow tends to be proportional to the pressure difference. So jets sized for full power tend to starve the engine at lower speed and part throttle. Most commonly this has been corrected by using multiple jets.

Carburetor is the device that used to mix air and fuel in an internal combustion engine. The main objective of the carburetor is to provide quality air-fuel mixture for cruising range and for other special requirements likes at starting, idling, acceleration, variable load, and speed operation condition. Above figure shows a simple carburetor. The main parts of a simple carburetor are carburetor air filter, float chamber, fuel discharge nozzle, metering orifice, choke valve, throttle valve and venture.

3D PRINTING CLASSIFICATION

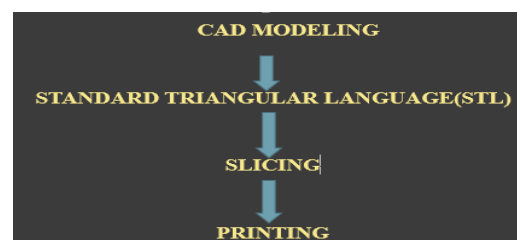


Figure: 1 3 D printing classification

CHOKE

During cold starts, fuel vaporizes less readily and tends to condense on the walls of the intake manifold, starving the cylinders of fuel and making the engine difficult to start, thus additional fuel is required (for a

given amount of air) to start and run the engine until it warms up.

A choke is used to supply this extra fuel. While the engine is warming up, a partially closed choke restricts the flow of air at the entrance to the carburetor, which increases the vacuum in the main metering circuit, causing more fuel to be supplied to the engine via the main jets. In older cars, the choke was manually operated by the driver, often using a lever or knob on the dashboard. Automatic chokes became more commonplace from the late 1950s, whereby a bimetallic thermostat was used to automatically close and open the choke based on the temperature of the engine's coolant liquid, an electrical resistance heater or air drawn through a tube connected to an engine exhaust source. A choke closed after the engine has warmed up increases the engine's fuel consumption and exhaust gas emissions and causes the engine to run rough and lack power.

However, excessive fuel (called a flooded engine) can prevent an engine from starting. To remove the excess fuel, many carburetors include an 'unloader mechanism', whereby the choke is held open to allow extra air into the engine in order to clear out the excess fuel. In order to activate the unloader mechanism, the driver holds the throttle pedal fully open while cranking the engine.

Another method used by carburetors to improve the operation of a cold engine is a fast idle cam. This cam is connected to the choke and prevents the throttle from closing fully while the choke is in operation. The resulting increase in idle speed provides a more stable idle for a cold engine (by better atomizing the cold fuel) and helps the engine warm up quicker.

History

In 1826, American engineer Samuel Morey received a patent for a "gas or vapor engine" which used a heated-surface carburetor to mix the turpentine fuel with air,[17][18] but the design did not reach production. In 1875, German engineer Siegfried Marcus produced a car powered by the first petrol engine to use a carburetor (along with the first magneto ignition system).[19][20][21] Karl Benz's Benz Patent-Motorwagen, built in 1885, also used a carburetor.[22][23]

The aforementioned carburetors were all "surface carburetors", which operate moving air across the top of a vessel containing the fuel.[24] However, the 1885 Grandfather Clock engine created by German engineers Wilhelm Maybach and Gottlieb Daimler introduced the float-fed carburetor design, which used an atomizer nozzle.[25] The Butler Petrol Cycle car - built in England in 1888 - also used a float-fed carburetor.[26][27]

The first carburetor for a stationary engine was patented in 1893 by Hungarian engineers János Csonka and Donát Bánki.[28][29][30]

The first 4-barrel carburetors were the Carter Carburetor WCFB and identical Rochester 4GC introduced in various General Motors models for 1952. Oldsmobile referred the new carburetor as the "Quadri-Jet" (original spelling)[31] while Buick called it the "Airpower".[32]

In the United States, carburetors were the common method of fuel delivery for most US-made gasoline (petrol) engines until the late 1980s, when fuel injection became the preferred method.[33] One of the last motorsport users of carburetors was NASCAR, which switched to electronic fuel injection after the 2011 Sprint Cup series.[34]

In Europe, carburetors were largely replaced by fuel injection in the late 1980s, although fuel injection had been increasingly used in luxury cars and sports cars since the 1970s. EEC legislation required all vehicles sold and produced in member countries to have a catalytic converter after December 1992. This legislation had been in the pipeline for some time, with many cars becoming available with catalytic converters or fuel injection from around 1990.

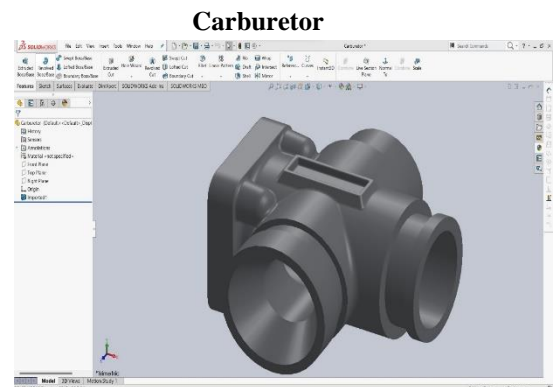


Figure: 2 CAD model of Carburetor diagram

SLM 280 MACHINE

A byproduct of the welding process is submicronic soot and condensate, which can be pyrophoric by nature. The permanent filter module traps soot and condensate particles from the process gas stream in a sintered plate filter. The filter is purged with gas, the waste material coated with an inhibitor and dropped in a bin for dry disposal, while clean gas returns to the process chamber.

- Long-life filter ensures part quality throughout builds without interruption
- No changing of filter cartridges
- Reduced consumable costs
- Safer operation by avoiding loaded filter housing exchange

- Dry mixture waste disposal without hydrogen formation with reactive materials



Figure: 3 SLM 280 machine

Results and discussions

3D printing simulation result for First Orientation

Displacement result for first orientation

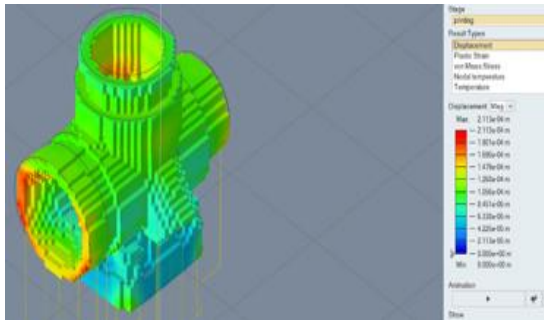


Figure: 4 Displacement for first orientation

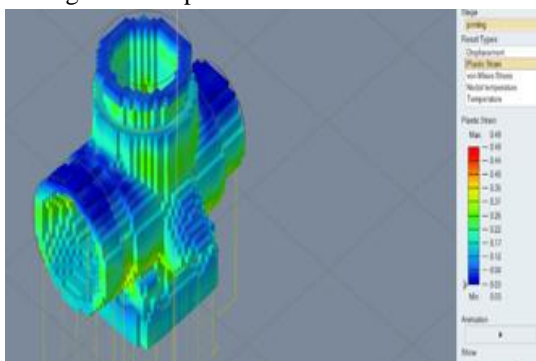


Figure: 5 Plastic strain for first orientation

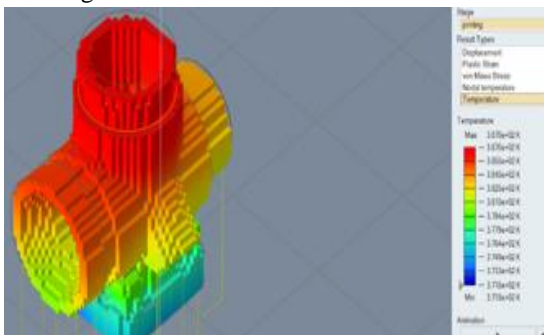


Figure: 6 Temperature distribution for first orientation

3D printing simulation result for Second Orientation

Displacement result for first orientation

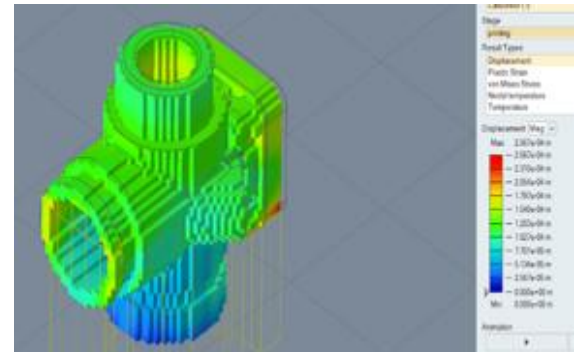


Figure: 7 Displacement for second orientation

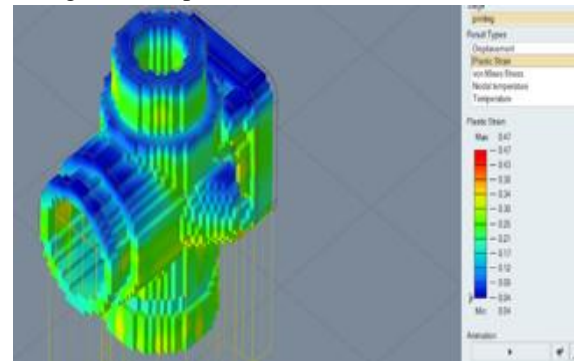


Figure: 8 plastic strain for second orientation



Figure: 9 Temperature distribution in second Orientation

3D printing simulation result for Third Orientation

Displacement result for third orientation

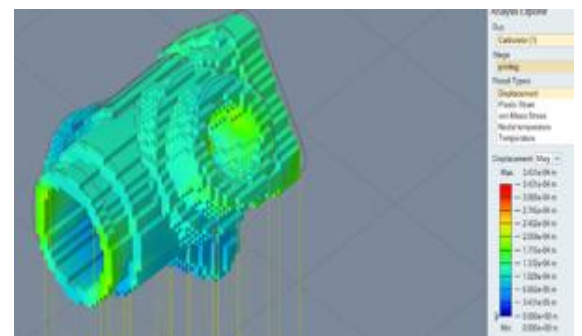


Figure: 10 Displacement for third orientation

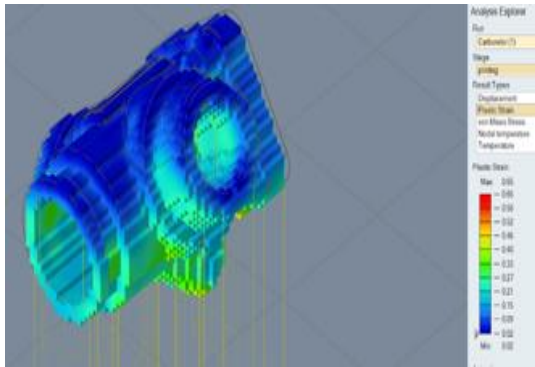


Figure: 11 plastic strain for third orientation

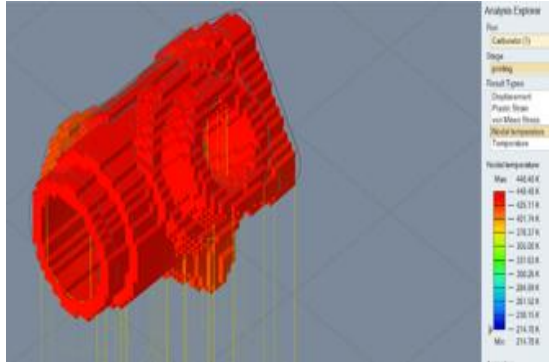


Figure: 12 Temperature distribution in second Orientation

RESULTS

Result	Orientation-1	Orientation-2	Orientation-3
Displacement	2.113e-04 m	3.431e-04 m	5.779e-04 m
Plastic Strain	0.49	0.65	0.94
Temperature	3.870e+02 k	448.48 k	857.49 k

CONCLUSION AND FUTURE SCOPE

We have simulated printing process for different orientations for carburetor to optimize the position for better accuracy in the final printing model. Since the carburetor has different cross sections, it has more chances to displace and circular cross sections will get ovality. To avoid this ovality we have simulated the carburetor in different orientations to decrease the displacement, plastic strain.

1. Out of three orientations third orientation giving the large displacements when compare first and second orientation.
2. Plastic strain in the second orientation is very less when compare to second and third orientation

From the above results we can conclude that **second orientation** giving us the better results when compared to other two orientations. To the extent of this work we would like to optimize the printing process parameters for better printing experience

REFERENCES

1. "Definition of CARBURETTOR". merriam-webster.com. Merriam-Webster. Retrieved 23 January 2023.
2. "carburettor noun - Definition, pictures, pronunciation and usage notes". oxfordlearnersdictionaries.com. Oxford University Press. Retrieved 23 January 2023.
3. "carburetor". dictionary.cambridge.org. Cambridge University Press. Retrieved 23 January 2023.
4. "What Is a Carburetor?". stateofspeed.com. 2018-11-05. Retrieved 2022-02-03.
5. "carburetor". www.etymonline.com. Retrieved 22 October 2022.
6. Woodford, Chris (23 October 2009). "How does a carburetor work?". Explain that Stuff. Retrieved 22 October 2022.
7. "Carburetors Explained". autoevolution. 1 August 2014. Retrieved 22 October 2022.
8. Beale, Paul; Partridge, Eric (2003), *Shorter Slang Dictionary*, Routledge, p. 60, ISBN 9781134879519
9. "SHIP MACHINERY PARTS | MEGA MARINE". ship machinery parts. Retrieved 2023-06-16.
10. <https://www.slm-solutions.com/products-and-solutions/machines/slm-280-production-series/>

ADVANCED FOOT STEP POWER GENERATION USING PIEZO-ELECTRIC SENSORS

I Sri Phani Sushma , K Bhavani , R.Chandu Naik

Department of Mechanical Engineering, University college of engineering jntuk -narasaraopet

Abstract - Power generation and its use is one of the issues. Now-a- days numbers of power sources are present, non renewable & renewable, but still we can't overcome our power needs. Among these human population is one of the resources. In this project we are doing generation of power by walking or running. Power can be generated by walking on the stairs. The generated power will be stored and then we can use it for domestic purpose. Advanced footstep power generator system that uses piezo sensors to generate power from human footsteps. The system allows for a platform for placing footsteps. The piezo sensors are mounted below the platform to generate voltage from footsteps. The sensors are placed in such an arrangement so as to generate maximum output voltage .The circuit is a microcontroller based monitoring circuit that allows user to monitor the voltage and charges a connected battery by it .It also displays the charge generated and displays on an LCD display. The micro-controller monitoring circuit that count the number of steps applied on the weighting plate and the voltage across the capacitor in the rectifier circuit. then is displays all the information on an LCD screen. This system can be installed at homes, schools, colleges, where the people move around the clock.

Keywords

Power utilization, Power generation, piezoelectric material, energy utilization

I.INTRODUCTION

Day by day, the population of the country increased and the requirement of the power is also increased. At the same time the wastage of energy also increased in many ways. So reforming this energy back to usable form is the major solution. As technology is developed and the use of gadgets, electronic devices also increased. Power generation using conservative methods becoming deficient. There is a necessity arises for a different power generation method. At the same time the energy is wasted due to human locomotion and many ways. To overcome this problem, the energy wastage can be converted to usable form using the piezoelectric sensor. This sensor converts the pressure on it to a voltage. So by using this energy saving method that is the footstep power generation system we are generating power. This project is used to generate voltage using footstep force. The proposed system works as a medium to generate power using force. This project is very useful in public places like bus stands, theaters,

railway stations, shopping malls, etc. So, these systems are placed in public places where people walk and they have to travel on this system to get through the entrance or exists.Then, these systems may generate voltage on each and every step of a foot. For this purpose, piezoelectric sensor is used in order to measure force, pressure and acceleration by its change into electric signals. This system uses voltmeter for measuring output, LED lights, weight measurement system and a battery for better demonstration of the system. In another way, we are also saving natural energy resource

II. LITERATURE SURVEY

Earlier developments in the piezo electric circuitry involved concentration on small vibrations and hence small strains. Also, few of them required external voltage supply and there were number of losses in the system which amounts to low voltage output. In December 1929, scientists in U.S Navy performed various researches on piezoelectric crystals. Their focus was primary on the dimensions of crystals. This research proved that by changing the dimension and orientation of crystal the output. considerably changed. They designed the crystal named "Curie cut" or "Zero Cut based on the changes made in the angles of the crystal. Thus, this proves that the crystals designed with such dimensions are effective in controlling oscillations of a 50watt vacuum tube. So, they act as a voltage controlling device too. In 1985, the concept of using handwriting dynamics for electronic identification was performed in Sandia Laboratories A piezoelectric sensor pen for obtaining the pen point dynamics during writing was studied.

P.Venkatesh : In this paper, we have presented the design of power generation using footstep based on available piezoelectric sensors. Human race requires energy at very rapid rate for their living and wellbeing from the time of their arrival on this planet, because of this reason power resources have been worn out and enervated. Proposal for the employment and

application of extravagant energy in foots of human is very much to the purpose for extremely populated nations like China and India.

III. NEED OF SYSTEM

The Utilization of the Waste Energy foot Power With human motion is very important and highly populated countries like India and China where the roads ,railway stations, temples ,etc, are all over crowded and millions of people move around the clock .This whole human/ bioenergy being wasted if can be made possible for utilization it will be great invention and crowd energy farms will be very useful energy sources in crowded countries .walking across a “crowd farm” floor, then, will be a fun for idle people who can improve their health by exercising in such farms with earning. The electrical energy generated at such farms will be useful for near by applications.

IV. PIEZOELECTRIC SENSOR

When a sensor works on the principle of Piezoelectricity, it is known as Piezoelectric Sensor. Piezoelectricity is a phenomenon where electricity is generated if mechanical stress is applied to a material. A sensor that employs the piezoelectric effect, to measure variations in acceleration, strain, pressure, and force by converting them into electrical charge is named a piezoelectric sensor. This piezoelectricity produced is proportional to the stress given to substrates of the strong piezoelectric crystal.

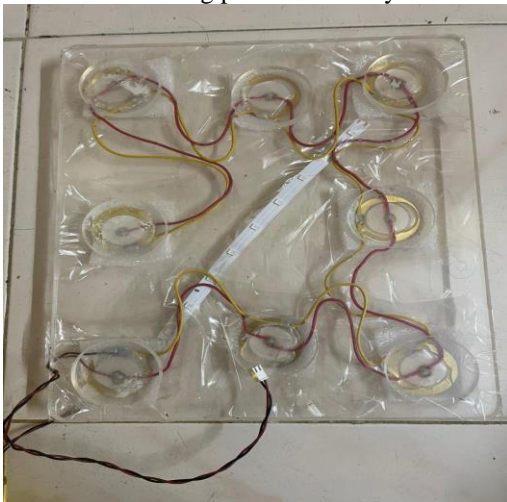
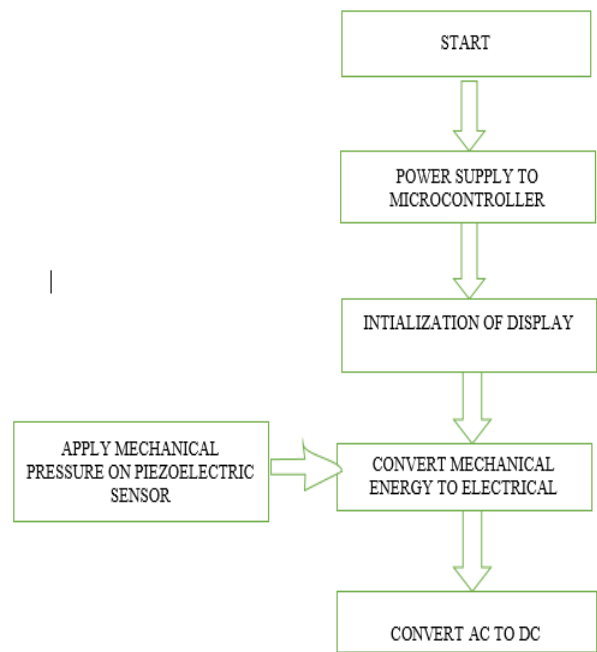


FIG.1. PIEZO-ELECTRIC SENSOR

V .MATERIALS USED

Category	Quantity	References	Value
Capacitors	2	C1,C3	22pf
Capacitors	1	C2	10uF
Capacitors	2	C4-C5	470uf
Capacitors	2	C6, 10UF	10uF
Resistors	7	R1,R3-R4,R6-R7,R14,R16	10k
Resistors	1	R2	1M
Resistors	1	R5	100k
Resistors	1	R8	330
Resistors	3	R10,R12-R13	1k
Resistors	1	R11	2k2
Resistors	1	R15	10R,2W resistor
Integrated Circuits	1	U1	atmega328
Integrated Circuits	2	U3-U4	7805
Transistors	1	Q2	BC547
Transistors	1	Q3	IRFZ44
Diodes	2	D1,D3,D4	RED-LED
Diodes	1	D2	5.1V zener
Diodes	1	D5	1N4007
Miscellaneous	4	BATTERY,J5,LED STRIP,PEIZO	2 pin relimate
Miscellaneous	1	BR1	Bridge
Miscellaneous	1	J1	LCD 16x2
Miscellaneous	1	J3	USBCONN
Miscellaneous	1	RESET	push button
Miscellaneous	1	RV3	10K POT
Miscellaneous	1		12V/1A DC Adapter
Miscellaneous	1		8-piezo footprint plate

VI.METHODOLOGY



VII. WORKING

- 1) The Footstep power generator works on the principle of piezoelectric effect.
- 2) Piezoelectric Effect is the ability of certain materials to generate an electric charge in response to applied mechanical stress.
- 3) Thus, squeeze certain crystals (such as quartz) and you can make electricity flow through them.
- 4) In most crystals (such as metals), the unit cell (the basic repeating unit) is symmetrical; in piezoelectric crystals, it isn't.
- 5) Normally, piezoelectric crystals are electrically neutral: the atoms inside them may not be symmetrically arranged, but their electrical charges are perfectly balanced: a positive charge in one place cancels out a negative charge nearby.
- 6) However, if you squeeze or stretch a piezoelectric crystal, you deform the structure, pushing some of the atoms closer together or further apart, upsetting the balance of positive and negative, and causing net electrical charges to appear.
- 7) This effect carries through the whole structure so net positive and negative charges appear on opposite, outer faces of the crystal.
- 8) Normally, the charges in a piezoelectric crystal are exactly balanced, even if they're not symmetrically arranged.
- 9) If you squeeze the crystal (massively exaggerated in this picture!), you force the charges out of balance.
- 10) Now the effects of the charges (their dipole moments) no longer cancel one another out and net positive and negative charges appear on opposite crystal faces. By squeezing the crystal, you've produced a voltage across its opposite faces and that's piezoelectricity!
- 11) In our project we have used the same phenomenon of producing piezoelectricity from piezoelectric crystal in the form of coin shaped disc.
- 12) When one steps on the weighing machine the piezoelectric disc gets compressed. After the leg is lifted the crystal is decompressed.
- 13) Thus a full vibration is sensed by the crystal disc and a voltage across it is produced.
- 14) This voltage is sensed by the voltmeter and displayed on its display.
- 15) Also, at the same time this voltage is used to charge the 12VDC Battery.
- 16) LED's have been mounted under the weighing machine that is switched on by relay through 555 timer IC whenever a voltage is generated.
- 17) This event is notified by a glowing LED on the PCB. (Also one can hear the switching sound of the relay)

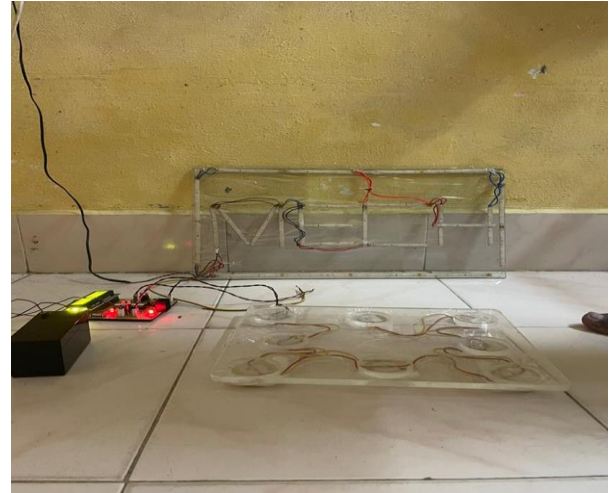


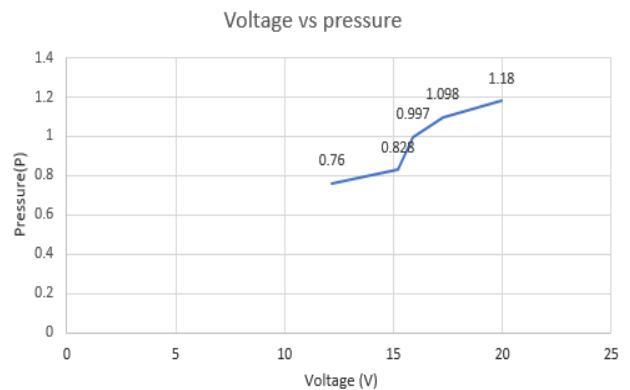
FIG.2. WORKING SET UP

VIII.RESULT:

VIII.1 Result Table

WEIG HT(W) (kg)	PRESS URE(P) (N/mm ²)	VOLTAGE(V)			
		Tr ail 1	Tr ail 2	Tr ail 3	Ave rage
45	0.760	7.0 9	13. 14	16. 3	12.1 7
49	0.828	12. 4	15. 2	18. 2	15.2
59	0.997	12. 7	14. 6	20. 6	15.9
65	1.098	13. 41	16. 3	22. 06	17.2 5
70	1.18	14. 8	18. 9	26. 2	19.9 6

VIII.2 GRAPH:



VIII.3 CALCULATIONS:

Area of a Footplate = Length*Breadth
 =27*21.5
 =580.5cm²
 Newton (N) = 9.81
 Pressure = weight*9.81/Area
 person1: weight = 45 kg

pressure at person 1 = $45 \times 9.81 / 580.5$
 = 0.760 N/mm²
 Person 2: weight = 49 kg
 Pressure at person 2 = $49 \times 9.81 / 580.5$
 = 0.828N/mm²
 Person 3: weight = 59 kg
 Pressure at person 3 = $59 \times 9.81 / 580.5$
 = 0.997N/mm²
 Person 4: weight = 65kg
 Pressure at person 4 = $65 \times 9.81 / 580.5$
 = 1.098N/mm²
 Person 5: weight = 70 kg
 Pressure at person 5 = $70 \times 9.81 / 580.5$
 = 1.18N/mm²

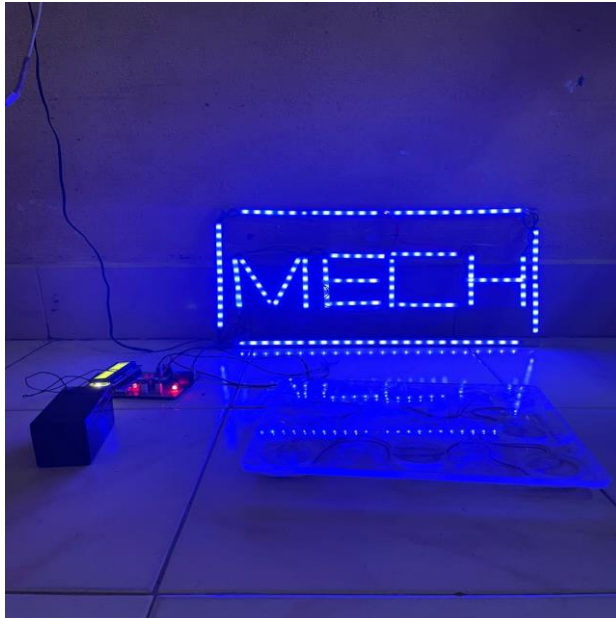


FIG.3.WORKING OUTPUT

CONCLUSIONS

In conclusion, it has been a long and interesting journey for us all. From the start when we picked the topic up to this moment writing the final report. We have had good and bad times putting this project together as we did not get to the goal we had set. On the other hand, we have gained a lot of knowledge with this project. we have set the goal to go for something different and better. As we have explained every aspect about the project in this report, we have partially done in the last step which is to have enough power to glow lights. but we have enough knowledge and experience to others who would like to work on such project. As well as the

knowledge that we have gained for us using this type of sensors which we worked with for the first time. Not only the sensors but so many components we have worked with for the first time.

REFERENCES

1. http://www.ijeit.com/Vol%203/Issue%2010/IJEIT1412201404_51.pdf Accessed 10/9/2018
2. <https://circuitdigest.com/electronic-circuits/foot-step-power-generation-circuit-usingpiezoelectric-sensor> Accessed 10/9/2018
3. https://www.researchgate.net/publication/308120087_Footstep_Power_production_using_Piezoelectric_Sensors Accessed 20/11/2018
4. <https://www.ijser.org/researchpaper/Footstep-Voltage-Generator-using-PiezoElectric-Transducers.pdf> Accessed 20/11/2018
5. <http://microcontrollerslab.com/foot-step-power-generation-system-using-picmicrocontroller/> Accessed 20/11/2018.

DESIGN AND FABRICATION OF STEERING GEAR MECHANISM FOR ELECTRIC VEHICLE

M. Sreenivasa Kumar, Mr. G. Gopi Chand, Mr. N. Bala Naveen, Mr. K. Pradeep, Mr. A. Yugandhar, Mr. M. Raja Sekhar

*Department of Mechanical Engineering,
Narasaraopeta Engineering College, Narasaraopet, Palnadu (Dist.), A.P., India*

Abstract - This Project aim the description and design the elements of the steering system for a electric vehicles. The steering system is one of the most important parts of the vehicle because has the task to control the car and guide by the desirable trajectory. The action starts on the hands of the pilot and is transmitted through several elements that have different tasks until turn the wheels.

Before start to design the elements of the steering system vehicle, it is required to study different aspects that have influence on the design of the steering system. It has good compilation of the general characteristics of a electric vehicles in order to know more about this kind of cars comparing with a other fuel that is known for the most of the people. Subsequently to study the theoretical knowledge and the technical fundamentals and general comments about the steering to understand better this system and applied on the electric vehicles.

The design of our steering system to separating the elements of the vehicle that have influence on the design of the steering and the elements. It has given begin giving a description of the mechanism and that will describe the function and the characteristics of each element. And also focus on the steering column, the rack and pinion and the steering arms and in order to design the elements, and using software's like fusion 360, solid works and Ansys and to calculate the stress that can support.

Keywords: Ackerman Steering Geometry, Motion transmission, Rack and Pinion Housing and Tie Rod Assembly.

1. INTRODUCTION

Steering is the term applied to the collection of components, linkages, etc. which will allow a vessel (ship or Boat) or vehicle to follow the desired course. An exception is the case of rail transport by which rail tracks combined together with railroad switches provide steering column, which may contain universal joints, to allow it to deviate somewhat from a straight line.

The most conventional steering arrangement is to turn the front wheels using a hand-operated steering wheel which is positioned in front of the driver.

The steering system acts a significant role of making car convenient to handle and enhance the vehicle stability. In the past one hundred years, the development of steering system has experienced many stages, and the

Steer-by-Wire system (SBW) is the newest technology of steering system for passenger cars. But the Steer-by Wire system has not yet accepted by public consumers and permitted by state regulations, in consideration of the reliability and safety of the system.

The steering system of a vehicle allows the driver to control the direction of the vehicle through a system of gears and linkages that connects the steering wheel with the front wheels. Steering Systems - Introduction The steering system must perform these functions:

- Change direction of vehicle.
- Provide a degree of 'feel' of the road for the driver.
- Not transmit excessive shock back to the driver due to an uneven road.
- Not cause excessive tire wear.

1.1 CONVENTIONAL STEERING SYSTEM

In this steering system, only the front wheels are steered towards right or left according to the requirement because at the rear their dead axle is present.

1.2 FOUR WHEEL STEERING SYSTEM

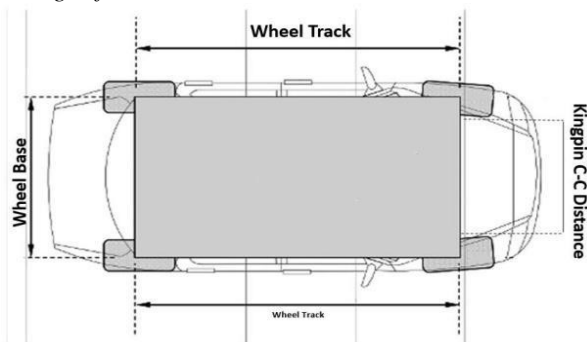
In this steering system, the all four wheels are to be steered according to the steer perform to drive towards left or right. Four-wheel steering, also called rear-wheel steering or all-wheel steering, provides a means to actively steer the rear wheels during turning maneuvers. It should not be confused with four-wheel drive in which all four wheels of a vehicle are powered. It improves handling and helps the vehicle make tighter turns. Production-built cars tend to under steer or, in few instances, over steer. If a car could automatically compensate for an under steer/over steer problem, the driver would enjoy nearly neutral steering under varying conditions.

In most active four wheel steering system, the rear wheels are steered by a computer and actuators, the rear wheels generally cannot turn as far as the front wheels. Some systems including Delphi's Quadra steer and the system in Honda's Prelude line allow the rear wheels to be steered in the opposite direction as the front wheels during low speeds. This allows the vehicle to turn in a significantly smaller radius sometimes critical for large trucks or tractors and vehicles with trailers.

1.3 ACKERMAN STEERING SYSTEM

According to Ackermann Steering geometry, the outer wheels moves faster than the inner wheels, therefore, the equation for correct steering is:

$$\cot \Phi - \cot \theta = b / l$$



In the image shown below,
 Φ = outer wheel angle
 θ = inner wheel angle
 b = track width
 L = wheelbase
 α = Ackermann angle

2. STATEMENT OF THE PROBLEM

.In conventional steering system we use the Ackermann geometry this is the arrangement of linkages in the steering of a car or other vehicle designed to solve the problem of wheel on the inside and outside of a turn needing to trace out circles of different radii.

In Anti-Ackermann geometry at low steering ratio and at high speed, handling capacity is low to eliminate this drawback we use the Ackermann geometry. In Ackermann geometry high speed handling increases and reduces the condition of over-steer and the vehicle handling capacity increases.

3. OBJECTIVES

The function of the steering system is clearly to afford the driver directional control of the vehicle, and to provide this control with sufficient accuracy to choose the best course around corners, to avoid other vehicles and stationary obstructions, and to maneuver the car efficiently at low speed. The following parameters need to be designed to minimize the steering effort.

1. Design of Steering arm angle.
2. Design Steering arm length.
3. Optimize Rack Position and placement of rack.
4. Optimize Steering effort, this factor should be designed according to wheel base and wheel track of the vehicle.

1. Design and Optimization of Steering System, Hardikkumar Gadher, Tejashkumar Patel, Chirag Modi, Zeel Bhojani Chandubhai S Patel Institute of Technology, CHARUSAT, Gujarat, India. 2017
2. Mohammad Kristamto - “Measuring geometric and kinematic properties to design steering axis to angle turn of the electric golf car.”, International Conference on Sustainable Energy Engineering and Application. 2015
3. R.S. Khurmi, J.K. Gupta - “Theory of Machines”, S Chand & Company Pvt. Ltd., Vol 1, 14th Edition, 2014

5. To study various wheel alignment related issues.
6. To understand the steering system in an automobile.
7. To study the components of steering systems and their configurations.

4. LITERATURE REVIEW

Rudolph Ackermann invented the steering mechanism allowing the vehicle to turn along the flow of the path in early 1800’s, called as Ackermann steering. The parallelogram steering mechanism was developed in late 1800’s. The major studies performed on the steering mechanisms and steering geometry optimizations are:

S.No	Author	Work	Year
1.	Hardikkumar Gadher, Tejashkumar Patel, Chirag Modi	Zeel Bhojani Chandubhai S Patel Institute of Technology, CHARUSAT, Gujarat, India.	2017
2.	Mohammad Kristamto	“Measuring geometric and kinematic properties to design steering axis to angle turn of the electric golf car.”, International Conference on Sustainable Energy Engineering and Application.	2015
3.	R.S. Khurmi, J.K. Gupta	“Theory of Machines”, S Chand & Company Pvt. Ltd., Vol 1, 14th Edition,	2014
4.	S.K. Gupta	“A Textbook of Automobile Engineering”, S. Chand & Company Pvt. Ltd., Vol 1, 1st Edition,	2014
5.	Saket Bhishikar, Vatsal Gudhka, Neel Dalal, Paarth Mehta, Sunil Bhil, A.C. Mehta	“Design and Simulation of 4 Wheel Steering System”, International Journal of Engineering and Innovative Technology (IJEIT), Volume 3, Issue 12,	June 2014
6.	Dr. Kirpal Singh	“Automobile Engineering”, Volume 1,	2013

4. S.K. Gupta - “A Textbook of Automobile Engineering”, S. Chand & Company Pvt. Ltd., Vol 1, 1st Edition, 2014
5. Saket Bhishikar, Vatsal Gudhka, Neel Dalal, Paarth Mehta, Sunil Bhil, A.C. Mehta - “Design and Simulation of 4 Wheel Steering System”, International Journal of Engineering and Innovative Technology (IJEIT), Volume 3, Issue 12, June 2014
6. Dr. Kirpal Singh, “Automobile Engineering”, Volume 1, 2013

5. MATERIALS SELECTION

The materials used in the steering system target precise operation and light weight components. Although precision and weight are the top priorities, cost, manufacturability, and reliability were also considered. Precision in the steering system is derived from high manufacturing tolerances and minimal deflection. Deflection in any component leads to steer compliance, resulting in an unresponsive steering system.

The pinion and idler gears were purchased, which limited material options but reduced manufacturing time. Although these gears are steel, they have a smaller face width than a comparable aluminium gear. The rack gear is Turned, Ground and Polished (TGP) 1042 carbon steel rod. The TGP material is more precise than standard round stock and the TGP finish removes surface tension inherent from standard extruding. This reduced the risk of the rack gear bending when the gear teeth were cut. The higher strength of the steel also allowed for extra material to be removed without introducing steer compliance. In addition to the precise material, the steel on steel gear mesh is advantageous for reliability. A softer material in the gear mesh would increase the possibility of galling, and compromise precision over time.

5.1 CHEMICAL COMPOSITION OF MATERIALS

<u>EN-19</u>	<u>EN-24</u>	<u>7075-AL ALLOY</u>
Carbon 0.35-0.45	C 0.36-0.44	Al 87.1-91.4
Manganese 0.50-0.80	Mn 0.45-0.70	Mn 0.3
Silicon 0.10-0.35	Si 0.10-0.35	Si Max. 0.4
Nickel ---	Ni 1.3-1.7	Zn 5.1-6.1
Molybdenum 0.20-0.40	Mo 0.2-0.35	Cu 1.2-2.0
Chromium 0.90-1.50	Cr 1.0-1.4	Cr 0.18-0.28
Sulphur 0.05	S 0.04	Fe Max 0.5

5.1 MECHANICAL PROPERTIES OF MATERIAL WITH REFERENCE TO HEAT TREATMENT PROCESSES (EN-19)

Forging

Pre heat carefully, then raise temperature to 850-1200°C for forging. Do not forge below 850°C. After forging cool slowly in air.

Annealing

Heat the EN19T slowly to 680-700°C. Cool in air.

Hardening

This steel grade is commonly supplied ready heat treated. If further heat treatment is required annealed EN19 should be

heated slowly to 860-890°C and after adequate soaking at this temperature quench in oil. Temper as soon as tools reach room temperature.

Tempering

Heat carefully to a suitable temperature selected by reference to a tempering chart or table. Soak at the temperature for 2 hours per 25mm of ruling section, and then allow to cool in air. Tempering between 250-375°C is not advised as tempering within this range will reduce the impact value.

Heat Treatment

Heat treatment temperatures, including rate of heating, cooling and soaking times will vary due to factors such as the shape and size of each steel component. Other considerations during the heat treatment process include the type of furnace, quenching medium and work piece transfer facilities. Please consult your heat treatment provider for full guidance on heat treatment of EN19T alloy steel

5.2 APPLICATION

EN19T was originally introduced for the use in the machine tool and motor industries for gears, pinions, shafts, spindles and the like. Later its applications became much more extended and it is now widely used in areas such as the oil and gas industries. EN19T is suitable for applications such as gears, bolts, studs and a wide variety of applications where a good quality high tensile steel grade is suited.

- A representative composition of AISI4140 steel also known as EN19 (medium carbon low alloy steel) is utilized to produce ferrite martensite dual phases of varied proportions by inter critical annealing treatment followed by heat treatment to different temperatures and rapid quenching. Mechanical test is essential part of any engineering activity. Mechanical test is applied to the materials, components and assemblies. It consists of measurement of fundamental properties or measurement of responses to particular influences such as load, temperature, etc. Types of mechanical tests carried out in EN19 (AISI4140) material are tensile test, Impact test and Hardness test. Table 1. shows the chemical composition of the material

6. CALCULATIONS

The geometry validation was done by performing the analytical treatment. The concept of reverse engineering was applied in order to validate the designed geometry.

The following calculations were performed in order to validate the geometry [1]:

Required conditions are:

6.1 ACKERMANN GEOMETRY

Angle of inside lock (θ) = 30^0

According to Ackermann Geometry for perfect steering is given by:

$$\begin{aligned} \cot \Phi - \cot \theta &= b / l \\ \cot \Phi &= \cot \theta + b / l \\ \cot \Phi &= \cot (30) + 1260/2032 \end{aligned}$$

Hence rearranging and substituting values in above equation;

$$(\Phi) = 23.02^0$$

Also,

Inner Turning Radius,

$$(R_{if}) = l / \sin \theta = 2032 / \sin$$

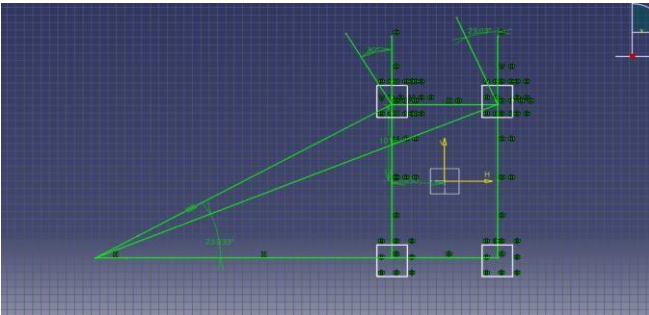
$$(30)(R_{if}) = 4064 \text{ mm}$$

Outer Turning Radius,

$$(R_{of}) = l / \sin \Phi = 2032 / \sin$$

$$(23.02)(R_{of}) = 5196.2 \text{ mm}$$

Hence by comparing both graphical and analytical data we can conclude that the both values are converging thus, the system design is accurate.



Model of Steering Angle Geometry

6.2 SELECTION OF GEAR TOOTH PROFILE

A gear tooth profile was selected based on BIS (Bureau of Indian Standard) recommendation and the manufacturability. A 20^0 full depth involute profile system was selected because of the following advantages:

It reduces the risk of undercutting It reduces the interference

Due to increase in pressure angle, the tooth becomes slightly broader at the root this makes the tooth stronger and increases its load carrying capacity. It provides better length of contact.

The properties of teeth of 20^0 full depth involute profile system are as follow:

Minimum number of teeth on pinion:

The minimum number of teeth required on pinion in order to avoid the interference was computed using following relation:

$$Z_p = 2h_a / m \cdot \sin^2 \Phi$$

Substituting values in above equation;

$$Z_p = 2h_a / m \cdot \sin^2 \Phi$$

$$\begin{aligned} &= 2 / \sin^2 \Phi \\ Z_p &= 17.09 = 18 \end{aligned}$$

Hence minimum numbers of teeth on pinion are: 18. Some

other details of gear teeth profile are given below,

- Module = 2
- 20^0 full depth involute system $\phi = 20^0$
- Addendum = $h_a = 1 \text{ m} = 2 \text{ mm}$
- Dedendum = $h_f = 1.25 \text{ m} = 2.5 \text{ mm}$
- Clearance = $C = 0.25 \text{ m} = 0.5 \text{ mm}$
- Working Depth = $2 \text{ m} = 4 \text{ mm}$
- Whole Depth = $2.25 \text{ m} = 4.5 \text{ mm}$
- Tooth thickness = $1.5708 \text{ m} = 3.14 \text{ mm}$

6.3 STEERING RATIO

The steering ratio is the ratio of how much the steering wheel turns in degrees to how much the wheel turns in degrees.

Approximating maximum turn to be of 25 degrees and steering wheel movement to be 180 degrees the steering ratio can be calculated as,

$$\begin{aligned} \text{S.R} &= 180/25 \\ &= 7.2 \end{aligned}$$

6.4 RACK TRAVEL

Once the steering ratio has been calculated the rack travel needs to be decided.

The steering wheel decided is AIM Formula steering wheel 2 which has a radius of 130 mm.

The steering wheel travel for one complete rotation,

$$\begin{aligned} &= 2\pi \times r \\ &= 0.6911 \text{ m} \end{aligned}$$

Considering maximum steer angle and max rack travel is reached at complete rotation of the steering wheel.

The steering ratio can be equated to steering wheel travel/rack travel

$$7.2 = 0.6911 / \text{Rack travel}$$

$$\text{Rack travel} = 95.98 \text{ mm}$$

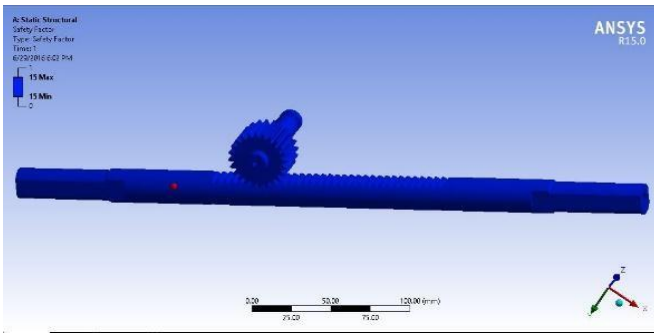
Therefore, required rack travel is around 96 mm.

6.5 RACK POSITION

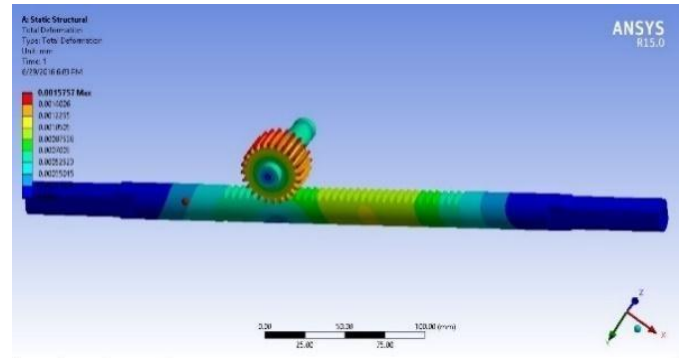
The rack can have two positions. It can either be in front of the front wheel center line or behind it. If the rack is placed forward of the front axle line it can be mounted easily on the frame giving wide range for choice of heights. However, this arrangement makes it difficult to have the steering rack, track rods and steering arms in a straight line which is required if Ackermann geometry is a goal for steering design. Fixing the rack behind the axle line is better from both a

geometrical and packaging viewpoint. Hence it is decided to

Three major analyses of rack and pinion on Ansys 15.0 are carried out here:



have the rack positioned behind the front axle line i.e. a rear steer is chosen.



7. DESIGN AND ANALYSIS

We are using rack and pinion mechanism because of oblivious advantages of reduced complexity, ease of construction and less space requirement compare to other steering mechanisms. The analytical steps involved in designing if rack and pinion systems are as follow:

- 1) Total Deformation
- 2) Equivalent Stress
- 3) Factor of Safety

a) Total Deformation

Fig. Total Deformation in Rack and Pinion

b) Factor of Safety

Fig. Factor of Safety in Rack and Pinion

7.3 CAD MODEL OF RACK AND PINION

We have designed complete assembly of rack and pinion in fusion 360, the complete design of rack and pinion and its assembly in fusion 360 is shown below:

c) Equivalent Stress

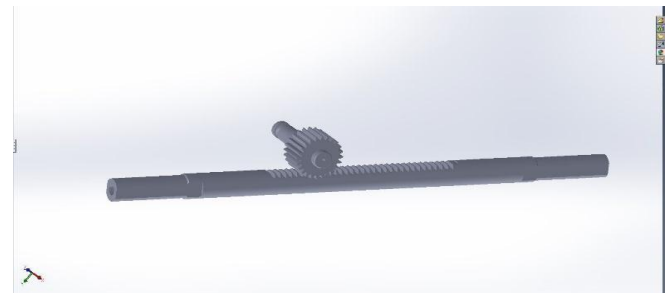
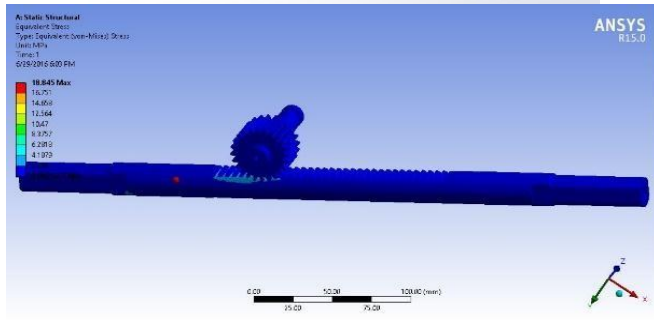


Fig. Cad model of Rack and Pinion in fusion 360

Requirements. "Today with electric power steering, the driver inputs some torque and we multiply it. With steer-by-wire, 100% of the effort to steer the vehicle has to come from the electric motor."

7.4 ANALYSIS OF COMPONENTS

Analysis is process of analysing the components by applying load, temperature, pressure etc. and obtaining the values such as stresses (bending, tangential and normal), deformations, safety factor etc. in order to determine the safety of the components when done in practical. These Analyses gives optimum result of safety of components and minimize the chances of failure.

8. CONCLUSION

The steering system was successfully 3D design and fabrication. Analysis was done one the steering system and identified rack and pinion of total deformation, factor of safety and stress. Also, to fit the steering system components in manually an electrical vehicle. To test the some tasks and to find the maximum turning radius is 3.5".

Fig. Stresses Generated in Rack and Pinion

Material Type: EN 19 Alloy Steel

Thus after the analyses of components The Design is Completely Safe.

9. SCOPE



An innovative feature of this steering linkage design is its ability to drive all four Wheels using a single steering actuator. Its successful implementation will allow for the development of a four-wheel, steered power base with maximum maneuverability, uncompromised static stability, front- and rear-wheel tracking, and optimum obstacle climbing capability.

The advanced system of “Four wheel steering” will work electronically with the help of microprocessors. The system will utilize an onboard computer to control and direct the turning left and right of the rear wheels.

One of the big challenges in moving to steer-by-wire is, Seeger said, communications. That's right: The internal network. Because a steer-by-wire system has no mechanical connection between the steering wheel and the front wheels, instead of creating a system that is fail-safe, one that is fault-tolerant is needed: If something goes wrong, the system still operates. This means data redundancy is the system. "Rather than the CAN communications that we used today, we need something like Flex Ray to allow high-speed communications

To improve the steering geometry i.e. Ackerman geometry, which helps the driver to avoid the negative effect of cornering forces acting on the vehicle & increases the space in cockpit area and the comfort of driver. Steering geometry can be optimized by using mathematical model for Ackerman condition for different inner wheel angles and select geometry for which percentage Ackermann as well steering effort is optimum. The composite material increases the strength of rack & pinion & reduces the weight of system which helps to reduce gross weight of vehicle. The weight Composite Material is reduced as compared to others material which is turn result in improved power transmission which overall improve the efficiency of the system

REFERENCES

[1] Borse, S., Chille, P., Dabhade, S., Deshmukh, S., Kulkarni, A.: Design and Manufacturing of an effective steering system for ATV and performance enhancement using yoke-nut assembly, special issue from national conference (NCMMM) in International Journal of Research in Advent Technology, 2016.
 [2] Zhao, J.-S., Liu, X., Feng, Z.-J., Dai, J. S.: Design of an Ackerman-type steering mechanism, Proceedings of Institution of Mechanical Engineering Part C: Journal of Mechanical Engineering Science, 227, 11, 2549–2562, 2013.
 [3] Jadoun, R. S., Kumar Choudhary, S.: Design and fabrication of variable steering ratio mechanism for light Motor vehicle, Innovative Systems Design and Engineering, 5, 9, 7–15, 2014.
 [4] Laxmi, N., Anil Kaumar, B., Kiran Varma, D.: Design and Fabrication of A Steering Controlled Headlights in Automobile, International Journal & Magazine of Engineering, Technology, Management and Research, 2, 7, 98–102, 2015.
 [5] Boby, G., Akhil, T. B., Albert, J., Aswin, J., Denny, F.: Design and Fabrication of Steering and Bracking System for All Terrain Vehicle, International Journal of Scientific & Engineering Research, 7, 3, 7–18, 2016.
 [6] Ahmed, A. K. W., Rawat, V., Bhat, R. B.: Vehicle Steering Mechanism for Active Independent Front Steering System, 3rd International Conference on Mechanical, Production and Automobile Engineering (ICMPAE'2013) January 4th to 5th Bali (Indonesia), 83 85,2013

Geometry	Ackermann geometry
Steering type	Rack & Pinion
Type of rack used	Right sided mounted
Steering ratio	7.2:1
Number of teeth	22
Length of knuckle	8.5”
Inner turning radius	3500mm
Outer turning radius	5200 mm
Inner wheel angle	26.6degree
Outer wheel angle	23 degree
Steering wheel travel	360 degree (691 mm)
Rack Travel	96 mm
Toe in (+ve)	1 degree
Camber angle	0 degree
Turning Radius	3.6 meter
Material for Rack and Pinion	EN-19
Material for Steering column	MS

Steering results at a glance

DESIGN AND ANALYSIS OF CONNECTING ROD USING ANSYS

K.Kiran Chand, CH. Ashok, V.Hemanth Kumar, B.Vishnu Vardhan Reddy, J.Sandleya, B.Prasanna Babu

Department of Mechanical Engineering, Narasaraopeta Engineering College, Narasaraopeta, Palnadu (Dist.), A.P., India

Abstract:

In this project it is proposed to do static analysis of a Connecting rod. Different materials are used for the analysis like structural steel, Titanium alloy, Aluminum alloy. Connecting rod is one of the most vital part of an I.C. engine and used to transfer the reciprocating motion of piston into the rotatory motion of crankshaft. It is heavily stressed during the operation subjected to compressive stress due to the gas pressure and tensile stress due to the Inertia force. The actual dimensions of the connecting rod are considered and the model of the connecting rod is designed in solid works and ANSYS is used for static and modal analysis for finding von mises stresses, frequencies for three materials and compared to choose the best material suitable for connecting rod.

It is observed that titanium alloy is the best material for manufacturing of connecting rod although it has more weight than the aluminum alloy, it has more factor of safety and high natural frequency which optimizes the design of connecting rod.

Key words: Connecting rod, Structural steel, Crank shaft.

I. INTRODUCTION

A Connecting rod is the part which connects the piston and the crank shaft. It is the link between both parts. Small end part of the rod is connected to piston with the help of the pin and the big end part of the rod is connected to the crank shaft. The purpose of the Connecting rod is to provide fluid movement between piston and crank.



Fig 1: Connecting rod

II. TYPES OF CONNECTING ROD

There are many types of connecting rod with different I section and H section. But there are basically two types of connecting rod.

- Connecting rod with nut and bolt
- Connecting rod without nut and bolt
- I-beam connecting rod
- Connecting rod with H-beam
- X-beam, cross beam

III. FAILURES IN CONNECTING ROD

The connecting rod connects the pistons to the crankshaft. It converts the linear motion of the pistons to the rotary motion of the crankshaft. On every stroke, the connecting rod is stretched and compressed. This pressure, plus other factors, can cause the connecting rod to break. The broken rod can go through the engine block completely, ruining the engine--a condition known as "throwing a rod."

- Fatigue
- Pin Failure
- Over Revving
- Hydro lock



Fig 2: Connecting rod that initially failed through fatigue, the further damaged from impact with crankshaft

IV. PROBLEM STATEMENT

The objective of the present work is to design and optimize a connecting rod based upon its material properties by using different materials (aluminum alloy, titanium alloy, structural steel). The material of connecting rod will be optimized depending upon the analysis result output. CAD model of connecting rod will be modelled in SOLID WORKS and then analyzed in ANSYS Software. After analysis a comparison will be made between existing material and alternate material which will be suggested for the connecting rod in terms of stresses, factor of safety and the desired output results can be achieved.

V. PROBLEM OBJECTIVE

1. Design and Analysis of the connecting rod based on the input parameters and then modelling of the connecting rod in the SOLID WORKS software.
2. FEM tool software ANSYS workbench is given model and material input based on the parameters obtained.
3. To determine the Von-Mises stresses, Shear stress, Total Deformation and to optimize in the existing Connecting rod design.

4. To calculate stresses in critical areas and to identify the spots in the connecting rod where there are more chances of failure.
5. To determine the structural analysis and modal analysis of the connecting rod with different materials.

XI. DESIGN FOR PRESSURE CALCULATION

Consider 150cc Engine Specifications

Engine type = Air cooled 4-stroke
 Bore x Stroke (mm) = 57 x 58.6mm2
 Displacement = 149.5 CC
 Maximum Power = 13.8 bhp @ 8500 rpm
 Maximum Torque = 13.4 Nm @ 6000 rpm
 Compression Ratio = 9.35:1
 Density of Petrol (C8H18) = 737.22 kg/m³
 Auto ignition temp. = 60°F = 288.85°K
 Mass = Density x volume = 737.22 x 10⁻⁹ x 149.5 x 10³ = 0.110214 kg
 Molecular weight of petrol = 114.228 g/mole = 0.11423 kg/mole
From gas equation, PV=m
 x *Rspecific* x T Where,
 P = Gas Pressure, MPa V = Volume
 m = Mass, kg
 T = Temperature, °k 11
Rspecific = Specific gas constant = R/M
Rspecific = 8.3144/0.114228
Rspecific = 72.788 Nm/kg K
 P = m x *Rspecific* x TV
 P = 0.110214 x 72.788 x (288.85 / 149.5) = 15.49 MPa ≈ 16 MPa
 Calculation is done for maximum Pressure of 16 MPa.

XII. DESIGN CALCULATION FOR THE CONNECTING ROD

Thickness of the flange & web of the section = t
 Width of the section, B = 4t
 Height of the section, H = 5t
 Area of the section, A = 11t²
 Moment of inertia about x-axis, I_{xx} = 34.91t⁴
 Moment of inertia about y-axis, I_{yy} = 10.91t⁴
 Therefore I_{xx}/I_{yy} = 3.2
 Length of the connecting rod (L) = 2 times stroke L = 117.2 mm
 Total Force acting F = FP - H
 Where,
 FP = force acting on the piston
 FI = force of inertia
 FP = (π/4) D² x Gas pressure
 Where,
 D = Bore Diameter
 FP = (π/4) 57² x 15.49 = 38275 N
 FI = m x ω² x r (cosφ + cos2φ/n)
 Where,
 M = Mass
 = 2 8500/60 = 890.118 = length of connecting rod(l) / crank radius(r)
 = (2 x /2)
 = 117.2/29.3
 = 4

The maximum gas load occurs shortly after the dead centre position at = 3.3 ° cos(3.3) = 0.9983 1

= 0.110214 x 890.1182 x 0.0293 (1 + 1/4)
 = 3200, F = 38275 - 3200 = 35075 N
 According to Rankin's - Gordon formula,
 = (σ /1+ ()²)
 Where,
 A = c/s area of connecting rod l
 = Length of connecting rod σc=
 Compressive yield stress
 F = Buckling load
 = Constant depending upon material and end fixity coefficient
 K_{xx} and K_{yy} = Radius of gyration of the section about x - x and y - y axis respectively. On substituting to Rankin's formula
 35075 = 170 x 112 / 1 + 0.002 (117.2 / 1.78)²
 By solving this, t
 = 5.5 mm
 Therefore,
 Width B = 4t = 22 mm
 Height H = 5t = 27.5 mm
 Area A = 11t² = 332.75 mm²

XIII. Design of small end

Load on the small end (Fp) = Projected area x Bearing pressure
 = d_{pl} x P_{bp}
 Where,
 Fp = 38275 N load on the piston pin
 d_p = Inner dia. of the small end
 l_p = length of the piston pin
 = 1.5bp to 2bp
 P_{bp} = Bearing pressure
 = 10.0 for oil engines.
 = 12.5 to 15.4 for automotive engines.
 We assume it is a 150cc engine, thus
 P_{bp} = 15.4 Mpa

Design of Big end:

Load on the big end (Fc) = Projected Area x Bearing pressure
 = d_{cl} x P_{bc}
 Where,
 Fc = 38275 N load on the crankpin
 dc = Inner dia. of the big end
 lc = length of the crankpin
 = 1.25 to 1.5
 = 5 to 12.6 Mpa
 Height at the small end H1 = 0.75H to 0.9 H
 H1 = 0.9 x 27.5 = 24.75 mm
 Height at the big end
 H2 = 1.1H to 1.25H
 H2 = 1.25 x 27.5 = 34.375 mm.
 Substituting,
 38275 = 2 x x 15.4
 = 35 mm
 = 2 = 70 mm
 Outer diameter of small end = + 2 + 2
 = 35 + [2x2] + [2x5]
 = 49 mm
 Where,
 Thickness of bush () = 2 to 5 mm
 Marginal thickness () = 5 to 10 mm
 Substituting,
 38275 = 1.5 x x 12.6, d = 45 mm
 = 1.5 = 67.5 mm
 Outer diameter of big end = + 2 + 2 + 2
 = 45 + [2x2] + [2x5] + [2x2]
 Outer diameter of big end = + 2 + 2 + 2

Marginal thickness (tm) = 5 to 10 mm
 Marginal thickness of bolt (db) = 2 to 5 mm

FINAL DIMENSIONS

Parameters	Size (mm)
Thickness of the connecting rod (t)	5.5
Width of the section ($B = 4t$)	22
Height of the section ($H = 5t$)	27.5
Height at the big end ($H1$)	24.75
Height at the small end ($H2$)	34.375
Inner diameter of the small end	35
Outer diameter of the small end	49
Inner diameter of the big end	45
Outer diameter of the big end	63

MODELLING

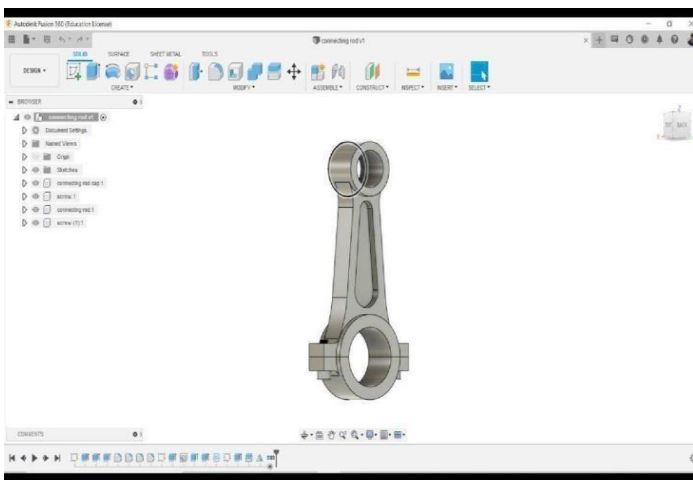


Fig 3 Fusion 360 drawing interface

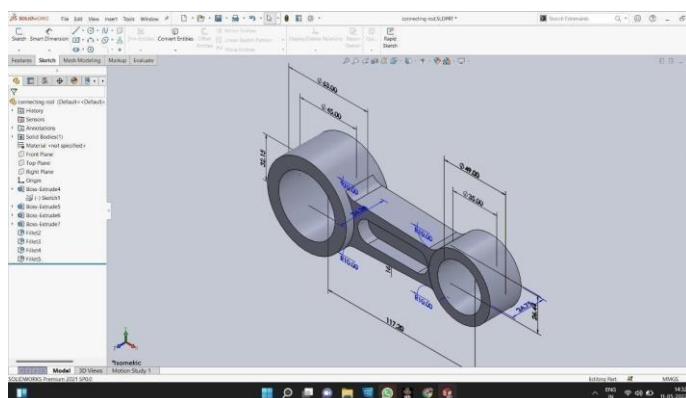


Fig 4: 3D structure of connecting rod

Introduction to ANSYS Workbench

ANSYS Workbench is the framework upon which the industry's broadest suite of advanced engineering simulation technology is built. An innovative project schematic view ties together the entire simulation process, guiding the user every step of the way. Even complex multi physics analysis can be performed with drag and-drop simplicity.

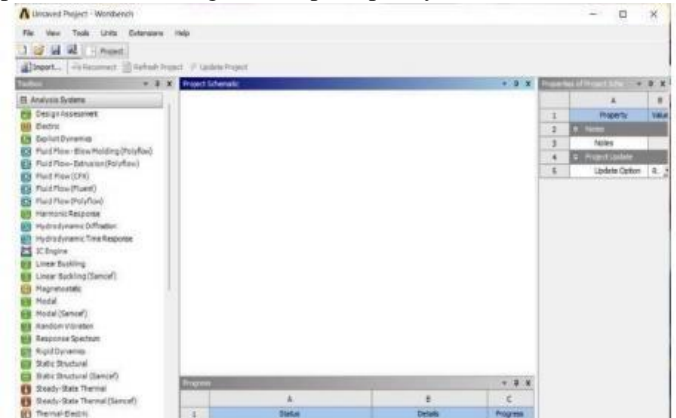


Fig 5: ANSYS work bench

Structural Analysis

Structural analysis is probably the most common application of the finite element method. The term structural (or structure) implies not only civil engineering structures such as bridges and buildings, but also naval, aeronautical, and mechanical structures such as ship hulls, aircraft bodies, and machine housings, as well as mechanical components such as pistons, machine parts, and tools.

Structural Steel:

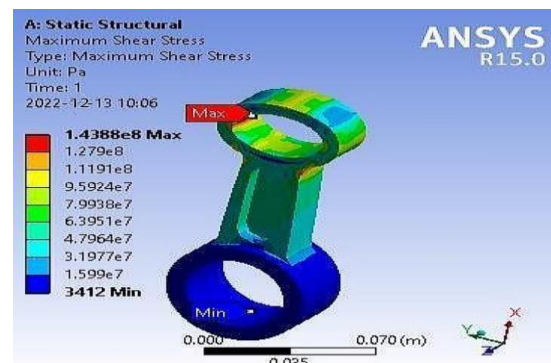


Fig 5: Maximum shear stress of Steel

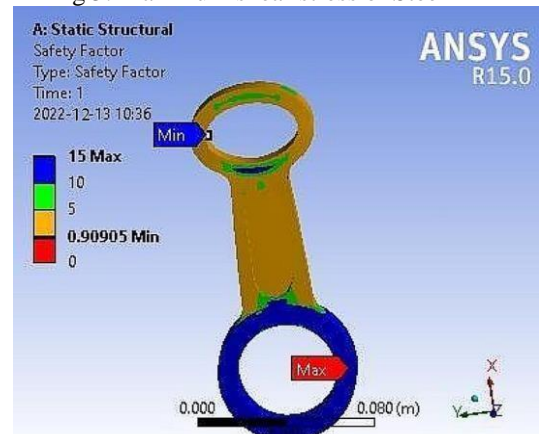


Fig 6: Factor of Safety

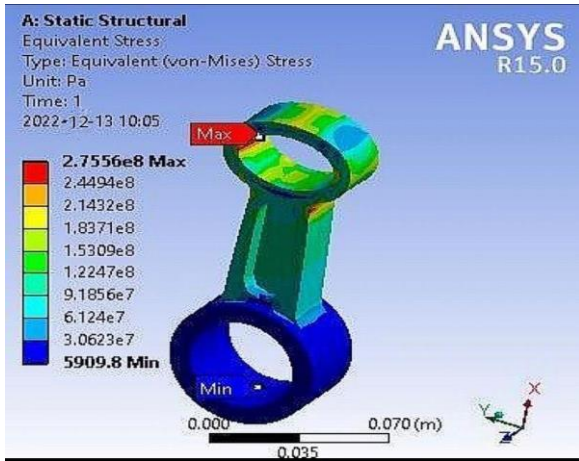


Fig 7: Equivalent stress

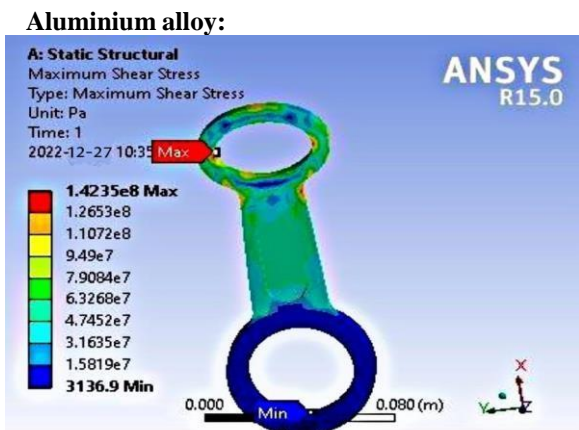


Fig 8: Maximum shear stress of Aluminium

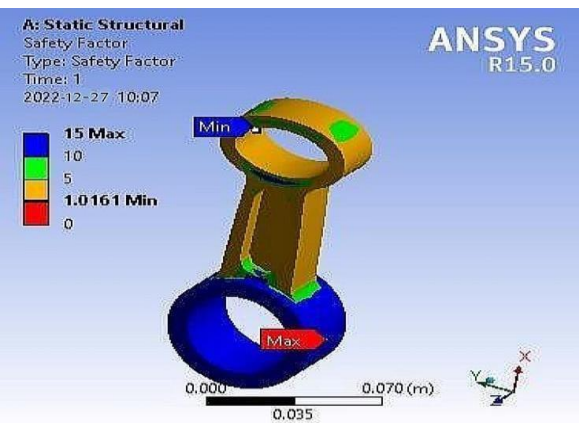


Fig 9: Factor of Safety

Results:

Materials	Structural steel	Aluminum alloy	Titanium alloy
Equivalent stress	275.56 MPa	275.01 MPa	275.68 MPa
Max. Shear stress	143.89	142.35 MPa	141.17 MPa
Factor of safety	0.90905	1.0161	3.375
Mass	0.79897 Kg	0.28193 Kg	0.47022 Kg

1. The Connecting rod model was safe for only for titanium alloy and aluminum alloy during the Static structural analysis and factor of safety is more than one for both aluminum and titanium alloy and having low density
2. Aluminum alloy has reduction in weight with respect to titanium alloy and structural steel
3. Max shear stresses for all materials are in range but structural steel has max shear stress
4. Von misses stresses for all materials are in range but structural steel has max shear stress.
5. Aluminum alloy has high natural frequency with respect to the other structural steel and titanium alloy.
6. Titanium has low natural frequency with respect to other aluminum alloy and structural steel.

CONCLUSION

1. With the help of fusion 360 software connecting rod was modelled.
2. Finally, analysis was done using Ansys software
3. From the analysis titanium alloy is best material for manufacturing of connecting rod although it has more weight than the aluminum alloy it has more factor of safety and high natural frequency which optimizes the design of connecting rod
4. Aluminum alloy is identified as second choice for production of manufacturing of connecting rod
5. Structural steel is not effective with regarding to mass and it increases the weight of connecting rod.

FUTURE SCOPE:

The analysis is focused on static structural and modelling analysis. So, further study may include dynamic loading and working conditions of the connecting rod. The thermal analysis can also be performed, by using Ansys. Buckling load can also be performed. Further one can investigate the behavior of connecting rod for the evaluation of performance of existing model by carrying out Experimental Stress Analysis (ESA) The above analysis can be performed assigning latest material composition to the connecting rod for the further optimization of design.

REFERENCE

1. [1] KULDEEP BASAVARAJAPPA, MOHAMMED FAHEEM, “Analysis and optimization of connecting rod using ALFASIC composites” International Journal of Innovative Research in Science Engineering and Technology 2(6):2480-2487, June 2013
2. [2] D. SOORYA PRABAKARAN AND P. RAMACHANDRAN, “Design and thermal analysis of Composite Connecting Rod ” International Journal of Engineering and Robot Technology. 4(1), 2017, 28-36.
3. [3] KUMBHA SAMBAIAH, DR. A RAMA RAO AND DR. M MAHESH “Optimization for thermal analysis connecting rod of internal combustion engine by using two different materials” , International Journal of Applied Research 2017; 3(12): 278-282
4. [4] ASHISH KUMAR, Er. SHUBHAM PARMAR “Analytical Study and Design Analysis of Connecting Rod of Mahindra Pijo by Finite Element Analysis”, International Journal of Scientific Development and Research (IJS DR) www.ijedr.org
5. [5] DR. B.K.ROY “Design Analysis and Optimization of Various Parameters of Connecting Rod using CAE Software’s” International Journal of New Innovations in Engineering and Technology (IJNIET)
6. [6] AISHA MUHAMMAD AND IBRAHIM HARUNA SHANONO “Finite Element Analysis of a connecting rod in ANSYS”, March 2020IOP Conference Series Materials Science and Engineering 736(2):022119
7. [7] MULUKUNTLA VIDYA SAGAR AND KANJARLA SHYAM KUMAR “Static analysis of Connecting Rod.” International Journal of Modern Trends in Engineering and Research (IJMTER)
8. [8] MR. H D. NITTURKAR, MR. S M. KALSHETTI, MR. A R. NADAF “Design and Analysis of Connecting Rod using Different Materials” International Research Journal of Engineering and Technology (IRJET).

DESIGN AND SIMULATION OF GYRO SPHERE

A.Pavan Kumar, M.S Willims, R.Satish Kumar, SK.Subhani, I.Prathap Reddy and M.Naga Lakshmaiah

Department of Mechanical Engineering, Narasaraopeta Engineering College, Narasaraopeta, Indi

Abstract— Fusion 360, a product introduced by design, structural design, mechanical by Autodesk and integrating industrial simulation, and CAM, turns out a design platform supporting collaboration and sharing both cross platform and via the cloud. In previous products, design and manufacturing use to be isolated. In the course of design, research and development, the communication between designers and engineers used to go on through different software products, tool commands, and even industry terms. Moreover, difficulty also lies with the communication between design thoughts and machining strategies. Naturally, a difficult product design and R & D process would trigger a noticeable gap between the design model and the actual product. A complete product development process tends to cover several major areas, such as industrial design, mechanical design, rendering and animation, computer aided emulation (CAE), and computer aided manufacturing (CAM). Fusion 360, a perfect design solving the technical problems of cross platform data exchange, realizes the effective control of cross an overview regional collaboration and presents of collaboration and breaks the barriers between art and manufacturing, and blocks between design and processing.

I. Introduction

We can see many kinds of different types of vehicles that runs on different types of the power sources. The Gyro Sphere Vehicle is the Eco friendly, Comfortable, simple and strongest Vehicle. The Gyro sphere is actually the idea which was brought into light for the purpose of the movie called the "Jurassic world". The design of this vehicle was designed by the designer called "Edward Verreaux" this vehicle is designed on the basis of the monster reptiles called the "Dinosaurs". According to the strength of the reptiles and the environmental conditions of and the land in past where this monster reptiles lived, are most harsh and the bite force is stronger than today's wild animals so it will be so strong and can withstand any type of the harsh conditions. The Gyro Sphere was the new technology based vehicle which runs on electricity and the latest technology is used in this vehicle and the difference between the ordinary vehicles and the gyro sphere is that it is a spherical vehicle surrounded with the thick hollow spherical fibre glass. The gyro sphere vehicle is the integrated future vehicle which contains the modern technology. The Gyro sphere is a simple type of the vehicle but the drawback is that it is an incomplete structure and design and also it is failed during the fabrication due to the design makes the vehicle the stable, strongest and the comfortable vehicle which reached our expectations as we assumed. When the force is applied to the axle, the section at the top of the gyroscope will try to move to the left, and the section at the bottom of the gyroscope will try to move to the right, as shown. If the gyroscope is not spinning, then the wheel flops over, as shown in the video on the previous page. If the gyroscope is spinning, think about what happens to these two sections of the gyroscope Newtons First Law of Motion states that a body in motion continues to move at a constant speed along a straight line unless acted upon by an unbalanced force. So, the top point on the gyroscope is acted on by the force applied to the axle and begins to move toward

the left. It continues trying to move leftward because of Newton's first law of motion, but the gyro's spinning rotates it, like this

NEED TO INVENT THE GYRO SPHERE VEHICLE: The main thing that gives an idea to invent the Gyro Sphere vehicle is that the Jurassic World movie, but before the plan is on progress to design the gyro sphere vehicle. Due to increase in fashion and the creativity and in accordingly the increase in the accident rate in places like jungle, air polluted areas, radioactive areas and the volcanic eruption areas. The gyro Sphere vehicle allows us to watch the nature very closely and peace fully and also to visit the harmful places like the jungle and other dangerous places for example the radioactive places. The Gyro sphere vehicle is designed based on the needs and the necessities of the modern present and the future world. So, there will be more demand to this vehicle and the main reason to invent this vehicle is to minimize the accidents and to give the better experience of watching the nature very closely and another important reason is that it is designed for the movie called the Jurassic World to encounter the wild beast lizards very closely. The Gyro Sphere uses an adaptive center-of-gravity automatic control system to enable the passenger to easily adjust the speed by handling the knob to change the center of gravity in the pod. the company suggested that the Gyro Sphere Vehicle is perfect for 'enclosed campuses such as airports, theme parks and malls.' it's no surprise then that segway-ninebot said the vehicle drew inspiration from the gyrosphere vehicles in the 2015 movie 'jurassic world' that transport visitors around the amusement park. the pod has been designed to offer wide-angle views that provide an expansive viewing field of passengers. the verge reported that it would likely be available During the shooting of "Jurassic World," a real Gyrosphere was loaded onto a specially constructed track, actors were put inside it, and it was controlled by a stagehand with a remote control. Trevorrow says that his son was even granted a ride during the shooting. The same chassis for the sphere was also used to simulate its bumpy movements by attaching it to an enormous mechanical arm that could flip it sideways and upside down like a real thrill ride, with actors strapped into it. The bumps were filmed against a green screen, and then digitally overlaid into the dinosaur enclosures. Trevorrow also filmed an empty sphere for a few shots, and then composited the actors into it after they, too, had been filmed against a green screen. The entire behind-the-scenes shoot of the sphere can be seen above.

II. About Fusion 360

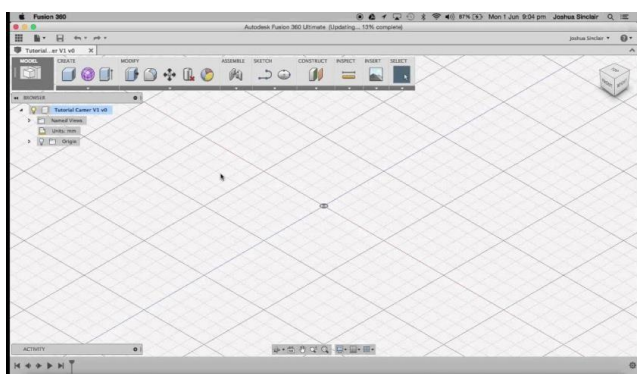
History: Fusion 360 is a Designing software which is used to design, Analyse, Render Animate the designed machine parts. Fusion 360 is a commercial computer-aided design

(CAD), computer-aided manufacturing (CAM), computer-aided engineering (CAE) and printed circuit board (PCB) design software application, developed by Autodesk. It is available for Windows and macOS, with simplified applications available for Android and iOS. Fusion 360 is licensed as a paid subscription, with a free limited home based, non-commercial personal edition available.

Features: Fusion 360 has built-in capabilities to do 3D modelling, simulation and documentation. It can manage manufacturing processes such as machining, milling, turning and additive manufacturing. It also has electronic design automation (EDA) features, such as schema design, PCB design and component management. The fusion 360 can also upload files to cloud directly in less time and it can save the files into our internal storage, it has some specific shapes which we can use directly without using sketch, for example we can create a sphere without using any sketch properties. Fusion 360 also enables some features like the shortcuts we can draw any sketch by just clicking one button it is the advanced feature of fusion 360, we can select rectangle by pressing 'R' and draw circle by selecting 'C' etc... There are also some features that makes fusion 360 very special that is it contain the analysis, rendering, animation and some other features, this enables us to do analysis like the thermal analysis, the load analysis and we can also animate the components by joining them.

Employed: Due to its special features and the simplicity, it is used in different areas where the design before the manufacturing is necessary. It is used in different kind of designing industries like the Car designing industry, the PCB designing industry, the Construction designing Industries etc..., the vehicle manufacturing industries use it for designing as well as the analysis. The Electronic industries uses them for designing the complicated parts like the microchips like the microcontrollers and the mi o analyse them coprocessors. The construction industries used it for designing the buildings and the beams and to analyse them.

Over view of Fusion 360 The Fusion 360 designing the was the designing app which was created by the auto desk for simple and the complicated many features components. It is the one of the software which as makes it different from other designing software. The layout of the is like...



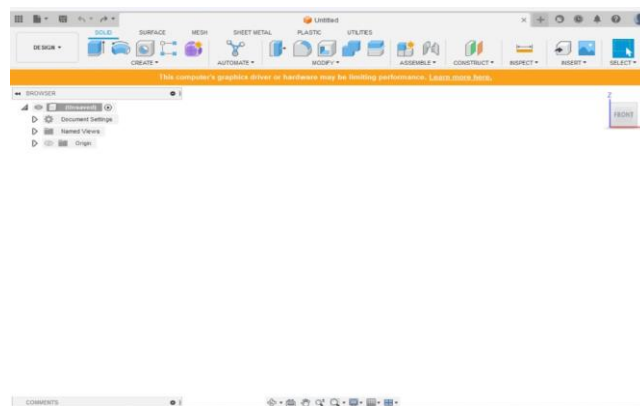
Layout of Fusion 360

The layout of fusion 360 3. 1 : Layout of Fusion 360 . has the Working toolbars a workbench, fusion 360 the animation panel, the toolbar panel and the design information like the re are some small bars on the screen which contains all the sketch of the 3D object, the dimensions, the two small boxes at bottom w origin etc..., it also have hich contains the tools which are used to rotate the 3D object or the sketch and to move the 3D sketch on the screen, there is also a zoom in and

zoom out option which enables us to see and correct the small mistakes while sketching and designing. The other options on the workbench are the save option, the re-do and un-do options which are the most common options seen any design software, there is a side panel which show the components and the projects we have done and it also plays a key role during the assembly and animations sections. There are some gridlines which looks like the graph paper and these lines gives us the accuracy in case of dimensions and for pointing the origin. Other special thing in fusion 360 is that it has offline mode option in which we can work even if there is no internet connection and when we connect the internet it will upload all the files to cloud so we can access them anywhere.

Tool Bars in Fusion 360: There are different types of tools used with different work abilities, Functionalities and specialities. They are divided into section named as, 1.) Solid. 2.) Surface. 3.) Mesh. 4.) Sheet Metal. 5.) Plastic. 6.) Utilities.

1.) Solid Section: The Solid tool bare is the first tool bar that is used to sketch any kind of the design and to add materials. And there are different kinds of sub tools which are the basis of any kind of the design, they are i.) Create. ii.) Automate. iii.) Modify. iv.) Assemble. v.) Construct. vi.) Inspect.



2.) Surface Modelling Section: The surface section contains the tools which are used to do all the surface work of the component like it is the skin of the component and it can be modified. Surface modelling is a way to display 3D objects in a CAD environment that is at times easier than solid modelling and more robust than wireframes. You can create and edit surfaces for repairing, patching, or designing geometry. Designers and engineers use this modelling method for product designs, organic form modelling, 3D gaming animations, and more. Unlike solid modelling, surface modelling requires the designer to define exterior curves and shapes. Without properties of thickness or mass, surface modelling gives the designer the unique ability to adjust the 3D model in ways solid modelling will not allow. However, this means that you cannot slice surface models open as they are virtually hollow. The Surface section contains the tools like, i.) Create. ii.) Automate. iii.) Modify. iv.) Assemble. V). VI) Construct. Inspect.

3.) Mesh Section: The Mesh tab use mesh Layout of the Surface Modelling Section contains mesh modelling tools within the Design 360, and supports both parametric and direct modelling modes. In workspace in Fusion Parametric modelling mode, a face group is the smallest selectable entity. In you can select individ ual faces. Direct Modelling mode, A mesh body is a collection of polygon faces

composed of vertices and edges. A mesh has no thickness. Meshes are commonly used in additive manufacturing. You can use the for Mesh manufacturing. Commands to insert, repair, and modify mesh bodies to prepare them

4.) Sheet Metal Section : ure 3. 4 : The Sheet Metal is the kind of metal which is in the form of sheets and can be bent in any direction Whether you have been bending sheet metal since the invention of the press brake or you just created your first flange, one flange command will improve you r design process. Those traditional CAD tools out there make you memorize when to use different sheet metal commands in different situations. But let’s be honest, no designer or engineer wants to remember that you have to use a base flange on a closed prof meter ile. We just want to be able to get the job done. Fusion 360 folds 5 sheet metal flange commands (base, edge, contour, , and swept) into one flange command. The command is aware of what is being selected and will automatically switch to the right comm .

5.) Plastic Section: The plastic section contain all the tools which enables us to The Assign Plastic Rule modify and features of the command lets you assign a specific plastic rule to components in your design. The plastic rule automatically controls certain properties of features within that component. These include physical material, thickness, and radii, using automatica and physical properties. lly generated parameters With this tool, you can quickly apply plastic material properties to any components in your design. Also, due to the parametric nature , you can edit these values at any time. And then have those changes propagate to any components with the respective material rule assigned to them. As a best practice, you must assign features the plastic rule prior to using subsequent such as Shell or Thicken to ensure those features in parametric herit settings and parameters from the plastic rule

6.) Utilities: In the utilities section we have the following features which are used to print and o make the different kinds of analysis like zebra anal make the 3D ysis, draft analysis, It very affective when it comes to the printing of the 3DS component etc... and to do the analysis which are used to analyse the strength of the material and the nature of the material

Selecting the Modelling software: After the selection of the project, it is very important to select the best Designing or Modelling software to execute the project. Fusion 360 is one of the famous Designing software used around worldwide, it was created by Auto Desk in the year 2013, due to its unique features, ability and the simplicity it is the first option for the designer in case of selecting the modelling software. The working complexity of this software is so good compared to the other software and the workbench contains all the necessary tools which are essential for Drafting, Modelling, for analysis and for animating the components.

Tools Used for the Project: The tools are the most important thing in designing the component the tools contains different specialities and features which are helpful to make the desired component, in this project we used the Two types of the sections, they are

I.) Solid Section. The above sections are the main tools we used for the project to design the Gyro Sphere Vehicle. These sections contain different types of the tools which played a major role in designing the project. These are further explained as, In this section we used the tools like,

i.) Create Toolbar

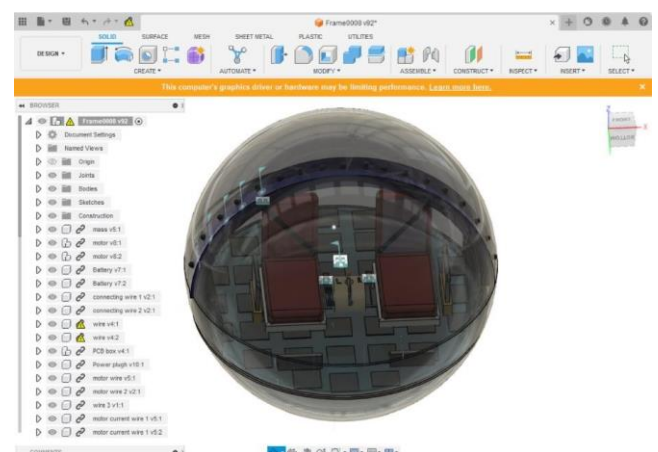
a.) Sketch. b.) Dimensions. c.) Extrude. d.) Loft. e.) Revolve. f.) Thread. g.) Hole. h.) Mirror. i.) Rectangle pattern. j.) Circular pattern.

Tool Library enables you to select existing tools from the standard Fusion 360 Library, create custom libraries, and create and copy tools and holders. With each tool, you can associate multiple Cutting Data parameters (feeds and speeds). The Sketch tools in the Edit Model contextual environment are the same tools available in the Design workspace. Sketches are typically two-dimensional entities (lines, circles, arcs, points or splines), created on a plane or existing flat face of a part.

Components Designed: Using the tool, we designed the Gyro Sphere Vehicle. There are different types of components which are assembled at one workbench to make it the whole Gyro Sphere Vehicle. The components are listed below, 1.) Hemispherical base. 2.) Spherical Hallow fibre glass cage. 3.) Motors. 4.) Wheels. 5.) PCB. 6.) Speed control rod and holder. 7.) Cover plate. 8.) Seats. 9.) Seat belts 10.) Batteries.

Material Used: The Spherical Hallow Fibre glass cage is the transparent cage which is made up of the fibre glass material. The strength of the fibre glass is 1307 KN m/Kg and the Quasi static penetration resistance of a composite structure represents the energy dissipating capacity of the structure under transverse loading without dynamic and rate effects. In this paper, a comparative study of the quasi-static penetration resistance behaviour of S-2 Glass/SC-15, S-2 Glass/HDPE and E-Glass/HDPE composite systems with varying thicknesses, i.e., 1.4–8.4-mm, is presented using the Quasi-Static Punch Shear Test (QS-PST) methodology developed earlier. The penetration resistance behaviour is usually presented by a series of force–displacement graphs at different support conditions, the integral of which is the energy dissipated by the composite during the quasi static penetration at corresponding support conditions.

Final Design of Gyro Sphere Vehicle



Final Design of the Vehicle

III. Actual Design of Vehicle

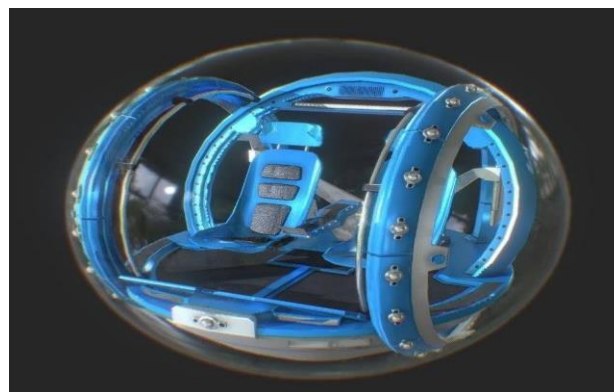
Type of Software Selected: To carry out the analysis like the load analysis and the thermal analysis we used the software called ANSYS. It is the most widely used and trust worthy software which gives the accurate readings and also contains many features which better and more efficient than other software. Due to its security of protecting the data, the process of an powerful.

About ANSYS Software: ansys is secured and ANSYS has been founded in 1970 and incorporated in 1994. Ansys predominantly offers engineering simulation software and ancillary services. The solutions provided by the company are used in a wide range of industries including aerospace, defence, automotive, biomedical and other industrial sectors. Ansys has been recognized as one of the world's most innovative companies by prestigious publications such as Bloomberg Businessweek and FORTUNE magazine for its engineering simulation software. Leveraging the power of today's Desktop, Ansys provides a common platform for product development, from design concept to final stage testing and validation. The company's product portfolio consists of platform offerings that are used in diverse multi physics simulation fields like heat transfer, fluid mechanics, statics, solid mechanics, etc. However, Ansys is best known for finite element analysis (FEA), which has gained popularity as a modelling and simulation tool over the years (and especially since the introduction of powerful computers) in solving a gamut of complex engineering problems. Ansys CAE software is popular with both academia and industry because of its multi physics capabilities, thorough institutes that provide online and in depth documentation and availability of training person Ansys courses. Since the ability to use Ansys software is a plus point, students too prefer getting certified in Ansys training

IV. Basic steps in the Finite Element Analysis:

- a) **Preprocessing phase:** create and discretize the solution domain into finite elements i.e. subdivide the real continuum into nodes and elements.
 - Assume a shape function to represent the physical behavior of an element; that is a approximate continuous function is assumed to represent the solution of an element.
 - Develop equations for all the elements in the mesh..
 - These generally take form. $[K][U] = [F]$
 - Where $[K]$ is a square matrix, known as stiffness matrix.
 - (U) is the vector of (unknown) nodal displacements or temperature.
 - $\{F\}$ is the vector of applied nodal forces
 - Assemble the elemental equations to obtain the equations of the whole problem. Construct the global stiffness matrix. Apply boundary conditions, initial conditions, and loading
- b) **Solution Phase:** Solve a set of linear or nonlinear algebraic equations simultaneously to obtain nodal results of primary degrees of freedom or unknowns, such as displacement values at different nodes in structural problem or temperature values at different nodes in heat transfer problem.
- c) **Post processing phase:**
 - Computation of any secondary unknowns or variables e.g., the gradient of the solution.
 - Interpretation of the results to check whether the solution makes sense.
 - Tabular and/or graphical presentation of the results
- b) **Solution Phase:** Solve a set of linear or nonlinear algebraic equations simultaneously to obtain nodal results of

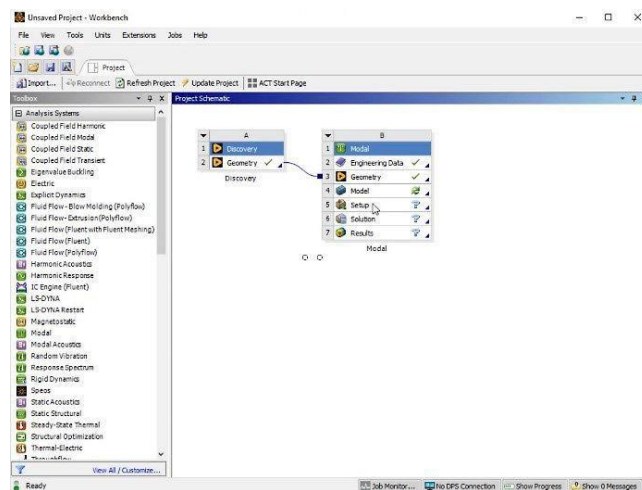
primary degrees of freedom or unknowns, such as



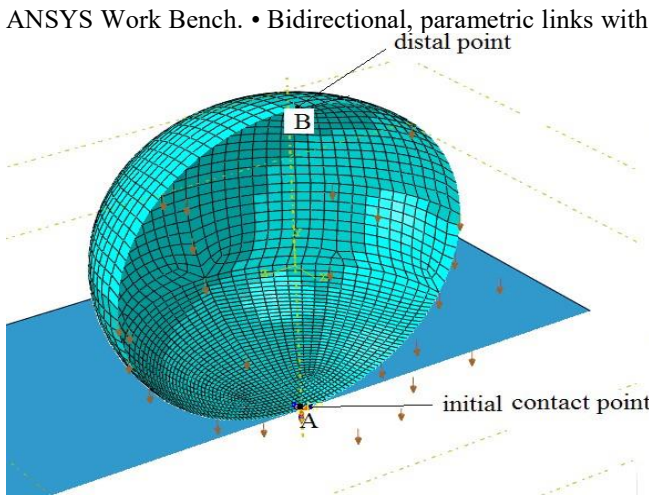
displacement values at different nodes in structural problem or temperature values at different nodes in heat transfer problem.

c) **Post processing phase:**

- Computation of any secondary unknowns or variables e.g., the gradient of the solution.
- Interpretation of the results to check whether the solution makes sense.
- Tabular and/or graphical presentation of the results the entire simulation process, guiding the user every step of the way. Even physics analysis can be performed with drag and drop simplicity. The ANSYS Workbench platform creates an automatic connection to share geometry for both the fluid and structural analyses, reducing data storage and making it easier to investigate the implications of geometry changes on both analyses. Furthermore, a link is established to automatically transfer pressure loads from the fluid to the structural analyses. The toolbox and the project Schematic are the two main parts of the ANSYS Workbench interface. The system templates in the toolbox can be used to create a project. The project Schematic is the interface section where we may manage our project. The new project schematic view provides a broad overview of the simulation project. Even for complex studies using many physics, engineering purpose, data relationships, and the status of the entire project are accessible at a glance. A navigation bar and a toolbar with frequently used functionalities will also be visible. Context menus on schematic items and cells can also be accessed by right clicking on them. Context menus allow you to add to and change your list



ANSYS Workbench Features:



all major

CAD • Integrated, analysis focused geometry modelling , systems. repair, and simplification via ANSYS Design Modeler.

- Highly-automated, physics-aware meshing.
- Automatic contact detection.
- Unequalled depth of capabilities within individual physics disciplines.
- Unparalleled breadth of simulation technologies.
 - Complete analysis systems that guide the user start-to-finish through an analysis.
 - Comprehensive multi physics simulation with drag-and-drop ease of use.
 - Flexible components enable tools to be deployed to best suit engineering intent.
 - Innovative project schematic view allows engineering intent, data relationships, and the state of the project to be comprehended at a glance. Complex project schematics can be saved for re-use.
- Pervasive, project-level parameter management across all physics.
- Automated what-if analyses with integrated design point capability.
- Adaptive architecture with scripting and journaling capabilities and API's enabling rapid integration of new and third-party solutions.

1) Static Analysis: Used to determine displacements, stresses, etc., under static loa of both linear and non ding conditions. It comprises linear static analysis. Non linearity can include plasticity, stress stiffening, large deflection, large strain, hyper elasticity, contact surfaces, and creep.

2) Modal Analysis: Used to calculate the n atural frequencies and mode shapes of a structure. Different mode extraction methods are available.

3) Harmonic Analysis: Used to determine the response of a structure to harmonically time

4) Transient Dynamic Analysis: Used to determine t he response of a structure to arbitrarily time mentioned under Static Analysis above are allowed.

5) Spectrum Analysis: varying loads. varying loads. All nonlinearity An extension of the modal analysis, used to calculate stresses and strains due to a response spectrum or a PSD input (random vibrations).

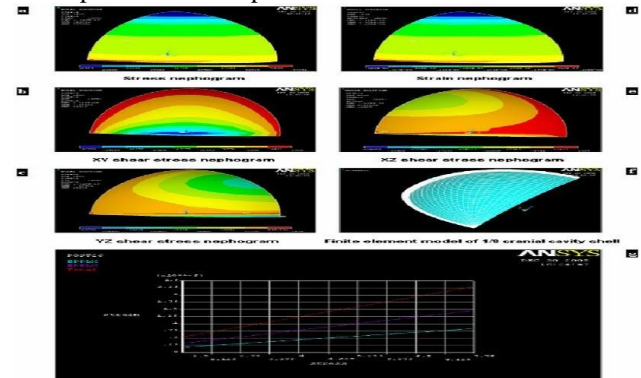
6) Buckling Analysis: Used to calculate the buckling loads and determine the buckling mode shape. Both linear (Eigen value) buckling and nonlinear buckling analyses are possible

V.ANALYSING THE STRESS DUE TO STATIC LOAD IN A HALLOW FIBRE GLASS SPHERE

INSERT. e to Static load. Then select force and click on apply. Then the force is defined by the component i.e., in which direction the force is to be applied.

FIBRE GLASS HALLOW SPHERE:

a.) and Strain Analysis: The Shear stress analysis is used to calculate the strength of the component when subjected to the impact and non impact loads.

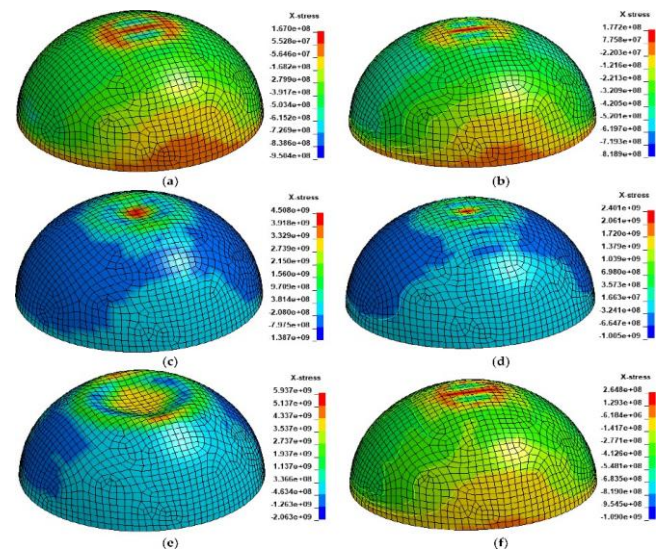


b.) Thermal Stress Analysis:

max = 53.12 N m/Kg The Thermal analysis on the Hallow sphere is done to analyse the flow of heat though the sphere when it goes through the extreme heat conditions.

Stress Analysis $\sigma_{max} = 74.32 \text{ N m/Kg}$

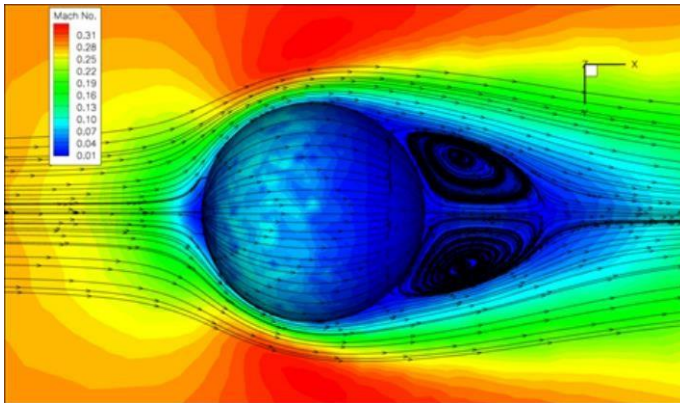
Strain Analysis $E_{max} = 53.12 \text{ N m/Kg}$



Thermal Stress Analysis on the hallow sphere shell

Thermal Stress Analysis Stress Induced=187.78 N/mm2

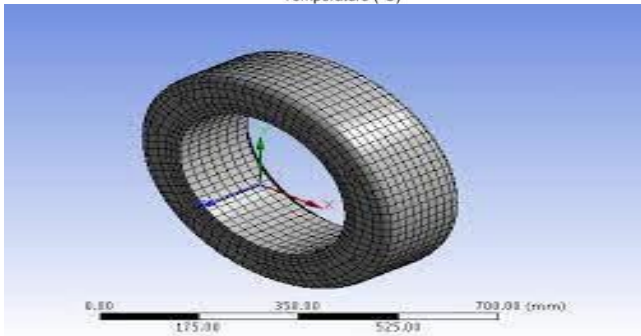
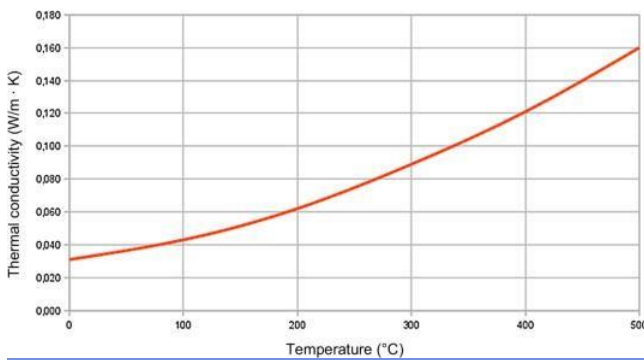
c.) **Fluid Analysis:** Induced = 187.78 N/mm² we have done the Fluid Analysis on the sphere because to observe the behaviour of the sphere when it is subjected to the heavy forceful wind during travelling.



Fluid Analysis Fluid (Air) Force= 423 m3/s

Wheels:

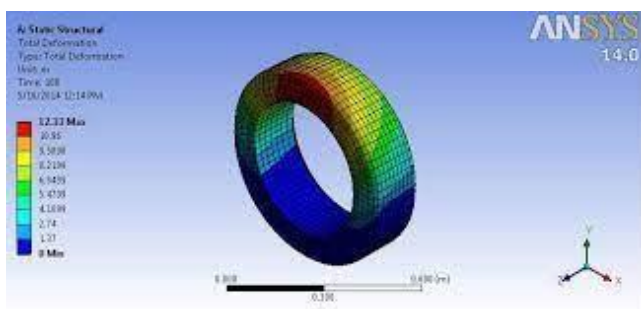
a.) **Static Analysis:** n = 2429.56 0 C The shear analysis is done on the wheels due to because if the wheels undergo to several stress and also may produce the heat.



Static analysis on the Wheels.

Static Analysis Load carrying Capacity= 615 Kg

Thermal Analysis on Wheels: The thermal analysis is done on the wheels to calculate the heat produced in the wheels during the rotating of wheels



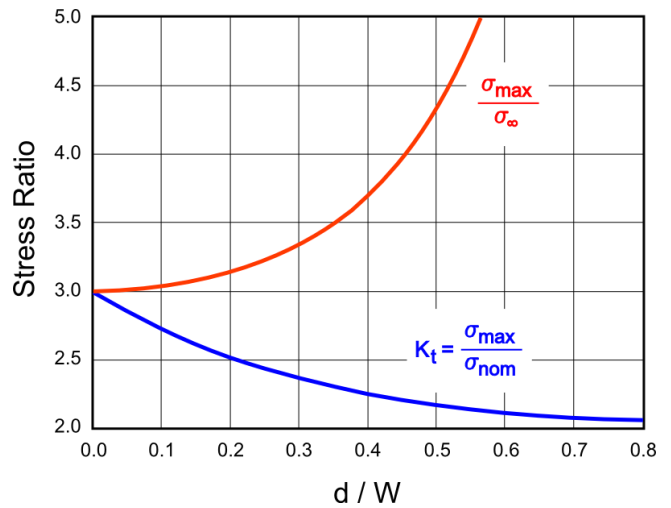
Thermal Analysis on wheels.

Thermal Analysis thermal Resistance= 221.88 0 C

Stress Concentration Calculation:

Stress Concentration in Fiber Glass: The Stress Concentration in the fiber glass can be calculated by the factor called the Stress Concentration Factor.

The, Stress Concentration Factor $\sigma_{max} = K_t \sigma_{nom}$. Where 'Kt' is the stress concentration factor. And, Therefore, $\sigma_{nom} = 1307 / (10-5) * 4$ $\sigma_{nom} = 130.7$ here, $K_t = 1$ therefore, $\sigma_{max} = 80$ N m/Kg $d/w = 2$, stress ratio (R)=3



Stress and Stress Concentration Factor Graph

Thermal Resistance of the fiber glass: The thermal resistance of the fiber glass can be obtained by the formula $T(0c) = 5/9[T(0F)-32]$

Therefore,
 $T(0C) = 5/9[1100-32]$
 $T(0C) = 600$ 0C

Thermal Resistance of the Fiber Glass

Thermal Stress for Fiber Glass

Thermal Stress: The Thermal Stress For the fiber glass can be obtained from the formula

$F/A = Y(L-L_0)$ Here

Y=Youngs modulus of the fiber glass.

Y for the fiber glass= 72 GPa.

L-L₀= $\alpha \Delta t$ α = coefficient of materials linear expansion. Therefore,

$\alpha \Delta t = 5.4 * 10^{-6}$ cm/cm/0C

The Thermal Stress for the fiber glass material is Thermal Stress = 250 N/m²

Stress Calculations on The Hemi-Spherical Metal Base:

Stress Calculation: The Stress induced on the Hemispherical Metal base due to the load acting on the metal base is:

Stress (σ) = F/A, Force (F)=250 N, Area (A) = $3.14 * 35 = 100$ mm²

Stress= $250 / 100 = 25$ N/mm²

ii.) Strain Calculations: The maximum elongation that the metallic base can endure is calculated by the formula:

Strain= $P_{max} * A$ Consider a Steel Specimen of the dimensions, Length= 30 mm, Width=10mm and thickness= 10 mm, load on the base is $P_{Max} = 10$ KN.

The maximum elongation after the tensile load is Elongation due to the tensile load= 1 mm Therefore,

Strain= $10 * 40 = 400$ MPa= $400 * 10^6$ N/mm²

iii.) Thermal Analysis Calculations on Metal Base: The thermal Analysis is carryout on this component because to analyse the strength of the component under certain hot conditions, the higher value indicates the strength and the heat resistance if the object. This can be calculated by the formula. $Q_n = hA_h(T_h - T_f)$ Where, $h =$ Convection Coefficient. $A_h =$ Surface area of the component. $T_f =$ Temperature of the surrounding fluid. $T_h =$ Temperature of the component. Here, value of $h = 25.32$, $A_h =$ Therefore, $q_n = 25.32 * 100 * (450 - 325)$ $Q_n = 2207$ OC

VI. Conclusions:

- 1.) With the help of the Design Software FUSION 360 we modelled a Vehicle named as the Gyro Sphere Vehicle.
- 2.) The Analysis was carried out in the analysis software called ANSYS.
- 3.) From the analysis we have observed that the vehicle and the parts of it are designed correctly that they can withstand all the load and other circumstances and keep the passenger safe.
- 4.) The Vehicle outer frame can bear the stress up to 74.35 N m/Kg.
- 5.) With changing different materials to model the parts we have selected the best materials like the fiber glass, steel.
- 6.) The theoretical Stress and Strain values for steel metal base 74.35 N m/Kg and $400 * 106$ N/mm².
- 7.) Hence the stress and strain caused by the loads on the steel base during analysis is 17.5 N/mm² and $150 * 106$ N/mm², so the design is safe and strong enough to bear the load caused by the people and the other components.
- 8.) The theoretical Stress concentration values for steel Fiber glass is 80 N m/Kg.
- 9.) The practical Stress concentration values for steel Fiber glass is 74.35 N m/Kg. Hence the design of Hallow Sphere Fiber glass is safe and it can withstand the impact loads which are caused during travelling.
- 10.) During the Thermal analysis the theoretical Thermal resistance value for the Fiber Glass is 600 OC and the thermal stress value for the fuber glass is 250 N/mm².
- 11.) The practical values obtained during the thermal stress and thermal resistance are 452 OC and 1897.78 N/mm², by considering the theoretical and practical values it is clear that the design is safe and perfect.
- 12.) The theoretical Thermal resistance value for the Hemispherical metal base is 2207 OC and the practical value is 2249 OC, from these values it is clear that the metal base can withstand thew higher temperature, so it can protect the inner delicate and heat sensitive components.
- 13.) The maximum heat resistance of the vehicle is $250 * 103$ N/mm²
- 14.) All the components fit into their places without errors and also the simulation process is done perfectly.

VII.FUTURE SCOPE The world is despite to invent new technology in the many fields importantly the Auto mobile field scientist's inventing a new technology every year to make the safety. models of the cars trendier and styles. These inventions also include the comfort, speed and Many people prefer safety than speed in these modern days and the automobile companies increasing the safety setup accordingly to the speed and there are more deaths that occur

due to the wild animal attacks in safaris, and people die due to the radioactive materials and the pollution so the World Health Organization (WHO) warns the world about the global warming. So, keeping an eye on this problem the Gyro Sphere Vehicle was designed to fulfil the wishes of the people and also to give safe ty to the people in the dangerous places like the wild (Jungle), Volcanic eruption areas, the radioactive places and the highly polluted areas and also it so comfortable and simple to drive

REFERENCES

- 1.) Introduction to the Gyro Sphere Vehicle : <https://www.youtube.com/watch?v=JyZwDbRiXkA>
- 2.) Detailed View: https://en.wikipedia.org/wiki/Jurassic_World:_Fallen_Kingdom
3. Review of the Vehicle: https://en.wikipedia.org/wiki/Action_film#References
- 4.) Developer of the Gyro Sphere Vehicle: <https://jurassicpark.fandom.com/wiki/Gyrosphere>
- 4.) About Fiber Glass: <https://www.phelpsgaskets.com/blog/fiberglass--types-properties-and-applications-across-industries>
- 5.) About the Motors: <https://www.nxp.com/docs/en/brochure/BBPRMMAGSYNART.pdf>
- 6.) PCB (Printed Circuit Board): <https://www.raypcb.com/motor-control-pcb/>
- 7.) Inventor: The inventor of the Gyro Sphere Vehicle is Ron Mendel and he is also the designer of the vehicle he designed the vehicle based on the that current situation, the main reason to design and fabricate the Gyro Sphere Vehicle is for the movie called the Jurassic World. Source: <https://www.youtube.com/watch?v=JyZwDbRiXkA>
- 8.) Product Designer: The Product Designer of the Gyro Sphere Vehicle Was Veeraux he is the main lead to develop and fabricate the design and also, he played a major role as the director for making this Vehicle. Source: <https://www.imdb.com/name/nm0894835/>
- 9.) Vehicle Art Designer: The art designer of the vehicle is Georg Fangeaux, he created the art called the Gyro Sphere Vehicle which was used in the movie Jurassic World for seeing the dangerous endangered species very closely in I spectacle view and it is the one of the greatest design arts that was created by him. Source: <https://www.youtube.com/watch?v=E5EigoNKkKo>

INVESTIGATION OF STRESS INTENSITY FACTORS AND J-INTEGRALS IN FRACTURE OF COMPOSITES USING FEM

Y.Ramamohan Reddy¹ and M.Venkanna Babu²

¹*Srinivasa Ramanujan Institute of Technology, Anathapuram, Andhra Pradesh*
²*Narasaraopeta Engineering College, Narasaraopet, Palnadu Dist., Andhra Pradesh*

Abstract: The need for high performance to weight ratio structures coming from the most advanced engineering fields is the main driver of the increasing usage of composite materials for critical applications. The special nature of composite materials makes it essential for the design analyst to be aware of certain types of material defects that occur during manufacture or fabrication. Fracture mechanics techniques are being applied to composite materials, primarily to determine the fracture parameters to aid in material development, selection and design. Fracture mechanics is employed to accommodate crack tip stress singularities in the assessment of defect criticality. Stress intensity factors are less well defined at interfaces than the strain energy release rate. Hence, the latter is utilized in most fracture tests and is experimentally measurable. Analysis of the strain energy release rate of a given geometry and loading is vital for the prediction of inter laminar flaw growth. Hence it is important to be familiar with the property of composite materials and their use in designing composite material structures. The objective of the present work is to analyze the behavior of composite beams and plates under different configurations of crack and loading conditions. The analysis is performed for uni axial and biaxial testing of composite beam to see the effect of loading ratio and strength of the member.

DESIGN AND FABRICATION OF ELECTRIC VEHICLE CHASSIS

D. Jagadish, K. Lakshmi Vara Prasad , A. Nagendra Babu, .M. Jesudasu, Shaik Sameer, T. Siva Reddy

Department of Mechanical Engineering, Narasaraopeta Engineering College, Narasaraopet, Palnadu (Dist.), A.P., India.

ABSTRACT: Nowadays, the world's most valuable resource is power. Hence, we must conserve power so that we can pass it on to the next generation. In electric vehicle Chassis is a major component of a vehicle system. It consists of internal framework that supports man-made object. It is the underpart of the vehicle which consists of frame and running gear like engine, transmission system, suspension system etc. The project work undertaken is design and fabrication of a Golf Cart Electric Vehicle. The chassis design of the EV is taken as the main objective. The type of chassis used for EV is ladder frame chassis. Modelling of the chassis is done through a Fusion 360 and analysis is done in Unigraphics. Chassis act as a framework for supporting various parts of a vehicle. It needs to withstand twist, shock, vibration, and other stresses caused due to acceleration, braking, road condition, and shock initiated by other parts of a vehicle. It should carry a maximum load under all operating conditions. The dimensions of the chassis were obtained from the design analysis. Later it was observed that the dimensions are in uniformity with the other parts of the Electric vehicle.

Keywords – Traction battery pack, Dc-Dc converter, electric motor, power inverter, controller, auxiliary batteries, charge port.

I. INTRODUCTION

Electric vehicles (EVs) are a promising technology for achieving a sustainable transport sector in the future, due to their very low to zero carbon emissions, low noise, high efficiency, and flexibility in grid operation and integration. The energy demand continues to rise on the back of relatively fast socioeconomic development. Growth in energy demand is predominately fulfilled by fossil fuel-based energy. The increase in greenhouse gas (GHG) and global warming resulting from extensive use of fossil fuel has now become a global phenomenon. It is estimated that CO₂ emissions from energy use continues to soar up and will increase by almost 10% by 2040. Moreover, due to resource depletion, fossil fuels are becoming more costly and their economic usefulness is diminishing. Thus, the global energy system faces a dual challenge: the need for 'more energy and less carbon'. The issues related to global energy crisis, limited availability and quality of conventional energy resources, increasing level of GHG emissions and ample potential of renewable energy.

II. PARTS OF ELECTRIC VEHICLE

A.Traction Battery Pack:



Fig.1: Traction Battery Pack

Traction applications have traditionally been jobs for Lead Acid batteries but the limitations of Lead Acid batteries, together with the high cost of alternatives, have in turn limited the range of potential battery powered traction applications. A typical family car would need a battery capacity of about 40 KWh to provide a one-way range of 200 miles and a 40 KWh Lead Acid battery weighs 1.5 tons. The situation is changing however as new battery chemistries and supporting technologies have brought with them new technical and economic benefits making battery power viable for traction applications that were previously uneconomic or impractical. In particular, the use of light weight Nickel Metal Hydride and Lithium batteries instead of the heavy and bulky Lead Acid batteries has made practical electric vehicles and hybrid electric vehicles possible for the first time.

B. DC-DC CONVERTOR

DC-to-DC converters are used in portable electronic devices such as cellular phones and laptop computers, which are supplied with power from batteries primarily. Such electronic devices often contain several sub circuits, each with its own voltage level requirement different from that supplied by the battery or an external supply (sometimes higher or lower than the supply voltage).

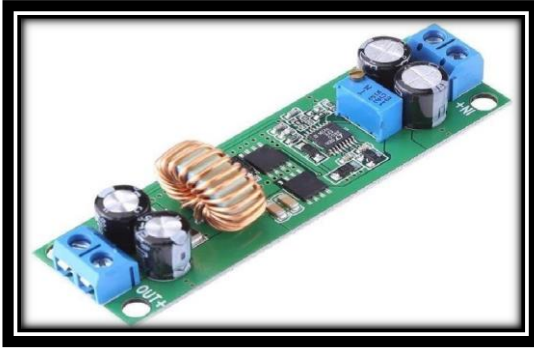


Fig.2: Dc-Dc Convertor

Additionally, the battery voltage declines as its stored energy is drained. Switched DC to DC converters offer a method to increase voltage from a partially lowered battery voltage thereby saving space instead of using multiple batteries to accomplish the same thing. Most DC-to-DC converter circuits also regulate the output voltage. Some exceptions include high-efficiency LED power sources, which are a kind of DC to DC converter that regulates the current through the LEDs, and simple charge pumps which double or triple the output voltage. DC-to-DC converters which are designed to maximize the energy harvest for photovoltaic systems and for wind turbines are called power optimizers.

C.POWER INVERTER:

A power inverter, inverter or invertor is a power electronic device or circuitry that changes direct current (DC) to alternating current (AC). The resulting AC frequency obtained depends on the particular device employed. Inverters do the opposite of rectifiers which were originally large electromechanical devices converting AC to DC. The input voltage, output voltage and frequency, and overall power handling depend on the design of the specific device or circuitry. The inverter does not produce any power; the power is provided by the DC source.



Fig.3: Power Inverter

A power inverter can be entirely electronic or may be a combination of mechanical effects (such as a rotary apparatus) and electronic circuitry. Static inverters do not use moving parts in the conversion process. Power inverters are primarily used in electrical power applications where high currents and voltages are present; circuits that perform the same function for electronic signals, which usually have very low currents and voltages, are called oscillators. Circuits that perform the opposite function, converting AC to DC, are called rectifiers. A typical power inverter device or circuit requires a stable DC power source capable of supplying enough current for the intended power demands of the system. The input voltage depends on the design and purpose of the inverter.

D.CONTROLLER:

A motor controller is a device or group of devices that can coordinate in a predetermined manner the performance of an electric motor. A motor controller might include a manual or automatic means for starting and stopping the motor, selecting forward or reverse rotation, selecting and regulating the speed, regulating or limiting the torque, and protecting against overloads and electrical faults. Motor controllers are used with both direct current and alternating current motors.

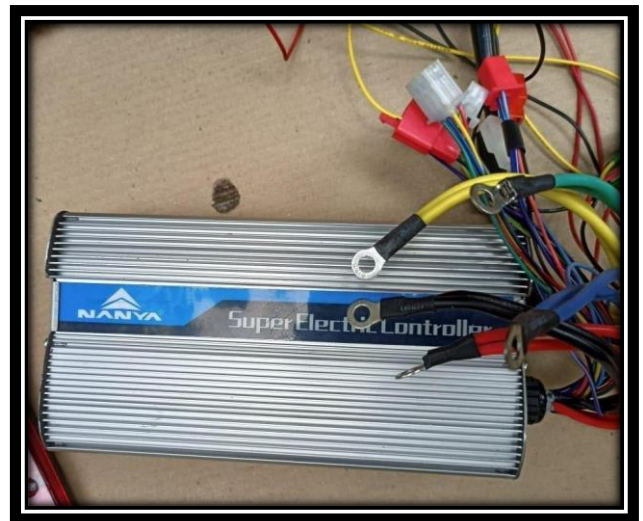


Fig:4 Controller

A controller includes means to connect the motor to the electrical power supply, and may also include overload protection for the motor, and over-current protection for the motor and wiring. A motor controller may also supervise the motor's field circuit, or detect conditions such as low supply voltage, incorrect polarity or incorrect phase sequence, or high motor temperature. Motor controllers may be manual, requiring an operator to sequence a starting switch through steps to accelerate the load, or may be fully automatic, using internal timers or current sensors to accelerate the motor.

E.AUXILIARY BATTERIES:

An electric vehicle battery (EVB, also known as a traction battery) is a rechargeable battery used to power the electric motors of a battery electric vehicle (BEV) or hybrid electric vehicle (HEV). Typically lithium-ion batteries, they are specifically designed for high electric charge (or energy) capacity. Electric vehicle batteries differ from starting, lighting, and ignition (SLI) batteries as they are 16 designed to give power over sustained periods of time and are deep cycle batteries. Batteries for electric vehicles are characterized by their relatively high power-to weight ratio, specific energy and energy density; smaller, lighter batteries are desirable because they reduce the weight of the vehicle and therefore improve its performance.



Fig: 5 Auxiliary Batteries

Compared to liquid fuels, most current battery technologies have much lower specific energy, and this often impacts the maximum all-electric range of the vehicles. The most common battery type in modern electric vehicles are lithium ion and lithium polymer, because of their high energy density compared to their weight. Other types of rechargeable batteries used in electric vehicles include lead acid ("flooded", deep-cycle, and valve regulated lead acid), nickel cadmium, nickel-metal hydride, and, less commonly, zinc-air, and sodium nickel chloride ("zebra") batteries. The amount of electricity (i.e. electric charge) stored in batteries is measured in ampere hours or in coulombs, with the total energy often measured in kilowatt-hours (kWh).

F. CHARGE PORT:

Green flash: battery not connected

Constant red light: in charge

Green light: charging field & onboard charger.

Red light flashes once and green light flashes once: battery reconnection

Red light flashes twice and green light flashes once: over temperature protection. Red light flashes three times and green light flashes once: over voltage protection.

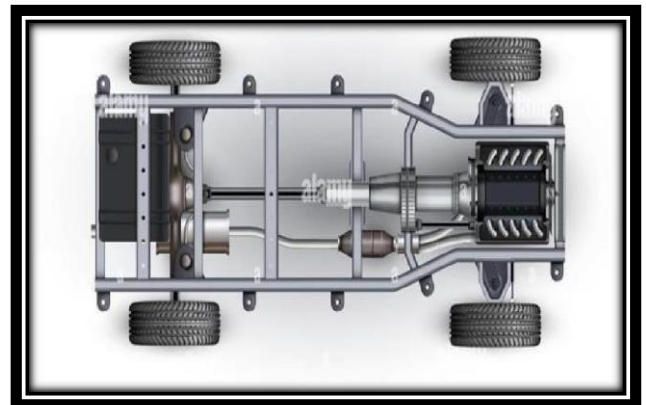
Red light flashes four times and green light flashes once: the battery voltage is too low or the battery fails.

III. CHASSIS FOR EV

Chassis is one of the important part that used in automobile industry. It is a rigid structure that forms a skeleton to hold all the major parts together. Chassis frames are made of "steel section" so that they are strong enough to withstand the load and shock. Chassis must be light in weight to reduce dead weight on the vehicles. The ladder chassis has few general standard sections which can be used in the construction. Like Channel Section, Tubular Section, Box Section.Etc. Chassis are five types are their like Ladder frame, Space frame, Torsion box, Monocoque, Combination.

Ladder Type of Chassis:

The most popular type of chassis is the ladder frame chassis. A lot of people know about this because of its heavy usage in SUVs, particularly the off roading capable SUVs. SUVs in India like the Fortuner, Endeavour, Thar, Gurkha are some of the most common large SUVs with quite impressive off roading capabilities. This is possible only because the cabin of the SUV is separated from the chassis. These chassis are generally accompanied by an All-Wheel (or 4 Wheel) Drive System. Following are the characteristics of a ladder frame chassis.



Ladder Type of Chassis

The ladder frame consists of two longitudinal beams with multiple cross members joining the beams. It is versatile as allows virtually anybody shape to be placed a top the chassis. The ladder frame chassis, as shown in fig is very durable due to its simplicity. If damage was occurred, it is much easier to repair than other types of chassis. The longitudinal beams are very stiff under bending through the use of closed section beams with a high second moment of area. While selecting the materials for the construction of automobile chassis, factors like safety and light-weight must be considered. Resources are valuable. So, materials which are chosen should be recyclable.

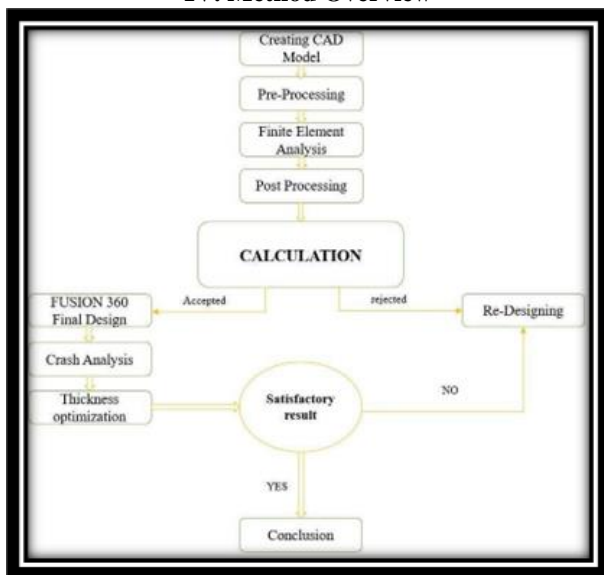
Mild Steel Materials:

The material should also absorb the impact energy by maintaining the safety of passengers. With the usage of light-weight materials in chassis, the overall weight of chassis decreases. Therefore, helps in reducing the consumption of fuel. Following materials are chosen for designing the ladder chassis in this study. Steel materials can be assigned to the automobile body, chassis, engine, and other parts also. One of the reasons in choosing steel is for its characteristic capability for absorbing impact energy during crash analysis. Hence, steel and its alloys are used in the market for the major variety of vehicles because of its material properties. Steel is a ductile material. For the construction of ladder chassis in this study, ‘A36’ steel is used. Welding and bolting can be used while joining two components of A36 steel material. Material properties of A36 steel can be seen in below Table.

Property	Values of steel (A36)
Density (tonne/mm ³)	7.8E-09
Modulus of Elasticity (MPa)	200000
Poisson’s Ratio	0.26
Yield strength (MPa)	250
Ultimate Tensile Strength (MPa)	500

Steel Properties Table

IV. Method Overview



Block Diagram Of The Ev Chassis

The method overview starts with designing a CAD model for the initial design of chassis by following the rules from design methodology. FEA is performed to this initial design to check whether it is satisfying acceptance criteria provided by ACB. If the torsional stiffness and

bending stiffness from acceptance criteria are not satisfied. Then, further design modifications are done by designing light weight cross-members. Until the design satisfies the acceptance criteria, modifications are done to chassis made by different materials to make it light-weight.

V. MODELING AND ANALYSIS

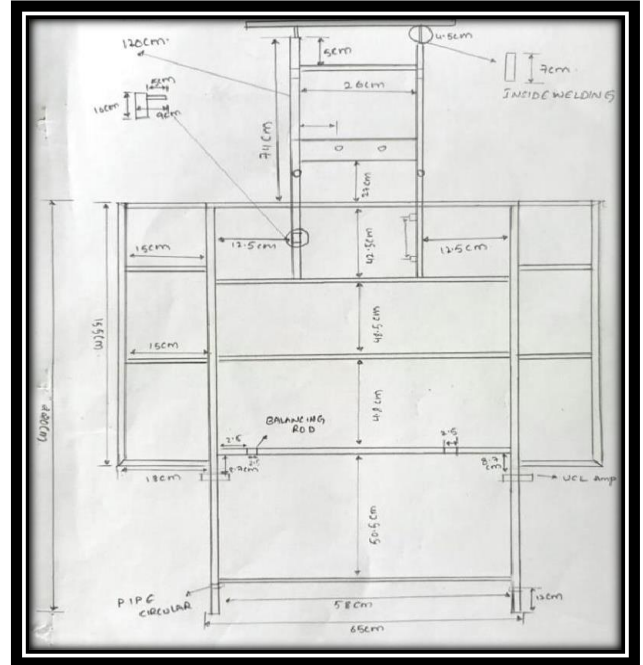


Fig: Layout of chassis

This model is designed by using Autodesk fusion 360. Fusion 360 is a commercial computer-aided design (CAD), computer-aided manufacturing (CAM), computer-aided engineering (CAE) and printed circuit board (PCB) design software application, developed by Autodesk.

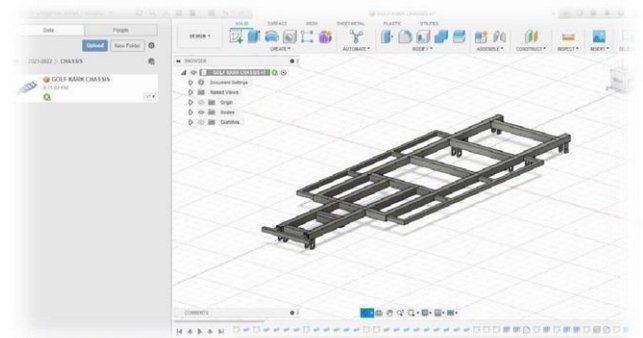


Fig: Isometric View of chassis

VI. CHASSIS FABRICATION, FITTING



The most important aspects to consider when it comes to the shape of the chassis is the strength, stiffness, ergonomics, space and the weight. Since the vehicle will be electrically driven by batteries, the allocation of space for batteries is of great importance. Since the vehicle will require a good number of batteries, it is essential that the batteries are evenly distributed over a relatively in given area. These chassis are generally accompanied by an All-Wheel (or 4 Wheel) Drive System. Following are the characteristics of a ladder frame chassis.



The ladder frame consists of two longitudinal beams with multiple cross members joining the beams. It is versatile as allows virtually anybody shape to be placed atop the chassis. Chassis Supports or bears the load of the vehicle body. Provide the space and mounting location for various aggregates of vehicle. Supports the weight of various systems of the vehicle such as engine, transmission etc. The ladder frame chassis is very durable due to its simplicity. If damage was occurred, it is much easier to repair than other types of chassis. The longitudinal beams are very stiff under bending through the use of closed section beams with high second moment of area.



Supports a load of passengers as well as the luggage. The brackets are provided in the frame to support the body also for mounting different parts such as suspension springs, engine, brake shaft etc. A typical chassis frame. Here the long sections which are located on either side are called longitudinal members. These longitudinal or side members are joined together with cross members with the help of rivets or bolts. Generally, five or six cross members are used to give good strength and stability to the chassis. Sometimes diagonal cross bracing is also provided for torsional rigidity. Body-on-frame, also known as ladder frame construction, is a common motor vehicle construction method, whereby a separate body or coach is mounted on a strong and relatively rigid vehicle frame or chassis that carries the powertrain (the engine and drivetrain) and to which the wheels and their suspension, brakes, and steering are mounted. While this was the original method of building automobiles, body-on-frame construction is now used mainly for heavy trucks, pickups, and predominantly large.

VII. ADVANTAGES

- No fuel required so you save money on gas.
- Environmental friendly as they do not emit Pollutants.
- Lower maintenance due to an efficient electric motor.
- Better performance.

VIII. APPLICATIONS

- Road ways
- Small weightage can be adopted
- industry • No emission
- Public places

IX. CONCLUSION

Electric vehicles are more efficient, and that combined with the electricity cost means that charging an electric vehicle is cheaper than filling petrol or diesel for travel requirements. Using renewable energy sources can make the use of electric vehicles more eco-friendly. Electric vehicles produce less life cycle emissions than traditional cars. Electric vehicles can be best in future because they are more energy efficient than internal combustion engines. Design the braking system of electric vehicle is carried out in this work. The vehicle is having four wheels and the brakes are provided at back two wheels. The brakes used are drum type. The length of the brake and the effort required to stop the vehicle are calculated using standard design calculations the vehicle is running at average speed of 20 mph, and the torque of the vehicle is calculated as 30 Nm. The effort of brakes is analysed and the brakes are arranged to the Electric vehicle. The brake size obtained as 32mm. Heat generated through the braking also estimated as 133 J. The values are within the range. Chassis act as a framework for supporting parts of a vehicle. It needs to withstand twist, shock, vibration, and other stresses caused due to acceleration, braking, road condition, and shock initiated by other parts of a vehicle. It should carry a maximum load under all operating conditions. The dimensions of the chassis were obtained from the design analysis. Later it was observed that the dimensions are in uniformity with the other parts of the Electric vehicle. The vehicle was run for trail purpose and observed that the chassis is fit to the vehicle weight and also as per the load carrying capacity of the vehicle.

REFERENCES

1. Assessment of Fuel Economy Technologies for Light-Duty Vehicles.”[Online]. Available: <https://www.nap.edu/read/1294/chapter/4> [Accessed: 03-Aug-2018].
2. “The Aluminium Automotive Manual.” [Online]. Available: https://www.europeanaluminium.eu/media/1543/1_aam_bodystructures.pdf [Accessed: 07-Jul2018].
3. A. E. Chambers, S. A. Rodriguez, R. M. Walsh, and D. Wootton, “Development of a Test Stand for Determining the Torsional
4. Rigidity of a Formula SAE Space Frame A36 Mild steel,” Wikipedia
5. Tomar and D. Singh, “Modelling and Analysis of a Chassis Frame by Using Carbon Fiber and E-Glass Epoxy as Composite Material: A Comparative Study.
6. Hamid, Umar Zakir Abdul (2022). "Autonomous, Connected, Electric and Shared Vehicles: Disrupting the Automotive and Mobility Sectors". Retrieved 11 November 2022.
7. Belles (2006) the early years the history of electric vehicles about.com archived from the original on 4 July 2021, retrieved 6 July 2006.
8. Asif Fazio Christopher S. Weaver; Michael P. Walsh (1996). Air Pollution from Motor Vehicles: Standards and Technologies for Controlling Emissions. World Bank Publications. p. 227. ISBN 978-0-8213-3444-7. Archived from the original on 4 July 2021. Retrieved 4 December 2017.
9. Mom, Gijs (15 February 2013). The Electric Vehicle: Technology and Expectations in the Automobile Age. JHU Press. ISBN 978-1-4214-1268-9.
10. Hamid, Umar Zakir Abdul (2022). "Autonomous, Connected, Electric and Shared Vehicles: Disrupting the Automotive and Mobility Sectors". Retrieved 11 November 2022.
11. Belles (2006) the early years the history of electric vehicles about.com archived from the original on 4 July 2021, retrieved 6 July 2006.

FINITE ELEMENT ANALYSIS OF SHEET MOULDING COMPOUND PANELS

Mr. K.Ravi Prasad, Mr. M Gangaraju, and Mr. Shaik Fahad,

Department of Mechanical Engineering, Mohan Babu University, Tirupati, India

Abstract: This panels made by SMC provide low light transmittance thus low light intensity on the inner surface of the panel thus prevents the growth of the algae, thus hygienic quality is maintained. In this work the panels of different configurations have been modeled by using Auto desk fusion 360 software as per the geometrical details and analyzed by using finite element analysis (FEA) software package ANSYS 15.0 at a specified pressure which is five times more than the actual working conditions. The panels are design with different geometrical shapes like flat, convex, and concave are arranged in different orientations as per the requirement. During the analysis the bottom panel is subjected to uniform pressure and the side panel is subjected to varying pressure. A comparison is made between panels of different configurations for normal displacements, Von-misses stresses, von-misses strains deflections are determined. Based on the results the best panel configuration is recommended for the desired applications.

Key words: Composite plate, SMC panels, Composite Design, Finite element method, Fibre length.

1. INTRODUCTION

1.1 SMC Composites:

Advanced composite materials, particularly continuous fibre-reinforced composites are currently being used in a wide variety of structural applications. These materials have now emerged as engineering materials, due to a number of attributes like low weight, high stiffens, large ultimate strength, excellent fatigue and corrosion resistance, ease in fabrication and so on. Sheet moulding compound (SMC) is a fibre composite material which contains 30% of organic ingredients and 70% of inorganic ingredients which curves by curing process by cross linking reaction. Sheet molding compound is the most commonly used composite material for manufacturing of water tanks. It is fibre reinforced material which primarily consists of inorganic ingredients.

1.2 Manufacturing of SMC materials:

SMC is usually manufactured by a highly automated continuous flow process by compression molding process. Continuous fibre glass is chopped into length of 20 to 50 mm length and deposited on a layer of resin filler paste which is travelling on a polyethylene film. Another layer of resin filler paste is deposited over the layer to form a continuous sandwich of fibre glass and resin filler. The sandwich with top and bottom covers of polyethylene is compacted and rolled in to a package sized rolls. The rolled up SMC is stored and then SMC rolls are moved to near the press and cut in to the proper charge pattern for the specific part and placed in a matched metal mold which is hot. Under the pressure of the press the system will flow to fill the complete

mould. In parallel the cutting process is started and after a short time the curved part will be remolded. This process is atomized and can be used for mass production i.e automotive industry. For series production the molds are metal dies which are heated with steam to temperature around 120 °C to reduce the curing time.

1.3 Material properties of SMC Materials:

SMC stands for Sheet Molding Compound, which is a type of composite material used in various industries. It is composed of a thermosetting resin, typically polyester or epoxy, reinforced with chopped glass fibers and other additives

All the properties of SMC material are taken from the Devi polymers Limited, Chennai; the properties are given as shown in table 1.

Table 1: SMC material properties

Sl.no	Material property	Value
1	Fibre Strength	20-50mm
2	Tensile strength	100-200gpa
3	Tensile Modulous	8-25gpa
4	Flexural Strengthth	200-600mpa
5	Impact Strength	300kj/mm ²
6	Density	1.9gm/cm ²
7	Young's modulous	10gpa
8	Possion's ratio	0.4990.449

1.4 Comparison table of the SMC material:

Table2: Water tank with other material water tanks

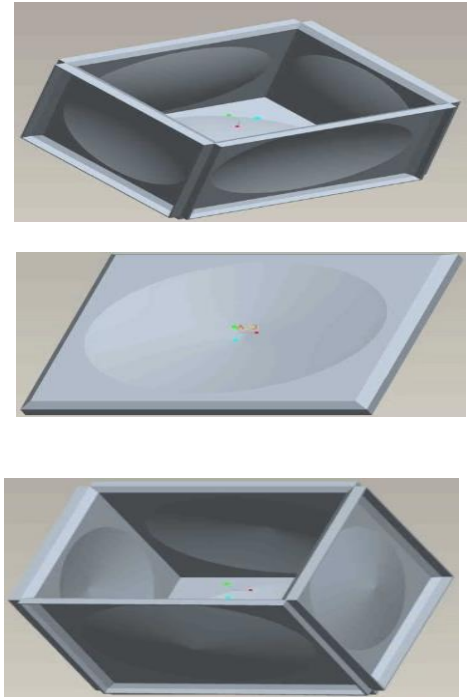
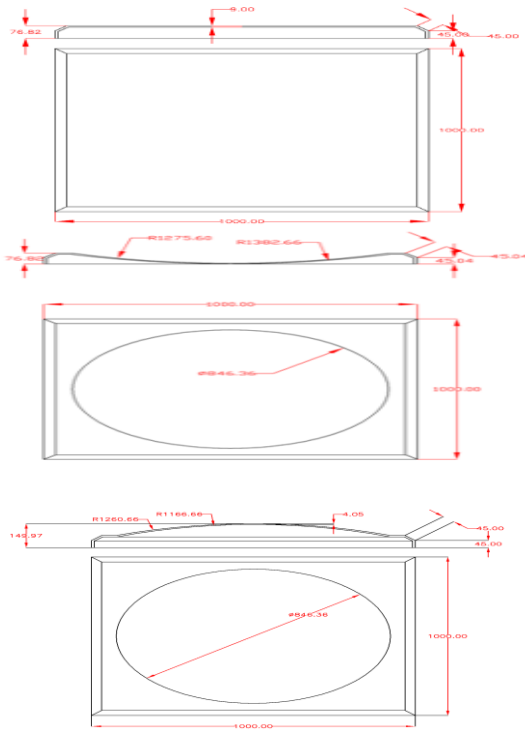
Kind of tank	Water quality	Leak Proof	durability	Transporta tion and assembly	maintenance	Adaptabil ity of design and size	Corrosion resistance
S.M.C.TANKS	⊙	⊙	⊙	⊙	⊙	⊙	⊙
CONCRETE TANKS	✦	△	△	✦	✦	△	⊙
STEEL TANKS	△	✦	△	△	✦	⊙	✦
STAINLESS STEEL TANKS	⊙	⊙	⊙	△	△	⊙	△
PVC TANKS	⊙	⊙	⊙	⊙	✦	✦	⊙

⊙ EXCELLENT ⊙ GOOD ✦ POOR △ FAIR

2. MODELING OF SMC PANELS

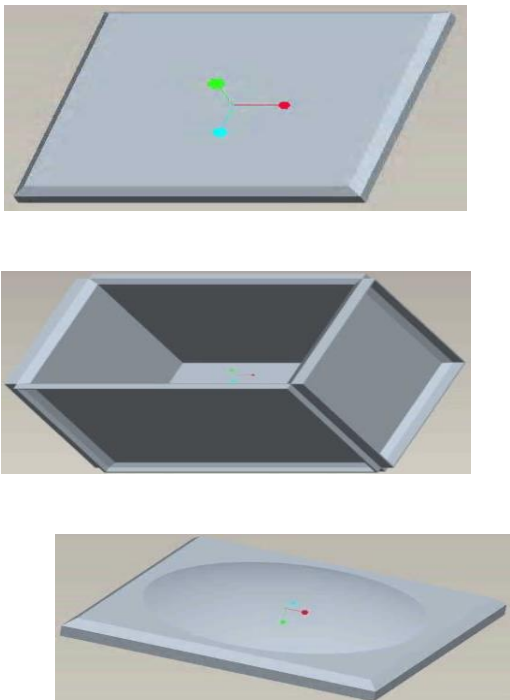
To have the realistic view of any component the solid model is essential. So the solid models of SMC water tank panels are modeled in special CAD software package like PRO/E.

The SMC water tank panels are of different configurations. We have selected the panels of three different configurations. They are a) flat panel b) Concave panel c) Convex panel. Two dimensional drawings of different configurations are given as follows.



a. Flat SMC Panel b. Concave SMC Panel
c. Convex SMC Panel

2.1 Modeled views



3. FINITE ELEMENT METHOD

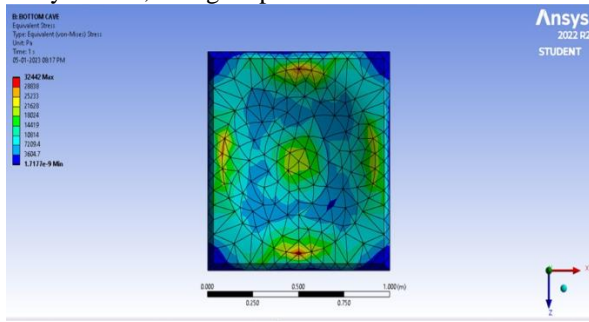
The Finite Element Method has become a powerful tool for the numerical solution of a wide range of engineering problems. With the advance in computer technology and CAD system, complex problems can be modeled with relative ease. Several alternative configurations can be tried out on a computer before the first prototype is built. All of this suggests that we need to keep pace with these developments by understanding the basic theory, modeling technique and computational aspects of the Finite Element Method. In this method of analysis, a complex region defining a continuum is discretized in to simple geometric shapes called finite Elements. The material properties and the governing relationships are considered over these elements and expressed in terms of unknown values at element corners. An assembly process, duly considering the loading and constraints, results in a set of equations.

3.1 Shell theory

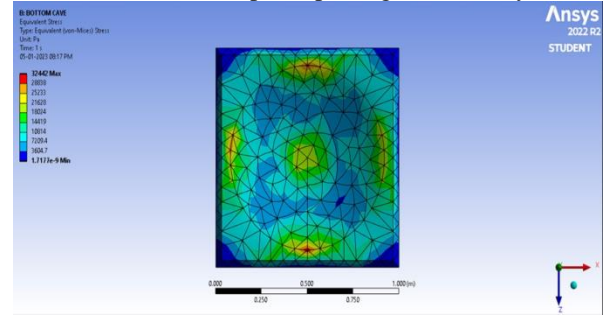
Thin shell theories are based on Love-Kirchoff assumption that as the shell deforms and the mid-surface stretches and bends the fibers of the shell initially straight and normal to the mid surface remain straight and normal to the mid-surface. Also it is usually assumed that the normal stress is zero. These assumptions permit to define the displacement of every point in terms of the displacement of the mid-surface of the shell. This in effect represent the reduction of a problem from a three dimensional to a two dimensional case. A shell may thus be thought of as the material form taken by enclosure of a volume bounded by curved surfaces. To analyze the internal forces, a small shell element is considered whose thickness is small in comparison with the other dimension of the shell and with its radii of curvature.

3.2 Overview of ANSYS

The ANSYS computer program is a large scale multipurpose finite element program which may be used for solving several classes of engineering analyses? The analysis capabilities of ANSYS include the ability to solve static and dynamic structural analyses, steady state and transient heat transfer problems, mode frequency and buckling, Eigen value problems, static or time varying magnetic analyses and various types of field and coupled field applications. The program contains main special features which allow nonlinearities or secondary effects to be include in the solution such as plasticity large strain, hyper-elasticity, creep, swelling, large deflections, contact, stress stiffening, temperature dependency, material anisotropy and radiation. ANSYS has been developed. Other capabilities ,sub structuring, sub modelling, random vibration, kineto statics, kineto dynamics, free convection, fluid analysis, acoustics, magnetic, piezoelectric, coupled field analysis and design analysis and, design optimization have been added to the

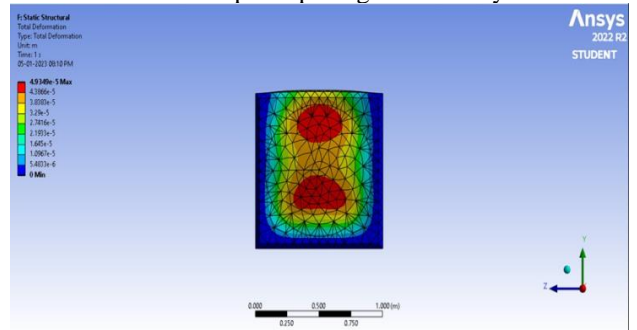


Deformation in concave panel placing horizontally



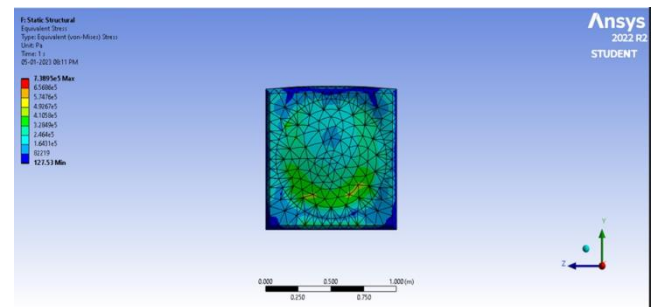
Stress in concave panel pacing horizontally

Strain in concave panel pacing horizontally



Deformation in convex panel placing vertically

program. These capabilities contribute further to making ANSYS a multipurpose analysis tool for varied engineering disciplines. The ANSYS program has been in commercial use since 1970, and has been used extensively in the aerospace, automotive, construction, electronic, energy services, manufacturing, nuclear, plastics, oil, and steel industries.

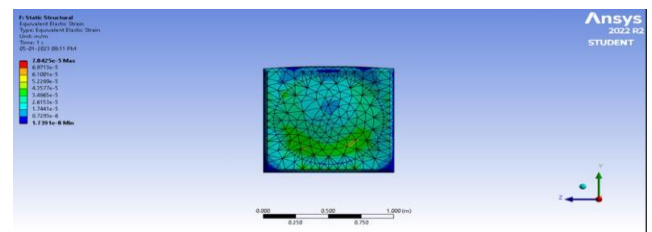


Stress in convex panel pacing vertically

4. FINITE ELEMENT ANALYSIS OF SMC PANELS OF DIFFERENT CONFIGURATIONS

Sheet Molding Compound (SMC) panels of different configurations for a water tank have been analyzed by FEA software package ANSYS 10.0 at a specified pressure of 0.04905 N/mm². The finite element idealization of the panel 1 is as shown in the figure. The side panel is subjected to simulated variable pressure and the bottom panel is subjected to simulated uniform pressure. The clamped edge conditions are simulated at the bolt hole locations. The material properties used are as follows

- Young's modulus – 10e3 N/mm²
- Poison's ration – 0.499
- Density – 1.9e-9 kg/mm³
- Element edge length – 50 mm
- Added mass per unit area – 10-3kg/mm²
- Average shell thickness – 9 mm



Strain in convex panel pacing vertically.

Results Type of the panel	Normal placement(mm)	Von misses ress(N/mm ²)	on misses strain
bottom panel	8.174×10 ⁻⁶	48276	5.11×10 ⁻⁶
Bottom side panel	3.39×10 ⁻⁴	15070000	1.67×10 ⁻⁴
oncave bottom panel	2.607×10 ⁻⁶	23244	3.31×10 ⁻⁶
concave side panel	7.02×10 ⁻⁵	788680	8.08×10 ⁻⁵
Convex bottom panel	1.8×10 ⁻⁶	9187	3.9×10 ⁻⁷
Convex side panel	4.93×10 ⁻⁶	738950	7.84×10 ⁻⁵

5. RESULTS AND DISCUSSION

For the flat panel made of SMC material:

Deformation = 8.174×10^{-6} mm

Stress = 48276 N/mm²

Strain = 5.11×10^{-6}

For the concave panel made of SMC material:

Displacement under uniform pressure = 0.04905N/mm²

Stress under uniform pressure = 23244 N/mm²

Deflection under varying pressure = 0.01635N/mm²

Strain = 3.31×10^{-6}

For the convex panel made of SMC material are:

Displacement under uniform pressure = 1.8×10^{-6} mm

Stress under uniform pressure = 0.04905N/mm²

Deflection under varying pressure = 0.01635N/mm²

These values were obtained using FEA solution package ANSYS 10.0.

Based on the calculations, the flat panel is not recommended as its Deflection values exceed the desired limit at both factor of safety 1 and factor of safety 5. On the other hand, the concave panel and convex panel both have thickness at the center that is less than 4mm, but their maximum stress values are within the actual tensile strength of the SMC material which ranges from 100-200 MPa. The values of both the concave and convex panels at factor of safety 1 and factor of safety 5 are within the desired limit, making them recommendable.

6. CONCLUSION

Sheet molding compounds (SMC) are composite materials that consist of a thermoset resin, usually polyester or vinyl ester, reinforced with glass fibers. SMC panels can be made in a variety of shapes, including flat, concave, and convex, and they are widely used in the automotive, construction, and aerospace industries, among others. Stress and strain are two important parameters used to describe the Deflection behavior of SMC panels. Stress is defined as the force per unit area applied to a material, while strain is the resulting Deflection of the material relative to its initial dimensions. The relationship between stress and strain is characterized by a material property known as the modulus of elasticity, or Young's modulus.

In SMC panels, the Deflection behavior will depend on the shape of the panel, the orientation of the fibers, the resin content, and the curing conditions. Flat panels will typically experience less Deflection than curved panels, due to the absence of curvature-induced stresses. Concave panels will tend to bulge outwards under load, while convex panels will tend to buckle inward. The Deflection behavior of SMC panels can be predicted using finite element analysis (FEA) software, which allows engineers to simulate the behavior of the panel under different loading conditions. FEA can also be used to optimize the design of SMC panels to minimize Deflection and improve their mechanical properties. The Deflection behavior of SMC panels depends on the shape of the panel, the orientation of the fibers, and the curing conditions. Stress and strain are important parameters used to describe the Deflection behavior of SMC panels, and finite element analysis can be used to predict their behavior under different loading conditions.

7. SCOPE OF THE WORK

There are still many areas on which we can extend our analyses work on different configurations of SMC panels based on day to day requirement. As the SMC material has got its applications in the field of automobile industry, which are traveling with high speeds, the air resistance on the body and other parts of the automobile may cause to temperature. So the thermal analysis of the composite structure should also be carried out and the thermal distribution can be analyzed for the thermal stability and safety. Depending on the fiber length from 20 to 50 mm length, the properties of SMC material varies, so we can apt different fiber lengths and checks the results and compare them. Depending on the fiber orientation i.e., Random fibers and continuous fibers, the properties of SMC material varies, so we can apt different orientation fibers and compare the results. Depending on the type of fiber i.e., longitudinal fiber, transverse fibers, the properties of SMC material varies, so consider different type of fibers and apply the load and compare the results among them. Not only above still, we can extend our analyses work by comparing the results obtained manually using displacement matrices, stiffness matrices, strain transformation matrices with the values obtained using FEA solution package.

8. REFERENCES

1. C.S. Krishna Murthy, Finite element Analysis, Tata Mc Graph Hill Ltd. New Delhi 1986.
2. Martin Fisk, Damage level calculation in SMC composite structures, master's thesis, Lulea University of Technology, Gothenburg, Sweden, 2006
3. Jones, R. M., Mechanics of Composite Materials, McGraw Hill, 1975.
4. Lagace, P. A., Jensen, D. W., and Finch, D. C., "Buckling of Unsymmetric Composite Laminates," Composite Structures, Vol. 5, 1986, pp. 101-123.
5. Ashton, J.E., J.C. Halpin and P.H. Petit, Primer on Composite Materials: Analysis, Technomic Press, Westport, CT, 1969.
6. Noor, A. et al. (eds.) (1989), \Analytical and Computational Models of Shells", ASME Special Publication, CED-3.
7. Bathe, K.J. and Dvorkin, E. (1986), \A Formulation of General Shell Elements | the Use of Mixed Interpolation of Tensorial Components", International Journal for Numerical Methods in Engineering, 22, pp. 697-722.
8. Koiter, W.T. (1959), A Consistent First Approximation in General Theory of Thin Elastic Shells", In Proc. IUTAM Symposium on the Theory of Thin Elastic Shells, Delft, pp. 12-33.
9. R. F. Gibson, Principles of Composite Material Mechanics, McGraw-Hill, New York, 1994.
10. Z. Vnučec, Engineering Properties and Applications of the Laminated Composite Materials, RIM'99 – Revitalization and Modernization of Production, Proceedings, pp 71- 78,

DESIGN AND FABRICATION OF MINI CNC DRILLING MACHINE

M.Balaji Naiak and B.Anand Kumar

Department of Mechanical engineering, University College of Engineering Narasaraopet, Palnadu Dist. Andhra Pradesh, India

Abstract: The development of small-scale industry has increased the demand of small-scale CNC machines since the implementation of machine in production of small-scale product shown a profitable economic value. The use of machines in the fabrication of small part has been proven to increase product production efficiency as well as reduce product costs. This is able to increase the business profits of small companies and push the business development to a higher level.

The main purpose of this project is to discuss the development of 3-axis CNC machines using integration between microcontroller as main controller and spindle drill. The main application of this built machine is to cut and carve low-hard materials such as wood. The design product to be fabricate is sent to the micro controller through a serial communication system. The microcontroller will control the movement of the spindle drill according to the point coordinates to perform the desired cutting according to the desired design. Three tests to determine the quality of product production are carry out. The results of tests carried out on the products produced by the 3-axis CNC machine.

I.INTRODUCTION

CNC stands for Computer Numerical Control and typically refers to a machine whose operation is controlled by a computer. It also is a specialized and versatile form of a Soft Automation, and its applications cover many kinds, although it was initially developed to control the motion and operation of machine tools. A CNC machine takes codes from a computer and converts the code using software into electrical signals. The signals from the computer are then used to control motors. Since the motors can turn very small amounts the machine is able to move in highly precise movements repeatedly. There are many types of CNC machine. The common CNC machines are two-axis and three-axis CNC machine. The two- axis machine can move on vertical and horizontal only which are X and Y axis. Three-axis machine can do movement starting with three primary axis which are X, Y and Z axis. The Z axis is being parallel with the spindle. By controlling a CNC machine through a PC, it is possible for the user to design a product on-screen, convert it to CNC-readable code and then send that data to CNC machine for it to produce a physical copy of the item designed. Mini CNC machine is described as it is based on Arduino controller and CNC shield. CNC is computer numerical control machine. G codes are preparatory Function. G codes are pre-define Function Associated with the movement on machine axes. In CNC Machine only G codes are used. G codes are giving the Direction to move the drill bit in X, Y and Z directions. The aim of over is to make a mini-CNC machine which is capable to draw difficult design in paper or surface of metal, to cut it with a great accuracy. We have used stepper motors with lead screw in Cartesian coordinate X, Y directions. Stepper motor is converting digital pulse into lead screw rotations. Stepper drivers are used to give command to the system. The main aim is to fabricate a

Mini CNC Machine to drill an object with using G codes. We also work on to reduced cost of the project and increase Reliability and Flexibility. This will be used for soft material cutting or machining We have reduced the cost, in the setup of mini-CNC machine (Computer Numerical Control).metal, to cut it with a great accuracy. We have used stepper motors with lead screw in Cartesian coordinate X, Y directions. Stepper motor is converting digital pulse into lead screw rotations. Stepper drivers are used to give command to the system. The main aim is to fabricate a Mini CNC Machine to drill an object with using G codes. We also work on to reduced cost of the project and increase Reliability and Flexibility. This will be used for soft material cutting or machining We have reduced the cost, in the setup of mini-CNC machine (Computer Numerical Control).



Figure 1. CNC MACHINE

Takes digitized data, a computer and CAM program is used to control, automate, and monitor the movements of a machine. The machine can be a milling machine, lathe, welder, and grinder, and laser, sheet metal stamping machine, robot, or two many other types of machines. For larger industrial machines, the computer is generally an on-board dedicated controller. But for more hobbyist types of machines, or with some retrofits, the computer can be an external PC. The CNC controller works together with a series of motors and drive components to move and control the machine axes, executing the programmed motions. On the industrial machines there is usually a sophisticated feedback system that constantly monitors and adjusts the cutter's speed and position.

CAM – Computer Aided Machining or Manufacturing – Refers to the use of various software packages to create toolpaths and NC code to run a Uncontrolled machine, based on 2D or 3D computer model. CAM does not actually run the CNC machine but just creates code for it to

follow. NC code –A special relatively simple computer language that a CNC machine can understand and execute. These languages were originally developed to program parts directly at the machine keyboard without the aid of a CAM program. They tell the machine what moves to execute, one by one, as well as controlling other machine functions such as spindle and feed speeds, coolant. The most common language is G-codes, a simple alphanumeric programming language developed for the earliest CNC machines in the 70s.

II. History

The early history of CNC machining is almost as complex as a modern CNC system. The earliest version of computer numerical control (CNC) technology was developed shortly after World War II as a reliable, repeatable way to manufacture more accurate and complex parts for the aircraft industry. Numerical control—the precursor to CNC was developed by John Parsons as a method of producing integrally stiffened aircraft skins. Parsons, while working at his father's Traverse City, Michigan-based Parsons Corp., had previously collaborated on the development of a system for producing helicopter rotor blade templates. Using an IBM 602. A multiplier to calculate air foil coordinates, and inputting this data to a Swiss jig borer, it was possible to produce templates from data on punched cards. Parsons' work led to numerous Air Force research projects at the Massachusetts Institute of Technology (MIT) starting in 1949. Following extensive research and development, an experimental milling machine was constructed at MIT's Servomechanisms Laboratory.

A 28-inch Cincinnati Hydro-Tel vertical-spindle contour milling machine formed the base of the experimental system. Extensive modifications were made, including the removal of all table, cross-slide, and head drives and controls, and the installation of three variable-speed hydraulic transmissions, which were connected to leadscrews.

Through gearing and lead screw, each transmission could produce a 0.0005 motion of the table, head, or cross-slide for each electrical pulse it received from the director. To ensure that this experimental machine was functioning as directed, a feedback system was added. Synchronous motors geared to each motion generated voltage in response to movement. This voltage was sent back to the detector for comparison to the original command voltage. By 1953, enough data had been collected through application studies to indicate the practical possibilities of the nascent technology. However, a different, less accurate, experimental NC machine also developed at MIT—one that utilized a Flex writer, eight column paper tape, a tape reader, and vacuum-tube. Electronic control systems became the true prototype for the future of CNC. Though the early CNC systems developed by Parsons, MIT, et al, were rudimentary by today's standards, they do share much in common with modern CNC equipment. All automated motion control machines, from that first modified Hydro-Tel to CMSNA's state-of-the-art Cronus moving bridge,

requires a command function, a drive/motion system, and a feedback system.



Figure 2. NC machine

ACNC machine 'command function could be anything from a simple cam follower to a fully digital interface. The motion/drive system could consist of an electric or hydraulic motor, a clutch, a cylinder, a brake, a valve, or any combination of these any sort of device that makes something move. The synchronous motor feedback system described above has been replaced with digital encoders and other similar technological advances. In 1968, John Parsons was the recipient of the Numerical Control Society's inaugural Joseph Marie Jacquard Memorial Award. In 1975, Parsons was honored as The Father of the Second Industrial Revolution by the Society of Manufacturing Engineers. In University Malaysia Pahang (UMP), especially at laboratory in manufacturing engineering faculty, there are a lot of machines can use CNC two axis programs for examples drilling machine and cutting machine, but those machines not yet using the technology. So that, staff and students have to do it manually, like marking and do some calculation. It will easily the lecturers, staff and student works by added programs into the machine. With the implement of CNC many people can shorten their task and works. For the improvements purpose, the machine must be added with CNC programs and converts the physical machine a little bit.

III. LITERATURE REVIEW

At this stage, the understanding of the machine's concept is needed. The basic of the project is very important. To understand the concept of the project, the research on the past journals, books, articles, and the experiment of the area of machine development. The resource is collect from the books which are CNC Machines by B. S. Pabla, M. Adithan, Programming of CNC Machines: Student Workbook by Ken Evans, CNC Programming: Principles and Applications by Micheal W. Mattson, Mike Mattson and Build Your Own CNC Machine by Patrick Hood-Daniel, James Floyd Kelly. The other resources are from journal and articles which are about the Mini CNC Machine. For example, A CNC Machining System for Education by A.A. Tseng, S.P. Kolluri and P. Radhakrishna, Computer Numerical Control by Dr. Aseel A. AlHamdany, and Evaluation of Performance Criteria of CNC Machine Tool Drive System by Venkatram Ramachandran.[1]

The importance of manufacturing and having skilled manufacturers in the United States industry has been apparent since the industrial revolution in the 1800's. The economic change that took place when production went from skilled craftsman to machines and factories has helped make the U.S. the superpower nation it is today. Since the modern industrial revolution took place in 1973 all areas of industry from technologies, politics, and the economy have all been influenced and changed dramatically (Scott, 2008; U.S. Department of Labor, Bureau of Labor Statistics, 2008). The skill of the manufacturing industry is to create a quality part that meets the consumer's specifications for the least amount of money. The progression and advances in manufacturing continue to decrease the cost of production and further decrease the overall cost of goods which, in turn, affects the national economy. Today the U.S. faces the difficult issue of overseas outsourcing manufacturing jobs to countries like China, Thailand, and Japan to save on production costs. Although this outsourcing may be useful in the short term and temporarily boost bottom line profit, the recent disaster in Japan shows us how dangerous outside reliance can be (Scott, 2008). United States companies are constantly looking for skilled manufacturing engineers and machine specialists to increase their productivity and lower machining costs.[2] For several years, rigorous research has been conducted in the area of CNC machine from diverse perspectives (Raksin and parnichkun, 2004; Siller et al., 2006; Omiru and Nearchou, 2009; Rahnama et al., 2009). Some investigators seem to contribute to the expansion of the frontier of CNC machine knowledge by focusing on system performance improvement tools such as sensors (Ertekin et al., 2003), neural and adaptive networks as well as fuzzy controllers (Chen and Jen 2000; Liang et al., 2002 Uros et al., 2009; Zuper et al., 2011; Kim and Jeon, 2011). Others applied optimization techniques to achieve their goals in CNC machine research (Ghani et al., 2004; Yang et al., 2009). Still, others have focused on different aspects such as hardenability (EL- 6 bestawi et al., 1997), nano surface generation (Cheng et al., 2008), new material study (Sharman et al., 2001), free from surface studies, thus the paragraphs follow contains a comprehensive review of existing studies in the literature in its disive modes, covering the various contributions of the authors till date. Mini CNC Machine is the small CNC Machine that can operate same likes another CNC machine. This machine is designed for the specific dimension. The CNC machines can be divided into two groups, which are turning machines and milling machine. A turning machine is generally made up of a device that spins a workpiece at high speed and the tool is moved back and forth and in and out until the desired shape is achieved. A milling machine is a machine that has spindle which is same as the router, with a special tool that spins and cuts in various directions and moves in two directions along the X, Y-axis. (Patrick Hood-Daniel, 2009) A CNC machine with several unique features, such as simplicity and reliability, was developed for studying computerized numerical control and its associated software. The machine is especially useful for educational and research purposes, and it is easy to integrate with other manufacturing systems. It can also be used to introduce the CNC aspect of CAM systems without involving too many complexities that are present in commercial systems.[3].

An important advance in the philosophy of NC machine tools was the shift toward the use of computers instead of proprietary controller units in the NC system of the early 1970s. This gave rise to the computer numerical control (CNC). CNC is a self-contained NC system for a single machine tool including a dedicated minicomputer controlled by stored instructions to perform some or all the basic NC functions. It has become widely used for manufacturing systems mainly because of its flexibility and less expensive. Computer Aided Manufacturing (CAM) software can be used to generate this part program. The service program is used to check, edit, and 12 correct the part program. It usually has a user interface that allows the user to operate the machine easily. The control program accepts the part program as input data and produces signals to drive the axes of motion. It performs interpolation, feed rate control, acceleration and deceleration, and position counters showing the current axes position. Most closed-loop CNC systems include both velocity and position control loops. The velocity feedback is usually provided by a tachometer and the position feedback is usually provided by an encoder or resolver. CNC software can also retrieve velocity feedback from encoder by differentiating the input signal. The computer output in CNC systems can be transmitted either as a sequence of reference pulses or as a binary word. If the reference pulse sequence is generated, each pulse generates a motion of 1 of axis travel. The number of pulses represents position, and the pulse frequency represents axis velocity. In an open-loop system, these pulses are the control signal of a stepper motor. In a closed-loop system, these pulses can be fed as a reference signal [4]

IV. NUMARICAL CONTROL MACHINE

Numerical Control (NC) refers to the method of controlling the manufacturing operation by means of directly inserted coded numerical instructions into the machine tool. It is important to realize that NC is not a machining method, rather, it is a concept of machine control. Although the most popular applications of NC are in machining, NC can be applied to many other operations, including welding, sheet metalworking, riveting, etc.

The major advantages of NC over conventional methods of machine control are as follows:

1. Higher precision
 2. Machining of complex three-dimensional shapes
 3. Better quality
 4. Higher productivity
 5. Multi-operational machining
 6. Low operator qualification
- Basic components of NC machine

An operational numerical control system consists of the following three basic components:

1. Program of instructions
2. Controller unit, also called a machine control unit (MCU)
3. Machine tool or other controlled process

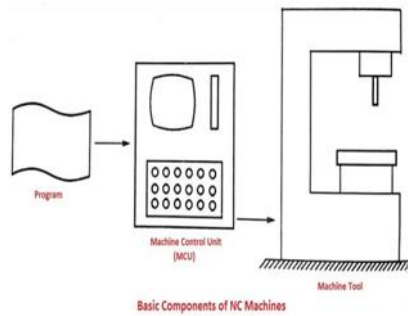


Figure 3. Basic components of NC machine
NC Procedure

To utilize numerical control in manufacturing, the following steps must be accomplished.

1. Process planning.

The engineering drawing of the work part must be interpreted in terms of the manufacturing processes to be used. This step is referred to as process planning and it is concerned with the preparation of a route sheet. The route sheet is a listing of the sequence of operations which must be performed on the work part. It is called a route sheet because it also lists the machines through which the part must be routed to accomplish the sequence of operations.

2. Part programming.

A part programmer plans the process for the portions of the job to be accomplished by NC. Part programmers are knowledgeable about the machining process, and they have been trained to program for numerical control. They are responsible for planning the sequence of machining steps to be performed by NC and to document these in a special format. There are two ways to program for NC:

- Manual part programming.
- Computer-assisted part programming

In manual part programming, the machining instructions are prepared on a form called a part program manuscript. The manuscript is a listing of the relative cutter/workpiece positions which must be followed to machine the part. In computer-assisted part programming, much of the tedious computational work required in manual part programming is transferred to the computer. This is especially appropriate for complex workpiece geometries and jobs with many machining steps.

3. Tape preparation.

A punched tape is prepared from the part programmer's NC process plan. In manual part programming, the punched tape is prepared directly from the part program manuscript on a typewriter like device equipped with tape punching capability. In computer-assisted part programming, the computer interprets the list of part programming instructions, performs the necessary calculations to convert this into a detailed set of machine tool motion commands,

and then controls a tape punch device to prepare the tape for the specific NC machine.

V. APPLICATIONS OF NUMERICAL CONTROL:

Numerical control systems are widely used in industry today, especially in the metalworking industry. By far the most common application of NC is for metal cutting machine tools. Within this category, numerically controlled equipment has been built to perform virtually the entire range of material removal processes, including:

- Milling
- Drilling and related processes
- Boring
- Turning
- Grinding

METODOLOGY

BLOCK DIAGRAM DISCRPTION



Figure 4. Block diagram

We have supplied the current in Arduino with USB DATA cable to transfer Data from Computer to Arduino Board, here we have used 2 Stepper Drivers to supply the G codes in Sequence to the stepper motors. Arduino will be mounted on PCB board. L293D will distribute the Current in the command of Arduino to the stepper motor to move to obtain the desire results. In X direction stepper motor will move left and right, Y direction stepper motor will move in front and back direction. Servo motor makes the pen moves up and down to plot the desire sketch. We can make many difficult designs via using this machine. The accuracy of this machines results is very high. So, we can use this machine in industry to reduce the cost of design printing and maintain accuracy level.

COMPONENTS USED IN CNC MACHINE:

ARDUINO UNO

Arduino UNO overview:

The Arduino UNO is a small, complete, and bread board-friendly board based on the ATMEGA328P which offers control of stepper and servo motors through motor drivers. It lacks only a DC power jack and works with a mini-B USB cable instead of a standard one. Arduino Nano is a surface mount breadboard embedded version with integrated USB. It is a smallest, complete, and breadboard friendly. Physically, it is missing power jack. The Nano is automatically sense and switch to the higher potential source of power, there is no need for the power select jumper. Nano's got the breadboard-ability of the Boarding and the Mini+USB with smaller footprint than either, so users have more breadboard space. It's got a pin layout that

works well with the Mini or the Basic Stamp (TX, RX, ATN, and GND on one top, power and ground on the other). This new version 3.0 comes with ATMEGA328 which offer more programming and data memory space. It is two layers. That make it easier to hack and more affordable.



Figure 5. Arduino UNO

VI. SOFTWARES USED

ARDUINO IDE

The Arduino IDE Is a cross-platform application written in java and is derived from the IDE for the processing programming language. It is designed to introduce programming to artists and other newcomers unfamiliar with software development. It includes a code editor with features such as syntax high lighting, brace matching, and automatic identification .and is also capable of compiling and uploading programs to the board with a single click. There is typically no need to edit make files or run programs on a command-line interface. The Arduino IDE comes with a C/C++ library, which makes many common input/output operation much easier. Arduino programs are written in C/C++, although users only need define two functions to make a run able program.

- Setup ()-a function run once at the start of a program that can initialize settings.
- Loop ()-a function called repeatedly until the board powers off.

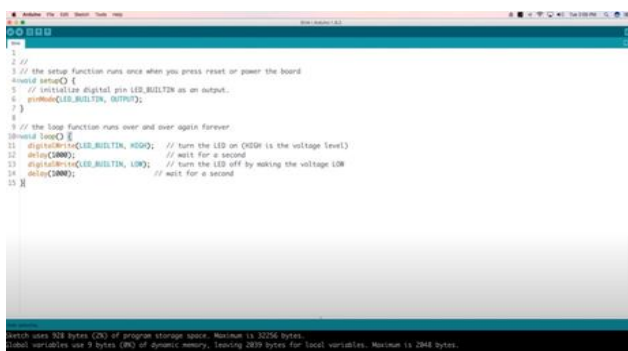


Figure 6. Arduino IDE Interface

Solid Edge

Solid Edge isa3D CAD, parametric feature and synchronous technology solid modelling software. It runs on Microsoft Windows and provides solid modelling,

Assembly modelling and 2D orthographic view functionality for mechanical designers. Through third party applications it has links to many other Product Lifecycle Management (PLM) technologies.

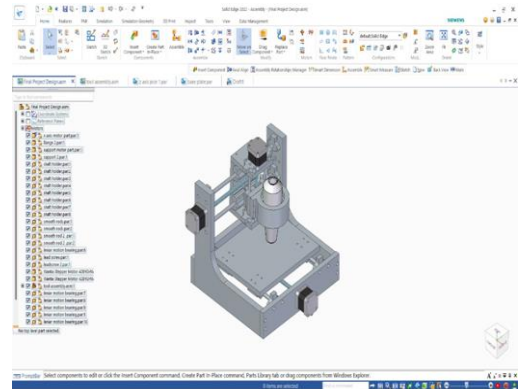


Figure 7. Solid Edge Design

WORKING AND CONSTRUCTION OF MINI CNC MACHINE STEP WISE

STEP 1: Connect Arduino with CNC shield and L293D motor driver with correct pin to pin.

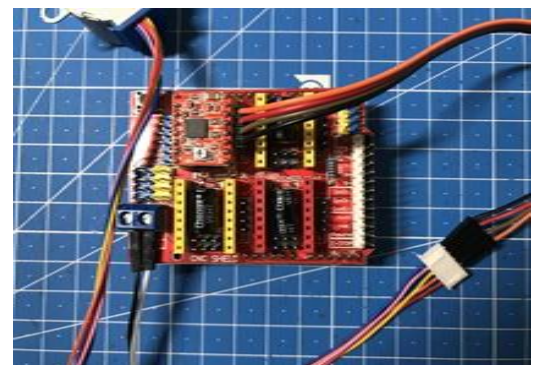


Figure 8. CNC shield with Arduino

STEP 2: Design a model with a solid edge and arrange the required components for hardware work. Take a piece of wood and prepare a base for the work, and the next step is to make an x, y, and z axis by using plywood, smooth rods, leadscrews, motors, shaft couplings, shaft holders, linear bearings, and flange bearings.



Figure 9. Hardware work

STEP 3: Now connect Stepper motor (x, y and z axis) to CNC shield and given power supply SMPE 12v and 10amps.

STEP 4: Open the Arduino ide software select port and Arduino bord.

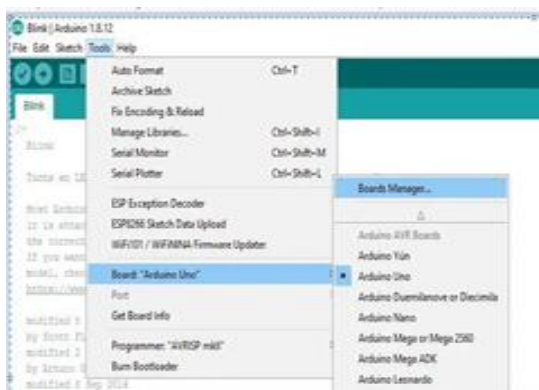


Figure 10. Selecting board and port in Arduino ide

STEP 5: Compile the code and upload GRBL into Arduino Uno.



Figure 11. GRBL uploading into Arduino ide

STEP 6: Open Fusion 360 software, design and manufacture the work piece and generate the G code and M codes of the workpiece.

G codes of the workpiece
(T1 D=3 CR=0 TAPER=118deg - ZMIN=-3 - drill)

G90 G94

G17
G21
G90
(Drill1)
T1
S1000 M3
G0 X60 Y40
Z5
Z0
G1 Z-3 F100
G0 Z5
G90
G28 G91 X0 Y0
G90
M5
M30

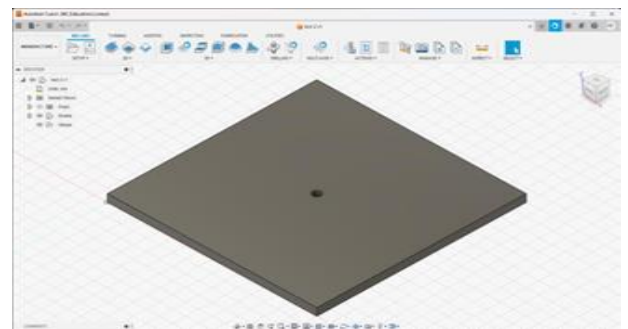


Figure 12. Workpiece model in fusion 360 software

STEP 7: Open the GRBL controller software, upload a G-code file, give the power supply to the Arduino board through a cable, and also give the power supply to the SMPE, place the work piece on the table, turn on the spindle, and perform a work.

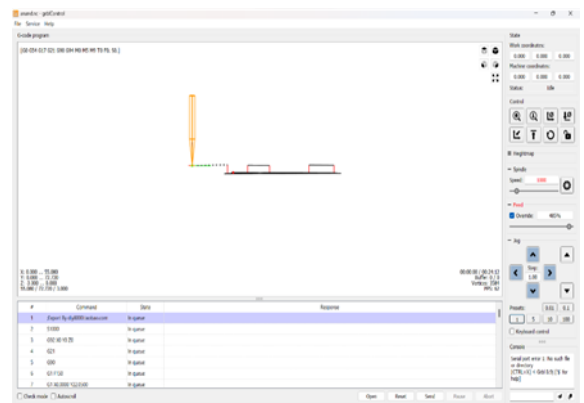


Figure 13. Uploading a file into GRBL controller.

VII. RESULT AND DISCUSSION

CALIBRATION OF THE MACHINE

After finishing the complete build-up of the machine, it is necessary to calibrate the movement of the axes. Test code for stepper motor is used where steps per revolution is 23 steps were allowed for the motor to move. On running the code, it is found that the motor is travelling 200 mm

which is indicating that the stepper motor takes 1 step to cover 10mm. This is calibration for both X and Y axes. And Z axis is 1 step to cover 5mm

DISCUSSION

After the testing and calibration, a machine was ready to operate. The machine is implemented and manufactured as planned, therefore it can drill, this CNC machine starts to collect data from programming that is derived from computer aided design (CAD) and computer aided manufacturing (CAM). The programs produce the computer file and will then extract the command to run the device. The program will be transferred via Arduino and then loaded into the CNC machine to start machining. After calibration and testing, the machine was fully functional ready to work.

WORKPIECE FILE: A file has been designed with Fusion 360 software and sent to the machine for drilling.

G codes and M codes

G90 G94

G17

G21

G90

(Drill1)

T1

S1000 M3

G54

G0 X33 Y38

Z3

Z2

G1 Z-5 F150

G0 Z3

X20 Y30

Z2

G1 Z-5 F150

G0 Z3

M5

M30

VIII. CONCLUSIONS

This project is about building a mechanical prototype of a mini-CNC. Machine which can drill on a given wood surface. It consumes low power and works with high accuracy due to precise controlling of stepper motors. This is a low-cost project as compared to other CNC product. It is made with easily available components and spare parts. It is designed for private manufacturing and small-scale applications in educational institutes. The machine is designed with a very simple construction scheme and can be carried anywhere without much effort. The algorithm used is simple. Software that has been used is open source and user- friendly. This is small machine which is easily

transportable and assembled everywhere as per the requirement. It will be free to make big size of design on paper. We have used G-code for giving commands. G-codes are language to give the command to the machine to move right, left, or up and down. These set of hardware with a combination of G-code gives a better accuracy and reduces the workload. G-code make easy to find the

information of all locations of all stepper motors moving as the status of our moving motors are directly shield on computer hence, we can start or stop the machine whenever we are needed. Making a small machine brings flexibility to do work.

This setup of hardware with a combination of G-code gives better accuracy and reduces the workload. G code make easy to find the information of locations of all stepper motor moving, as the status of our moving motor are directly seen on computer hence, we can start or stop the machine whenever we are needed. Making a small machine brings a flexibility to do work.

REFERENCES

- [1] H. Ferdinando, I. N. Sandjaja, G. Sanjaya, DzAutomatic Drilling Machine for Printed Circuit Board Proceedings of the 6th Symposium on Advanced Intelligent Systems, Surabaya Indonesia 2005, pp. 218-222.
- [2] N.Balasubramanyam and Prof. Smt. G. Prasanthi DzDesign and Fabrication of an Automatic PC-Based Drilling Machine, HCTL Open International journal of Technology Innovations and Research, Volume 7, January 2014
- [3] Shrikant Bhange, Lochana Ahire, Madhuri Gadkari, Asmita Bhosale, Mansi Shrimali PC CONTROLLED PCB DRILLING Machine International Journal of Engineering Technology and Computer Research (IJETCR), Volume 3; Issue 1
- [4] D.S. Bernstein, "Setting up and running a control research laboratory", IEEE Control Systems Magazine, vol. 23, pp. 14-19, 2003.
- [5] K. Nagai, "Learning while doing: Practical robotics education", IEEE Robotics & Automation Magazine, vol. 8, pp. 38-43, June 2001.
- [6] N. Raju, N. Beedu, N. Lakshminarasamma, and V. Ramanarayanan, "A do-it-yourself (DIY) switched mode power conversion laboratory", Proc. India Int. Conf. Power Electronics, Chennai, pp. 289-292, 2006.
- [7] V.K. Pabolu and K.N.H. Srinivas, "Design and Implementation of a three-dimensional CNC Machine", Int. J. Computer Science and Engineering, vol. 2, pp. 2567-2570, 2010.
- [8] T. Andrei and I. Nae, "Practical applications Performed by a stepper motor CNC router", Seria Technical, vol. LXII, pp. 127-138, 2010.
- [9] I. Nae and T. Andrei, "Designing and building a CNC router using stepper motors", Seria Technica, vo. LXII, pp. 55-62, 2010.
- [10] I. Pahole, L. Rataj, M. Ficko, S. Klančnik, S. Brezovnik, M. Brezocnik, and J. Balic, "Construction and evaluation of low-cost table CNC milling

DESIGN AND FABRICATION OF 360 DEGREE DESKLAMP

S.Kamala kumar, T.Ashok Kumar and P.Govardhan Babu

*Department of Mechanical Engineering,
Narasaraopeta Engineering College, Narasaraopet, Palnadu (Dist.), A.P., India*

Abstract — now a day's smart work is best result for the output. The Additive manufacturing is the advanced product manufacturing process of producing 3-dimensional objects from a computer file. 3D Printing is a novel method of manufacturing parts directly from digital model by using layer by layer material build-up approach. A desk lamp is a portable task light that sits on a desk or table to provide targeted illumination for accomplishing tasks such as computer work, reading, writing, drafting, crafting, bookkeeping, sewing, knitting, and painting.

The aim of this project is to design and fabrication the 360 degree desk lamp. In this project Desk Lamp designed with the help of fusion 360 software and fabrication is by using 3D printer. Generation of G-Codes and estimating time is done by using Cura Ultimate S5. Acrylonitrile Butadiene Styrene (ABS) material issued for fabrication. This project deals with the study of additive manufacturing, cura software and polymer's.

INVESTIGATION INTO THE COMBINED INFLUENCE OF INCLINATION AND PARTIAL FINS ON PHASE CHANGE MATERIAL MELTING IN A RECTANGULAR ENCLOSURE UTILIZING COMPUTATIONAL FLUID DYNAMICS (CFD)

D. Kondala Rao and Srinivas Kolla

Department of Mechanical Engineering, R.V.R. & J.C. College of Engineering, Guntur, Andhra Pradesh, India

ABSTRACT: In this research, we investigate the combined impact of inclination and internal fins on the melting rate of phase change material (PCM) in a rectangular enclosure measuring 8.89cm×6.35cm. The enclosure consists of a hot wall maintained at a temperature of 311K, a cold wall at 301.3K, and the remaining two walls are thermally insulated. The PCM used in this study is gallium, which possesses an extremely low Prandtl number. Initially, we analyze the individual effects of different inclinations (0°, 45°, and 90°) of the enclosure on the melting rate of the PCM. Subsequently, we examine the influence of internal fins on the system. Next, we introduce a combined setup involving both inclination and partial fins to investigate its impact on the liquid fraction, velocity contours, and temperature distributions. Plots depicting the liquid fraction and average temperatures as functions of time are also generated. Finally, we compare the results and plots obtained from the combined effect with those obtained under other conditions. Through this comparative analysis, we deduce that the combined effect of inclination and partial fins, in the presence of constant normal gravity, significantly enhances heat transfer within the PCM.

Keywords: Computational Fluid Dynamics; Phase Change Materials; Thermal behavior; Partial Fins.

I. INTRODUCTION

Nowadays, there is a growing interest in phase change materials (PCMs) due to their ability to store thermal energy. This energy can be stored as sensible heat by raising the temperature of the PCM, or as latent heat during the phase change process. PCMs exhibit high energy storage capacity and demonstrate isothermal behaviour during melting and solidification processes. They find a wide range of applications, including refrigeration [1], solar energy storage [2], building materials [3], desalination [4], thermal stability of electronics [5], and more. To improve the heat transfer efficiency of systems utilizing PCMs, it is crucial to

have a comprehensive understanding of the thermal behaviour of the PCM.

Several techniques have been developed to enhance the thermal performance of PCMs. These techniques include the use of high-conducting materials, extended heat transfer surfaces [6], intermediate heat transfer mediums, heat pipes, multiple PCMs [7], micro-encapsulation [8], and others. Among the major heat transfer enhancement techniques for PCMs are the incorporation of partial fins [9] and providing inclination to the enclosure [10]. Previous studies have established that these two techniques individually enhance the thermal performance of PCMs. However, there is a scarcity of studies focusing on the combined effect of partial fins and inclination on the thermal performance of PCMs.

This study aims to compare the combined effect of partial fins and inclination on the thermal performance of PCMs under constant gravity conditions, while also examining their individual effects. By investigating these factors, a deeper understanding of how they influence the thermal behaviour of PCMs can be obtained. Such knowledge can contribute to further advancements in optimizing the heat transfer mechanisms of PCM systems, ultimately enhancing their overall performance.

II PROGRESSION OF THE STUDY

Firstly, the melting of PCM under normal conditions is studied. Then, the individual effect of partial fins and inclination of the enclosure are studied. For the case of inclination we only take the case of horizontal hot wall

(90° inclination) because the heat transfer enhancement for the horizontal enclosure is higher than that of any other inclined configuration. Finally, both partial fins and 90° inclination are provided to the enclosure containing the PCM and the results are compared with all the individual effects.

III MODELLING PHASE CHANGE MATERIALS

Phase-change processes (melting and solidification) are modelled primarily in three different ways; empirical, classical and enthalpy-based methods. In the empirical method, higher conductivity values are assigned for the liquids to account for convection effects and purely conduction treatment is considered. Classical method accounts for the convection by solving suitable governing heat and mass transfer equations. Enthalpy-Porosity technique [11] is widely followed now-a-days to model solidification/melting problems which uses the latent heat and assigns every computational cell a nodal latent heat value according to the temperature. When a phase-change occurs in the material (computational domain), the latent heat value is adjusted accordingly. In this method, instead of tracking melt-interface, liquid fraction, which is the liquid fraction of cell volume, is assigned to each cell in the domain. Liquid fraction is computed at each iteration through which energy source term is obtained.

We assume boussinesq model to be valid in our problem. This model treats density as a constant value in all solved equations, except for the buoyancy term in the momentum equation. Thus, along with momentum sink term we add buoyancy source term (boussinesq treatment) to account for natural- convection effects. In this work

Enthalpy-Porosity technique is modelled using FLUENT 15.0 CFD code. The governing heat transfer and fluid flow equations are:

$$\text{Mass conservation equation } \partial\rho/\partial t + \nabla \cdot (\rho V) = 0 \quad (1)$$

$$\text{Momentum equation: } \rho (DV^{\rightarrow})/\partial t - \nabla p + \mu \nabla^2 V^{\rightarrow} + \rho g + S \quad (2)$$

$$\text{Energy conservation equation: } \rho Dh/\partial t = k \nabla^2 T \quad (3)$$

Where, ρ is the density, k is the thermal conductivity, μ is the dynamic viscosity, is the momentum source term, is velocity vector, T is temperature and h is specific enthalpy. Other auxiliary equations are

prohibitively long to mention here, and therefore can be found in Ref. [11].

In this study we consider a 2-dimensional rectangular computational domain of dimensions 8.89cm × 6.35cm. A uniform mesh of 42×32 node in x- and y- directions is used. Gallium is used as the PCM. Thermo-physical properties of gallium used in the simulation are listed in the table.1.

Table 1: Thermo-physical properties of Gallium

Property	Value
Specific heat capacity	381.5 kJ/kg K
Melting temperature (Reference)	302.78 K
Latent heat of fusion	80160 J/kg
Thermal conductivity	32 W/m-K
Density (Reference)	6095 kg/m3
Dynamic viscosity	1.81E-3 kg/m-s
Volume thermal expansioncoefficient of liquid	1.2E-4
Prandtl Number	2.16E-2

In this study, four cases are simulated, and results are analysed: 1) melting of gallium in normal conditions of the enclosure 2) with the enclosure inclined at 90° 3) with partial internal fins and 4) both inclination and partial internal fins (all the cases with normal gravity). The temperatures of hot wall are fixed at 311K and that of cold is fixed at 301.3K. Other walls are insulated. The PCM is considered to be at 301.3K initially and simulations are conducted with normal gravity. Fig (2), comprises of four internal fins, each with a length of 1.0 cm and height of 0.71 cm.

Monitors are created for liquid fraction and average temperature of the enclosure as the time progresses. Vertex average of liquid fraction and average temperature of each element of the computational domain is calculated and plots are generated with time (seconds) on x-axis.

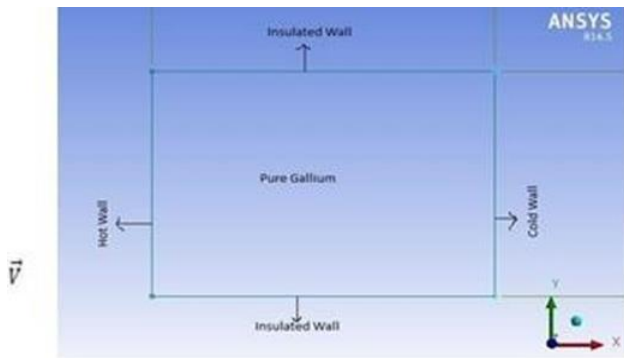


Figure 1: Computational domain without fins.

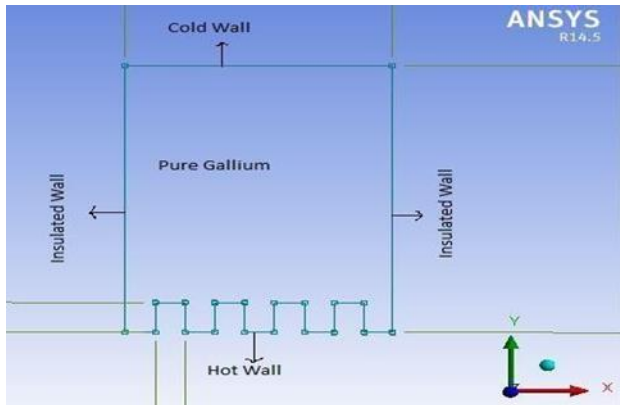


Figure 2: Computational with 90° inclination and partial fins.

The computational domains for case (2) and case (3) are the derivatives of Fig2. So they are not shown separately.

IV Results and Discussion

Figures (3, 6, 9, 12) show the advancement of solid-liquid interface, streamlines and temperature distribution. Fig3 for normal conditions, Fig4 for inclined enclosure, Fig5 for the enclosure with partial fins and Fig6 for the combination of inclination and partial fins, at different melting times, $t=180$ s (Fig. 3,7,10,12a, d, g), $t=360$ s (Fig. 3,7,10,12b, e, h), and $t=540$ s (Fig. 3,7,10,12c, f, i).

During the melt down of Gallium in the enclosure, initially, conduction dominant melting occurs along the hot wall resulting in uniform propagation of melt interface as the viscous forces oppose the movement of the liquid PCM. Later the thickness of the liquid at the top of the enclosure increases due to which mobility increases leading to the domination of buoyancy forces over viscous forces. Buoyancy forces trigger the natural convection currents in the enclosure. This being said, we can say from velocity contours that the liquid rises along the hot wall and crawls down along the melt interface causing clockwise currents.

At early melting stages the melt interface is almost flat and heat conduction is the main melting source. Later the interface shape becomes wavy and is controlled by convection currents to a large extent. As the conduction turns into convection many small vortices start originating overlapping each other increasing the turbulence in the flow. As the melting progresses they merge together with each other forming large sized vortices bringing back the 2-dimensionality of the flow (reduces the turbulence).

At early stages the melting is governed by heat conduction which changes to convection dominant. Buoyant forces dominate the viscous forces in order to do so. Increased surface area of heat transmission increases the melting rate. The liquid PCM rises along the wall and get diverted right by the fin where its separated into two streams. One directly impinges on the melt interface and the other rises along the tip to upper part of the enclosure. There will also thermal plumes originating from the top surface of the fin. The melting rate is enhanced by the vortex motion of thermally driven flows above the fin surfaces.

Initially the heat conduction dominant melting takes place due to viscous forces opposing the liquid flow. Later vortex induced melting occurs due to convection domination, which is caused by buoyancy forces domination over viscous forces. Direct impingement of thermal plumes originating from the hot wall on to the melt interface has some effect on melting rate. Large number of small vortices originate in the fin grooves and the hot surfaces. These combine to form large sized vortices as the time passes. A wavy type interface is formed at the beginning of the convection which is caused by the small sized vortex motions of the liquid. This increases the turbulence in the flow. As the melting time progresses these vortices mix with each other to form large sized vortices. As the vortices become large the waviness of the flow reduces decreasing the turbulence in the flow. Adding fins increased the vortex motion of the flow and surface area of the hot wall to boost the melting rate. Inclination increased the 3-dimensionality of the flow by generating more number of vortices and also produced thermal plumes, which effect the rate of melting in a great manner. One disadvantage of using the internal fins is that it reduces amount of PCM that can be fit into a normal enclosure.

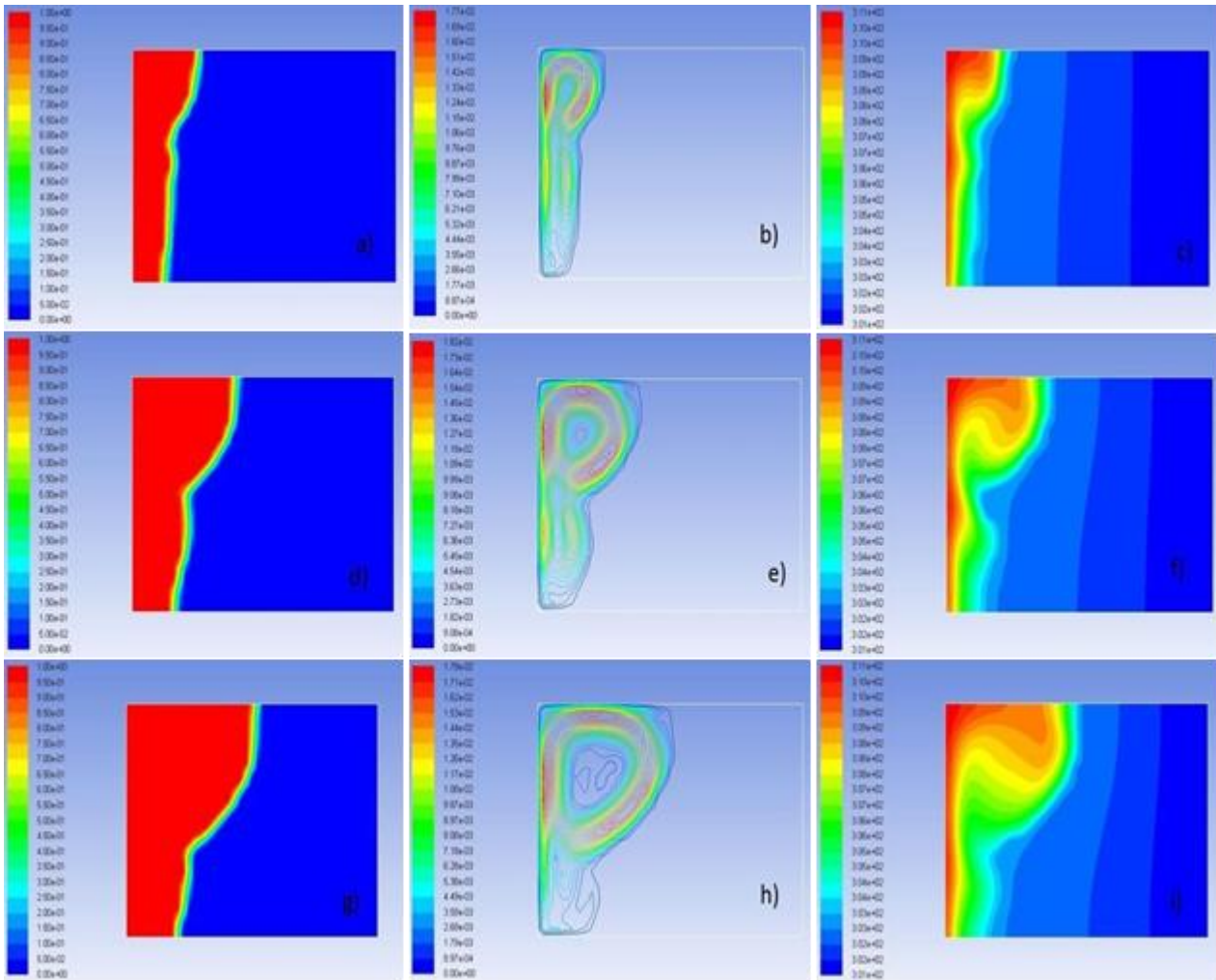


Figure 3: Melting of gallium under normal conditions, after time, $t= 180$ s (top), 360 s (middle) and 540 s (bottom); (a, d, g) are solid-liquid interface propagation, (b, e, h) are stream lines and (c, f, i) are isotherms.

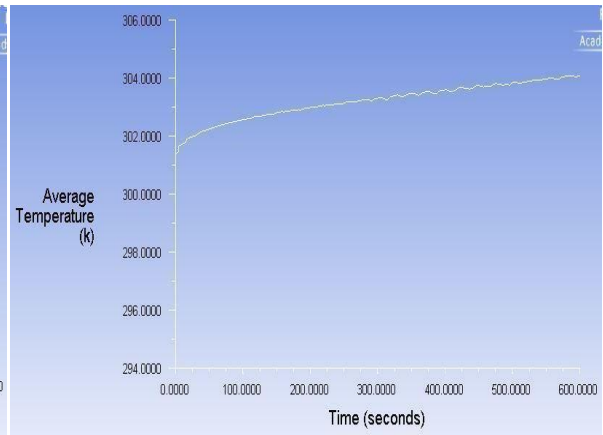
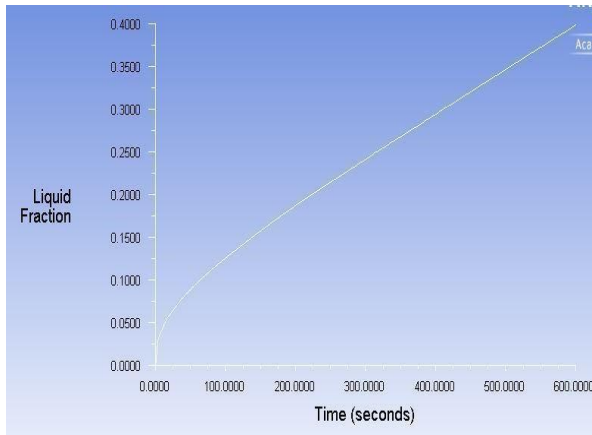


Figure 4: Liquid fraction vs time graph for melting of Gallium under normal conditions.

Figure 5: Average temperature vs time graph for Gallium under normal conditions.

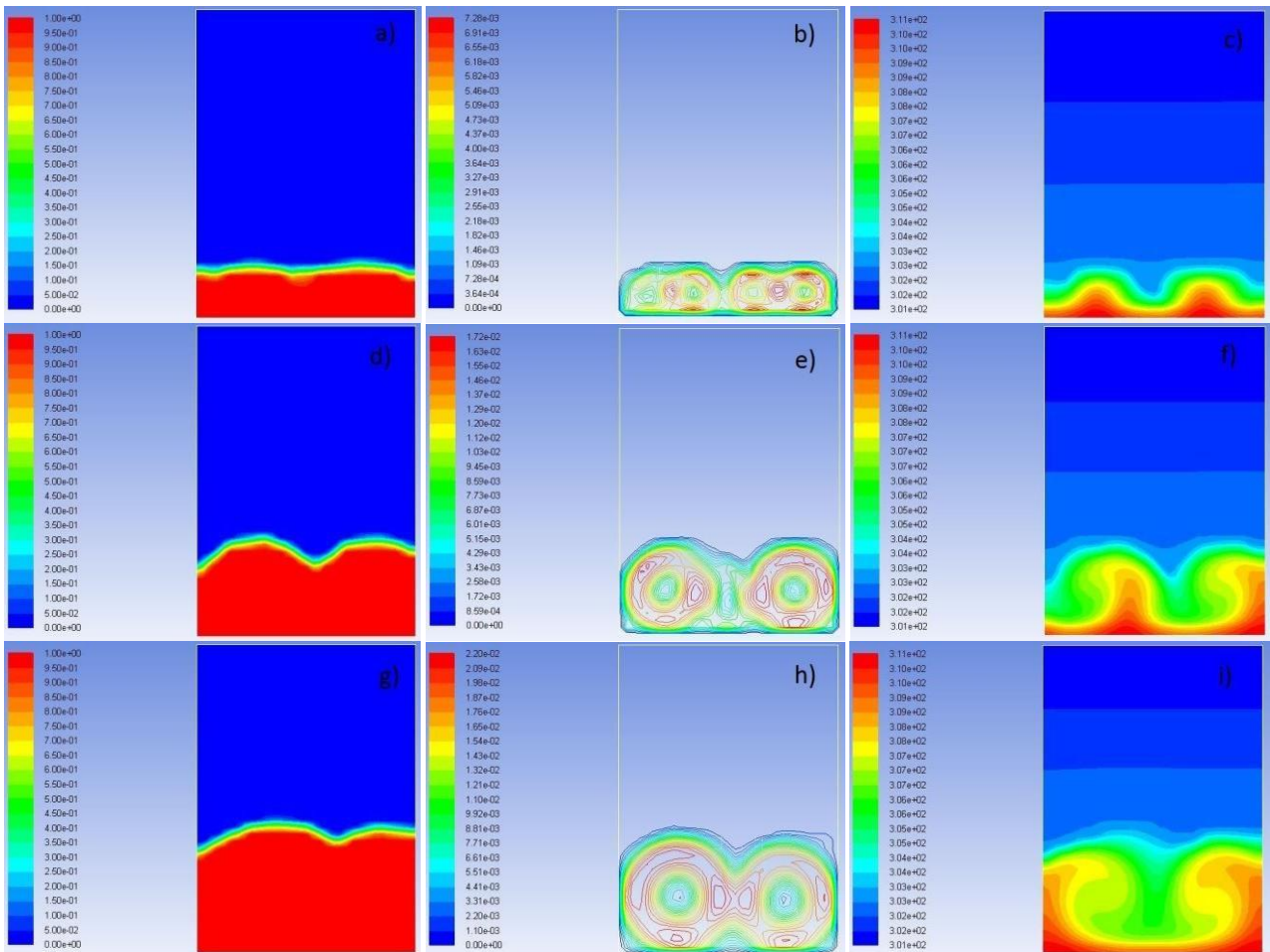
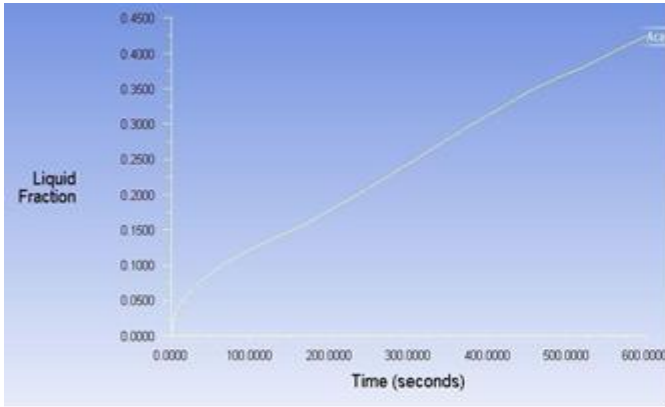
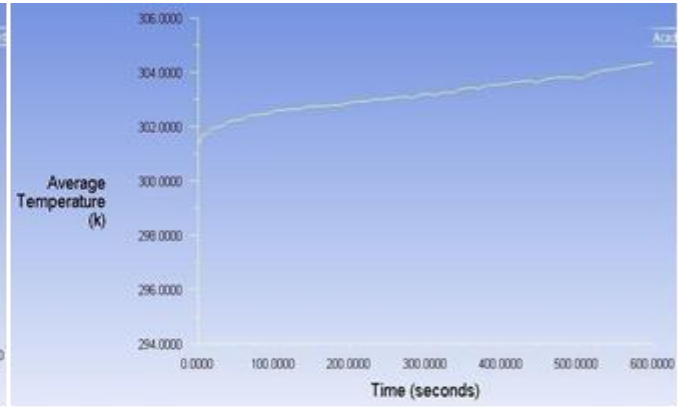


Figure 6: Melting of gallium in an enclosure inclined at 90° , after time, $t = 180$ s (top), 360 s (middle) and 540 s (bottom); (a, d, g) are solid-liquid interface propagation, (b, e, h) are stream lines and (c, f, i) are isotherms



in a 90°inclined enclosure.



Gallium in a 90°inclined enclosure.

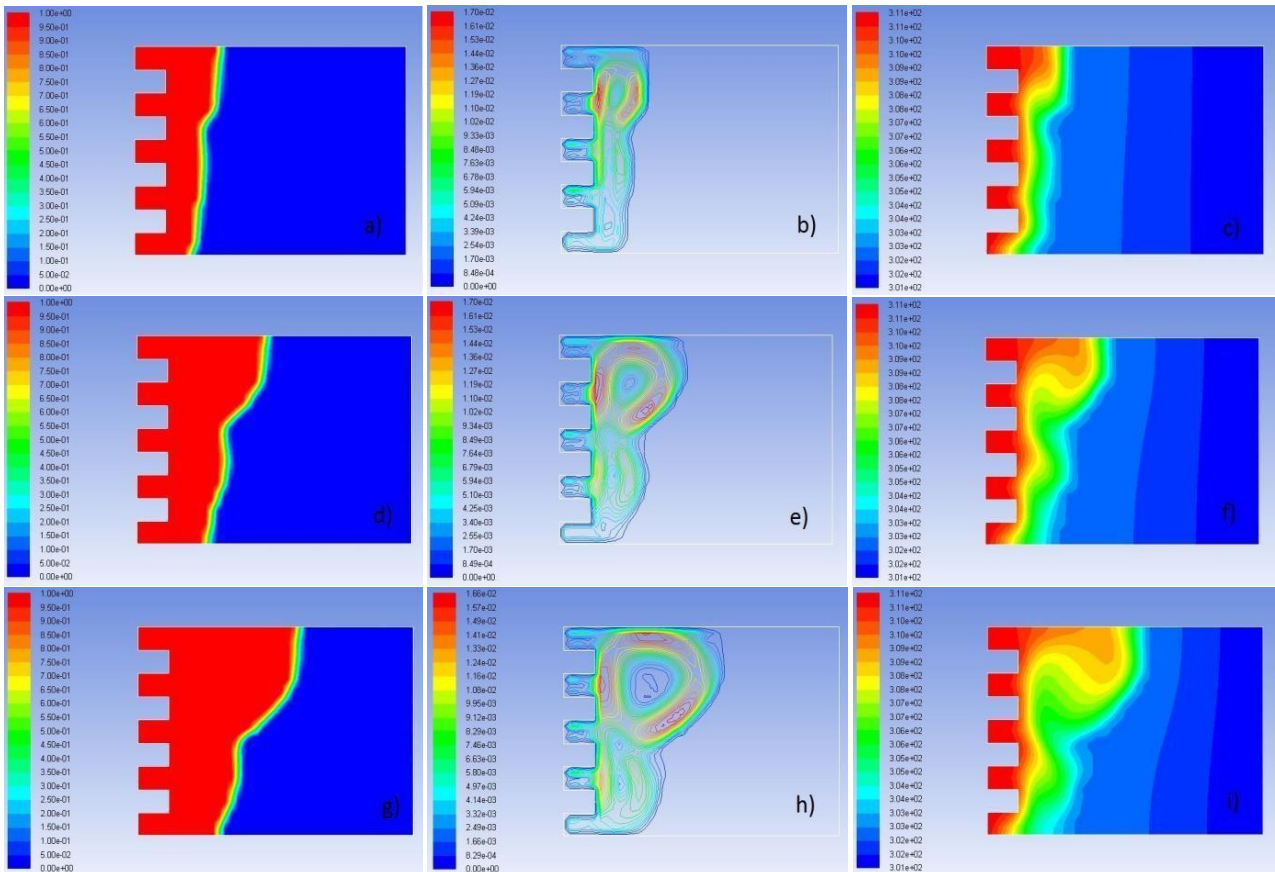


Figure 9: Melting of gallium in an enclosure with partial fins, after time, $t= 180$ s (top), 360 s (middle) and 540 s (bottom); (a, d, g) are solid-liquid interface propagation, (b, e, h) are stream lines and (c, f, i) are isotherms.

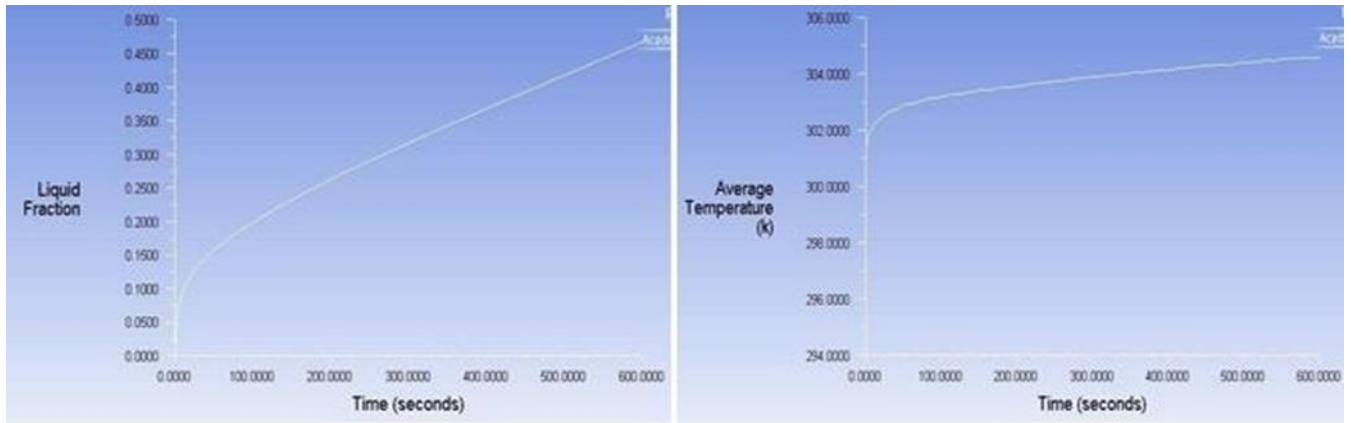


Table 2: Comparative tabulation of liquid fraction of all the four cases at different times.

Time(seconds)	Liquid Fraction			
	Melting under normal conditions	Melting in a 90° inclined enclosure	Melting in an enclosure with partial fins	Melting in a 90° inclined enclosure with partial fins
180s	0.175	0.165	0.254	0.245
360s	0.273	0.285	0.347	0.358
540s	0.368	0.392	0.4375	0.464
600s	0.400	0.425	0.442	0.493

Table 3: Comparative tabulation of average temperature of all the four cases at different times.

Time(seconds)	Average Temperature			
	Melting under normal conditions	Melting in a 90° inclined enclosure	Melting in an enclosure with partial fins	Melting in a 90° inclined enclosure with partial fins
180s	302.8 K	302.75 K	303.5 K	303.5 K
360s	303.4 K	303.4 K	304.1 K	304.0 K
540s	303.9 K	304.05 K	304.45 K	304.6 K
600s	304.15K	304.45 K	304.6 K	304.8 K

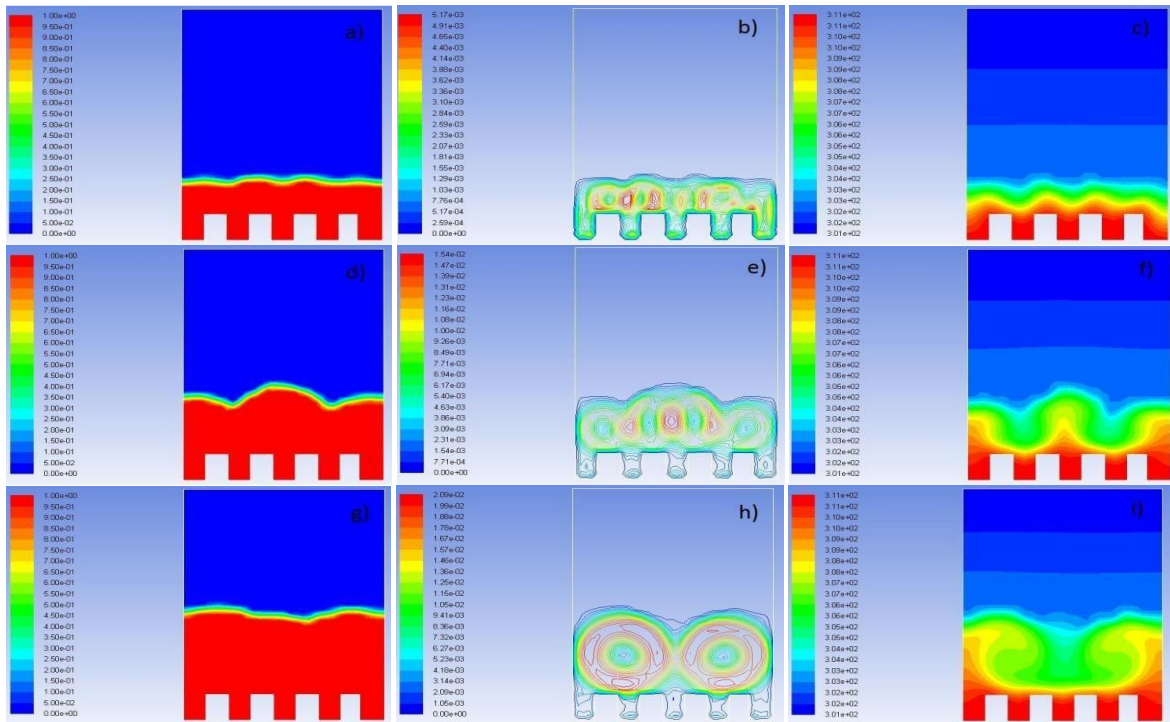


Figure 12: Melting of gallium in a 90° inclined enclosure with partial fins, after time, $t= 180$ s (top), 360 s (middle) and 540 s (bottom); (a, d, g) are solid-liquid interface propagation, (b, e, h) are stream lines and (c, f, i) are isotherms.

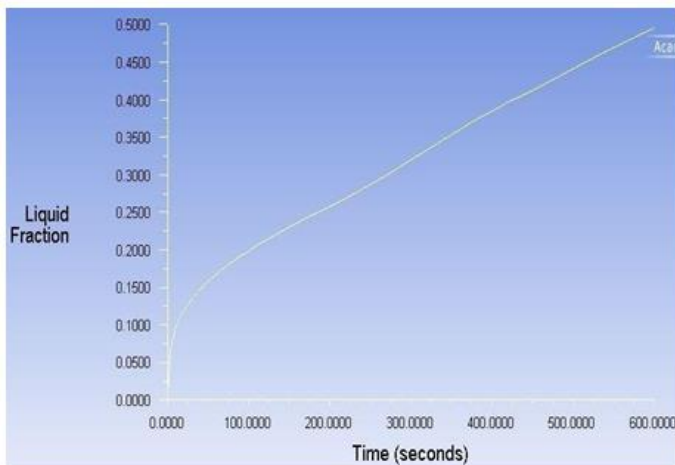


Figure 13: Liquid fraction vs time graph for a 90° inclined enclosure with partial fins.

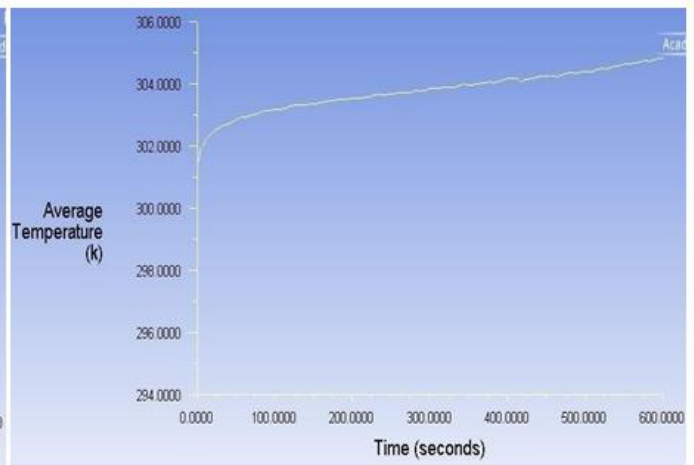


Figure 14: Average temperature vs time graph for a 90° Inclined enclosure with partial fins.

V Conclusions

From this study we can conclude that both application of partial fins and providing inclination to the enclosure enhance the melting rate of PCM by empowering the

heat transfer mechanisms. The initial conduction dominant melting is turned into convection dominant melting by the buoyant force's domination over viscous forces. The combined effect has increased the melting rate of PCM significantly by enhancing the convection

currents. By using the combined effect of inclination and fins under normal gravity conditions we can extract large amount of energy from the PCM in a small time period, whose applications can be used extensively. If we take a step further and increase the gravity of the domain by applying electromagnetic field, we can get exceptional results.

References

- [1] Liu, M.; Saman, W.; Bruno, F., (2012). Development of a novel refrigeration system for refrigerated trucks incorporating phase change material. *Appl. Energy.*, 92, 336–342.
- [2] Pistocchini, L.; Motta, M., (2011). Feasibility study of an innovative dry-cooling system with phase-change material storage for concentrated solar power multi-MW size power plant. *J. of Solar Energy Engineering.*, 133(3), pp: 10.
- [3] Stritih, U.; Butala, V., (2010). Experimental investigation of energy saving in buildings with PCM cold storage. *Int. J. Refrig.*, 33 , 1676–1683.
- [4] Arunkumar, T.; Denkenberger, D.; Ahsan, A.; Jayaprakash, R., (2013) The augmentation of distillate yield by using concentrator coupled solar still with phase change material. *Desalination*, 314 , 189–192.
- [5] Kandasamy, R.; Wang, X., Mujumdar, A.S., (2007). Application of phase change materials in thermal management of electronics. *Appl. Therm. Eng.*, 27 , 2822–2832.
- [6] Varol, Y.; Okcu, M., (2013). Numerical investigation of fins effect for melting process of phase change materials. *ASME 2013 International Mechanical Engineering Congress and Exposition, San Diego, California, USA, November 15-21, 2013.*
- [7] Liu, M.; Saman, W.; Bruno, F., (2014). Review on storage materials and thermal performance enhancement techniques for high temperature phase change thermal storage systems. *Renewable and Sustainable Energy Reviews.*, 16 (4), 2118-2132.
- [8] Agyenim, F.; Hewitt, N.; Eames, P.; Smyth, M.,(2010) A review of materials, heat transfer and phase change problem formulation for latent heat thermal energy storage systems (LHTESS). *Renewable and Sustainable Energy Reviews.*, 14 (2), 615-628.
- [9] BabakKamkari.; Hossein Shokouhmand.,(2014). Experimental investigation of phase change material melting in rectangular enclosures with horizontal partial fins. *International Journal of Heat and Mass Transfer.*, 78 , 839–851.
- [10] Babak Kamkari, Hossein Shokouhmand.; Frank Bruno., (2014) Experimental investigation of the effect of inclination angle on convection-driven melting of phase change material in a rectangular enclosure. *International Journal of Heat and Mass Transfer.*, 72, 186–200.

- [11] Brent, A.; Voller, V.; Reid, K.T.J., (1988) Enthalpy-porosity technique for modeling convection-diffusion phase change: Application to the melting of a pure metal. *Numerical Heat Transfer-part A.*, 13 (3), 297-318.

DUAL AXIS SOLAR TRACKING SYSTEM

P.Durga Neeharika¹, D.Radha², P.Sravani³, P.Sai Kiran Yadav⁴

¹*Narasaraopeta Institute of Technology, Narasaraopet, Palnadu Dist., Andhra Pradesh*

²*Kshatriya College of Engineering, Nizamabad, Telangana*

^{3,4}*Narasaraopeta Engineering College, Narasaraopet, Palnadu Dist., Andhra Pradesh*

Abstract- As population is increasing globally; we are very concerned for Electricity. There are various ways of electricity generation like Hydro power plant, Nuclear power plant, Windmill plants and also solar power plants. The former two are Non Renewable source of energy; hence we cannot depend only on such technology. Also Harnessing Energy from Hydro and Nuclear is equally difficult. The latter two are Renewable source of Energy; nowadays we have lots of power plants established on Solar and Wind Technology. Our project aims at Dual axis or Dual direction tracker. The Solar panel used in this system can adjust its direction both in X-Y co-ordinates. This helps better directivity with Sun rays, thus increasing the efficiency of the solar system.

DEVELOPING FACE RECOGNITION SYSTEM USING AI & ML

Mr.K.Kiran chand¹, Mr.M. Venkateswarlu², Mr.D.VeeranjiReddy³,

Assistant Professor¹, Department of Mechanical Engineering, Narasaraopeta Engineering College, Narasaraopet, Palnadu(Dist.), A.P., India.

Assistant Professor², SKN Sinhgad Institute Of Technology And Science -[SknSits] Lonavala, Pune, India.

Student, Department of Mechanical Engineering, Narasaraopeta Engineering College, Narasaraopet, Palnadu(Dist.), A.P., India.

Abstract: Facial recognition technology is a computer-based system that can identify or verify a person's identity by analyzing and comparing their facial features with a database of known faces. This technology has gained significant attention and use in recent years, and is being deployed in various settings such as security and surveillance systems, access control systems, and marketing analysis. This section describes a sample model of possible data organization that can be implemented to support this protocol. The purpose of this description is simply to help explain how this aspect of the protocol works. This specification does not prescribe that implementations adhere to this model as long as their external behavior is consistent with what is described throughout this document.

This is a protocol document specifying the File Replication Service (FRS) Protocol. The FRS Protocol is used to replicate files and folders among servers on the network. This protocol enables duplicate files and folders to be maintained on multiple servers. Microsoft operating systems use FRS to maintain duplicate copies of data files in system volume (SYSVOL) system folders on multiple domain controllers in a domain. Microsoft operating systems also use FRS to replicate data files among Distributed File System (DFS) shares.

This document provides detailed technical reference material for the Remote Procedure Call (RPC) interfaces, packet formats, and data structures required for interoperation using FRS.

Key Words: File Replication Service, network, Microsoft operating systems.

Advantages of Facial Recognition Systems

High accuracy: Facial recognition systems have become highly accurate due to advancements in artificial intelligence and deep learning algorithms.

Convenience: Facial recognition systems provide a convenient and contactless way of identification or verification, which is especially useful in situations where physical contact is not desirable, such as during a pandemic.

Security: Facial recognition systems can improve security measures by detecting and preventing unauthorized access to restricted areas or devices.

Efficiency: Facial recognition systems can save time and reduce human errors in identification or verification processes, which can be especially beneficial in large organizations or public institutions.

Customization: Facial recognition systems can be customized to specific requirements or scenarios, such as detecting certain expressions or emotions.

Disadvantages of Facial Recognition Systems

Privacy concerns: Facial recognition systems have raised concerns over privacy and potential misuse of personal data.

Bias: Facial recognition systems can be biased against certain groups of people, such as people of color or women, due to biases in the data used to train the algorithms.

Cost: Facial recognition systems can be expensive to implement and maintain, which may be a barrier to adoption for some organizations or individuals.

Reliability: Facial recognition systems may not work properly in certain conditions, such as poor lighting or low-quality images, which can lead to errors in identification or verification.

Ethical concerns: Facial recognition systems have raised ethical concerns over issues such as consent, accuracy, and potential misuse for surveillance purposes

Applications of Face Recognition System

- **Security:** Facial recognition systems are commonly used for security and surveillance purposes. They can be used to control access to secure areas, such as airports, government buildings, and data centers, and to identify or track suspicious individuals in public spaces.
- **Law Enforcement:** Facial recognition systems are widely used by law enforcement agencies to identify suspects and wanted criminals from surveillance footage or images captured at crime scenes.
- **Retail and Marketing:** Facial recognition systems can be used in retail stores and marketing campaigns to analyze customer demographics and preferences, as well as to personalize the shopping experience for customers.
- **Healthcare:** Facial recognition systems are used in healthcare facilities to identify patients and to ensure the correct treatment is administered to the right patient. They can also be used to track patient movement within the facility to improve care delivery.
- **Education:** Facial recognition systems can be used for attendance tracking, student identification, and campus security purposes in educational institutions.
- **Banking and Finance:** Facial recognition systems are used in banking and finance to identify customers during transactions and to prevent fraud and identity theft.
- **Transportation:** Facial recognition systems are used in transportation, particularly in airports, to enhance security and expedite check-in and boarding processes.
- **Entertainment:** Facial recognition systems can be used in entertainment venues, such as concert halls and stadiums, for access control and to detect potential security threats.
- **Personal Devices:** Facial recognition systems are used in personal devices, such as smartphones and laptops, for user authentication and access control.

SOFTWARE

PYTHON VERSION 3.9

MODULES OF PYTHON:

- OPENCV-PYTHON
- FACE_RECOGNITION
- CVZONE
- NUMPY
- OPERATING SYSTEM(OS)
- PICKLE
- FIREBASE_ADMIN

INSTALLATION OF PYTHON

Here are the general steps to install Python 3.9 on a Windows operating system:

- Go to the official Python website at <https://www.python.org/downloads/> and download the latest version of Python 3.9 for Windows.
- Once the download is complete, open the installation file and run it as an administrator.
- In the first window, make sure to select the checkbox that says "Add Python 3.9 to PATH".
- Choose a destination folder for the installation. The default location is usually fine.
- In the next window, select the "Customize installation" option.
- In the next window, make sure that all checkboxes are selected, including pip (a package installer for Python).
- Click "Next" and wait for the installation to complete. This may take a few minutes.
- Once the installation is complete, open the command prompt by pressing Windows key + R, then type "cmd" and press enter.

In the command prompt, type "python" and press enter. This should open the Python interpreter, indicating that Python 3.9 has been installed successfully.

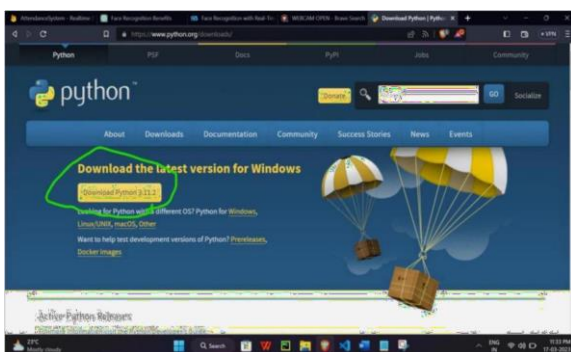


Figure: 1 start using Python 3.9

INSTALLATION OF MODULES

Here are the general steps to install modules in Python:

- Open a command prompt or terminal window on your operating system.
- Type "pip install <module_name>" and press enter. Replace "<module_name>" with the name of the module you want to install.
- Wait for the installation to complete. The command prompt will display the progress of the installation.
- Once the installation is complete, you can import the module in your Python code using the "import" statement.
- For example, if you want to install the "numpy" module, you would type "pip install numpy" in the command prompt.
- Note that some modules may have dependencies that need to be installed first. In this case, you may need to install the dependencies separately before installing the main module.
- Also, it's a good practice to create a virtual environment for your Python projects to isolate the dependencies and avoid conflicts with other projects on your system. You can use the "virtualenv" or "venv" module to create a virtual environment. Once the virtual environment is activated, you can install the required modules using pip as described above.

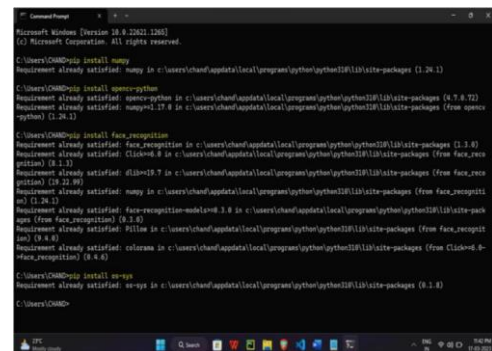


Figure: 2 Python 3.9 installation PROCEDURE

The procedure of a face recognition system involves the following steps:

- Capture an image or video of a person's face using a camera or other imaging device.
- Pre-process the image or video by adjusting the brightness, contrast, and other parameters to enhance the facial features.
- Detect and locate the face in the image or video using object detection algorithms. This involves identifying the face's boundaries, such as the position of the eyes, nose, and mouth.
- Extract the facial features from the detected face, such as the distance between the eyes, the shape of the jawline, and the distance between the nose and mouth. This is usually done using feature extraction algorithms.
- Create a unique facial signature for the person by encoding these facial features into a digital format using complex algorithms and machine learning techniques.

- Store the facial signature in a database for future comparisons.

When a person presents their face to the facial recognition system, the system captures an image or video of their face and repeats steps 2-5 to extract the facial features and create a unique facial signature.

Compare the facial signature of the person to the stored facial signatures in the database using complex algorithms and machine learning techniques.

If the system finds a match, it will identify or verify the person's identity and provide a result indicating the match. If there is no match, the system will not identify or verify the person's identity.

Overall, the procedure of a face recognition system involves capturing and analyzing various facial features to create a unique facial signature, which is then compared to the stored facial signatures in a database for identification or verification purposes.

Webcam:

A webcam captures digital images or videos of human faces, which are then processed by the face recognition system.

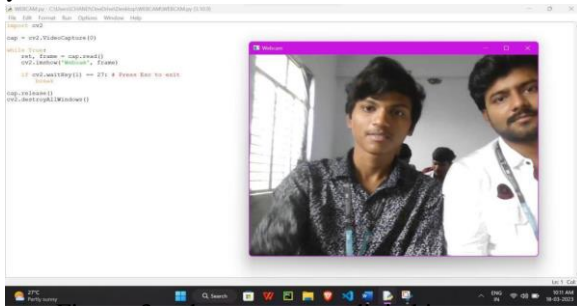


Figure: 3 webcam captures digital images

Graphics:

Graphics are used to display the captured images or videos, as well as the results of the face recognition analysis.



Figure: 4 Graphic captured images

Encoding generator:

An encoding generator creates a unique digital representation of each face, which is used to compare against known faces in the database.

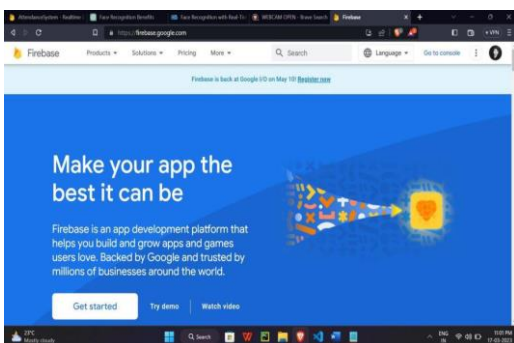


Figure: 5 Encoder images

Face recognition:

Face recognition software compares the digital representation of a face against known faces in a database to identify the individual.

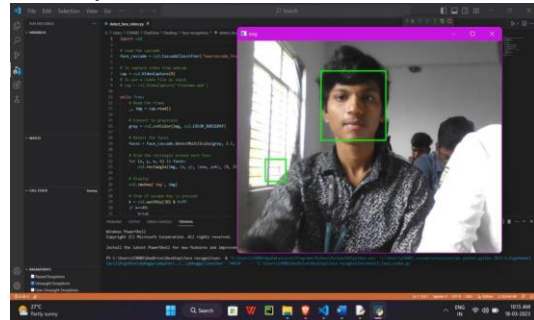


Figure: 6 Face recognition image

Database setup:

A database is set up to store the digital representations of known faces, along with associated data such as name, ID, and other relevant information.

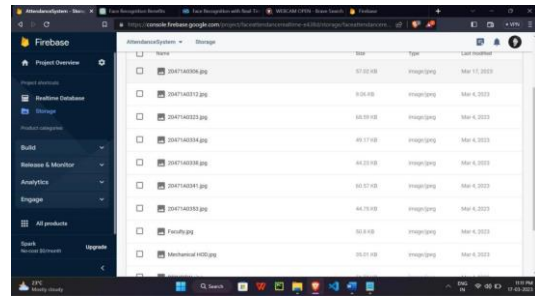


Figure: 7 Digital Representations

Adding data to database:

Data on individuals is added to the database, including their name, ID, and digital representation of their face.

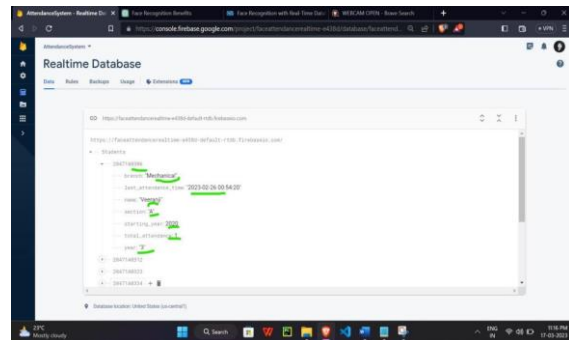


Figure: 8 Adding data to data base

Adding images to database:

Images of individuals are added to the database to improve the accuracy of the face recognition system.

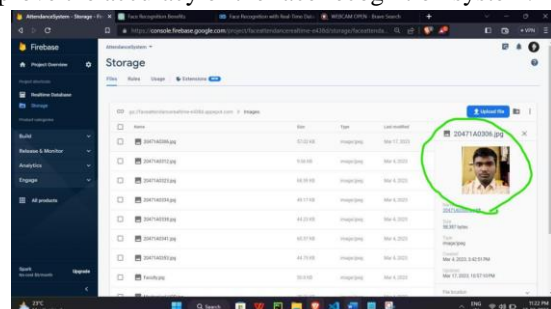


Figure: 9 Data base to image

Real-time database update:

The database is updated in real-time as new individuals are added or removed, or as changes are made to the data associated with known faces.

Limit number of attendance per day:

To limit the number of attendance per day, the system can be programmed to restrict entry after a certain number of entries have been recorded.

In summary, face recognition using Python involves a range of components and steps, from capturing images or videos using a webcam to comparing digital representations of faces against known faces in a database. The system can be customized to include additional features such as real-time updates and limitations on attendance.

RESULT

When a person presents their face to the facial recognition system, the system captures an image or video of their face and extracts their facial features.

The system then compares the person's facial signature to the stored facial signatures in its database using complex algorithms and machine learning techniques.

If the system finds a match, it will identify or verify the person's identity and provide a result indicating the match. If there is no match, the system will not identify or verify the person's identity.

Overall, the software procedure and result of facial recognition systems involve capturing and analyzing various facial features to create a unique facial signature, which is then stored in a database for future comparisons. The result of the system is a match or no match, indicating whether the person's identity has been identified or verified.

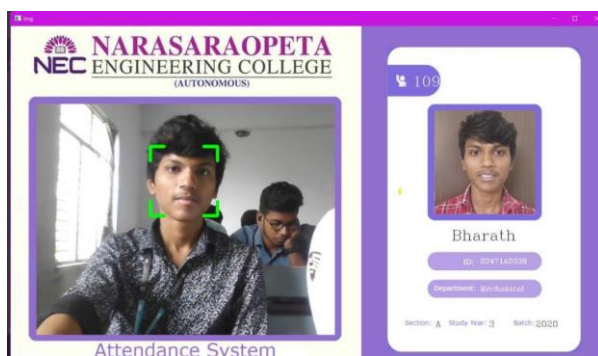


Figure: 10 software system identifying the student

CONCLUSION & SCOPE FOR FUTURE WORK

The conclusion of a face recognition system is that it is a powerful technology that has the potential to revolutionize security and surveillance. It uses computer algorithms to analyze and recognize human faces from digital images or videos.

There are many advantages of face recognition technology, including its accuracy, speed, and ability to work in various lighting conditions. It can be used for a range of applications, including security, law enforcement, and

marketing.

However, there are also concerns about privacy and potential misuse of the technology. It is important to develop appropriate regulations and ethical guidelines to ensure that face recognition technology is used responsibly and in accordance with human rights.

In conclusion, face recognition technology has the potential to bring many benefits to society, but it is important to weigh the benefits against the potential risks and to develop appropriate safeguards to protect individuals' privacy and rights.

SCOPE FOR FUTURE

As technology continues to advance, face recognition systems will become even more powerful and versatile. Here are some potential areas of development for the future of face recognition technology:

Better accuracy: Researchers are constantly developing new algorithms and techniques to improve the accuracy of face recognition systems, and we can expect this trend to continue.

Enhanced security: Face recognition systems are already being used for security purposes, but future developments could include real-time tracking of individuals and the ability to detect and prevent potential threats.

Virtual reality and gaming: Face recognition technology could be used to enhance the gaming experience by tracking facial expressions and allowing for more realistic interactions.

Healthcare: Face recognition systems could be used to help diagnose certain medical conditions based on facial features.

Education: The technology could be used in education to monitor student attendance and engagement, as well as to personalize learning experiences based on individual facial expressions and behaviors.

Overall, the future of face recognition technology is exciting and full of possibilities, and we can expect to see many new applications and advancements in the years to come. However, it is crucial that we continue to prioritize ethical considerations and ensure that the technology is used responsibly to protect individual privacy and rights.

REFERENCES

[1] C Rahmad, R A Asmara, D R H Putra, I Dharma, H Darmono and I Muhiqqin (Jan. 2020). "Comparison of Viola-Jones Haar Cascade Classifier and Histogram of Oriented Gradients (HOG) for face detection." The 1st Annual Technology, Applied Science, and Engineering Conference 29–30 August 2019, East Java, Indonesia. 28 January 2020.

[2] M. Turk and A. Pentland (Jun. 1991). "Face Recognition Using Eigenfaces." Proceedings of CVPR IEEE Computer Society

[3] Navneet Dalal and Bill Triggs (Jun. 2005). "Histograms of Oriented Gradients for Human Detection." IEEE Computer Society

[4] Dadi HS, Pillutla GM. Improved face recognition rate using HOG features and SVM classifier. IOSR Journal of Electronics and Communication Engineering. 2016 Apr;11(04):34-44.

[5] Geng C, Jiang X. Face recognition using SIFT features. In2009 16th IEEE international conference on image processing (ICIP) 2009 Nov 7 (pp. 3313-3316).IEEE.

[6] Albiol A, Monzo D, Martin A, Sastre J, Albiol A. Face recognition using HOG–EBGM. Pattern Recognition Letters. 2008 Jul 15;29(10):1537-43.

DESIGN AND OPTIMIZATION OF HTV FUEL TANK ASSEMBLY BY FINITE ELEMENT ANALYSIS

K.Prakash Babu¹ and M.Venkanna Babu²

¹Department of Mechanical Engineering, Azad College of Engineering, Hyderabad

²Department of Mechanical Engineering, Narasaraopeta Engineering College, Narasaraopet

Abstract: *A fuel tank (or petrol tank) is a safe container for flammable fluids. The functions of a fuel tank are Storage of fuel, filling, and venting. A Fuel tank must provide a method for determining level of fuel in tank and Anticipate potentials for damage. The present study is a methodology to improve the first natural frequency of a fuel tank brackets for heavy duty vehicles using FEA. To improve the performance of the fuel tank bracket series of design iteration was carried out by taking the account of base model structure.*

1. INTRODUCTION

The first heavy duty trucks were developed in United States in the late 1890s. During World War I heavy duty truck played an important role in moving supplies at home and overseas. Fuel tanks in the heavy duty trucks were made with steel because of high strength and durability. Fuel tank is a safe container for flammable fluids. The fuel system of automobile vehicles should perform within major safety parameters related to the importance of flammable substances such as diesel fuels which is extensively consumed worldwide. Important consideration in designing a fuel tank are determining placement choosing the shape and determining the required volume. The fuel system of automobile chassis body system may undergo undesirable vibration due to disturbance from road and fuel tank system. In order to control the road induced vibration the fuel tank bracket should be stiff and damped. Fuel tank mounting is accomplished with use of brackets, straps or a combination of both for the purpose of attaching the fuel tank to the truck frame. Let us consider an example of high speed vehicle boat, at high speeds the sloshing that occur in the tank can drastically affect center of gravity of the vehicle, depending on the size of the fuel tank severity of the sloshing can negatively affect a control system.

1.1 FUEL TANK CONSTRUCTION:

While most tanks are manufactured, some fuel tanks are still fabricated by metal craftsmen or hand-made in the case of bladder-style tanks. These include custom and restoration tanks for automotive, aircraft, motorcycles, and even tractors. Construction of fuel tanks follows a series of specific steps. The craftsman generally creates a mockup to determine the accurate size and shape of the tank, usually out of foam board. Next, design issues that affect the structure of the tank are addressed - such as where the outlet, drain, fluid level indicator, seams, and baffles go. Then the craftsmen must determine the thickness, temper and alloy of the sheet he will use to make the tank. After the sheet is cut to the shapes needed, various pieces are bent to create the basic shell and/or ends and baffles for the tank.

1.2 AUTOMOTIVE FUEL TANKS:

The maximum distance a combustion-engine powered car with a full tank can cover is the product of the tank capacity and its fuel efficiency (as in miles per gallon). While larger tanks increase the maximum distance, they also take up more space and (especially when full) add to the total weight, requiring higher fuel consumption for the same performance. Fuel-tank capacity is therefore the result of a trade-off in design considerations. For most compact cars, the capacity is in the range 45–65 liters (12–17 US gal); the original model Tata Nano is exceptional with its 15 liters (4 US gal) fuel tank. SUVs and trucks tend to have considerably larger fuel tanks.

1.3 SAFETY:

Proper design and construction of a fuel tank play a major role in the safety of the system of which the tank is a part. In most cases intact fuel tanks are very safe, as the tank is full of fuel vapor /air mixture that is well above the flammability limits, and thus cannot burn even if an ignition source were present (which is rare).

2. LITERATURE SURVEY

2.1 LITERATURE SURVEY:

Initial assessment through value engineering and comparative study of the reference vehicles have led to the listing out of various parameters and components which affect the price of the vehicle. Literature survey therefore is concentrated towards the study of those parameters which affects the price of the vehicle and the methods of quantifying the parameters of the vehicle and also various testing procedures and standards.

Fatigue Behavior Analysis and Durability Evaluation of Plastic Fuel Tank, by Himeki. H, Kumagai.H and Morohoshi.K Plastic materials are often used for automotive fuel tanks today because of their light weight, freedom for forming complicated shapes and corrosion resistance. The fatigue behavior of the high-density polyethylene applied to fuel tanks was analyzed under the low-level cyclic loading that simulated fuel tank pressure changes.

The rollover threshold of the articulated vehicle carrying a compartmented tank is investigated and an optimal order of unloading various compartments is presented. [5] Fuel Tanks for the automotive vehicle by Corrodi, R and Gordon, H Steel tank or plastic tank that is the question. Like Shake spear's "Hamlet, Prince of Denmark" this is probably what all those responsible for fuel tanks have asked themselves, time and time again. [6] Minimum Weight Design of Tank Structures by Jones. This paper defines the geometry of minimum weight tank structures of giving the enclosed volume.

Fishbone Diagram is applied to analyze the causes that lead to accidents. Corrective actions are also provided to help

operating engineers handling similar situations in the future. The results show that 74% of accidents occurred in petroleum refineries, oil terminals or storage. Fire and explosion account for 85% of the accidents. There were 80 accidents (33%) caused by lightning and 72 (30%) caused by human errors including poor operations and maintenance. Other causes were equipment failure, sabotage, crack and rupture, leak and line rupture, static electricity, open flames etc. Most of those accidents would have been avoided if better engineering have been practiced. [9]

3. DESIGN OF A FUEL TANK MOUNTING BRACKET

3.1 INTRODUCTION TO CAD/CAM/CAE:

The Modern world of design, development, manufacturing so on, in which we have stepped can't be imagined without interference of computer. The usage of computer is such that, they have become an integral part of these fields. In the world market now the competition in not only cost factor but also quality, consistency, availability, packing, stocking, delivery etc. So are the requirements forcing industries to adopt modern technique rather than local forcing the industries to adapt better techniques like CAD / CAM / CAE, etc.

3.2 COMPLETE DESIGN OF A FUEL TANK MOUNTING BRACKET:

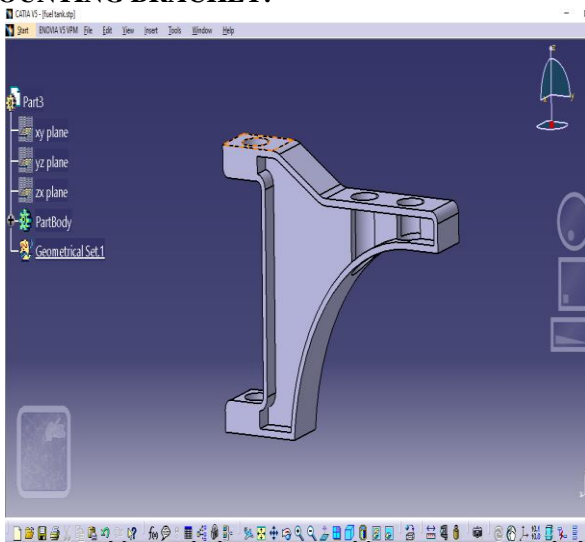


Figure: 3.1 Complete Design of a Fuel Tank Mounting Bracket

4. FINITE ELEMENT METHOD

4.1 FINITE ELEMENT METHOD:

The finite element analysis (finite element method) is a numerical technique for finding approximate solutions of partial differential equations as well as of integral equations. The solution approach is based on either eliminating the differential equation completely (steady state problems) or rendering the partial differential equation into an approximating system of ordinary differential equations, which are then numerically integrated using standard techniques such as Euler's method, Runge-Kutta method etc.

4.2 HISTORICAL DEVELOPMENT:

Development of the finite element method closely parallels the timetable of the Development of the digital computer.

Prior to the advent of the digital computer, work during the 1940's involved the approximation of continuous solids as a collection of line elements (bars and beams). However, due to the lack of computation tools, the number of line elements had to be kept to a minimum.

The first appearance of two-dimensional elements appeared in a paper published in 1956 by Turner, Clough, Martin, and Top [1]. However, Clough did not use the term finite element until 1960 in a paper. The 1960's were an era in which most large corporations began installing mainframe computers. However, most finite element analysis work was done as a research exercise, rather than being part of the normal product design cycle.

During the 1980's, many finite element software packages were running on minicomputers along with highly interactive graphically oriented pre-and post-processors. The late 1980's and 1990's found many of these finite element packages being moved onto personal computers. However, even today, some finite element analysis is still done on large scale computers for problems which involve very large models, such as fluid flow computations, casting solidification and some non-linear Structural analysis.

4.3 SPECIFIC CAPABILITIES OF ANSYS: STRUCTURAL ANALYSIS:

Structural analysis is probably the most common application of the finite element method as it implies bridges and buildings, naval, aeronautical, and mechanical structures such as ship hulls, aircraft bodies, and machine housings, as well as mechanical components such as pistons, machine parts, and tools.

5. ANALYSIS OF FUEL TANK ASSEMBLY

5.1 OBJECTIVE OF THE PRESENT WORK:

The Objectives Of The Project Are As Follows:

- To develop structural modeling of fuel tank and bracket using CATIA
- To perform Modal analysis of fuel tank and bracket by using Ansys 15 for finding natural frequency for basic design
- To perform finite element analysis of fuel tank and bracket by using Ansys 15 for structural steel material for the basic design
- Perform design modifications on basic design to improve natural frequency and avoid high stress locations.
- Perform Modal and Static structural analysis on modified designs.
- Investigate the maximum stress of fuel tank and bracket using ANSYS 15 software
- Results description in terms of factor of safety, stiffens, deformation and stress.

5.2 SCOPE OF PROJECT:

To improve the first natural frequency of a fuel tank brackets for heavy duty vehicles using FEA. To improve the performance of the fuel tank bracket series of design iteration was carried out by taking the account of base model structure. Normal modal analysis for base model is carried out to find the first natural frequency. Normal modal analysis was carried for all the design iteration to improve the first natural frequency of the fuel tank bracket. Static analysis is carried out for all modified designs to find out the Maximum displacement and von misses stress at critical location.

5.3 STATIC STRUCTURAL & MODAL ANALYSIS:

The computer aided design of base model fuel tank mount bracket is shown in figure 5.1. This bracket has been assigned to various design modification by adding stiffeners to base design. Finite Element Analysis is carried out by using ANSYS software.

5.4 HYPERMESH:

ALTAIR HYPERMESH is widely used for meshing for gas turbine rotor blades. It is almost used in all automobile-leading industries. For complex geometries it is best suited. The effective mesh generation is done. The main objective is to check all the element quality checking such as aspect ratio, warpage angle, skew angle, and jacobian. So tetra mesh and mapped mesh of gas turbine rotor blade is done.

5.5 MESHING OF FUEL TANK:

Model is meshed with tetrahedrons second order elements. The meshed model is shown in below figure.

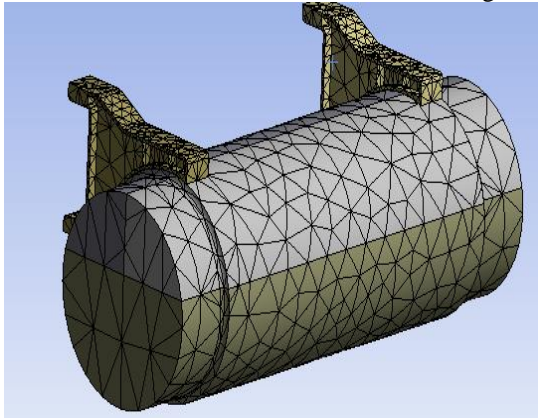


Figure: 5.1 Meshing of fuel tank in Tetrahedral

MESH DETAILS:

Statistics	
<input type="checkbox"/> Nodes	11279
<input type="checkbox"/> Elements	5733
Mesh Metric	None

ELEMENT TYPE:

Solid 187(Tetrahedral second order element)

5.5 LOADS & BOUNDARY CONDITIONS:

Bolt holes of the brackets are fixed in all degrees of freedom. Gravity load applied to the model. Loads & Boundary conditions applied to the model is shown in below figure.

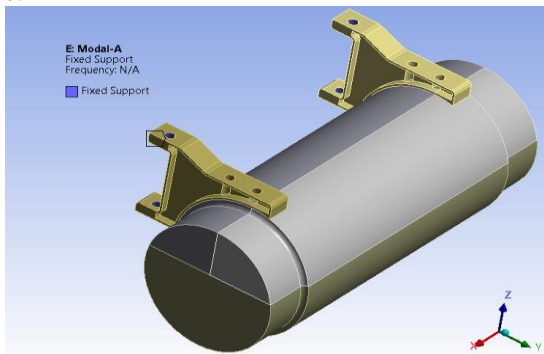


Figure: 5.2 Loads and Boundary Conditions

The above mesh settings and loads & boundary conditions are used for all modified designs in static & modal analysis.

6. RESULTS AND DISCUSSIONS

6.1 STATIC STRUCTURAL ANALYSIS RESULTS:

6.1.1 BASIC DESIGN:

GEOMETRY:

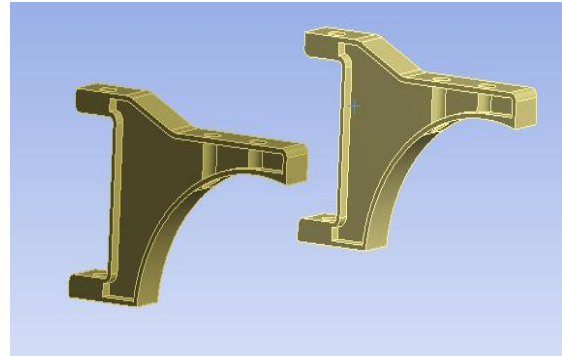


Figure: 6.1 Geometry for the basic design

TOTAL DEFORMATION:

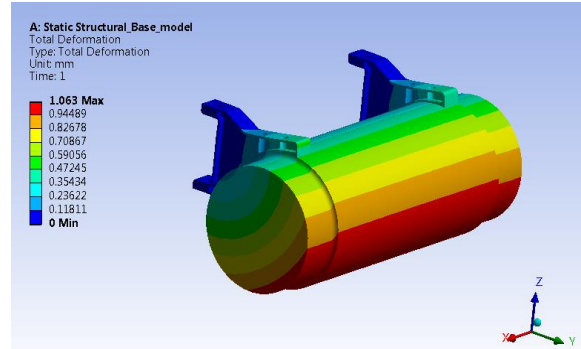


Figure: 6.2 Total deformation in the basic design

The total deformation observed in the structure is 1mm. The result of deformation is as expected behavior and is accepted.

EQUIVALENT STRESS:

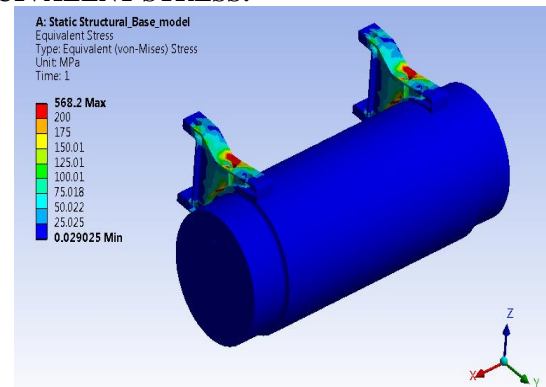


Figure: 6.3 Equivalent Stress structure

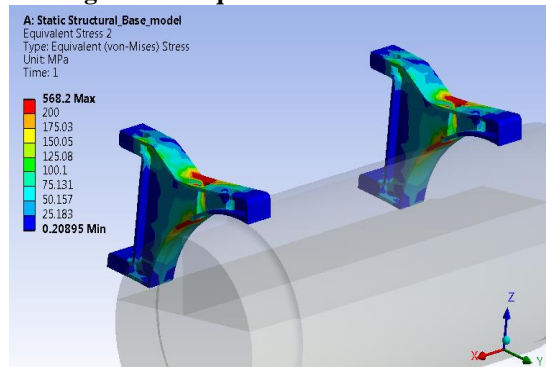


Figure: 6.4 Equivalent Stress brackets

The total equivalent (von mises) stress observed in the structure is **568MPa**.

6.1.2 DESIGN MODIFICATION -1:

GEOMETRY:

From the results observed in the basic design the brackets are getting high stress, to avoid the high stress the following design modification is proposed with adding one stiffener to the existing bracket and FE analysis performed on the modified design.

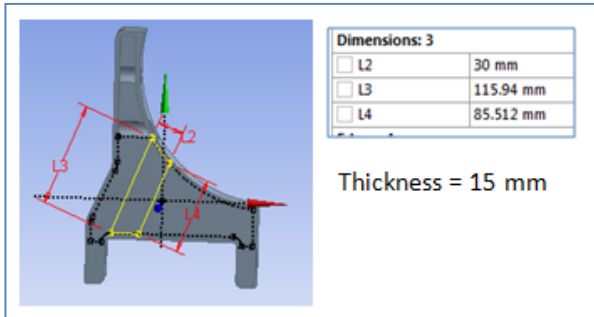


Figure: 6.5 Modified design-1 dimensions

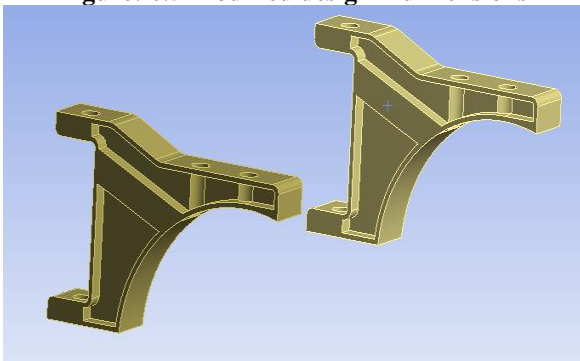


Figure: 6.6 Geometry for the modified design-1

TOTAL DEFORMATION:

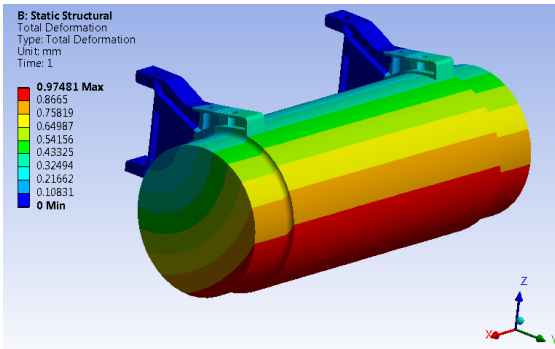


Figure: 6.7 Total deformation in the design modification -1
 The total deformation observed in the structure is **0.97mm**.
 The result of deformation is as expected behavior and is accepted.

EQUIVALENT STRESS:

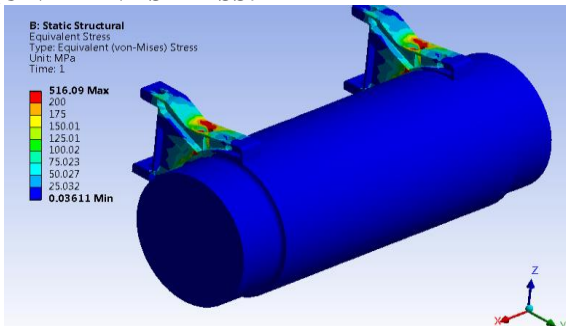


Figure: 6.8 Equivalent Stress structure

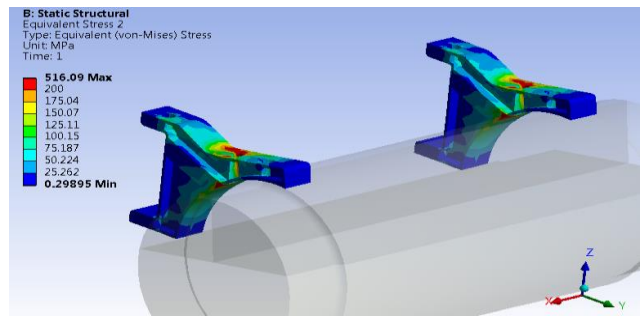


Figure: 6.9 Equivalent Stress brackets

The total equivalent von mises stress observed in the structure is **516MPa**.

6.1.3 DESIGN MODIFICATION -2:

GEOMETRY:

From the results observed in the basic design the brackets are getting high stress, to avoid the high stress the following design modification is proposed with adding two stiffeners to the existing bracket and FE analysis performed on the modified design.

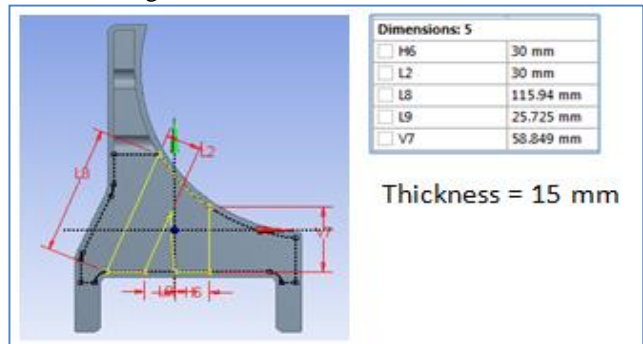


Figure: 6.10 Modified design-2 dimensions

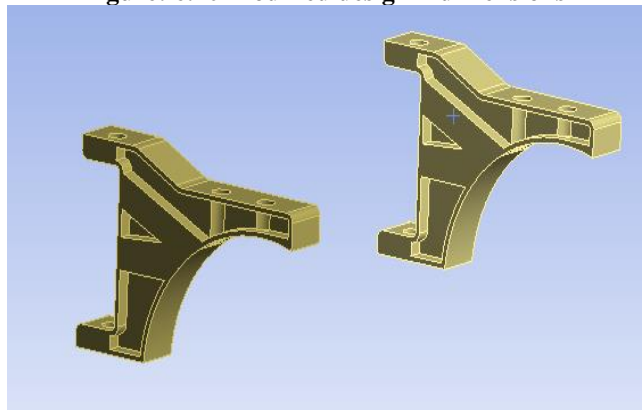


Figure: 6.11 Geometry for the modified design-2

TOTAL DEFORMATION:

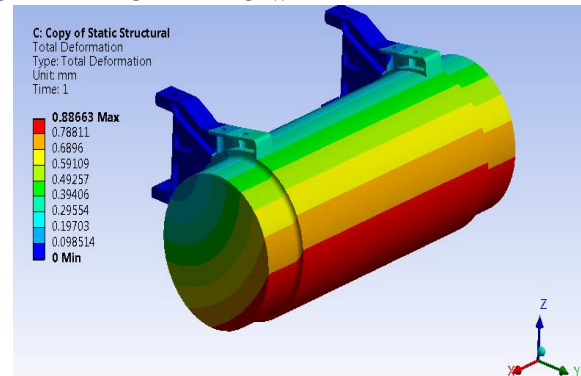


Figure: 6.12 Total deformation in the design modification -2

The total deformation observed in the structure is 0.88mm. The result of deformation is as expected behavior and is accepted.

EQUIVALENT STRESS:

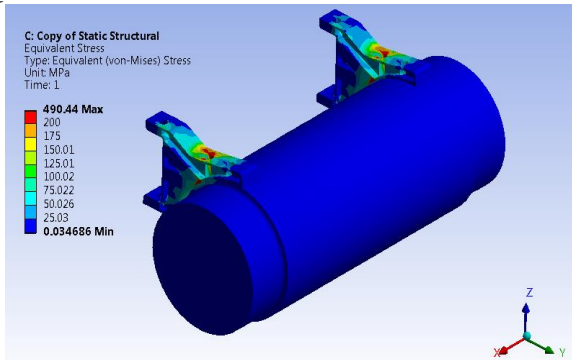


Figure: 6.13 Equivalent Stress structure

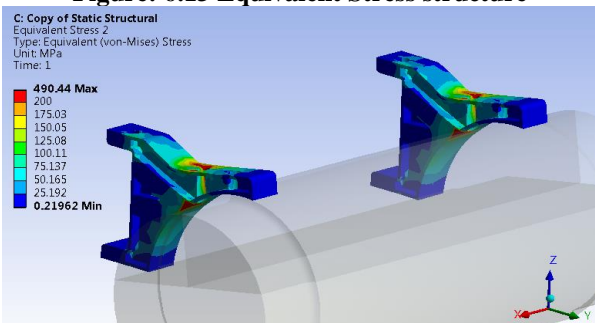


Figure: 6.14 Equivalent Stress brackets

The total equivalent von mises stress observed in the structure is 490MPa.

6.1.4 DESIGN MODIFICATION -3: GEOMETRY:

From the results observed in the basic design the brackets are getting high stress, to avoid the high stress the following design modification is proposed with adding multi stiffeners to the existing bracket and FE analysis performed on the modified design.

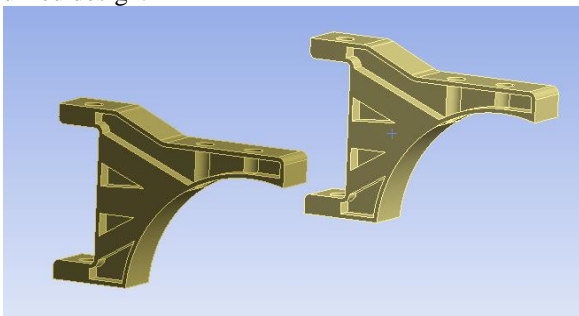


Figure: 6.15 Geometry for the modified design-3

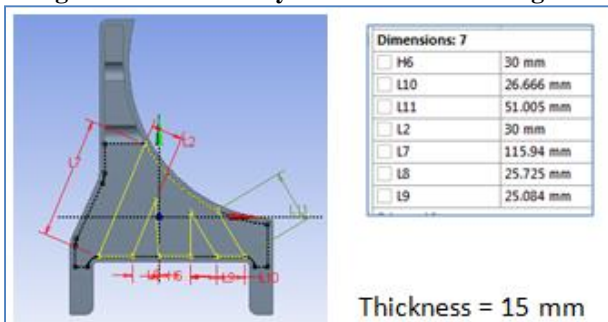


Figure: 6.16 Modified design-3 dimensions

TOTAL DEFORMATION:

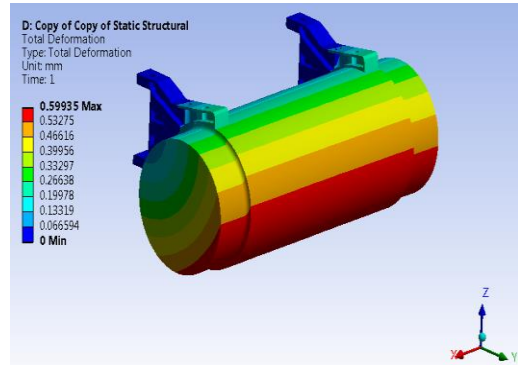


Figure: 6.17 Total deformation in the design modification -3

The total deformation observed in the structure is 0.59mm. The result of deformation is as expected behavior and is accepted.

EQUIVALENT STRESS:

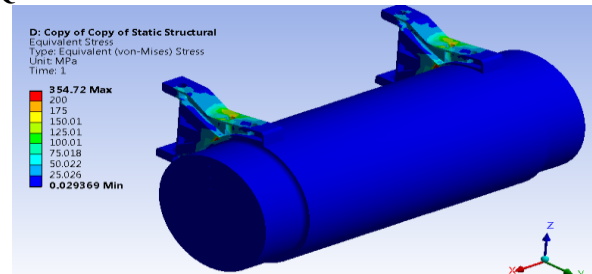


Figure: 6.18 Equivalent Stress structure

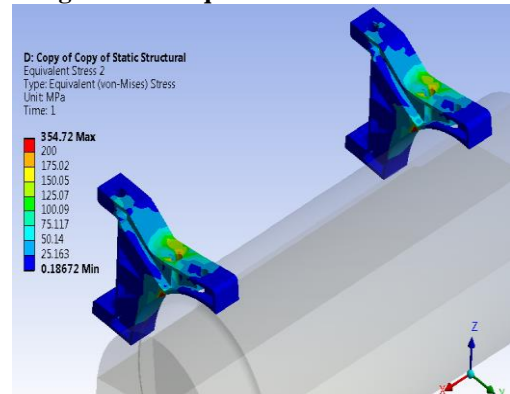


Figure: 6.19 Equivalent Stress brackets

The total equivalent von mises stress observed in the structure is 354MPa.

6.2 MODAL ANALYSIS RESULTS:

Modal analysis performed for the structure to finding the natural frequencies. The frequency results for the basic design and design modifications are presented in below tables.

Tabular Data		
	Mode	Frequency [Hz]
1	1.	70.183
2	2.	112.86
3	3.	371.6
4	4.	410.04
5	5.	568.46
6	6.	746.15

Basic Design

Tabular Data		
	Mode	Frequency [Hz]
1	1.	71.745
2	2.	129.39
3	3.	379.73
4	4.	438.17
5	5.	605.27
6	6.	756.37

Design modification - 1

Tabular Data		
	Mode	Frequency [Hz]
1	1.	72.285
2	2.	132.14
3	3.	384.62
4	4.	440.04
5	5.	607.7
6	6.	763.73

Design modification - 2

Tabular Data		
	Mode	Frequency [Hz]
1	1.	73.284
2	2.	135.33
3	3.	398.51
4	4.	442.72
5	5.	611.98
6	6.	789.1

Design modification - 3

6.3 RESULTS SUMMARY:

The results for the basic design and design modifications are represented in below table.

Design	Deformation (mm)	von Mises Stress (MPa)
Basic Design	1.06	568
Design Mode 1	0.97	516
Design Mode 2	0.88	490
Design Mode 3	0.59	354

7. CONCLUSION

- A successful effort has been made to predict the Eigen values and Eigen vectors of fuel tank mounting brackets assembly by numerical simulation. By comparing the results of all design iterations the following conclusions are made.
- static structural analysis we came to the conclusion that the brackets with multi stiffeners i.e. design modification 3 are giving good results of deformation of 0.59mm and von mises stress of 384MPa. Which are minimal values as compare with basic and other design modifications.
- From the Normal mode analysis that the first natural frequency of multi stiffener fuel tank mounting bracket is 73Hz is good compare to other stiffeners.

8. REFERENCES

- 1) Umesh s ghorpade, Mahendra gaikwad “ FEA and natural frequency optimization of engine bracket” IJMIE, Vol-2, Iss-3, 2012.
- 2) Tatsuo kasuga, Eisei higuchi, “method and structure for mounting a fuel tank” US5794979 A.
- 3) Pavan B. chaudhari, “comparison of Mg, Al and cast iron to obtain optimum frequency of engine bracket using FEA” IJERA, Vol-2, sep-oct 2012.
- 4) Jasvir Singh Dhillon, Priyanka Rao, ”design of engine mount bracket for FSAE car using finite element analysis” IJERA, Vol-4, Iss-9(version 6), September 2014.
- 5) Michael Davis, Zhingxing fu, Qunhui Han, “optimizing fuel tank design for high speed vehicles ”June 9-12 2009.
- 6) Howstuffworks "Transmission Basics" Norton 2004, p. 462
- 7) Lewis, M. J. T. (1993). "Gearing in the Ancient World".*Endeavour* 17 (3): 110–115 [p. 110]. doi:10.1016/0160-9327(93)90099-O.
- 8) "The Antikythera Mechanism Research Project: Why is it so important?", Retrieved 2011-01-10 Quote: "The Mechanism is thought to date from between 150 and 100 BC"
- 9) *ANSI/AGMA 1012-G05*, "Gear Nomenclature, Definition of Terms with Symbols".
- 10) Khurmi, R.S, *Theory of Machines*, S.CHAND
- 11) Schunck, Richard, "Minimizing gearbox noise inside and outside the box.", *Motion System Design*.
- 12) Doughtie and Vallance give the following information on helical gear speeds: "Pitch-line speeds of 4,000 to 7,000 fpm [20 to 36 m/s] are common with automobile and turbine gears, and speeds of 12,000 fpm [61 m/s] have been successfully used." – p.281.,*Helical gears*, retrieved 15 June 2009.
- 13) *McGraw Hill Encyclopedia of Science and Technology*, "Gear", p. 742.
- 14) Canfield, Stephen (1997), "Gear Types", *Dynamics of Machinery*, Tennessee Tech University, Department of Mechanical Engineering, ME 362 lecture notes.
- 15) Hilbert, David; Cohn-Vossen, Stephan (1952), *Geometry and the Imagination* (2nd ed.), New York: Chelsea, pp. 287,ISBN 978-0-8284-1087-8.
- 16) *McGraw Hill Encyclopedia of Science and Technology*, "Gear", p. 743.
- 17) Vallance Doughtie, p. 287,Vallance Doughtie, pp. 280, 296.
- 18) Doughtie and Vallance, p. 290; McGraw Hill Encyclopedia of Science and Technology, "Gear", p. 743.
- 19) *McGraw Hill Encyclopedia of Science and Technology*, "Gear", p. 744.
- 20) Kravchenko A.I., Bovda A.M. Gear with magnetic couple. Pat. of Ukraine N. 56700 – Bul. N. 2, 2011 – F16H 49/00.

FIRE AND GAS SAFETY ALARM PROTOTYPE USING ARDUINO

B. Venkata Siva, P. Gopinadh, D.Santhosh, O.Veeranjanyulu, S. Manikumar and L. Rajasekhar

Department of Mechanical Engineering, Narasaraopeta Engineering College, Narasaraopeta, Palnadu (Dist.), A.P.

Abstract - Public security and environment safety is a big issue in the present day. Smoke, fire, gas, can cause too many issues and causes accidents at home and industrial areas. To decrease chances of such accidents it is essential to take necessary steps such like entertain security-based projects. GSM based smart safety system is a solution to such necessary problems. It provides the fool proof security to industries and homes. The system consists of alarming system, smart SMS alert. The system observes the environment using sensors for smoke, gas, flame, vibration and in case any problem it alerts the related person. The system uses the Arduino UNO as micro-controller and sensor used for smoke is MQ-2, gas MQ-5. The system acquire data using sensors and then transmit to Arduino. Arduino further transmit data to the c#based application and a GSM module is used which send SMS to the relevant person. The alarm device is added to alarm.

Keywords: *IoT, Arduino IDE, Fire Sensor, Gas Sensor, GSM module, Buzzer.*

I. INTRODUCTION

Nowadays, securing one's property and business against fire is becoming more and more important. Monitoring commercial and residential areas all-round is an effective method to reduce personal and property losses due to fire disaster. Home fire detection is a matter of great concern, and thus many efforts are devoted in most developed countries to the design of automatic detection systems. A fire alarm system should reliably and in a timely way notify building occupants about the presence of fire indicators, such as smoke or high temperatures. A fire detector is usually implemented as a smoke sensor due to its early fire detection capability, fast response time and relatively low cost. Other options for the fire detection are based on gas sensors or temperature sensors fire detectors that use a single sensor, generally a smoke sensor, and present high false-alarm rates due to temperature changes. In order to prevent fires from occurring or minimize their impact, accurate and early detection is essential, and automatic fire detection is becoming very essential to reduce the fire in the building and industry. Automatic fire alarm system provides real-time surveillance and monitoring. A key aspect of fire protection is to identify a developing fire emergency in a timely manner, and to alert the building's occupants and fire emergency organizations. This is the role of fire detection and alarm systems. Generally, fire detectors are designed to respond at an early stage to one more of the four major characteristics of combustion, heat, smoke, flame or gas. No single type of detector is suitable for all types of premises or fires. Heat detectors respond to the temperature rise associated with a fire and smoke detector respond to the smoke or gas generated due to fire. Fire alarm system plays an important role in maintaining and monitoring the safe of all kind Environments and situations. However, the usability of many existing fire

Alarm system is well known but could be produce with high cost. Subsequently, it is not affordable for the low-income users. The main objective of this project is to make a fire control system with low cost. The project has three main systems the detection system the monitoring system and the appliance system. The detection system operates as the fire detector and smoke detector. This paper discusses the design and implementation of a fire alarm system using the ARDUINO UNO R3 which operates the entire system. The detectors are placed in parallel in different levels. The entire system is controlled by microcontroller. The microcontroller is programmed in such way by using C-Programming with ARDUINO IDE. From the project done, the System can detect smoke, flame, heat etc. sensed by the detector, followed by the monitoring system which indicates smoke, light, flame, heat etc. at that particular level. Finally, when the sensors form each level triggered individually, the main Buzzer operates, send SMS.

II. LITERATURE SURVEY

The device which is used to detect the gas is already present the market which is widely used in many places like industries where there is plenty of chances of the explosion which may lead to massive destruction and the loss of man power; in homes, where the LPG gas used most widely in our daily necessity where it can detect the leakage of LPG gas; in cars, where most of the vehicles contains the cylinder and many more places.

Authors of [1] proposed system defines that detection and monitoring of the LPG gas is sensed using MQ 5 sensors. In the system, when the leakage of gas is detected, the buzzer will be on, along with that the alert message will be displayed in the LCD. And while monitoring of gas based on the cylinder weight, which is measured using the load sensor, it will send the message to the owner of the application or system. Authors of [2] proposed system, the authors used the push bullet for the rapid transfer of the data of the message using the Wi-Fi module which functions when there is leakage of gas which is connected to the Arduino UNO. Authors of [3] proposed system, the sensor which is used to detect LPG gas is MQ 6, for methane gas, the sensor used is MQ 4, and benzene is detected using the sensor using MQ 135 respectively. The output of the sensors will be given in form of PPM. Further, ESP32 is used for the sending and receiving of the messages. Authors of [4] proposed system, the application is for the monitoring of the gas where it sends the message. Node MCUs is powered as the sensors where the load sensors always monitor the cylinder. If the weight is less, then it will be displayed using Arduino. Authors of [5] proposed system, where the LPG gas management is

proposed for the cost which is low. Along with detection and monitoring, the system also calculates the temperature and humidity concentration. Authors of [6] For sites where fire occurrences are unavoidable, the improvement and revolution of fire monitoring using information and communication technologies has strategic significance. Automated fire detection and alert system (FDAS) technology is a very promising green technology for the future in sensing fires efficiently compared with the traditional systems of fire detection. Authors of [7] The potential value of integrating fire safety considerations as one of the many variables that should be optimized during building design processes, has been revealed by several decades of advances in fire safety science but in some cases, fire safety prescriptive considerations are still unknown among some building design community. Authors of [8] The role of fire detection and alarm systems are to identify a developing fire emergency in a timely manner, and to alert the building's inhabitants and fire emergency establishments. Fire detection and alarm systems can provide several main functions. First, they provide means to identify a developing fire through either manual or automatic methods. Second, alerts building occupants to a fire condition and the need to evacuate. Lastly is the transmission of an alarm notification signal to the fire department or other emergency response organization. They may also shut down electrical, air handling equipment or special process operations, and they may be used to initiate automatic suppression systems. Authors of [9] Fire alarms in absence of a real fire condition in terms of fire safety engineering are false alarms. False alarms occur as side effect of system technologies and the alerting process. Considering damages often associated to fire, time is a critical factor in fire detection that is often accomplished by installed fire detection and fire alarm systems. Authors of [10] Some fire detectors are based on the detection of smoke by scattering lights and during combustion process, most but not all fires emit smoke aerosols. False alarms will almost certainly occur as smoke particles are only one sort of airborne particulate matter. It is coherent to upgrade photoelectric fire detectors or even replace them for specific settings with gas sensor-based technologies as every fire is producing specific gases.

III. BASIC IDEA OF THE PROJECT

Gas leakage and fire accident are the main problems in industrial area and also in residential area causes many health issues and accidents. Thus, to prevent such disasters happen, the atmosphere of a workplace should be regularly monitored and controlled, in order to maintain the clean air environment. However, efforts in industrial air quality control have been impeded by the lack of science-based approaches to identify and assess atmosphere air quality and level of dangerous gas. Therefore, a monitoring system for gas leakage detection needs to be developed. The project is about GSM based Gas Leakage Monitoring system. In this project GSM module is used to send the alert message and, in this project, we used buzzer it is also to alert nearby people.

IV. HARDWARE INTEGRATION

MQ2 Gas Sensor:

The MQ2 gas sensor is an electronic sensor which is used to detect ambient gas concentrations such as LPG, propane, methane, hydrogen, alcohol, smoke, and carbon monoxide. It contains a sensing material whose resistance, when in contact with the gas, changes. The MQ-2 Gas detection

sensor module has four pins VCC, GND, Aout, and Dout that can be used to get the needful information out of the sensor. It will sense the gas percentage and sends the value to the Arduino in that having microcontroller from that it will display the value and any issues came means it will send to some output signals like SMS by using gsm and sound by using buzzer.



Fig.1:MQ2 Gas Sensor

FIRE SENSOR:

There are many types of flame sensors available in the market but we will use IR infrared flame sensor module in this tutorial. A picture of this flame sensor is shown below. As you can see in the picture, the main component of this sensor is an IR receiver that is a photodiode. This photodiode is used to detect flame and fire. The flame sensor is used to detect fire or other light sources which are in the range of wavelength from 760nm to 1100nm. The module consists of an IR sensor, potentiometer, OP-Amp circuitry, and a led indicator. When a flame will be detected, the module will turn on its red led. This module is sensitive to flame but it can also detect ordinary light. The detection point is 60 degrees. The sensitivity of this sensor is adjustable and it also has stable performance.

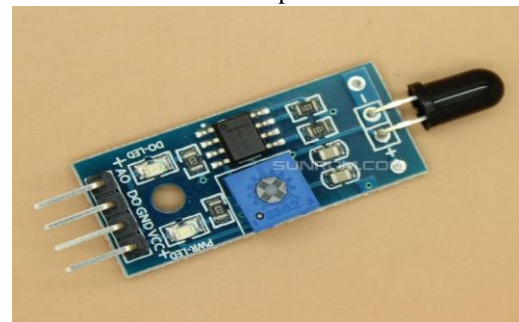


Fig.2: IR Fire Sensor

Ribbon Cable:

A ribbon cable is a collection of flat small-grade cables that are seemingly connected together and made to form a ribbon. The core of the insulator connects each lane of cable together making it seem like they are one single cable but are actually single sized independent cables. The ribbon cable is also known as the multi-wire planar cable is basically used for short distance peripheral connection such as is seen in most tech gadgets such as computers, mobile phones, and hard drives.



Fig.3: Ribbon cable

Arduino UNO:

Arduino UNO is a low-cost, flexible, and easy-to-use programmable open-source microcontroller board that can be integrated into a variety of electronic projects. This board can be interfaced with other Arduino boards, Arduino shields, Raspberry Pi boards and can control relays, LEDs, servos, and motors as an output.

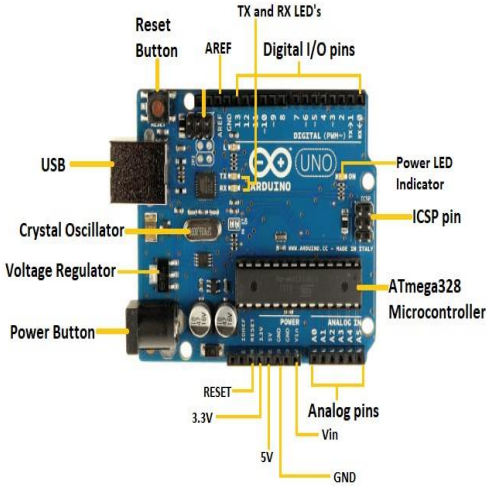


Fig.4: Arduino UNO

Gsm Module:

SIM900A GSM Module is the smallest and cheapest module for GPRS/GSM communication. It is common with Arduino and microcontroller in most of embedded application. The module offers GPRS/GSM technology for communication with the uses of a mobile sim. It uses a 900 and 1800MHz frequency band and allows users to receive/send mobile calls and SMS. The keypad and display interface allow the developers to make the customize application with it. Furthermore, it also has modes, command mode and data mode. In every country the GPRS/GSM and different protocols/frequencies to operate. Command mode helps the developers to change the default setting according to their requirements. It will send the alert message to desired number.



Fig.5: Gsm module

Buzzer:

An Arduino Buzzer is basically a beeper. The Arduino buzzer is a device that produces sound when an electric current is passed through it. The Arduino buzzer can be directly connected to the Arduino and produce different tones by giving different frequency electric pulses to the buzzer. As a type of electronic buzzer with integrated structure, buzzers, which are supplied by DC power, are widely used in computers, printers, photocopiers, alarms, electronic toys, automotive electronic devices, telephones, timers and other electronic products for voice devices. Buzzers can be categorized as active and passive ones (see the following picture). Turn the pins of

two buzzers face up, and the one with a green circuit board is a passive buzzer, while the other enclosed with a black tape is an active one.



Fig.6: Buzzer

V.SOFTWARE INTEGRATION

The Arduino Integrated Development Environment or Arduino Software (IDE) contains a text editor for writing code, a message area, a text console, a toolbar with buttons for common functions and a series of menus. The language used is based on C and C++, there are a couple of small differences designed to make Arduinos as easy to use as possible. The Arduino IDE will do some pre-processing to the code to avoid some unwanted errors but other than that it's C and C++.

Installation of Software:

To begin, download the Arduino IDE from the Arduino website. Make sure to select the right version for your Operating System (OS). For a full getting started guide for each OS, please refer to the Arduino guide. Once the arduino.zip file has been downloaded, extract the file to a folder somewhere on your computer.



Fig.7: Arduino Software

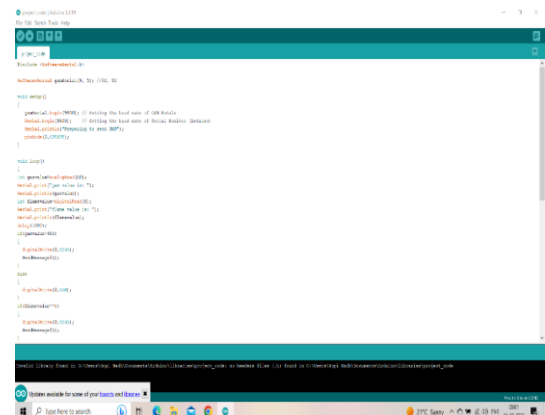


Fig.8: Arduino Code

VI.RESULT



Fig.9: Final Output

VII.ADVANTAGES

- Get real-time alerts about the gaseous presence in the atmosphere
- Prevent fire hazards and explosions
- Supervise gas concentration levels
- Ensure worker’s health
- Real-time updates about leakage
- Cost-effective installation
- Data analytics for improved decisions
- Measure oxygen level accuracy
- Get immediate gas leak alerts

VIII.APPLICATIONS

- Hydrogen stations
- Household and Industries
- Textile industries
- Combustion monitors for burners
- Oil and gas pipelines
- Turbine enclosures

IX.CONCLUSION & FUTURE SCOPE

In recent days, the Internet of Things has acquired its broad prominence. Thanks to its diverse sources of applications that have paved the way for human beings to live in a smooth, healthy and simpler way. The suggested detector of gas leakage in the area of security seems promising. The goal to make this model has always been to introduce a revolution on safety to reduce and therefore eliminate any large or little risk that may arise from the leaking of toxic and hazardous gases. One such application area is monitoring of gas reservations and gas leakages and fire accident for both household and industrial applications. While the identification of gas leak and fire accident has been one of the main problems, while there are numerous

ways. This study therefore provided a new approach, depending on microcontroller, for gas reservation and gas detectors. The sensor employed in this version is capable to monitor, identify and inform the client to the remainder of the pressurized gas, and to also take certain actions without obstructing the prebooking of the new cylinder. It is a low cost but extremely efficient device for detecting gas leakage and may play a key role in avoiding Gas leakage exploration. The major aim of this effort is to maintain security and to make it simpler to reserve gasses and detect leaks to prevent tragedies caused by carelessness. In this project GSM module was successfully implemented and hence, in the any emergency situation alert message will be received. The buzzer alarm was also successfully implemented to provide extra safety in the system. Finally, the developed system can be useful to house hold and industries.

REFERENCES

- [1] Suma V, Ramya R Shekar, Akshay Kumar A, “Gas Leakage Detection Based on IOT,” Proceedings of the Third International Conference on Electronics Communication and Aerospace Technology [ICECA 2019] IEEE Conference Record # 45616; pp.no 1312 – 1315.
- [2] M Athish Subramanian, Naveen Selvam, Rajkumar S, R Mahalakshmi, J Ram Prabhakar , “Gas Leakage Detection System using IoT with integrated notifications using Pushbullet-Control (ICISC 2020) IEEE Xplore Part Number: CFP20J06-ARTI; pp.no 359 – 363.
- [3] Ravi Kishore Kodali, Greeshma, R.N.V, Kusuma Priya Nimmanapalli, Yatish Krishna Yogi Borra, “IOT Based Industrial Plant Safety Gas Leakage Detection System”, International Conference on Computing Communication and Automation (ICCCA), pp.no,
- [4] Nagib Mahfuz, Shawan Karmokar, Md. Ismail Hossain Rana, “A Smart Approach of LPG Monitoring and Detection System Using IoT”, 11th International Conference on Computing and Communication and Networking Technologies (ICCCNT), published in 2020
- [5] Asmita Varma, Prabhakar S, Kayalvizhi Jayavel, “Gas Leakage Detection and Smart Alerting and Prediction Using IoT”, 2017 Second International Conference On Computing and Communications Technologies (ICCT’17) 2017 IEEE, pp.no, 327-333.
- [6] Kechar Bouabdellah, Houache Nouredine, Sekhri Larbi, Using Wireless Sensor Networks for Reliable Forest Fires Detection, Procedia Computer Science, Volume 19, 2013, Pages 794-801,ISSN1877-0509, <http://dx.doi.org/10.1016/j.procs.2013.06.104>.
- [7] Cristian Maluk, Michael Woodrow, Jose Luis Torero, the potential of integrating fire safety in modern building design, Fire Safety Journal, Volume 88, 2017, Pages 104-112, ISSN 0379-7112, <http://dx.doi.org/10.1016/j.firesaf.2016.12.006>.
- [8] Northeast Document Conservation Centerr <https://www.nedcc.org> Date Access: September 9, 2017.
- [9] Sebastian Festag, False alarm ratio of fire detection and fire alarm systems in Germany – A meta-analysis, Fire Safety Journal, Volume 79, 2016, Pages 119-126, ISSN 0379-7112, <http://dx.doi.org/10.1016/j.firesaf.2015.11.010>.
- [10] Ulrich Hofer, Daniel Gutmachera, Fire Gas Detection, Procedia Engineering, Volume 47,2012,Pages1446-1459,ISSN1877-7058,<http://dx.doi.org/10.1016/j.proeng.2012.09.430>.

Characterization of Sugarcane Fiber Reinforced Composite

SK. Riyaz Shalikhhan¹, UCEN Narasaraopet, JNTUK Kakinada. Ch. Venkata Prasad², Assistant Professor, V R Siddhartha Engineering college, Dr.G Sulochana³, Assistant Professor, UCEN Narasaraopet, JNTUK Kakinada.

Abstract- Natural fiber composites expected to be in great demand in the coming years due to increased consumer awareness to reduce the waste and environmental pollution. Bagasse fibers available in plenty as an agro-residue and bio composites derived from such renewable resources offer potential for scale-up and value addition.

The natural, bio-degradable features and chemical constituents of the sugarcane bagasse (SCB) have been attracting attention as a highly potential and versatile ingredient in composite materials. Eco-friendly and low-cost considerations have set the momentum for material science researchers to identify green materials that give low pollutant indexes. Various components of SCB are shown to possess the ability of being applied as raw material for manufacturing of composite materials at multiple levels of properties and performances. Studies on the impacts, performances and applications of SCB in its original condition; transformed forms; treated with appropriate chemicals and/or processes; in combination with materials of distinct properties and manipulation of manufacturing methodologies have been duly considered. This paper attempts to summarize the fabrication methodology for the SCB fiber reinforced composite.

The present work is focused on fabrication of sugarcane fiber reinforced composite, where the sugarcane bagasse are the renewable resources, which are used to create useful and biologically sustainable materials.

By doing this, obtain the properties of sugarcane fiber reinforced composites and the variation of properties according to the densities are observed. The properties of the composite materials are directly depended on the material density and the denser fiber material is available the greater mechanical properties are obtained.

I. INTRODUCTION

Composite materials with natural fibers have gained significant attention in recent years due to their numerous advantages over traditional materials. These composites are a combination of natural fibers and a matrix material, typically a polymer, resulting in a material that possesses enhanced properties and a reduced environmental impact.

Natural fibers, such as jute, flax, hemp, bamboo, and sisal, are derived from renewable resources and offer several benefits. They are lightweight, biodegradable, have excellent mechanical properties, and exhibit low density and high specific strength. These fibers also have good thermal and acoustic insulation properties, making them suitable for a wide range of applications.

When combined with a matrix material, natural fibers create a composite material that capitalizes on the strengths of both components. The matrix material, often a polymer resin like epoxy or polyester, provides improved toughness, durability, and dimensional stability to the composite. The

natural fibers, on the other hand, reinforce the matrix, adding strength, stiffness, and impact resistance.

One of the significant advantages of composite materials with natural fibers is their reduced environmental impact. Compared to traditional composites that rely on synthetic fibers, the production of natural fiber composites requires fewer fossil fuel resources and emits less greenhouse gases. Additionally, at the end of their life cycle, these composites can decompose naturally, minimizing their environmental footprint.

These materials find applications in various industries, including automotive, aerospace, construction, and consumer goods. In the automotive sector, natural fiber composites can be used for interior components, such as door panels and dashboard trims, reducing the overall weight of the vehicle and improving fuel efficiency. In the construction industry, they can be employed in the manufacturing of eco-friendly building materials, like boards, panels, and insulation. Despite their numerous benefits, natural fiber composites also have some limitations. They can be susceptible to moisture absorption, which can affect their mechanical properties and dimensional stability. Furthermore, their production and processing techniques are still evolving, and achieving consistent quality and performance can be challenging.

However, ongoing research and development efforts are addressing these challenges and expanding the applications of composite materials with natural fibers. With their environmentally friendly nature, excellent mechanical properties, and versatility, these composites have the potential to revolutionize various industries while promoting sustainability and reducing our dependence on non-renewable resources.

Krishpersad Manohar et.al.[1] investigates the apparent thermal conductivity for bio-degradable coconut and sugarcane fiber were investigated. *Phanindra et.al.*[2] tested thermal conductivity by varying the volume fraction and by treating fibers with chemicals such as NaOH and Acetone. *Rahul Khantwal et.al.*[3] investigated the flexural and tensile modulus of the polypropylene composites were noticeably improved by the addition of walnut shell flour. *Deepa G. Devadiga et.al.*[4] reviewed various chemical treatment methods and processing techniques used to improve the mechanical, thermal, acoustic, and aging properties of sugarcane bagasse reinforced composites. *Fasika Abedom et.al.*[5] study focuses on the experimental study of composites developed from bagasse fiber/bamboo charcoal for technical applications by investigating its diverse mechanical and thermal insulating properties. *S. S. Bhattacharyya et.al.*[7]

discusses the mechanical and physical properties of sugarcane-based composites, including their tensile strength, flexural strength, and impact strength, and compares them to other natural fibers used in composite materials. The authors conclude that sugarcane-based composites have a promising future in various industries, including the automotive and construction industries, due to their desirable properties and eco-friendliness. *Albuquerque et.al.*[8] discusses the study conducted on the mechanical and thermal properties of sugarcane bagasse fiber reinforced epoxy composites. The authors examine the manufacturing process and evaluate the mechanical properties of the composites, including tensile, flexural, and impact strength, and find that the inclusion of sugarcane bagasse fibers improves the mechanical properties. Additionally, the article examines the thermal properties of the composites, including the glass transition temperature and thermal stability, and concludes that the composites show potential for use in applications requiring high mechanical strength and good thermal stability.

II MATERIALS AND METHODOLOGY

Bagasse is used for multiple purposes, but there is a specific method involved in the fabrication of sugarcane fibre reinforced composite. After the sugarcane plant has been harvested and the liquid has been extracted, the leftover substance (bagasse) is kept wet and then blended with water to form a pulp.

The properties of sugarcane fibre are

- It is 100% biodegradable.
- High tenacity, bulkiness, sound & heat insulation property, low thermal conductivity.
- Moisture - 1.34 %
- Volatile matter - 85.34 %
- Ash - 1.89 %
- High crack control capacity

Sugarcane (*Saccharum officinarum*) is cultivated in considerable quantities in tropical countries. It is used in sugar mills and alcohol mills. But it cannot be consumed entirely by those mills as about 30% pulpy fibrous residue is produced after being utilized in those mills. These residues are called bagasse. The bagasse is used in various applications, including paper industries, as feedstock, as biofuel, etc. Sugarcane bagasse is a lingo cellulosic material. It is generally a kind of waste, which may have some particular uses. Since it contains quite a fair amount of cellulose, this cellulose can be extracted, and that cellulose can have different applications. The fibrous materials may also be used as fiber in the textile and civil engineering sector, too though they may need some unique treatments before being used. More specifically, this bagasse can be used to reinforce composite materials for

creating a totally new type of material. The main advantage of using bagasse is, it is pure waste material, and if this material can be utilized in any application even after a few simple pre-treatments, the process still produces a very economical product, and also the product will surely be fully or partially biodegradable, which is quite an important factor these days. Also, the extracted fiber can show quite good mechanical properties if an appropriate technique is used. The sugar cane stalk can be divided into two portions, the outside rind and an inner pith. The outside rind portion contains longer and finer bundles of fibers, while the inner portion contains the short fibers.



Fig. 1 Sugarcane Bagasse

Here we use 0.1N NaOH solution. The NaOH solution has a normality of 0.1 N which is equal to 0.1 M of NaOH, thus we can say that $N a^+$ and $O H^-$ also have a molarity of 0.1 M. As we know that pOH (strength of base or OH^-) = $-\log(OH^-)$ That is, $pOH = -\log(0.1) = 1$
As we know $pH + pOH = 14$
 $pH = 14 - pOH = 13$.

Methods for effectively extracting fibre from bagasse were investigated in this study by comparing alkaline and enzymatic extraction. Alkaline extraction was performed using different concentrations of sodium hydroxide (NaOH).

The cleaned fibre is soaked in to the solution for 3 to 5 hrs to remove the bacteria and dust from the bagasse and to soften the fiber for extraction. It helps to easily extraction of fiber from the bagasse of the sugarcane and the continuous fiber is easily extracted from the bagasse after drained in atmosphere for 5 to 6 days. The fibre extraction can be easily obtained after the draining process.

A. Fiber Extraction

The bagasse fibres are collected from streets is cleaned in water and dried in 40°C temperature for 5 days. And then chemically treated by submerging them in 500 ml alkaline solution with 10% NaOH at 60–70% for 3 hours. Then, they were rinsed with distilled water to cleanse them from excess

alkaline remnant on the surface then followed by drying up in an oven at temperature of 200°C for 30 seconds.

To extract fibre from plant strips a process called retting is employed. This process involves the action of bacteria and moisture on dried sugarcane strips to dissolve and rot away cellular tissues that surround the fibre in the strips. And this soaking process loosens the fibres and can be extracted out easily. Finally, the fibres were washed again with water and dried at room temperature for about 5 days.



Fig. 2 Fiber Extraction

B. SPECIMEN PREPARATION:

The specimens are prepared according to the standard specimen specification required to perform the required test. The properties of the material are to be found on the different specimen pieces to observe the behaviour of the material. Three number of sample pieces collected with different density values to observe how the properties of the materials is depend on the density values.

The tests are performed to find the mechanical properties are

- i. Tensile test
- ii. Impact test
- iii. Hardness test



Fig. 3 Specimens

III RESULTS AND DISCUSSION

A. Tensile Test

Tensile testing, also known as tension testing, is a fundamental science and engineering test in which a sample is subjected to

a controlled tension until failure. Properties that are directly measured via a tensile test are ultimate tensile strength, breaking strength, maximum elongation and reduction in area. From these measurements the following properties can also be determined: Young's modulus, Poisson's ratio, yield strength.

**TABLE I
TENSILE TEST RESULTS**

S.No	% of Fiber	% of Resin	Tenile Strength(kN/m ²)
1	60	40	0.382
2	70	30	0.396
3	85	15	0.4

B. IMPACT TEST

In materials science, the Charpy impact test, also known as the Charpy V-notch test, is a standardized high strain rate test which determines the amount of energy absorbed by a material during fracture. Absorbed energy is a measure of the material's notch toughness.

The apparatus consists of a pendulum of known mass and length that is dropped from a known height to impact a notched specimen of material. The energy transferred to the material can be inferred by comparing the difference in the height of the hammer before and after the fracture.

**TABLE 2
IMPACT TEST RESULTS**

S.No	Trail Number	Impact of power of specimen 1	Impact of power of specimen 2	Impact of power of specimen 3
1	1	0	0.03	0.06
2	2	0.01	0.02	0.05
3	3	0	0.03	0.06

C. HARDNESS TEST

In materials science, hardness is a measure of the resistance to localized plastic deformation induced by either mechanical indentation or abrasion.

The Rockwell hardness test uses a specific type of indenter, either a diamond cone or a hardened steel ball, which is pressed into the surface of the material under a specified load. The depth of penetration is measured and used to calculate the Rockwell hardness number (RHN) of the material.

The Rockwell scale ranges from A to C, with each scale representing a different combination of load and indenter type. The most common scale is the Rockwell C scale, which

uses a 150kg load and a diamond cone indenter. The RHN is **Specimen Three** expressed as a number, with higher numbers indicating greater hardness.

TABLE 3
HARDNESS TEST RESULTS

S.No	Trail Number	R.H.N. Value of Specimen One	R.H.N. Value of Specimen Two	R.H.N. Value of Specimen Three
1	1	35	42	55
2	2	36	43	56
3	3	35	42	57

TABLE 4
SUMMARY OF TEST RESULTS

S.No	Properties	Specimen One	Specimen Two	Specimen Three
1	Tensile strength	0.509	0.517	0.53
2	Strain	0.135	0.147	0.15
3	percentage of elongation	13.5	14.5	15
4	percentage reduction in area	51	52.5	53
5	Yield Strength	0.352	0.396	0.4
6	Specific Impact Power	0.01	0.03	0.06
7	R.H.N. Value	35	43	57

IV. CONCLUSIONS

The sugarcane fiber reinforced composite material is obtained by required mechanical properties. These are the modern advancements towards the composite materials. The properties which are developed by these sugarcane composites are widely flexible and can be used as alternating materials to various mechanical applications.

By the observations, the properties of specimen three have high Tensile Strength, Specific Impact Power and R.H.N. Values. Therefore, it is better to use the composite material

with high fiber to resin ratio to obtain the greater mechanical properties.

The properties of the composite materials are directly depended on the material density and the denser fiber material is available the greater mechanical properties are obtained. By

doing this project we obtain the properties of sugarcane fiber reinforced composites and the variation of properties according to the densities are observed.

REFERENCES

- [1] Krishpersad Manohar, Dale Ramlakhan, Gurmohan Kochhar, Subhas Haldar, (2006), "Biodegradable fibrous thermal insulation" Journal of Braz. Society of mechanical science and engineering.
- [2] Phanindra, T. Vidyasagar, N. Prabhu Kumar, D. Sai Teja (2014) "Thermal Characterization of Sugarcane Fibre Reinforced Composite", International journal of Engineering Research & Technology (IJERT)
- [3] Rahul Khantwal, Gourav Gupta, Ripudaman Singh Negi (2016) "Walnut Shell Reinforced Composite; A Review", International Journal of scientific & engineering Research, volume 7.
- [4] Deepa G. Devadiga, K. subrahmanya Bhatt, GT Mahesha (2020), "Sugarcane bagasse fiber reinforced composites: Recent advances and applications"
- [5] Fasika Abedom, S. Sakthivel, Daniel Asfaw, Bahiru Melese, Eshetu Solomon, S. Senthil Kumar, (2021) "Development of Natural Fiber Hybrid Composites Using Sugarcane Bagasse and Bamboo Charcoal for Automotive Thermal Insulation Materials"
- [6] Ramakrishnan. S (2022), "Fabrication and Characterization Of Composite From Sugarcane Bagasse, Waste Plastics And Saw Dust For Car Roof Liner Thermal Insulation", International Research Journal of Modernization in Engineering Technology and Science
- [7] "Sugarcane-based composites: An overview" by S. S. Bhattacharyya and S. Rana, published in Journal of Reinforced Plastics and Composites (2012)
- [8] "Sugarcane bagasse fiber reinforced epoxy composites: Mechanical and thermal properties" by P. T. P. Albuquerque, G. C. R. Oliveira, and A. B. de Menezes, published in Polymer Composites (2018)
- [9] "Sugarcane bagasse reinforced polypropylene composites: Effect of fiber content on mechanical and thermal properties" by P. T. P. Albuquerque, G. C. R. Oliveira, and A. B. de Menezes, published in Journal of Reinforced Plastics and Composites (2019)
- [10] "Sugarcane bagasse as a potential reinforcement for thermoplastic composites: A review" by V. C. Aranguren, S. E. Mazzanti, and M. A. Nazareno, published in Journal of Applied Polymer Science (2016)

- [11] "Sugarcane bagasse reinforced thermoset composites: A review" by A. G. Zampaloni and E. L. Lima, published in *Polymer Composites* (2017)
- [12] "Effect of sugarcane bagasse fiber loading on mechanical properties of recycled polypropylene composites" by S. S. Bhattacharyya, S. Rana, and A. K. Mohanty, published in *Polymer-Plastics Technology and Engineering* (2011)
- [13] "Sugarcane bagasse fiber reinforced polypropylene composites: Effect of fiber surface treatments on mechanical properties" by P. T. P. Albuquerque, G. C. R. Oliveira, and A. B. de Menezes, published in *Materials Research Express* (2019)
- [14] El-Hajjar, R., Abou-Kheira, A., & Hassan, A. (2018). Recent advances in sugarcane-based composites: A review. *Journal of Renewable Materials*, 6(1), 1-20.
- [15] Prado, L. A. S. A., Leite, M. C. A. M., Santos, M. S., & Dos Santos, J. F. (2020). Sugarcane Bagasse Reinforced Composites: A Review. *Polímeros: Ciência e Tecnologia*, 30(2).
- [16] Corrêa, A. C., & Telis, V. R. N. (2019). Sugarcane bagasse fiber reinforced composites: A review of processing and properties. *Journal of Polymers and the Environment*, 27(11), 2326-2338.
- [17] A. Ramesh Babu, A. (2018). Sugarcane fiber composites: a review. *Journal of Applied Polymer Science*, 135(3), 45688.
- [18] Sánchez-Sáez, S., Espinach, F. X., & Mutjé, P. (2019). Sustainable sugarcane bagasse reinforced composites. *Industrial Crops and Products*, 139, 111538.
- [19] Khorami, M., & Ganjian, E. (2011). Comparing flexural behaviour of fibre–cement composites reinforced bagasse: Wheat and eucalyptus. *Construction and Building Materials*, 25(9), 3661–3667. <https://doi.org/10.1016/j.conbuildmat.2011.03.052>
- [20] Kordkheili, H. Y., Hiziroglu, S., & Farsi, M. (2012). Some of the physical and mechanical properties of cement composites manufactured from carbon nanotubes and bagasse fiber. *Materials & Design*, 33, 395–398
- [21] La Mantia, F. P., & Morealle, M. (2011). Green composites: A brief review. *Composite Part A: Applied Science and Manufacturing*, 42(6), 579–588.
- [22] Lila, M. K., Shukla, K., Komal, U. K., & Singh, I. (2019). Accelerated thermal ageing behaviour of bagasse fibers reinforced Poly (Lactic Acid) based biocomposites. *Composites Part B*, 156, 121–127.
- [23] Lopez, R., Poblano, V. M., Licea-Clavere, A., Avalos, M., Alvarez-Castillo, A., & Castano, V. M. (2012). Alkaline surface modification of sugarcane bagasse. *Advanced Composite Materials*, 9(2), 99–108.
- [24] Luz, S., Del Tio, J., Rocha, G., & Gonçalves, A. (2008). Cellulose and cellulignin from sugarcane bagasse reinforced polypropylene composites: Effect of acetylation on mechanical and thermal properties. *Composites. Part A, Applied Science and Manufacturing*, 39(9), 1362–1369.
- [25] Mahesha, G. T., Shenoy, B. S., Kini, M. V., & Padmaraj, N. H. (2018). Effect of fiber treatments on mechanical properties of *Grewia serrulata* bast fiber reinforced polyester composites. *Materials Today Proceedings*, 5 (1), 138–144.
- [26] Mahesha, G. T., Shenoy, B. S., Vijaya Kini, M., & Subrahmanya Bhat, K. (2017). Mechanical characterization and water ageing behavior studies of *Grewia serrulata* bast fiber reinforced thermoset composites. *Journal of Natural Fibres*, 14(6), 788–800. Mahesha,
- [27] G. T., Subrahmanya Bhat, K., & Padmaraja, N. H. (2019). Biodegradable natural fiber reinforced polymer matrix composites: Technical updates. *AIP Conference Proceedings*, 2166, 020001.
- [28] Manzoor, A., Khokhar, Z., Hussai, A., Manzoor, A., Uzma, A., Sh., A., Syed, Q., & Blag, S. (2012). Dilute sulphuric acid: A cheap acid for optimization for bagasse treatment. *Science International (Lahore)*, 41–45.
- [29] Mathews, J. F., Skopec, C. E., Nason, P. E., Zuccato, P., Torjet, R. W., Sugiyama, J., Himmel, M. E., & Brady, J. W. (2006). Computer simulation studies of microcrystalline cellulose, Carbohydrate Research. *Carbohydrate Research*, 341(1), 138–152.
- [30] Mooney, C. A., Mansfield, S. D., Touhy, M. G., & Saddler, J. N. (1998). The effect of initial pore volume and lignin content on the enzymatic hydrolysis of softwoods. *Bioresource Technology*, 64(2), 113–119.
- [31] Motaung, T., Linganis, L., John, M., & Anandjiwala, R. (2015). The effect of silane treated sugar cane bagasse on mechanical, thermal and crystallization studies of recycled polypropylene. *Materials Sciences and Applications*, 6(8), 724–733.
- [32] Moubarik, A., Grimi, N., & Boussetta, N. (2013). Structural and thermal characterization of Moroccan sugar cane bagasse cellulose fibers and their applications as a reinforcing agent in low density polyethylene. *Composites Part B: Engineering*, 52, 233–238.
- [32] Mulinari, D. R., Voorwald, H. J. C., Cioffi, M. O. H., Da Silva, M. L. C. P., Da Cruz, T. G., & Saron, C. (2009). Sugarcane bagasse cellulose/HDPE composites obtained by extrusion. *Composites Science and Technology*, 69(2), 214–219.
- [33] Onesippe, C., Passe-Coutrin, N., Toro, F., Delvasto, S., Bilba, K., & Arsene, M. (2010). Sugarcane bagasse fibres reinforced cement composites: Thermal considerations. *Composites. Part A, Applied Science and Manufacturing*, 41(4), 549–556.
- [34] Pandey, A., Soccol, C. R., Nigam, P., & Soccol, V. T. (2000). Biotechnological potential of agro-industrial residues. I: Sugarcane bagasse. *Bioresource Technology*, 74(1), 69–80.

- [35] Pickering, K. L., & Le, T. M. (2016). A review of recent developments in natural fibre composite and their mechanical performance. *Composite Part A: Applied Science and Manufacturing*, 83, 98–112
- [36] Ramleea, N. A., Jawaid, M., Zainudinb, E. S., & Yamani, S. A. K. (2019). Tensile, physical and morphological properties of oil palm empty fruit bunch/ sugarcane bagasse fibre reinforced phenolic hybrid composites. *Journal of Materials Research and Technology*, 8(4), 3466–3474.
- [37] Rodrigues, E. F., Maia, T. F., & Mulinari, D. R. (2011). Tensile strength of polyester resin reinforced sugarcane bagasse fibers modified by esterification. *Procedia Engineering*, 10, 2348–2352.
- [38] Rossignolo, J. A., Rodrigues, M. S., Santos, S. F., & Junior, H. S. (2017). Improved interfacial transition zone between aggregate-cementitious matrix by addition sugarcane industrial ash. *Cement and Concrete Composites*, 80, 157–167.
- [39] Shenoy, B. S., Mahesha, G. T., Kini, M. V., & Padmaraj, N. H. (2019). Effect of chemical treatments on hardness and toughness properties of grewia serrulata reinforced polymer composites. *Journal of Mechanical Engineering Research and Developments*, 42(4), 228–230.
- [40] Thangaraju, R., & Kannan, G. (2016). Evaluation of mechanical characteristics of treated and untreated sugarcane fiber composites. *Journal of Chemical and Pharmaceutical Sciences*, 9(1), 652–656.
- [41] Timung, R., Deshvath, N. N., Goud, V. V., & Dasu, V. V. (2016). Effect of subsequent dilute acid and enzymatic hydrolysis on reducing sugar production from sugarcane bagasse and spent citronella biomass. *Journal of Energy*, 2016, 1–12.
- [42] Trindade, W. G., Hoareau, W., Megiatto, J. D., Razera, I. A. T., Castellan, A., & Frollini, E. (2005). Thermoset phenolic matrices reinforced with unmodified and surface-grafted furfuryl alcohol sugarcane bagasse and curaua fibres: Properties of fibres and composite. *Biomacromolecules*, 6(5), 2085–2496.
- [43] Verma, D. (2012). Bagasse fibre Composite-A Review. *Journal of Materials and Environmental Science*, 3(6), 1079–1092.

SMART AUDITORIUM USING ARDUNIO

Mr.CH.Sekhar, Mr.K.PrudhviYashwanthReddy, Mr.V.Avinash, Mr.B.Jagadeesh, Mr.B.Rambabu, Mr.P.Hussian, Mr.J.Madhu

Associate Professor, IV B.Tech., Department of Mechanical Engineering, Narasaraopeta Engineering College, Narasaraopet, Palnadu(Dist.), A.P., India

Abstract -Nowadays, the world's most valuable resource is power. Hence, we must conserve power so that we can pass it on to the next generation. Systems that operate automatically are preferred over those that operate manually. Electric and electronic appliances, as well as other equipment, can be controlled by the power managing and saving project design. In this project, an effort was made to demonstrate a clever technique to manage power usage and power savings in theatres, malls, and other public spaces. The project was created with a low power usage in mind. The Arduino IDE, a four-channel relay, and an Infrared sensor were used to make it happen. The Arduino received the data from the IR sensor and made a wise judgement based on the situation before turning on the lights and air conditioning turned on.

Keywords – IoT, Arduinio IDE, Infrared Sensor, IR Sensor

I. INTRODUCTION

Electrical energy conservation is a top priority in the twenty-first century. Because lights are expensive but vital, the system must be optimised to be both inexpensive and energy efficient. Manually controlling the lights requires a lot of time and effort. Working in this way can result in significant catastrophes and devastation. The major problem with manual light switches is that they waste a lot of energy in the morning because they can't all be switched off at once, and they waste a lot of time talking in the evening when they should be on. When lights are left on at maximum brightness at midnight, that is another instance of waste. The technology starts working by counting the number of individuals present and detecting when they enter the theatre. This quantity is the fan-like devices' control parameter. The entrance gate's buzzer and metal detector will both be activated to look for metal. A signal is sent to the microcontroller by the entry sensor and exit sensor, which are installed at the entrance and exit gates, respectively, to detect persons entering and leaving the auditorium. The microcontroller then uses this signal to display the number of people inside on the LCD panel. The route light points patrons towards an open seat beginning in the first row as they enter the theatre. The temperature sensor in the auditorium senses input and output, turns on the fan, and modifies its velocity dependent on temperature. It also generates a temperature-related voltage that controls the fan's speed inside the auditorium. The system needs a constant power source to function properly.

II. EXISTING DESIGN



Figure.1:Normal Auditorium

In the present days auditorium when the people are in the Single Count also all the Lights & Fans will get turned on. By this wastage of the power will become more. When we are leaving the room also we need to turn OFF all the Switches.

III. PROPOSED METHOD

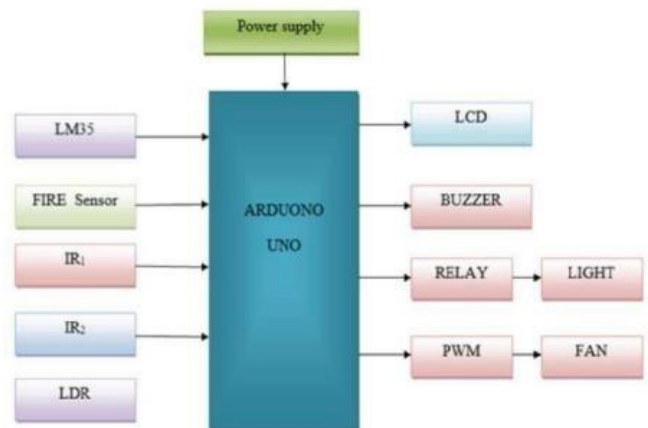


Figure.2: Block diagram of the Smart Auditorium

The first step in the system's operation is identifying each person who enters the auditorium and keeping count of how many individuals are present. This count serves as the control parameter for devices like fans. The buzzer will activate if metal is detected by the metal detector, which is located at the entrance door. To monitor who enters and leaves the theatre, entry sensors and exit sensors are placed at the entrance and exit doors. This sends a signal to the microcontroller, which then displays the number of people

inside on the LCD panel. When someone enters the theatre, a path light will direct them towards an empty seat, beginning in the first row. The temperature sensor will measure the temperature in the auditorium and provide a voltage in accordance with temperature, which regulates the speed of the fan there.

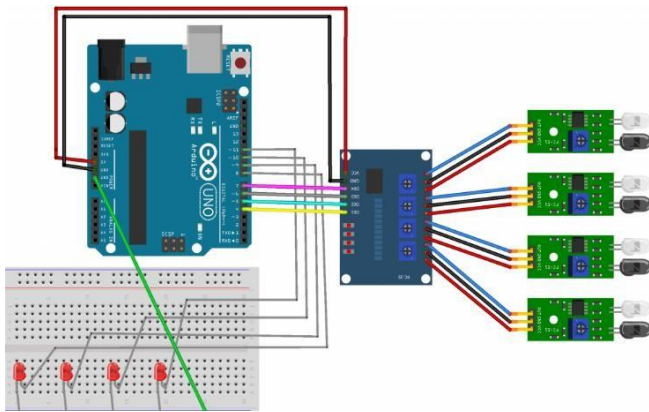


Figure.3: Circuit diagram of the Smart Auditorium

The ATmega328P-based Arduino UNO is a microcontroller board. It has 14 digital I/O pins (of which 6 can be used as PWM outputs), 6 analogue inputs, a ceramic resonator operating at 16 MHz, a USB connection, a power jack, an ICSP header, and a reset button. It comes with everything you need to support the microcontroller; simply connect it to a computer via USB or power it via an AC-to-DC adapter or battery to get started.

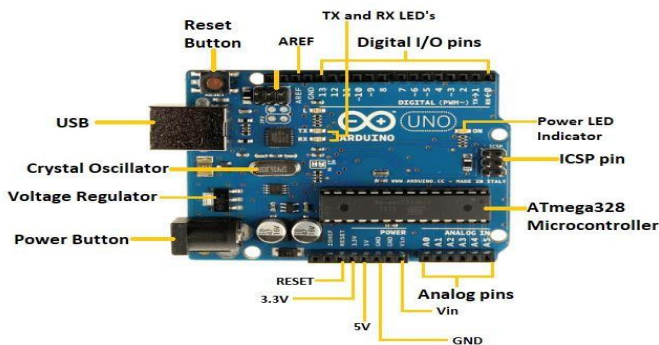


Figure.4: Arduino Uno

IR sensor is an electronic device, that emits the light in order to sense some object of the surroundings. An IR sensor can measure the heat of an object as well as detects the motion. Usually, in the infrared spectrum, all the objects radiate some form of thermal radiation. These types of radiations are invisible to our eyes, but infrared sensor can detect these radiations. The emitter is simply an IR LED (Light Emitting Diode) and the detector is simply an IR photodiode. Photodiode is sensitive to IR light of the same wavelength which is emitted by the IR LED. When IR light falls on the photodiode, the resistances and the output voltages will change in proportion to the magnitude of the IR light received. There are five basic elements used in a typical infrared detection system: an infrared source, a transmission

medium, optical component, infrared detectors or receivers and signal processing. Infrared lasers and Infrared LEDs of specific wavelength used as infrared sources.

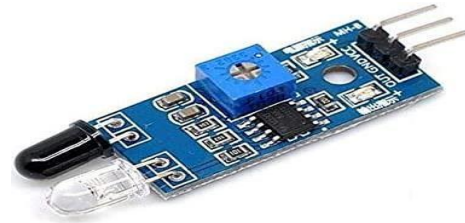


Figure.5. IR Sensor

The 4 Channel Relay Module is a convenient board which can be used to control high voltage, high current load such as motor, solenoid valves, lamps and AC load. It is designed to interface with microcontroller such as Arduino, PIC and etc. The relays terminal (COM, NO and NC) is being brought out with screw terminal. It also comes with a LED to indicate the status of relay. A simple relay consists of wire coil wrapped around a soft iron core, or solenoid, an iron yoke that delivers a low reluctance path for magnetic flux, a movable iron armature and one or more sets of contacts. The movable armature is hinged to the yoke and linked to one or more set of the moving contacts. Held in place by a spring, the armature leaves a gap in the magnetic circuit when the relay is de-energized. While in this position, one of the two sets of contacts is closed while the other set remains open.

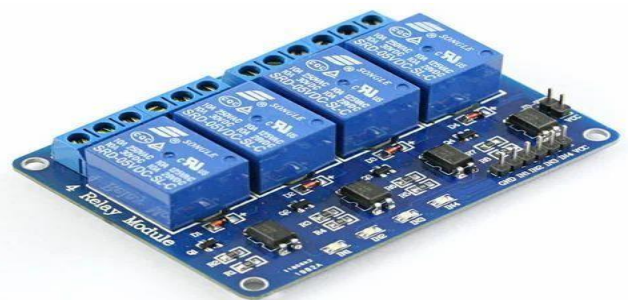


Figure.6. Four-Channel Relay

An LCD (Liquid Crystal Display) screen is an electronic display module and has a wide range of applications. A 16x2 LCD display is very basic module and is very commonly used in various devices and circuits. A 16x2 LCD means it can display 16 characters per line and there are 2 such lines. In this LCD each character is displayed in 5x7 pixel matrix. The 16 x 2 intelligent alphanumeric dot matrix display is capable of displaying 224 different characters and symbols. This LCD has two registers, namely command and data.



Figure.7: LCD Display

A ribbon cable is a collection of flat small-grade cables that are seemingly connected together and made to form a ribbon. The core of the insulator connects each lane of cable together making it seem like they are one single cable but are actually single sized independent cables. The ribbon cable is also known as the multi-wire planar cable is basically used for short distance peripheral connection such as is seen in most tech gadgets such as computers, mobile phones, and hard drives.



Figure.8.Ribbon Cable

A buzzer or beeper is a mechanical, electromechanical, or piezoelectric audio signalling device. Buzzers and beepers are frequently used as alarm clocks, timers, and to validate human input such a mouse click or keyboard.



Figure.9: Buzzer

SOFTWARE IMPLEMENTATION:

The Arduino Integrated Development Environment or Arduino Software (IDE) contains a text editor for writing code, a message area, a text console, a toolbar with buttons for common functions and a series of menus. The language used is based on C and C++, there are a couple of small differences designed to make Arduinos as easy to use as possible. The Arduino IDE will do some pre-processing to the code to avoid some unwanted errors but other than that it's C and C++

Installation of Software:

To begin, download the Arduino IDE from the Arduino website. Make sure to select the right version for your Operating System (OS). For a full getting started guide for each OS, please refer to the Arduino guide. Once the arduino.zip file has been downloaded, extract the file to a folder somewhere on your computer. There is no install - simply open the folder and double click the .exe

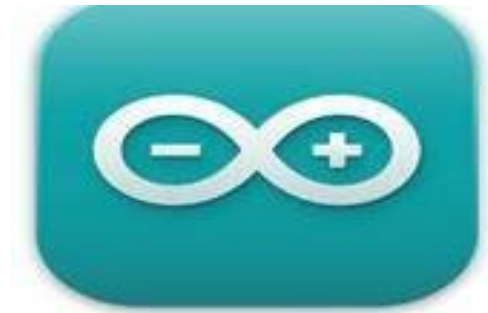


Figure.10:Arduino Software

IV. RESULT

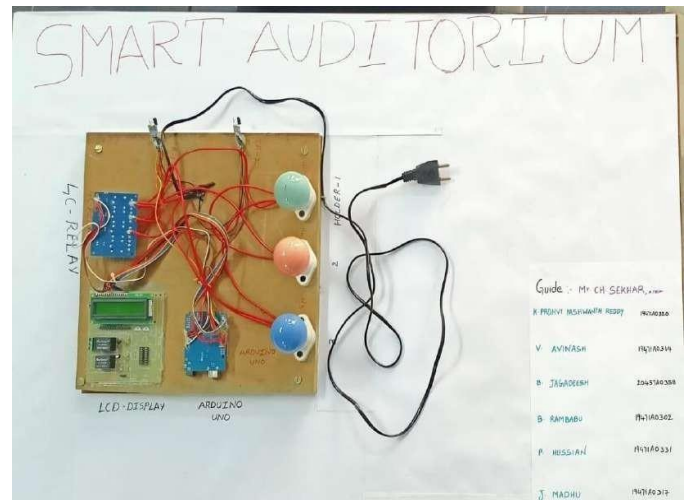


Figure.11: Implemented circuit

A microcontroller, IR and photodiode, and LCD are used in this project. The IR sensor continuously generates a signal, which is observed by the photodiode. If any barriers appear between the IR and the photodiode, the photodiode output is given. On liquid crystal displays, the entire number of people in the room is presented.



Figure.12.Output when the Kit is ON

The microcontroller is responsible for receiving the signals from the sensors mentioned above. A microcontroller, IR and photodiode, and LCD are used in this project. The IR sensor continuously generates a signal, which is observed by the photodiode.



Figure.13. Output when the People are in the Room

V. ADVANTAGES

- Depending on how the PIR sensor is adjusted, they can detect infrared light at a far distance.
- PIR sensors are typically small and adaptable to almost any electrical gadget.
- They have a wide lens range, are quite durable, need little power, and can be readily interfaced with other devices.
- The same item can serve two distinct functions, offering multifunctional qualities.

VI. APPLICATIONS

- Super markets
- Shopping Malls
- Auditorium
- Seminar halls
- Public places

VII. CONCLUSION & FUTURE SCOPE

The primary purpose of the project is to save energy that is wasted in the auditorium when it is empty due to the fan running. The guidance system is a simple technique that is eventually used in order to save energy. Security is provided via the metal detector at the entrance gate. Our system's cornerstone is the Arduino controller, which handles everything from sensing input and output to turning on the fan and adjusting its velocity based on temperature. To keep the system working smoothly, a continual power source is required.

In the future, we will create a scalable distributed architecture to integrate all of the campus's rooms, such as the auditorium, offices, laboratories, meeting rooms, refectories, and so on. We will use artificial intelligence to cure data and monitor sensors in terms of failures, derives, and predict the evolution of environmental parameters to improve temperature management. We will include LoRaWan, an outdoor protocol used to connect devices such as weather stations.

REFERENCES

[1] K. Gupta, S. K. Arora (2007), Industrial Automation and Robotics, 348 pages, Laxmi Publications, ISBN-10: 8131801810
 [2] J. Burroughs (2010), "X-10 Home Automation Using The PIC16F877A" Lamp, vol. 10, article 10
 [3] F. J. Perez-Pinal, C. Nunez and R. Alvarez (2005), "A Novel Speed Control Approach In parallel-connected Induction Motor By Using A Single Inverter And Electronic Virtual LineShafting", IEEE 36th Power Electronics Specialists Conference, (PESC '05), pp. 1339- 1345

[4] D.V. Nicolae and A. A. Jimoh (2007), "A Three-Phase Induction Motor with Power Electronic Controlled Single-

[5] The Internet of Things (The MIT Press Essential Knowledge series) – 20 March 2015.
 [6] The Fourth Industrial Revolution Hardcover – January 3, 2017, by Klaus Schwab(Author).
 [7] Getting Started with the Internet of Things: Connecting Sensors and Microcontrollers to the Cloud (Make: Projects) 1st Edition, Kindle Edition by Cuno Pfister(Author)
 [8] X. Fang, S. Misra, G. Xue, and D. Yang, "Smart grid -The new and improved power grid: A survey," IEEE Communications Surveys and Tutorials. 2012
 [9] Y. Yan, Y. Qian, H. Sharif, and D. Tipper, "A survey on smart grid communication infrastructures: Motivations, requirements and challenges," IEEE Communications Surveys and Tutorials. 2013.
 [10] "The Smart Grid," in The Internet of Things: Key Applications and Protocols, 2011.
 [11] N. Komninos, E. Philippou, and A. Pitsillides, "Survey in smart grid and smart home security: Issues, challenges and countermeasures," IEEE Communications Surveys and Tutorials. 2014.
 [12] J. L. Hernández-Ramos, M. V. Moreno, J. B. Bernabé, D. G. Carrillo, and A. F. Skarmeta, "SAFIR: Secure access framework for IoT-enabled services on smart buildings," in Journal of Computer and System Sciences, 2015.
 [13] A. R. Metke and R. L. Ekl, "Security technology for smart grid networks," IEEE Trans. Smart Grid, 2010.
 [14] M. Yigit, V. C. Gungor, and S. Baktir, "Cloud Computing for Smart Grid applications," Computer Networks. 2014.
 [15] E. O. B. Ogedengbe, O. I. Saka, G. E. Azeez, and N. A. Tihamiyu, "Minimum energy performance assessment of air-conditioners in a university indoor environment," in 15th International Energy Conversion Engineering Conference, 2017, 2017

FATIGUE CHARACTERIZATION OF A356-SiC METAL MATRIX NANO COMPOSITES BY USING STIR CASTING METHOD

Dr.D. Suneel, Mr.R. Anil, Mr.T.Radha krishna, Mr.V. Yoganjaneyulu, Mr.P.Kalyan..

Vice Principle1, IV B.Tech.2-6, Department of Mechanical Engineering, Narasaraopeta Engineering College, Narasaraopet, Palnadu(Dist), A.P, India.

Abstract - Composite materials are now a major field of research and development activity. Composites are rapidly becoming important and useful structural materials, and probably the next major area for polymer applications is in the field of composite materials. Aluminum matrix composites (AMCs) become choice for automobile and aerospace industries due to its tunable mechanical properties such as very high strength to weight ratio, superior wear resistance, greater stiffness, better fatigue resistance, controlled co-efficient of thermal expansion and good stability at elevated temperatures.

In the present work an attempt was made to understand the mechanical behavior of composite, Pure Aluminum alloy, reinforced with Boron Carbide and silicon carbide. Composites are casted using stir casting method. Castings are prepared with a percentile range from 0%,2% ,4% and 6%. An investigation is made on studying the mechanical behavior of the pure base metal when compared with different weight percents of reinforcements. The composites were by varying the weight of percentage of copper particles in aluminum, ranging from 5% and 20%.

The results showed that the addition of copper particles improved the hardness, tensile strength and wear resistances of the composites. However, the density of the composites decreased with increasing copper content. The study provides valuable insights into the potential of using copper as a reinforcement material for aluminum metal matrix composites, which can be used in a variety of engineering applications.

Keywords- Aluminum matrix composites, wear resistance,Hardness, Stir Casting Technique. ,

INTRODUCTION

The choice of the right materials is an arduous engineering challenge to the materials engineer and, if done carefully, can be a springboard to the proper and successful implementation and subsequent operation of the design. There are a host of materials available to the designer, and making the right decision is a vital achievement in putting forth a successful design. Materials are required to perform according to the designer's expectations and must possess and retain the right properties in the working environment throughout the working period Material selection is in most cases a contradictory decision-making process. Lightweight materials will most likely not possess sufficient strength, and brittle materials will not necessarily be good in fatigue resistance, stiffness or toughness The process parameters in various manufacturing processes are controlled in order to avoid the agglomeration of reinforcement particles in the matrix A356 aluminum casting alloy is a 7% Si, 0.3% Mg alloy with 0.2 Fe (max) and 0.10 Zn (max).This has very good casting and machining characteristics.A356 aluminum casting alloy is used for aircraft parts, pump housings, impellers, high velocity blowers and structural castings where high strength is required increased strength, stiffness, wear resistance, and corrosionresistance.



Figure 1: A356 Material

Silicon carbides are advanced composite materials that combine silicon carbide (SiC) ceramic particles or fibers with a metal matrix, typically aluminum, magnesium, or titanium have exceptional mechanical properties, including high strength, stiffness, and wear resistance, as well as excellent thermal conductivity and low coefficient of thermal expansion. The production of SiC typically involves powder metallurgy or casting processes. In powder metallurgy, SiC particles or fibers are mixed with metal powders, compacted into a desired shape, and then sintered to create a dense composite material. In casting, molten metal is poured into a mold containing SiC particles or fibers, and then cooled to solidify into a composite material. SiC offer a unique combination of properties that make them attractive for various high-performance applications. However, they can be more expensive to produce than traditional metal alloys, which can limit their widespread use in some industries. Some examples of SiC include aluminum-SiC, magnesium-SiC , and titanium-SiC. Each type has its own set of unique properties and advantages, making it suitable for different applications.



Figure 2: Silicon Carbide

LITERATURE SURVEY

Two groups of specimens were made in this research, including aluminum alloy specimens reinforced with nano-clay particles and the original un-reinforced alloys for comparison. The fabrication method of original aluminum alloys is a permanent mould gravity casting method described in the following paragraph: The aluminum ingots

were first melted and the temperature was held at 700 °C for 2 hours in an electrical resistance furnace [1] before pouring them into a permanent steel mould. For the production of 1 wt. %, nano-clay particles reinforced specimens with the stir-casting process, as nanoparticles with the chemical composition according to Tab. It should be noted that high stirring time and rotational speed can result in better dispersion of nanoparticles in the melt. On the other hand, it caused the degradation of mechanical properties because of the formation of some undesired chemical components and increasing the gas entrapment in the melt. It should be noted that for the nanocomposite, it took 20 minutes to put the molten aluminum in the steady-state condition after adding the nano clay particles [2]. As a first observation, the finer microstructure of AlSi₉Mg_{0.5} compared to Al-Si alloys could be observed. It was commonly confirmed that the addition of hard particles to the metal-matrix materials resulted in reduction of the grain size [4], which was generally related to the pinning role of particles at the grain boundaries during the solidification. Such a phenomenon in the nano-composites can improve the mechanical strength of the matrix material through the Hall-Petch effect [5] Other researchers investigated the effects of adding SiC nanoparticles on the tensile properties of an Al 7075-T6 alloy and found that the SiC was beneficial in enhancing the tensile properties of the Al alloy. Hamedan and Shamir reported the synthesis of A356 reinforced by SiC nanocomposite using a modified stir casting approach by studying the effects of the main parameters of this approach such as stirring temperature, stirring rate, and the main powder type on the mechanical properties and microstructure of nanocomposites. Their results indicate that with optimized parameters of modified stir casting (stirring temperature and stirring speed are at 750 °C and 700 rpm, respectively, and master powder reinforced by 20 wt.% SiC nanoparticles), tensile tests demonstrated that with 1.0 wt.% nanosized SiC, the yield strength and ultimate tensile strength of the nanocomposite improved, while the ductility is slightly decreased [6]. The optical images of the A356 aluminum alloy and Al-nanocomposites are shown in Figure 3. When nanoparticles were added to the base alloy, the grain size decreased, as reported earlier by Hamedan and Shahmiri [7] According to the research by Bradbury et al. [8], with the decrease in grain size, the specimen's hardness was improved. Hence, the SiC particulates added with Al7075 was studied and found that 20 min stirring time was used for obtaining the maximum strength [9]. In another work, a stirring temperature of 750°C and stirring speed of 700 rpm were used for improving the results of A356/SiC composite [10]. In this work, the primary aim is to explore the microstructure, mechanical properties and wear rate of various combinations of AA7075/SiC/Cu-Fe-Ni hybrid composites. More works showed that the addition of SiC reinforcement with aluminium matrix materials is enhancing the microstructure and mechanical properties of aluminium hybrid composites [11]. However, it has been found that few works have been carried out to find the effect of adding SiC and Cu-Fe-Ni alloy with AA7075 hybrid composites. Hence, the SiC particulates added with Al7075 was studied and found that 20 min stirring time was used for obtaining the

of mechanical stirring. The liquid composite material is then cast by conventional casting methods and may also be processed by conventional metal forming technologies. In stir casting we use stirrer to agitate the molten metal matrix. The stirrer is generally made up of a material which can withstand at a higher melting temperature than the matrix temperature. Generally, graphite stirrer is used in stir casting. The stirrer is consisting of mainly two components cylindrical rod and impeller. The one end of rod is connected to impeller and other end is connected to shaft of the motor. The stirrer is generally held in vertical position and is rotated by a motor at various speeds. The resultant molten metal is then poured in die for casting. Stir casting is suitable for manufacturing composites with up to 30% volume fractions of reinforcement.



Figure 3: Stir casting machine

In this case study, we have used the Horizontal CNC milling machine in CITD, Vijayawada to machine the required dies to produce fatigue specimen. The machining of MS (mild steel) die involves several steps such as cutting, roughing, finishing, and heat treatment.



Figure 4: MS steel die block

maximum strength [12]. In another work, a stirring temperature of 750°C and stirring speed of 700 rpm were used for improving the results of A356/SiC composite [13].

EXPERIMENTATION

Stir Casting is a liquid state method of composite materials fabrication, in which a dispersed phase (ceramic particles, short fibers) is mixed with a molten matrix metal by means

When ensuring Die temperature to the normal room temperature, Die has been disassembled and solidified casting was removed carefully from it. Casting was subjected to fettling to separate specimen from it.



Figure 5: removing specimen from die

Heat treatment (T6) was performed for the castings to increase their mechanical properties and to remove residual stresses if any. To attain it Electric Muffle Furnace was used. A356 alloy and A356- SiC Composite samples are heated to 540°C followed by water quenching till room temperature. After that those samples are reheated to 150°C to 200°C and then cooled in air to room temperature.



Figure 6: Heat treatment process

Specimens were prepared as per ASTM E 8/E 8M - 08 Standard. After being heat treated as stated earlier, the A356 and A356-SiC rods are machined as per the standards to attain the required shape on the lathe machine



Figure 7: Machining

The Dog Bone Shapes of both alloy and composites material are fixed between two centers and then loaded for fatigue test.



Figure 8: Fatigue testing

The test specimens are machined to the dimensions of impact test specimens (IZOD & CHARPY) by milling operation. Izod test specimen is of 75x10 mm petry and having a 45 degree notch (2mm depth) at a distance of 28 mm from one end. Charpy specimen is of length 55x10mm having notch at the middle



Figure 9: Impact test

Since the specimen for hardness testing is of having no specifications, the specimens made for either of above tests are used. Brinnel hardness and rockwell hardness tests are conducted with a load of 100 Kgf.



Figure 10: Hardness test

The specimens are placed under electronic microscope and check the microstructure by using software. The specimens could be seen under magnification about 100x and 400x



Figure 11: Microstructure

RESULT

Fatigue testing is defined as the process of progressive localized permanent structural change occurring in a material subjected to conditions that produce fluctuating stresses and strains at some point or points and that may culminate in cracks or complete fracture after a sufficient number of fluctuations. The following are calculations done to find Fatigue Failure Stress for Pure alloy and composite from fundamentals.

Calculation for A356 alloy:

Fatigue test $(\sigma_x) = 32/\pi D^3$

WERE,

M = Bending Moment

W = Load On The Specimen

L = Length Of The Specimen Between Chuck

And Point Of Load D = Minimum Diameter Of

The Specimen

Diameter Of Test Piece (d) = 18.5mm

Bending Moment (M) = Load Applied \times Bending Distance

= 65.850 \times 40

= 2701.732

Load Applied = Dead Load \times Load Ratio \times 9.81

= 1.6 \times 4 \times 9.81

= 62.850N

Bending Distance(B) = 40Mm

$\sigma_b = 32/\pi D^3$

= 12.88 N/mm²

Calculation For A356-SiC:

WERE,

M = Bending Moment

W = Load On the Specimen

L = Length of The Specimen Between Chuck

And Point Of Load D = Minimum Diameter Of

The Specimen

Diameter Of Test Piece (d) = 18.5mm

Bending Moment (M) = Load Applied \times Bending Distance

= 75.340 \times 40

= 3013.632

Load Applied = Dead Load \times Load Ratio \times 9.81

= 1.6 \times 4 \times 9.81

= 75.340 N

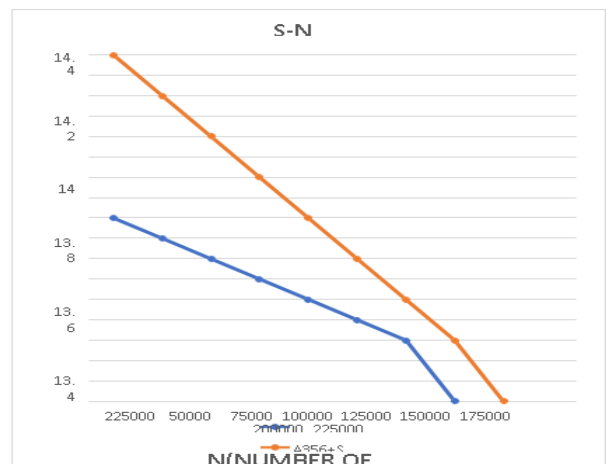
Bending Distance(B) = 40Mm

$\sigma_b = 32/\pi D^3$

= 32 \times 75.85 \times 40/ $\pi \times 133$

= 96436.224 / $\pi \times 133$

= 14.48 N/mm²



s-n curve

The impact test is a method for evaluating the toughness, impact strength and notch sensitivity of engineering materials. The notched test specimen is broken by the impact of a heavy pendulum or hammer, falling at a predetermined velocity through a fixed distance. The quantity usually measured is the energy absorbed in breaking the specimen in a single blow, as in the Charpy impact test and Izod impact test. Specifications are: 55mm \times 10mm; V-notch kept at 27.5mm from any end; V-notch 2mm depth, 2mm width, V-angle-45°. The following calculations are to know the impact strength of pure alloy and composite.

CALCULATIN OF A356:

For Charpy Test

Charpy test = (A-B)/S

Were,

A= without specimen hammer energy

B = specimen after breaking energy

S = cross sectional area of notch

Therefore,

S = 80mm²

A = 300

B = 110

300–110

Charpy = $80 + 190 / 80$

= 1.41 N/mm

For Izod Test

Izod Test = $(A-B)/S$

A= without specimen hammer energy

B = specimen after breaking energy

S = cross sectional area of notch

Therefore,

S = 80mm^2

A = 164

B = 35

Izod Test = $A-B/S$

= $164 - 35 / 80$

= $129 / 80$

= 1.625 N/Mm

Calculation For A356-SiC

For Charpy Test:

Charpy test = $(A-B)/S$

Were,

A= without specimen hammer energy

B = specimen after breaking energy

S = cross sectional area of notch

Therefore,

S = 80mm^2

A = 300

B = 110

Charpy test = $A-B/S$

= $300 - 110 / 80$

= $190 / 80$

= 2.61 N/mm

For Izod Test

Izod Test = $(A-B)/S$

A= without specimen hammer energy

B = specimen after breaking energy

S = cross sectional area of notch

Therefore,

S = 80mm^2

A = 164

B = 35

Izod Test = $A-B/S$

= $164 - 35 / 80$

= $129 / 80$

= 1.85 N/Mm

Hardness is the property of a material that enables it to resist plastic deformation, usually by penetration. However, the term hardness may also refer to resistance to bending, scratching, abrasion or cutting. Hardness here measured using Brinell hardness number.

Brinell Hardness Test for A356:

Were

F = Applied Load IN Kilogram Force

D= Diameter of Indenter (Mm)

d= Diameter of Indentation (Mm)

Hardness(H) = F/A

Hardness (H) = Force/Area

$$HBW = \frac{2P}{\pi D(D - \sqrt{D^2 - d^2})}$$

= $2 \times 1.587 / \pi \times 8.70 (8.70 - \sqrt{8.70^2 - 0.82^2})$

= 72.17 BHN

Rockwell Hardness Test for A356:

Where Ball diameter (D) = 1.587 Mm

= 1/16-inch

Load (W) = 100kg

Hardness Value at first indentation = 60

Hardness value at second indentation = 50

Hardness value at third indentation = 75

The hardness value should be calculated by three values divided by

three

$$\text{Hardness value} = 60+50+75/3$$

$$= 185/3$$

$$= 61.6 \text{ RC}$$

Brinell Hardness Test for A356-SiC

Were

F = Applied Load IN Kilogram Force

D= Diameter of Indenter (Mm)

d= Diameter of Indentation (Mm)

$$\text{Hardness(H)} = F/A$$

$$\text{Hardness (H)} = \text{Force/Area}$$

$$= 2 \times 1.587 / \pi \times 9.70 (9.70 - \sqrt{8.702 - 0.82})$$

$$= 82.17 \text{ BHN}$$

Rockwell Hardness Test for composite:

Where:

For Al356+SiC Specimen:

Ball diameter (D) = 1.587 Mm

$$= 1/16 \text{ inch}$$

Load (W) = 100kg

Hardness Value at first indentation = 80

Hardness value at second indentation = 60

Hardness value at third indentation = 65

$$\text{Hardness value} = 80+60+65/3$$

$$= 205/3$$

$$= 68.8 \text{ Rc}$$

The microstructure of fracture was carried out to make out microstructural degradations after machinability for A356/SiC metal matrix composites for different percentage of reinforcements. Fractures were observed for A356/SiC composites shown in Figure below.

CONCLUSION & FUTURE SCOPE

Fabricated Al MMNCs by taking A356 as a matrix material and nano SiC at 5% weight as reinforcing material by using stir casting. T6-heat treatment is carried out to the castings for improvement in mechanical properties and to remove residual stresses. These heat-treated samples are machined and tested as per ASTM standards for several characterizations like fatigue, hardness, microstructure studies and impact strength.

The fatigue test revealed that the A356-SiC Composite given 14.4 MPa as fatigue stress against to pure alloy of 12.8 MPa with same cyclic load. So, the prepared A356-SiC composite showed good results in Fatigue property.

The impact test reveals that the A356-SiC composites given 2.61 N/mm as toughness value against to pure alloy of 1.41 N/mm with same load .so the prepared A356-sic composites showed good results in impact strength.

Rockwell and Brinell hardness are tested for A356 alloy and A356-SiC composite, the average values are 61.6 RC, 72.17 BHN and 68.33 RC, 82.17 5BHN respectively.

The microstructure of pure alloy and composites are tested under a microscope by visualizing the microstructure to the pure alloy and composites with the help of monitor.

In Current work, fatigue Characterization of A356 metal Matrix Nanocomposite targeted through stir casting technique at a weight Parentage of 0.5. along with other properties like micro-Structure, hardness, Impact, Fatigue strength.

In all above tests, the properties are improved for nanocomposite Compared to Pure alloy. But for microstructure observation, SEM (scanning electron microscope) is to be used as reinforcements are nano particles.

Also, it is observed that reinforcement of nan-particles is becoming a tedious task with an increase in wt.%. Hence an alternate method for stir casting is suggested as a scope for future work.

Due to limited time, composite was prepared with 5% Weight of

reinforcements and the same work may be extended for different weight percentages and with variety of reinforcement materials. Also, low cycle fatigue testing only done in current work. It may be extended for High Cycle and High Temperature Fatigue esting also.

REFERENCES

1. K.A. Venkatesha, K. Suresha, S. Sharma, and S. Sridhar, "Fatigue Behavior of Aluminium 6061 Matrix Composite Reinforced with Alumina and Silicon Carbide Particles using StirCasting Technique," *Procedia Materials Science*, vol. 6, pp. 522- 531, 2014.
2. V. T. Desai, R. K. Vyas, and R. K. Goyal, "Fatigue behavior of Al 6061/SiCp composites fabricated by stir casting," *Materials Science and Engineering A*, vol. 567, pp. 125-130, 2013.
3. S. K. Nath, K. S. K. Narayan, P. S. Robi, and S. M. Waliullah, "Fabrication and Fatigue Behavior of Al/SiCp Composites Prepared by Stir Casting Technique," *Journal of Materials Science Research*, vol. 2, no. 4, pp. 28-36, 2013.
4. V. A. Kodali, R. K. Gangwar, A. Kumar, and R. K. Goyal, "Fabrication and Fatigue Behaviour of Al-MMC Composites Prepared by Stir Casting," *Materials Today: Proceedings*, vol. 5, no. 3, pp. 6645-6652, 2018.
5. S. L. Dharani and T. V. Venkatesha, "Fatigue behavior of AA6061/SiC metal matrix composite fabricated by stir casting," *Journal of Materials Science and Technology*, vol. 28, no. 8, pp. 689-695, 2012.
6. Ramesh, M. R., & Ranganath, M. S. (2014). Fabrication of fatigue specimens by stir casting technique. *International*

Journal of Engineering Research and Technology, 3(7), 2049-2055.

7. Wang, Y., & Zhang, H. (2016). Fabrication of aluminum alloy fatigue specimens by stir casting. *Procedia Engineering*, 148, 1208-1214.

8. Ahsan, M. R., Hoque, M. M., & Shams, M. M. (2018). Fabrication of fatigue specimen by stir casting process for aluminum alloy. *International Journal of Mechanical Engineering and Technology*, 9(11), 1749-1756.

9. Khedkar, M. K., & Kamble, R. R. (2019). Fabrication of aluminum alloy 7075 fatigue specimens using stir casting technique. *International Journal of Innovative Technology and Exploring Engineering*, 8(10), 2739-2743.

10. P. C. P. de Carvalho, A. F. Silva, F. V. Silva, and R. N. Faria Jr, "Influence of stirring speed on the fatigue properties of A356/SiCp composites," *Materials Research*, vol. 16, no. 6, pp. 1298-1303, 2013.

FABRICATION OF FATIGUE SPECIMEN BY USING STIR CASTING METHOD

Penugonda Suresh Babu, G. Hashwanth Praveen Reddy, S. Narendra Babu, V. Yashwanth Sai, SK.MD. Riyaz, G. Vamsi. Department of Mechanical Engineering, Narasaraopeta Engineering College, Narasaraopet, Palnadu (Dist) A.P, India.

Abstract - In this modern world consumers demand for systems and machines that are more energy efficient, stronger, light-weight, cost-effective, etc. In this search for new and advanced materials will remain a subject of interest all the time. The difficulty in designing materials for such stringent specifications cannot be overstated, owing to the conflicting nature of these specifications. Aluminium metal matrix composites are light in weight, highly resistive to corrosion and durable. Due to these properties, aluminium metal matrix composites lead to have various applications in aeronautical, automobile and marine industries. With a variety of reinforcement materials and flexibility in their primary processing, Aluminium metal matrix composites offer great potential for the development of composites with the desired properties for certain applications. The fabrication of fatigue specimens is critical in determining the fatigue properties of materials. Stir casting is a widely used method for fabricating metal matrix composites (MMCs). In this study, a stir casting machine is used to fabricate fatigue specimens from an aluminium alloy reinforced with SiC particles as per ASTM standards. The process parameters, including stirring speed, stirring time, and SiC particle content, were optimized to achieve a uniform distribution of the reinforcement particles in the matrix. The fabricated specimens are tested for surface roughness and microstructure. The results showed that the fabricated specimens of both unreinforced and reinforced fatigue specimens came as per requirements.

Keywords – Aluminium, Silicon Carbide, Dies, Stir Casting.

INTRODUCTION

A356 is an aluminium alloy widely used in engineering applications due to its high strength, good ductility, and excellent casting properties. By incorporating ceramic particles or fibers into the A356 matrix, the resulting composite material exhibits improved mechanical, physical, and thermal properties. The most commonly used reinforcement materials for A356s are ceramic particles such as silicon carbide (SiC) or alumina (Al₂O₃), or fibers such as silicon carbide or alumina. The manufacturing methods for A356 include powder metallurgy, casting, and infiltration. The choice of manufacturing method depends on the desired properties and the application requirements.

In summary, A356 offer improved mechanical, physical, and thermal properties compared to the base A356 alloy, making them suitable for various applications across multiple industries. The incorporation of ceramic particles or fibers into the A356 matrix results in a material with increased strength, stiffness, wear resistance, and corrosion resistance.



Figure: 1. A356 Alloy

Silicon carbides are advanced composite materials that combine silicon carbide (SiC) ceramic particles or fibers with a metal matrix, typically aluminum, magnesium, or titanium have exceptional mechanical properties, including high strength, stiffness, and wear resistance, as well as excellent thermal conductivity and low coefficient of thermal expansion. The production of SiC typically involves powder metallurgy or casting processes. In powder metallurgy, SiC particles or fibers are mixed with metal powders, compacted into a desired shape, and then sintered to create a dense composite material. In casting, molten metal is poured into a mold containing SiC particles or fibers, and then cooled to solidify into a composite material. SiC offer a unique combination of properties that make them attractive for various high-performance applications. However, they can be more expensive to produce than traditional metal alloys, which can limit their widespread use in some industries. Some examples of SiC include aluminum-SiC, magnesium-SiC, and titanium-SiC. Each type has its own set of unique properties and advantages, making it suitable for different applications.



Figure: 2. Silicon Carbide powder

LITERATURE SURVEY

S. Kumar et al. investigated the effect of various parameters on the mechanical properties of Al/SiC composites fabricated by stir casting. The results showed that the addition of SiC particles improved the mechanical properties of the composites. Moreover, the optimum casting parameters for obtaining the highest tensile strength and hardness were identified [1]. N. Venkatesan et al. focused on the fabrication of SiC reinforced A356 composites using stir casting. The results showed that the addition of SiC particles improved the mechanical properties of the composites, including the tensile strength and hardness. The microstructure analysis showed that the SiC particles were uniformly distributed in the matrix [2]. H. Sun et al. compared the microstructure and mechanical properties of A356/SiCp composites fabricated by stir casting and squeeze casting. The results showed that the stir casting process produced composites with a more uniform distribution of SiC particles and better mechanical properties [3]. X. Li et al. investigated the effect of SiC particle size on the microstructure and mechanical properties of A356/SiCp composites fabricated by stir casting. The results showed that the addition of SiC particles improved the mechanical properties of the composites, and smaller SiC particles produced composites with higher strength and hardness [4]. X. Li et al. investigated the effect of stirring speed on the microstructure and mechanical properties of A356/SiCp composites fabricated by stir casting. The results showed that the optimum stirring speed for obtaining the highest mechanical properties was 400 rpm, and higher stirring speeds resulted in decreased mechanical properties due to particle agglomeration [5]. Li et al. proposes a design for a high-cycle fatigue test specimen suitable for small samples, which can be used to test a variety of materials. The authors discuss the fabrication process and the testing methodology for this type of specimen [6]. Al-Badour et al. presents a novel fatigue specimen design that can be used to evaluate the fatigue life of welded structures. The authors discuss the fabrication process and the testing methodology for this type of specimen [7]. Fan et al. investigates the effect of fabrication method on the fatigue performance of titanium alloy components. The authors compare the fatigue performance of components fabricated using traditional casting methods and additive manufacturing methods [8]. Chen et al. presents a novel notched specimen design that can be used to evaluate the fatigue behavior of high-temperature materials. The authors discuss the fabrication process and the testing methodology for this type of specimen [9]. Hua et al. proposes a novel fatigue specimen design for composite materials. The authors discuss the fabrication process and the testing methodology for this type of specimen, and evaluate its performance using experimental testing [10].

EXPERIMENTATION

Initially verified the die design and ensured that it met the necessary requirements, such as material specifications, manufacturing constraints, and functional requirements. Also verified the design using simulation and testing tool to ensure that it meets the necessary performance criteria and thus the die is designed using CATIA.

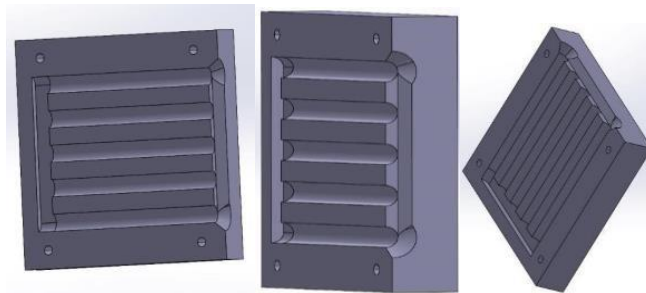


Figure 3. Designed die using CATIA

In this, we have used the Horizontal CNC milling machine at CITD, Vijayawada to machine the required dies to produce fatigue specimen. The machining of MS (mild steel) die involves several steps such as cutting, roughing, finishing, and heat



treatment.

Figure 4. MS steel die block.

For fabrication of fatigue specimen, A356 taken as matrix material and reinforced with silicon carbide (SiC) particles to produce A356/SiC composites through a stir casting process. In this process, heated SiC particles are added to the molten A356 alloy while melting and stirred to distribute the particles uniformly throughout the A356 matrix. The addition of SiC particles to A356 can significantly improve its mechanical properties, such as hardness, strength, and wear resistance, while maintaining its excellent castability. SiC particles act as reinforcing agents, and their high stiffness and strength help to resist deformation and cracking under load. The resulting A356/SiC composite material has a higher strength-to-weight ratio than the A356 alloy alone, making it suitable for use in high-performance applications. The heated liquid material is poured into the preheated metal dies and allowed to solidify to get the required composite bars.

This process creates a fine, uniform microstructure that results in improved mechanical properties compared to traditional casting methods. The use of silicon in A356 alloy promotes the formation of a fine eutectic structure, which enhances the strength and ductility of the material

However, the addition of SiC particles can also affect the casting process, as the particles can settle at the bottom of the melt and create non-uniformity in the material. Therefore, careful control of the stirring

process is necessary to ensure uniform distribution of the SiC particles and to prevent agglomeration or clustering..

Additionally, the production cost of A356/SiC composites can be higher due to the cost of the SiC particles and the additional processing steps required. Nonetheless, A356/SiC composites have a wide range of applications in the aerospace, automotive, and defense industries due to their high strength and wear resistance properties.

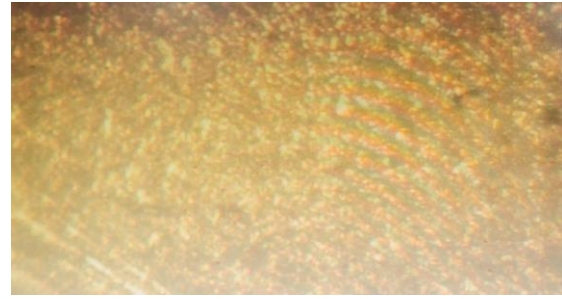


Fig: 7. Micro structure of Pure A356

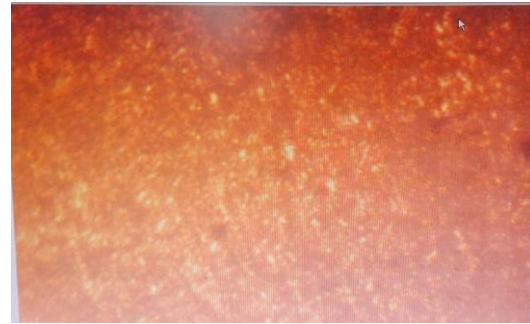


Fig: 8. Micro structure of A356+SiC

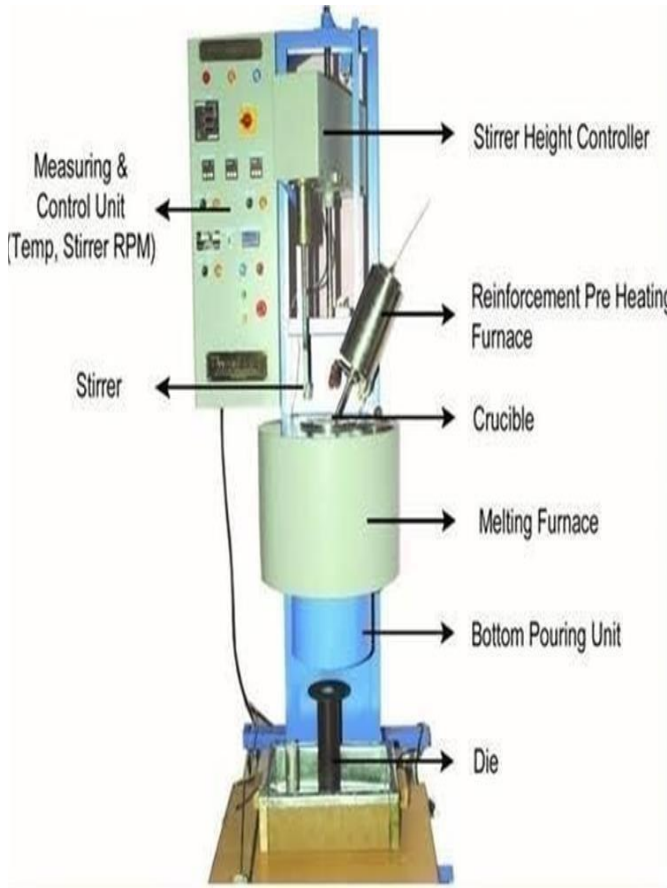


Fig: 5. Stir Casting Setup

RESULT

Due to high strength and hardness of A356 with the reinforcement as SiC of various percentages (with step of 0.05% i.e., 0.05%, 0.1%, 0.15%, 0.2%) and with the help of stir casting machine we have taken four melts and produced A356+SiC MMCs.

Once the molten metal is cooled and solidified composite bars are then collected and inspected for quality. Any defects or imperfections can be identified and addressed before the bars are sent to further processing or assembly.



Fig:6. Produced A356-SiC Composite bars

S.NO	COMPOSITE	ROUGHNESS VALUE (Ra value)
1.	Pure A356	0.540 (µm)
2.	A3556+SiC(0.05%)	0.597(µm)
3.	A356+SiC(0.1%)	0.648(µm)
4.	A356+SiC(0.15%)	0.692(µm)
5.	A356+SiC(0.2%)	0.796 (µm)

Table: 1. Surface roughness values

ADVANTAGES

- For a given weight, composites give higher performance and increase fuel savings. Stiffness weight and strength-to-weight are key metrics in aerospace manufacturing, and composite materials can help boost them.
- Part count gets reduced.
- Minimized production costs since composites production is done through a broad array of processes.

APPLICATIONS

- These composites are being used in
- Automotive industry
- Aerospace and aircraft industry
- Rail transport
- Building and construction industry
- Medical
- Firearms
- Machine making

Microstructures and surface roughness tests are conducted for the obtained specimens and the results were obtained as follows:

Conclusion & Future Scope

The fabrication of fatigue specimens by using stir casting involves incorporating a reinforcement material such as ceramic particles into a metal matrix using a stirring process. First of all the combination of A356 and SiC is selected as a metal and reinforcement material. Then the dies are machined used CNC Milling machines according to the requirement. Then by using stir casting setup A356-SiC fatigue specimen are fabricated successfully and the produced specimens were made to test for the surface roughness and microstructure analysis. The results shows that as the percentage of reinforcement material of SiC increases the surface roughness. Hence, successfully completed work titled as "Fabrication of Fatigue Specimen By Using Stir Casting Method".

Further these fatigue specimen can be tested for fatigue and Impact strengths for future use.

REFERENCES

- 1.K.A. Venkatesha, K. Suresha, S. Sharma, and S. Sridhar, "Fatigue Behavior of Aluminium 6061 Matrix Composite Reinforced with Alumina and Silicon Carbide Particles using StirCasting Technique," *Procedia Materials Science*, vol. 6, pp. 522- 531, 2014.
- 2.V. T. Desai, R. K. Vyas, and R. K. Goyal, "Fatigue behavior of Al 6061/SiCp composites fabricated by stir casting," *Materials Science and Engineering A*, vol. 567, pp. 125-130, 2013.
- 3.S. K. Nath, K. S. K. Narayan, P. S. Robi, and S. M. Waliullah, "Fabrication and Fatigue Behavior of Al/SiCp Composites Prepared by Stir Casting Technique," *Journal of Materials Science Research*, vol. 2, no. 4, pp. 28-36, 2013.
- 4.V. A. Kodali, R. K. Gangwar, A. Kumar, and R. K. Goyal, "Fabrication and Fatigue Behaviour of Al-MMC Composites Prepared by Stir Casting," *Materials Today: Proceedings*, vol. 5, no. 3, pp. 6645-6652, 2018.
- 5.S. L. Dharani and T. V. Venkatesha, "Fatigue behavior of AA6061/SiC metal matrix composite fabricated by stir casting," *Journal of Materials Science and Technology*, vol. 28, no. 8, pp. 689-695, 2012.
- 6.Ramesh, M. R., & Ranganath, M. S. (2014). Fabrication of fatigue specimens by stir casting technique. *International Journal of Engineering Research and Technology*, 3(7), 2049-2055.
- 7.Wang, Y., & Zhang, H. (2016). Fabrication of aluminum alloy fatigue specimens by stir casting. *Procedia Engineering*, 148, 1208-1214.
- 8.Ahsan, M. R., Hoque, M. M., & Shams, M. M. (2018). Fabrication of fatigue specimen by stir casting process for aluminum alloy. *International Journal of Mechanical Engineering and Technology*, 9(11), 1749-1756.
- 9.Khedkar, M. K., & Kamble, R. R. (2019). Fabrication of aluminum alloy 7075 fatigue specimens using stir casting

technique. *International Journal of Innovative Technology and Exploring Engineering*, 8(10), 2739-2743.

10. P. C. P. de Carvalho, A. F. Silva, F. V. Silva, and R. N. Faria Jr, "Influence of stirring speed on the fatigue properties of A356/SiCp composites," *Materials Research*, vol. 16, no. 6, pp. 1298-1303, 2013.

Bending of Composite Plates Using Classical Laminate Plate Theory

Mr. M Gangaraju, Mr. K.Ravi Prasad and Mr. Shaik Fahad, Department of Mechanical Engineering, Mohan Babu University, Tirupati, India

Abstract— Most important aim of this current study is to build up a MATLAB program on fiber Reinforced Composite (FRC) laminates and to investigate how mechanical loading would affect the deflection and the stress & strain distribution of the FRC. The program is established by comparing the computed values with the literature. Laminated composite plates have found widespread applications in the building of engineering structures due to the several attributes of the composites such as light weight, high strength, high stiffness as well as excellent fatigue and corrosion resistance properties. purpose of this work is to develop frequently used laminate plate theory namely the classical laminated plate theory (CLPT) to determine effect of stacking sequence on transverse deflections and stresses in specially orthotropic square laminate subjected to various types of mechanical loads. This work deals with the generation of MATLAB script files that assists the user in the design of a composite.

Index Terms— Composite Laminates, ABD Matrix, Fibre Angle, MATLAB, Stiffness, Composite Design.

I. INTRODUCTION

Composites are extremely versatile materials and may be customized to suit any function. They have found uses from the aerospace industry to common everyday applications. However, one drawback of these materials is tedious design processes [2]. Therefore, in an attempt to reduce this time consuming phase, it was decided to develop a computer program that assisted the user in designing a composite structure. The program needed to perform the necessary calculations in the fraction of the time it would take if done using conventional techniques. Conventional methods for designing composite structures involve the use of Hooke's law for two-dimensional unidirectional composites [1]. Equations relating the stresses and strains in these materials have been developed and are available from various texts. However, these equations are limited to flat unidirectional laminates. The procedure to follow is quite laborious. The material properties, material limits, number of fibre layers, and the fibre orientation and thickness of each layer as well as the loading conditions need to be known.

II. LITERATURE REVIEW

The different methods used to examine the fibre reinforced composite laminate of varying thickness. In the current study, the software MATLAB is used. It provides an easy way to analyze lamina and laminate of fibre reinforced composite by programming the formulae commonly used. The classical

laminated theory is based on the Kirchhoff assumptions, in which transverse normal and shear stresses are neglected. This

implies that the normal stress through the thickness is ignored; an assumption which is also called the "plane stress" condition. This leads to a situation where the displacement through-the-thickness is not necessarily linear and where the plate thickness may change during deformation. While depending on the stacking sequence of varying thickness layers, laminate may also exhibit different response in terms of stress and moment. Therefore, this research will focus on analyzing the fibre reinforced composite laminate of varying thickness where the stress strain, and deflections of laminate will be computed by means of programming approach which based on the classical laminate theory with MATLAB procedure. This method is used to analyze the fibre reinforced composite laminate of varying thickness. It provides an easy way to analyze lamina and laminate of fibre reinforced composite by programming the formulae commonly used.

Each and every data concerning each layer (E_1 , E_2 , G_{12} , ν_{12} , θ , t , $[Q]$, $[T]$, and $[Q]$) were stored in an array. The data in this array was used to calculate the $[A]$, $[B]$, and $[D]$ matrices. Using these matrices and the applied loading conditions, the global and local stresses and strains were computed. The local stresses were compared to the material limits, via the Tsai-Wu failure criterion, to determine whether the composite will fail. A script file was written that controlled the use of each function. The purpose of the functions was to enable easier programming in future. This program was tested against manually calculated examples in the various texts [2] and the results were exactly comparable to the manual computations. In an example (Example 4.3) by Kaw [3], the stresses and strains in a graphite/epoxy composite laminate were examined correspondingly. The resulting global strains, global stresses, local strains and local stresses at the top, middle and bottom of each layer are shown in Table I to V respectively. From this the Conventional Approach program can accurately determine the stresses and strains in a flat unidirectional composite structure. The Conventional Approach script file was further extended to include failure analysis via the Tsai-Wu failure theory. The resulting SR values for the top, middle and bottom of each layer is shown in figure I. The rows represent the layers and columns 1 to 3 represent the top, middle and bottom of each layer. The final aspect involved in the design of a composite structure is the failure analysis. There are various failure theories; however, the Tsai-Wu failure criterion is only one that closely correlates with experimental data.

In order to better facilitate the use of this failure theory. Each stress component was multiplied by a variable [2]. This variable is referred to as the strength ratio (SR) combining

resulted Equation is given as follows.

$$(H_{11}*\sigma_1 + H_{22}*\sigma_2 + H_{66}*\tau_{12})SR + H_{11}*\sigma_1^2 + (H_{22}*\sigma_2 + H_{66}*\tau_{12}^2 + 2H_{12}*\sigma_1*\sigma_2) SR^2 < 1 \tag{1}$$

The purpose of SR is to directly determine by what ratio the local stresses must be increased or decreased to avoid failure. This also directly relates to the applied forces. The criterion for SR is that it can only be positive. If SR is less than 1, then failure occurs because it means that the loading needs to decrease to avoid failure. A SR value of 1 implies that the composite structure is perfectly suited for the applied loading conditions. A value of greater than 1 means that the structure is more than capable of carrying the applied loading and that the loading may also be increased. For example, a SR value of 1.5 means that the loading may be increased up to 50% without failure occurring.

Table I: Material properties, limits and loading conditions for graphite/ epoxy composite Example in Kaw [3].

Material Properties				Material Limits				Forces	Moments	
$E_1(GPa)$	$E_2(GPa)$	$G_{12}(GPa)$	ν_{12}	$(\sigma_1^T)_{ult}$	$(\sigma_1^C)_{ult}$	$(\sigma_2^T)_{ult}$	$(\sigma_2^C)_{ult}$	$(\tau_{12})_{ult}$	N	M
181	10.3	7.17	0.28	1500	1500	40	246	68	1000	0
									1000	0
									0	0

Table II: Analytical values of global strains [3]

Ply #	Position	ϵ_x (m/m)	ϵ_y (m/m)	γ_{xy} (m/m)
1 (0°)	Top	8.944×10 ⁻⁸	5.955×10 ⁻⁶	-3.836×10 ⁻⁶
	Middle	1.6371×10 ⁻⁷	5.134×10 ⁻⁶	-2.811×10 ⁻⁶
	Bottom	2.380×10 ⁻⁷	4.313×10 ⁻⁶	-1.785×10 ⁻⁶
2 (30°)	Top	2.380×10 ⁻⁷	4.313×10 ⁻⁶	-1.785×10 ⁻⁶
	Middle	3.123×10 ⁻⁷	3.492×10 ⁻⁶	-7.598×10 ⁻⁷
	Bottom	3.866×10 ⁻⁷	2.670×10 ⁻⁶	2.655×10 ⁻⁷
3 (-45°)	Top	3.866×10 ⁻⁷	2.670×10 ⁻⁶	2.655×10 ⁻⁷
	Middle	4.609×10 ⁻⁷	1.849×10 ⁻⁶	1.291×10 ⁻⁶
	Bottom	5.352×10 ⁻⁷	1.028×10 ⁻⁶	2.316×10 ⁻⁶

TABLE III: ANALYTICAL VALUES OF GLOBAL STRESSES. [3]

Ply #	Position	σ_x (Pa)	σ_y (Pa)	τ_{xy} (Pa)
1 (0°)	Top	3.351 (10 ⁴)	6.188 (10 ⁴)	-2.750(10 ⁴)
	Middle	4.464 (10 ⁴)	5.359 (10 ⁴)	-2.015(10 ⁴)
	Bottom	5.577 (10 ⁴)	4.531 (10 ⁴)	-1.280(10 ⁴)
2 (30°)	Top	6.930 (10 ⁴)	7.391 (10 ⁴)	3.381 (10 ⁴)
	Middle	1.063 (10 ⁵)	7.747 (10 ⁴)	5.903 (10 ⁴)
	Bottom	1.434 (10 ⁵)	8.102 (10 ⁴)	8.426(10 ⁴)
3 (-45°)	Top	1.235 (10 ⁵)	1.563 (10 ⁵)	-1.187(10 ⁵)
	Middle	4.903 (10 ⁴)	6.894 (10 ⁴)	-3.888(10 ⁴)
	Bottom	-2.547(10 ⁴)	-1.840(10 ⁴)	-4.091(10 ⁴)

TABLE IV: ANALYTICAL VALUES OF LOCAL STRAINS. [3]

Ply #	Position	ϵ_1 (m/m)	ϵ_2 (m/m)	γ_{12} (m/m)
1 (0°)	Top	8.944 (10 ⁻⁸)	5.955 (10 ⁻⁶)	-3.836(10 ⁻⁶)
	Middle	1.637 (10 ⁻⁷)	5.134 (10 ⁻⁶)	-2.811(10 ⁻⁶)
	Bottom	2.380 (10 ⁻⁷)	4.313 (10 ⁻⁶)	-1.785(10 ⁻⁶)
2 (30°)	Top	4.837 (10 ⁻⁷)	4.067 (10 ⁻⁶)	2.636 (10 ⁻⁶)
	Middle	7.781 (10 ⁻⁷)	3.026 (10 ⁻⁶)	2.374 (10 ⁻⁶)
	Bottom	1.073 (10 ⁻⁶)	1.985 (10 ⁻⁶)	2.111(10 ⁻⁶)
3 (-45°)	Top	1.396 (10 ⁻⁶)	1.661 (10 ⁻⁶)	-2.284(10 ⁻⁶)
	Middle	5.096 (10 ⁻⁷)	1.800 (10 ⁻⁶)	-1.388(10 ⁻⁶)
	Bottom	-3.766(10 ⁻⁷)	1.940 (10 ⁻⁶)	-4.928(10 ⁻⁷)

TABLE V: ANALYTICAL VALUES OF LOCAL STRESSES. [3]

Ply #	Position	σ_1 (Pa)	σ_2 (Pa)	τ_{12} (Pa)
1 (0°)	Top	3.351 (10 ⁴)	6.188 (10 ⁴)	-2.750(10 ⁴)
	Middle	4.464 (10 ⁴)	5.359 (10 ⁴)	-2.015(10 ⁴)
	Bottom	5.577 (10 ⁴)	4.531 (10 ⁴)	-1.280(10 ⁴)
2 (30°)	Top	9.973 (10 ⁴)	4.348 (10 ⁴)	1.890 (10 ⁴)
	Middle	1.502 (10 ⁵)	3.356 (10 ⁴)	1.702 (10 ⁴)
	Bottom	2.007 (10 ⁵)	2.364 (10 ⁴)	1.513(10 ⁴)
3 (-45°)	Top	2.586 (10 ⁵)	2.123 (10 ⁴)	-1.638(10 ⁴)
	Middle	9.786 (10 ⁴)	2.010 (10 ⁴)	-9.954(10 ³)
	Bottom	-6.285(10 ⁴)	1.898(10 ⁴)	-3.533(10 ³)

A. Tsai-Wu failure criterion and SR values:

The program asks the user to enter the following: (a) material properties (b) material limits (c) loading conditions. The [Q] matrix and the Tsai-Wu parameters can be calculate straight away as these do not vary with fibre angle but rather with material properties and limits. The program begins with one layer at an angle of 0° and computes the [T], [Q], [A], [B] and [D] matrices. Thereafter the mid-plane strains and curvatures, and, the global and local stresses and strains are calculated. The Tsai-Wu failure theory is applied and a value for SR is obtained for each layer. The program then analyzes the SR values and confirms whether it is in a certain range. The lower limit of this range is 1 as any value below this would mean failure. The upper limit in this range is 1.2 and this is to avoid over designing. If the SR value for each layer is between 1 and 1.2, then the design of the composite structure is complete.

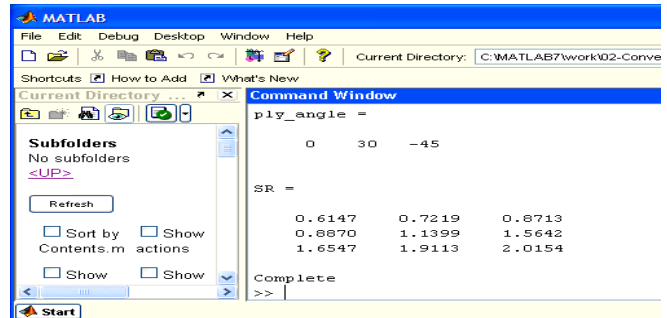


FIGURE I: SR VALUES FROM CONVENTIONAL APPROACH [2]

III. MECHANICAL BEHAVIOR OF COMPOSITE PLATE WITH CLPT:

The Kirchhoff's hypothesis stated that the line AA' remains straight and normal to the geometric mid-plane after deformation as in figure 1 and also the length of the line AA' remains the same. The first assumption implied that the line AA' does not deform but instead it only rotates and translates.

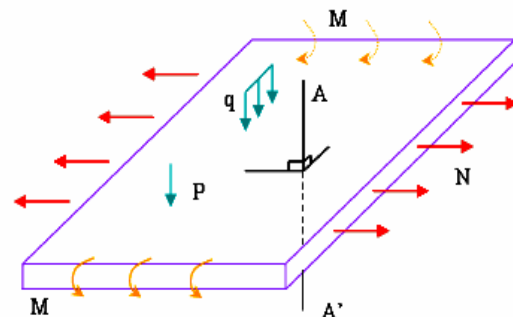


Figure.2: Laminated plate acted up on by loads

In other words, the effect of transverse shear is neglected. The fact that the length remains the same means that there is no strain in z direction. With these two implications, the strains and displacements at any points can be expressed in terms of the displacements of points on the composite mid plane. This also implied that the problem has been reduced from three dimensional to the two dimensional problem.

IV. RESULTS AND DISCUSSION

This chapter presents the code used for the analysis and the results. First of all, in order to verify and make sure that the code is correct, verification with an example in the book will be shown. Such a comparison is made to ensure that the written program is error - free and can be used in the analysis. Once the code is verified, an anisotropic control material with predetermined plies and varying thickness is first selected and the stress and strain of the material is calculated and investigated. The results of the control material will hence be compared to the composite material made of fibre and matrix. The plies and number of varying thickness follow that of the isotropic control material. During this step, different sets of laminate with different orientation are set up, and their stress and strain would be calculated. Also, in order to study the behavior of the varying thickness of laminate, the thickness arrangement of the laminate would be rearranged into symmetric laminate.

A. MATLAB Program

Program for the project is done using MATLAB version 7.8.0.324 (R2009a). The program can be divided into 2 parts. First of all, the code starts from the initial statement of the engineering properties of the material, and then the number of plies, following with the insertion of fibre orientation and the thickness of the laminate, the first step ends with the computational of the ABD matrix. The second part of the program takes the ABD matrix obtained from the first part as initial input. The program continues with the definition of the mechanical load on the laminate. With the load applied, the program calculates the lamina stresses and strains globally and locally of the laminate and the lamina respectively. The first three values the users provide represent the forces in the x, y and z- direction, while the others three values are the moment acting on the laminate about x , y and z axes respectively. After the values of the loading are inserted the program would then calculate the stress and strain distribution for the laminate globally and locally along with the parameters for the Tsai-Wu failure criterion using these parameters and the local stresses for each layer. Once SR has been determined, the designer will know whether the structure will fail or not. If failure occurs, the fibre angles and possibly the number of layers have to be adjusted; finally, the program ends with the computation of the stress ratio and the strain ratio. This program was tested against manually calculated. Examples in the various texts [2, 3] and the results were exactly comparable to the manual computations. In an example (Example 4.3) [2], the stresses and strains in a graphite/epoxy composite laminate were examined. This

laminate consisted of three layers, with fibre angles of 0°, 30° and -45°, and each layer had a thickness of 5 mm. Following are the MAT LAB script file generated results.

Table VI: Global strains from Conventional Approach

S No	Present Results(1.0e ⁰⁰⁵)			
Ply #	Position	ϵ_1 (m/m)	ϵ_2 (m/m)	γ_{12} (m/m)
1 (0°)	Top	0.0089	0.5955	-0.3836
	Middle	0.0164	0.5134	-0.2811
	Bottom	0.0238	0.4313	-0.1785
2 (30°)	Top	0.0238	0.4313	-0.1785
	Middle	0.0312	0.3492	-0.0760
	Bottom	0.0387	0.2670	0.0266
3 (-45°)	Top	0.0387	0.2670	0.0266
	Middle	0.0461	0.1849	0.1291
	Bottom	0.0535	0.1028	0.2316

Table VII: Global stresses from Conventional Approach

S No	Present(1.0e ⁰⁰⁵)			
Ply #	Position	σ_x (Pa)	σ_y (Pa)	τ_{xy} (Pa)
1 (0°)	Top	0.3351	0.6188	-0.2750
	Middle	0.4464	0.5359	-0.2015
	Bottom	0.5577	0.4531	-0.1280
2 (30°)	Top	0.6930	0.7391	0.3381
	Middle	1.0633	0.7747	0.5903
	Bottom	1.4336	0.8102	0.8426
3 (-45°)	Top	1.2353	1.5628	-1.1826
	Middle	0.4903	0.6894	-0.3888
	Bottom	-0.2547	-0.1840	-0.4091

Table VIII: Local strains from Conventional Approach

S No	Present(1.0e ⁰⁰⁵)			
Ply #	Position	ϵ_1 (m/m)	ϵ_2 (m/m)	γ_{12} (m/m)
1 (0°)	Top	0.0089	0.5955	-0.3836
	Middle	0.0164	0.5134	-0.2811
	Bottom	0.0238	0.4313	-0.1785
2 (30°)	Top	0.0484	0.4067	0.2636
	Middle	0.0778	0.3026	0.2374
	Bottom	0.1073	0.1985	0.2111
3 (-45°)	Top	0.1396	0.1661	-0.2284
	Middle	0.0510	0.1800	-0.1388
	Bottom	-0.0377	0.1940	-0.0493

Table IX: Local stresses from Conventional Approach

S No	Present(1.0e ⁰⁰⁵)			
Ply #	Position	σ_1	σ_2	τ_{12}
1 (0°)	Top	0.3351	0.6188	-0.2750
	Middle	0.4464	0.5359	-0.2015
	Bottom	0.5577	0.4531	-0.1280
2 (30°)	Top	0.9973	0.4348	0.1890
	Middle	1.5024	0.3356	0.1702
	Bottom	2.0075	0.2364	0.1513
3 (-45°)	Top	2.5858	0.2123	-0.1638
	Middle	0.9786	0.2010	-0.0995
	Bottom	-0.628	0.1898	-0.0353

Table X: Local stresses from Conventional Approach

S No	Present(1.0e ⁰⁰⁵)			
Ply #	Position	σ_1	σ_2	τ_{12}
1 (0°)	Top	0.3351	0.6188	-0.2750
	Middle	0.4464	0.5359	-0.2015
	Bottom	0.5577	0.4531	-0.1280
2 (30°)	Top	0.9973	0.4348	0.1890
	Middle	1.5024	0.3356	0.1702
	Bottom	2.0075	0.2364	0.1513
3 (-45°)	Top	2.5858	0.2123	-0.1638
	Middle	0.9786	0.2010	-0.0995
	Bottom	-0.628	0.1898	-0.0353

From above results one part of the work is done successfully. In the second part of the work we generate MATLAB code to determine the transverse deflections and

in plane stresses in especially orthotropic square symmetric laminates subjected to various types of mechanical loads. For this we follow the first part of the work up to calculating ABD matrices after that finally the force and moment resultants in the laminate can be computed using the stresses.

B. Tsai-Wu failure criterion and SR values:

The Tsai-Wu failure theory is applied and a value for SR is obtained for each layer. The program then analyzes the SR values and confirms whether it is in a certain range. The lower limit of this range is 1 as any value below this would mean failure. The upper limit in this range is 1.2 and this is to avoid overdesigning. If the SR value for each layer is between 1 and 1.2, then the design of the composite structure is complete. If we observe the SR values for the 0, 30, -45 degree fiber orientations are as follows.

Table XI: Layer wise failure results by the Tsai-Wu failure theory

Layer	Strength ratio (SR) values for the angles					
	0°	Tsai-Wu criterion	30°	Tsai-Wu criterion	45°	Tsai-Wu criterion
Top	0.6147	failure	0.7219	failure	0.8713	failure
Middle	0.8870	failure	1.1399	safe	1.5642	overdesign
Bottom	1.6547	Over design	1.9113	overdesign	2.0154	Over design

The Conventional Approach script file was further extended to include failure analysis via the Tsai-Wu failure theory. The resulting SR values for the top, middle and bottom of each layer is shown in table I. The rows represent the layers and columns 1 to 3 represent the top, middle and bottom of each layer, respectively. The SR values in table 5.5 indicate that the composite structure will fail first on layer 1 (SR = 0.6147) and then layer 2 (SR = 0.8870). It is clear from this that the input angles and number of layers were insufficient to carry the applied loads. Previously the SR value on the first layer was less than 1 and lower than the other two layers indicating earliest failure. The following table shows transverse deflections and stresses in orthotropic square laminates subjected to various types of mechanical loads for the properties of the material are given [9]. All laminates are of same thickness. $E_1/E_2=25$, $G_{12}=G_{13}=0.5E_2$, $G_{23}=0.2E_2$, $\nu_{12}=0.25$. The number in parentheses denotes the number of terms used in the double Fourier series to evaluate the series. The transverse shear stress σ_{xz} is the maximum at $(x,y,z)=(0,b/2,0)$, σ_{yz} is the maximum at $(x,y,z)=(a/2,b/2,h/2)$, those are the results obtained by the MATLAB script file generated are compared.

Table XII: Transverse deflections and stresses in especially orthotropic square laminates by using CLPT

Laminate	Mechanical loading [J N Reddy JNREDDY]				Mechanical loading[MATLAB]			
	W	σ_{xx}	σ_{yy}	σ_{xy}	W	σ_{xx}	σ_{yy}	σ_{xy}
	SSL*				SSL*			
0°	0.4312	0.5387	0.0267	0.0213	0.4312	0.5387	0.0267	0.0213
(0/90/0)	0.4312	0.5387	0.0267	0.0213	0.4312	0.5387	0.0267	0.0213
	UDL (19)				UDL (19)			
0	0.6497	0.7866	0.0244	0.0463	0.6497	0.7866	0.0244	0.0463
(0/90/0)	0.6660	0.8075	0.0306	0.0425	0.6659	0.8075	0.0306	0.0425

V. CONCLUSIONS

A MATLAB code is developed to study the static response of laminated composite plates. The computations of stress strain and deflections are made using classical laminate plate theory. The developed code is capable to take up variations in both thickness of lamina and sequence of laminate. The results are found to be in good agreement with published results. A study also been carried out the influence of number of layers in a laminate. It is observed that the central deflection decreases as the number of layers increases up to certain number of layers only further no change is noticed in result. First ply failure analysis is done using Tsai Wu failure criterion. The first ply failure analysis results indicate that the ply in which stresses are maximum.

VI. RECOMMENDATIONS

There are numerous recommendations for future research in terms of the analysis of the varying thickness of fibre reinforced composite laminate. The data input for the MATLAB program can be enhanced. If possible, implementing the user interfaces where users can have more freedom when using the program. Expand the scope of studies of the research if possible; try increasing the number of cases of orientation and layers and thickness so that users would have clearer views on the behavior of the varying thickness composite laminate.

VII. REFERENCES

- [1] S. K. Mazumdar, "Composite Manufacturing: Materials, Product, and Process Engineering," CRC Press LLC,
- [2] Avinash Ramsaroop, Krishnan Kenny, Using MATLAB to Design and Analyze Composite Laminates.doi:10.4236/eng.2010.211114 published Online November 2010 (<http://www.scirp.org/journal/eng>)
- [3] A. K. Kaw, "Mechanics of Composite Materials," CRC Press LLC, Boca Raton, 1997.
- [4] C. T. Herakovich, "Mechanics of Fibrous Materials," John Wiley & Sons Inc., Hoboken, 1998.
- [5] R. M. Christensen, "Mechanics of Composite Materials," Dover Publications, New York, 2005.

- [6] M. Akbulut and F. O. Sonmez, "Optimum Design of Composite Laminates for Minimum Thickness," *Computers and Structures*, Vol. 86, No. 21-22, 2008, pp.1974-1982
- [7] *Mechanics of Composite Materials with MATLAB* by George Z. Voyiadjis Peter I. Kattan.
- [8] Rodrigo Silva- Munoz and Roberto a. lopez-anido "effect of transverse shear deformation on elastic Response of sandwich composite plates".
- [9] J N Reddy "Mechanics of laminated composite plates and shells theory and analysis"
- [10] Cesar Augusto Rojas, "structural analysis of fiber reinforced composite materials", the University of Texas at Arlington December
- [11] MediaWiki, "MATLAB,"2008.<http://en.wikipedia.org/wiki/MATLAB>
- [12] R. V. Dukkipati, "MATLAB for Mechanical Engineers," New Age International (P) Limited, New Delhi, 2008
- [13] S. Nageswara , S. Lakshmi Narayana, Dr. Y. Venkata Mohan Reddy, Dr. B. Chandra Mohan Reddy, , "Mechanical Properties of
- [14] Glass, Bamboo and Sisal with Reinforced Epoxy Composite: An Experiment" *International Journal of Engineering & Technology Research* Volume 4, Issue 3, May-June, 2016,PP 01-13.
- [15] M. Naghipour, H.M. Daniali and S.H.A. Hashemi Kachapi "Numerical Simulation of Composite Plates to be used for Optimization of Mobile Bridge Deck". *World Applied Sciences Journal* 4 (5): 681-690, 2008
- [16] SHE WAI WAI "Thermo mechanical behavior of fiber reinforced composite laminate plate, University technology Malaysia 2010"
- [17] S. Nageswara, Dr. T. Hariprasad P. Mallikarjuna Rao "Structural Analysis of Crane Hook Using the Finite Element Analysis (FEA) Approach" *International Conference on Advances in Design and Manufacturing (ICAD&M'14)* 303 ISBN 978-93-84743-12-3 © 2014 Bonfring.
- [18] S. Nageswara, Dr. T. Hariprasad "A Study on the Fracture and Fatigue Behaviour of an Aluminium Alloy: Finite Element Analysis (FEA) Approach" *International Journal of Research in Mechanical Engineering* Volume 1, Issue 2, October-December, 2013, pp. 11-18
- [19] K. Sivakumar, N. G. R. Iyengar and K. Deb, "Optimum Design of Laminated Composite Plates with Cutouts Using a Genetic Algorithm," *Composite Structures*, Vol. 42, No. 3, 1998, pp. 265-279.
- [20] A Gnanarathinam, D Palanisamy, M Gangaraju... - *Materials Today: Proceedings*, 2022 , Investigation of corrosion behavior of welded area of austenitic stainless steel under different environments
- [21] G Moopuri, S Victor, MR Francis *Microstructural Analysis and Enhancement of Mechanical Properties in AA2219 Composite by In-Situ TiB2 and Sub-Micron ZrB2 Particles.*

THE AUTOMATIC DETECTION OF FISHING VESSELS FOR INDIAN FISHERMEN

*Tumati Venkateswara Rao, Department of Electronics and Communications Engineering
Sir C R Reddy College of Engineering Eluru, India*

Abstract— With the evolution of the technology over the various sectors communication is possible at ease. However, due to lack of awareness about ocean frontiers and advanced alert instruments, fishermen are facing trouble in knowing weather updates and border limits. In order to protect the fishermen and to assist them about the sea/ocean frontiers and weather updates during fishing, we are proposing vessel monitoring system, in which automatic identification is done using a GPS module and a communication established is between ship-ship, ship-shore using a Very High Frequency (VHF) equipment. This marine VHF set is a Two-way radio transceiver on ships and watercraft used for two way/bidirectional voice communication. [The VHF radio band operates at frequencies ranging from 156 to 174 MHz. Its transmitter power is limited to 25 watts, and with the range of 100 kilometers (62 mi).] A panic switch is also installed to call out for help during emergency situations. Thus, this provides an effective navigation by preventing the fishermen from the border crossing and taking necessary actions during severe weather conditions and panic situations.

Keywords— *VHF communication module, Raspberry Pi 3 Model B+, DHT11 sensor, GPS module*

I. INTRODUCTION

Fishing is one of the world’s most dangerous professions since it is vulnerable to a variety of oceanographic and climatic circumstances [1]. The issues that most fishermen face are being imprisoned or shot by the neighboring country's officials and perishing due to storms or cyclones. Indian fishermen too face these problems/cases quite often with our neighboring countries like Sri Lanka. The India-Sri Lanka border stretches approximately 288km (155nm) from the Maldives tripoint in the west, i.e., the Gulf of Mannar, to approximately 200nm (370km) in the east, i.e., Palk Strait. The regions of the Gulf of Mannar and Palk Strait have been the regions of dispute for over a long time, despite the discussions between the two nations. So, it requires providing a proper navigation system to the fishermen in order to have an idea or alert about frontiers and also feed them with frequent weather updates.

Weather Updates

TABLE I. DIFFERENCE IN WEATHER CONDITIONS

Conditions	Temperature	Atmospheric Pressure & Humidity
------------	-------------	---------------------------------

Normal Conditions	20° C (68 F)	800 millibars
During Cyclone	26° C (79 F)	1013.2 millibars

To address these problems, we are proposing a system that keeps track of the fishermen's location while also establishing communication between the fishermen and coast guards to provide weather updates and request assistance in case of an emergency or a panic situation [2]. In the proposed system, we use the Global Positioning System (GPS) module for keeping track of the location of the fishing vessel and providing these location coordinates to the coast guards at regular intervals, so that the kit can give out an alert if the fishermen are crossing or close to crossing the positions.

1. Position: 09° 13'.0 North, 79° 32'.4 East.
2. Position: 08° 53'.8 North, 79° 29'.3 East.
3. Position: 08° 31'.2 North, 79° 04'.7 East.
4. Position: 08° 12'.2 North, 78° 53'.7 East. ([1] [3])

On the other hand, the weather monitoring sensors are used in the kit to provide real-time weather updates, and the coast guards feed the alerts regarding cyclones or storms in advance so that the fishermen can reach a safer location [4]. It is a very high frequency (VHF) set, which is used for communication purposes. This VHF set supports about 16 commercial channels with an operating frequency range of 156-174 MHz. In these 16 channels we are using 3 channels those are channel 9 is primary channel with operating frequency 156.450 MHz, channel 13 is bridge to bridge communication between vessels with operating frequency 156.650MHz, channel 16 is emergency and distress call with operating frequency 156.80 MHz through these dedicated channels the information regarding the weather, cyclones and storms information is fed to the fishermen in critical situations. In case of critical emergencies like health issues or unexpected accidents there exist a panic switch that helps in sending out a message to coast guards about the emergency so that the nearby officials can reach them in time to provide assistance to them

II. MATERIALS AND METHODS

- This proposed paper is an embedded system is implemented using the Raspberry Pi 3 micro-controller. The Raspberry Pi 3 has different components where the interfacing across sensors and actuators can be connected. The Raspberry Pi 3 is interfaced with GPS module, VHF module, temperature and humidity sensors and others.

- If the boat crosses the sea borders and is apprehended by the coast guard, or if they lose their way within the nautical borders, the GPS module allows them to be identified.

- For this, an algorithm is written so that the vessel can be monitored continuously and tracked down efficiently. The algorithm is based on the threshold values set before the boat reaches the borders, and thus an alarming signal is sent.

- The system comprises of weather forecasting sensors to notify the changes in weather at stipulated time intervals.

Raspberry Pi 3 Model B+

This is a micro-controller device whose operation is similar to that of a CPU in a computer. This device consists of 40 GPIO pins to connect to external components and in-built memory capacity. To facilitate efficient connectivity, the device also contains HDMI and Ethernet ports.

VHF communication module

A VHF communication module is a two-way communication device used to transfer and receive messages between the coastal authorities and fishing vessels. This marine VHF module works by operating on MHz that fall anywhere between 156 and 172, which is a small fragment of the MHz used in high frequency radios that work with radio waves between 30 to 300. Here we use three channels, 9, 13, and 16. For the primary communication channel, we tune to channel 9. For distress calls and emergencies, tune into channel 16. Tune into channel 13 for communication between boats.

GPS module

In this system, we are using the NEO-6M GPS module that can track up to 24 satellites on 50 channels with the highest level of sensitivity, i.e., -161dB and identifies locations anywhere in the world. These are low-power and inexpensive modules. The module supports a baud rate from 4800bps to 230400bps with a default baud of 9600. They're pre-programmed to know exactly where the GPS satellites are at all times. Satellites send radio signals to the Earth that contain information about their location and current time. These signals identify satellites and provide information about their locations to the receiver. By calculating the time, it takes for the signals to arrive, the receiver may determine how far away each satellite is. It can pinpoint

your location on Earth once it has information on how far away you are and where at least three satellites are in space. This process is known as trilateration.

DHT11 sensor

The DHT11 is a part of the DHTXX series of humidity sensors that measure both humidity and temperature. There are three primary parts to the DHT11 Humidity and Temperature Sensor. A resistive humidity sensor, an NTC (negative temperature coefficient) thermistor (for temperature measurement), and an 8-bit microprocessor that translates the analogue outputs from both sensors into a single digital signal. Any microcontroller or microprocessor may read this digital signal and analyze it further.

Voice recorder and playback module APR33A3

In this system, we are using the APR33A3 voice record and playback module that senses and reads out pre-recorded voice notes through the speaker to alert the fishermen. This is a powerful audio processor along with high-performance audio analog-to-digital converters (ADC) and digital-to-analog converters (DAC). This is a high-quality analogue to digital and PWM module which averagely uses up to eight voice messages per recording and playback.

LCD display

In LCD 16×2, the term LCD stands for Liquid Crystal Display that uses a plane panel display technology. This is a 16-pin electronic device used to display data and messages. It includes 16 Columns & 2 Rows so it can display 32 characters (16×2=32) in total. The role of this LCD display is to display the messages/alerts from coastal authorities and to view humidity and temperature values.

III. METHODOLOGY

The automatic identification system of fishing vessels for Indian fishermen is an embedded system device which is interfaced with a physical tracking device, a communication device and some sensors. In this system, physical tracking is done by using the global positioning system (GPS) Module. The latitude and longitude coordinates of the location is received from the GPS receiver and is compared to the previously defined threshold coordinates from the algorithm. There are two threshold values set one at 5km from the border line and the other at 2km from the border line. Using the GPS module, the current location coordinates of the fishing vessel are considered and compared to the threshold values set at the 5km. If the boat is near the threshold limit of 5km, then the system sends out an alert message to the fishermen. Now if the boat enters the critical area i.e., the threshold limit of 2km, another alarm is set, and an SMS is sent out to the coast guards. After receiving the message, the coast guard makes a communication with the fishermen to manually alert them.

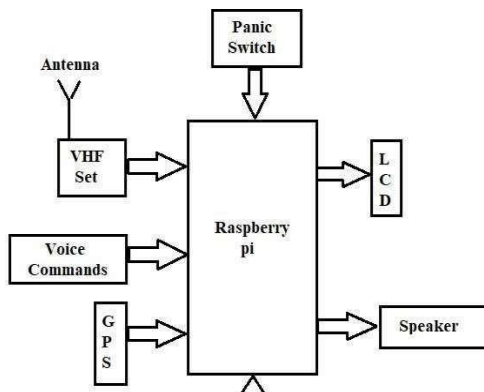


Figure 2: Proposed system for automatic identification of fishing vessels



Figure 1: Transmitted block in proposed System

The fishermen need to be aware of the changing weather conditions in order to make best use of the conditions and have good yield so we can use the DHT11 sensor which gives humidity and temperature levels at stipulated time intervals, but it is still not possible for the sensors to detect cyclones or tsunamis in real time, so we make use of a VHF communication set to feed this information to the fishermen in real time. The coast guard is made available with a VHF set to transmit and receive messages and same is the case with the fishermen. The coast guard's duty is to send out the alerts regarding the cyclones or tsunamis or any other natural calamities through a dedicated channel i.e., channel 16.

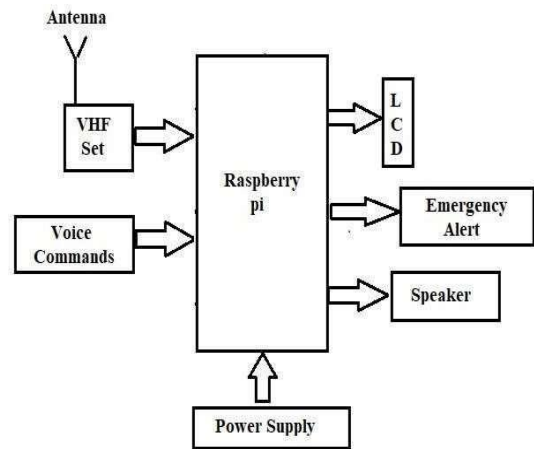


Figure 3. Receiver block in proposed System

In case of any medical emergencies like heart stroke or any other serious injuries during fishing, the fishermen require a quick medical assistance. So, we can make use of the channel 13 to send out a message to the fishing boats and coast guards nearby for medical help. Due to unforeseen circumstances if the boat is met with an accident, there exist a panic switch which when turned on sends out a message to the coast guards to quickly reach and help them so that there wouldn't be loss of life. This panic switch can also be used for medical emergencies well.

IV. RESULTS AND DISCUSSIONS

Present paper is designed using Raspberry Pi 3 microcontroller. It is proposed to design an embedded system which is used for automatic identification of fishing vessels where the Raspberry Pi 3 is interfaced to various hardware peripherals as shown in fig. The Raspberry Pi 3 microcontroller is interfaced serially to a GPS transceiver. There will be a reference GPS location. When the current location exceeds reference location of the first threshold(5km), the fishermen are intimated as shown in the fig 4 and when reference location of second threshold(2km) is exceeded, then the intimation is sent to both the fishermen and the coast guard as shown in the fig 4 and fig 5. This intimation is be using a buzzer for first threshold and for second threshold we will be using a VHF communication set and also the buzzer.

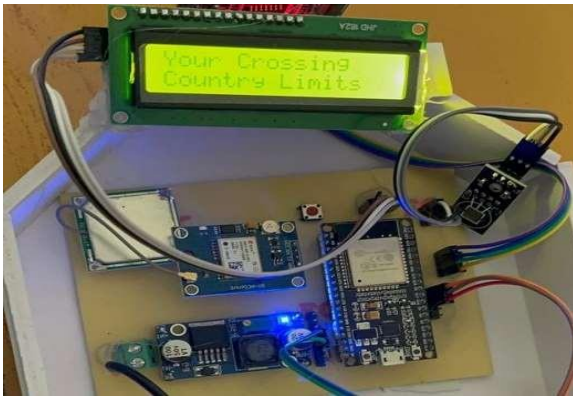


Figure 4: Received alert message and associated circuit setup



Figure 7. Temperature measurement

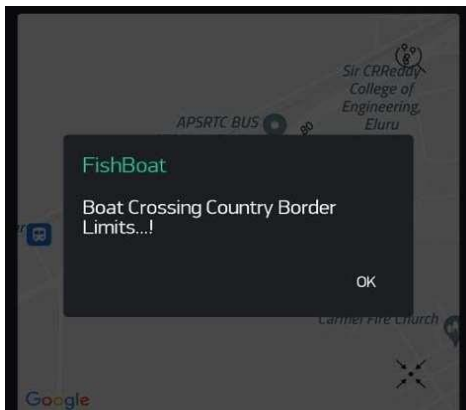


Figure 5: Message to Coastal Guard

The fishermen will also be requiring weather updates for a safe hunt. So, by interfacing a DHT11 sensor to the microcontroller we are giving humidity and temperature values regularly as shown in the below fig 6 and fig 7. The intimation for natural calamities like cyclone is given using the VHF communication set. In this communication set the common channel 16 is used by the coast guard to send an alert to all the fishing vessels that had gone to the hunt.



Figure 6. Received message according to Weather Information

When there is an emergency situation during the hunt, we use a panic switch. This panic switch when pushed on sends out a message to the coast guards when the fishing boat met with an accident as shown in the fig 8.

In case of any medical emergency like heart stroke or attack, the fishermen can make use of the VHF communication set to communicate with the coast guards or other fishing boats for emergency assistance.

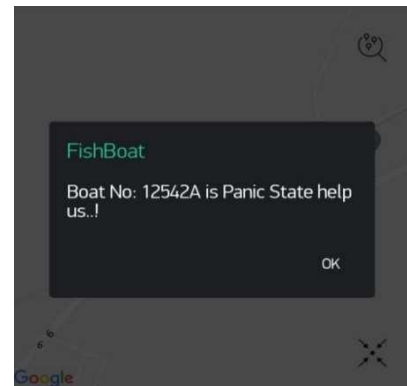


Figure 8. Emergency message to Coast guard from fishermen

When the communication process used in the proposed system is compared to other communication techniques like LoRa, GSM, the VHF communication module provided better results in terms of bandwidth usage, wavelength and data rate as shown in table below. So, it would be more effective and efficient when VHF communication is used for communication.

TABLE II. DATA RATE COMPARISON AMONG TECHNOLOGIES

Technologies	LoRa	GSM	VHF
Bandwidth	500KHz	45MHz	270MHz
Wavelength	16 Cm	33 Cm	1 M

Data rate	22.7 Kbps	21.6 Kbps	31.4 Kbps
-----------	-----------	-----------	-----------

V. CONCLUSION

The proposed system assists the fishermen from not crossing the international maritime borders by giving alerts when they are close to the border and weather updates/alerts regarding rains/cyclones/storms are also provided by the coast guards directly using flexible processes as discussed in the above sections. The panic switch comes handy during emergency situations in providing suitable assistance thereby preventing the loss of life. By this the fishermen caught/shot/arrested by neighboring countries navy forces can be controlled and the lives of the Indian fishermen will also be saved

REFERENCES

[1] Sureshkumar, R. & Ilakkiya, C. (2021). An Intelligent communication system for fisherman. Journal of Physics: Conference Series. 1916. 012053. 10.1088/1742-6596/1916/1/012053.

[2] R.G.T. Prabhudesai et al., "GPRS based Real Time Reporting and Internet Accessible Sea Level Gauge for Monitoring Storm Surge and Tsunami," OCEANS2006-AsiaPacific, 2006, pp. 1-4, Doi:10.1109/OCEANSAP.2006.4393979.

[3] Miranji Katta, R Sandanalakshmi, "Static and Dynamic Analysis of Carbon Nano Tube Cantilever for Nano Electro Mechanical Systems Based Applications", Journal of Computational and Theoretical Nano science, Volume: 17, Issue: 5, Pp: 2151-2156, Year: 2020, ISSN: 1546-1955, DOI: https://doi.org/10.1166/jctn.2020.8862.

[4] Miranji Katta, R Sandanalakshmi, "Geometrical Sensitivity Analysis of Bio-Nano Electro Mechanical Systems Using FEM Analysis For Disease Detection" Bioscience and Biotechnology Research Communications, Volume:13, Issue:2, Pp:49-58, Year:2020, ISSN:2321-4007, DOI:10.13140/RG.2.2.30372.81282.

[5] P. Satyanarayana, V. B. K. L. Aruna and P. N. V. S. Kumar, "International boundary scanning and ship surveillance system," 2017 International Conference on Electrical, Electronics, Communication, Computer, and Optimization Techniques (ICEECCOT), 2017, pp. 212-215, doi: 10.1109/ICEECCOT.2017.8284669.

[6] Katta M, R Sandanalakshmi, "Simultaneous tropical disease identification with PZT-5H piezoelectric material including molecular mass biosensor microcantilever collection", Sensing and Bio-Sensing Research-Elsevier, Volume:32, Pp:1-6, Year:2021, ISSN:2214 - 1804, DOI:https://doi.org/10.1016/j.sbsr.2021.100413.

[7] B. Kamalakannan, K. Naresh and P. Sakthivel, "Protecting fishermen's by detecting and warning them while crossing sea borders using GSM and RFID technologies," 2016 Online International Conference on Green Engineering and Technologies (IC-GET), 2016, pp. 1-6, doi: 10.1109/GET.2016.7916655.

[8] R. G. Prabhudesai et al., "GPRS based Real-Time Reporting and Internet Accessible Sea Level Gauge for Monitoring Storm Surge and Tsunami," OCEANS 2006 - Asia Pacific, 2006, pp. 1-4, doi: 10.1109/OCEANSAP.2006.4393979.

[9] N. Mitra, A. Maji and P. Agarwalla, "Integrated maritime security & surveillance," 2017 Devices for Integrated Circuit (DevIC), 2017, pp. 766-768, doi: 10.1109/DEVIC.2017.8074055.

[10] https://lora-developers.semtech.com/documentation/tech-papers-and-guides/lora-and-lorawan/

[11] https://en.wikipedia.org/wiki/GSM_frequency_bands

MODELING AND REINFORCEMENT OF A HEAVY VEHICLE LEAF SPRING FOR THE MATERIALS OF E-GLASSES AND EPOXY COMPOSITES

Mrs. Narasimhala Hymavathi, Mrs.S.Vaneela

Assistant Professor, Department of Mechanical Engineering, Eswar College of Engineering, Narasaraopet, A.P. India.

Abstract: Leaf spring are mainly used in suspension system to absorb shock loads in automobiles like light motor vehicles, heavy duty trucks and in rail system. It carries lateral loads, breaker torque in addition to shock absorbing. The advantage of leaf spring over helical spring is that the ends of spring may be guided along a definite path as is deflects to act as structural member in addition to energy absorbing device. Reducing weight while increasing or maintaining strength of products is getting highly impotent research issue in this modern world Composite materials are one of the material families. which are attracting reaches and being solution of such issue in this project we describe design of leaf spring. The design constraint is stiffness. The auto mobile industry has great interest for replacement of steel leaf spring with that of composite leaf spring. Since the composite material has high strength to weight ratio, good corrosion resistance. The design parameters were selected and analyzed with the objective of minimizing weight of the composite leaf spring as compared to that families. The design parameters of spring are in catia v5 r20 is used as a cad tool for designing leaf spring suspension. Catia is a advanced cad software which is used for a good sketcher design. Leaf spring is designed using part design workbench and later on it is assembled in assembly workbench. The analysis of heavy vehicle leaf spring is going to do in ansys workbench with the composite materials of e-glass and epoxy.

Key points: Stiffness, steel, epoxy and e-glass.

INTRODUCTION:

A spring is defined as an elastic body, whose function is to distort when loaded and to recovers its original shape when the load is removed. Semi- elliptic leaf springs are almost universally used for suspension in light and heavy commercial vehicles. For cars also, these are widely used in rear suspension. The spring consists of a number of leaves called blades. The blades are varying in length. The blades are us usually given an initial curvature or cambered so that they will tend to straighten under the load. The leaf spring is based upon the theory of a beam of uniform strength. The lengthiest blade has eyes on its ends. This blade is called main or master leaf, the

remaining blades are called graduated leaves. The leaves of the leaf spring require lubricant at periodic intervals. If not, the vehicle is jacked up so that the weight of the axle opens up the leaves. The spring is then cleaned thoroughly and sprayed with graphite penetrating oil. However, it is important to remember that in some vehicles, (e.g. Ambassador) it is specified that the lubricant of spring leaves should not be done.

OBJECTIVE:

The automobile industry is showing increased interest in the replacement of steel spring with fiber-glass composite leaf spring due to high strength to weight ratio. Therefore; this project aims at comparative study of design parameters of a traditional steel leaf spring assembly and mono composite leaf spring with bonded end joints. By performing static analysis using ANSYS software and mathematical calculations, the maximum bending stress and corresponding payload have to be determined by considering the factor of safety.

LITERATURER REVIEW:

ZliahuZahavi [1] the leaf spring works is very complicated from the point of view of mechanics and numerical computations. The magnitude of loading is high as well as spring deformations. Multi-surfaces 3D contact between subsequent leafs also takes place. The main advantage of leaf springs is that the ends of the spring are guided along a definite path as it deflects to act as a structural member in addition to energy absorbing device. Practically, a leaf spring is subjected to millions of load cycles leading to fatigue failure. Free vibration analysis determines the frequencies and mode shapes of leaf spring

OVERVIEW OF LEAF SPRING:

Semi-elliptic leaf springs are almost universally used for suspension in light and heavy commercial vehicles. For cars also, these are widely used in rear suspension. The spring consists of a number of leaves called blades. The

blades are varying in length. The blades are usually given an initial curvature or cambered so that they will tend to straighten under the load. The leaf spring is based upon the theory of a beam of uniform strength. The lengthiest blade has eyes on its ends. This blade is called main or master leaf, the remaining blades are called graduated leaves. All the blades are bound together by means of steel straps.

SUSPENSION SYSTEM:

The automobile chassis is mounted on the axles, not direct but some form of springs. This is done to isolate the vehicle body from the road shocks, which may be in the form of bounce, pitch, roll or sway. These tendencies give rise to an uncomfortable ride and also cause additional stress in the automobile frame. The part, which performs the function of isolating the automobile from the road shocks, is collectively called a suspension system. It includes the springing device used and various mountings for the same.

TYPES OF SUSPENSION SYSTEMS:

PLASTIC SUSPENSION:

Viberitis P.A of TURINE has developed a new type of suspension based upon the use of resilient plastic rings in compression. The suspension consists of a cylindrical container secured to the chassis, a shaft attached to the axle and free to slide within the plastic rings contained in the cylinder, there are two centering rings, the bottom one fixed to the lower end of the cylinder and the upper one is arranged as high as possible keeping in consideration that in the rebound position shaft must remain supported by it by the plastic rings and absorb the vertical dynamic load. **Independent Suspension:** When a vehicle with rigid axle suspension encounters road irregularities the axle tilts and the wheels no longer remain vertical. This causes the whole of the vehicle to tilt on one side. Such a state of affairs is not desirable. Apart from causing rough ride, it causes „wheel wobble“. The road adhesion is also decreased. To avoid this, the wheels are sprung independent of each other, so that tilting of one does not affect the other. Besides the independent suspension also have the following advantages over rigid axle type suspension.

1. Front Wheel Independent Suspension:
2. Rear Wheel Independent Suspension:

Wishbone type suspension: The wishbone arms are like the chicken wishbone or letter V in shape, because of which the system is so called, because of this V-shape. The wishbones not only position the wheels and transmit the vehicle load to the springs. But these also resist acceleration, braking and cornering (side) forces. The upper arms are shorter in length than the lower ones. This helps to keep the wheel track constant, thereby avoiding tyre scrub thus minimizing tyre wear. However a small change in the camber angle does occur with such an arrangement.

Mac Pherson Strut Type of Suspension:

A strut containing shock absorbing and the spring carriers also the stub axle on which the wheel is mounted. The wishbone is hinged to the cross member and positions the wheel as well as resists accelerating, braking and side forces. This system is simpler than double wishbone type described above and is also lighter, keeping the unsprung weight lower. This type of suspension gives the maximum room in the engine compartment and is, therefore commonly used on front wheel drive cars. In India this system has been used in Maruti (Suzuki) 800 cars. This type of suspension with anti-roll bar as employed in Volkswagen Jetta and Passat cars. This is claimed to provide increased road safety, improve ride comfort and light and self-stabilizing steering which means that car continues along its chosen line of travel when the brakes are applied even though the road surface may vary.

Air Suspension:

Air suspension systems are coming into prominence because of certain advantages they possess over the conventional metal springs.

The advantages are:

1. A vehicle space for wheel deflection is put to optimum use by virtue of the

automatic control devices.

2. Because of the vehicle is also constant, changes in headlamp alignment due to varying loads are avoided.
3. The spring rate varies much less between the laden and unladen conditions, as compared with that of conventional steel springs. This reduces the dynamic loading.
4. The improved standard for ride comfort and noise reduction with air springs reduces both driver and passenger fatigue.

Hydro elastic Suspension:

In this system a displacer unit is fitted at each of the four wheels. The displacer units are all interconnected by means of fluid. In the displacer unit, rubber (under compression and shear) is used as a spring where as fluid rubber pressure acts as damping medium. The stem is connected to the wheel through suitable linkage so that its movement is proportional to the up and down movement of the wheel. A two way valve assembly controls the up and down flow of the fluid. The upper valve opens when the fluid pressure below rises sufficiently. Similarly the lower valve allows the fluid to pass in the downward direction under pressure.

Bending Stress of Leaf Spring:

Consider a single plate fixed at one end and loaded at the other end. This plate may be used as a flat spring.

Let t = thickness of Plate

b = width of plate, and

L = length of plate or distance of the load W from the cantilever

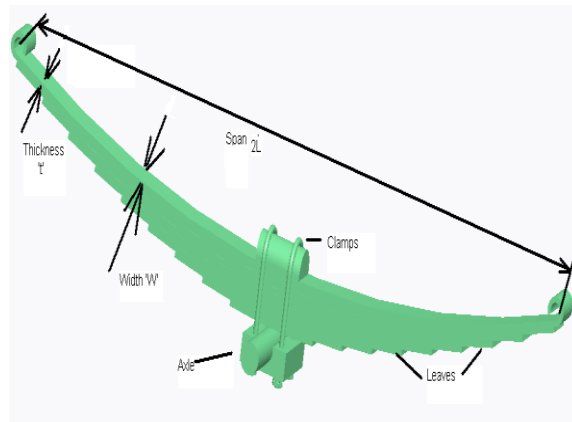


Figure: 1. elements of leaf spring

DESIGN CALCULATION OF LEAF SPRING:

Step (1):
Material of leaf spring:

- Material selected steel : 50 Cr 1 V 23
- Composition of material : 0.45% C,
0.1-0.3% Si,
0.6-0.9 % Mn,
0.9-1.2 % Cr

Step (2): Basic data of Force Motors Trax Cruiser leaf spring:

- Total length of the spring (Eye to Eye)
- No. of full length leaves (n)
- No. of graduated leaves (n_g)
- Thickness of leaf (t)
- Width of the leaf spring (w)
- Young's modulus (E)
 $= 2 \times 10^5 \text{ N/mm}^2$
- Central band 110 mm wide (Ineffective length)
- Tensile strength (σ)
- Yield strength (σ_y)
- Total load
- BHN

Step (3): Basic requirement of load:

- Maximum capacity = 10000 Kg
 $= 10000 \times 10$

$$=100000 \text{ N}$$

Force Motors Trax Cruiser is equipped with 4 nos. of semi elliptical leaf spring,

So load acting on the leaf spring assembly
 $=100000/6$

$$= 16,666.6 \text{ N}$$

Step (4): Calculation of the loaded leaf spring:

□ Consider the leaf spring is cantilever beam. So the load acting on the each assembly of the leaf spring is acted on the two ends of the leaf spring. Load acted on the leaf spring is divided by the two because of consideration of the cantilever beam

$$2 \times W = 16,666.6 \text{ N} = 8,333.33 \text{ N}$$

□ For support and clamping of the leaf spring the “U” bolt is use and the distance between the “U” bolt is 110 mm. This is considered as an unbent portion of the leaf spring. In effective length of the leaf spring is as under :

$$i = 110.00 \text{ mm}$$

Step (5): Calculations of the stress generated in the leaf spring are as under :

□ Material of the leaf spring is 50 Cr 1 V 23

□ Property of the material are as under:

$$\begin{aligned} \text{Tensile strength (} \sigma_t \text{)} &= 190 - 240 \text{ Kgf/mm}^2 \\ &= 1900 - 2400 \text{ N/mm}^2 \end{aligned}$$

$$\begin{aligned} \text{Yield strength (} \sigma_y \text{)} &= 180 \text{ Kgf/mm}^2 \\ &= 1800 \text{ N/mm}^2 \end{aligned}$$

$$\text{Modulus of elasticity (E)} = 200000 \text{ N/mm}^2$$

BHN = 500 – 580 HB with hardened and tempered

□ By considering the factor of safety for the safety purpose of the leaf

spring is 1.5 for automobile leaf spring [20]. So the allowable stress for the leaf spring is as under :

$$\begin{aligned} \text{Tensile strength (} \sigma \text{)} &= 1900/1.5 \\ &= 1266.66 \text{ N/mm}^2 \end{aligned}$$

$$\begin{aligned} \text{Yield strength (} \sigma_y \text{)} &= 1800/1.5 \\ &= 1200 \text{ N/mm}^2 \end{aligned}$$

□ Bending stress generated in the leaf spring is as under :

$$\begin{aligned} \sigma_b &= \frac{6 \times W \times L}{n \times b \times t^2} \\ \sigma_b &= \frac{6 \times 8333.33 \times 852.33}{6 \times 60 \times 25 \times 25} \\ \sigma_b &= 189.453 \text{ N/mm}^2 \end{aligned}$$

□ So, the stress generated in the leaf spring is lower than the allowable design stress. So design is safe.

Deflection generated in the assembly of leaf spring is as under :

$$\begin{aligned} y &= \frac{6 \times W \times L^3}{n \times b \times t^3} \\ y &= \frac{6 \times 3562.5 \times 852.34^3}{6 \times 200000 \times 60 \times 25^3} \\ y &= 322.052 \text{ mm} \end{aligned}$$

Step (6): Calculation of the pin of the leaf spring is as under : Allowable bearing pressure of the eye [20] (p) = 8 N/mm² Take length of the eye (i) = 60 mm . Load acting on the ye are as under:

$$\begin{aligned} W &= d \times i \times p \\ \frac{W}{d} &= \\ i \times p &= 8333.33 \\ d &= \frac{8333.33}{60 \times 8} \end{aligned}$$

$d=17.42 \text{ mm}$

$D=18 \text{ mm}$

- Considering factor of safety is 2.
- Calculation of the bending moment of the pin is as under :Length of the pin = Length of the eye + (2 □ Clearance)

(Take the clearance 2.50 mm per side [20])

$$l_p = 60 + (2 \times 2.50)$$

$$l_p = 65 \text{ mm}$$

Maximum bending moment acting on the pin is as

$$1, 35,411$$

$$0.0982 * d^3$$

(Considering bending stress 43.00 N/m)

Shear stress generated in the pin is as under:

Inassembly of the leaf spring pin acting under the double shear action due to assembly structure of the leaf spring. Scope of application:

CATIA:-

Commonly referred to as a 3D Product Lifecycle Management software suite, CATIA supports multiple stages of product development (CAx), including conceptualization, design (CAD), engineering (CAE) and manufacturing (CAM). CATIA facilitates collaborative engineering across disciplines around its 3DEXPERIENCE platform, including surfacing & shape design, electrical fluid & electronics systems design, mechanical engineering and systems engineering. CATIA facilitates the design of electronic, electrical, and distributed systems such as fluid and HVAC systems, all the way to the production of documentation for manufacturing. There are different modules in CATIA using which different tasks can be performed. The main window and modules of CATIA shown in figure-

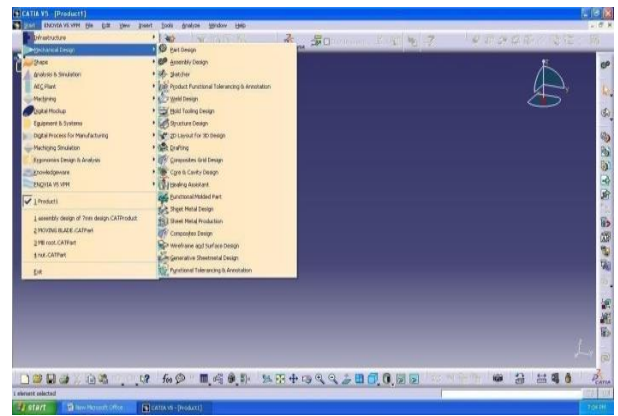


Figure 2. Catia-v5 Interface

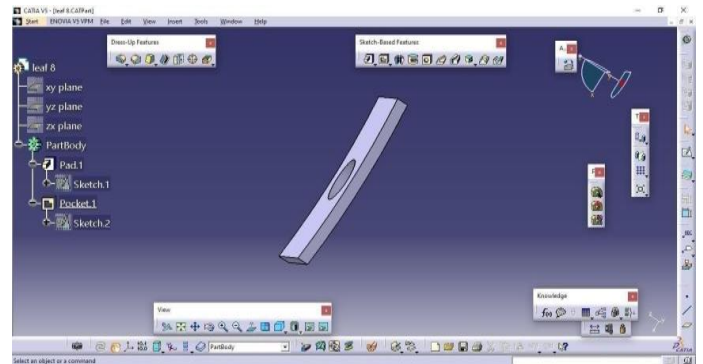
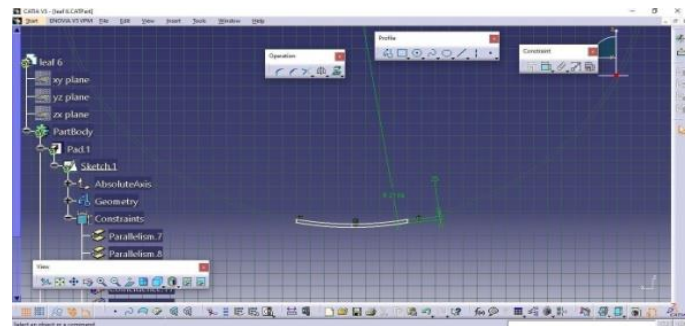


Figure 3: Half Leaf

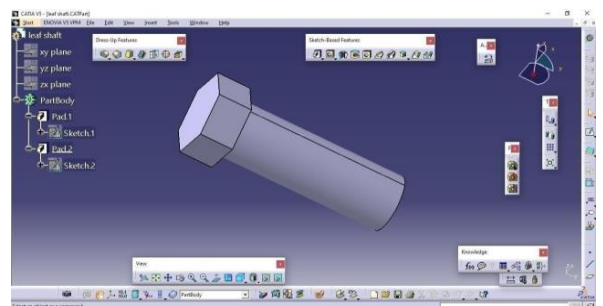


Figure 4. bolt design in catia



Figure 5: Full length Leaf

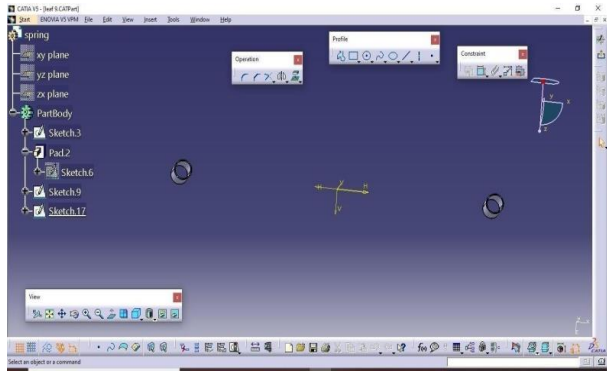


Figure 6: leaf spring eye joints

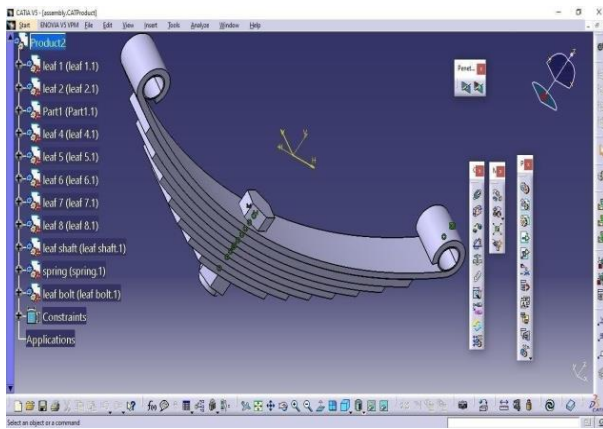


Figure 7: Catia-v5 assembly of leaf spring

MESHING:

MESHING: Before lattice the model and even before building the model, it is essential to consider whether a free work or a mapped cross section is proper for the examination. A free work has no limitations as far as component shapes and has no predefined example connected to it. Contrast with a free work, a mapped cross section

is confined as long as the component shape it contains and the pattern of mesh. Mapped area mesh contains either quadrilateral or just triangular components, while a mapped volume cross section contains just hexahedron components. In the event that we need this kind of lattice, we must form the geometry as arrangement of genuinely normal volumes and/or regions that can acknowledge a mapped network.

**DESIGN ANALYSIS OF LEAF SPRING
3D Model of a Leaf Spring**

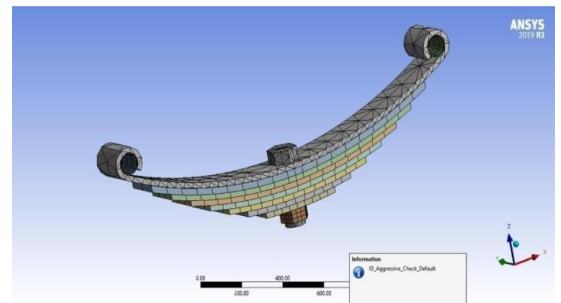
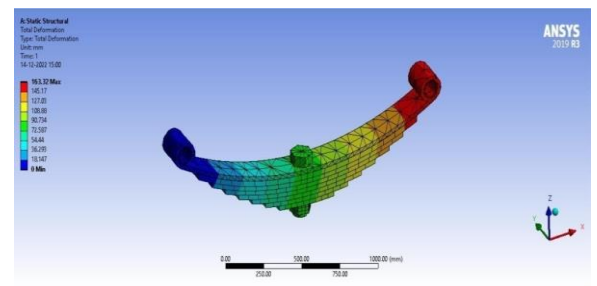
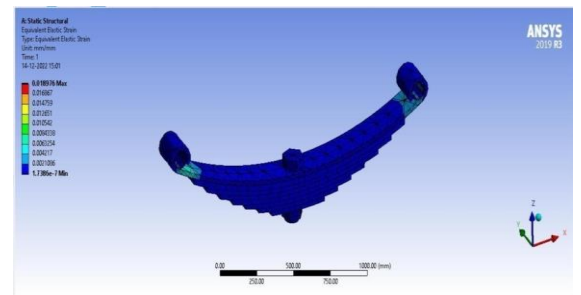


Figure 8: Mesh of leaf spring



workbench 2019. In workbench we analysed the leaf spring with static structural and we got best results in epoxy

Epoxy E-Glass UD

Property	Value	Property	Value
Density	2e-06 kg/mm ³	Shear YZ	0.016
Structural			
Orthotropic Elasticity			
Young's Modulus X direction	4000 MPa	Coupling Coefficient XY	-1
Young's Modulus Y direction	10000 MPa	Coupling Coefficient XZ	-1
Young's Modulus Z direction	10000 MPa	Coupling Coefficient YZ	-1
Puck Constants			
Poisson's Ratio XY	0.3	Material Classification	Glass
Poisson's Ratio YZ	0.4	Compression Inclusion YZ	0.25
Poisson's Ratio XZ	0.3	Compression Inclusion XZ	0.2
Shear Modulus XY	5000 MPa	Tension Inclusion XZ	0.3
Shear Modulus YZ	3042.2 MPa	Tension Inclusion YZ	0.2
Shear Modulus XZ	5000 MPa		
Orthotropic Stress Limits			
Tensile X direction	1100 MPa	Other	
Tensile Y direction	35 MPa	Ply Type	
Tensile Z direction	35 MPa	matrix	ACP
Compressive X direction	-475 MPa	Type	Regular
Compressive Y direction	-120 MPa	Additional Puck Constants	
Compressive Z direction	-120 MPa	Interface Weakening Factor	0.8
Shear XY	80 MPa	Degradation Parameter s	0.5
Shear YZ	48154 MPa	Degradation Parameter M	0.5

E-Glass

Fibers only

Density: 2.6e-06 kg/mm³

Structural

Isotropic Elasticity

Derive from	Young's Modulus and Poisson's Ratio
Young's Modulus	73000 MPa
Poisson's Ratio	0.22
Bulk Modulus	43452 MPa
Shear Modulus	29918 MPa

Result Summary

Results	Minimum	Maximum	Units	Time (s)
Total Deformation	0.	59.889	mm	1.
Equivalent Elastic Strain	1.2274e-007	8.4016e-003	mm/mm	1.
Equivalent Stress	2.1274e-002	1453.6	MPa	1.

CONCLUSION

As compare to the materials epoxy, e glass, s glass for leaf spring, epoxy is the best material it has less weight and good efficiency. The design of ling spring parts are designed in solid works. We used solid works 2019 for design and for analysis we used ANSYS

Materials	Total Deformation (mm)		Equivalent Elastic Strain		Equivalent Stress(MPa)	
	Minimum	Maximum	Minimum	Maximum	Minimum	Maximum
Steel	0	59.889	1.2274e-007	8.4016e-003	2.1274e-002	1453.6
S-Glass	0	132.47	1.7386e-007	1.8976e-003	1.1775e-002	1497.5
E-glass	0	162.32	2.1435e-007	2.3395e-002	1.1775e-002	1497.5
Carbon epoxy	0	609.94	1.1596e-006	0.14272	1.0652e-002	2207.4

References:

- [1]. K. Krishnamurthy, P. Ravichandran; Sci-Hub | Modeling and structural analysis of leaf spring using composite materials |
- [2]. Pradip Kumar; Sci-Hub | Analysis and optimization of mono parabolic leaf spring material using ANSYS | 10.1016/j.matpr.2020.06.605
- [3]. Birhan Alemu Tadesse, O. Fatoba; Design optimization and numerical analyses of composite leaf spring in a heavy-duty truck vehicle -
- [4]. D. Lydia Mahanthi; 23 IJAERS-FEB-2017-46-Design and analysis of composite Leaf Spring for light Weight Vehicle.
- [5]. K.S. Ashraff Ali; Sci-Hub | Analysis of composite leaf spring using ANSYS software | 10.1016/j.matpr.2020.08.068 (hkvisa.net)

Multi Response Optimization of Mechanical Properties of Sponge Gourd Fiber Reinforced Polypropylene Composites Using Grey Relational Analysis

Ch. Ranga Rao¹, N. Ravi Kumar, B. Raghava Rao², M. Venkaiah³, P. Srikant⁴

¹Department of mechanical Engineering, Andhra Loyola Institute of Engineering and Technology, Vijayawada, Andhra Pradesh, India.

²R. Siddhartha Engineering College, Mechanical engineering, Vijayawada, 520007, Andhra Pradesh, India.

³Narasaraopeta Engineering College, Mechanical engineering, Kotappakonda Rd, Narasaraopeta, 522601, Andhra Pradesh, India.

⁴Research scholar in Andhra university, Mechanical engineering, Vizag, 530003, Andhra Pradesh, India.

Abstract: In the present study, sponge gourd fiber polypropylene (PP) composites fabricated and tested for their mechanical properties. Maleic anhydride grafted polypropylene (MAPP) added to the matrix and the effect of matrix modification investigated. The mechanical properties of treated composites found to increase considerably when compared with untreated composites. Experiments conducted by using L₁₂ - orthogonal array considering the two-design parameters viz. weight fraction of the fiber (X) and treatment (Y). From Grey rational analysis, a grey relational grade find, based on this value an optimum level of strength parameters identified. The Analysis of variance (ANOVA) carried out to obtain the significant values of tensile strength, flexural strength and impact strength at 95 % confidence level. Confirmation test conducted to validate the test result.

Keywords: *Natural Fiber; Polypropylene composites; Maleic anhydride grafted polypropylene; Mechanical properties; Grey rational analysis; ANOVA.*

INTRODUCTION

There has been a developing enthusiasm for using fibers as support to create composite materials. Researchers lean toward thermoplastic polymeric lattices than thermosets because of the low generation cycle, lower expense of preparing and high reparability of thermoplastics. Different natural fibers are generally utilized as support as a part of thermoplastic polypropylene (PP) matrix material to get ready composites (Shubhra, Alam, and Quaiyyum 2011). The utilization of

regular fiber polypropylene composite materials in basic applications expanding in the most recent years due to their points of interest in bio degradability, recyclability, ease, eco-friendly and low thickness (Marques et al. 2014). Because of the adhesion between matrix and fibers, the mechanical properties of natural fiber polypropylene composites affected mainly. Distinctive Chemical alteration strategies used to improve the fiber and matrix adhesion, due to the improvement of adhesion between matrix and fiber the mechanical properties of the composites increased (Malkapuram, Vivek, and Negi 2009). A short jute fibre reinforced polypropylene composites have been developed by injection moulding technique with varying parameters like fibre loading (0%, 5%, 7.5%, 10%, 12.5% & 15% by weight) and fibre condition (untreated, NaOH treated followed by bleaching with H₂O₂) at constant fibre length of 3mm (Gunti, and Atluri V 2013). Taguchi method of design of experiments, genetic algorithm, and artificial neural network are some of the important tools used for robust design to produce high quality products quickly and at low cost. Taguchi method based on performing evaluation or experiments to test the sensitivity of a set of response variables to a set of control parameters (or independent variables) by considering experiments in “orthogonal array”. Orthogonal arrays provide a best set of well-balanced experiments (Phadke 2009). The S/N ratios, which are log functions of desired output, serve as the objective functions for optimization,

help in data analysis and the prediction of the optimum results. There are three forms of S/N ratio that are of common interest for optimization of static problems. 1. Smaller-the-better, 2. Larger-the-better and 3. Nominal-the-best (Rahul, Kaushik, and Sumit 2014). The grey relational analysis can be used for solving the complicated inter relationships between the multi responses. From the grey relational analysis, the grey rational coefficients calculated from S/N ratio of each output parameter. From grey rational coefficients (GRC's), grey rational grades calculated for each experiment. From grey rational grades (GRG's) find the ranks for each experiment after that GRG of each input parameters calculated (Noorul Haq, Marimuthu, and Jeyapaul 2008). Analysis of

variance (ANOVA) is a better feel for the relative effect of the different factors obtained by the decomposition of variance. Different factors affect the strength to a different degree (Rahul et al. 2014). The main objective of this work is to determine the suitability of Sponge gourd fibers as reinforcement in the polypropylene matrix for making composites. Composites comprising of polypropylene fortified with Sponge gourd fiber arranged by injection moulding with shifting weight divisions of fiber (0%, 5%, 10%, 15%, 20%, and 25%). In this present study, maleic anhydride grafted polypropylene (MAPP) copolymer used as a chemical agent to improve the adhesion between matrix and fiber. The effect of the fiber content and the interfacial adhesion on the mechanical properties of Sponge gourd Fiber/PP composites investigated. The design of experiments carried out with the help of L12 orthogonal array. The experimental data analyzed using Grey Rational Analysis for optimal conditions of input parameters. ANOVA carried out on experimental data to find the significant effect of the input parameters. Predicted values of the output parameters calculated for considering significant input parameters. Confirmation test conducted to validate the test result.

EXPERIMENTAL

Materials

The sponge gourd fiber collected from the local resources and soaked in water for two weeks. Later the purified fibers dried for a week. The extracted fiber then chopped into short fiber. The

matrix material, Polypropylene had melting temperature of 180 °C and melt flow index of 11 gm/10 min at 230 °C. The matrix material, Polypropylene had density of 0.9 gm/cm³ at room temperature. A commercially available Maleic anhydride grafted polypropylene (MAPP) copolymer used as a coupling agent. It had a softening point of 163 °C and a density of 0.91 gm/cm³.

Processing

The extracted fiber dried in an oven at a temperature of 80 °C for 2 hours to expel the moisture. The composite samples prepared in two levels. In the first level, proper proportions of fibers (0, 5, 10, 15, 20 and 25%) by weight and polypropylene pellets have properly mixed to get a homogeneous mixture. Composites of different weight fractions of fiber fabricated using Injection moulding machine. Five specimens made for each weight fraction of sponge gourd composites. At the second level, to improve fiber matrix adhesion, MAPP (2 %) added to the matrix material and composites of different fiber weight fractions prepared with a mixture of polypropylene pellets and the sponge gourd fibers.

Design of experiments

The design of experiments carried out with L12 orthogonal array. The array contained twelve rows and two columns, with 11 degrees of freedom (df) to treat one parameter (weight fraction of the fiber X) with six levels and another parameter (treatment Y) with two levels. Each parameter level set as according to the L12 orthogonal array. The different levels of variables used in the experiments listed in Table 1.

Tensile, flexural and Impact tests

An electronic tensometer used to find the tensile and flexural properties of the composite specimens. Dog bone shaped tensile test specimens made in accordance with ASTM-D 638M to measure the tensile properties. For flexural properties, three point bend tests performed in accordance with the ASTM D790M test method. The samples tested at a crosshead speed of 1 mm/min. An Izod impact test machine used to find the impact properties of the composite specimens. The impact specimens prepared in accordance with ASTM D256-97.

RESULTS AND DISCUSSION

Tensile, flexural and impact strength test results

The tensile, flexural and impact properties found out from six different weight fraction of fibers (0%, 5%, 10%, 15%, 20%, and 25%) for without MAPP and with MAPP. For each weight percentage, five specimens tested to achieve the repeatability of results. The variations of mean tensile strength, flexural strength and impact strength with weight fraction of fiber (%) shown in the Figure 1. (a), (b) and (c) respectively.

The tensile, flexural and impact strength of the sponge gourd fiber reinforced with and without Maleic anhydride polypropylene composites increases up to 15% and then decreased which is because of the expansion in the likelihood of agglomeration, which adversely adds to the property of the composite. Table 2, Table 3 and Table 4 showed the experimental results of various tests respectively. It observed that all the composites have shown a moderate increase in tensile, flexural and impact strength with the addition of MAPP. Maleic anhydride grafted polypropylene improves the adhesion between fiber and matrix by chemically bonding to available OH groups on the fiber surface and then adhering to the matrix through molecular chain entanglement. The incorporation of fibers into thermoplastics leads to poor dispersion of fibers due to strong inter fiber hydrogen bonding which holds the fibers together. Improper adhesion hinders the considerable increment of tensile strength (Beckermann, Pickering, and Foreman 2004). Thus, as fiber percentage increases, gathering of fibers takes place instead of dispersion and melted polypropylene cannot wet them properly due to non-entrance of melt through the adjacent two fibers. Since no adhesion is present between the fibers and fibers also not bonded with matrix, failure occurs before attaining the theoretical strength of composite. The reasons for the lower flexural properties at higher fiber weight fractions are possibly due to the lower fiber to fiber interaction, void and poor dispersion of fiber in the matrix (Asri and Abdul 2002). High fiber content increases the probability of fiber agglomeration, which results in regions of stress concentration requiring less energy for crack propagation (Karmakar et al. 2007). This results in lower energy dissipation and hence impact strength decreases at higher fiber weight percentages.

Signal to Noise Ratio for tensile, flexural and impact strength

The experimental results transformed into S/N ratios to quantify the quality characteristics deviating from the desired value. In the present work, the S/N ratio calculated by using the following Larger-the-better formula.

$$\eta = -10 \log_{10} \left(\frac{1}{n} \sum_{i=1}^n \left(\frac{1}{y_{ij}^2} \right) \right) \quad (1)$$

The S/N ratio of Experiment results (tensile strength, flexural strength and impact strength) calculated and shown in Table 5, Table 6 and Table 7 respectively.

Grey Rational Analysis for tensile, flexural and impact strength

In the Gray Rational Analysis, the era of grey relations connected to the test information identified with quality attributes, the aftereffects of which used to acquire the grey relational grades consequently to rank every information arrangement. In the grey relations, the S/N ratio normalized as N-S/N ratio ($0 \leq \eta_n \leq 1$) by utilizing the following equation to keep away from the impact of receiving diverse units and to decrease the variability.

$$N - S/Nratio = \eta_n = \frac{\eta_i - \min(\eta_i)}{\max(\eta_i) - \min(\eta_i)} \quad (3)$$

In the grey relations, the quality loss function (Δ) calculated by using the N-S/N ratio.

$$Quality Loss = \Delta = \max(\eta_{n_i}) - \eta_{n_i} \quad (4)$$

Computed the grey relational coefficient (GRC) form the quality loss function (Δ).

$$GRC = \frac{\min(\Delta_i) + \xi * \max(\Delta_i)}{\Delta_i + \xi * \max(\Delta_i)} \quad (5)$$

Where ξ = Distinguishing coefficient, which defined in the range $0 \leq \xi \leq 1$ (the value of ξ can be adjusted on the practical needs of the system).

The N-S/N ratio (η_n), quality loss function (Δ) and grey rational co-efficient (GRC) of Experiment results (tensile strength, flexural

strength and impact strength) calculated and shown in Table 5, Table 6 and Table 7 respectively.

The grey rational grade (GRG) Computed for each experiment by using the following formula, the results showed in Table 8.

$$GRG = \frac{1}{m} \sum_{k=1}^m GRG_{ik} \quad (6)$$

Where

$$m = \text{number of output parameters} = 3$$

The higher grey relational grade infers the better output quality; along these lines, on the premise of grey relational grade, the parameter effect can be evaluated and the ideal level for each controllable parameter can be resolved. The Grey Rational Grades of input parameters (Weight fraction of the fiber (X) and Treatment (Y)) calculated by using the total mean of the grey relational grade for the 12 experiments and listed in Table 9. Considering maximization of grey rational grade (GRG) values (Table 9/Figure 2), the optimal input parameters obtained at X4Y2, i.e. at 15 % of the Weight fraction of the fiber (X) and with treatment (Y).

Analysis of variance

The purpose of the statistical analysis of variance is to investigate which design parameter significantly affects the strength of the composites. The analysis carried out for the level of significance of 5% (the level of confidence is 95%). Using the grey grade value (GRG), ANOVA formulated for identifying the significant factors. Two-way ANOVA allows comparing the grey rational grades (GRG) of the population when the populations classified according to two (categorical) factors (weight fraction of the fiber (X), treatment (Y)). Analysis of variance results listed in Table 10 and Figure 3.

From ANOVA it can be concluded that the weight fraction of the fiber (X) is significant since corresponding F value is higher than F-crit. This analysis is acceptable since corresponding p value is less than 0.05. From the ANOVA, the significant contribution of weight fraction of the fiber (X) is 85.75 % followed by treatment (Y) is 7.615 %.

Predicted optimum condition:

In order to predict the optimum condition, the expected mean at the optimal settings (μ) calculated by using the following model

$$\mu = X_4 + Y_2 - GRG_{AVG} \quad 7$$

Where X4 and Y2 are the mean values of the grey relational grade with the parameters at optimum levels and GRGAVG is the overall mean of average grey grade.

The expected mean (μ) at the optimal settings found to be 0.9094.

Confidence interval (CI) calculated as

$$CI = \sqrt{(F(1, f_e) * V_e * (\frac{1}{n_{eff}} + \frac{1}{R}))} \quad 8$$

Where

F(1,fe) is the F ratio at a significant level of 95% = 6.61,

Fe is the error degrees of freedom = 5,

Ve is the error mean square = 0.004348,

n_{eff} is the effective total number of test

n_{eff}

$$= \frac{\text{Total number of observations}}{1 + (\text{Total degrees of freedom associated with } \mu)}$$

$$= \frac{12}{1 + 6} = 1.7142857$$

and R is the number of confirmation tests = 5.

The confidence interval (CI) value for the error is ± 0.15 .

The Grey rational grey value at the optimum (X4Y2) is lies between $\mu + CI$ and $\mu - CI$.

$$(0.9094 - 0.15) \leq \text{Final GRG} \leq (0.9094 + 0.15)$$

$$(0.7594) \leq \text{Final GRG} \leq (1.0594).$$

Therefore, the final GRG value lies between 0.7594 and 1.0594.

Confirmation experiment

The confirmation experiment conducted at the optimum settings (X4Y2) to verify the optimum mechanical properties of sponge gourd reinforced polypropylene composites. The average responses by the confirmation experiment trial at the optimal settings are Tensile Strength = 25.25366 MPa, Flexural Strength = 54.67 MPa, and Impact Strength = 53.58 J/m showed in Table 11. The grey relational grade value as per above discussion is found to be 0.994. This result is within the 95% confidence interval of the predicted optimum condition and grey grade value of confirmation experiment improved by 9.303% from the predicted mean value (μ). Hence, the grey relational analysis for the optimization of the multi response problems is a very useful tool for predicting the tensile strength, flexural strength and impact strength of the sponge gourd reinforced polypropylene composites.

CONCLUSIONS

The effect of reinforcement of sponge gourd fiber into the polypropylene matrix investigated based on the fiber loading and the addition of a coupling agent (treatment). The experimental results supported the successful fabrication of sponge gourd fiber reinforced polypropylene composites and confirmed that sponge gourd fiber can be used as filler as it improved the mechanical properties of the composite when compared to polypropylene. The tensile strength, flexural strength and impact strength values collected under different fiber loading conditions without and with MAPP treatment.

From this Grey Rational analysis, it is revealed that weight fraction of the fiber is the prominent factor which affects the mechanical properties of polypropylene composites. Weight fraction of the fiber (X=85.75%) is more and followed by Treatment (Y=7.61%). The best performance characteristics were obtained at X4Y2, i.e. at 15% of the weight fraction of the fiber (X) and with treatment (Y). Confirmation test was conducted to validate the results. In perspective of the great appearance of sponge gourd composites arranged with

short filaments, their utilization as decorative boards, linings and items without auxiliary capacity can be conceived.

REFERENCE

- 1) Asri, S. M., and Abdul Khalil H. P. S. 2002. "Utilization of oil palm fibers thermoplastic prepreg in polyester hybrid composites." Proceedings of 3rd National Symposium on polymeric materials 160-166.
- 2) Beckermann, G. W., K. L. Pickering, and N. J. Foreman. 2004. "The Processing, Production and Improvement of Hemp-Fiber Reinforced Polypropylene Composite Materials." Proceedings of SPPM 257-265.
- 3) Gunti Rajesh, and A. V. Ratna Prasad. 2013. "Advanced Materials Manufacturing & Characterization" Advanced Materials Manufacturing & Characterization Vol 3 Issue 2.
- 4) Karmakar, A., S.S. Chauhan, J.M. Modak, and M. Chanda. 2007. "Mechanical properties of wood-fiber reinforced polypropylene composites." Composites. A 38: 227-233.
- 5) Maria de, Fatima, V. Marques, Renato P. Melo, S. Rafael da, Araujo, N. Juliana do, Lunz, O. Vincius de and Aguiar. 2014 "Improvement of mechanical properties of natural fiber-polypropylene composites using successive alkaline treatments," Journal of Applied Polymer Science DOI:10.1002/app.41710.
- 6) M. S. Phadke. 2009. "Quality engineering using robust design," 2nd edition. Pearson.
- 7) Noorul Haq, A., P. Marimuthu, and R. Jeyapaul. 2008. "Multi-response optimization of machining parameters of drilling Al/SiC MMC using grey relational analysis in the Taguchi method." International Journal of Advanced Manufacturing Technology 37: 250-255. doi:10.1007/s00170-007-0981-4.
- 8) Quazi, T.H.Shubhra, AKMM.Alam, and MA.Quaiyyum. 2011. "Mechanical properties of polypropylenecomposites A review," Journal of Thermoplastic Composite Materials 0892705711428659.
- 9) Ramakrishna, Malkapuram, Vivek Kumar, and Yuvraj Singh Negi. 2009. "Recent Development in Natural Fiber Reinforced Polypropylene Composites," Journal of Reinforced Plastics and Composites vol. 28 no.10:1169-1189.
- 10) Rahul, Kumar, Kaushik Kumar, and Sumit Bhowmik. 2014. "Optimization of Mechanical properties of epoxy based wood dust reinforced green composite using Taguchi method," Procedia Materials science 5: 688-696.
- 11) Rahul, Kumar, Kausik Kumar, Prasanta Sahoo, and Sumit Bhowmik. 2014. "Study of Mechanical Properties of Wood Dust Reinforced Epoxy Composite," Procedia Materials Science 6: 551 - 556.

Experimental Investigation of AZ31 Metal Matrix Composites

Itha Veeranjanyulu, T Durga Prasad, T. Chandra Shekhar Reddy

Department of Mechanical Engineering, Aditya Engineering College, Suram palem, Kakinada, A.P. India.

Abstract— The AZ31 alloy is used as the matrix material in the current investigation, with silicon carbide (SiC) and graphite (Gr) particles used as reinforcement. The stir casting technique was used to create AZ31-SiC-Gr hybrid composites with various SiC and Gr compositions (0, and 2 wt%). The produced hybrid composite density, hardness, tensile, and compressive properties were assessed. The experimental findings demonstrate that adding reinforcements enhanced the mechanical properties of the created hybrid composites. By adding 2% SiC and Gr to the base alloy, the mechanical properties were raised.

Keywords— AZ31, Hybrid composites, stir casting

I. INTRODUCTION

The developments in the area of magnesium (Mg) based composites particularly AZ (Aluminum Zinc) series Mg alloy based composites are reviewed in this chapter. The literature that is relevant to the present research is summarized and presented. Significant findings from the earlier published scientific information are described in detail.

MAGNESIUM BASED COMPOSITES

The existing literature has used both pure magnesium and various magnesium alloys as matrix materials. The two most popular magnesium alloys from the AZ series alloys, together with pure magnesium, are AZ31 and AZ91. To create magnesium-based composites, a variety of reinforcements with varying size, shape, morphology, and quantity are disseminated throughout the matrix. The qualities that are desired to be introduced into the composite determine the reinforcement to be used. The additional reinforcements can be divided into the three categories below in order to create composite materials based on magnesium.

- i. Ceramics
- ii. Intermetallics
- iii. Metallic powders

SiC is a significant reinforcement that is frequently utilised in creating composites made of magnesium. Strong bonds between the dispersed particles and matrix, which SiC

demonstrates greater wettability for in molten Mg, aid in improving the composite's mechanical characteristics.

Another ceramic phase that has been extensively employed in the creation of composites based on magnesium is Al₂O₃. The development of Mg-based composites is also using carbon nanotubes (CNTs), a new and promising material, as reinforcement because of their high strength (150 GPa) and high Young's modulus (1 TPa).

The specifics of material preparation, processing, and characterization are covered in this chapter. All of the characterisation methods employed in the current investigation are fully described. Details of the preparation of the AZ31 Mg alloy and the AZ31-SiC-Gr composite, as well as their characterisation, are described.

II. SAMPLE PREPARATION

Development of AZ31 Mg alloy and AZ31-SiC-Graphite Composites

The AZ31Mg alloy, which contains 3% aluminium, 1% zinc, and the rest percentage being magnesium, has been chosen for the current research project and will be created using the stir casting method. Pure Mg billet has been obtained from Exclusive Magnesium, Hyderabad, in order to create the AZ31 Mg alloy. Base alloy was created through stir casting using the proper weights of pure Mg, Al, and Zn (Swam equipment, Chennai, India). SiC and Gr were added to create composites.

In the current study, the AZ31 matrix was reinforced with 25 m of Gr. Table 1 displays the AZ31's basic elemental composition in weight percentages. SiC and graphite were imported in powder form, and AZ31 alloy was purchased in ingot form.

Table 1. Elements of AZ31D in wt %

Elements	Al	Zn	Mn	Cu	Fe	Mg
Wt%	3	0.98	0.20	0.02	0.02	Rest

Materials were created in the current work using a bottom pouring type stir casting machine. A picture of a typical stir casting machine used in this work is shown in Fig. 1. It has a moving stirrer with a ceramic-coated impeller blade fastened to the stirring rod and a variable-speed motor connected to it. When the material is liquid in the furnace, the stirrer is used. In order to feed the preheated reinforcing powder into the furnace, where the materials are melted, a feeder is positioned above the mouth of the furnace. Preheating is done to clean the materials of any contaminants or moisture. The mixed slurry is then poured into metal mold.

The furnace is constructed of 310-grade stainless steel for increased heat and corrosion resistance. Since there is a danger that the furnace could be damaged while stirring, a mild steel sleeve with a graphite coating is kept inside the furnace. The furnace has a 2 kg capacity and can melt magnesium or aluminium. It can sustain temperatures of up to 950 C as measured with the Kanthal APM. Heating coils with ceramic fibre insulation are used. A three phase AC motor is used to automatically open and close the stir casting furnace's gate valve. Mild steel is used to construct the machine's outside casing. Mild steel is used to construct the machine's outside casing. The stirrer blade has two fins and is constructed of 310-grade stainless steel. It can rotate at speeds ranging from 100 to 1500 rpm and is controlled by a DC motor with a 4 to 20 mA control and a separate digital indication. It is of the motorised control variety and has the ability to automatically stop at the most extreme top and bottom side positions in order to prevent mishaps.

Before beginning the procedure, the furnace is preheated. The stir casting equipment has a heating chamber with stainless steel tubes and a bottom gate valve to control the flow of reinforcement into the melt. The reinforcement powder is delivered on the top side of the equipment during preheating. The reinforcement can be

pushed into the melt using an electromagnetic vibrator as well. In a similar manner, a separate portable heater is set up to heat the mould to 3500 C before the melt is poured into it. A separate set of argon cylinders is available for the delivery of shielding gas.



Figure 1: Photograph of stir casting setup

Magnesium is extremely flammable despite having good machinability. As a result, caution must be used when working with magnesium and its alloys. Liquid paraffin was used as a coolant for the machining process, which was done on a wire cut EDM machine. In order to conduct microstructural research, evaluate mechanical characteristics like density, hardness, tensile strength, and compression, as well as for scanning electron microscopy, samples were cut across the cast rods.

III. EXPERIMENTAL DATA

A. Density measurement

The rule of mixture and the Archimedes principle were used, respectively, to compute the theoretical and observed densities of the S1, and S2 samples.

B. Hardness Measurements

Hardness of a material is described as its resistance to long-term deformation, surface abrasion, or scratching under various stresses. Hardness is typically evaluated using the indentation method, which presses a hard indenter with a predetermined form on the surface of the workpiece while delivering the proper loads. The workpiece's surface

imprint is measured, and the hardness value is computed taking the applied load value into account. In Vickers indentation method, the opposite faces of the diamond indenter contains an angle of 136 °. A suitable load is applied on the indenter to produce an impression on the surface of the workpiece. Then the lengths of the diagonals of the diamond shape indent produced on the surface of the workpiece are measured.

C. Tensile and Compression Measurements

Tensile and compressive tests were performed using UTM (INSTRON 8801 UTM) on cylindrical specimens of S1, and S2 with a ram speed of 3 mm/min. The experiment was conducted for three samples of each specimen and the value was averaged over three readings.

IV. RESULTS AND DISCUSSION

A. DENSITY and MICRO HARDNESS

The incorporation of reinforcements in the semi-solid condition as the contract to the monolithic alloy is responsible for the rise in the density of hybrid composites. Comparing the measured density to the theoretical density, lower values were found. The increase in density of hybrid nanocomposites is credited to the inclusion of reinforcements in the semi-solid condition as compared with the monolithic alloy which is shown in Table 2. The measured density was lower values as compared with the theoretical density. The addition of SiC and Gr particles leads to an enhanced porosity and increased density, which contributes to raising the hardness of the nanocomposite.

Table 2. Density and Micro hardness

Sam ple	Alloy and Composites	Theore tical Densit y (g/cc)	Measur ed Density (g/cc)	Micro Hardness (VHN)
S1	AZ31	1.8	1.799	71.89
S2	AZ31+2%SiC+2%Gr	1.84	1.834	80.97

B. TENSILE AND COMPRESSION PROPERTIES

The UTS, YS, and CS of composites are improved when the volume ratio of SiC and Gr particles is changed. The bonding between the reinforcements and matrix may be impacted by the grain size of the reinforcements. In comparison to the monolithic alloys of UTS and YS, respectively, and as shown in figure 3, the 2 weight percent of AZ31/SiC/Gr composite has improved the strength overall. With more reinforcement, the composites' ability to withstand stress and strain is improved.

Due to the reinforcement of SiC and Gr particles in composites, the compression outcomes of the materials are improved. The composite's strength varies depending on the reinforcements' grain size and how well they are bonded to the matrix. Grain refining is what allows for the greater strength. The interfacial holding between the reinforcement and matrix is acceptable, and once pressure is applied, the formed SiC and Gr particles may transform to a magnesium combination lattice.

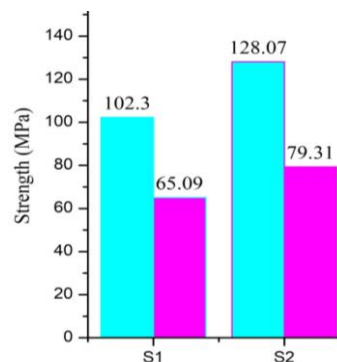


Figure 2: Variation of YS and UTS of hybrid composites

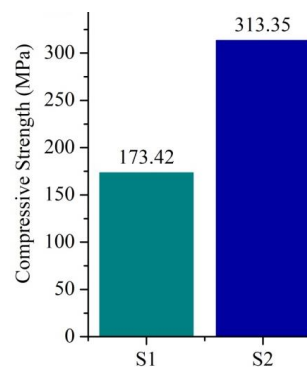


Figure 3: Variation of compressive strength of hybrid composites

V. CONCLUSIONS

- Development of AZ31 Mg alloy and composites of AZ31 Mg alloy – Silicon Carbide and Graphite were successfully done by stir casting method.
- The material with the highest density of 1.84 g/cc and Vickers hardness number of 80.97 was AZ31-2%SiC-2%Gr. This was brought on by the presence of SiC and shows the increase in density and hardness vs the AZ31 alloy.
- The AZ31-2%SiC-2%Gr hybrid composite outperformed compared to base alloy in terms of ultimate tensile strength and compressive strength. This resulted from the matrix's reinforcements being distributed consistently.
- When compared to the base alloy, the mechanical properties were greatly enhanced. The S1 hybrid composite yielded superior outcomes overall.

REFERENCES

- [1] R. Vara Prasad Kaviti, D. Jeyasimman, G. Parande, M. Gupta, R. Narayanasamy, P.G. Koppad, Improving the friction and wear characteristics of AZ31 alloy with the addition of Al₂O₃ nanoparticles, *Mater. Res. Express*. 6 (2019).
- [2] U. Rokkala, S. Bontha, M.R. Ramesh, V. Krishna, A. Srinivasan, S. V Kailas, Tailoring surface characteristics of bioabsorbable Mg-Zn-Dy alloy using friction stir processing for improved wettability and degradation behavior, *J. Mater. Res. Technol.* 12 (2021) 1530–1542.
- [3] A. Khandelwal, K. Mani, N. Srivastava, R. Gupta, G.P. Chaudhari, Mechanical behavior of AZ31/Al₂O₃ magnesium alloy nanocomposites prepared using ultrasound assisted stir casting, *Compos. Part B Eng.* 123 (2017) 64–73.
- [4] Dinaharan, I., Zhang, S., Chen, G.; Shi, Q. Development of titanium particulate reinforced AZ31 magnesium matrix composites via friction stir processing. *Journal of Alloys and Compounds*, April 2020, Volume 820, 153071.
- [5] Zang, Q., Chen, H., Zhang, J.; Wang, L., Chen, S., Jin, Y. Microstructure, mechanical properties and corrosion resistance of AZ31/GNPs composites prepared by friction stir processing. *Journal of Materials Research and Technology*. October 2021, Volume 14, Pages 195–201.
- [6] Kumar, K.C.K., Kumar, B.R. & Rao, N.M. Microstructural, Mechanical Characterization, and Fractography of AZ31/SiC Reinforced Composites by Stir Casting Method. *Silicon* 14, 5017–5027 (2022).
- [7] Gangadhara Rao, Vundavilli, P.R., Meera Saheb, K. Microstructural and Mechanical Behaviour of Al6061/Gr/WC Hybrid Metal Matrix Composite. *Advances in Materials and Manufacturing Engineering* pp 525–531.
- [8] M. Subramani, S. J. Huang, K. Borodianskiy. Effect of SiC Nanoparticles on AZ31 Magnesium Alloy. *Materials*, 15(2022)1004.

CONSTRUCTION OF A MOTORIZED ROTARY WELDING TABLE

Ch. Ranga Rao¹, K. Sathwik, E. Durgesh, M.Venkaiah²

Associate Professor¹, Student, Assistant Professor, ¹Department of mechanical Engineering, Andhra Loyola Institute of Engineering and Technology, Vijayawada, Andhra Pradesh, India.

⁴Department of mechanical Engineering, Narasaraopeta Engineering College, Narasaraopet Andhra Pradesh, India.

Abstract: A Specialized piece of machinery made specifically for the welding business is the motorized rotary welding table. This table provides a rotary motion to the workpiece which can improve the efficiency and the accuracy of the welding. The apparatus is made with a robust foundation, which provides stability while welding operations are being done. It has a robust motor that makes the rotating motion possible, and it has an intuitive user interface. The table is very adaptable for various welding applications because it has features like variable speed control. Use of a motorized rotary welding table can speed up welding and produce welds of higher quality.

INTRODUCTION

Welding is a joining process used to join two materials by using the heat and the mechanical moments which is having the ability to melt and it is being left in the air to cool and form a strong joint. There are different types of welding process like Arc welding, TIG Welding, MIG welding, and Spot Welding. Where the Arc Welding refers to the process of welding using an alternating current (AC) power supply.

AC periodically changes its direction, typically at a frequency of 50 to 60 cycles per second. AC welding is commonly used for a variety of welding applications, including metal fabrication, construction, and repair works. AC Welding offers a few advantages over DC Welding. It can provide better cleaning action and improve penetration, especially for certain materials like aluminum.

However, AC Welding can be more challenging than DC Welding due to the Constantly Changing polarity.

Mostly Welding may be linear, circular. In some of the cases the welding may not be carried properly carried out in the circular components to rectify this problem the fabrication of the motorized rotary welding table is done. Where the motorized rotary welding table consists of a motor and where the speed is being controlled by knob.

The advantages of the ARC welding are: -

1. Flexibility in positioning: Arc welding can be performed in various positions. Including flat, horizontal, vertical, and overhead. This flexibility allows welders to tackle projects with different welding orientations.
2. Wide range of processes: Arc welding encompasses several welding processes, such as shielded metal arc welding, Gas tungsten arc welding, flux Cored Arc welding and more.
3. Suitable for thick materials: Arc welding is well suited for thicker sections of metal. By adjusting the welding parameters and using appropriate electrode types, it is possible to achieve deep penetration and create robust welds in thicker materials.
4. Strong and durable welds: Arc welding produces welds with excellent strength and durability. The fusion of metals the joint creates a bond that is often as strong, if not stronger, than the base metal.
5. Portability: Arc welding machines come in various sizes, including compact and portable models. This portability allows for flexibility in welding applications. Especially on situations where the workpiece cannot be easily moved.

PROBLEM STATEMENT

The current welding process involves manually rotating the workpiece on a welding table to access different welding angles. This manual rotation not only consumes valuable time but also requires additional manpower. Moreover, the human operator may face challenges in maintaining consistent rotation speed and precision, resulting in variations in weld quality.

table that automates the rotation process can significantly increase work efficiency and reduce

the lead time.

COMPONENTS

The components that are needed for fabrication of motorized rotary welding table are being classified as:

- 1.Zinc Hollow pipes
- 2.Compound gears
- 3.Bearing
- 4. DC Motor
- 5.DC Battery
- 6.Iron sheet
- 7.Regulator
- 8.Toggle Switch
- 9.Shaft

ZINC HOLLOW PIPES

These are also known as zinc-coated or galvanized hollow pipes are metal pipes that have been treated with a protective layer of zinc to prevent corrosion. These are commonly used in various applications where corrosion resistance is essential, such as plumbing, construction and outdoor structures.

COMPOUND GEARS

Compound gears also known as double gears or combination gears are a type of gear arrangement that consist of two or more gears. In a compound gear system, each gear is in contact with the adjacent gears and teeth of the gears are mesh together.



Figure:1: Compound gears

BEARING:

A Bearing is a mechanical component that supports and facilitates the rotation of another component, typically a shaft or an axle with reduced friction. It helps in reducing the friction forces between moving parts and enabling smooth and efficient motion.

These are used in wide range of applications from small household applications to large industrial machinery.

DC MOTOR

. A DC Motor is a type of electric motor that converts electrical energy into mechanical rotational motion. It operates on principal of electromagnetic induction utilizing the interaction between a magnetic field and electric current to produce motion.

The basic components of a DC motor include a stator and a rotor. When a electric current is passed through the armature a magnetic field is generated around it due to interaction between magnetic field of stator and current flowing through the armature windings

Fig no 2: DC Motor

DC BATTERY

A DC battery often referred to as direct current battery is a device that stores electrical energy chemically and releases it as direct current when needed. It is a portable source of power commonly used in wide range of applications, from small electronic devices to large scale systems

DC batteries are designed to provide a steady and reliable source of electrical energy. They consist of one or more electrochemical cells connected in series or parallel to achieve the desired voltage and capacity.

Each cell within the battery typically consists of two electrodes an electrolyte and a separator.



Figure 3: DC Battery

IRON SHEET

An Iron sheet also being known as sheet metal or steel sheet refers to a flat thin plate of iron in various sizes and thicknesses. It is a versatile material widely used in construction, manufacturing, and various industries for its strength, durability, and ease of fabrication.

These sheets are typically made of carbon steel or mild steel, which is an alloy of iron and a small amount of carbon. They can also be made from Stainless Steel which contains additional elements like chromium for enhanced corrosion resistance.

The IMP point that needs to be considered is that Iron sheet can be susceptible to corrosion if not properly protected.

REGULATOR

A regulator is a device or mechanism that controls or regulates the flow, pressure, or voltage of a system to maintain a desired and the consistent output.

TOGGLE SWITCH

A Toggle switch is a type of electrical switch that is commonly used to control the flow of electric current in a circuit. It is name TOGGLE because it can be flipped or toggled between two positions, typically an ON position and an OFF position.

SHAFT

A shaft is a mechanical component that is used to transmit rotary motion and power between different parts of a machine or system. It is a long, cylindrical rod or bar that usually rotates along its axis. Shafts are commonly found in various mechanical systems, including engines, motors, pumps and industrial machinery.

- Material: Mild steel [MS]
- Diameter: 25mm
- Length: 120mm

OBJECTIVES

1. To Reduce the welding cost and to increase the weld quality
2. Increased the weld access
3. Operator Safety and ergonomics
4. Flexibility and acceptability
5. Integration with the weld systems

CHALLENGES

1. Equipment maintainer
2. Equipment Complexity
3. Compatibility and Integration
4. Programming and control
5. Workpiece Adaptability
6. Workpiece Limitations

CONSIDERATIONS

1. Workpiece size and weight
2. Rotary speed and torque requirements
3. Safety features
4. Integrations with welding processes
5. Workspace requirements
6. Maintenance and Serviceability
7. Training and operator skills
8. Cost and Return Investment

LITERATURE SURVEY

Kamesh S et al. [1] this project is preplanned that it provides flexibility in operation. 360° welding cutting rotary turn table welding positioner' in this

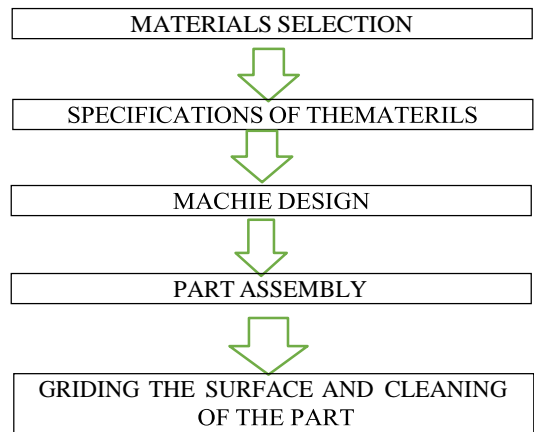
Equipment it reduces the time required to complete the operation and reduce fatigue. Nisarg Shete, et al [2] Friction welding is a non- conventional pressure welding where it is considered most variables to overcome the difficulties faces in conventional joining technique. These are mostly used for joining the materials which has varying like mechanical and physical properties. In friction welding the kinetic energy is converted into heat energy by producing high quality of weld and a high efficiency

Ashish Deiokar [3] In order to do automatic, they have used advance gas metal arc welding with the automated kit. In order to make the brake pedal automatic they have used circular weldings successfully

Vijaykumar. P et al [4] In order for the flexibility in the 360° welding. The invention of 360° Rotary welding Table rotary welding table has been created, where these are useful for the variety of the industries. These help us to steps needed to create the welding table.

Prabhakaran. S et al [5] Optimization of the welding parameters for the shielded metal arc welding in the fabrications of the metals in fabrication industries is by the simulant software

METHODOLOGY



RESULT

The Result of implementing a motorized rotary welding table can vary depending on specific application and the welding operations requirements. Some of the potential outcomes that

are achieved with a motorized rotary welding table are: -

1. Increased Productivity
2. Improved weld quality
3. Enhanced welding access
4. Operator safety and ergonomics
5. Reduction in Rework and scrap

CONCLUSION

In this a motorized rotary welding table offers several advantages and benefits for welding operations. It enhances productivity by reducing manual handling and repositioning of workpieces, leading to increase efficiency and throughput. The controlled rotation of the workpiece ensures uniform heat distribution resulting in improved weld quality and reduced defects.

REFERENCE

1. Vijaykumar, P. Varsan, M.M, et al (2022). Design and fabrication of Automatic Welding Table, International Journal of research Publication and Reviews, 3(5), 778-784.
2. Prabhakaran, S., et al (2020). Optimization of welding parameters for shielded metal arc welding parameters for shielded metal arc welding in metal fabrication industries simufact software, IRJETT, 7(4).
3. Kamesh, S, Karthik, M, et al (2021) 360° Welding Cutting Rotary turn table positioner. International Research Journal of Engineering and Technology (IRJET), 8(3).
4. Ravisankar, A., Velaga, S. K. Rajput, G., & Venugopal, S. (2014). Influence of welding speed and power on residual stress during gas tungsten arc welding of thin sections with constant heat input: A study using numerical simulation and experimental validation.
5. Deokar, A., Bhujbal, C., et al (2020). Manufacturing and designing of the Job. (IRJET), 7(6).
6. Jamadar, N. S., et al (2021). The fabrication of the Standing desk rotary ais welding table. International journal of advanced research in science, Engineering and technology, 8(8)
7. Shete, N, Deolar, S.U. (2017). A review paper on the rotary friction Welding, (ICHIIME).

Preparation and Characterization of Al-Cu Composite by using Stir Casting Technique

*Mr. K. Krishna kishore, Mr N.Rammohanarao, Ms. M.Mariyambi, Ms. K.Surekha, Mr. K.Rajesh
Asst.Professor, IVB.Tech., Department of Mechanical Engineering, Seshadri Rao Gudlavalleru Engineering College,,
Gudlavalleru, A.P., India.*

Abstract - Composite materials are now a major field of research and development activity. Composites are rapidly becoming important and useful structural materials, and probably the next major area for polymer applications is in the field of composite materials. Aluminum matrix composites (AMCs) become choice for automobile and aerospace industries due to its tunable mechanical properties such as very high strength to weight ratio, superior wear resistance, greater stiffness, better fatigue resistance, controlled coefficient of thermal expansion and good stability at elevated temperatures.

In the present work an attempt was made to understand the mechanical behavior of composite, Pure Aluminum alloy, reinforced with Boron Carbide and silicon carbide. Composites are casted using stir casting method. Castings are prepared with a percentile range from 0%, 2%, 4% and 6%. An investigation is made on studying the mechanical behavior of the pure base metal when compared with different weight percents of reinforcements. The composites were by varying the weight of percentage of copper particles in aluminum, ranging from 5% and 20%.

The results showed that the addition of copper particles improved the hardness, tensile strength and wear resistances of the composites. However, the density of the composites decreased with increasing copper content. The study provides valuable insights into the potential of using copper as a reinforcement material for aluminum metal matrix composites, which can be used in a variety of engineering applications.

Keywords- Aluminum matrix composites, wear resistance, Hardness, Stir Casting Technique. ,

INTRODUCTION

Anything composed of one or more substances that is comprised of matter is called material. Some examples of materials include water, air, hydrogen, wood, cement, and air. When used more specifically, the word "material" can refer to substances or parts that have particular characteristics and are employed as inputs in production or manufacturing. In this sense, materials are the components needed to create something else, such as structures, works of art, stars, and even computers. In the modern world, metal-matrix composites (MMCs) are regarded as the most beneficial and advanced composite materials. Due to its high strength-to-weight ratio, high young modulus, and strong abrasive characteristics, MMCs are particularly essential.

MMCs are materials made by combining a matrix such as AL or Cu with reinforcing materials, such as ceramics, carbon fibers or metallic particles. The resulting material has improved mechanical, thermal, and electrical properties compared to the base metal. Both AMCs and CMCs have the potential to replace conventional materials in many applications, as they offer a unique combination of properties that cannot be achieved with single phase metals.

I. LITERATURE REVIEW

[1] Hassan (2007) studied the effect of mechanical and microstructural properties of Al-Cu composite. The authors concluded that the reinforcement improves the hardness, tensile strength and porosity whereas it lowers density and impact strength.

[2] Kumar et al. (2010) examined mechanical, physical, metallography and tribological performance Pure Al and Cu and Pure Al-Cu composites. The composites are made with 0%, 2%, 4% and 6% volume of Cu and Pure Al by a stir casting route.

[3] Vannan et al. (2014) fabricated Pure Al composites reinforced with short basalt fibre by compocasting technique. It was observed that the increase of fibre proportion increases mechanical properties and reduces the density. Moreover, the interface bonding between matrix and fibre are examined with optical and SEM

[4] Aku et al. (2013) evaluated microstructure, hardness and density of CSA composites with 3% to 15% volume. It was found that by increasing the volume percentage of reinforcement, density decreases by 7.16% and hardness increases 17.95%. From the literatures, it was observed that, the wear mechanism was mainly influenced by the load, volume or weight percentage (%) of reinforcement, sliding distance, sliding speed, contact surface and temperature.

[5] Sahin (2010) optimised the wear behaviour of Pure Al and Cu-MMCs and reported that the effect of abrasive particles plays a key role in wear mechanism, followed by the percentage of reinforcement. However, the effect of sliding distance is not significant parameter on wear loss of materials.

II PREPARATION OF COMPOSITE

Place the molding material and reinforcing material in an oven and preheat to a temperature of 330-360 °C for 30 minutes. Pure AL alloy is placed in the furnace section of a stir casting plant and can be heated to 640 °C. Gradually add Copper-(CU) reinforcement from the pouring chamber to the melt to achieve uniform mixing and set the rotor speed to 600 rpm. The reinforcement is then inserted by weight into the molten metal from the same chamber. Rotate the agitator for approximately 25 minutes and move it up and down to evenly mix the molten metal. Remove the mold from the preheating furnace and set it in the furnace throat. When the valve is open, the melt is poured into the mold through the lander and riser pipes. Allow the die to cool for some time before removing the cast sample from the die. Finishing work removes unnecessary parts with a whetstone. The sample is now ready for testing and characterization.



Figure 1: Stir Casting Machine

III EXPERIMENTAL PROCEDURE

COMPRESSION TEST:

Compressive strength is the ability of a material or structure to resist stresses that tend to shrink in size, as opposed to tensile strength, which resists stresses that tend to stretch. In other words, compressive strength resists compression (pushing together) and tensile strength resists tension (pulling apart). When investigating the strength of a material, tensile strength, compressive strength and shear strength can be analyzed separately.



Figure 4: Universal Testing Machine



Figure 2: Pre Heating Furnace



Figure 5: Samples Before Compression



Figure 3: Casting Specimens

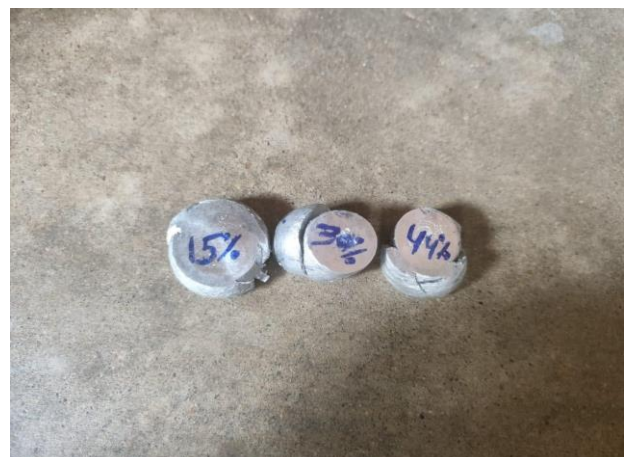


Fig.6: Samples After Compression

TENSILE TEST

Tensile testing is a procedure used to determine the mechanical properties of a material, particularly its strength and elasticity. It involves applying tensile force to a sample of the material, typically a long, thin cylinder, until the material breaks or undergoes permanent deformation. The test is usually performed using a machine called a universal testing machine. Which apply the force and measures the resulting deformation



Figure 7: Samples of Tensile Before and After Testing

HARDNESS TEST:

The hardness of a material can be determined by Brinnel’s, Rockwell and Vicker’s hardness test. In Vicker’s hardness test, diamond indentation is used to determine the hardness. Vicker’s test determines the hardness by the measurement of the depth of penetration of an indenter under load more than compared to the penetration made by a preload. There are different scales, denoted by a single letter, that use different loads or indenters. The hardness of the Pure Al and composites was determined with Vickers Micro Hardness Tester (LECOAT700Microhardness Tester). The dimension of each specimen for hardness testing was 10x10mm and each specimen was grinded and polished to obtain a flat smooth surface. During the testing, a load of 100gm. was applied for 10s on the specimen square based diamond indenter and the hardness readings taken in a standard manner.



Figure 8: Vickers MicroHardnessTester

IV RESULTS & DISCUSSIONS

Compression behavior of Composite (Pure Al + Cu (2%,4%6%)

The compressive strength of composites is measured on specimens using a universal testing machine. The compressive strengths of composites from C1 to C3 are shown in Table 1. The strength of composites has been found to increase with increasing reinforcement loading. The maximum compressive stress obtained was 362 N/mm² for the C3 composite.

Sample	Composite	Compression Strength(N/mm ²)
C1	Pure (Al) + Cu (2%)	199.98
C2	Pure (Al) + Cu (4%)	251.36
C3	Pure (Al) + Cu (6%)	361.82

Table 1. Compression Strength

Tensile behavior of Composite (Pure Al + Cu (2%,4%6%)

The Tensile strength of composites is measured on specimens using a universal testing machine. The Tensile strengths of composites from C1 to C2 are shown in Figure 4.2.1. The strength of composites has been found to increase with increasing reinforcement loading. The maximum compressive stress obtained was 197 N/mm² for the C2 composite. But 4% and 6% of tensile samples are failed due to the induced brittleness of the material.

Sample	Composite	Tensile Strength(N/mm ²)
C1	Pure (Al) + Cu (2%)	56.63
C2	Pure (Al) + Cu (4%)	196.33

Table 2. Compression Strength

Hardness behavior of Composite (Pure Al + Cu (2%,4%6%)

The hardness test values observed that due to increase of percentage of reinforcement hardness was increased.

Sample	Composite	Hardness (VHN)
C1	Pure (Al) + Cu (2%)	69.45
C2	Pure (Al) + Cu (4%)	75.09
C3	Pure (Al) + Cu (6%)	84.13

CONCLUSION

Pure Al reinforced with copper with various proportions of 0%, 2%, 4% and 6% are tested to determine the mechanical, Cu metallurgical and tribological properties such as compressive strength and micro structure, hardness, tensile strength and Charpy impact strength. It is observed that due to increase of percentage of reinforcement compression was increased. It is observed that due to increase of percentage of reinforcement tensile was increased. But 4%, 6% of tensile samples are failed due to the induced brittleness of the material. The hardness of the composite increases with increase in composition of the material.

REFERENCES

- [1] Deepak Kumar, Pradeep K. Singh, "Investigation of Tribological Behaviour of Pure AL Based Metal Matrix Composite using Taguchi's Optimization Approach", 2019 Materials today
<https://doi.org/10.1016/j.matpr.2019.07.365>
- [2] Deepak Kumar, Pradeep K. Singh, "Microstructural and Mechanical Characterization of Pure AL based Metal Matrix Composites" 2019 Materials today
- [3] <https://doi.org/10.1016/j.matpr.2019.07.114>
- [4] Avinash Gudimetla, Surapaneni Sambhu Prasad, Dumpala Lingaraju, "Influence of RHA reinforcements on mechanical and wear behaviour of Pure AL composite", 2020 Emerging Materials Research
- [5] <https://doi.org/10.1680/jemmr.20.00104>
- [6] Pardeep Saini and Pradeep K Singh, "Fabrication and characterization of CU-reinforced metal Pure AL matrix composites", 2020 Engineering Research Express
- [7] <https://doi.org/10.1088/2631-8695/ac4831>
- [8] Deepak Kumar and Pradeep K Singh, "Sliding wear characteristics of Pure AL/CU/GMP hybrid composites using L-16 orthogonal array", 2022 Engineering Research Express
<https://doi.org/10.1088/2631-8695/ac6488>
- [9] Kumar, D., Singh, P.K. Effect of Control Parameters on Tribological Performance of Pure- AL/GP Composites. J Bio Tribo Corros 8, 41 (2022).
- [10] <https://doi.org/10.1007/s40735-022-00639-3>
- [11] [7] S. Senthil Kumaran et al., "High Temperature Sliding Wear Behaviour of Pure AL- ZrB2 in situ composite", 2009 International Journal of Materials Science
- [12] Kolusu Varalakshmi et al., (2019) [8], "Analysis dry sliding wear behavior of Al-coconut shell ash metal matrix composite using stir casting", 2019 Applied Engineering Letters
<https://doi.org/10.18485/aeletters.2019.4.2.3>
- [13] M. Uthayakumar et "Wear performance of Al-CU-B4C hybrid composites under dry sliding conditions, 2013 Elsevier
- [14] <https://doi.org/10.1016/j.matdes.2012.11.059>
- [15] Pardeep Saini and Pradeep K Singh, "Optimization of end milling parameters for rough and finish machining of Pure AL/3%CU metal matrix composite", Eng. Res. Express 3 (2021) 045009
<https://doi.org/10.1088/2631-8695/ac2e11>
- [16] [11] S. Suresha, B.K. Sridhara, Wear composite characteristics of hybrid aluminium matrix reinforced with graphite and Copper particulates, 2010 Composites Science and technology.
- [17] <http://dx.doi.org/10.1016/j.compscitech.2010.06.013>

CRUISE CONTROL SYSTEM USING FUZZY LOGIC FOR AUTONOMOUS VEHICLE

K.Anupama Francy, S.V.Sai Sudheer and S. Rohit

Vishnu Institute of Technology, Bhimavaram, West Godavari, Andhra Pradesh, India

ABSTRACT: The cruise control system has turned out to be a common feature in automobiles at present. And this control system automatically controls the throttle to maintain a set speed. Therefore, the cruise control method can help decrease a driver's tiredness in driving a long road trip. This project works based on Fuzzy Control System and our main aim is to drive alone on the track from 300cm and stop 8cm before the stop block with less rising time and settling time and to follow the variable speed front car and stay 15cm of distance. And the process is first, the IR sensor and motor are calibrated for the initial information to control. Then using my RIO interface Motor controller, motors, and IR sensor are connected. In Lab VIEW, the required circuit is prepared with a fuzzy control model. Rule base and Membership functions for input and outputs are assigned. By conducting several iterations, the optimal Membership function and rule base is formulated for getting the required control. Finally, a fuzzy-based control system is obtained, and real-time tests have conducted.

Keywords: Fuzzy Control, IR sensor and variable speed.